IMPERIAL INSTITUTE
OF
AGRICULTURAL RESEARCH, PUSA

PROCEEDINGS

OF THE

ROYAL SOCIETY OF LONDON

SERIES A

CONTAINING PAPERS OF A MATHEMATICAL AND
PHYSICAL CHARACTER

VOL CXXVII

314729
IARI

LONDON
PRINTED FOR THE ROYAL SOCIETY AND SOLD BY
HARRISON AND SONS, LTD, ST MARTIN'S LANE,
PRINTERS IN ORDINARY TO HIS MAJESTY

JUNE, 1930

LONDON
HARRISON AND SONS, LTD., PRINTERS IN ORDINARY TO HIS MAJESTY,
ST. MARTIN'S LANE

CONTENTS.

SERIES A. VOL. CXXVII.

No. 804.—April 1, 1930.

Antimonial Analogues of the Carbazole Series. By G. T. Morgan, F.R.S., and C. R. Davies ... 1

A Thermal Method of Measuring the Vapour Pressure of an Aqueous Solution. By A. V. Hill, F.R.S. ... 9

Quantitative Analysis by X-Ray Spectroscopy. By C. F. Eddy and T. H. Laby. (Plate 1.) Communicated by Sir Ernest Rutherford, P.R.S. ... 20

The Theory of Metallic Corrosion in the Light of Quantitative Measurements.—Part III. By G. D. Bengough, J. M. Stuart and A. R. Lee. (Plate 2.) Communicated by Sir Harold Carpenter, F.R.S. ... 42

Correction Factors in the Photographic Measurement of X-Ray Intensities in Crystal Analysis. By E. G. Cox and W. F. B. Shaw. Communicated by Sir William Bragg, F.R.S. ... 71

Measurement of Absorbing Power of Materials by the Stationary Wave Method. By A. H. Davis and E. J. Evans. Communicated by Sir Joseph Petavel, F.R.S. ... 89

Characteristic Energy Losses of Electrons Scattered from Incandescent Solids. By E. Rudberg. Communicated by O. W. Richardson, F.R.S. ... 111

The Effect of a Nucleus Spin on the Optical Spectra.—II. By J. Hargreaves. Communicated by R. H. Fowler, F.R.S. ... 141

The Effect of Water Vapour on Diffusion Coefficients and Mobilities of Ions in Air. By J. J. Nolan and T. E. Nevin. Communicated by A. W. Conway, F.R.S. ... 155

Measurements on the Ranges of α Particles. By G. I. Harper and E. Salaman. Communicated by Sir Ernest Rutherford, F.R.S. ... 175

The Effect of Rotation upon the Lift and Moment of a Joukowski Aerofoil. By W. G. Bickley. Communicated by G. I. Taylor, F.R.S. ... 186

On the Spectrum of Bromine in Different Stages of Ionisation. By S. Chandra Deb. Communicated by M. Saha, F.R.S. ... 197

The Kinetics of the Oxidation of Gaseous Benzene. By R. Fort and C. N. Hinshelwood, F.R.S. ... 218

The Conductivity of Thiocyanates in Methyl Alcohol. By A. Unmack, D. M. Murray Rust and Sir Harold Hartley, F.R.S. ... 228

No. 805.—May 7, 1930.

PAGE

Discussion on Catalytic Reactions at High Pressures. Opened by G. T. Morgan 240

The Origin and Nature of Coals and Chars. By H. E. Armstrong, F.R.S. 268

The Optical Rotatory Power of Quartz on either side of an Infra-Red Absorption Band. By T. M. Lowry, F.R.S., and C. P. Snow 271

Study of Electrolytic Dissociation by the Raman Effect. I.—Nitric Acid. By I. Ramakrishna Rao. (Plate 3.) Communicated by O. W. Richardson, F.R.S. 279

The Splitting Strength of Mica. By J. W. Obreimoff. (Plate 4.) Communicated by P. Kapitza, F.R.S. 290

The Mobility of Ions in Air. By J. L. Hamshere. Communicated by Sir Joseph Thomson, F.R.S. 298

The Kinetics of the Heterogeneous Thermal Decomposition of Methyl Formate. By E. W. R. Steacie. Communicated by A. S. Eve, F.R.S. 314

The Spectra of Trebly ionised Oxygen (O IV) and Trebly ionised Nitrogen (N IV). By L. J. Freeman. Communicated by A. Fowler, F.R.S. 330

The Group Properties of Dirac's Operators. By G. Temple. Communicated by A. S. Eddington, F.R.S. 339

The Operational Wave Equation and the Energy Levels of the Hydrogen Atom. By G. Temple. Communicated by A. S. Eddington, F.R.S. 349

The Raman Spectra of some Organic Halogen Compounds. By S. Bhagavantam and S. Venkateswaran. Communicated by Sir Venkata Raman, F.R.S. 360

The Liberation of Electrons from Metal Surfaces by Positive Ions. Part I.—Experimental. By M. L. E. Oliphant. Communicated by Sir Ernest Rutherford, P.R.S. 373

The Liberation of Electrons from Metal Surfaces by Positive Ions. Part II.—Theoretical. By M. L. E. Oliphant and P. B. Moon. Communicated by Sir Ernest Rutherford, P.R.S. 388

The Effect of a Nuclear Spin on the Optical Spectra.—III. By J. Hargreaves. Communicated by R. H. Fowler, F.R.S. 407

The Crystal Structure of the Normal Paraffins at Temperatures Ranging from that of Liquid Air to the Melting Points. By A. Müller. (Plates 5 and 6.) Communicated by Sir William Bragg, F.R.S. 417

The Behaviour of a Single Crystal of Antimony subjected to Alternating Torsional Stresses. By H. J. Gough and H. L. Cox. (Plates 7 to 11.) Communicated by Sir Thomas Stanton, F.R.S. 431

Further Experiments on the Behaviour of Single Crystals of Zinc subjected to Alternating Torsional Stresses By H J Gough and H L Cox (Plates 12 to 15) Communicated by Sir Thomas Stanton F R S 453

Structure in very Permeable Collodion Gel Films and its Significance in Filtration Problems By W J Elford (Abstract) Communicated by J E Barnard F R S 479

No 806 — June 2 1930

Researches on the Chemistry of Coal Part VI —Its Benzenoid Constitution as shown by its Oxidation with Alkaline Permanganate By W A Bone, F R S, L Horton and S G Ward 480

The Interaction of Oxygen with Nitrogen after Collision with Electrons By O H Wansbrough Jones Communicated by T M Lowry F R S 511

The Formation of Ozone from Oxygen after Collision with Electrons By O H Wansbrough Jones Communicated by T M Lowry F R S 530

On the Coefficient of Heat Transfer from the Internal Surface of Tube Walls By A Eagle and R M Ferguson Communicated by G G Stoney, F R S 540

Vertical Electric Currents below Thunderstorms and Showers By T W Wormell (Plates 16 and 17) Communicated by C T R Wilson, F R S 567

The Spread of Vorticity in the Wake behind a Cylinder By L Rosenhead Communicated by H Jeffreys, F R S 590

Photo conductance Phenomena in the Silver Halides and the Latent Photographic Image —Introduction and Part I By F C Toy and G B Harrison (Plate 18) Communicated by T Slater Price, F R S 613

Photo conductance Phenomena in the Silver Halides and the Latent Photographic Image—Part II By F C Toy and G B Harrison Communicated by T Slater Price, F R S 629

The Absorption Band Spectrum of Chlorine —II By A Elliott Communicated by O W Richardson, F R S 638

The Scattering of Electrons by Atoms By N F Mott Communicated by W L Bragg F R S 658

Scattering of Fast Electrons and Nuclear Magnetic Moments By H S W Massey Communicated by R H Fowler F R S 666

Remarks on the Anomalous Scattering of α Particles from the Quantum Mechanical Point of View By H S W Massey Communicated by R H Fowler, F R S 671

An Application of the Stern Gerlach Experiment to the Study of Active Nitrogen By L C Jackson and L F Broadway Communicated by A P Chattock, F R S 678

The Energy of Crystal Lattices By H Jones Communicated by R H Fowler, F R S 689

The Geographical Representation of the Mountains of Tibet By Colonel Sir Sidney Burrard, F R S 704

OBITUARY NOTICES

	PAGE
Henry John Horstman Fenton	i
Sir Henry Bradwardine Jackson (with Portrait)	vi
Percy Alexander MacMahon (with Portrait)	x
Sebastian Ziani de Ferranti (with Portrait)	xix
Index	xxiii

PROCEEDINGS OF
THE ROYAL SOCIETY.

SECTION A.—MATHEMATICAL AND PHYSICAL SCIENCES.

Antimonial Analogues of the Carbazole Series.

By GILBERT T. MORGAN, F.R.S., and GLYN REES DAVIES, Chemical Research Laboratory, Teddington, Middlesex.

(Received January 17, 1930.)

Although arsenic and antimony exhibit certain similarities in regard to their combinations with hydrocarbon radicals, yet the organic chemistry of the latter metalloid is still in a much more fragmentary condition than that of the former element because of the greater experimental difficulties which attend the preparation of organic antimonials. These difficulties are two-fold: the first is the ease with which antimony is dislodged from its attachment to carbon, the second arises from the amorphous and colloidal nature of organic stibinic acids.

In a former communication* we discussed the antimonial analogues of the cacodyl series, whereas in the present one we describe certain organic derivatives in which antimony replaces nitrogen in the carbazole nucleus, these compounds being analogues of the arsenical carbazole series already studied by Aeschlimann, Lees, McClelland and Nicklin.†

The starting material in this research was *o*-aminodiphenyl prepared preferably from commercially available diphenyl. This hydrocarbon was nitrated to a mixture of *o*- and *p*-nitrodiphenyls which were separated and reduced to the corresponding bases.‡

---

* 'Roy. Soc. Proc.,' A, vol. 110, p. 523 (1926).

† 'J. Chem. Soc.,' vol. 127, p. 66 (1925).

‡ *Nomenclature of Diphenyl Derivatives.*—The literature of diphenyl and its derivatives shows that this term is often used to designate either the hydrocarbon or its univalent radicals, $C_6H_5 \cdot C_6H_4$, although certain authors employ "diphenylyl" for these radicals and "diphenylylene" for the corresponding bivalent groups. Such expressions tend, however, to become cumbersome when employed for compounds containing two or more

Antimony is introduced into the diphenyl nucleus by converting *o*-xenylamine (*o*-aminodiphenyl) through the diazo reaction into *diphenyl-*o*-diazonium antimony tetrachloride* C_6H_5 C_6H_4 N_2 $SbCl_4$,* and this diazonium salt when digested with cold aqueous caustic soda until the diazo-nitrogen is eliminated yields *xenyl-*o* stibinic acid* (formula v) obtained as an amorphous white precipitate on acidifying the alkaline solution Reduction of the stibinic acid in presence of hydrochloric acid leads to *xenyl-*o* stibine dichloride* (vi) and by eliminating hydrogen chloride from this dichloride ring closure occurs with formation of *xenylene-2 2′-stibine chloride* (ii) A similar closure of the ring is effected by removing the elements of water from xenyl *o* stibinic acid (v)

By double decomposition with sodium iodide, xenylene 2 2′-stibine chloride yields the corresponding *iodide* (ii) which by Grignard condensations gives rise to the antimonial analogues of the *N* alkylcarbazoles Thus magnesium methiodide furnishes *2 2′ xenylene methylstibine* (iii) corresponding with *N*-methylcarbazole This tertiary stibine does not combine additively with methyl iodide although it furnishes a dibromide (iv) When treated with ammonia or aqueous alkalis xenylene - 2 2′ stibine chloride and iodide (ii) lose their halogen and become converted into *bis 2 2′ xenylenestibine oxide* (i) which has been obtained crystalline from organic solvents

The accompanying diagram illustrates a feature in which aromatic antimonials differ from the corresponding arsenicals When *xenyl *o* stibine dichloride* (vi) is rendered slightly alkaline or ammoniacal the primary xenyl-*o*-stibine dihydroxide thus produced is unstable and by elimination of half its combined antimony as antimonious oxide it passes into a secondary oxide, *tetrakis *o* xenyldistibine oxide* (viii) In this complex oxide each antimony

---

of these diphenyl residues and more euphonious names are extant and applicable, for when A W von Hofmann first isolated the base $C_{12}H_9$ NH_2 from certain "aniline tailings" ('C R,' vol 55, p 901 (1852), 'Roy Soc Proc,' A, vol 12, pp 393, 576 (1862-3)) he decided on the name "xenylamine" after a brief use of the more obscure term "martylamine" (compare 'Jahresbericht p 344 (1862))

Xenylamine was identified concurrently as *p* aminodiphenyl by Schultz ('Ann Chem', vol 174, p 212 (1874)) and by Osten ('Ber D Chem Ges,' vol 7, p 171 (1874)), and later by Hübner (Ann Chem,' vol 209, p 342 (1881)) who like the two preceding investigators referred to Hofmann's xenylamine Moreover, in the 4th edition of Beilstein's 'Handbuch der Organischen Chemie" (vols 5-7, 9, 10, 12) xenyl is employed as a synonym for diphenylyl We propose therefore to follow and extend this usage by adopting another suggestion of Hofmann's to employ the term "xenylene" for the bivalent radical of diphenyl Accordingly there are three xenylamines (*o*, *m* and *p*) and twelve xenylene diamines to be further specified by the notation commonly adopted for diphenyl derivatives

* May, Trans Chem Soc,' vol 101, p 1037 (1912)

atom is now combined with two aromatic radicals and when dissolved in alcoholic hydrochloric acid it furnishes crystalline *di-o-xenylstibine chloride* (VII) which can be utilised as the starting point for another series of antimonial

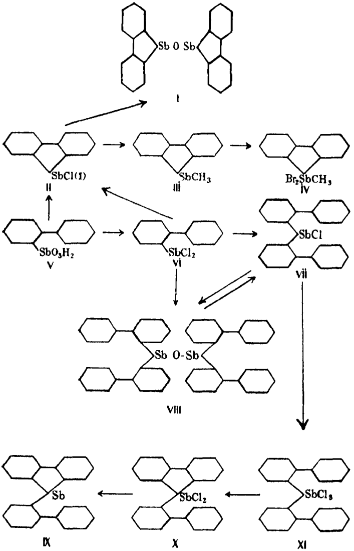

analogues of carbazole *Di-o-xenylstibine trichloride* (IX) produced by direct addition of chlorine to the preceding monochloride (VII) loses hydrogen chloride on gently warming under reduced pressure and passes with ring closure into 2 2′-*xenylene o-xenylstibine dichloride* (X) whilst this cyclic antimonial on prolonged treatment with zinc dust loses its chlorine and gives rise to 2 : 2′-*xenylene-o-xenylstibine*, a tertiary aromatic stibine, which is an analogue of the *N*-arylcarbazoles.

Experimental.

The *o*-aminodiphenyl required in this investigation was prepared by the two following processes :—

1. *Pyrolysis of diazoaminobenzene in presence of aniline.** Owing, however, to the small yield of *o*-aminodiphenyl (about 18 per cent.) and to the tedious nature of the isolation of the base from other products of reaction this preparation was abandoned in the favour of the second process.

2. *Reduction of o-nitrodiphenyl.*—The starting point was commercially available diphenyl which was nitrated to a mixture of *o*- and *p*-nitrodiphenyls, the latter predominating. A comparatively simple method of separation was devised and the isomeric nitro compounds were reduced with iron borings and acidified water.†

Xenyl-o-stibinic acid, $C_6H_5 \cdot C_6H_4SbO(OH)_2$.—50 g. of *o*-aminodiphenyl in 300 c.c. of water and 160 c.c. of hydrochloric acid (D 1.16) were diazotised with 22 g. of sodium nitrite in 100 c.c. of water and to this diazo solution were added 46 g. of antimony trioxide dissolved in 200 c.c. of hydrochloric acid (D 1.126) the temperature being kept between 0° and 25° when *diphenyl-o-diazonium antimony tetrachloride* separated as a light yellow crystalline precipitate (Found : Cl 30.9, Sb 27.3. $C_{12}H_9N_2Cl_4Sb$ requires Cl 31.9, Sb 27.4 per cent.). This complex diazonium salt after washing with water was suspended in 1500 c.c. of water containing 300 g. of ice the mixture being cooled to 0°; 160 to 200 c.c. of glycerin were added and 5*N* caustic soda was introduced slowly with stirring until the mixture was faintly acid for which about 300 c.c. of the alkali were required. After froth had subsided a further 30 c.c. of 5*N* caustic soda were added and the liquid stirred until a sample no longer gave an azo coloration with H acid. The filtered solution was then acidified with dilute hydrochloric acid and warmed to complete the precipitation of the stibinic acid which was freed from inorganic antimony compounds by repeated washing with hydrochloric acid (D 1.126). The viscid residue was extracted with warm 2.5*N* caustic soda and the filtrate acidified with acetic acid. The precipitated stibinic acid dried to a white amorphous powder only very slightly soluble in hot water but dissolving more readily in boiling alcohol from which solution it separated in small colourless crystals (Found C 43 93, H 3 1 Sb 37 42, $C_{12}H_{11}O_3Sb$ requires C 44 3, H 3 39, Sb 37 50 per cent)

---

* Hirsch, 'Ber. D. Chem. Ges.,' vol. 23, p. 1923 (1893) and Aeschlimann, Lees, McClelland and Nicklin, *loc. cit.*

† Morgan and Walls, 'J. Soc. Chem. Ind.,' vol. 49, p. 15 T (1930).

When warmed with concentrated hydrochloric acid the stibinic acid yielded *xenyl o-stibine tetrachloride* $C_6H_5 \cdot C_6H_4 \cdot SbCl_4$ as a yellow oil which on shaking with a saturated solution of ammonium chloride in hydrochloric acid (D 1 126) gave a light yellow crystalline *xenyl* o *stibine ammonium pentachloride* $[C_6H_5 \cdot C_6H_4 \cdot SbCl_5]NH_4$ which after washing with hydrochloric acid was dried on porous tile (Found Cl 37 1 Sb 26 2, 25 8, $C_{12}H_{13}NCl_5Sb$ requires Cl 37 7, Sb 25 9 per cent) *Xenyl* o *stibine dichloride* $C_6H_5 \cdot C_6H_4 \cdot SbCl_2$ was prepared by passing sulphur dioxide into a solution of xenyl-*o* stibinic acid in methyl alcoholic hydrochloric acid containing a trace of potassium iodide On concentrating a chloroform extract of these reagents the dichloride remained as an oily residue which was dissolved in ether and the solution diluted with petroleum (b p 60–80°) when it deposited by slow evaporation rosettes of colourless needles melting at 76° (Found Sb 34 2 $C_{12}H_9Cl_2Sb$ requires Sb 35 2 per cent)

The dichloride was very soluble in the ordinary organic media and showed a great tendency to separate as an oil from these solutions and it was not found possible to convert it into the corresponding xenyl-*o* stibine hydroxide since on treatment with alkali half the antimony was eliminated as trioxide

*Xenyl-*o *stibine diiodide*, $C_6H_5 \cdot C_6H_4 \cdot SbI_2$ was preferably obtained on reducing xenyl-*o*-stibinic acid to the oily dichloride as in the preceding preparation when addition of sodium iodide in acetone solution yielded the solid diiodide which crystallised from alcohol in dark yellow needles melting at 95–96° (Found C 27 58, H 2 0, I 47 5, Sb 23 2, $C_{12}H_9I_2Sb$ requires C 27 23, H 1 7, I 48 0, Sb 23 0 per cent)

Xenylenestibine Chloride (formula II) – This chloride has been prepared by two methods similar to those employed in the preparation of its arsenical analogue* –

1 *Removal of Hydrogen Chloride from Xenyl* o-*stibine Dichloride* —On heating this dichloride at 100° under 25 mm pressure hydrogen chloride was evolved and a dark resinous mass remained which was extracted with chloroform Addition of alcoholic hydrochloric acid to this extract precipitated a grey crystalline powder which was recrystallised from alcohol or chloroform when greenish white diamond shaped plates were obtained

2 *Dehydration of Xenyl-*o *stibinic Acid* – A more satisfactory method consisted in adding 4 g of the stibinic acid to 10 c c of cold concentrated sulphuric

---

* Aeschlimann Lees McClelland and Nicklin *loc cit*

acid to which were subsequently added a further 5 c c of the same acid the mixture was warmed for 10 minutes on the water bath and then poured into a large volume of water The greyish white precipitate was washed, dried and dissolved in warm hydrochloric acid with the minimum quantity of methyl alcohol A fragment of potassium iodide was added to the cooled solution and sulphur dioxide bubbled in until crystals appeared The mixture was then left until deposition of the cyclic chloride was completed The product was recrystallised from alcohol with addition of animal charcoal

Xenylenestibine chloride was thus obtained in greenish white acicular crystals melting at 209° It was moderately soluble in hot chloroform alcohol, acetone or benzene but less soluble in carbon disulphide or light petroleum (Found C 46 35, H 2 87, Cl 11 20, Sb 39 40 (99 82 per cent), $C_{12}H_8ClSb$ requires C 46 56, H 2 59, Cl 11 47, Sb 39 38 per cent)

In the foregoing reduction it is important to avoid excess of sulphur dioxide and to keep the solution cold, otherwise antimony is entirely eliminated from the organic molecule with formation of diphenyl

Xenylenestibine Iodide $(C_6H_4)_2$ SbI prepared by interaction of the preceding chloride and sodium iodide (1 mol) in acetone solution, crystallised from benzene in lemon yellow needles melting at 222° (Found C 36 07, H 2 28, I 31 20, Sb 30 43, $C_{12}H_8ISb$ requires C 35 93, H 1 99, I 31 68 Sb 30 39 per cent)

Xenylenemethylstibine $(C_6H_4)_2$ Sb CH_3 Magnesium (3 6 g) was added to 1 c c of methyl iodide in 25 c c of dry ether, and the solution added to a cooled suspension of 4 g of xenylenestibine iodide in 30 c c of dry ether During this addition the colour of the iodide was discharged and the reaction completed by heating on the water bath for 15 minutes after which the product was poured into water Ether was removed and the residual oil extracted with chloroform The tertiary stibine was obtained as an oil which solidified in a vacuum desiccator Crystallisation was facilitated by adding petroleum (b p 40 60°) to the evaporating solution, but in the presence of air this concentration was accompanied by slight oxidation The product crystallised from petroleum in pale yellowish white leaflets melting at 57° (Found C 53 70, H 3 46, Sb 41 75, $C_{13}H_{11}Sb$ requires C 54 02, H 3 81, Sb 42 18 per cent)

This stibine did not combine additively with methyl iodide although it decolourised a chloroform solution of bromine with deposition of a dibromide

Xenylenemethylstibine Dibromide $(C_6H_4)_2$ $Sb(CH_3)Br_2$ a pale yellow microcrystalline powder was slightly soluble in alcohol or acetone but not appreciably so in other organic media, it melted at 207° (Found Br 35 97 Sb 26 91, $C_{13}H_{11}Br_2Sb$ requires Br 35 65, Sb 27 14 per cent)

Tetrakis o-xenylstibine Oxide $(C_6H_5\ C_6H_4)_2Sb\ O\ Sb(C_6H_4\ C_6H_5)_2$ produced together with antimony trioxide when crude xenyl-*o* stibine dichloride was digested with warm dilute alkali, but was preferably prepared by adding an acetone solution of purified chloride (vii) to a large volume of water containing sufficient ammonia to remain alkaline after heating the mixture on the water bath The viscid oxide after washing with warm water was dissolved in hot acetone, and the solution rendered turbid by addition of water when on evaporation large colourless flattened needles separated melting at 157° and sparingly soluble in alcohol (Found C 66 18, H 4 14, Sb 27 90, $C_{48}H_{36}OSb_2$ requires C 66 10, H 4 13 Sb 27 94 per cent)

Di-o xenylstibine Chloride $((C_6H_5\ C_6H_4)_2SbCl$ The crude oily xenyl-*o*-stibine dichloride was poured into water and the liquid made slightly alkaline with caustic soda or ammonia The mixture containing precipitated xenyl-*o* stibine oxide was warmed on the water bath to complete the elimination of antimony trioxide corresponding with the change from primary to secondary stibine derivative The precipitate dissolved in hot alcoholic hydrochloric acid and on cooling di-*o* xenylstibine chloride separated in colourless needles melting at 125 5° (Found C 61 83, H 3 96, Sb 26 30, $C_{24}H_{18}ClSb$ requires C 62 16, H 3 89, Sb 26 29 per cent)

This chloride dissolved in the ordinary organic media with the exception of light petroleum

Di-o xenylstibine Iodide $((C_6H_5\ C_6H_4)_2SbI$ was obtained either by treating the preceding oxide with hydriodic acid or preferably by interaction of the corresponding chloride and sodium iodide in acetone solution When crystallised from chloroform or alcohol the iodide separated in light yellow prisms melting at 156–157°, it dissolved only sparingly in light petroleum (Found C 52 05, H 3 52, I 23 20, Sb 21 74, $C_{24}H_{18}ISb$ requires C 51 94, H 3 24, I 22 89, Sb 21 95 per cent)

Bis-2 2′-xenylenestibine Oxide (formula i) An acetone solution of 2 2′-xenylenestibine chloride when poured into water containing a slight excess of ammonia gave a white flocculent precipitate of the complex stibine oxide which was coagulated on warming and crystallised from alcohol in yellowish white spangles melting at 177 179° (Found C 51 29, H 3 28, Sb 43 03, $C_{24}H_{16}OSb_2$ requires C 51 10, H 2 84, Sb 43 22 per cent)

This oxide was readily soluble in chloroform, less so in alcohol, acetone or benzene and insoluble in water or 2*N*-sodium hydroxide

Di-o-xenylstibine Trichloride ($(C_6H_5\cdot C_6H_4)_2SbCl_3$) obtained by adding chlorine to the preceding monochloride in chloroform solution, crystallised from a mixture of this solvent and alcohol in small colourless needles melting at 177° (Found C 54·28, H 3·7 Cl 19·80, Sb 22·92 ; $C_{24}H_{18}Cl_3Sb$ requires C 53·91, H 3·37, Cl 19·92, Sb 22·80 per cent.)

Xenylene-o-xenylstibine Dichloride (formula x). When warmed to 50° above its melting point under 20 mm. pressure di-*o*-xenylstibine trichloride commenced to froth vigorously and heating was continued until evolution of hydrogen chloride ceased. On cooling the residue set to a jelly which was extracted with warm chloroform. The product after removing the solvent was crystallised from a mixture of chloroform and alcohol with addition of animal charcoal; it separated in small white nodules melting at 212°. Although dissolving freely in chloroform the dichloride was only moderately soluble in other organic media. (Found C 57·34, H 3·12 Cl 14·20 Sb 24·22 $C_{24}H_{17}Cl_2Sb$ requires C 57·85, H 3·41, Cl 14·26, Sb 24·47 per cent.)

2:2′-Xenylene-o-xenylstibine (formula ix). The foregoing chloride was suspended in 20 parts of alcohol and boiled for 2 hours with 2 parts of zinc dust. The filtered solution was then concentrated when the aromatic stibine was obtained in large rosettes of colourless needles melting at 106–107° (Found C 67·23, H 3·92, Sb 28·27 (99·62 per cent.), $C_{24}H_{17}Sb$ requires C 67·48, H 3·98, Sb 28·54 per cent.) This tertiary stibine was readily soluble in ordinary organic media.

A Thermal Method of Measuring the Vapour Pressure of an Aqueous Solution

By A. V. Hill, F.R.S., Foulerton Research Professor

(Received January 16, 1930.)

(From the Department of Physiology and Biochemistry, University College, London.)

The method described below of measuring the difference of vapour pressure between any two aqueous solutions, or between a solution and the solvent, arose from experiments on isolated surviving muscles, in which it was noticed that stimulation in nitrogen led to a large increase in the rate of resting heat production. This increment in heat rate was traced finally to condensation of moisture on the muscle due to the lowering of vapour pressure caused in the muscle by the accumulation of the products of activity. These experiments are described elsewhere.* The unexpected sensitivity of the apparatus to a change of vapour pressure led to its trial with solutions of various concentrations held by strips of filter paper: the results were so promising that a special instrument was designed and constructed, which alone is referred to in the following pages.

The method has various advantages: (*a*) it is direct† and fairly exact, *e.g.*, the difference of vapour pressure between water and a not too dilute aqueous solution can be measured at any required temperature, within 1 to 2 per cent.; (*b*) it is fairly rapid: a reading is obtained in 30 to 45 minutes and four or five measurements can be made at the same time if desired by a single observer; (*c*) it has a wide range, *e.g.*, one can measure, on the one hand, the difference of vapour pressure between 0.1 M NaCl and 0.2 M cane sugar, or on the other between 5 M NaCl (5 g. molecules NaCl to 1000 g. H_2O) and water, the latter difference being of the order of 500 times the former; (*d*) very small quantities of the solutions are required, enough namely to moisten 1 to 2 sq. cm. of filter paper, say 0.2 c.c.

Apparatus

The thermopile shown in the figure is symmetrical; it has one set of junctions in a line down the middle of one face, the other set in a similar line down the middle of the opposite parallel face It is wound upon a hollow brass rectangular frame insulated with "bakelite" varnish The elements are of

---

* 'Roy. Soc. Proc.,' B, vol. 105, p. 298 (1929), and *ibid.* (in preparation).

† That is, the difference of vapour pressure is measured directly and not obtained by subtraction of two separate measurements.

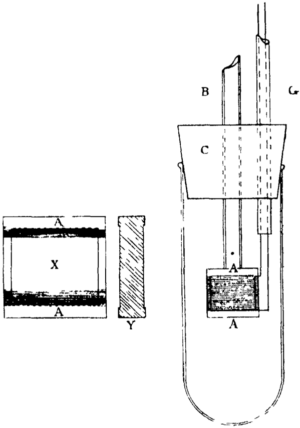

Vapour Pressure Thermopile in Chamber X, insulated brass frame shown enlarged and partly wound with wire, Y side view of same AA, line of junctions B, brass tube C, rubber stopper G, glass tube carrying leads to galvanometer Dimensions of thermopile 23 × 23 × 6 mm, wound with 71 turns of 38 S W G constantan wire, *half of each turn being electroplated*

silver-constantan, made by electroplating constantan wire as suggested by Hamilton Wilson * The wires should be wound as regularly and as close together as possible, and should cover the whole of each face of the frame They are insulated by "bakelite" varnish, each coat of which requires careful baking to harden it and render it insoluble During the baking a little hole in the frame is left open, afterwards this is sealed with shellac Each face is finally trimmed up with flaked or dissolved shellac, and the whole instrument is dipped for a few seconds into a mixture of melted paraffin wax and bees-wax, to render it waterproof by a thin film over its surface The thermopile is not unlike that employed for measuring the heat production of nerve * but simpler and more robust Fuller details for constructing such instruments are given elsewhere †

---

* 'Proc Phys Soc,' vol 32, p 326 (1920)

The thermopile is mounted on a brass tube, which passes through a rubber stopper, it is covered during use by a glass tube forced on to the stopper The leads pass out through a glass tube to two copper terminals on a vulcanite platform above A small hole is drilled at the thermopile end of the brass tube, to allow pressure equalisation to occur with the outside

On one face (A) of the thermopile is laid a small strip of filter paper of suitable size dipped in solution (*a*), on the other face (B) a similar strip of filter paper dipped in solution (*b*) The chamber is kept moist by covering its walls with a large strip of filter paper dipped in any solution (*c*) Let p_a, p_b, and p_c be the water vapour pressures of the three solutions Then the solution (*c*) being in large excess, the water vapour pressure in the chamber will approximate to p_c, except in the immediate neighbourhood of faces A and B The rate of condensation of moisture, therefore, on face A is equal to $k(p_c - p_a)$, where k is some constant depending on (i) the instrument, (ii) the temperature, and (iii) the barometric pressure Similarly the rate of condensation of moisture on face B is $k(p_c - p_b)$, the k being the same since the instrument is symmetrical Now owing to the condenstion of water on the two faces of the thermopile the temperatures of these tend to rise above that of the surroundings After a few minutes the tendency is balanced by heat loss, due to conduction, etc, and a steady state is reached in which face A attains a temperature $k'(p_c - p_a)$ above the surroundings, and face B a temperature $k'(p_c - p_b)$ above the surroundings, the constant k' depending (like k) upon the instrument the temperature and the pressure The final *difference* of temperature, therefore, between face A and face B is $k'(p_b - p_a)$, and is independent of the vapour pressure of solution (*c*) Thus the E M F developed in the thermopile is $K(p_b - p_a)$ where K is a constant (which can be determined for any given instrument by calibration with solutions of known vapour pressures, but depends upon temperature and pressure) and p_a and p_b are the vapour pressures of the two solutions on the faces of the thermopile

A large water bath is employed, stirred with an air stream and kept automatically at a temperature in the neighbourhood of 20° C by a large gas regulator The jet from which the gas emerges is ground off at an angle so that the mercury rising in the tube of the regulator in response to a rise of temperature of the bath diminishes the gas supply gradually There is no " off " and " on " but continuous adjustment The temperature, read by a Beckmann thermometer graduated in 0 002°, remains constant all day long within 0 001° It is found that the reading due to two given solutions on the faces of the thermopile is approximately doubled by a rise of 10° This implies a 7 2 per cent increase per 1°, a 0 007 per cent increase per 0 001° The temperature regulation, therefore, is more than sufficient It is desirable, however, to have it as good and as steady as possible, since sudden changes of temperature—even small ones—produce appreciable disturbances in the readings

---

* Downing and Hill, 'Roy Soc Proc,' B, vol 105, p 147 (1929)

† Hill, 'Roy Soc Proc,' B, vol 103, p 117 (1928)

The difference of temperature between the two faces due to their unequal rates of evaporation (or condensation) is small, but still sufficient to reduce the difference of vapour pressure between the two solutions on them to a just perceptible degree This, of course, does not affect the accuracy, which depends upon direct calibration with solutions of known vapour pressure For example, a 1 per cent NaCl solution on one face, against water on the other, gives a reading at 20° C with thermopile No 1 of about 12 microvolts This instrument has 71 couples of electroplated silver constantan, each giving (say) 35 microvolts per 1° C, a total of about 2500 microvolts per 1° C Thus the 12 microvolts due to the difference between 1 per cent NaCl and water betokens a temperature difference of about 0 0048° C This corresponds to a relative change of vapour pressure of 0 000340 (0 00007 per 0 001°) which is about 6 per cent of the difference between water and the NaCl solution A corresponding relation exists for other concentrations

The rate of dilution of the solution on the face of the thermopile, by the condensation of vapour on it, is not so great, except when large differences of vapour pressure exist in the chamber, as to produce any considerable effect during the time necessary to obtain a reading It is possible, in any case, to avoid such dilution when measuring the difference of vapour pressure between a solution and water, by placing on the wall of the chamber either the solution itself or another solution judged to be approximately isotonic with it Practically no evaporation of, or condensation on, the experimental solution will then occur, while the gradual evaporation of water from the opposite face is found to produce no effect on the reading until the filter paper has become perceptibly drier, this takes several hours to occur It is often convenient, and accurate, to work differentially, *i e*, to measure the small difference between the experimental solution (*a*) (*e g*, blood) and a known solution (*b*) (*e g*, 0 96 per cent NaCl) approximately isotonic with it In that case the same solution (*b*) can be placed on the wall, and no perceptible dilution or concentration will occur on either face during the attainment of a reading The only error of importance, due to evaporation, is caused by delay in placing the strip of wet filter paper on the face of the thermopile and mounting the latter in its chamber in a hot dry room this error might be considerable if the time taken were too long It is advisable to prepare everything beforehand, and to be as quick as possible in the final stages of laying the strip of filter paper containing the experimental solution on the face of the thermopile and of placing the cover in position

The chamber should be connected to the atmosphere by a small hole or a narrow pipe Initial temperature differences due to handling, etc, while setting up the apparatus, and the process of forcing the cover on to the stopper, may otherwise cause the pressure in the chamber to settle down finally to some unknown and arbitrary value Mr B Topley, of the Department of Chemistry University College, informs me that the reading should be inversely proportional to the total pressure in the chamber, provided that it depends mainly on diffusion, as it probably does, thus a constant pressure is necessary The changes of barometric pressure which occur from day to day, or even during a single day, may be allowed for approximately by assuming what has not yet been verified experimentally the inverse relationship referred to above, or their effects can be eliminated by standardising the apparatus, or a similar one, on the day of the experiment by an observation made on a solution of known vapour pressure

The galvanometer employed has been a Zernicke moving coil instrument (Zc) by Messrs Kipp en Zonen of Delft, Holland reading (at $2\frac{1}{2}$ m distance) to $1\ 5 \times 10^{-10}$ amp Except when the readings have been very small they have not been made directly on the scale, but by a null method employing a Pye rotary potentiometer led off into a 1 3000 potential divider constructed with copper wire The arrangement was calibrated with an accurate potentiometer

Standards

The instrument described does not give absolute readings of the vapour pressure, it is necessary to calibrate it on a solution of known vapour pressure The best available data appear to be those of Berkeley, Hartley and Burton* on cane sugar Assuming (i) the results obtained at 30° C with "Apparatus D," as corrected by Berkeley (*loc cit*, p 347), (ii) the results obtained at 0° C (*loc cit*, p 344), and (iii) a value of the relative molal depression of vapour pressure of 0 0180 for very dilute solutions,* two curves for the relatively molal depression were constructed for 0° C and 30° C respectively The data employed are as follows —

---

* 'Phil Trans,' A, vol 218, p 295 (1919)

	Concentration g cane sugar per 100 g water							
	0	34	56 5	81 2	112	141	183	217 5
$\frac{p_0 - p}{[S] p_0} \times 10^2$ at 0° C	[1 800]	—	2 094	2 207	2 344	2 456	2 558	2 602
$\frac{p_0 - p}{[S] p_0} \times 10^2$ at 30° C	[1 800]	1 921	—	2 131	—	2 372	2 476	

Here p_0 is the vapour pressure of water and p that of the solution, while [S] is the concentration of sugar in g molecules per 1000 g of water

The curves for 0° C and for 30° C differ appreciably, but not considerably, from one another, so that a linear interpolation between them is allowable The interpolated data for 20° C are as follows —

Table I

	Concentration g cane sugar per 100 g water						
	0	10	20	30	40	50	60
$\frac{p_0 - p}{[S] p_0} \times 10^2$	1 800	1 845	1 890	1 935	1 980	2 025	2 070
	70	80	90	100	110	120	130
$\frac{p_0 - p}{[S] p_0} \times 10^2$	2 115	2 160	2 204	2 247	2 288	2 328	2 365
	140	150	160	170	180	190	200
$\frac{p_0 - p}{[S] p_0} \times 10^2$	2 398	2 427	2 454	2 477	2 497	2 515	2 530

---

* This theoretical number is justified experimentally, at least at 0° C, by freezing point measurements made on dilute solutions of cane sugar (see Bedford, 'Roy Soc Proc,' A, vol. 83, p 459 (1910)) which allow the calculation of the identical value

If desired sodium chloride solutions can be used instead of cane sugar as standard Data contained in the 'International Critical Tables,' vol 3, allow us to interpolate the following smoothed values for a temperature of 20° to 25° C

Table II

	Concentration g NaCl to 100 g water						
	0.5	1.0	1.5	2.0	2.5	3.0	3.5
$\frac{p_0 - p}{[S]p_0} \times 10^2$	3.317	3.285	3.275	3.269	3.267	3.268	3.270
	4.0	4.5	5.0	6.0	7.0	8.0	9.0
$\frac{p_0 - p}{[S]p_0} \times 10^2$	3.273	3.278	3.285	3.302	3.320	3.339	3.359
	10.0	11.0	12.0	13.0	14.0	15.0	
$\frac{p_0 - p}{[S]p_0} \times 10^2$	3.380	3.401	3.423	3.447	3.471	3.495	

These values were found to be in good agreement with those given above for cane sugar * A similar set of data for KCl gives the following smoothed interpolated values, the effect of temperature being stated to be negligible

---

* The results for NaCl published by Bousfield ('Roy Soc Proc ' A, vol. 103, p 429 (1923)) appear to be considerably in error, if we accept the calibration with cane sugar as correct, see below

Table III

	Concentration g. KCl per 100 g. water						
	0.5	1.0	1.5	2.0	2.5	3.0	3.5
$\frac{p_0 - p}{[S] p_0} \times 10^3$	3.319	3.251	3.220	3.203	3.191	3.183	3.177
	4.0	4.5	5.0	6.0	7.0	8.0	9.0
$\frac{p_0 - p}{[S] p_0} \times 10^3$	3.173	3.169	3.167	3.163	3.161	3.159	3.158
	10.0	11.0	12.0	13.0	14.0	15.0	
$\frac{p_0 - p}{[S] p_0} \times 10^3$	3.158	3.159	3.161	3.163	3.165	3.168	

These again, so far as they have been tested, have been found to be in good agreement with those for cane sugar and for NaCl.

Accuracy

Random errors, at present uncontrollable, perhaps due to variations in setting up, appear to affect the readings, on the average to about 1½ per cent with not too dilute solutions. An early trial in which a solution of cane sugar, 5 g. to 100 g. water, was compared several times with water, led to the following series of readings on the galvanometer scale:—

No.	1	2	3	4	5	6
Reading, mm.	608	605	606	601	601	602
Constant after, minutes	30	35	52	31	33	60

The agreement is unusually good, but shows what may sometimes be attained. The tests shown in Table IV, carried out at various times, give a fairer impression of the average accuracy.

Table IV—In this table percentage concentrations are given as grammes of solute to 100 grammes of water, molal concentrations as gramme-molecules to 1000 grammes of water Readings are given as turns of the rotary potentiometer (in the last experiment as millimetres on the scale)

Experiment of December 16, 1929—

NaCl 1 per cent *versus* water gave 9 29 turns
NaCl 6 per cent *versus* water gave 55 50 turns
Ratio —Observed, **5 98**, from Table II, **6 03**

Experiment of December 17, 1929—

Number	1	2	3	4
Cane sugar per cent	10	60	—	—
NaCl, per cent	—	—	1	6
Reading *versus* water	9 57	65 18	9 63	58 33

The ratio of reading (2) to reading (1) is **6 81**, from Table I, **6 73**
The ratio of reading (4) to reading (3) is **6 06**, from Table II, **6 03**
The ratio of reading (4) to reading (2) is **0 89**, from Tables I and II, **0 93**

Experiment of December 18, 1929—

(*a*) NaCl 1 per cent *versus* cane sugar 10 per cent
Ratio —Observed, **1 036**, from Tables I and II, **1 042**
(*b*) NaCl 6 per cent *versus* cane sugar 60 per cent
Ratio —Observed, **0 917**, from Tables I and II, **0 933**

Experiment of December 21, 1929—

NaCl 0 25, 1 and 6 per cent *versus* respectively, cane sugar 2 5, 10 and 60 per cent
Ratios —Observed, **1 17, 1 06** and **0 90**, from Tables I and II, **—, 1 04** and **0 93**

Experiment of December 30 1929

Number	1	2	3	4	5	6
Cane sugar, per cent	60	—	—	—	—	10
NaCl, per cent	—	-	6	-	1	—
KCl, per cent	-	10	-	—	—	--
Glucose, per cent	—	—	—	10	—	-
Reading *versus* water	63 00	75 35	60 50	17 82	10 01	10 13

Ratio —

Reading (1) to (6) Observed, **6 21**, from Table I, **6 73**
Reading (3) to (5) Observed, **6 04** from Table II, **6 03**
Reading (2) to (3) Observed, **1 244**, from Tables II and III **1 249**
Reading (3) to (1) Observed, **0 96**, from Tables I and II, **0 93**.

Readings (4) and (1) lead to a molal relative depression of 0 0185 for 10 per cent glucose There are no data for glucose in the 'International Critical Tables,' but, if glucose and cane sugar may be compared, Table I gives for a solution of the latter of equivalent strength 0 01885

Experiment of December 31, 1929—

NaCl 6 per cent and 1 per cent *versus*, respectively, cane sugar 60 per cent and 10 per cent
Ratios —Observed, **0 924** and **1 067**, from Tables I and II, **0 93** and **1 042**.

Experiment of January 2, 1930 —Comparison of NaCl 1 M and KCl 1 M

Face A	NaCl	KCl	Water
Face B	KCl	NaCl	NaCl
Reading turns	−2 45	+2 45	+59 3

$$\frac{\text{V P depression KCl}}{\text{V P depression NaCl}} = 1 - \frac{2\ 45}{59\ 3} = \mathbf{0\ 959}$$

For 1 M solutions Tables II and III give a ratio of **0 957**

Table IV -- (continued)

Experiment of January 3, 1930—Comparison of $CaCl_2$ 2M/3 and NaCl 1 M

Face A	NaCl	$CaCl_2$	Water
Face B	$CaCl_2$	NaCl	NaCl
Reading turns	+0 80	1 80	+58 6

$$\frac{\text{V P depression CaCl}}{\text{V P depression NaCl}} = 1 + \frac{1\ 3}{58\ 6} = \mathbf{1\ 022}$$

There are no data in the Tables for $CaCl_2$ to check this comparison.

Experiment of January 6 1930 *and January* 7, 1930 —Comparison of 1 per cent NaCl and 10 404 per cent cane sugar, these, from Tables I and II, should be isotonic The experiment was set up anew 10 times in succession, as follows —

Face A	Water	NaCl	C S	NaCl	C S	NaCl
Face B	NaCl	C S	NaCl	C S	NaCl	C S
Reading mm	+1223	−1	+14	+16	−20	−8
Ratio NaCl/C S	—	1 001	1 011	0 987	0 984	1 007

Face A	C S	NaCl	C S	NaCl	C S
Face B	NaCl	C S	NaCl	C S.	NaCl
Reading, mm	+4	−34	−32	−36	+16
Ratio NaCl/C S.	1 003	1 028	0 974	1 029	1 013

Mean value of ratio **1 004**

Average divergence from mean ±0 014 or 1 4 per cent

Discussion

The principle of the method described above is clearly nothing but that of the wet-bulb thermometer, increased in sensitivity It is interesting to record that A W Reed* in 1913 demonstrated the lowering of vapour pressure of a solution by two wet-bulb thermometers, moistened with a sodium chloride solution and with water respectively Reed used ordinary thermometers and gave no quantitative results

Other methods of measuring the depression of vapour pressure in small quantities of solutions have been described, *e g*, by Barger and by Whytlaw-Gray and Whitaker † These have their advantages for special purposes The present method has, up to the present, been used only for aqueous solutions For solvents other than water it will be necessary to test, and perhaps to modify, the insulation of the thermopile One possible difficulty, which was expected, has not hitherto been encountered, viz, the adsorption of the solute by the filter paper, it would clearly be possible to avoid the effect of this on the vapour pressure by leaving the filter paper for a long time in an excess of the solution to come into equilibrium with it When this has been done no effect on the reading has been noticed with the solutions employed

---

* 'Chem. News,' vol 107, p 64 (1913)

† Barger, 'Trans Chem Soc,' vol 85, p 286 (1904), Whytlaw Gray and Whitaker, 'Leeds Phil Soc Proc,' vol 1, p 97 (1926)

If the method proves to be useful for more dilute solutions, or to a higher degree of accuracy, the possible effects of adsorption must be further examined

By increasing the number of observations and taking a mean, as in the last experiment of Table IV, it is clearly possible to attain a greater accuracy than by a single observation That experiment shows clearly that the data of Tables I and II, for cane sugar and for sodium chloride respectively, are in close agreement Accepting the value for the molal relative depression of cane sugar as correct, that for sodium chloride (1 g to 100 g H_2O) is calculated to be 0 0330 Interpolated from the data in the ' International Critical Tables ' it should be 0 03285 The value calculated from the data of Bousfield and Bousfield is 0 0359, which is apparently in error to the extent of nearly 9 per cent The value for sodium chloride, 6 g to 100 g H_2O, calculated from the results of Table IV, assuming the value 0 0330 for 1 g to 100 g H_2O to be correct, is 0 0330, or, assuming the value for 60 g cane sugar to 100 g H_2O to be correct, 0 0332 The value interpolated from Bousfield and Bousfield is 0 03425, which is 3½ per cent greater than the mean of these Bousfield and Bousfield measured vapour pressure directly as pressure, a procedure which is apparently more liable to error than the weighing of the losses by evaporation from solution and solvent respectively when brought into equilibrium with the same slow stream of air (Berkeley, Hartley and Burton)

Summary

A thermoelectric method is described by which the difference of vapour pressure between two solutions, or between a solution and the pure solvent, can be measured The principle involved is simply that of a differential wet-bulb thermometer of high sensitivity A reading is obtained in 30 to 45 minutes and the average error of a single observation is of the order of 1½ per cent of the difference read

My thanks are due to Mr A C Downing for the construction of the thermopile employed.

Quantitative Analysis by X-Ray Spectroscopy

By C E Eddy, M Sc, Chamber of Manufactures Research Physicist, and Prof T H Laby, M A, Sc D, F Inst P, University of Melbourne

(Communicated by Sir Ernest Rutherford, P R S – Received December 9, 1929)

[Plate 1]

Summary

The previous work of the authors on analysis by X ray spectroscopy, which was shown to be highly sensitive and capable of general application, has been developed as a method of quantitative analysis It has been tested in the first place on alloys of elements of nearly equal atomic number with widely varying concentrations, and is found to have an accuracy of about 1 in 200 , successful preliminary experiments have been made with alloys of elements of unequal atomic number

It is assumed that the ratio of the number of atoms of two elements in an alloy of metals of nearly equal atomic number is equal to the ratio of the intensities of corresponding lines (say the $K\alpha_1$ lines) in the spectra of the elements provided the lines are excited under equivalent conditions The intensities have been determined photographically, and the great advantages of the photographic method for line intensity measurements are pointed out

The effect on the assumption stated above of (*a*) the potential applied to the X-ray tube, (*b*) the variation with wave-length of the absorption and the photographic action of the lines measured, and (*c*) the inhomogeneity of some of the targets used are discussed and tested by experiment

The results obtained are not in agreement in certain respects with those of previous workers Coster and Nishina found that the presence of a third element affected the results of an X-ray analysis, which we have not confirmed for alloys, and came to conclusions unfavourable to the direct method used successfully in this investigation The ratio of the intensities of two lines of a given element is found to be independent of their absolute intensities, contrary to the results of Gunther and Stranski

The X-ray method of analysis has been applied to alloys obtainable only in small amounts, in which the element to be estimated was present in from 0 1 to 0 01 per cent In such cases it is difficult to apply other methods The X-ray method was tested in a series of alloys containing traces of lead in zinc

As these elements differ widely in atomic number, the method described above was replaced by one in which a comparison was made of the intensity of the lead $L\alpha_1$ lines from each alloy with those obtained with an equal exposure from an alloy of known composition

X-ray analysis should be of value in testing the purity of metals to be used in the accurate determination of their physical properties

Introduction

In a previous paper* the qualitative detection of elements by X-rays was discussed and the method, although involving a complicated technique, was shown to be very sensitive and generally applicable In this paper,† experiments will be described which had as their aim the investigation of the possibilities of quantitative analysis by X ray spectroscopy In order to have, in the initial experiments, conditions to which existing theory is applicable alloys of metals of nearly equal atomic number were studied , some results however, are given for alloys without this restriction in their composition

If two elements are present together in the focal spot, the ratio of the intensities of corresponding lines in their spectra should be equal to the ratio of the number of atoms of each element excited and if the elements are present in a homogeneous mixture, this should be equal to the ratio of the number of atoms of each element present If the percentage of one element is known, and the ratio of the intensities of corresponding lines be measured, then it might appear that the percentage of the second element could be calculated The following factors, however, render the position much less simple than this

1 *Line Intensity and Applied Potential*—The intensity of an emission line is dependent upon the voltage applied to the tube If V be the applied potential, and V_K the critical voltage required to excite the line, then the intensity of the line has been found to be a function of $V - V_K$ The exact nature of this function is in some doubt , Table 1 shows the values obtained by several investigators using various spectra , in the fifth column the method used for measuring the intensity is indicated, I denoting the ionisation method and P the photographic method The large discrepancies between the values shown may be due to variations in the applied voltage (even small variations produce a large effect) and to difficulties in the measurement of spectral line intensities

---

* Eddy, Laby and Turner, 'Roy Soc Proc ,' vol 124, p 249 (1929)

† Mr Turner shared in the initial stages of the present investigation, and assisted in checking the photographic line intensity measurements

Table I

Author	Date	Spectra investigated		Method.	Intensity proportional to	Reference
		K series	L series			
Webster and Clarke	1917	Rh	Pt	I	$(V - V_K)^{1.5}$	'Phys Rev,' vol 9 p. 571 (1917)
Wooten	1919	Mo Pd	—	I	$V^2 - V_K^2$	Phys Rev vol. 13 p. 71 (1919)
Kettmann	1923	Cr Rh Cu Ag	Pb La Pr	P	$V^2 - V_K^2$	Z Physik,' vol 18, p 359 (1923)
Stumpen	1926	Mo Cu	W	I	$(V - V_K)^2$	'Z Physik,' vol 36 p. 1 (1926).
Jonsson	1926	Cu	W Pt	I	$(V - V_K)^{1.7}$	'Z Physik,' vol 36 p. 426 (1926)
Allison	1927	—	Th	I	$(V - V_K)^2$	'Phys Rev vol 30, p. 245 (1927)
Nasledow and Scharawsky	1927	Ag Pd Mo	—	I	$V^2 - V_K^2$	'Phys Z vol 28, pp 549, 625 (1927)
Lorentz	1928	Al	—	P	$(V - V_K)^2$	Z Physik vol 51, p 71 (1928)
Allison	1928	—	Ur	I	$(V - V_K)^{1.8}$	'Phys Rev vol 32 p. 1 (1928)

Whatever the real relation may be, only in the case of two elements lying close together in the periodic table will their critical voltages be so nearly equal that this factor will not be of considerable importance The intensity of the lines of the L series is further dependent upon whether the applied voltage is sufficient to excite the K series or not It must also be remembered that the emission line is superimposed upon a continuous spectrum, and the intensity of this must be taken into account when measuring the intensity of the line

2 *Non-homogeneous Targets* —The ratio of the numbers of atoms of each element in the focal spot may not be the same as in the whole target, since the focal spot is generally less than 5 mm^2 in area and the cathode rays penetrate only a few hundredths of a millimetre the target should be sensibly homogeneous if accurate results are to be obtained Further, where one element is more volatile than another (e g, if an amalgam is used as a target) the ratio of the number of atoms may change as the target becomes heated

3 *Comparison of Lines of different Wave Length* The two lines to be compared will have different wave lengths The absorption of a beam of X-rays in passing out of the target, through the tube window, the air in the spectrometer, and the film wrapping will be different for the wave lengths under comparison, and the ratio of the intensities of the two lines when they reach the film will not be the same as the ratio of the intensities of the lines as they are produced in the target Further, the photographic effect produced by the lines* is a function of their wave length It has been shown also† that the intensity of an emission line may be reduced by critical absorption in the target material itself, when the wave-length of the line is less than that of an absorption edge of another constituent The different lines, too, will be reflected by different parts of the crystal, and, in general, the reflecting power of a crystal will vary over its surface The effect of this variation can be reduced by (1) using a narrow incident beam of X-rays, (2) having this beam accurately centred about the rotation axis, and (3) using a uniformly rotating crystal The reflecting power of a crystal is further not wholly independent of the wave-length,‡ but it does not vary appreciably over small wave-length ranges

It is therefore evident that any method of quantitative analysis utilising a direct comparison of the intensities of two corresponding lines must take into account (as far as this is possible) the action of all these factors It may be noted here also that, since the relative intensities of two lines in the same series may change with the atomic number of the emitting element,* neither existing theory nor observation enable the relative amounts of two elements to be deduced from the ratio of the intensities of two lines in different series or of two different lines in the same series Although it is obvious that there are many inherent difficulties, it is evident from the reasons indicated by us previously (*loc cit*, p 267) that the development of any spectroscopic method capable of giving reasonably accurate results is of considerable importance, particularly if it could be applied to the estimation of elements present in quite small amounts

---

* The photographic method only is discussed here because (1) it has the advantages stated on pp 26, 27, and (2) the ionisation method has not been used by previous workers for the purposes under consideration

† Gunther and Stranksi, 'Z Phys Chem,' vol 118 p 257 (1925)

‡ Wagner and Kulenkampf 'Ann Physik,' vol 68, p 369 (1922)

Previous Work--A number of workers have made quantitative analyses of materials by X-ray spectral methods, and conflicting conclusions have been drawn from the various results Hadding† showed that the values given by X-ray analysis are erroneous when the factors influencing the intensity of the spectral lines are not taken into account Gunther and Stranski (*loc cit*), in an analysis of an alloy containing 50 per cent each of nickel and cobalt, obtained, from different photographs, values for nickel varying between 46 and 56 per cent In further experiments to discover the reason for these divergent results, they arrived at the conclusion that the ratio of the intensities of two lines in the same series of an element was not constant but varied with the intensity of one of them This result, if true, would make quantitative X-ray analysis difficult, if not impossible but reasons are given later for believing Gunther and Stranski to be in error

Coster and Nishina,‡ in a series of careful experiments on the determination of the hafnium content of several zirconium minerals, came to a conclusion unfavourable to the direct method of determining amounts of an element, and evolved an empirical method which gave accurate results In their experiments however, the materials to be analysed were in the form of powders rubbed into the roughened copper surface of the target, and this may have introduced errors due to causes discussed later

Several writers§ have shown that a fairly good idea of the quantity of an element present can be obtained from a direct comparison of line intensities

---

* Coster, 'Phil Mag,' vol 43, p 1102 (1922)

† Hadding, 'Z Anorg Chem,' vol 122, p 195 (1922)

‡ 'Chem News,' vol 30, p 149 (1925)

§ Gunther and Wilche 'Ann Chem,' vol 440, p 203 (1924), 'Phys Chem,' vol 119 p 219 (1926), Gunther 'Z Angew Chem,' vol. 37, p 355 (1924), Thomassen, 'Staatens Raastoffkomite Publications' vol 21, p 108 (1925)

Unfortunately all the factors which introduce errors have not been considered and in some cases the spectrographs used have not been suitable for precise measurements The method has not been tested however, for small quantities of an impurity (amounts less than 1 per cent), and it is in this region that a spectroscopic method is likely to prove most valuable A great deal of interest has been shown in the discussion* of the possibilities and limitations of the X-ray method, particularly because the necessity for some physical means of rapidly and accurately analysing materials for small amounts of impurities has arisen in recent years

The possibility of analysis using X-ray absorption spectra for determining the amount of an element has been investigated by Glocker and Frohnmeyer Delauney, and Gunther † In this method the material to be analysed is placed in the path of the X-ray beam and absorption edges due to the elements present are obtained If the ratio of the intensities of the continuous radiation on each side of the absorption edge is measured, then the amount of the element can be calculated This method has many advantages (1) the results do not depend upon the voltage‡ applied to, or the current through, the tube (2) no corrections for differences in absorption or photographic action are required, since the wave lengths compared are practically the same , (3) no special X-ray tube is required, as an ordinary commercial tube can be used, thus the troublesome evacuating system is not necessary , and (4) the material to be investigated may be a metal in sheet form or it may be a powder or a solution Unfortunately, however, it is much more difficult to detect a faint absorption edge than a faint emission line and therefore the absorption method is not so readily applicable to the estimation (or detection) of small amounts of an impurity as the emission method It was therefore decided to investigate the accuracy with which analyses could be made by the emission method when the errors due to the various factors mentioned above were made as small as possible

---

* Gunther, 'Naturwiss ' vol 14 p 1118 (1926), Gunther and Stianski 'Z Phys Chem ,' vol 106, p 433 (1923), Stintzing, 'Z Phys Chem ,' vol 107, p 154 and vol 108, p 51 (1924) 'Phys Z vol 23, p 464 (1922) and vol 27 p 844 (1926), Becker 'Metallborse,' vol 14 p 297 (1924), Sterzel, 'Z Tech Phys ,' vol 5, pp 22, 52, 84 and 125 (1924), Glocker, 'Fortschr Geb Roent ,' vol 31 p 90 (1923) Reis 'Z Angew Chem ,' vol 38, p 249 (1925), Hovesy, 'Chem Rev ' vol 3, p 321 (1927), Borg 'Siemens Z ,' vol 6, pp 135, 187 (1926)

† Glooker and Frohnmeyer 'Ann Physik,' vol 76 p 369 (1925), Delauney, 'C R ,' vol 180, p 1658 (1925), and 'Bull Soc Chem ,' vol 39 p 805 (1926), Gunther, 'Naturwiss ,' vol 14, p 1118 (1926)

‡ It is only necessary that the voltage should be less than that required to excite second order radiation

Measurement of Intensity of X-ray Lines The measurement of X-ray intensity can be made in two ways (1) by determining the rise in temperature caused by the total absorption of the X-ray beam, but this is unsuitable when faint X-ray beams are to be measured, (2) by measuring the effects of the electrons ejected from the atoms due to the passage of the X-ray beam This latter method is equivalent to counting the number of X ray quanta, which may be done in three ways by the use of (*a*) an ionisation chamber, in which the X rays pass through a gas and the resultant ionisation is measured (*b*) the Geiger counter, in which the photo and the recoil electrons produce a sudden electrical discharge, (*c*) a photographic plate or film, in which the electrons ejected in the emulsion render the silver halide grains developable

The ionisation method has usually been used for measuring X-ray intensity Recent measurements of the energy required to form a pair of ions in air, however, differ considerably amongst themselves, and discussions of the recently adopted unit of X ray exposure (the roentgen) have emphasised the difficulty of measuring X-ray energy by ionisation methods * The characteristic features of the ionisation method are (*a*) the fraction of the energy absorbed per unit volume of the gas used is very small, (*b*) this absorption depends on the wave length of the radiation being measured, (*c*) the currents produced in the ionisation chamber vary with variation of the source, and are generally very small and consequently difficult to measure For accuracy in the ionisation method, the photo-electrons ejected by the X-rays should not in general be incident on the electrodes, and there should not be critical absorption by the gas The characteristics (*a*) and (*c*) make the measurement of a narrow beam of X rays of small intensity, such as occur in spectroscopy, very difficult

The photographic method has usually been regarded as less trustworthy than the ionisation method, although it is well known that self-consistent results, and results in agreement with the ionisation method, have been obtained for spectral line intensities Experiments carried out in this laboratory, however, have shown that the photographic method possesses definite advantages under certain conditions, and Dr L H Martin using the photographic method for the measurement of X ray absorption coefficients, is obtaining values in very good agreement with ionisation determinations The features of the photographic method are (*a*) the absorption per unit volume in the emulsion is very much larger than in a gas*, (*b*) the absorption is dependent upon the wave-length, (*c*) the effect of X-ray beams of very small intensity are cumulative, and so with sufficient exposures give measurable photographic densities, and (*d*) permanent records of intensity are made simultaneously at a number of places on the plate As in the ionisation method, errors are introduced by critical absorption in the emulsion The characteristics (*a*), (*c*) and (*d*) give the photographic method great advantages for measuring spectral line intensities Although the relation between density and the intensity of the radiation producing it is not the same for all wave-lengths, it is an easy matter to determine this relation for the wave lengths used The degree of photographic density can be measured rapidly to an accuracy of rather better than 1 per cent by means of a Moll recording micro-photometer

---

* Crowther 'Brit J Radiology,' vol 2 p 175 (1929), Taylor, 'Bur Standards Res,' vol 2 p 771 (1929)

Experiment

The apparatus described previously was used, only the few modifications rendered necessary by the nature of these experiments will be mentioned here

The X ray Tube -The hot-cathode, watercooled, metal type of tube with easily replaceable targets previously described,† was modified by the introduction of a brass tube connected to the central metal portion and surrounding both electrodes in the manner described by Martin‡, this cylinder has the effect of "hardening" the tube and ensures steadier running conditions, which is especially necessary for quantitative work The running of the tube was further improved by the substitution of a four-stage Gaede mercury diffusion pump in place of the smaller Gaede pump used previously, and the mercury vapour was absorbed in a liquid air trap instead of a potassium trap In some of the later experiments, a Philips demountable Metallix X-ray tube type "B"§ (presented to the laboratory by the Philips Lamp Company of Australia) was used, and proved very satisfactory, the rubber gaskets enable joints to be made rapidly and surely and the tube is quite leak-tight For the rather special problem we were engaged in, however, this tube had two disadvantages In order to run the tube continuously on a load of half a kilowatt, it was found necessary to attach watercooling jackets to the anode block, possibly the necessity for this extra cooling would not arise if well degassed targets of high melting point were used Further, in spectral analysis work it is essential that the only radiation entering the spectrometer should arise in the target material itself, and in the tube of our own design this was provided for The Philips tube is so constructed that some scattered radiation from the chrome-iron window support can enter the spectrometer and thus lines which are due to materials in the tube, and not in the target, may be obtained, this objection could easily be overcome by slightly modifying the window support to enable it to be faced either with a pure element or the material under examination

---

* A rough calculation shows that the absorption in the photographic film used is about 12,000 times as great as that of an equal thickness of air, and an ionisation chamber con taining air at atmospheric pressure would need to be over 3 metres in length if the same absorption as in the emulsion is produced

† Eddy, Laby and Turner, *loc cit*, fig 3, p 255

‡ 'Proc Camb Phil Soc,' vol 23, p 785 (1927)

§ For a description of this tube see Bouwers, 'Physica,' vol 5, p 8 (1925)

Calibration of the Photographic Films —Two kinds of films were used, at first Kodak "superspeed" duplitised X-ray film with a Wratten hydrokinone developer was employed, and later ' Agfa " double-coated rontgen film with the special metol-hydrokinone developer recommended for it The Agfa film was found to be very satisfactory for quantitative work, as it has a very fine and well distributed grain, and a further advantage arises from the fact that the emulsion surface is particularly hard and is not easily scratched

Standardised developing and fixing conditions were adopted It is particularly important to develop at a constant temperature, this was accomplished by developing in a large test tube immersed in water contained in a Dewar flask The film was held in a vertical position in the solution and constantly agitated, this precaution is necessary when using duplitised film, as the products of decomposition are removed and development is complete and uniform, and chemical fog is also decreased The development of duplitised film in flat trays is unsatisfactory, as the density obtained is less than for the vertical position, probably because fresh developer does not reach the underside

The density produced in an emulsion is not only a function of the intensity of the X-rays incident upon it, but also of the time of exposure t, the wave-length λ, the nature of the developer, its temperature and time of action As is well known, the Hurter and Driffield relation $D = a + \gamma \log E$ holds for X-rays as well as light, where D is the photographic density produced by an exposure E ($E = It$), and a and γ are constants for a given wave-length and emulsion developed under fixed conditions I is the intensity of the X rays measured as the energy incident per unit time per unit area on the film, and t is the time of exposure The photographic action has been found* to be determined by It^p. Values of p less than unity have been observed, but for intermittent exposures such as we have used $p = 1$ within the limits of experimental error.*

---

* Schwarzschild, 'Astrophys J,' vol 11, p 89 (1900)

The Hurter and Driffield curve for a given photographic film and for X-rays of a definite wave-length (*e.g.*, the Kα doublet of zinc) was determined in these experiments by photographing these lines with about 15 exposures, four or five films being used. The potential applied to the tube was a mechanically-rectified alternating potential, the R.M.S. value of the intermittent impulses being measured by an Abraham and Villard electrostatic high-tension voltmeter in parallel with the tube. This potential was kept at a definite value during an exposure by means of a fine-adjustment rheostat in the primary circuit of the transformer. The time mean of the intermittent current through the tube was given by a moving coil milliammeter, the value being read at intervals of 5 seconds to take into account any small fluctuations. The intensity of the X-rays emitted for constant conditions of applied potential was taken as I = constant $(i\ \ t)$ where i is the mean tube current. During an exposure the crystal was rocked symmetrically with uniform speed over both lines.

The photographic density was measured with a Moll registering microphotometer. The density is defined as the logarithm of the ratio of the intensity of the light incident on the film to that of the transmitted light, the light intensities being proportional to the galvanometer deflections. The density due to the line is superimposed on a background due to the celluloid and emulsion, the chemical fog and the continuous radiation, and it can readily be shown that the density of the line alone is given by the logarithm of the ratio of the light transmitted by that part of the film affected by fog and continuous radiation to that transmitted through the line. Times of exposure were selected so that the resultant line densities were such that the incident and transmitted light beams produced galvanometer deflections of the order of 10 and 5 cm. respectively, so that errors introduced in measuring the density were small. The Moll galvanometer possesses excellent zero-keeping qualities and the time lag of the thermopile and galvanometer combined was of the order of 1 second, enabling films to be passed through the instrument quite rapidly.

On plotting the value of the density of the α_1 line against the logarithm of the exposure, the usual Hurter and Driffield curve was obtained, the points lying well on a smooth curve (see figure) It will be noticed that a straight line part of the curve is not so much in evidence for X-rays,* and for small

---

* Glocker and Traube, 'Phys. Z.,' vol. 22, p. 345 (1921); Bouwers, "Over het meten der intensiteit van Röntgenstralen," Eindhoven, 1924.

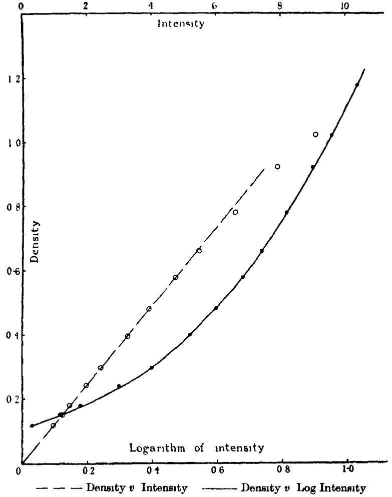

values of the density a straight line is obtained when density is plotted against exposure (or intensity) Graphs constructed from the α_2 line were found to lie parallel to those for the α_1 line From the graph could be read the intensity corresponding to any measured density for any radiation with a wave length near to that of the zinc lines Similar calibrations were carried out for other wave lengths when required, but the variation in photographic action for the film used over a wave length range from 1800 to 500 X U was so small that the curves could be fitted together by suitably altering the intensity ordinates *

---

* See also Dobson, Griffith and Harrison, 'Photographic Photometry,' p 25

The accuracy with which the calibration curve could be constructed was determined by the steadiness of the tube current and voltage during an exposure and by the accuracy with which the current, exposure time, and density were measured As the relative intensities of certain X-ray lines are known, it was decided to test the photographic method by measuring some of these ratios It is to be noted that the spectrometer adjustments (particularly setting the crystal in the rotation axis, and centering the X-ray beam through the axis) must be carried out very accurately for precise measurements of relative intensities Further the crystal must be rocked symmetrically at a uniform speed over both lines , by using an unsymmetrical sweep, or by setting a stationary crystal a little away from the mean reflecting angle, it is possible to alter erroneously the observed ratio of the intensities of the Kα_2 to α_1 lines from 0 5 to 1 5

The results for the ratio of the intensity of the α_2 to that of the α_1 line, with the intensity of the α_1 line, are shown in Table II for zinc and silver in the K series, and for tungsten in the L series, as well as the ratio of the β_1 to α_1 in the K series of zinc The values obtained agree well with the previous determinations and with the theoretical values of 0 50 for the α doublet in K series and of 0 10 for the L series, showing that the photographic method is reliable in comparing spectral line intensities

Table II

							Mean.
Zinc Kα lines	Intensity α_1	14 8	15 5	16 0	17 3	18 1	
	Ratio α_2/α_1	0 50	0 51	0 50	0 53	0 52	0 51
Zinc K lines	Intensity α_1	14 2	16 8	19 4	24 6	31 2	
	Ratio β_1/α_2	0 28	0 26	0 29	0 27	0 26	0 27
Silver K lines	Intensity α_1	17 0	17 8	21 5	25 5	31 6	
	Ratio α_2/α_1	0 52	0 53	0 51	0 50	0 51	0 51
Tungsten Lα lines	Intensity α_1	16 4	19 7	25 1	28 5	30 4	
	Ratio α_2/α_1	0 11	0 11	0 11	0 11	0 10	0 11

The contention of Gunther and Stranski that these ratios vary with the intensity of one line is fundamental to quantitative analysis by X-rays

---

* Dr L H Martin, working in this laboratory has developed a more accurate method of film calibration employing a balance method, and has confirmed this observation over the same wave length range

Determinations of the relative intensities of different pairs of lines in the same series of a particular element have been made by Unnewehr, Siegbahn and Zacek, Allison and Armstrong, and Webster,* but none of these writers record any evidence of a variation of these ratios with the intensity of one line Theoretically, the ratio of the intensities of the lines is the ratio of the probabilities of the electronic transitions which give rise to the lines, and this is constant for a given element Our results given in Table II show that over the range of intensities considered the ratio remains constant, and there is no evidence of the systematic variation found by Gunther and Stranski

Method of Analysis —An attempt was then made to estimate quantitatively the amount of an element present in an alloy In order to reduce as far as possible the errors due to the factors previously discussed, the following experimental plan was followed —

1 *Applied Potential* —In view of the uncertainty of the relation between the intensity of a line and the exciting voltage, the lines due to each element were photographed separately, the voltage being adjusted in each case to exceed the critical voltage for the element by the same amount (usually 10,000 volts) This did not entirely remove the error, however, for the penetration of the cathode rays into the target would be greater when the lines of the element of higher atomic number were being photographed, and thus a greater number of atoms of that element would be excited Since the elements considered were of nearly the same atomic number, this difference in applied voltage was so small that the increase in the range of the cathode rays (as calculated from the formula of Bohr†) was very small, and since further the increased voltage would tend to diminish the area of the focal spot by virtue of the sharper focusing of the cathode rays, the resultant error was negligible

2 *Homogeneity of the Target* —Both homogeneous and heterogeneous alloys, as shown by the appearance of the focal areas in the microscope, were used The elements selected had melting points high compared with the temperature of the focal spot, so that errors would not be introduced by the volatilisation of one element It was found, moreover, that with satisfactory watercooling of the target, alloys with melting points as low as 160° C could be used

3 *Wave lengths of the lines compared* —Since elements of nearly the same atomic number were used, the spectral lines which were compared were nearly

---

* Unnewehr, 'Phys Rev,' vol 22, p 529 (1923), Siegbahn and Zacek, 'Ann Physik,' vol 76, p 369 (1925), Allison and Armstrong, 'Phys Rev,' vol. 26, p 701 (1925), Webster, 'Proc Phys Soc,' vol 41, p 181 (1929)

† 'Phil. Mag,' vol 30, p 603 (1915)

of the same wave length, so that differences in absorption and photographic action introduced no appreciable error Care was taken that no line was used which could undergo a selective absorption either in the target material or in another part of the apparatus

Composition of the Alloys — The various alloys were prepared from the pure elements obtained from Kahlbaum The melting was carried out *in vacuo* to prevent oxidation and to produce a ' gas-free " target The elements were thoroughly mixed by keeping them in a molten state for about half an-hour and vigorously shaking them The target faces were prepared in the manner described previously to prevent contamination The composition of some of the alloys was determined by careful chemical analysis, the others by synthesis this could be done very accurately when the melting points of the components were not too greatly different and oxidation was prevented The success of a synthesis was established when the mass of the alloy obtained equalled the total mass of the components used

During the operation of the tube, the target face became contaminated with a deposit of tungsten from the filament, as this film of metal of high atomic number appreciably absorbed the comparatively soft X-rays used, the target faces were frequently cleaned by removing the top layer In this way two or more focal areas were used during an analysis

Exposures —Usually the α lines of either the K or the L series were used in a comparison Photographs were taken of the lines due to each element in turn, the portion of the film where the lines due to one element would fall being screened with a lead strip while the lines of the other were being photographed This is particularly necessary when the percentage of one element is small, as during the longer exposure required the film is affected by scattered or badly focussed radiations The exposures for the two sets of lines were adjusted so that nearly equal densities of a value suitable for the photometer were obtained

Calculation of the Amount of an Element —If I be the intensity of a line as determined from the measured density by using the Hurter and Driffield graph, n the number of atoms of the emitting element per unit volume in the target and i the tube current passing during the exposure time t, then $\mathrm{I} \propto itn$ If two elements are present together in the focal spot, then the ratio of the intensity of corresponding lines in their spectrum is given by

$$\frac{\mathrm{I}_1}{\mathrm{I}_2} = \frac{\phi_1}{\phi_2} \frac{i_1 t_1 n_1}{i_2 t_2 n_2} \frac{v_1}{v_2},$$

where ϕ represents the efficiency of production of characteristic radiation for the element, and v_1, v_2 represent the volumes of the target in which the radiation is excited. As has been pointed out earlier for elements of near atomic number, ϕ_1/ϕ_2, v_1/v_2 can be written as unity without the introduction of appreciable error, and we have

$$\frac{n_1}{n_2} = \frac{I_1 i_2 A_2}{I_2 i_1 A_1}$$

The ratio of the weights of two elements present W_1/W_2 is given by a_1n_1/a_2n_2 where a_1, a_2 are the respective atomic weights. When a binary alloy is considered, W_1/W_2 can be replaced by $W_1/(100 - W_2)$, and the percentage of each element can be calculated directly.

Results of Analyses

The results of analyses of several alloys are given in Table III. In general, four films were measured for each alloy, and each film was photometered at four different places across the lines. Part of the variation between the results from the different films is due to the experimental errors in determining the exposure time and the tube current, and in holding the voltage constant. In addition, since all films were not taken with the same target face part of the variation may be due to differences in the composition of the alloy from place to place in the target. Experiments showed that exposures which from the measured values of iA were equal produced equal photographic action to within 1 per cent. The variation in the results obtained from different places on the same film may be due to (1) inequalities in the emulsion and (2) heterogeneity of the target. Experiment showed that the second factor was actually present; while the intensity of a line varied along its length, the ratio of intensities at points on the same level on two lines of a given element was constant, but it was not constant for lines of different elements in the same target. It will be noticed that there is a better agreement between the values obtained at different levels when the target is homogeneous than when it is not.

Table III *—Alloy 1 - Cu in Zn Cu 73 00, Zn 27 00† , homogeneous

Film				
1	2	3	4	
72 8	72 7	73 4	73 0	Grand mean 73 1_8 per cent
73 0	73 5	72 8	72 9	
73 3	73 3	73 1	73 4	Mean dep ,‡ ± 0 2 per cent
73 4	73 2	73 3	73 5	
Mean 73 1_1	73 1_7	73 1_5	73 2_0	C – X,§ 0 16 per cent

Alloy 2 —Cu in Zn Cu 73 00, Zn 27 00† , homogeneous

Film				
1	2	3	4	
72 6	73 0	73 1	73 3	Grand mean, 73 1_1 per cent
73 0	72 8	73 3	73 6	
72 9	73 1	73 3	73 1	Mean dep 0 2 per cent
72 8	73 2	73 5	73 3	
Mean 72 8_2	73 0_2	73 3_0	73 3_2	C – X, 0 11 per cent

Alloy 3 - Cu in Zn Cu 1 12 per cent , heterogeneous

Film				
1	2	3	4	
1 13	1 16	1 04	1 18	Grand mean 1 13 per cent
1 11	1 06	1 07	1 16	
1 09	1 19	1 19	1 16	Mean dep , ± 0 05 per cent
Mean 1 11	1 14	1 10	1 17	C - X, 0 01 per cent

* The compositions given in this table are from chemical analysis

† These alloys had the same composition , alloy 1 was annealed, alloy 2 had a cored structure produced by rapid cooling

‡ The " mean departure from the mean " calculated from the 16 readings, is used in preference to the " probable error," as the probable error indicates an accuracy greater than our experimental errors would permit

§ C — X represents the difference between the results given by chemical and X ray methods

Table III —(continued)

Alloy 4 Cu in Zn Cu 0 112 per cent , heterogeneous

	Film				
	1	2	3	4	
	0 110 0 103 0 130	0 101 0 108 0 129	0 126 0 121 0 126	0 109 0 106 0 134	Grand mean, 0 117 per cent Mean dep , ± 0 011 per cent
Mean	0 114	0 113	0 124	0 116	C — X, 0 005 per cent

The variation in the individual results for alloys 3 and 4 is very marked, the results falling close to either one or the other of two well defined values Both these alloys show, under the microscope, evidence of two different solid solutions, and it may be that the variation in the results is due to the predominance of one or the other of these throughout the focal spot The values can be divided in the following way

							Mean	
Alloy 3	1 13 1 16	1 11 1 19	1 09 1 19	1 06 1 18	1 04 1 16	1 07 1 16	1 08 1 17	± 0 03 ± 0 01
Alloy 4	0 110 0 129	0 103 0 126	0 101 0 130	0 108 0 121	0 109 0 126	0 106 0 134	0 106 0 128	± 0 003 ± 0 003

If it is to be inferred that the two sets of values give the composition of the two types of crystals, then the X-ray method must be very sensitive to variations in the composition of the target This might appear to be a serious disadvantage, since usually materials for analysis are heterogeneous, and results obtained from small portions of the area of the focal spot (about 3 square millimetres) and a few hundredths of a millimetre thick would not necessarily be true for larger portions An improvement can be made by substituting a flat spiral cathode giving a circular focus of as much as 5 mm diameter, thus enabling a much larger sample to be used , if the spectrometer slit system is placed at glancing incidence to the target face, no great diminution in the energy being analysed results It has been found, however, that even with coarse grained targets no large errors are introduced On the other hand, it would appear to be possible to develop an X-ray method, using a pin-hole spectrum of the target, which would give information concerning the variation in the chemical composition of the crystals forming the surface of a metal, such as is required in investigating problems in corrosion

The results of the analyses of four other alloys are shown together in Table IV As in the previous table four readings were taken for each film but for the sake of brevity only the mean for each film is given

Table IV

Alloy	Composition	Type	X ray results		Mean
5	70 8 per cent Sn* 29 2 per cent Cd (eutectic)	Homogeneous	71 1 71 2	70 9 71 3	70 8 ± 0 3 per cent
6	60 45 per cent Pb 39 55 per cent Bi (synthesis)	Heterogeneous	60 1 60 6	60 1 60 1	60 2 ± 0 4 per cent
7	12 21 per cent Zn in a ZnCuSn alloy (chemical analyses)	Heterogeneous	12 1 12 1	12 2 12 2	12 2 ± 0 2 per cent
8	17 05 per cent Sn 82 95 per cent Zn (chemical analyses)	Heterogeneous	47 9 48 0	47 8 48 1	48 0 ± 0 5 per cent

* Mean of the published values for the composition of the eutectic

The third column of the table indicates the nature of the target, while in the fourth are given the mean values for the composition obtained from each film The final mean, as well as the mean departure from the mean calculated from the 16 results obtained for each alloy, are in the last column

The target used for alloy 5 was the eutectic of cadmium-tin It was found difficult to prepare a sample of this eutectic which was uniform throughout, but an ingot was obtained which had a central core of eutectic of about 1 cm diameter surrounded by a layer containing excess cadmium The centre was then used as the target, but unfortunately the composition of the core could not be calculated from the synthesis The published values for the composition of the cadmium-tin eutectic are not in good agreement, that given in the Landholt-Bornstein Tabellen (1912) is 71 9 per cent tin, in 1927 70 0 per cent, and the International Critical Tables 72 0 per cent, so we have used in preference the mean (70 8 per cent) of the following values Stoffel 70 59, Schleicher 71 4, Lorentz and Plumbridge 70 0, Manzatto 70 0, and Bucher 72 0 *

* Stoffel 'Z Anorg Chem,' vol 53, p 14 (1907), Schleicher, 'Inter Z Metall,' vol 2, p 76 (1912), Lorentz and Plumbridge, 'Z Anorg Chem,' vol 83, p 235 (1913), Manzatto, 'Inter Z Metall,' vol. 4, p 13 (1913), Bucher, 'Z Anorg Chem,' vol 98, p 106 (1916)

Alloy 5 is (with the exception of alloy 8) the only one in which the two elements compared are not of adjacent atomic number Here the difference in atomic number (Cd = 48, Sn = 50) is associated with a difference in excitation voltage of 2,400 volts compared with differences of only 800 volts for the copper zinc, and 600 volts for the lead-bismuth alloys, and this would possibly increase the radiation from the tin as the penetration of the cathode rays would be a little deeper when the tin lines were being photographed, further, the K lines of tin will be subject to slightly less absorption than those of cadmium The effect of these two factors would make the X-ray analysis value for the tin content a little higher than the true value, and we conclude that the cadmium tin eutectic does not contain more than 71 1 per cent of tin, and possibly a little less

With this alloy an analysis was also made by comparing the intensities of the $K\alpha_2$ lines, the mean value of 71 3 per cent agreeing well with that of 71 1 per cent derived from the α_1 lines

A further result of interest was obtained with this alloy The critical absorption edge of cadmium is of longer wave-length than that of the $K\beta_1$ line of tin, and the line would therefore suffer selective absorption, it is to be expected that the result obtained from a comparison of the β_1 lines of the two elements would give too low a value for the tin content Measurements showed the apparent amount of tin as 63 4 per cent, illustrating the magnitude of the error due to selective absorption This error would be increased when dealing with alloys of greater cadmium content

The ternary mixture of copper, zinc and tin in alloy 7 was investigated to determine whether the relative intensities of the lines of two elements would be influenced by the presence of a third Coster and Nishina found that the presence of a third component changed the relative intensities of the lines due to the other two elements, for example, with a mixture of SnO and Sb_2O_3 containing equal numbers of tin and antimony atoms, the ratio of the $L\alpha$ lines of antimony to tin was found to be unity when 88 per cent of $CaSO_4$ was added, but increased to six when the amount of $CaSO_4$ was reduced to zero The reason for this result is not at all obvious, but as Coster and Nishina had used the "rubbed powder" method of preparing their targets it was thought advisable to test this point with an alloy target

With this mixture of three components it was not possible to determine directly the amount of one element present, instead the ratio $K\alpha_1Zn$ $K\alpha_1Cu$ was determined and the zinc content calculated from the known copper content The results obtained show no evidence of the effect found by Coster and Nishina

The analysis of alloy 8 was carried out to determine the errors involved when two elements of very different atomic number are compared In this case, tin (N = 50) requires an excitation potential of 29 1 kilovolt, while zinc (N = 30) needs only 9 65 kilovolt The depth of the focal spot when the tin lines were being photographed was consequently a great deal larger than for the zinc lines, in addition the absorption experienced by the zinc lines (λ = 1435 X U) was much greater than by the tin lines (λ = 494 X U) the total effect of these two factors being to greatly increase the apparent value of the tin content

A survey of all the results obtained shows that the mean departure from the mean is about 0 5 per cent when the element occurs in amounts of 50 per cent or more, and is as little as 0 01 per cent when impurities of about one-tenth of 1 per cent are being estimated * While the accuracy reached with larger proportions does not approach that obtainable under favourable conditions by chemical analysis it appears that for lower proportions than 1 per cent the method may be extremely useful

It is evident that the intensity of the emission lines is directly proportional to the amount of the element present in an alloy, and results of reasonable accuracy can be obtained when elements of adjacent (or nearly adjacent) atomic number are being compared Direct determinations of amounts of elements of widely different atomic number would only be possible when preliminary experiments determining the effect of the variation of the penetration of the cathode rays of various velocities into the particular target material being investigated, and the variation of the absorption and photographic action with wave-length have been carried out A simple scheme for performing routine analyses, such as would be needed in most general applications of the method, and which is not affected by differences in atomic number and wave-length, is at present being developed The theory of the method will be given in a later paper, but the results of some preliminary experiments are of interest At the request of the Electrolytic Zinc Company of Australia the lead content of a series of zinc-lead alloys was determined The amount of lead present varied between 0 1 and 0 01 per cent, and, as each sample was not more than 5 grams in weight, chemical analysis was difficult and would involve micro-chemical methods One sample with a lead content of

---

* The agreement between the values given by chemical analysis and by X rays using the photographic method is very good evidence that the photographic plate can be used to measure the intensity of even very weak X ray beams to an accuracy of rather better than 1 per cent

0 087 per cent taken from a large ingot for which the same difficulty of analysis did not arise was used as standard, and the Lα lines due to it were photographed with a given exposure Equal exposures were then made with the other samples, and the amount of lead present in each calculated from the ratio of the intensities of the lines obtained from the unknown and standard samples Results for the alloys of unknown lead content ranged from 0 064 to 0 008 per cent, and although no analysis by another method was carried out, these values were in good agreement with other evidence as to the composition of the samples

This method has the very great advantage that, provided equal exposures are given, the results are not affected by any of the factors discussed earlier as the incident cathode rays have the same velocity, the volume of the focal spot is constant, and the same wave-length is used throughout It is necessary that the voltage should be maintained at the same average value during each exposure, and that the average current and the time of exposure should be measured accurately The disadvantage that a sample of similar composition containing a known amount of the element being estimated is required may be overcome after further work has been done

The Effect of Heterogeneity of the Target—The degree of heterogeneity of each alloy studied was found by microscopic examination In Plate 1, fig 2 the micro-photographs of the more relevant specimens are shown We have to thank Prof Greenwood and Mr G B O'Malley of the metallurgical laboratory for advice and assistance in preparing the alloys, and Mr H P Russell and Mr R S Matthews for polishing the specimens and taking the photographs As several of the alloys were very soft, it was difficult to polish and etch the surfaces to show their structure and to obtain photographs with satisfactory contrast The photographs show a number of casting flaws due to casting small ingots *in vacuo* With the exception of C, the area shown in each photograph is about one-fifth of that of the focal spot, the width of the focal spot is approximately equal to the diameter of the photograph

The structure of alloy 1 (copper 73 per cent in zinc, homogeneous) is shown in A, with that of alloy 2 (the same composition, but cored by rapid cooling) in B The X ray analysis showed no evidence of the effect of the different structures for these two alloys

The structure of alloy 4 (0 1 per cent copper in zinc, heterogeneous) is shown in C, which is a macro-photograph Microphotographs of this alloy show crystals of two different solid solutions, but with poor contrast A similar structure was found for alloy 3 (1 1 per cent copper in zinc) and it is

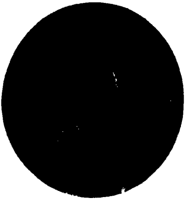

A. Alloy 1. 73 per cent. Cu in Zn, homogeneous.

B. Alloy 2. 73 per cent. Cu in Zn, heterogeneous.

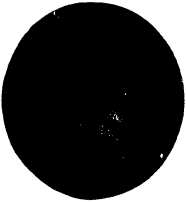

C. Alloy 4. 0·1 per cent. Cu in Zn, heterogeneous.

D. Alloy 5. 70·8 per cent. Sn in Cd, homogeneous.

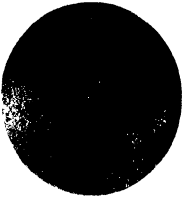

E. Alloy 6. 60·2 per cent. Pb in Bi, heterogeneous.

F. Alloy 7. Cu, Zn, Sn, heterogeneous.

(Facing p. 40.)

probable that the two concentrations given by the X-ray analysis of alloys 3 and 4 correspond to these two solid solutions In this photograph, the area shown is 1,200 times that of the focal spot In spite of the large apparent size of these crystals, microscopic examination showed that it was impossible to find an area on the surface as large as the focal spot which did not contain several crystals of each kind

The central core of cadmium tin eutectic (about 70 8 per cent of tin) of alloy 5 is shown in D The last two photographs show the most heterogeneous alloys used, in E the lead bismuth alloy 6 (60 2 per cent lead) shows crystals of widely different composition, and in F the copper-zinc tin alloy 7 (copper 73 per cent, zinc 12 2 per cent, tin 14 8 per cent) with crystals of three different compositions Even with such heterogeneous targets as these, no difference was noticed between analyses from different focal spots indicating that only with heterogeneous alloys with very large crystals would the X-ray method of analysis be likely to give inaccurate results

Comparison of the X ray Emission with other Methods of Spectral Analysis Results obtained with the X-ray absorption method* agree to within 5 per cent with those of chemical analysis, and are therefore less accurate than those obtained with the emission method The method has advantages when liquids and powders are being investigated, but it does not appear to be applicable to mixtures in which the amount of the impurity is less than 1 per cent, as the absorption edges are not then well defined With mixtures containing elements of both high and low atomic number, long exposures are required to record the long wave length absorption edges, as the X-ray beam is greatly reduced in intensity by the elements of high atomic number Further, it is impossible to analyse metals unless they are in the form of thin sheets, and during the preparation of these sheets it is very easy to introduce impurities

The X-ray emission method of quantitative analysis possesses definite advantages over an optical method particularly as the optical methods are generally not satisfactory above 1 per cent, and the lower limit of detection of some elements is about 0 01 per cent Where it is applicable, however, the optical method is more rapid, requires a less expensive equipment, and the technique is simpler It is to be expected, therefore, that until the X-ray emission method is simplified it will be applied more particularly in cases where other methods fail, and where expensive apparatus and skilled workers are available It should be of value also in testing the purity of samples of the metallic elements intended for the accurate determination of physical

* Glocker and Frohnmeyer, *loc cit*, Gunther, ' Naturwiss,' vol 14, p 1118 (1926)

properties such as electrical and thermal conductivities, which are greatly changed by the presence of small amounts of impurity

We again desire to thank Dr Ian Wark for carrying out the chemical analysis of the alloys and we are indebted to Mr H C Webster for correcting the proofs of this paper Part of the cost of the investigation was met by the gift of the Victorian Chamber of Manufactures to the University of Melbourne

---

The Theory of Metallic Corrosion in the Light of Quantitative Measurements — Part III

By G D Bengough, J M Stuart, and A R Lee

(Communicated by Sir Harold Carpenter, F R S — Received December 18, 1929)

[Plate 2]

The present paper describes an investigation into the degree of reproducibility obtainable by the oxygen absorption method of measuring corrosion, and gives comparative results for this and the loss of weight method The work described in Part II* which dealt with the corrosion of zinc in dilute potassium chloride has been extended up to 4N solution, and to a series of potassium sulphate solutions from N/10,000 to N

Slight vibration of the apparatus has been found to have been the source of error in three of the experiments described in Part II, namely those performed in N/200 and N/10 KCl The corrosion time curves for these solutions show too steep a slope owing to convection of oxygen set up by the vibration. Curves more nearly representing corrosion in truly stagnant conditions are given in fig 4 of the present paper The effect of vibration was only important in those experiments which were controlled by the rate of oxygen supply whereas most of the experiments of Part II were controlled by the concentration of chlorine ions

Most of the experiments for the present paper were performed in conditions in which the rate of oxygen supply was the controlling factor Accordingly special precautions have been taken against vibration

In the latest apparatus the thermostats are mounted on brick pillars, built up from the concrete ground floor of the laboratory, which carry three 3-inch steel girders covered with planks, 1 5 inch thick All accessory gear, such as motors and stirrers, is carried independently of the thermostats on shelves attached to the laboratory wall The corrosion vessel is seated in a recess in a brass holder placed on the bottom of the thermostat and is held above the water level in a clamp attached to the wooden casing of the thermostat lagging

---

* 'Roy Soc Proc,' A, vol 121, p 88 (1928)

The manipulation and general conditions of the experiments have been kept similar to those used for the earlier work with the following alterations The electrode vessel shown in fig 1 is now used instead of that shown on p 439 of

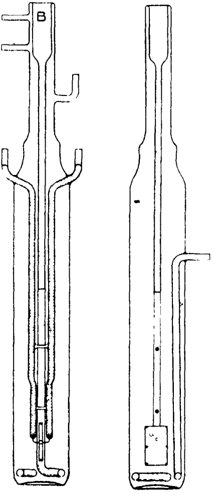

FIG 1 —Electrode Vessel

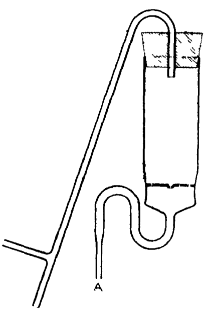

FIG 2

the Proceedings,' A, vol 116, 1927, the new design is preferred for its greater strength For dissolving the salt for strong solutions the apparatus shown in fig 2 is used The salt required is weighed directly into this vessel, and A of fig 2 is attached to B of fig 1 by a rubber stopper The salt contains entangled air and the vessel should be swept out with purified air after making connections with the electrode vessel as described in Part II Conductivity water is then passed to and fro from the electrode vessel, till all the salt is dissolved For making up dilute solutions a vessel is used similar to that shown at 1 of fig 2 of Part I, except that glass baffles have been attached to the central tube, for the purpose of checking loss of spray during evaporation, the baffles are notched to permit the insertion of a fine tube down the side of the vessel

Reproducibility

Much of the literature on corrosion work on totally immersed specimens shows failure to maintain a reasonable degree of agreement between supposedly duplicate experiments Occasionally remarkable agreement is obtained,* while another series of experiments performed under apparently similar conditions, shows wide discrepancies Sometimes the discrepancies are put down to variations in the metal samples but without evidence independent of the corrosion results, though it is clear that the discrepancies may be due mainly to factors of the environments, some of which are difficult to control Few papers purporting to give quantitative results state quantitatively the controlling factors under which they were obtained or provide evidence that a reasonable degree of reproducibility was maintained throughout One of the principal objects of the present research is to ascertain the degree of reproducibility attainable in the presence of defined controlling factors, which, so far, have been (1) oxygen control (2) ion control

The duplicate experiments of Table I and fig 3 show the order of reproducibility reached with zinc The general table of results at the end of the paper gives further details of these and other experiments

A *Reproducibility in Conditions of Oxygen Control*--The term "oxygen control" is used in this paper in the following sense

A metal is said to be corroding under oxygen control when the rate of corrosion is increased by an increase in the rate of oxygen supply (by such means as alteration of partial pressure, size of vessel or convection currents) The

---

* Heyn and Bauer, 'Mitteil König Materialprüfungsamt,' vol 46, p 100, etc, Newton Friend, 'J Iron & Steel Inst,' vol 117, p, 644 (1928), Evans, 'J Chem Soc,' p 123 (1929)

Table I

Experiment															
A 89		A 105		A 84		A 85		A 98		A 104		A 86		A 87	
N/200 KCl		N/200 KCl		N/1000 KCl		N/1000 KCl		N/10 K_2SO_4		N/10 K_2SO_4		N/1000 K_2SO_4		N/1000 K_2SO_4	
t days	Oxygen c.c.	*t* days	Oxygen c.c.	*t* days	Oxygen c.c.	*t* days	Oxygen c.c.	*t* days	Oxygen c.c.	*t* days	Oxygen c.c.	*t* days	Oxygen c.c.	*t* days	Oxygen c.c.
0.7	0.5	0.75	0.90	0.79	0.44	0.8	0.44	0.75	0.58	0.76	0.75	0.73	0.61	1.75	2.28
18.7	29.47	12.75	20.35	7.79	10.75	7.8	10.65	10.75	14.81	17.75	24.16	1.73	2.08	7.75	10.92
27.7	40.87	18.75	30.29	10.79	14.86	10.8	14.80	19.75	24.60	23.75	32.30	5.75	7.67	11.75	14.01
36.7	47.02	24.75	38.12	14.79	19.79	14.8	19.72	31.75	41.55	30.75	41.97	10.75	13.12	21.75	16.23
51.7	53.30	30.75	43.30	17.79	23.25	19.8	25.47	35.75	51.50	37.75	52.96	14.75	15.78	28.75	16.84
—	—	37.75	47.29	22.79	27.78	23.8	28.66	46.71	62.88	47.75	67.41	21.75	17.41	34.75	17.17
—	—	44.75	49.98	28.79	30.10	36.8	32.67	51.71	73.41	52.75	75.90	28.75	18.36	41.75	17.39
—	—	—	—	37.79	32.34	46.8	34.16	—	—	—	—	38.75	19.04	—	—
—	—	—	—	46.79	33.63	—	—	—	—	—	—	—	—	—	—

Note.—Intermediate readings between these given in the table were taken, usually daily, for "apparent oxygen

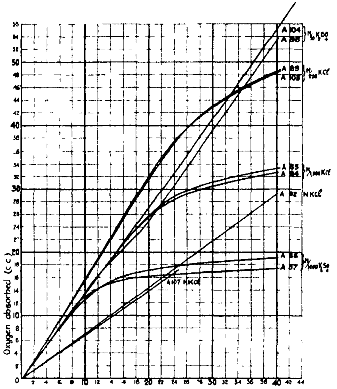

FIG 3 —Curves showing Reproducibility (Oxygen Absorption)

corrosion-time curve is a straight line the slope of which is determined by the rate of oxygen supply The maximum possible rate of corrosion under oxygen control for a given metal is fixed by the partial pressure of the oxygen, the configuration of the apparatus, the nature of the liquid, the uniformity of conditions and mechanical stability, but within this rate the same metal may corrode at different rates in different solutions The different rates of corrosion of the same metal in different solutions of the same salt which possess differences of oxygen solubility too small to account for the different rates seem to be most simply explained on the hypothesis of effectively restricted cathodic areas As the concentration, and therefore the conductivity of the solution is increased the effective cathodic area is also increased The restriction of a cathodic area may be due to its characterisation by a special kind of metallic surface or film, or to a rapid fall of hydrogen concentration outwards from the anode, so that depolarisation takes place very slowly beyond a certain distance

Fig 3 shows that in N/KCl the slopes of the curves for experiments A92

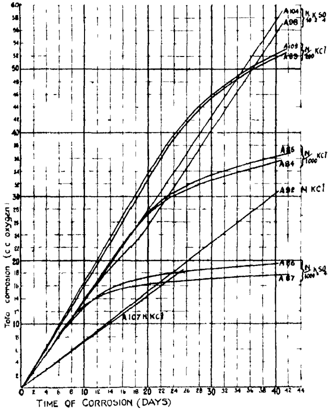

FIG 3A.—Curves showing Reproducibility (Total Corrosion)

and A107 correspond to an oxygen absorption of 0.725 and 0.714 c c per day, the difference of these from the mean value is ± 0.76 per cent.

Experiments A89 and A105 in N/200 KCl show that oxygen control was maintained for the period of 1 to 20 days. The slopes correspond to a rate of oxygen absorption of 1.606 and 1.635 c c per day respectively. These duplicates differ from the mean value by ± 0.95 per cent.

In experiments A84 and A85 with N/1000 KCl oxygen control was only maintained for the period between about 1 and 14 days, and the slopes correspond to 1.382 and 1.377 c c per day.

The difference from the mean value is ± 0.2 per cent.

The slopes for N/10 K_2SO_4 in experiments A98 and A104 correspond to 1.41 and 1.38 c c per day respectively, the difference from the mean is ± 1 per cent. The slope for A98 has been taken from the curve between 20 and 40 days, this is closely similar to that between 1 and 12 days, between

12 and 20 days the slope is slightly different, but the authors can suggest no reason for this temporary alteration

Straight line curves for A86 and A87 in N/1000 K_2SO_4 were only obtained for 5 or 6 days, after which control passes over to the (SO_4) ion concentration The slopes are 1 41 and 1 44 c c per day and the difference from the mean is less than ± 1 per cent

The fact that the slope of the curve for N/1000 KCl agrees with those for N/1000 and N/10 K_2SO_4 means that in all three solutions approximately the same proportion of the total metallic area is functioning as cathode

The above results with others summarised in fig 8 show that the rate of oxygen supply to the specimens in the present series of experiments varies with the concentration of the solution from a maximum of 1 75 c c per day in N/10 KCl to a minimum of 0 19 in 4N KCl, and that in experiments controlled by oxygen in this range it is possible to obtain reproducibility such that the difference from the mean of two experiments is not greater than ± 1 per cent Any difference greater than this may reasonably be set down to some factor or factors connected with the metal

B *Reproducibility in Conditions of Ion Control*—Data have already been given in Part I of this research on reproducibility under control by chlorine ion concentration In N/20,000 KCl it was less than ± 1 per cent This was exceptionally good, for in N/10,000 it was only ± 4 per cent and was worse for the first few days when the possible errors in observation were large in proportion to the total corrosion Table II shows more recent results for N/10,000 KCl taken from Part II, here again the reproducibility is poor for the first 5 days, but improves and becomes satisfactory after about 10 days

Table II

Days	Cubic centimetres of oxygen			Mean value	Maximum difference	Per cent variation from mean
	A 50	A 67	S 2			
5	4 24	4 00	4 61	4 28	0 61	±7 0
10	7 50	7 15	7 75	7 47	0 60	±4 0
20	10 92	10 35	10 38	10 55	0 57	±2 5
30	12 04	11 47	11 42	11 64	0 43	±2 0
40	12 41	12 00	12 03	12 15	0 41	±1 7
50	12 58	12 25	12 50	12 44	0 33	±1 3

Fig 3 of the present paper shows that in N/1000 solutions after oxygen control has ceased and ion control begun reproducibility is liable to vary

For A84 and A85 the variation from the mean value is ± 1, for A86 and A87 it is ± 4 It is possible that part of these variations between duplicates may be due to small differences in the total volume of liquid used, which becomes important in conditions of ion control Special precautions were taken to ensure constancy of depth of immersion and cross section of vessel in all experiments, since these dictate the rate of oxygen supply, in the authors' apparatus it is difficult at the same time to keep the total volume of liquid absolutely similar in all the experiments, and there has been a possibility of about 1 per cent variation in volume in these experiments Precautions are now being taken to eliminate this source of error, which only affects those few experiments which are under ion control

Factors which limit Reproducibility

The necessity for annealing the metal after shaping has been shown in the earlier parts of this research For metal so treated the principal factors which limit reproducibility are

1 *The Presence of Metallic Impurities*—Even the small quantities of metallic impurities which occur in high-grade electrolytic zinc may affect the corrosion process It has already been shown in Part II of this research that there is no appreciable evolution of hydrogen gas from the "spectroscopically pure" grade A zinc of the New Jersey Zinc Company in N/10,000 KCl solution, whereas measurable quantities of gas are evolved from the less highly purified electrolytic zinc In N/10 KCl about one fifth of the volume obtained from the latter was obtained from the spectroscopically pure metal, the comparison being made when a total corrosion of 265 mgms had taken place It was shown in Part II that the rate of evolution of the gas was proportional to the total corrosion* in the range 0–125 c c of oxygen absorption in N/10 KCl, and this was interpreted to mean proportionality to the production of films of metallic impurities of low over potential The fact that a small amount of hydrogen can be evolved from zinc which contains no metallic impurity which can be definitely detected by the spectroscope suggests that this interpretation must be modified, evidently a slow rate of hydrogen evolution can occur when over-potential has been reduced by the fine-scale roughening of the zinc produced by a relatively large amount of corrosion In ordinary samples of zinc the rate of evolution of the gas will, nevertheless, be determined mainly by the presence of metallic films of low over-potential, and since hydrogen gas evolution is responsible for from 5 to nearly 18 per cent of the total corrosion

---

* See fig 3, 'Roy Soc Proc,' A, vol 121, p 96 (1928)

the quantity, distribution, and physical nature of these films may be a factor which limits reproducibility It seems unlikely that the small amount of impurity present in the electrolytic zinc affects appreciably the rate of oxygen absorption since this is closely similar to that for the spectroscopically pure zinc

2 *The Presence of Convection Currents* – Convection currents are considered to be the most important factors in preventing reproducibility in conditions of oxygen control The authors' experiments are conducted in conditions in which these currents have been reduced to an amount that is constant for each solution They have not been eliminated altogether because of the nature of the corrosion process which is characteristic of stagnant solutions beneath an atmosphere of oxygen Corrosion removes oxygen from the layers of the liquid next the metal , this oxygen is ultimately replaced by solution at the liquid surface, and a gradation of oxygen concentration is set up throughout the body of the liquid This gradation gives rise to —

(1) Oxygen diffusion owing to the concentration gradient

(2) Convection owing to the increased density of the highly oxygenated surface layers of the liquid

It is possible to calculate approximately the proportion of the total oxygen conveyed by each method in certain experiments From the measurements of Hüfner* it was shown in Part II of this research that nearly 0 5 c c of oxygen per day could reach the metal surface by diffusion The maximum amount of oxygen that can be supplied for corrosion of zinc per day is about 1 75 c c in solutions within the concentration range N/50 to N/10, *i e* , when the corrosion rate is at its maximum In these solutions, therefore, nearly one-third of the oxygen used may be supplied by diffusion and about two thirds by convection , actually convection currents are probably responsible for a greater proportion since they tend to lessen diffusion In strong solutions the proportion will be different owing to the lowered solubility of oxygen which will diminish convection currents more than diffusion rates

The principal sources of convection currents in corrosion experiments are —

1 Temperature changes
2 Movement set up in the liquid by vibration, etc
3 Density changes in surface layers set up by evaporation
4 Density changes in surface layers set up by oxygen absorption

(1) Temperature changes of a magnitude of two or three degrees have

---

* 'Ann Phys Chim ,' vol 60, p 134 (1897)

occurred, at rare intervals, during the course of these experiments , normally the variation from the mean temperature of 25° C , does not exceed ± 0 05° C , which is without appreciable effect on the measurements The larger variations always produce a temporary increase in oxygen absorption in conditions of oxygen control because the effect of the resulting convection currents is far greater than the effect of the alteration of oxygen solubility In conditions of ion control no important change is produced by a temporary variation of one or two degrees A slow rate of temperature change such as 2° C per day has not shown any advantage over a rapid change of 2° C per hour Table III illustrates some of the points just mentioned

Table III —Effect of Temperature Variations Normal Temperature 25° C

	Control by chlorine ion concentration			Control by oxygen		
	Temperature ° C	Days	Daily oxygen abs c c	Temperature (	Days	Daily oxygen abs c c
Temperature rise to	25 0	2 9	1 10	25 0	2 7	1 41
	25 0	3 9	0 96	25 0	4 7	2 74 (for 2 days)
	26 95	→		*25 9*	→	
	25 0	4 9	1 05	25 0	6 7	3 32 (for 2 days)
	25 0	6 0	0 91	25 0	7 7	1 39
			N/10000 KCl			N/200 KCl
Temperature fall to				25 0	1 75	0 25
				25 0	2 75	0 19
				23 6	→	
				25 0	4 75	1 31 (for 2 days)
				25 0	5 75	0 37
				25 0	6 75	0 20
						4N KCl

(2) It seems probable that the great effect of slight vibration on corrosion in apparently stagnant water under conditions of oxygen control has not been generally realised In the ordinary type of corrosion experiment the effect would be entirely masked by the much larger convection currents due

to evaporation and temperature changes Vibration is not necessarily absent when no movement of the surface of the liquid can be seen—the sensitive mercury horizon test should be applied to the supports which carry the thermostats

(3) The effect of evaporation has probably been one of the most important factors in diminishing the reproducibility of experiments carried out in open beakers except when special arrangements have been made, such as those of U R Evans*, even with these, changes of atmospheric pressure might affect results In the present series of experiments evaporation has been reduced to a negligible factor by the use of closed vessels kept at nearly constant temperature and pressures

(4) The density changes produced by the absorption of oxygen in the surface layers of liquid are regarded as an essential part of the corrosion process and no attempt has been made to interfere with them

In Part II of this research the statement was made that "reproducibility is artificially favoured by cutting down the oxygen supply to a small fraction of that which could be utilised by the metal under test Even moderately large differences of reactivity may then be masked, in fact only metals which corrode so slowly that they cannot make full use of even the restricted supply of oxygen will be clearly distinguished from others" The experimental evidence now available requires modification of this statement If the whole or an exactly similar proportion of the surfaces of the metals under comparison function as cathodes then the relative rates of corrosion of these metals will remain the same whatever the numerical value of oxygen control Reproducibility will only be 'artificially favoured' if the amount of corrosion is so reduced that the absolute difference between two experimental results is too small to be detected by the methods of measurement employed When zinc and mild steel are tested by the standard method of this research, no such artificial favouring occurs

Comparison between Oxygen-Absorption and Loss of Weight Methods of Measuring Corrosion

In Part II of this research Tables II and IIA gave some comparative measurements of corrosion by oxygen absorption and by loss of weight The latter method requires a correction for the attack on the metal by the acid used in removing corrosion products This was obtained by measurement of the hydrogen gas evolved during the acid treatment and a calculation of the corresponding weight of metal attacked, this was then deducted from the total loss of weight, and the result was called corrected loss of weight. An additional series of comparative measurements are given in Table IV.

---

* 'J Chem Soc,' p 120 (1929)

Table IV.—Comparison between two methods of Measuring Corrosion.

I Specimen No.	II Corroding liquid	III Zinc by oxygen absorption Mgrs.	IV Zinc by loss of weight (corrected) Mgrs.	V Mean value of zinc corroded	VI Percentage variation of columns III and IV from mean
A93	KCl N/2	2059.9	2029.71	2044.8	0.74
A94	KCl N/5	655.0	657.72	656.4	0.2
A95	KCl N/50	489.7	481.53	485.6	0.8
A96	KCl N/10	1578.9	1582.33	1580.6	0.11
A97	K_2SO_4 N	541.6	546.21	543.9	0.4
A98	K_2SO_4 N/10	1050.5	1022.28	1036.4	1.38
A99	K_2SO_4 N/50	821.1	790.17	805.7	1.9
A100	K_2SO_4 N/10000	25.7	24.00	24.9	3.4
A101	K_2SO_4 N/200	315.1	314.13	314.6	0.2
A102	K_2SO_4 N/5	591.1	592.06	591.6	0.1
A103	KCl N/5	691.7	703.46	697.6	0.9
A104	K_2SO_4 N/10	450.8	451.54	451.2	0.1

In nine pairs of measurements out of twelve the differences of each from the mean of the two does not exceed ± 1 per cent.; in the two others the difference is less than ± 2 per cent., and in the other the actual difference measured is less than 2 milligrams, though the percentage difference is 3.38. The discrepancy with specimen A98 is probably due to the oxygen absorption experiment in which the hydrogen measurements gave rather erratic readings during the last few days. The cause of the discrepancy with A99 is unknown, for both the oxygen absorption and total-corrosion curves seem quite satisfactory, and no residual corrosion products could be detected by the microscope after the loss of weight determinations.

The results of Table IV as a whole show appreciable improvements over the comparative results of Table IIA of Part II of this research. The fact that two different methods of measuring the corrosion of a single specimen show such satisfactory agreement over a series of experiments, and that two different specimens show satisfactory agreement when tested by one of these methods, appears to foreshadow a sound quantitative basis for corrosion research.

The Effect of Concentration on Corrosion

Corrosion-time curves for true oxygen absorption and total corrosion are given in figs 4 and 5 for potassium chloride solution, and in figs 6 and 7 for potassium sulphate Rates of corrosion are plotted against concentration in fig 8

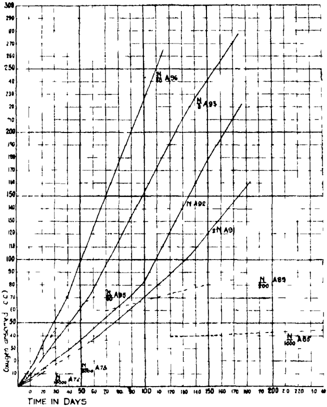

FIG 4 —Variation of True Oxygen Absorption with Concentration of KCl

In chloride solutions it will be seen that —

1 The rate of corrosion increases with concentration up to a maximum which occurs over the range N/50 to N/10 This corresponds to the "critical concentration" of Heyn and Bauer's work on iron *

2 The maximum rate is not reached immediately oxygen control replaces ion control, i e, at about N/5000

3 The rate of corrosion falls over the range N/10 to 4N

---

* 'Mitt K Material prüfungsamt,' vol 26, p 2 (1908)

4 The curve for the solubility of oxygen is related to the curve for the rate of corrosion in a rather complicated manner which is discussed below

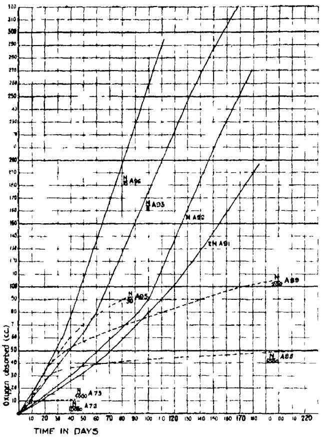

Fig 5 —Variation of Total Corrosion with Concentration of KCl

5 An increase in corrosion rate occurs during a period which corresponds roughly to 70 80 c c of true oxygen absorption throughout the range N/10 to 2N KCl

6 After this period the curves in this range are approximately straight lines for periods extending up to at least 200 days from the beginning of the experiment

7 In dilute solutions the straight line curves characteristic of oxygen control, change to short branches which are probably exponential in form, and these into straight lines of low inclination to the time axes

The reason why the rate of corrosion increases with concentration up to a maximum seems to be that the increase in the concentration of chlorine ions increases the active cathodic area, so that a greater amount of oxygen can be utilised in the corrosion process When the whole of the area of the metal is

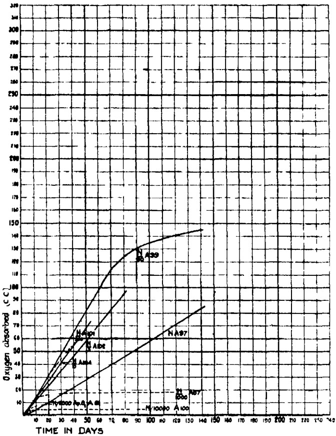

Fig 6 —Variation of True Oxygen Absorption with Concentration of K_2SO_4

active either as anode or cathode the maximum rate of corrosion is reached and this occurs in the range N/50–N/10 Between N/5000 and N/200 a range occurs in which only a portion of the total metallic surface is developed as anode or cathode, and the rate of oxygen supply to the relatively restricted cathodes dictates the rate of corrosion, since there is a sufficient supply of chlorine ions to feed the corresponding anodes in the early stages of the experiment In still more dilute solutions and in the later stages of stronger ones the supply of chlorine ions becomes so diminished that they cannot feed the anodes as fast as the oxygen supply can reach even the relatively restricted cathodes, consequently the rate of corrosion falls with, and is solely controlled by, the concentration of the chlorine ions

Throughout the range 0 to N/10 KCl the alteration in the solubility of oxygen with concentration is so small that it has a negligible influence on the

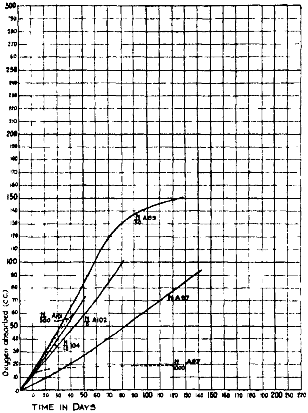

FIG 7 —Variation of Total Corrosion with Concentration of K_2SO_4

rate of corrosion, but beyond this range its influence causes a decrease in the corrosion rate Finally the rate is so diminished that in 4N solution it amounts to less than one-fifth of the maximum rate

The increase in corrosion rate which occurs when corrosion corresponding to about 70–80 c c of oxygen has been reached is connected with the increased rate of hydrogen evolution which occurs at about the same time This evolution sets up convection currents which probably cause an increased supply of oxygen at the cathodes, and, consequently, an increased corrosion rate This explanation of the increased slope of the corrosion-time curves appears preferable to the suggestion made in Part II that it was due to increased cathodic efficiency due to roughening of the zinc surface

The falling over of the oxygen controlled straight line curves in strong

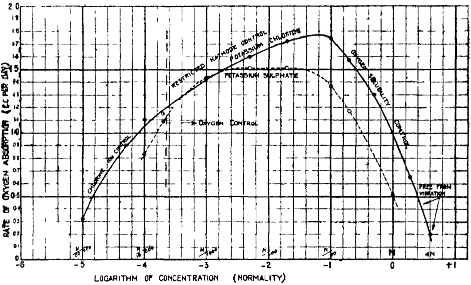

Fig 8 —Variation of Corrosion Rate with Concentration of KCl and K_2SO_4

solutions which still contain a considerable concentration of Cl′ or SO_4'' ions such as N/50 K_2SO_4 (A99 of fig 6) is apparently due to the gradual accumulation of corrosion products which increase the electrical resistance to the corrosion current

During the period of oxygen control the slope of a curve is determined by the rate of cathodic depolarisation and any slight increase of resistance introduced into the circuit does not therefore alter the current, nor consequently, the corrosion rate , but when the increase of resistance passes a certain value the current is lessened and cuts down the cathodic displacement of hydrogen to an amount that is less than the amount that can be oxidised in the conditions of experiment, and a fall in corrosion rate occurs

Corrosion in Potassium Sulphate Solutions

In general the phenomena are similar to those in potassium chloride The corrosion-time curve for N/5000 K_2SO_4 was found to be exponential between 2 and 15 days, as shown in fig 9 , in stronger solutions oxygen control obtains after the first day or two and straight line curves persist for considerable periods In some details the curves differ from those for similar chloride solutions, as shown by comparison of figs 6 and 7 with figs 4 and 5 These differences may be summarised as follows —

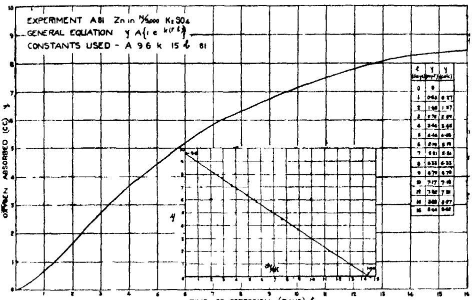

FIG 9

1. In conditions of oxygen control the slopes of the straight lines are usually less in equivalent solutions, but the initial rates which are characteristic of the first day are usually slightly greater (see Table V)
2. In dilute solutions the straight line curves are not maintained for so long as in equivalent chloride solutions
3. The maximum corrosion rate occurs approximately over the range N/200–N/50, i e, in more dilute solutions than in chlorides (see fig 8)
4. Increases in the slopes of the straight lines, such as normally occur in the range 70–80 c c of oxygen absorbed in chloride solutions are less pronounced and generally occur in the range 40–50 c c

The principal causes of these differences seem to be —

1. The slightly lower solubility of oxygen in sulphate solutions (see fig 10)
2. The greater rate at which the sulphate ion is withdrawn from the weak solutions
3. The tendency to develop a smaller number of definite pits in sulphate solutions

In Plate 2 the two photomicrographs show that the number of definite pits is much greater in N/10,000 chloride solution than in sulphate Microscopic study has shown that corrosion begins at quite as many points in the sulphate as in chloride solutions, and may spread more superficially, but a greater proportion of the original points of attack develop into definite pits in the latter The whole question of the causes which determine the distribution of pits is being further investigated microscopically

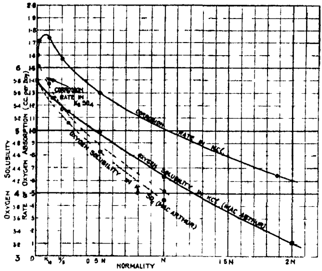

Fig 10 —Variation of Corrosion Rate with Concentration of KCl

Table V

Average corrosion rates for first 18 hours
Cubic centimetres of oxygen absorbed

	Potassium sulphate		Potassium chloride	
		Mean	Mean	
N/10000	0 32	0 32	0 18	0 17, 0 12 0 24
N/5000	0 48 0 40	0 44	0 23	0 23, 0 20, 0 25
N/1000	0 92, 0 61	0 76	0 41	0 38, 0 41, 0 44
N/200	0 67	0 67	0 71	0 90, 0 53
N/50	1 09	1 09	0 68	0 68
N/10	0 75, 0 58	0 66	0 68	0 68, 0 75, 0 57
N/5	1 00	1 00	0 73	0 70, 0 75
N	0 31	0 31	0 27	0 32, 0 21

The Relation of Oxygen Solubility to Corrosion Rate

Explanations of the fact that the corrosion rate of some metals is less in highly concentrated than in dilute solutions of certain salts have been proposed by several authors Adie in 1845 suggested* that the reduced solubility of oxygen in saturated brine solutions was the cause of the relatively slight corrosion action Walker, Cederholm and Bent† stated, that the rate of corrosion is directly proportional to the concentration of dissolved oxygen, and Speller‡ gives a few experimental data confirming this result for iron in flowing water Friend§ considered that 'whilst this" (*i e*, oxygen solubility) "is undoubtedly an important factor it cannot be the only one, in as much as experiment shows that the reduction in corrosion is usually very much greater than the above theory demands" Friend's experiments were mainly carried out with iron, and he drew attention to the fact that while his curve connecting corrosion with salt concentration showed a close similarity with the curve for oxygen solubility in sodium chloride solutions it did not do so in potassium sulphate solutions, in these he stated that corrosion fell off more rapidly than oxygen solubility, a fact previously suggested by Heyn and Bauer's experiments || Friend's tables of results also showed a less rate of corrosion in solutions of sulphates of potassium and sodium than in similar chloride solutions and he proposed an explanation based on the different precipitating power of the two anions for colloidal ferric hydroxide catalyst

The views stated above have been based upon experiments which could not reasonably be expected to provide more than first approximations to the truth since none of them was carried out in strictly defined conditions The matter has, therefore, been re-examined and the results for zinc are given in fig 11 which is derived from the curves shown in fig 10 Within the range N/5 to 2N the curve showing the relation between true oxygen absorption y (*i e*, corrosion) and oxygen solubility x, is found to be a parabola for which the equation is

$$y = \mathrm{K}(x + \mathrm{A})^2 + \mathrm{B},$$

where

$$\mathrm{K} = 0\ 08,\ \mathrm{A} = 1\ 56,\ \mathrm{B} = 0\ 39$$

There is, therefore, a striking difference between the relation found in the present research and that proposed by the previous authors, and the differences appear to be due to the experimental methods adopted In the present research the supply of oxygen to cathodes is mainly due to the very gentle convection currents set up by the increased density of the surface layers of the solution

---

* 'Proc Inst Civ Eng,' vol 4 p 323 (1845)

† 'J Amer Chem Soc' vol 29, p 1251 (1907)

‡ 'Trans Am Electrochem Soc,' vol 39, p 141 (1921)

§ 'Carnegie Res Memoirs,' vol 11, p 135 (1922)

|| *Loc cit*, Table II

In these conditions a square law would be expected since the supply would depend not only directly upon the solubility but also upon the fact that increased solubility would increase convection currents For this reason an equation of the form $y = Kx^2$ would be expected if diffusion be ignored

Fig 11 shows that the parabola obtained experimentally does not pass through the origin, but is displaced relatively to both axes, hence the appearance of the two constants A and B, the physical meanings of which were not at first apparent It was then found that two points corresponding to 4N and 3N KCl solutions lay well below the parabola The experiments with these two solutions were carried out in a thermostat placed on the solidly constructed piers described on p 43 of this paper, whereas most of the experiments upon which the parabola was based were performed on a reinforced table which appeared to give perfectly stagnant and stable conditions until it was examined by the mercury-horizon test It seemed possible, therefore, that the displacement of the parabola was due to vibration, and if this were true the points for 4N and 3N solution would lie on another parabola, which might pass through the origin To test this two more experiments were started under stable conditions in N/2 and N KCl, and the results for all four experiments are shown in the lower curve in fig 11 It is a parabola of the type $y = Kx^2$ and the value of constant k is 0 041

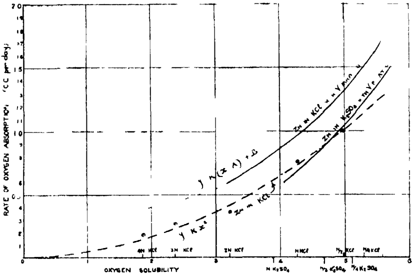

Fig 11 —Variation of Oxygen Absorption with Oxygen Solubility

The parabolic form of curve will only be obtained in conditions in which major convection currents due to changes in temperature, pressure, liquid flow, evaporation and possibly other causes have been eliminated Such currents tend to equalise the oxygen concentration throughout the liquid, to diminish the effect of diffusion, and to give a straight line relation between corrosion and oxygen solubility The parabolic relation will only be obtained when the main source of oxygen supply is the slow convection due to the slight density changes caused by surface solution of oxygen, since it is only the oxygen supplied by this convection which increases as the square of the solubility

The above conclusions require that the curves giving the relation between salt concentration and corrosion rate in fig 8 be corrected if they are to represent truly stagnant conditions As they stand they represent corrosion rates in *apparently* stagnant conditions such as may be expected on a good laboratory bench on which there is no moving apparatus The correction for vibration can be obtained from the difference between the two curves for potassium chloride given in fig 11

The rate of Evolution of Hydrogen Gas

Curves showing the rate of evolution of hydrogen gas are given in figs 12 and 13 In strong KCl solutions the curves become nearly parallel straight

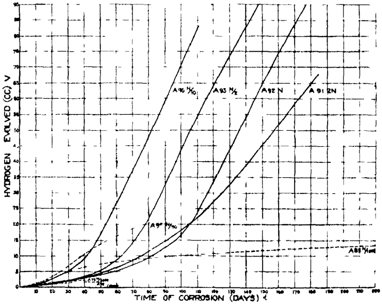

Fig 12 —Hydrogen Gas Curves Zn in KCl Solutions

lines, though that for 2N solution has a rather less slope than the others In Part II of this research a curve was given showing the relation of the rate of gas evolution to total corrosion for N/10 KCl Curves are now given in fig 14 for four chloride solutions For N/10 and 2N the slopes resemble that given in Part II Each is composed of two straight lines, the first of which extends from 0 to about 130 c c of oxygen and the second is parallel to the horizontal axis between 130 and 200 c c of oxygen The curves for N/2 and N show a curious break at about 75 c c, but both finally join the curve for N/10 at about 120 c c

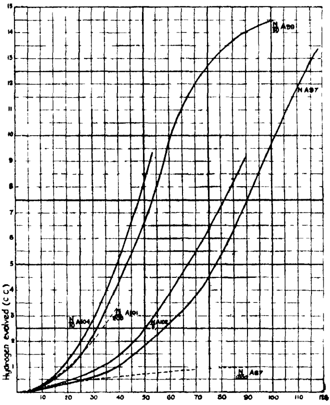

FIG 13 —Variation of Hydrogen with Concentration of K_2SO_4

The interpretation proposed in Part II for the proportionality of rate of gas evolution and total corrosion was the gradual formation of films of metallic impurities of low over-potential as corrosion proceeds The experiment with "spectroscopically pure" zinc in N/10 KCl mentioned earlier in this paper shows that a small evolution of gas can take place in the absence of such films

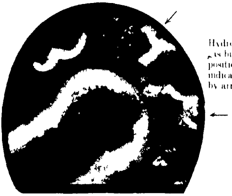

(*a*) Zinc in N/10000 KCl for 9 days (× 6) White masses are corrosion products

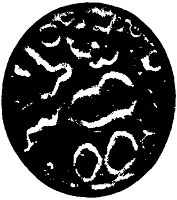

(*b*) The same as (*a*) showing whole specimen (× 2·5)

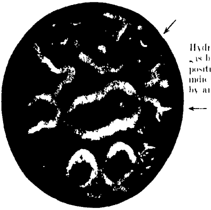

(*c*) Zinc in N/10000 KCl for 13 days (× 2·5)

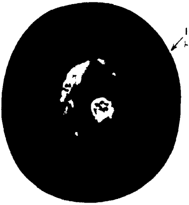

(*d*) The same as (*c*) showing hydrogen bubble trapped in corrosion products (× 2·5)

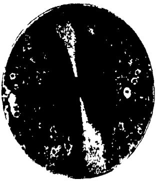

(*e*) Zinc in N/10000 KCl for 12 days Corrosion products removed (× 2·5)

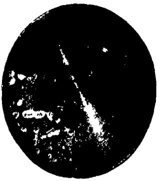

(*f*) Zinc in N/10000 K_2SO_4 for 7 days Corrosion products removed (× 2·5)

(*Facing p* 64)

when zinc has been heavily attacked in strong solutions It seems possible, **therefore, that the rate of evolution may be determined to a small extent by**

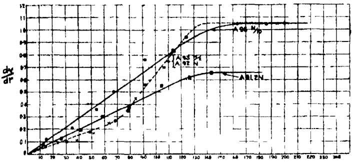

FIG 14 —Rate of Hydrogen Evolution and Total Corrosion

○ A96 N/10 KCl ⊕ A92 N/2 KCl
A93 N/2 KCl □ A91 2N KCl

the development of a roughened zinc surface which has a low over potential relative to an uncorroded surface in very dilute solutions the roughening is insufficient as shown by the result recorded in Part II for N/10,000 KCl

In strong solutions when a definite minimum area of metallic film and roughened metal has been developed all the hydrogen that can be evolved in the experimental conditions can find suitable cathodic area, the maximum rate of evolution is then reached and further deposit of metal and roughening of surface has no effect, *i e*, the gas evolution time curves become straight lines The cause of the break in the curves for N/2 and N KCl does not seem to be readily explainable on these lines

The hydrogen-time curves for N/10 and stronger solutions do not remain straight lines for infinite time but begin to fall over at similar times to the oxygen absorption curves this is clear from fig 9 of Part II for N/10 KCl, and fig 13 of the present paper for N/50 K_2SO_4 If the presence of films and roughened surfaces were the sole determining factors in hydrogen gas production this would not happen, and some other factor must be operative which is probably connected with the oxygen absorption type of corrosion

The Mechanism of Hydrogen Production

Observations have been made with the microscope upon zinc specimens placed in conditions similar to those of the quantitative work, except that about 350 c c of solution were used instead of 100 c c The work was confined to **dilute solutions from N/10,000 to N/200, and it showed clearly that hydrogen**

gas is evolved from the pits, which must be formed mainly by the oxygen absorption process, for in this range the corrosion due to hydrogen gas is less than 14 per cent of the total Plate 2 shows a bubble of gas *in situ* in a pit, also bubbles which have risen up from the pit and are resting against the cover glass of the microscope Bubbles have never been seen to rise from the area surrounding the pits which must be presumed to be their corresponding cathodes for the oxygen absorption process The films of metallic impurity must, therefore, form at the anode and may consist either of residual metal or metal redeposited after temporary solution on the less anodic parts of the anode in similar fashion to copper in "dezinced" brass When once formed the metallic film is likely to be fairly stable and the falling off of the rate of hydrogen evolution is unlikely to be connected with a gradual removal of the film

The facts about the mechanism of hydrogen production which have been reasonably well established may be summarised thus —

1 The gas is evolved from the pits which form the anodes of the oxygen absorption process
2 The rate of evolution is dependent upon the presence of films of metallic impurities and of roughened metal
3 In any solution within the range N/10-2N the rate rises to a maximum at which it stays for a time, it then falls and approximately follows the rate of the oxygen absorption process, lagging behind it in the earlier stages, but maintaining itself rather better in the later stages
4 The rate of evolution is much less in sulphate than in chloride solutions of equivalent concentration
5 The proportion of the total corrosion due to the hydrogen gas process increases with concentration (see Table VI)

Some evidence points to the conclusion that the mechanism of hydrogen evolution is not merely a question of greater or less access of oxygen to the seat of production of atomic hydrogen If it were, an exponential curve would be expected for *total* corrosion in dilute solutions since the whole process would depend on the access of chlorine ions to the anodes The exponential curves are actually obtained for the oxygen absorption process only, and the curves for hydrogen evolution are of such a form that they could not give another exponential by addition The hypothesis suggested in the previous paper was that hydrogen evolution was connected with the local formation of caustic potash, but no support for it could be found when pieces of zinc were

Table VI —Proportion of Total Corrosion due to Hydrogen Gas Evolution

Potassium chloride						Potassium sulphate.					
Concentration.	Specimen No	Days corroded	Total corrosion.	Hydrogen evolved.	Per cent of total corrosion.	Specimen No	Days corroded.	Total corrosion	Hydrogen evolved.	Per cent of total corrosion.	Concentration
			c c of O_2.	c.c				c c of O_2	c c		
N/10000	A72	47	11 2	1 53	6 9	A100	125	4 8	0 18	1 9	N/10000
N/5000	A73	53	15 9	2 1	6 5	A81	20	8 8	0 19	1 1	N/5000
N/1000	A85	235	51 0	13 4	13 4	A87	119	19 1	1 10	2 9	N/1000
N/200	A62	75	83 4	16 3	9 7	A101	40	58	3 10	2 7	N/200
N/10	A96	100	260	70	13 4	A99	50	83	6 6	4 0	N/50
N/2	A93	140	267	83	15 7	A104	50	71	8 2	5 8	N/10
N	A92	170	251	84	16 7	A102	81	100	7 5	3 75	N/5
2N	A91	180	190	65	17 4	A97	100	63	9 7	7 7	N

Note.—The figures for total corrosion have been taken either when the corrosion time curve has become nearly parallel to the time axis or when both oxygen absorption and hydrogen gas curves are straight lines.

placed in N/50 KOH This failure might be due to absence of freshly deposited metallic iron formed by the corrosion process To test this, pieces of zinc were placed in dilute ferrous sulphate solution, washed and then transferred to N/50 KOH , hydrogen gas was freely evolved Pieces of zinc similarly treated were also placed in conductivity water (exposed to air), N/50 $ZnCl_2$ and N/50 $ZnSO_4$, and gas was evolved in the proportion approximately of 0 1, 1 0 and 0 75 These results explain the fact that the exponential curve does not conform with total corrosion which evidently includes a process not directly connected with chlorine ion concentration, but do not explain quantitatively the much greater evolution of hydrogen from chloride solutions than from sulphate shown in Table VI

Summary of Results

1 Reproducibility In Part I of this research it was stated that—" it is not clear (from a study of the literature) whether the discrepancies between supposedly duplicate experiments are due to some inherent characteristic of the corrosion process or to the fact that in the experiments control has not been kept over all the controllable factors , ' but it can be now definitely stated that when adequate control has been kept over temperature, pressure, mechanical stability and chemical purity of the closed system in which the experiments have been conducted, the corrosion rates of horizontally supported annealed zinc specimens with a total area of 14 9 sq cm were reproducible within the limits ± 1 per cent from the mean of two duplicates, throughout the whole range of potassium chloride and sulphate solutions Similar limits of accuracy have been found for commercially produced mild steel in similar dilute solutions Corrosion of these metals is therefore a suitable subject of investigation by the ordinary methods of physical chemistry and the results obtained are of the same order of accuracy as those in many other branches of that subject

The very large number of points at which attack occurs on zinc specimens of the size stated, allows smooth and reproducible curves to be obtained For metals on which the number of points of attack is much less, reproducibility would probably be reduced unless much larger specimens were used

2 Comparative measurements made by the oxygen absorption and loss of weight methods of measuring corrosion did not generally differ from the mean of the two by more than ± 1 per cent , except when small amounts were measured

3 In very weak potassium sulphate solutions the time-corrosion curves have

General Table of Results

Specimen No	Metal sample	Treatment	Corroding liquid	Conductivity of liquid	Time of experiment	Total hydrogen evolved	Total oxygen consumption	Total corrosion expressed in oxygen	Chlorine or sulphate in liquid after experiment	Effect of glass supports
				mhos	days	c c	c c	c c	mgrs	
A72	Australian electrolytic zinc	Turned and annealed in argon	KCl N/10000	15.6×10^{-6}	47	1.53	10.4	11.2	Nil	Marked
A73	,,	,,	KCl N/5000	31.3×10^{-6}	68	2.54	14.7	16.0	Nil	Noticeable
A81	,,	,,	K_2SO_4 N/5000	31.1×10^{-6}	22	0.19	8.39	8.79	Trace	Noticeable
A84		,,	KCl N/1000	15.1×10^{-5}	143	11.5	41.6	47.3	0.46	Marked.
A85	,,	,,	KCl N/1000	15.1×10^{-5}	235	13.4	44.3	51.0	0.41	Noticeable
A86	,,	,,	K_2SO_4 N/1000	15.0×10^{-5}	57	1.04	19.7	20.2	0.63	Marked
A87	,,	,,	K_2SO_4 N/1000	15.0×10^{-5}	119	1.10	18.5	19.1	Trace	Marked
A89	,,	,,	KCl N/200	73.0×10^{-5}	205	36.5	89.3	107.6	3.15	Not definite
A91	,,		KCl 2N	—	218	88.7	197.3	241.6	6528.0	Noticeable
A92		,,	KCl N	—	196	103.9	248.7	300.7	3032.0	—
A93		,,	KCl N/2	—	206	131.1	319.5	385.0	1556.0	Noticeable
A95		,,	KCl N/50	—	83	20.7	81.2	91.5	40.77	Marked
A96	,,		KCl N/10	—	112	83.1	253.6	295.1	288.11	None
A97			K_2SO_4 N	—	156	19.6	91.4	101.2	4335.0	Not definite
A98	,,		K_2SO_4 N/10	—	147	30.0	181.4	196.4	405.30	Not definite
A99			K_2SO_4 N/50	—	142	15.8	145.6	153.5	58.65	Not definite
A100			K_2SO_4 N/10000	15.0×10^{-6}	125	0.18	4.71	4.80	Trace	Not definite
A101			K_2SO_4 N/200	—	42	3.30	57.3	58.9	6.16	Noticeable
A102	,,		K_2SO_4 N/5	—	89	8.97	106.0	110.5	825.90	Noticeable
A104	,,	,,	K_2SO_4 N/10	—	55	10.1	79.2	84.3	432.80	Noticeable
A105	,,	,,	KCl N/200	73.0×10^{-5}	60	12.2	56.0	62.1	6.38	—
S3	New Jersey grade A zinc	As cast	KCl N/10	—	42	0.91	49.8	50.2	310.28	—

been found to be exponential, *i e*, of similar form to those in weak chloride solutions

4 The changes of corrosion rate with concentration have been determined quantitatively for zinc in two series of solutions The different slopes of the straight line curves are due to the different rates at which oxygen reaches the metal owing to changes in oxygen solubility and available cathodic area

5 In strong solutions the curve connecting oxygen solubility and corrosion rate is a parabola in stagnant or nearly stagnant liquid in which convection currents have been reduced to a minimum It is probable that a straight line relation would be obtained in the presence of vigorous convection currents or moving water

6 Hydrogen gas is evolved during the corrosion of electrolytic zinc in all the solutions tested stronger than N/20,000 The proportion of total corrosion due to this evolution increases with concentration in both chloride and sulphate solutions and reaches 17 4 per cent of the total corrosion in 2N KCl and 7 7 per cent in N K_2SO_4

7 From spectroscopically pure zinc hydrogen evolution is greatly reduced—in N/10,000 KCl to zero This change is determined by the removal of approximately one part in ten thousand of total metallic impurity

8 In neither of the series of solutions was a straight line corrosion-time curve obtained which passed through the origin

The thanks of the authors are due to Miss Ruth Pirret who has rendered them much valuable assistance The research was carried out for the Corrosion of Metals Research Committee of the D S I R, and the thanks of the authors are due to the Chairman, Prof Sir Harold Carpenter, and to Prof G T Morgan for facilities afforded and permission to publish

Correction Factors in the Photographic Measurement of X-Ray Intensities in Crystal Analysis

By E. G. Cox, B.Sc., and W. F. B. Shaw, B.A.

(Communicated by Sir William Bragg, F.R.S.—Received December 21, 1929.)

1. *Introduction*

For the complete solution of the structures of complex crystals, and in particular of organic substances, it is essential to be able to measure at least the *relative* intensities of reflexion of homogeneous X-rays from the more important lattice planes with some degree of accuracy. In most crystal problems a number of parameters governing the positions of the atoms in the lattice remain to be found after the geometrical requirements of the symmetry have been satisfied. These can only be determined from intensity measurements, so that in general, the greater the number of reflexions measured the more closely will the deduced structure approach to the truth.

Until comparatively recently the only instrument of precision available for X-ray intensity work has been the Bragg ionisation spectrometer.* It has, however, three disadvantages when used for this purpose, which may be briefly summarised:—

(1) Only the strongest planes are measurable with any degree of accuracy, owing to the "swamping" effect of the unremovable background radiation in the case of the weaker reflexions.

(2) It is clearly impossible to use it, without very special technique, in the case of crystals which are volatile or even liquid at normal temperatures.

(3) The measurement of the true *integrated intensity* is a somewhat lengthy operation in practice, with the result that experimenters are tempted to determine the *peak* values of the intensities instead; these, in general, are not in the same ratio as the integrated reflexions, so that a false idea of the reflexions may be obtained.

The solution of the problem lies in the use of rotation or oscillation photographs, on which planes of perhaps only 1/100th of the intensity of the strongest planes are registered Until recently no quantitative method was available for the measurement of the intensities of spots on X-ray photographs, and only visual estimation was possible This makes it possible to arrange planes in their correct order of intensity, but does not permit the estimation of intensity ratios to more than 20–30 per cent Even this accuracy is only obtainable with care within a limited range of intensities, and the results, of course, are still uncorrected for the errors discussed in this paper

---

* The mode of use of the ionisation spectrometer for intensity measurement is fully described in a paper by W. L. Bragg, James and Bosanquet, 'Phil. Mag.,' vol. 41, p. 309 (1921).

The development of the Astbury radioactive photometer * however, has made accurate quantitative measurements possible, and all planes sufficiently strong to register on a photograph can now be determined to an accuracy of 1 or 2 per cent It thus becomes very important to investigate whether the relative intensities as measured from the photograph are in reality the true relative intensities of reflexion from the crystal planes In this paper the authors discuss two corrections which have to be applied for this to be the case These arise in the following ways —

(1) When the reflecting plane does not contain the axis of rotation of the crystal (in other words, when the spot does not lie on the equatorial line of the photograph), the angular velocity of rotation for the plane is effectively decreased This results in reflexion for a longer time in each rotation or oscillation than for planes reflecting on the zero layer-line

The problem will be discussed in detail in section 2, and it is sufficient to state here that the effect is purely geometrical, depending only on the angle of reflexion and the orientation of the reflecting plane with respect to the axis of rotation It will be shown that to every point on a photograph there corresponds a correction factor by which the measured intensity must be multiplied in order to eliminate this effect, this will give the intensity that the spot would have if it lay on the equatorial line

This factor will be referred to as the *Geometrical Correction Factor*, and will be denoted by the symbol D_1

(2) In general, the reflected X-ray beam will pass obliquely through the photographic film or plate, and it is clear that for a given intensity falling on the film, the density of the spot produced will depend on the angle of incidence, obliquity of incidence presents a thicker layer of sensitised material to the action of the X-rays, with consequent increased photographic action This makes it necessary to multiply each measured intensity by a correction factor which will eliminate the effect of the obliquity The use of the factor is

---

* 'Roy Soc Proc,' A vol 115, p 640 (1927) and vol 123, p 575 (1929)

equivalent to the reduction of all spots to the case of normal incidence for the purposes of comparison Its magnitude will depend —

(i) On the angle at which the X ray beam is incident on the photograph
(ii) On the particular type of photographic film or plate which is used
(iii) On the wave-length of the monochromatic X-ray beam employed

The theoretical and experimental investigation of the effect will be described in section 3 The factor will be called the *Film Absorption Factor*, and will be denoted by D_2

Of the remainder of the paper, section 4 is a discussion of the validity of the ordinary polarisation factor while in section 5 some experimental figures are quoted to show how the factors give reasonably concordant results when applied to actual measurements on X ray photographs The discussion of the polarisation factor is considered necessary in view of the somewhat confused state of the literature of the subject, and in view also of the fact that various writers have used arbitrary polarisation factors with no reference to actual experimental data

2 *The Geometrical Correction Factor*

The theory of this factor was worked out by the authors before they were aware of previous mention of it in papers by Ott and by Hoffmann and Mark * These writers gave the correction in forms which made it necessary to calculate the factor separately for each spot Hoffmann and Mark, moreover, assuming that the divergence of the incident beam of X-rays was entirely responsible for the geometrical error, gave a definite value to the divergence and calculated their correction on that basis The following theory is derived without any assumptions as to the nature of the phenomena which make it necessary

It is known† that when a crystal is rotated or oscillated, a given lattice plane reflects characteristic X-rays, not at a definite angle θ, but over a range of angle $\delta\theta$ from $(\theta - \frac{1}{2}\delta\theta)$ to $(\theta + \frac{1}{2}\delta\theta)$, where θ is given by the Bragg law

$$n\lambda = 2d \sin \theta$$

The principal cause of this is undoubtedly the divergence of the X ray beam, but even in the case of a parallel beam the effect would still persist owing to internal imperfections of the crystal, and, in a lesser degree, because the characteristic radiation is not strictly homogeneous It would be difficult to estimate $\delta\theta$

---

* Ott, 'Z Physik,' vol 22, p 201 (1924), Hoffmann and Mark, 'Z Phys Chem,' vol 111, p 321 (1924)

† Darwin, 'Phil Mag,' vol 27, p 675 (1914)

theoretically from these various factors, the correction, however, since it is concerned only with the geometry of the rotation, is independent of $\delta\theta$, as will be seen later

Now the total intensity of the beam reflected from a crystal plane is proportional to $\delta\theta/\omega$, where ω is its angular velocity about an axis perpendicular to the plane of reflexion,* *i e*, the intensity is proportional to the time during which reflexion takes place If the intensities of different planes are to be compared, quantities such as ω which do not depend upon the nature of the crystal, but vary from plane to plane according to the particular axis of rotation chosen, must be eliminated This is done by multiplying the observed intensity by a factor $D_1 = \omega/\Omega$, where Ω is the angular velocity of the crystal itself Thus D_1 is equal to unity for planes passing through the axis of rotation, and is less than unity for all other planes

The value of D_1 is obtained as follows Fig 1 represents a stereographic projection of the crystal O being the axis of rotation, A the incident beam of X rays, B the normal to the reflecting plane, and C the reflected beam Suppose that the normal makes an angle α with the axis, and let the angle between the planes AO and BO be ν The angle BA is ϕ the complement of the glancing angle θ

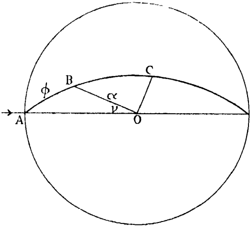

Fig 1

Since ABC is the plane of reflexion, and B the normal to the reflecting plane, ω is the rate of change of the angle AB, while Ω is the rate of change of the angle ν

---

* Here "reflecting plane" is the lattice plane of the crystal giving rise to the reflexion The expression "plane of reflexion" has its ordinary optical significance

Thus

$$D_1 = \frac{\omega}{\Omega} = \frac{d\phi}{d\nu} \tag{1}$$

From the quadrantal spherical triangle ABO

$$\cos \nu = \frac{\cos \phi}{\sin \alpha} \tag{2}$$

and so

$$\frac{d\phi}{d\nu} = \frac{\sin \nu \sin \alpha}{\sin \phi} \tag{3}$$

But from equation (2)

$$\sin \nu = \frac{\sqrt{\sin^2 \alpha - \cos^2 \phi}}{\sin \alpha}$$

whence from equation (3)

$$\frac{d\phi}{d\nu} = \frac{\sqrt{\sin^2 \alpha - \cos^2 \phi}}{\sin \phi}$$

i e,

$$\frac{d\phi}{d\nu} = \frac{\sqrt{\sin^2 \alpha - \sin^2 \theta}}{\cos \theta}$$

since ϕ is the complement of θ

Thus finally

$$D_1 = \frac{\sqrt{\sin^2 \alpha - \sin^2 \theta}}{\cos \theta} \tag{4}$$

This may easily be transformed to the expression

$$D_1 = 1 \Big/ \sqrt{1 - \left(\frac{\sin \chi}{\sin 2\theta}\right)^2}, \tag{5}$$

where χ is the complement of the angle between the reflected beam and the axis of rotation Equation (5) is the form in which the correction was given by Ott (*loc cit*)

To calculate the correction factor separately for each spot on a photograph from this equation would be very laborious, the authors have therefore constructed charts on which have been plotted curves of constant D_1 The appropriate chart is placed over the photograph (or an enlargement of it) and the value of D_1 for each spot can be read off directly, an accuracy of 1 per cent being easily obtainable in most cases Two charts have been made, one for cylindrical films of radius 5 cms, and the other for flat films It will be seen later that the form of the latter chart is independent of the distance between the crystal and the film These correspond with the two interpretative charts given by Bernal *

---

* 'Roy Soc Proc,' A, vol 113, p 117 (1926)

For plotting the curves of $D_1 =$ constant the equation (4) must be expressed in the form

$$x = f(D_1, y),$$

x and y being the co-ordinates of the spot on the film, and the form of f being different for flat and cylindrical films

(*a*) *Flat Film*—The form of the function f is very simply derived in this case Suppose ψ to be the angle which the radius vector from the centre of the film to the spot makes with the y-axis, then

$$\cos \psi = \frac{\cos \alpha}{\cos \theta}$$

whence

$$\sin \psi = \sqrt{1 - \left(\frac{\cos \alpha}{\cos \theta}\right)^2}$$

$$= \frac{\sqrt{\sin^2 \alpha - \sin^2 \theta}}{\cos \theta}$$

$$= D_1$$

Thus the equation of the curve is

$$\psi = \text{arc} \sin D_1,$$

i e, the curves of constant D_1 are straight lines passing through the origin, and are independent of the distance between the film and the crystal

The equation in rectangular co-ordinates is

$$\frac{x}{y} = \frac{D_1}{\sqrt{1 - D_1^2}} \qquad (6)$$

(*b*) *Cylindrical Film*—The equation is best obtained in this case from equation (6) Suppose X and Y are the co-ordinates of the spot on the cylindrical film, corresponding to x and y on the flat film Then

$$x = D \tan \phi, \qquad y = D \sec \phi \tan \chi,$$

and

$$X = R\phi, \qquad Y = R \tan \chi,$$

where R is the radius of the cylindrical film, and D the distance of the flat film from the crystal.

From these it follows that

$$\frac{x}{D} = \tan \frac{X}{R}, \qquad \frac{y}{D} = \sec \frac{X}{R} \ \frac{Y}{R},$$

i e,

$$\frac{x}{y} = \frac{R}{Y} \sin \frac{X}{R},$$

Box and Shaw.

I.—Cylindrical Film   Radius 5 cms.

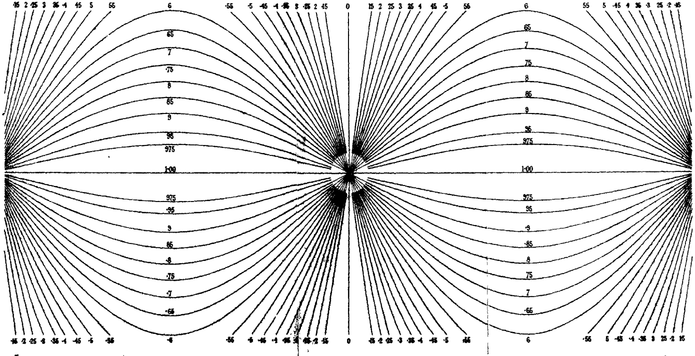

(Facing p. 74.)

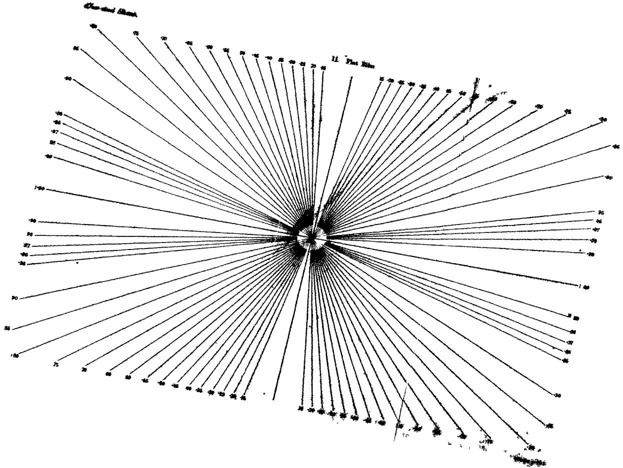
II. Flat Ribs

or, from equation (6)

$$Y \frac{D_1}{\sqrt{1 - D_1^2}} = R \sin \frac{X}{R},$$

i.e.,

$$Y = \frac{R}{D_1} \sqrt{1 - D_1^2} \sin \frac{X}{R} \tag{7}$$

The curves of constant D_1 are thus sine curves for the case of the cylindrical film, the maxima being given by

$$Y = \frac{R}{D_1} \sqrt{1 - D_1^2}$$

Reproductions of the two charts accompany this paper.

3 *The Film Absorption Factor*

The action of X-rays incident obliquely on photographic films was investigated experimentally. The problem was to send the same amount of monochromatic radiation on to the film first normally and then at an angle, and measure by means of the radioactive photometer the apparent intensities of the spots so produced. Preliminary work showed that the use of direct X-ray beams was not possible, as even the most efficient filtering arrangements let through sufficient residual general radiation to produce a considerable effect. A truly monochromatic beam was therefore obtained by using the reflexion of copper K_α-rays from a crystal (actually the 022 reflexion from a small diamond was employed), with nickel filters in the primary beam to remove the K_β spot and cut down the intensity of the background.

The whole of this investigation was carried out using Schleussner Doneo duplitised X-ray films, which have been found in this laboratory to be the most suitable for photographic intensity work. The development in all cases was for a period of 7 minutes in a solution 1 in 20 of Agfa Rodinal at 18° C.

A piece of film was mounted in the quarter plate holder of the X-ray spectrometer, which can be swung round on a turn-table over a graduated circle to make any desired angle with the beam reflected from the crystal. The holder was first arranged so that the reflected beam was incident normally on the film, and exposure for a suitable time was made with the crystal oscillating about the reflecting position with constant angular velocity. The holder was then turned so that the beam struck the film at a known angle and an equal exposure was given. The X-ray tube was maintained in as steady a condition as possible during this period, and lead screens were placed in suitable positions over the film in order to prevent scattered radiation from falling on the exposed portions On a shielded part of the film were also registered six uniform spots corresponding to X-ray intensities in known ratios These are obtained by passing a uniform beam (from a distant tube) through six equal apertures in a lead plate, in front of which rotates a sector so cut that the times of exposure for the holes are in the ratios of 100 80 60 40 20 10 Since the Schwarzschild constant p is equal to unity for all X-ray frequencies,* this procedure gives a series of uniform spots whose total intensities are also in the ratios of 100 80 60 40 20 10, moreover, it is not necessary to use copper radiation for the production of these spots These are the "calibration spots" which serve as standards of intensity ratio for this particular film

These operations were repeated, using different strips of film, for various angles of incidence For convenience the films were all developed at the same time and in the same tank of developer in a special holder made for the purpose which prevented contact of the negatives with one another or with the tank, constant stirring made it certain that the entire batch was developed uniformly and under exactly the same conditions With these precautions it was possible to make one carbon tissue with all the spots from different pieces of film printed on it, together with one of the sets of calibration spots, with a reasonable certainty that once the radioactive photometer has been adjusted to give a linear relation between α ray and X-ray intensities for these calibration spots, the linearity will hold for all the specimens of film The photogravure tissue G 12 was printed and developed in the manner described by Astbury (*loc cit*), and measured up in the photometer Each individual photograph gives the ratio of the *photographic intensities* produced by the same X ray beam falling normally, and at an angle, on the film This is the correction factor D_2 by which the observed intensities must be multiplied to eliminate the obliquity effect

The experimental measurements of D_2 for different angles are represented in fig 2 The possible error in each value is estimated at about 2 per cent, mainly owing to variations in the intensity of the primary X ray beam and in the velocity of rotation of the crystal

A tentative explanation of this effect may be obtained in the following manner The duplitised film consists of two layers of sensitised material, mainly silver halides and gelatine, separated by a thickness of celluloid The problem is to investigate the total photographic action in the two layers as a function of the angle of incidence of the radiation

* Bouwers 'Z Physik,' vol 14 p 374 (1923)

According to Silberstein's quantum theory of photographic action,* the sensitive emulsion may be regarded as composed of a number of discrete

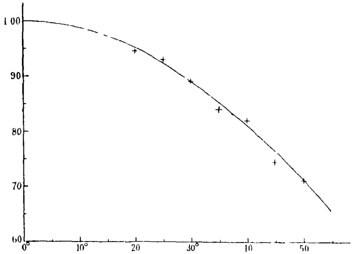

Fig. 2.—The Relation between the Film Absorption Factor D_2 and the Angle of Incidence

grains, each of which becomes "activated" and developable on absorbing a quantum of energy. An area of film is thus to be thought of as a series of targets presented to the firing action of the incident quanta, so that the absorption of a quantum by a grain takes place according to the laws of probability. For a single layer of grains of uniform size Silberstein finds the relation

$$k = N(1 - e^{-na}), \tag{1}$$

where

k = number of grains activated

N = number of grains exposed to the radiation

n = number of incident quanta

a = area of each grain normal to the incident beam

For an emulsion composed of grains of different sizes this law holds for each individual grain class, so that

$$K = \int f(a)\ da\ (1 - e^{-na}), \tag{2}$$

where K = total number of grains activated, $f(a)\ da$ = number of grains having areas between a and $(a + da)$.

---

* 'Phil. Mag.,' vol. 44, p. 257 (1922).

The law may also be extended to the case of a thickness of emulsion containing more than one layer of grains the grains in the lower layers are effectively shielded by those above and the net result is merely an alteration in the law of grain size distribution It may then be assumed that the expression (1) holds for each set of grains of a particular area in the duplitised film under consideration *

If now a beam of X rays be projected on the film first normally and then at an angle ψ with the normal the numbers of grains of a particular area activated in the two cases will be in the ratio

$$k_N/k_\psi = \cos\psi$$

where

k_N = number of activated grains in normal exposure

k_ψ number of grains activated at an angle ψ,

since the number of grains exposed to the beam is $\cos\psi$ times as great for the oblique exposure as for the normal This will be the case for all sizes of grain so that the total numbers of grains blackened in the two cases will also be in the ratio $\cos\psi$

Now Bouwers (*loc cit*) has found experimentally the relation

$$D = D_0 (1 - e^{-AX})$$

where D is the photographic density produced by an X ray intensity X, D_0 and A being constants This is of exactly the same form as equation (1), so that the photographic density must be proportional to the number of activated grains It follows that the densities corresponding to the incidence of the X ray beam obliquely and normally are also in the ratio $\cos\psi$

It will now be assumed that the densities under consideration are small so that approximately

Photographic density $\propto$ X ray intensity

Under these conditions it is clear that the oblique beam of intensity X is equivalent in its action on the film to an intensity $X/\cos\psi$ incident normally This may be expressed by the statement

$$\text{Action} = A \quad X/\cos\psi,$$

---

* It should be noted that this result is true only if two conditions are satisfied (i) That the thickness of emulsion is such that it contains a number of layers of grains, (ii) That the individual grains have a random distribution in orientation, otherwise the effective area presented to the X ray beam is altered by oblique incidence There is no reason to believe that these conditions are not fulfilled in the case of the Dooco films used

where action denotes the X-ray intensity equivalent to the photographic blackening actually produced, as measured by the radioactive photometer. The production of this action will be accompanied by a loss of intensity from the beam proportional to the number of grains activated, and therefore to the action produced, so that

$$\text{Loss of intensity} = C \ X/\cos\psi$$

Here C and A are constants, which are proportional to one another.

It is now possible to investigate the behaviour of the entire duplitised film. An X-ray intensity X incident at an angle ψ will produce an action $A\ X/\cos\psi$ in the upper layer of emulsion, and will enter the celluloid backing with intensity $X(1 - C/\cos\psi)$. A further absorption will take place in the celluloid, if this has thickness t and an absorption coefficient μ (for the particular radiation considered), the beam reaching the second sensitive layer will have intensity

$$X(1 - C/\cos\psi)\ e^{-\mu t/\cos\psi}$$

This, as before, will produce an action given by

$$A\ X/\cos\psi\,(1 - C/\cos\psi)\ e^{-\mu t\cos\psi}$$

so that the total action is

$$A\ X/\cos\psi\ \left[1 + e^{-\mu t/\cos\psi}(1 - C/\cos\psi)\right] \qquad (3)$$

The same intensity X incident normally would give rise to an action equal to the value of equation (3) with $\psi = 0$, this is

$$A\ X\left[1 + e^{-\mu t}(1 - C)\right] \qquad (4)$$

Then the ratio of expressions (3) and (4) is the correction factor D_2 giving the relation

$$D_2 = \cos\psi\left[1 + e^{-\mu t}(1 - C)\right] / \left[1 + e^{-\mu t/\cos\psi}(1 - C/\cos\psi)\right] \qquad (5)$$

The values of the constants C and (μt) in this expression were easily obtained in the following manner. A crystal was mounted on an ionisation spectrometer fitted with a copper target X-ray tube, and arranged so that the K_α reflexion from a certain plane was entering the ionisation chamber. The ionisation produced was then measured with and without a piece of film in the path of the reflected beam; this gave the total absorption in the two layers of emulsion and the celluloid. A specimen of film was thoroughly soaked in hydrochloric acid and washed in hot water to remove the emulsion, and the absorption of the celluloid which remained was measured in the same way The results of these experiments gave the values $(\mu t) = 0\ 204$, and $C = 0\ 220$ Using these values of the constants the theoretical relation between D_2 and ψ has been calculated and is represented graphically in fig 2, together with the experimental results It will be seen that the agreement is quite good

The assumption was made earlier that the photographic densities concerned were small This will not always be the case but it is easy to see what kind of error is introduced by the assumption For large densities an increase of incident intensity results in a smaller fractional increase of the number of grains blackened Conversely, an increase of activated grains in the ratio k_ψ/k_N will correspond to an increase of apparent intensity in a greater ratio than k_ψ/k_N In other words, D_2 will have a smaller value than is indicated by the formula (5) for large photographic densities Reference to fig 2 shows that the experimental points, on the whole lie a little below the theoretical curve, as would be expected from this reasoning, but the discrepancy is small

Tables of values of D_2 have been constructed in a form suitable for use in experimental work With a cylindrical film the angle of incidence and so D_2 depends only on the co ordinate ζ of the particular reflected spot in the reciprocal lattice, and Table I gives D_2 for various values of ζ, up to $\zeta = 0\ 8$

Table I —Absorption Factor D_2 for Cylindrical Films
For Doneo Films and Copper K_α Radiation

ζ	D_2	ζ	D_2
0 00	1 00	0 42	0 925
0 02	1 00	0 44	0 915
0 04	1 00	0 46	0 905
0 06	1 00	0 48	0 90
0 08	0 995	0 50	0 89
0 10	0 995	0 52	0 88
0 12	0 995	0 54	0 87
0 14	0 99	0 56	0 86
0 16	0 99	0 58	0 85
0 18	0 985	0 60	0 835
0 20	0 985	0 62	0 825
0 22	0 98	0 64	0 81
0 24	0 975	0 66	0 80
0 26	0 97	0 68	0 785
0 28	0 965	0 70	0 77
0 30	0 96	0 72	0 755
0 32	0 955	0 74	0 735
0 34	0 95	0 76	0 715
0 36	0 945	0 78	0 695
0 38	0 94	0 80	0 675
0 40	0 93		

With a plane film D_2 depends upon the glancing angle of reflexion θ, and so upon the distance of the photographic spot from the centre of the film for a given distance from the crystal, Table II gives D_2 in terms of θ and the distance x of the spot from the centre for the film at a distance of 10 cms from the crystal This table is continued as far as $\theta = 26°$, and $x = 13$ cms

Table II—Absorption Factor D_2 for Flat Films
For Doneo Films and Copper K_α Radiation, film at a distance of 10 cms from the crystal

Distance between spot and centre of film x	D_2	Glancing angle of reflexion θ	D_2
cms		°	
0.0	1.00	0	1.00
0.5	1.00	1	1.00
1.0	0.995	2	0.995
1.5	0.99	3	0.995
2.0	0.985	4	0.99
2.5	0.975	5	0.985
3.0	0.965	6	0.98
3.5	0.955	7	0.975
4.0	0.94	8	0.97
4.5	0.925	9	0.96
5.0	0.915	10	0.95
5.5	0.90	11	0.94
6.0	0.885	12	0.93
6.5	0.87	13	0.915
7.0	0.85	14	0.905
7.5	0.835	15	0.89
8.0	0.82	16	0.875
8.5	0.805	17	0.86
9.0	0.79	18	0.845
9.5	0.78	19	0.83
10.0	0.765	20	0.81
10.5	0.75	21	0.79
11.0	0.735	22	0.775
11.5	0.72	23	0.755
12.0	0.71	24	0.735
12.5	0.695	25	0.71
13.0	0.685	26	0.69

Values of D_2 for other types of photographic films, or for X rays other than copper K_α radiation, may be measured experimentally if required, or may be calculated from equation (5), using the easily determined values of (μt) and C It may be noted that for small values of ψ, D_2 may be taken equal to $\cos\psi$ with little error, and this approximation is increasingly accurate the smaller (μt) and C, and so the greater the frequency of the X radiation used It may be considered applicable for Doneo films, to an accuracy of about 1 per cent, for wave-lengths not greater than that of copper K_α radiation (1 539 × 10^{-8} cms), up to $\psi = 20°$ at least

4 *The Polarisation Factor*

The measured intensity of a crystal reflexion must also be divided by a factor which takes into account the state of polarisation of the primary X-ray beam If this radiation is unpolarised, the " polarisation factor " is*

$$\tfrac{1}{2}(1 + \cos^2 2\theta),$$

θ being the glancing angle of reflexion If, however, there is a plane-polarised component present, the factor has a different value It is important, therefore, to know the state of polarisation in all intensity work in order to have an accurate knowledge of the factor to be employed Since the experimental work which has been published on this subject in the past few years has been somewhat contradictory, the writers have thought it advisable to make a critical examination of the various results which have been obtained

The work of Kirkpatrick, and of Wagner and Ott,† has shown that " white " radiation, from a tube run at a potential insufficient to excite the characteristic radiation of the anticathode, is partially plane-polarised The electric vector of the polarised component lies in the plane containing the cathode-ray stream and the X-ray beam, as would be expected

On the other hand Barkla and Sadler, and more recently, A H Compton, and Mark and Szilard‡ have shown in different ways that fluorescent X-rays, *i e*, characteristic radiation excited from a secondary source by an X-ray stream of higher frequency, are unpolarised As little is known of the fundamental differences between the modes of production of characteristic, general, and fluorescent radiation, no prediction can be made from these results as to the probable state of polarisation of characteristic rays

The first experimental investigation was made by Bishop § A water-cooled Coolidge tube with a molybdenum anticathode was used, filters of zirconium or strontium being inserted in the beam to remove the general radiation and leave the K_α or K_β rays, respectively Reference should be made to Bishop's paper for details of the experiment, it is sufficient to state here that a considerable percentage of plane-polarisation was found. Realising the extreme importance of removing as completely as possible the background radiation, Bearden and Wollan* isolated a truly monochromatic beam of molybdenum K_α radiation by reflexion from a crystal and examined it for polarisation. They agreed in finding that the X-rays were unpolarised within the limits of experimental error (about 1 per cent.). Haas† has recently examined iron K_α radiation, and Mark and Wolf‡ have investigated copper K_α rays, both using pure beams obtained in this way: in neither case was any polarisation observed, the possible error again being about 1 per cent.

---

* W H Bragg and W L Bragg, " X Rays and Crystal Structure," chap 13

† Kirkpatrick 'Phys Rev ,' vol 22, p 226 (1923), Wagner and Ott, 'Ann Physik,' vol 85, p 425 (1928)

‡ Barkla and Sadler, 'Phil Mag ,' vol 16, p 550 (1908), Compton, 'Proc Nat Acad Sci ,' vol 14, p 425 (1928) Mark and Szilard, 'Z Physik,' vol 35, p 732 (1926)

§ 'Phys Rev ' vol 28, p 625 (1926)

In view of these results there can be little doubt that Bishop's system of filters was in reality inefficient, and that the polarisation which he observed was due to the residual white radiation. It is significant that the percentage of polarisation which he found agrees reasonably closely with that predicted by extrapolation from, Kirkpatrick's measurements on general radiation.

It may be concluded that there is not more than 1 per cent. of plane polarisation in the characteristic K_α radiations of molybdenum, iron, and copper; presumably this will be true of all characteristic X-rays of the K series.

The effect of the presence of a small amount of plane polarisation will now be investigated. Kirkpatrick§ has derived an expression for the factor which is to be used in the case of a partially polarised beam, for measurements on the ionisation spectrometer. Defining the state of polarisation by a factor

$$P = (I_0 - I_P)/(I_0 + I_P)$$

where I_P and I_0 are respectively the intensity of the polarised component and the total intensity, he finds

$$\text{Polarisation factor} = [\sin^2\alpha + P\cos^2\alpha + (P\sin^2\alpha + \cos^2\alpha)\cos^2 2\theta]/(1 + P),$$

where α = the angle between the plane of reflexion and the plane containing the cathode stream and the incident X-ray beam.

In the experiments of Bearden, Wollan, Haas, and Mark and Wolf (*loc. cit.*), P was found equal to unity, with a possible error of 1 per cent. If $\alpha = 0°$, which is the most common arrangement of tube and spectrometer in practice, and $P = 0.99$, the factor assumes the value

$$(0.99 + \cos^2 2\theta)/1.99$$

---

* Bearden, 'Proc. Nat. Acad. Sci.,' vol. 14, p. 539 (1928); Wollan, *ibid.*, p. 864.

† 'Ann. Physik,' vol. 85, p. 470 (1928).

‡ 'Z. Physik,' vol. 52, p. 1 (1928).

§ 'Phys. Rev.,' vol. 29, p. 632 (1927).

involving a maximum error of $\frac{1}{2}$ per cent (for $\theta = 45°$), in using the ordinary factor $\frac{1}{2}(1 + \cos^2 2\theta)$.

This formula is applicable only to reflexions on the zero layer-line, as photographic work is concerned with reflexions at any angle to the axis of crystal rotation, it is necessary to see if an error of more than $\frac{1}{2}$ per cent can be introduced in the general case. The general expression is found to be

$$\text{Polarisation factor} = 1/I_0 [\tfrac{1}{2}(I_0 - I_1) + I_1 \sin^2\beta\,(1 + \cos^2 2\theta) + I_P \cos^2\chi \cos 2\beta],$$

where β = the angle between the axis of rotation of the crystal and the electric vector of the polarised component

χ = the complement of the angle between the reflected beam and the axis of rotation.

For $\beta = 90°$ (which corresponds to $\alpha = 0°$ in Kirkpatrick's expression), and $P = 0.99$ as before, this gives

$$\text{Factor} = 0.5025\,(1 + \cos^2 2\theta) - 0.00503 \cos^2\chi$$

On the zero layer-line $\chi = 0°$, so that the difference between the true value of the polarisation factor and $\frac{1}{2}(1 + \cos^2 2\theta)$ decreases with increase of χ, the maximum error which can occur is thus $\frac{1}{2}$ per cent, for reflexions by planes which contain the axis of rotation.

If there were any appreciable amount of polarisation in monochromatic X-ray beams, it would show up in the measurement of the intensities of the spots on single crystal rotation photographs. With the same lattice plane, or planes equal in reflecting power, of a small single crystal, giving reflexions in different directions, the spot with the larger value of χ should have the greater measured intensity (corrected with the appropriate factors D_1 and D_2) if there is polarisation. The figures quoted in section 5 to test the validity of D_1 and D_2 show that there is no systematic difference of this kind, and consequently no evidence from these photographs in favour of plane-polarisation in the beam.

Two conclusions may be drawn from the discussions of this section —

(i) That characteristic X ray beams contain not more than 1 per cent of plane polarised radiation.

(ii) That the maximum error involved in assuming the polarisation factor to have the value $\frac{1}{2}(1 + \cos^2 2\theta)$ is $\frac{1}{2}$ per cent.

5 *Experimental Evidence*

It sometimes happens that in the rotation or oscillation of a crystal, two (or more) lattice planes of equal reflecting power give reflected spots in different regions of the same photograph A photograph of this type may be used to test the accuracy of the correction factors D_1 and D_2 The integrated intensities of the spots are measured by means of the photometer multiplied by the appropriate values of the factors, and the resultant corrected intensities should be equal

In a series of measurements on an organic hexagonal crystal by Mr B W Robinson of this laboratory, the following four pairs of equivalent lattice plane reflexions were determined

Equivalent planes	ξ	ζ	Measured intensity	D_1	D_2	Corrected intensity
110	0 103	0 176	73	0 50	0 99	36
020	0 205	0 000	45	1 00	1 00	45
111	0 281	0 176	158	0 83	0 99	130
021	0 332	0 000	125	1 00	1 00	125
221	0 332	0 352	162	0 65	0 95	100
041	0 487	0 000	98	1 00	1 00	98
201	0 261	0 352	247	0 57	0 95	134
131	0 404	0 176	155	0 91	0 99	140

As extra confirmation a small diamond was rotated about a random axis, and the intensities of the photographic spots given by the (111) planes were measured These gave the results

ξ	ζ	Measured intensity	D_1	D_2	Corrected intensity
0 700	0 285	100	0 90	0 97	87 3
0 64	0 42	(111 114, 120 116) Mean = 115	0 80	0 925	86 1

The corrected intensities in the last column, for a pair of planes, cannot be expected to be exactly the same, since the paths of the reflected beams in the crystal, and therefore their losses of intensity by absorption, are not in general equal The absorption in organic crystals is usually small, and as may be seen above, the application of the corrections D_1 and D_2 is sufficient to give intensities which are correct within 2 or 3 per cent Since the uncorrected intensities may be as much as 100 per cent too great, the importance of the corrections is at once apparent

Summary

Possible sources of error in the measurement of the integrated intensities of X ray reflexions by crystals from photographic records are discussed, and correction factors developed for their elimination These are —

(i) A factor dependent upon the geometrical arrangements of the crystal and the X-ray spectrometer

(ii) A correction introduced by obliquity of incidence of the reflected X-rays on the photographic film

The ordinary polarisation factor $\frac{1}{2}(1+\cos^2 2\theta)$ is examined critically and found to be valid in practice Experimental figures are quoted illustrating the use of the correction factors

The authors wish to express their gratitude to Sir William Bragg for his interest in the investigation, and to the Managers of the Royal Institution for providing facilities for the work They also wish to thank Mr B W Robinson for numerous fruitful discussions on the subject of the absorption factor, and for providing some of the experimental data used in section 5

Measurement of Absorbing Power of Materials by the Stationary Wave Method

By A H DAVIS, D Sc , and E J EVANS B Sc , Physics Department, National Physical Laboratory Teddington, Middlesex

(Communicated by Sir Joseph Petavel, F R S —Received December 23, 1929)

1 *Introduction*

The stationary wave method of determining the absorption coefficient of a material employs plane waves of sound at perpendicular incidence It requires the use of only small samples of material and provides a rapid and convenient means of obtaining useful information

The principle of the method has been previously described, so that a brief outline is sufficient A long pipe is provided with a source of sound at one end and is closed at the other by the test specimen Sound waves from the source travel down the pipe and are reflected by the specimen to an extent depending on its absorbing power The superposition of the incident and reflected waves gives rise to a stationary wave system, and the pressure amplitude varies continuously along the pipe, going through a series of maximum and minimum values The same description applies to the velocity amplitude, with the difference that the pressure maxima coincide in position with the velocity minima and *vice versa*

To determine the absorption coefficient "a" of a material it is sufficient to determine the ratio N/M which the minimum amplitude—either of pressure or of velocity—bears to the maximum The absorption coefficient, defined as the ratio of absorbed to incident energy, is then given by

$$a = 1\Big/\left(2 + \frac{M}{N} + \frac{N}{M}\right)$$

Various methods of measuring this ratio have been adopted Tuma who first suggested the stationary wave method used the ear as detector Subsequently Weisbach used a telephone earpiece inserted in the pipe and Hawley Taylor employed a Rayleigh disc placed outside the pipe and communicating with the interior by means of a narrow tube A description of this earlier work has been given by Paris * Later Paris, using as detector a hot wire microphone placed in the pipe, gave results for frequencies of 380 512, 650

---

* 'Proc Phys Soc,' vol 39 pp 269 295 (1927)

He found in many cases a measurable change of phase on reflection, and that there was no appreciable absorption of sound at the walls of the pipe Early experiments were carried out in 1924* at the N P L using a telephone earpiece for measuring the sound No details were published, but exploring tubes were found desirable, and a square test pipe did not give such perfect nodes and antinodes as were later obtained with a circular pipe Eckhardt and Chrisler† used as detector a telephone earpiece communicating with the interior of the pipe by means of a long narrow tube They tuned the pipe to resonance at each frequency, a procedure which, as Paris has pointed out, appears unnecessary They found no evidence of change of phase on the reflection of sound by the test material, and apparently concluded that such change would only occur in the case of diaphragm-like vibration of the specimen They found it was necessary to correct for absorption of energy at the walls of the pipe, and gave results for frequencies in the range from 297 to 3,200 cycles per second

Heimburger‡ compared coefficients for various materials, using a Rayleigh disc placed in the pipe as detector, the pipe being tuned Assuming the values for certain standard substances the coefficients of the remainder were then calculated The standard coefficients taken appear to have been obtained by the reverberation method and were assumed to be the same as the stationary wave coefficients In general such an assumption is unjustifiable and his procedure is open to criticism on this account

Wente and Bedell,§ using as source an electrically driven diaphragm occupying the whole section of the pipe measured the pressure amplitude immediately in front of the diaphragm by a short narrow tube leading to a microphone The specimen was moved along the pipe and the maximum and minimum pressure amplitude determined They assumed that, in consequence of the specially massive diaphragm used the velocity of the diaphragm was unchanged when the specimen was moved along the tube They did not find it necessary to correct for absorption at the walls of the pipe Results were given from 60 to 4 000 cycles per second

2 *Theory*

(*a*) *General* -- It will be convenient to have the following brief statement of theory Neglecting dissipative effects at the walls in the first instance and taking the face of the specimen as the origin $x = 0$, let the wave incident upon the specimen be the real part of

---

* N P L Annual Report, 1924

† 'Bur Stds Sci Papers,' No 526 (1926)

‡ 'Phys Rev,' vol 31, p 275 (1926)

§ 'Bell System Technical J,' vol 7, p 1 (1928)

$$\phi_1 = \mathrm{A}\, e^{i\beta x} e^{i\omega t} \tag{1}$$

Then, confining our attention throughout to real parts the reflected wave may be written

$$\phi_2 = \mathrm{B}\, e^{-i\beta x} e^{i\omega t}, \tag{2}$$

where ϕ is the velocity potential, $\omega = 2\pi \times$ frequency $\beta = \omega/c = 2\pi/\lambda$, $c =$ velocity of sound, and $\lambda =$ wave-length

The resultant potential in the pipe is

$$\phi = \phi_1 + \phi_2 = \mathrm{A}\, e^{i\beta x} e^{i\omega t} + \mathrm{B}\, e^{-i\beta x} e^{i\omega t} \tag{3}$$

If A and B are wholly real, so that there is no phase change on reflection, the pressure amplitude P at any point is

$$\mathrm{P} = \left| \rho \frac{\partial \phi}{\partial t} \right| = \rho\omega \left[\mathrm{A}^2 + \mathrm{B}^2 + 2\mathrm{AB} \cos 2\beta x \right]^{\frac{1}{2}} \tag{4}$$

Thus P^2 varies harmonically with x, maximum values $\rho^2\omega^2 (\mathrm{A} + \mathrm{B})^2$ occurring at $x = 0$, $\frac{1}{2}\lambda$, λ, $\frac{3}{2}\lambda$, etc, minimum values $\rho^2\omega^2 (\mathrm{A} - \mathrm{B})^2$ at $x = \frac{1}{4}\lambda$, $\frac{3}{4}\lambda$, $\frac{5}{4}\lambda$, etc

The absorption coefficient

$$a = 1 - \frac{\mathrm{B}^2}{\mathrm{A}^2} = 4 \bigg/ \left(2 + \frac{\mathrm{P}_{\max}}{\mathrm{P}_{\min}} + \frac{\mathrm{P}_{\min}}{\mathrm{P}_{\max}} \right) \tag{5}$$

If we have reflection with change of phase, B is complex $(\mathrm{B} = \mathrm{B}_0 e^{-i\beta\delta})$, and the velocity potential is given by the real part of

$$\phi = \mathrm{A}\, e^{i(\omega t + \beta x)} + \mathrm{B}_0\, e^{i(\omega t - \overline{\beta x + \delta})}$$

If, as pointed out by Paris, we substitute $x_1 = x + \delta/2$, $t_1 = t - \beta\delta/2\omega$, we find

$$\phi = \mathrm{A} e^{i(\omega t_1 + \beta x_1)} + \mathrm{B}_0 e^{i(\omega t_1 - \beta x_1)}, \tag{6}$$

which is identical in form with (3), and A and B_0 are both real Thus the effect of the phase change δ is to shift the whole of the stationary wave system a distance of $\frac{1}{2}\delta$ towards the origin Accordingly, the phase change can be determined from a knowledge of the position of the stationary system relative to the material

To obtain an estimate of the effect of dissipation at the walls, we assume* that the amplitude of a progressive wave in the pipe decays exponentially and write for the incident and reflected wave respectively —

---

* Crandall, 'Theory of Vibrating Systems and Sound,' p 95, Eckhardt and Chrisler 'Bur Stds Sci Papers' No 526 (1926)

$$\phi_1 = A e^{(\alpha+i\beta)x} e^{i\omega t} \quad \text{and} \quad \phi_2 = B e^{-(\alpha+i\beta)x} e^{i\omega t},$$

where α is the attenuation coefficient, assumed to be small The total potential is

$$\phi = \phi_1 + \phi_2 = A e^{(\alpha+i\beta)x} e^{i\omega t} + B e^{-(\alpha+i\beta)x} e^{i\omega t},$$

and the pressure amplitude

$$P = \rho\omega \left[A^2 e^{2\alpha x} + B^2 e^{-2\alpha x} + 2AB \cos 2\beta x\right]^{\frac{1}{2}}$$

The positions of the maximum and minimum values of P, given by $\partial (P^2)/\partial x = 0$ are found to be very nearly the same as for no dissipation

Let

$$\rho\omega A = P_i \qquad \rho\omega B_0 = P_r$$

denote 1st, 2nd, 3rd, , maxima by M_1, M_2, M_3
and 1st, 2nd, 3rd, , minima by N_1, N_2, N_3
Then

$$M_1 = P_i + P_r, \quad M_2 = P_i + P_r + \tfrac{1}{2}\alpha\lambda (P_i - P_r)$$

$$M_n = P_i + P_r + \tfrac{1}{2}(n-1)\,\alpha\lambda\,(P_i - P_r) \tag{7}$$

and

$$N_1 = (P_i - P_r) + \tfrac{1}{4}\alpha\lambda (P_i + P_r) \quad N_2 = (P_i - P_r) + \tfrac{3}{4}\alpha\lambda (P_i + P_r),$$

$$N_n = (P_i - P_r) + (2n-1)\,\tfrac{1}{4}\alpha\lambda\,(P_i + P_r) \tag{8}$$

We see then that the effect of absorption is to cause both the maxima and minima to increase with their distance from the closed end, this increase being negligible in the case of the maxima, but appreciable for the minima, especially with highly reflecting specimens The correction $\frac{1}{4}\alpha\lambda$ was therefore determined by preliminary measurements with the highly reflecting steel plate and was applied to the minima obtained with test specimens

Actually in any test, as a check on the regular behaviour of the apparatus four successive minima were measured and the average of the corrected values of these minima were taken

The above theory is general We now consider the special case of reflection from a material placed in the pipe at different distances l from a perfect reflector closing one end Let the front surface of the material be the origin $x = 0$ and let the distance from the back surface to the backing plate be l For simplicity consider an incident wave of unit pressure amplitude $p = e^{i\beta x} e^{i\omega t}$ where p is pressure in the wave Of this a fraction $R e^{-i\beta x} e^{i\omega t}$ is immediately reflected and, after transmission through the thickness of the material, a fraction $Te^{i\beta x}e^{i\omega t}$ emerges on the other side, where R and T are coefficients of reflection and transmission respectively The transmitted part is reflected to and fro between the steel plate and the material, and at each arrival at the material a fraction emerges again on the side of the incident wave As a consequence, the final expression for the pressure in the reflected wave at a point x cm from the front of the specimen is given by the sum of geometrical progression,

$$p = e^{-i\beta x}e^{i\omega t}[\mathrm{R} + \mathrm{T}^2 e^{-2i\beta l} + \mathrm{RT}^2 e^{-4i\beta l} + \mathrm{R}^2\mathrm{T}^2 e^{-6i\beta l} \quad]$$

$$= e^{-i\beta x}e^{i\omega t}\left[\mathrm{R} + \frac{\mathrm{T}^2 e^{-2i\beta l}}{1 - \mathrm{R}e^{-2i\beta l}}\right] \tag{9}$$

R and T are in general complex Writing $\mathrm{R} = \mathrm{R}_0 e^{-i\delta}$, $\mathrm{T} = \mathrm{T}_0 e^{-i\epsilon}$ the amplitude of reflected wave is

$$\mathrm{P} = \mathrm{R}_0 e^{-i\delta} + \frac{\mathrm{T}_0{}^2 e^{-2i(\beta l+\epsilon)}}{1 - \mathrm{R}_0 e^{-i(2\beta l+\epsilon)}} \tag{10}$$

If $\mathrm{P}_{2\pi}$ and P_{π} are values of P for special cases when $2\beta l = 2\pi$ and π respectively, *i e*, $l = \frac{1}{2}\lambda$ and $l = \frac{1}{4}\lambda$, we find

$$\mathrm{R}_0 e^{-i\delta} = \frac{\mathrm{P}_{2\pi} + \mathrm{P}_{\pi}}{2 + \mathrm{P}_{2\pi} - \mathrm{P}_{\pi}} \tag{11}$$

$$\mathrm{T}_0{}^2 e^{-2i\epsilon} = \tfrac{1}{2}(\mathrm{P}_{2\pi} - \mathrm{P}_{\pi})(1 - \mathrm{R}_0{}^2 e^{-2i\delta}) \tag{12}$$

Thus, from a knowledge of $\mathrm{P}_{2\pi}$ and P_{π} we can calculate R_0, δ, T_0, ϵ, and hence find the reflected wave for any position of the absorbing material

The arrangement employed in the measurements referred to below is that shown in fig 1 The test pipe was of wrought iron 1 2 cm thick, of 30 cm

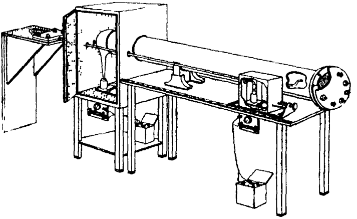

FIG 1 —General Arrangement of Apparatus

internal diameter, and 250 cm long, with a flange at one end The interior of the pipe was scoured and painted to ensure a smooth rust free surface The pipe wall was comparatively thick to avoid appreciable vibration or yielding of the walls The pipe diameter was chosen to be as wide as possible both with a view to minimising any absorption effect at the walls, and to using a specimen large compared with any irregularities of the surface This width however is such that radial vibrations of the contained air may be set up for a number of frequencies above 1290 cycles per second, and may thus impose an upper limit on the working of the apparatus A moving-coil horn type loud-speaker, excited by a valve oscillator, was used as source The mouth of the horn, which was of the same diameter as the unflanged end of the pipe, was placed close to that end of the pipe, but not in actual contact The loud-speaker, together with the adjacent end of the pipe, was enclosed in a felt-lined box

Arrangements were made whereby the test specimen was mounted within a wooden ring bolted to a steel disc 0 9 cm thick, which served as a backing wall to the various materials In many cases the specimen was cemented to the backing wall Crevices between the specimen and the wooden ring were filled up with cement suited to the material, or with plasticene An airtight joint between the flange and the ring was ensured by a rubber washer which was placed between them before they were bolted together

For the measurements of sound amplitude at points within the pipe an exploring tube of 1 2 cm internal diameter and 2 mm wall was employed, communicating with a moving coil loud-speaker movement placed on the table outside the pipe At any frequency, the electrical E M F generated at the terminals of the moving coil instrument was proportional to the acoustic pressure communicated to the diaphragm by the exploring tube Incidentally resonances of the air column in the tube were of no importance for at any frequency the column was equally in resonance when the maxima and minima were measured, and the E M F was proportional to the pressure at the mouth of the system irrespective of whether it was in resonance or not By bending the exploring tube into U form (like a trombone slide) space was saved The exploring tube was supported within the test pipe upon a light framework with rubber wheels Whilst the position of the open end of the tube could be varied when desired over the cross section of the pipe, it normally occupied a position on the axis To suppress certain lateral vibrations of the exploring tube which were found to give rise to sound leakage into the conduit, the tube was passed through grooves tightly packed with cotton wool, and separately supported just behind the loud-speaker cabinet Care was taken that the tube did not touch the loud-speaker horn, nor the sides of the cabinet The loud-speaker and its cabinet were completely insulated from the rest of the apparatus To prevent leakage of sound and vibration to the microphone it was connected to the exploring tube by a short length of rubber tubing, and was carried on string suspensions in a rubber wheeled carriage to which the exploring tube was rigidly attached The adjustments were such that, at all frequencies, when the open end of the exploring tube was stopped up, the microphone reading was zero

In taking readings at various points the whole microphone system was moved along Near minima of amplitude where variation with distance was very sharp, a slow motion device attached to the microphone box was employed enabling the minima to be determined accurately and conveniently to within ± ½ mm or less A second microphone and tube (not shown) was used as a check in order to detect any changes of the loud-speaker output when the exploring microphone system was moved For each frequency this second tube was in a fixed position near a maximum at the loud-speaker end

The electrical system for measuring the relative microphone E M F was similar to that described by Davis and Fleming * The microphone E M F was applied to a tuned amplifier the rectified output being passed through a galvanometer By means of a two-way switch an E M F from a variable calibrated mutual inductance was substituted for the microphone E M F, the mutual inductance being adjusted to give the same galvanometer reading as the microphone The current through the inductometer primary was derived from the oscillator by a potentiometer, and remained constant Accordingly, the microphone E M F was always proportional to the mutual inductance Since for this microphone the E M F is proportional to the pressure amplitude of the incident sound, it follows that the sound amplitude is proportional to inductometer reading The electrical leaks were rendered inappreciable by the use of earthed leads

3 *Procedure*

Measurements were made of the first four maxima and minima to avoid error, because it was found that in a few cases the first minimum was markedly different from the succeeding ones, which were more uniform This irregularity is probably due to lack of planeness in the reflected wave from a non-homogeneous surface, and disappeared as the pipe was traversed The procedure accordingly was as follows The positions and values of the first four minima were determined, then the maxima, and finally the determination of the first minimum was repeated Readings of the fixed check microphone were then taken for each position of the exploring microphone Corrections were then applied to the values of the minima for any change of output of the loud-speaker arising from moving the microphone from the maxima position and for the absorption of sound by the walls of the pipe The output of the loud-speaker was taken to be proportional to the check microphone readings, a procedure which receives some justification later The variations in output were found to be small, increasing at the higher frequencies, and did not exceed 5 per cent in amplitude The correction for absorption was applied as described in Section 2, and from the mean value of $(A_0 - B_0)/(A_0 + B_0)$ thus obtained the absorption coefficient was calculated

---

* 'Phil Mag,' vol 2, p 51 (1926)

4 *Results*

Standard Steel Plate —The general behaviour of the apparatus was subjected to a rigorous overall test by using a steel plate —practically a perfect reflector to close the pipe This should have given rise to practically perfect nodes and antinodes, and to a sine-wave distribution of amplitude along the pipe It was necessary to take great precautions to avoid leaks, both electrical and mechanical, the latter being extremely troublesome Finally they were satisfactorily eliminated by the devices enumerated above This was shown by the measurements on steel plate, which gave an extremely low value for the absorption coefficient

It was observed by locating the minima that the exploring tube measured the pressure at a point a short distance outside its mouth The distance varied with frequency, being approximately 0 3 cm at 500, 0 4 at 800, 0 4 at 1000, and 0 5 cm at 1200 cycles per second This end effect was verified by measurements by another tube, bent at the end, so that the mouth faced the other way It may be mentioned that the effect does not enter into the measurements of absorbing power or phase displacement, since only relative magnitudes and positions are respectively required

The response of the microphone system was tested by taking readings at a large number of points between distance $\frac{1}{4}\lambda$ and $\frac{3}{4}\lambda$ from the plate, readings of the fixed check microphone also being taken Theoretically, for a perfect reflector and for linear response of the microphone, the relation between microphone E M F and distance should be very nearly a sine curve, as is seen by putting $A = B$ in equation (4) As an example, experimental results are shown in fig 2 for a frequency of 1,200 cycles per second in comparison with a true sine curve The microphone readings have been corrected for variation in loud speaker output due to movement of microphone tube in the pipe The precision with which the corrected experimental results agree with the sine curve indicates satisfactory response of the microphone system and justifies the correction for loud-speaker variation It may be noted that the loud-speaker variation experienced in this particular case was much greater than that usually encountered, and the uncorrected experimental curves themselves, usually lay very near the sine curve

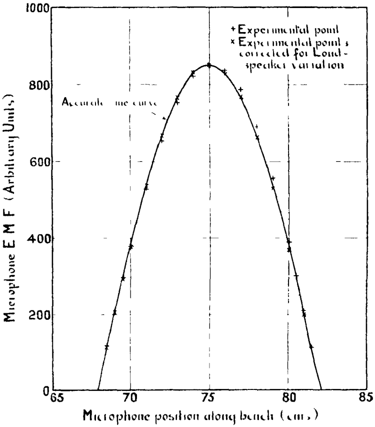

Fig 2 — Steel Reflector Relation between microphone reading and distance along pipe at frequency of 1 200 cycles per second

Accurate determination of maxima and minima for the steel plate showed that the maxima were all substantially uniform, but that the minima, although always very small compared with the maxima, showed definite increase with distance from the plate. The results were the same whether readings were taken on the axis or near (within 1.5 cm.) the wall of the pipe, showing that conditions were uniform over the cross section to within a short distance of the wall. This increase of minima is in general accordance with equations (8) and is probably due to slight absorption at the walls.

The magnitude of the effect observed is also of the right order. According to a theoretical treatment by Helmholtz, Kirchoff and Rayleigh, the decay factor for sound propagation in a pipe, when viscosity only is considered, is given by $\alpha = \frac{1}{rc}\sqrt{\frac{\omega\mu}{2\rho}}$ where r is radius of pipe, μ/ρ is kinematic viscosity of air. The effect of heat conduction is to increase the decay factor, which remains of the same order of magnitude. The following table shows values of α calculated from this formula, together with α calculated from experimental results by use of equations (8).

Table I

Frequency	500		800	
	Theoretical	Experimental	Theoretical	Experimental
α	5.8×10^{-5}	3.8×10^{-5}	7.3×10^{-5}	5.8×10^{-5}
Frequency	1,000		1,200	
	Theoretical	Experimental	Theoretical	Experimental
α	8.1×10^{-5}	6.3×10^{-5}	8.9×10^{-5}	7.3×10^{-5}

It is seen that the experimental and theoretical values are of the same order of magnitude, and we conclude that the dissipative effects at the boundary are sufficient to account for the progressive increase of minima observed, and that corrections on the lines of equation (8) are justifiable.

As expected from the possible occurrence of radial vibrations of the air in the test pipe at frequencies above about 1,200 cycles per second, good minima were not obtained with the steel plate above this frequency. Accordingly, all determinations made with the apparatus have been confined to notes below this pitch.

General Absorbents.—Absorption coefficients have been determined for a large number of materials Chief interest centres in the behaviour of the more efficient materials, and, in view of the fact that such materials as glass plaster, hard wood etc , all reflect about 97 per cent or more of the incident sound, no special attention has been paid to them A list of results is given in Tables IVA and IVB Table IVA relates mainly to simple absorbents employed under various conditions suggested by theoretical considerations Unfortunately, however, absorbents used in the correction of acoustical defects of auditoriums are almost exclusively proprietary articles with special features and in Table IVB results for a variety of these absorbents are collected together

In many cases the absorption coefficient determined for samples of acoustical absorbents depended on whether or not the sample was rigidly fixed to the backing plate, the difference being greater in the case of stiff board-like materials than soft materials like felt, in which the difference was often negligible Presumably it is due to occurrence of diaphragm-like vibrations of the free specimen The following results indicate the magnitude of the effect

Table II

Material	Absorption coefficient at frequency of				
	250	500	800	1,000	1,200
Cane fibre board 1 1 cm thick free	0 04	0 05	0 08	0 11	0 17
Cane fibre board 1 1 cm thick, cemented	0 03	0 03	0 04	0 05	0 07

Accordingly absorption coefficients were always determined for the material rigidly fixed unless otherwise stated This coefficient gives the absorption due to porosity and yielding of the material when movement as a whole is prevented

It was also found, in agreement with Paris, that there was a definite phase change on reflection even when diaphragm-like vibrations of the specimen were prevented by rigid fixing to the backing plate The shift of the stationary wave system was frequently of the order of 1 cm and was easily measurable

It may be desirable to mention here that when test materials are reasonably homogeneous and undamaged, results obtained by the apparatus described above are satisfactorily reproducible for different samples For example, a number of measurements on different samples of ½-inch felt always gave practically the same results This was true also of certain cotton waste results which were repeated, and indeed the manner in which results given later (for different thicknesses of cotton waste, and different positions of felt) agree with the theoretical formulæ, indicates that the apparatus functions satisfactorily Results obtained for a large number of varied absorbents are collected together in Table IV It is convenient to notice a few general points which are revealed

Variation of Absorption Coefficient with Thickness —Results given by Paris and Wente and Bedell, indicated that in general absorption increased with thickness, up to a limit when the absorption became constant

Experiments were made with the present apparatus on various materials, including cotton waste, a material which was used at the Laboratory as a material for thickly lagging the walls of sound chambers

In many cases, for certain regions of thickness, an increase of thickness produced a decrease of absorption coefficient This effect, which does not appear to have been noted before, can be explained on theoretical grounds by taking account of the interference between sound reflected directly from the front surface and that emerging from the material after reflection at the backing surface The phenomenon is analogous to the reflection of light by plane parallel surfaces in optics

A formula has been worked out by Crandall,* under certain assumptions, for the variation of absorption with thickness He obtained the result

$$\xi = \frac{r - e^{-2(\alpha+i\beta)l}}{1 - re^{-2(\alpha+i\beta)l}} \tag{13}$$

where ξ is the displacement amplitude (complex) of reflected wave for thickness l r the reflected amplitude for infinite thickness, and $\alpha + i\beta$ is the propagation constant of the material, α expressing the attenuation and β the phase factor in the material

If we refer to pressure amplitudes instead of displacement the formula becomes

$$\xi = \frac{r + e^{-2(\alpha+i\beta)l}}{1 + re^{-2(\alpha+i\beta)l}} \tag{14}$$

By measuring both the amplitude and the phase of the reflected wave, ξ was determined for various thicknesses of absorbing material A test of the formula was made for cotton waste at a frequency of 1,200 by calculating the constants r, α, β, from the results at this frequency They were found to be $r = 0{\cdot}2$, $\alpha = 0{\cdot}12$, $\beta = 0{\cdot}36$ From these three constants the reflection coefficients for various thicknesses were calculated The theoretical curve thus obtained is exhibited in fig 3 and shows good agreement with the experimental results

---

* 'Theory of Vibrating Systems and Sound,' p 195, equation (270A)

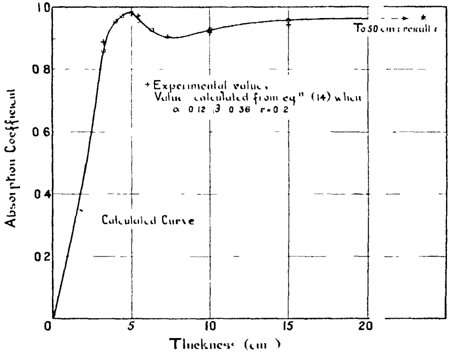

FIG 3 — Absorption Coefficient of Cotton Waste Variation with thickness at frequency of 1,200 cycles per second

It is of interest to note that the velocity of sound in cotton waste, calculated from β, is approximately 21,000 cm per second

Measurements were also made at frequencies of 250, 500, 1 000, and experimental results are exhibited together in fig 4 It is seen that the behaviour is generally the same in all cases, the absorption rising to a maximum at roughly $\frac{1}{4}\lambda$ for each frequency, then falling away and finally becoming constant

Results were also obtained for felt and for cotton wool in layers They are shown in fig 5, where the same effect is again evident, but in these cases it is seen that the final constant value is reached much more quickly than in the case of cotton waste

Variation with Distance of Specimen from the Backing Plate - Measurements of amplitude and phase of the sound reflected from $\frac{1}{2}$-inch felt placed at different distances from the plate were made at frequencies of 800 and 1,200 The felt was chosen because its absorption coefficient did not depend on whethe

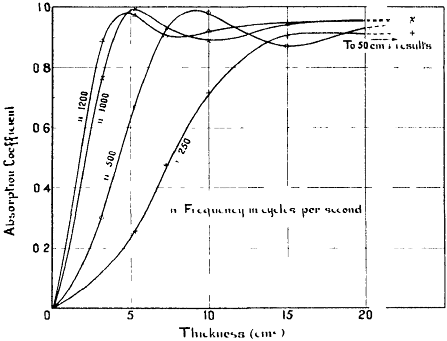

Fig 4 Absorption Coefficient of Cotton Waste Variation with thickness at different frequencies

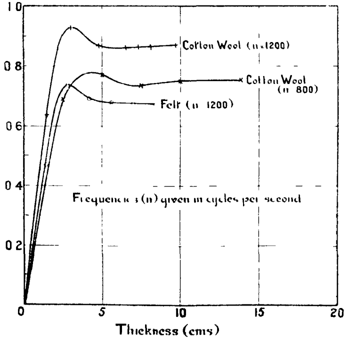

Fig 5 —Variation of Absorption Coefficient with thickness

or not it was rigidly fixed to the backing plate In each case the theoretical curves for variation were calculated from measurements at two distances by formulæ (9), (10), (11) Figs 6 and 7 show the comparison between the

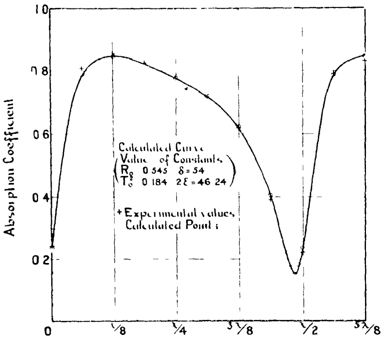

FIG 6 —Absorption Coefficient of ½ inch felt at different distances from backing plate (frequency of 800 cycles per second)

theoretical and the experimental results The agreement at 800 is excellent, while that at 1,200 is also satisfactory It will be noted that both theory and experiment agree that the absorbing power increases very rapidly within a short distance of the plate, and that the results are repeated for positions $\frac{1}{2}\lambda$ apart

Effect of Perforations in Substance —It was observed that when perforations were made in the surface of a board-like material, the absorbing power was very much increased As an example, this is shown in Table III, which relates to a ½-inch cane fibre board, before and after perforation

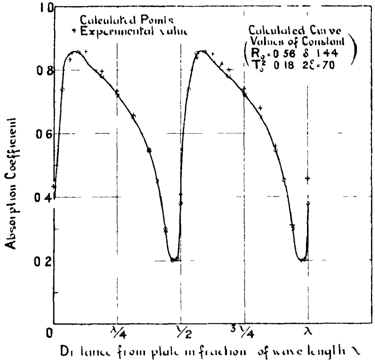

Fig. 7.—Absorption Coefficient of ½ inch felt at different distances from backing plate (frequency of 1,200 cycles per second).

Table III.

Material	Absorption coefficient at frequency of			
	500	800	1 000	1 200
Cane fibre board 1.1 cm. thick	0.03	0.04	0.05	0.07
Cane fibre board 1.1 cm. thick perforated with 480 holes per square foot, each $\frac{1}{32}$ inch diameter	0.175	0.356	0.36	0.53

Effect of Membranes fastened to Surface.—It will be seen, on referring to Table IV, that the effect of fixing various membranes to the front surface of soft felt-like materials was frequently to increase the absorption coefficient, the increase being greatest at lower frequencies. As a result the absorption is more uniform over the frequency range employed.

Table IV.—Sound Absorption Coefficients determined by the Stationary Wave Method. (*Figures in brackets relate to the phase change on reflection, and give in centimetres the displacement ($\frac{1}{2}\delta$ of equation (6)) of the stationary wave system towards the specimen.*)

A.—General Absorbents

Material	Thickness (cms.)	Absorption coefficient for frequency (cycles per second) 250	500	800	1,000	1,200
Steel backing plate	0.9	0.01	0.002	0.006	0.004	0.002
Cotton waste*	3.2	—	0.30 (4.0)		0.76 (4.3)	0.89 (4.3)
	5.3	0.25 (7.4)	0.67 (6.8)	—	1.0 (−6.7)	0.97 (−3.1)
	7.3	0.48 (9.7)	0.93 (7.9)		0.93 (−1.2)	0.91 (−0.6)
	10	0.72 (11.7)	0.98 (2.4)	—	0.89 (0.3)	0.92 (0.7)
	15	0.91 (5.7)	0.87 (1.3)		0.94 (0.8)	0.95 (0.5)
	50	0.92 (6.0)	0.95 (2.0)	—	0.93 (0.3)	0.97 (0.1)
Cotton wool* (in layers)	1.5		—	—	—	0.64 (1.7)
	3.0			—	—	0.93 (1.0)
	4.8		—	—	—	0.87 (0.4)
	6.5	—		—	—	0.86 (0.4)
	7.3		—	—	—	0.86 (0.4)
	8.1	—		—	—	0.86 (0.7)
	9.7			—		0.87 (0.7)
Cotton wool* (in layers)	2.5			0.69 (2.0)		—
	5.0	—		0.77 (0.6)	—	
	7.5	—	—	0.74 (0.8)		—
	10.0	—		0.75 (1.1)	—	—
	13.9	—	—	0.75 (1.1)	—	—
Felt (hair)* (in layers)	1.4	—		—	—	0.47 (1.4)
	2.8	—	—	—	—	0.74 (1.0)
	4.2	—		—	—	0.69 (0.6)
	5.6	—	—	—	—	0.68 (0.7)
	7.0	—	—	—	—	0.68 (0.7)
	8.4	—	—	—	—	0.67 (0.7)
Different samples	2.8	—	—	—	—	0.76 (0.8)
	2.8	—	—	—	—	0.75 (1.0)
Felt (hair)—						
1st sample	1.3	0.03	0.10	0.26	0.35	0.46
(2nd sample)	1.3	0.04	0.11	0.25	0.35	0.15
Felt (hair)	1.9	0.07	0.21	0.41	0.43	0.63
Felt (red hair)	2.5	0.08	0.19	0.36	0.35	0.45
Felt* at distance from backing plate in cms.—						
0	1.3	—		0.244 (1.2)		0.435 (1.15)
1.8	—		—	—		0.835 (0.8)
2.7	—	—	—	0.81 (1.6)	—	—
3.6		—	—	—	—	0.86 (−0.1)
5.4	—	—	—	0.854 (0.3)	—	0.795 (−0.3)
7.2	—		—	—	—	0.735 (−0.4)
8.1	—	—	—	0.825 (−0.6)	—	—
9.0	—	—	—	—	—	0.66 (−0.5)
10.8		—	—	0.781 (−0.6)	—	0.545 (−0.4)
12.6	—	—	—	—	—	0.292 (−0.05)
13.5	—	—	—	0.718 (−0.9)	—	—

* Not cemented to backing plate.

Table IV A —(continued)

Material	Thickness (cms)	Absorption coefficient for frequency (cycles per second)				
		250	500	800	1 000	1 200
Felt* at distance from backing plate in cms —						
14 3	—	—	—	—	—	0 41 (1 2)
16 2	—	—	—	0 62 (-0 9)	—	0 84 (0 8)
18 0	—	—	—	—	—	0 85 (0 0)
18 9	—	—	—	0 39 (—0 6)	—	—
19 8	—	—	—	—	—	0 80 (—0 3)
21 5	—	—	—	—	—	0 74 (—0 2)
21 6	—	—	—	0 22 (1 2)	—	—
23 3	—	—	—	—	—	0 68 (—0 5)
24 2	—	—	—	0 79 (1 6)	—	-
25 1	—	—	—	—	—	0 56 (-0 3)
26 9		-	—	0 83 (0 3)	—	0 30 (—0 0)
28 7	—	-	—	—	—	0 46 (1 2)
Felt (effect of coverings)—						
Hair felt (bare)	1 3	0 03	0 10	0 26	0 35	0 46
Hair felt, same sample with brown paper glued to front surface	1 3	0 16	0 30	0 41	0 46	0 49

Table IV B - Special Absorbents

Material	Thickness (cms)	Absorption coefficient for frequency (cycles per second)				
		250	500	800	1,000	1,200
Akousti celotex Type—						
BB*	—	0 19 (2 8)	0 37 (2 0)	0 56 (1 2)	0 61 (1 2)	0 69 (1 1)
BB (later specimen)	3 2	0 17	0 40	—	0 65	0 73
B	2 1	0 12 (1 6)	0 23 (1 1)	—	0 45 (1 0)	0 53
B (different sample)	2 1	—	—	—	0 50	0 63
C	0 95	—	0 12	0 24	0 30	0 37
C*	0 95	—	0 12	0 23	0 29	0 37
Celotex	1 1	—	0 03 (0 15)	0 04 (0 05)	0 05 (0 2)	0 07 (0 2)
Celotex*	1 1	-	0 05 (0 15)	0 08 (0 2)	0 11 (0 3)	0 17 (0 1)
Balsam wool, sound, absorbent	2 5	0 05	0 13 (2 5)	0 24 (2 5)	0 31 (2 5)	0 40 (2 5)
Cabot quilt	1 5	0 09	0 18	0 43	0 66	0 91
(2nd sample)	1 5	0 07	0 19	0 55	0 84	0 87
Carpet	0 6	—	0 02	0 04	0 05	0 06
***Felt** (effect of coverings)*						
Asbestos akousticos felt, bare	1 3	0 03	0 07	0 14	0 18	0 22
Do , covered with brown paper	1 3	0 11	0 38	0 58	0 61	0 59
Asbestos akousticos felt, bare	1 0	0 10	0 23	0 44	0 54	0 63

* Not cemented to backing plate

Table IV B —(continued)

Material	Thickness (cms)	Absorption coefficient for frequency (cycles per second)				
		250	500	800	1 000	1 200
Asbestos akousticos felt, covered with brown paper	1 9	0 21	0 37	0 44	0 46	0 65
Do , covered with perforated brown paper	1 9	—	0 23	0 51	0 66	0 81
Flaxlinum	2 8	0 15 (2 6)	0 40 (2 1)	0 68 (0 8)	0 68 (0 3)	0 65 (0 2)
Do (2nd sample)	2 8	0 20	0 55	0 66	0 60	0 58
Masonite	1 1	0 07	0 09	0 11	0 11	0 14
Do (2nd sample)	1 1	0 08 (0 3)	0 10 (0 2)	0 13 (0)	0 13 (0 05)	0 15 (0 15)
Masonite*	1 1	0 09 (0 3)	0 12 (0 3)	0 19 (0 2)	0 30 (0 1)	0 26 (0)
Nashkote Type—						
B332	1 2	0 04	0 09	0 21	0 29	0 40
B332	1 9	0 09	0 26	0 59	0 76	0 86
B316	1 9		0 19	0 39	0 52	0 70
Do , with cover removed	1 9	—	0 15	0 30	0 39	0 54

* Not cemented on backing plate

Appendix Short Description of Materials

Material	Description
Akousti celotex BB	Perforated cane fibre board $1\frac{1}{4}$ inch thick, 1 67 lb per square foot, 441 holes per square foot $\frac{3}{16}$ inch diameter, $1\frac{1}{8}$ inch deep Perforations exposed
, B	Perforated cane fibre board $\frac{13}{16}$ inch thick, 1 11 lb per square foot, 441 holes per square foot, $\frac{3}{16}$ inch diameter, $\frac{1}{2}$ inch deep Perforations exposed
C	Perforated cane fibre board $\frac{5}{8}$ inch thick, 0 48 lb per square foot Completely perforated
Balsam Wool Sound Absorbent	Soft wood fibre faced with open meshed muslin, backed with asphalted kraft paper 1 inch thick 0 22 lb per square foot
Cabot quilt	Eel grass quilted in envelope of brown paper $\frac{3}{8}$ inch thick, 0 32 lb per square foot (No covering membrane)
Celotex	Cane fibre board $\frac{7}{16}$ inch thick
Hair felt	$\frac{1}{2}$ inch thick, 0 54 lb per square foot
,,	$\frac{3}{4}$ inch thick, 0 81 lb per square foot
Flaxlinum	Semi stiff flax fibre board 1 inch thick, 1 17 lb per square foot
Masonite	Pressed board about $\frac{1}{4}$ inch thick of fine wood fibres
Hair felt (red)	1 inch thick, 0 48 lb per square foot
Nashkote B332	Asbestos hair felt with cover of perforated oil cloth cemented on surface Perforations $\frac{3}{32}$ inch diameter, 10 per square inch, $\frac{1}{2}$ inch thick, 0 47 lb per square foot
,, B332	As above, but thickness $\frac{3}{4}$ inch Two samples gave 0 71 and 0 77 lb per square foot respectively

Relation between Stationary Wave Results and Values obtained by Reverberation Method – In the stationary wave method of measuring absorbing power a small specimen is used, and the sound is incident perpendicularly, whereas in actual practice, when absorbents are used in auditoriums, the sound is incident in a random manner upon large areas Again the method of mounting materials in an auditorium on studding or otherwise may allow vibration of the absorbent, with some consequent effect upon the absorption, not covered by the stationary-wave test in which specimens are usually adherent to the backing plate It is to be noted that a certain method of testing absorbents – the reverberation method—uses large samples mounted under practical conditions in a large test room, and gives results directly applicable to auditorium requirements In view, however, of the cheapness and convenience of the stationary-wave method for comparing materials on a small scale, it is desirable to consider what relations hold between the coefficients determined by the two methods

A theoretical formula for the relation has been given by Dr Paris,* which, strictly speaking, should apply only to hard porous materials such as porous plasters As a matter of interest it was applied to results obtained for ½-inch felt at 500 cycles per second as obtained at the N P L The average stationary wave value was 0 11 From this Dr Paris's formula indicated that the reverberation coefficient should be 0 17, measurements upon three different samples agreeing to ± 0 005 Actually the reverberation coefficient of a large sheet of the same felt carried out under somewhat adverse conditions was found to be considerably greater than this Also a reverberation coefficient for Akousti-celotex BB at 500 cycles per second, estimated in the same way from an observed stationary wave value of 0 40, was calculated to be 0 49 Watson, however, found 0 70 for this material by the reverberation method

Clearly the reverberation coefficient for these materials at 500 cycles per second is greater than the stationary wave value, but the difference is greater than that calculated from Dr Paris's formula

Comparison between Stationary Wave and Reverberation Results for various Materials —In the absence of a theoretical formula applicable to all types of materials and in view of the importance of reverberation figures, Table V has been compiled from such data as is available, showing the actual experimental ratios between the two The stationary wave coefficients employed in calculating the tables are those given in Table IVB The reverberation results have been compiled from various sources indicated It should be clearly understood that, whilst the materials are proprietary articles which have the same name, the samples were tested at widely different times in different countries and may well differ appreciably In this connection, for instance, two samples of the same felt like material weighed at the Laboratory varied some 8 per cent in weight per square foot, and occasional samples of a compressed board-like absorbent were found to be specially absorbent owing to loosening of surface layers Indeed, published reverberation figures for commercial materials of the same name obtained by different laboratories differ themselves in extreme cases by as much as ± 20 per cent as is illustrated in Table V by the ratios given for akousti-celotex B and BB Variation is also shown in the two sets of values for balsam-wool For these reasons appreciable variability is to be expected in the ratios for given frequency in Table V

---

* 'Phil Mag,' vol 5, p 489 (1928)

Table V —Relation between Stationary Wave and Reverberation Results

Material	Ratio $\frac{\text{Reverberation coefficient}}{\text{Stationary wave coefficient}}$ at frequency			
	250–256	500–512	1 000–1,024	Source of reverberation figure
Akousti celotex				
BB	1 8	1 8	1 2	Watson, 1927
C		2 5	1 6	Watson, 1927
B	2 0	2 0	1 1	Watson
B	2 2	1 7	1 0	P E Sabine
B	2 2	1 7	1 4	Bur Standards
BB	2 2	1 6	1 2	P E Sabine
Balsam wool sound, absorbent—				
1 inch	3 6	3 4	2 0	Watson
1 inch	5 4	3 8	2 2	P E Sabine
Celotex*	—	6 3	1 6	
Felt, asbestos hair -				
½ inch	4 7	4 4	2 8	P E Sabine
¾ inch	2 4	2 0	1 2	P E Sabine
Flaxlinum, 1 inch	2 7	1 2	1 0	Watson
Nashkote—				
B332, ½ inch thick	4 8	4 8	2 3	P E Sabine
B332, ¾ inch thick	2 7	2 0	1 0	P E Sabine
B316, ¾ inch thick	—	2 5	1 4	P E Sabine
Masonite	3 7	3 8	3 3	P E Sabine

* Information concerning the reverberation coefficient of celotex was received too late for these points to be included in figs 8 and 9 They are, however, in good agreement with the curves

An inference from the table is that the reverberation coefficient in the ordinary practical range is generally greater than the stationary wave coefficient, the ratio being greatest for low frequencies

In fig 8 the ratio between the reverberation coefficient and the stationary-wave coefficient has been plotted against the absorbing power determined by the stationary wave method In the case of the materials akousti celotex B and BB already referred to (stationary wave coefficients 0 23 and 0 40,

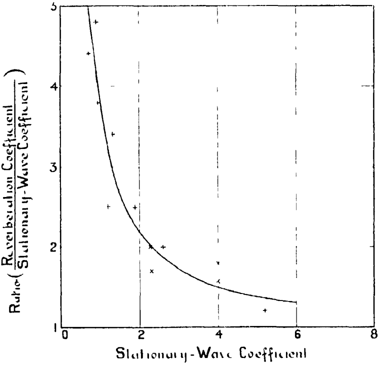

FIG 8 —Showing the Ratio (reverberation coefficient/stationary wave coefficient) plotted against the stationary wave coefficient for a frequency of about 500 cycles per second

respectively), ratios obtained from two sources of reverberation figures have been plotted A curve has been drawn to indicate the trend of the results, but in view of the miscellaneous nature of the materials a definite relation is not to be expected Similar results were obtained at other frequencies

The experiments were carried out in the Physics Department of the National Physical Laboratory The authors express their acknowledgments to Dr G W C Kaye, O B E , Superintendent of the Physics Department, for interest and encouragement Mr R Berry, Observer, assisted in the early stages of the work and constructed parts of the apparatus

Characteristic Energy Losses of Electrons Scattered from Incandescent Solids

By Erik Rudberg, Nobel Institute, Stockholm, Sweden

(Communicated by O W Richardson, F R S —Received January 13, 1930)

Introduction

The electron emission produced when solid conductors are bombarded with electrons of controlled speed has formed the subject of a great number of investigations It is now generally recognized that this emission consists of three different parts (1) Primary electrons, truly reflected without loss of energy , (2) electrons scattered back with reduced energy , and (3) secondary electrons proper, with very low velocities, which would seem to be produced from the atoms of the target by the same collision processes that give rise to the second group In recent years considerable attention has been paid to the reflected electrons, the angular distribution of which reveals their wave character, if the target is a definitely orientated crystal of the substance in question [*] Some time ago I made some measurements on the velocity spectrum of the emission produced by electron bombardment, using a magnetic deflection apparatus of fairly high resolving power [†] The principal object of this investigation was to look for evidence of groups of electrons with characteristic velocities related to the soft X ray levels of the substance From certain theoretical considerations such electrons might be expected to be present in the emission [‡] Targets of lithium, beryllium, boron, carbon and aluminium were tried but in no case was there any evidence of electrons of the kind in question These results are discussed in the paper mentioned The distribution curves obtained for different targets and bombarding voltages ranging from 40 to 900 volts were all similar in shape The reflected electrons produced a sharp and narrow peak separated from the rest of the curve by a very deep minimum The curve then rapidly rose to a maximum, corresponding to scattered electrons which had lost an energy equivalent to 25 volts in the collision In addition to these, some experiments were made with targets of platinum and carbon, which could be kept at incandescence also when readings were taken It was found that new maxima appear at high temperature, nearer to the reflected peak, and that the 25 volt maximum becomes very faint but reappears after some time on cooling These changes were repeated several times It was concluded that the 25 volt maximum was produced by an adsorbed layer formed on the cold target in the high vacuum, whilst the new maxima with hot targets should probably be regarded as characteristic of the target substance itself Somewhat similar effects have been observed by Brown and Whiddington using a photographic method *

---

[*] Davisson and Germer, 'Phys Rev,' vol 30, p 705 (1927), vol 33 p 760 (1929), 'Nat Acad Sci Proc,' vol 14, p 317 (1928), Davisson, 'J Franklin Inst,' vol 205 p 597 (1928), and vol 208, p 571 (1929) D C Rose 'Phil Mag,' vol 6, p 712 (1928)

[†] Rudberg, 'K Svenska Vet Akad Handl' vol 7 No 1 (1929)

[‡] Richardson 'Roy Soc Proc,' A, vol 119 p 531 (1928), Rudberg 'Roy Soc Proc,' A, vol 121, p 421 (1928), and *loc cit*

The present investigation is a continuation of these experiments with heated targets The influence of the magnetic field set up by the heating current for the targets in the earlier apparatus made it necessary to work with fairly high bombarding voltages, and owing to the limited resolving power in this region the characteristic features of the curves near the reflected peak could not be traced accurately The apparatus used in the present work is essentially an improved form of the earlier one To avoid complications I have only studied targets of non magnetic material, these are copper, silver gold platinum, and the oxides of magnesium, calcium, strontium and barium

Description of Apparatus

The various parts of the experimental arrangement employed are all mounted on a large glass stopper, provided with a tube of large bore, joined to the pumping system, and several narrow tubes for wire connections A long, 80 mm wide glass tube, closed at one end, surrounds the whole, it is joined to the stopper by hard sealing-wax The inside construction consists of three parts the electron gun, the small box containing the target, and the large deflexion box, to which the tube shielding the electron collector is directly attached These are all shown in fig 1, *a*, *b* represents a horizontal section through the plane of the slits in the deflexion box, *c* gives vertical sections showing details of the mounting of the target box and the target holder All metal parts are made of pure copper, silver soldered or bolted together by copper screws The particular shape of the target holder was chosen in order to reduce the magnetic field of the heating current to a minimum For this purpose connexion to the ends of the thin strip used as a target is made through strips of sheet copper in the plane of, and parallel to the target, the direction

---

* Brown and Whiddington, 'Leeds Phil Lit Soc Proc,' vol 1, p 162 (1927), Whiddington *ibid*, vol 1, p 242 (1928)

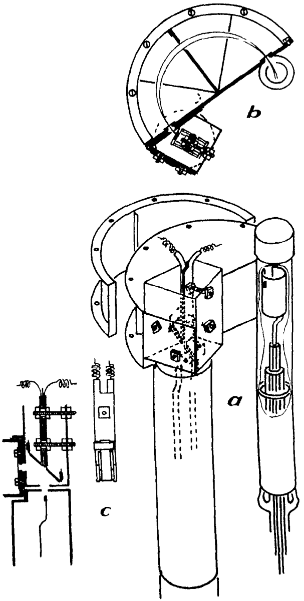

FIG 1

of the current in these strips being opposite to that in the target The leads for the heating current are insulated from each other and from the target box by thin pieces of mica and very short bits of quartz tubing The target box is insulated from the deflexion chamber by sheets of mica

The semi-cylindrical wall of the deflexion box is made removable to allow adjustment of the inside parts; it is provided with flanges which fit very closely to the other walls of the box, to which it is fastened by 10 screws. The entrance and exit slits are cut by a sharp razor in thin sheet copper and examined under the microscope. They are attached by screws to the inside of the box in such a way that they cover the corresponding wider slits in the rigid base plate of the box. The correct adjustment of the slits is checked and their distance apart measured with the aid of a dividing machine. The width of the electron beam which is analysed in this apparatus, is determined by a third slit in the central partition of the box, the two extra screens merely serving the purpose of cutting down the effect of stray electrons. The dimensions of the slits used in the present research are: entrance slit 2.5 × 0.083, exit slit 2.5 × 0.073, central slit 2.5 × 3.5, all in millimetres. The slit in the target box is 3.0 × 0.7 mm. The distance between entrance and exit slit was found to be 49.95 mm, the mean radius hence very nearly 25.0 mm. From these data the greatest relative interval of velocity $\Delta v/v$, within which electrons are collected for a given value of the deflecting field, may be calculated*; the smallness of this quantity measures the resolving power. In the present case maximum $\dfrac{\Delta v}{v} = 0.6$ per cent.

After a good many readings had been taken with this apparatus, in which only electrons scattered in a direction at right angles to the primary beam are studied, it was thought desirable to try similar experiments for electrons scattered in other directions. For this purpose the apparatus was altered in such a way as to allow measurements of the velocity distribution among the scattered electrons to be taken for a series of different angles in succession, keeping other conditions constant. The change in the former design consists essentially in the introduction of a new construction, which replaces the electron gun and the target box and which is rigidly attached to the deflexion chamber in the same way as the latter. The new construction is shown in position in fig. 2, *a* and *b*; in *a* the nearest corner of the apparatus is to be imagined cut open, as indicated, in order to show the interior parts; *b* is a top view. Fig. 2, *c* represents a vertical section through the centres of the two wheels to be seen in fig. 2, *b*. The upper one of these wheels, the axis of which coincides with the axis of the whole tube, merely serves the purpose of transmitting a rotating motion to the similar pulley attached to the electron gun and target to be rotated. A simple coupling enables the first pulley to be turned from the outside, when the tube is mounted in position, by acting on a ground joint at the top this joint is lubricated by a special vacuum oil* of a very low

---

* Rudberg, *loc. cit.*

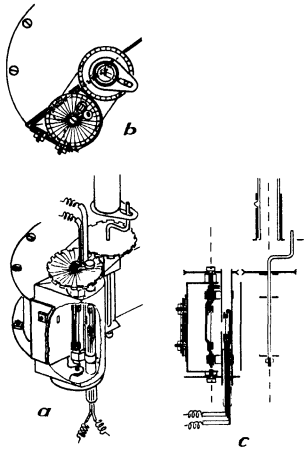

FIG 2

vapour pressure made by the Metropolitan-Vickers Electrical Company When lubricated in this way the joint worked very satisfactorily

The long, very narrow electron gun of this apparatus constitutes a rigid stem to which the other revolving parts, particularly the target holder, are attached It is fixed to the pulley with its upper end and to another wheel with its lower part in such a way that it remains parallel to the slit when it is made to pivot round the common axis of these two wheels, which is also parallel to the slit The target is a narrow strip, stretched as nearly as possible along the axis of rotation The target holder is insulated by strips of mica, and the construction is such as to reduce the magnetic field due to the heating current to a minimum The same precaution has been taken in the construction of the hot filament source, which is insulated by a quartz tube fitting snugly into the gun tube Electrical connexion is made to the foil at the top and to the filament at the bottom, by means of very soft copper springs, which do not impede the motion appreciably The position of the gun with respect to target and slit can be read from the outside by the aid of a fixed index and a circle divided in 24 parts, which is drawn on the top wheel

---

* C R Burch 'Roy Soc Proc,' A vol 123, p 271 (1929) I am much indebted to Prof Siegbahn of Upsala who very kindly let me have some of the oil given to him

Methods

Keeping the bombarding voltage constant, there are two different methods which may be used to obtain the velocity distribution of the fast electrons from the target In the first of these the target box and the target are directly connected to the deflexion chamber The magnetic field, parallel to the slits is varied by small steps over the region corresponding to the velocities in question according to the relation

$$v = erH/m, \tag{1}$$

where v is the velocity an electron must possess to be able to follow the semi circular path of radius r defined by the three slits, when the deflecting field is H For each setting of the slit, the current to the collector behind the exit slit is measured This method which was the one adopted in the previous work referred to, will be called the method of the varied field Since the energy of the electrons is proportional to the square of the velocity, and the latter proportional to the first power of the field and hence to the coil current, it is necessary to plot the results against the square of the current in the magnetic coils to obtain the distribution with respect to energy A further disadvantage with this method is that the magnitude of the velocity interval selected by the slits is proportional to the velocity, which means that the electrometer readings must be divided by a quantity proportional to the square of the coil current to give the actual number of electrons of the corresponding energy in the distribution

The second method consists in keeping the deflecting field fixed at a value slightly higher than that which would focus the fastest—truly reflected—electrons on to the exit slit, and lowering the potential of the entire system target box and electron gun, by small, measured steps In this way the bombarding voltage remains the same all the time, but the electrons emerging from the slit in the target box are accelerated in the narrow space between this and the entrance slit, so that they enter the deflexion chamber with an energy which is greater than their initial energy by an amount equivalent to the applied potential difference If the total energy of the electron on entering the deflexion box corresponds to the particular velocity which satisfies equation (1) for the value of the fixed magnetic field in question the electron is captured by the collector As the applied potential difference is increased electrons which have lost a greater amount of energy in the collision are directed to the collector for the gain of kinetic energy in the accelerating field makes up for the loss in the target Obviously the applied potential difference provides a measure of the energy loss and it is only necessary to determine the true zero of the energy scale This is done by observing the value of the applied potential for which the truly reflected electrons are directed to the collector This method which will be referred to as the method of accelerating potential, has another advantage besides that of the linear scale It is obvious that the electrometer readings give a direct measure of the number of electrons which have suffered the corresponding energy loss, since the magnetic field remains the same all the time But there is also a disadvantage with this method In the method of the varied field, the emission which is analysed derives exactly from the same spot of the target, whatever the value of the field, this is easily recognised, if the two limiting trajectories in fig 1, *b*, are extended back into the target box In the second method this is no longer the case, for whereas the path inside the deflexion chamber is the same for all electrons analysed, the trajectories in the target box are more curved the lower the initial energy of the electrons Hence an electron, if it is to be counted, must start from a point nearer to the axis of the apparatus the greater the energy loss In the first apparatus the bombardment is sufficiently uniform over the area of the target required by the differences in speed in the region investigated, for the rotating target, however, the area bombarded is so narrow that this shift often produces a considerable distortion of the distribution curves obtained by the method of accelerating potential For this reason I have used both methods alternatingly As regards the first of the two, the range of velocities of the scattered electrons which is studied in the present case is so small relatively, that the readings may be plotted directly against the coil current without recalculation and the corresponding voltage scale marked down

Experimental Procedure

As a support for the different substances investigated, strips of platinum foil, 0 003 mm thick, have been used throughout When targets of the other metals were studied, small rectangular pieces were cut from a thin foil of the metal, two parallel slits were made in the small piece and the platinum strip passed through, finally the projecting edges were turned back and the whole was pinched tight together Such a platinum strip with a coating of a less refractory metal in the middle, is easy to heat and does not burn through if overheated for a moment as does a simple strip of the metal in question The oxides were deposited on a platinum surface, roughened with a piece of emery paper, by evaporating solutions of the nitrates in the usual way

After assembly the tube received a heat treatment in an electric furnace the temperature of which was raised to 400° C A cooling mixture carbon dioxide and acetone—was then applied to the mercury trap and the filament and the foil heated for some time, then the bombardment was started with the foil still kept at incandescence In general the experiment with any particular target extended over a period of 4 days at least, during which time readings were taken several hours every day, sometimes an experiment would last more than a week In these experiments, not only were the pumps and the mercury trap maintained in operation during the whole time, but both the filament and the foil were kept glowing continuously, day and night It would therefore appear that the targets must have been rather well degassed in these experiments As a matter of fact, the McLeod—of the large type, calibrated down to 10^{-5} mm—always indicated "sticking pressure" under these conditions A few runs taken with pressures considerably higher than this, of the order 10^{-5} mm, did not reveal any change in the curves due to the increased pressure It should also be mentioned, that in no case was there any trace of a tungsten deposit to be found on the targets when removed at the end of an experiment As a matter of fact a deposit of this kind soon formed on the inside of the target box, and in such a position as to suggest that the particles of sputtered tungsten from the filament were largely specularly reflected at the hot surface of the target In some of the experiments with copper and silver the temperature in the first degassing was raised to such a point that the metal evaporated freely, forming a bright deposit on the surrounding walls, but when readings were taken it was tried to use such a heating current that the vapour pressure in front of the surface of the target could be neglected

A diagram of the electrical connexions is given in fig 3, where the essential metal parts of the apparatus are indicated schematically by heavy lines The

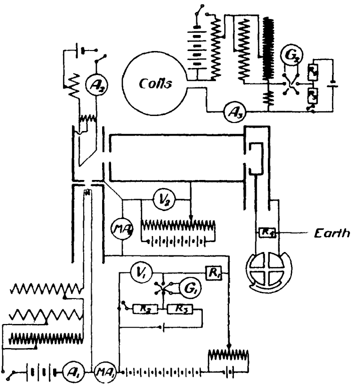

Fig 3

heating currents for the foil and the filament and the current for the production of the magnetic field are supplied by three separate batteries of large accumulators The last two of these currents can be adjusted very accurately by means of sliding resistances of different orders of magnitude The total current to the target and surrounding box (MA_2) is kept constant, with the rotating target, where the microammeter MA_2 is omitted, the total emission from the filament (MA_1) is instead maintained the same in taking a curve, but the difference is very small The bombarding voltage, supplied by a high tension battery with a potentiometer for fine adjustment, is measured by the precision voltmeter V_1 with a high series resistance R_1 Except in the first measurements with the method of the varied field, the voltage was kept very sensibly constant by balancing the potential drop across the instrument by the aid of an extra circuit, comprising an accumulator and a high resistance box R_2 R_3, G_1 is a galvanometer The accelerating potential difference used in the second method is supplied by a battery of small accumulators adjusted by a sliding resistance potentiometer and measured by the precision voltmeter V_2

The first measurements of the current to the collector were made by timing the motion of the electrometer needle as the quadrants charged up (electrometer sensitivity, 3000 mm /m for 1 volt) Later this method has only been used in the region of the true reflection, where the currents become very large For the rest of the distribution curves the quadrants are shunted with a high resistance R_4—a quartz fibre with a thin film of sputtered platinum—and the steady deflection of the needle is observed

To supply the magnetic field I have used the pair of Helmholtz coils previously employed, giving 56 52 gauss per ampere A precision ammeter is included in the circuit, but the current is measured with a higher accuracy by employing the usual method of balancing the potential drop across a small resistance in series with the coils R_5 R_6 is a potential divider of the dial pattern and G_2 a galvanometer, used to check the balance The earth's magnetic field I have compensated in all experiments by means of a large pair of Helmholtz coils, mounted in the appropriate position They have been omitted in the diagram

Results

I have confined the investigation to such scattered electrons for which the energy lost in the collision does not exceed 50 volts A typical curve is shown in fig 4 for a platinum target, this was obtained by varying the magnetic field and timing the swing of the electrometer The dots represent the measured points The sharpness of the peak due to reflected electrons and its height compared with that of the rest of the distribution curve should be noticed In all the other curves reproduced in the following, the ordinates of the part due to reflected electrons have been plotted in a scale which is roughly 1/10 of that of the rest of the curve, for the sake of convenience Of the two further maxima exhibited by the platinum curve the one corresponding to the smaller energy loss is fairly sharp Sometimes this maximum is accompanied by one for a 3 volts greater loss, which may become so large that it almost suppresses the first one

The curve in fig 5, for copper, was obtained in the same way as that for platinum There are maxima at 7 0 and 25 4 volts loss, and indications of similar features at 3 5 and, although very feeble in this curve, at about 12 and 35 volts

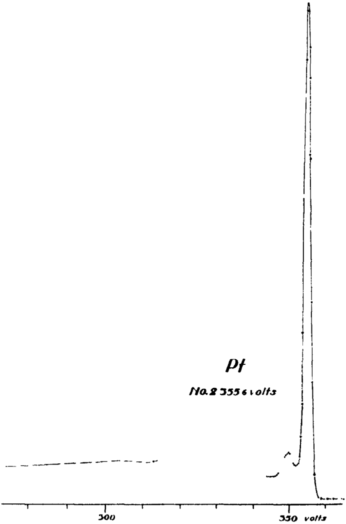

FIG 4

The curve for a silver target, shown in fig 6, was obtained by the method of accelerating potential, as indicated by the manner in which the voltage scale is marked off in this case Since this curve was taken with the rotating target apparatus, it is believed to come down a little too quickly on the side of higher energy losses, for the reasons mentioned in the discussion of the method There are three maxima in this curve, and the rise to the first one is remarkably steep

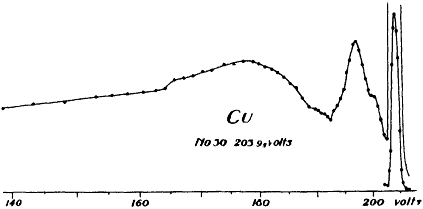

Fig 5

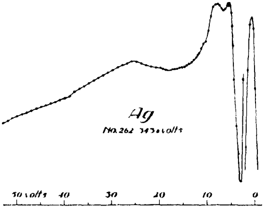

Fig 6

Two different specimens of gold have been tested (fig 7) The first contained 96 per cent of pure gold, the rest being presumably copper The second held 99 9 per cent of the pure metal On the whole there is a fair agreement between the curves for the first specimen, which like the upper curve in fig 7 were all obtained with a fixed target and accelerating potential, and the results for the pure metal, secured in the second form of apparatus and using a varied magnetic field In the former case, however, there is near the first maximum a further hump for a somewhat higher energy loss, which will be seen to be competing with the first maximum in the curve

Still more salient features are exhibited by the curves rendered by the oxides, particularly those of the metals calcium, strontium and barium With calcium oxide, for example, four different deposits have been tested and the different

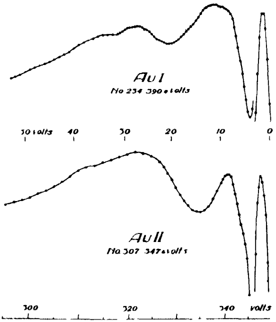

FIG. 7

methods employed using both types of apparatus. Altogether more than 30 distribution measurements have been secured with this substance, all of which show the same kind of curve. In figs. 8 and 9 distribution curves are given for the oxides of the four metals mentioned. They were all obtained with the method of accelerating potential. Each of the three oxides CaO, SrO and BaO gives rise to two conspicuous maxima, which appear to shift in the same direction from one element to the next in proceeding down the series. Besides these main maxima, there appears to be several small ones, particularly in the case of calcium oxide. The curve for magnesium oxide in fig. 9 has at least one well developed maximum at 22.7 volts. Of the others the one in the neighbourhood of 17 volts is usually brought out fairly well in the curves.

Before proceeding to give the numerical results of the different experiments to fix the position of these maxima in the curves, a few words must be said about the question how the distribution depends on the angle of scattering. This has been studied with the apparatus where the target and electron gun could be rotated, in the case of targets of copper, silver, gold and calcium oxide. It should be mentioned that the angle at which the bombarding electrons

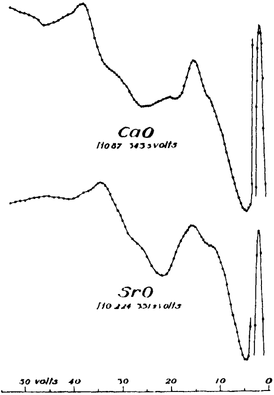

Fig 8

strike the plane surface of the target remains constant in these experiments since the latter rotates together with the gun This angle was about 30° in all the measurements A typical series of distribution curves for different angles of scattering measured from the initial direction of the primary electrons, is shown in fig 10 These seven curves were all obtained by the method of varying the magnetic field, using a copper target The bombarding voltage was the same in all seven cases, the very slight shifts of the scale which some of these curves exhibit, when compared with the others, are probably due to a small error in the adjustment of the rotating system, with the effect that the scattering studied does not take place at exactly the same points of the target for different settings This may produce a small change in the energy of the bombarding electrons, on account of the voltage drop across the strip and the filament The inclusive potential drop, measured between the leads outside the tube, was generally about 1 volt for the strip, and about 1 5 volts for the filament

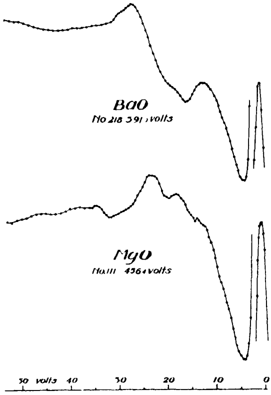

Fig 9

Fig 10 clearly shows that the position of the maxima is independent of the angle of scattering, at any rate for this range of some 70° All the other measurements support this conclusion In fact, the shape of the distribution curve is almost exactly the same for all angles It is doubtful if any meaning should be attached to the variation of the relative intensities of the maxima, which may be found in these curves, and which sometimes occurred in other experiments of the same kind Such changes would frequently take place for the metal targets also in the measurements where the scattering angle remained fixed, owing to uncontrollable changes in the conditions

In my first paper on this subject, I was able to show that, if the distribution is plotted as a function of the energy, maxima of this kind retain a fixed position with respect to the reflected peak over a considerable range of the bombarding voltage In the present experiments I have hence mostly restricted the range of the bombarding potential to such values as were favourable for a determination of the position of the characteristic humps in the curves Notwithstand

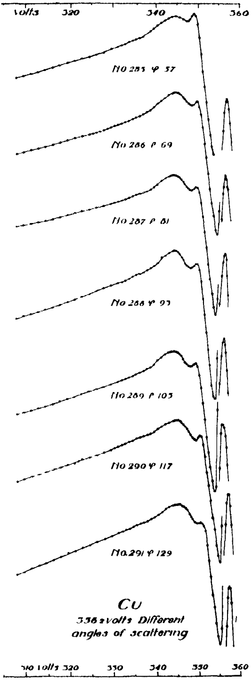
Volts 320 340 360
No 285 φ 57
No 286 φ 69
No 287 φ 81
No 288 φ 93
No 289 φ 105
No 290 φ 117
No. 291 φ 129
Cu
356.2 volts Different
angles of scattering
310 Volts 320 330 340 350 360

Fig 10

ing, the data presented in the following tables supply valuable additional proof of this statement.

Numerical Data

The following tables give the position of the different maxima, or indications of maxima, in the curves, measured in volts from the centre of the peak due to reflected electrons. The bombarding voltage and the kind of method employed are also stated. The different curves are numbered in chronological order. Where several targets of the same substance have been tested they are distinguished as I, II, etc. The symbol Pt′ refers to a silver target backed with platinum, from which the silver had been distilled off completely, before the measurements were started.

Table I. Copper

Target	No	Voltage	Method	V_1	V_2	V_3	V_4	V_5
I	33	91.6	var field	3.3	6.9		27.5	
	29	137.2		3.1	7.1		26.8	
	35	166.4		3.0	7.2		28.0	
	30	204.0		3.5	7.0		25.4	
	27	232.4		3.5	7.1		26.1	
	32	275.3		3.8	7.0		25.2	
	34	305.3		3.3	6.7		24.2	
	28	340.7		3.8	7.5		24.9	
	31	411.8			6.3		24.1	
				3.4	7.0		25.8	
II	172	303.7	acc pot		8.1			
	171	325.6			8.1			
	170	346.9			8.6			
					8.3			
III	179	280.9	acc pot		7.0	12.8	24.5	34.9
	186	375.6			6.5	12.6	24.7	33.7
	185	395.9			6.8	12.7	24.7	34.4
	183	434.4			6.8	12.6	25.1	35.1
					6.8	12.7	24.8	34.5
			acc pot					
IV	280	254.0	45		6.5	12.9		
	279		69		6.1	11.9		
	277		81		6.7	12.8		
	281		93°		6.6	13.0		
	282		105°		6.6	13.1		
	276		117		6.5	12.9		
	278		137°		6.8	13.0		
					6.5	12.8		

Table I (continued)

Target	No	Voltage	Method	V_1	V_2	V_3	V_4	V_5
			var field					
	284	254 0	57°		6 3	10 7		
	283		137°		6 4	12 7		
	285	356 2	57°		6 5	11 0		
	286		69°		6 8	11 8		
	287		81°		6 8	12 2		
	288		93°		6 6	12 0		
	289		105°		6 5	11 8		
	290		117		6 8	12 2		
	291		129°		6 9	12 0		
					6 6	11 8		
Mean of all measurements				3 4	6 9	12 3	25 5	34 5

Table II —Silver

No	Voltage	Method	V_1	V_2	V_3
		acc pot			
258	261 8	69°	4 3	7 2	
257		81°	4 3		
260		93°	4 4	7 3	
256		105	4 4		
261		117°	4 6	7 1	
259		136°	4 7	7 0	
265	343 8	69°	4 6	7 4	
264		81	4 6	7 5	
267		93°	4 8	7 6	
263		105	4 7	7 6	
268		111	5 0	8 0	25 1
266		117°	4 6	7 4	
262		136°	4 8	7 2	24 6
			4 6	7 4	24 8

Table III – Gold

Target	No	Voltage	Method	V_1	V_2	V_3	V_3	V_3	V_4
I	229	298 9	acc pot	8 1			25 6		35 1
	228	316 0		8 1		24 6		27 1	34 6
	227	336 1		8 2		24 3			
	237	348 8		8 7		24 7			34 6
	226	356 4		7 4	9 2	25 2			35 2
	236	365 1		8 9		24 9			
	225	376 1		7 1	11 0	25 0			34 6
	235	377 9		7 5	9 8		25 9		34 2
	234	390 0		7 3	10 3		25 6		34 7
	233	401 9		7 2	10 7		25 8		34 5
	232	417 5		8 4			25 6		35 4
	231	438 6		7 3	9 4	24 5		27 6	35 0
	230	458 9		8 6		25 0		27 4	
				7 3	10 1	24 8	25 7	27 3	34 8
							25 5		
			var field						
II	301	256 8	69	7 0			26 6		
	300		81°	7 2					
	299		93°	7 3			24 3		
	302	295 8	69	7 0			27 1		
	303		81	7 5			27 1		
	304		93	7 3			27 3		
	307	347 6	69	7 1			26 0		36 5
	306		81°	7 8			26 3		35 9
	305		93	8 0			26 6		36 8
	308	375 8	69°	6 9			24 6		35 4
	309		81	7 4			27 1		35 0
	310		93°	7 5			27 7		36 3
				7 3			26 4		36 0
Mean of all measurements				7 3	10 1		25 9		35 2

Table IV —Platinum

Target	No	Voltage	Method	V_1	V_2	V_3	V_4
I	3	93 0	var field	6 3			
	9	135 1		6 3			
	1	190 1		5 8		26 2	
	5	256 6		6 4		25 9	
	2	355 6		5 9		25 7	
	4	540 2		5 9		25 9	
				6 1		25 9	
II	125	203 6	acc pot	6 5			
	124	224 6			9 1		
	115	240 0		5 9	9 7		
	116	262 0		6 5	9 8		
	117	283 4		6 7	9 5	23 8	
	118	304 0		7 0	9 3	24 3	
	119	324 8		6 8	9 4	24 2	
	120	344 1		6 3	8 9	24 3	
	122	385 2		6 4	9 3	24 1	
	123	416 0			8 9	24 2	
	126	437 3		6 6			
				6 8	9 3	24 1	
III	164	260 0	acc pot	6 1	8 7	25 4	33 1
	154	270 3		6 2	10 3	24 5	33 7
	163	282 2		6 8	9 4	25 5	
	153	296 5		6 5	10 0	24 1	34 1
	162	317 1		7 0	9 4	25 5	33 9
	156	332 9		7 6	9 7	24 1	33 8
	155	359 9		6 8	9 4	23 8	
	161	370 1		7 4	9 4	25 6	33 9
	160	385 0			9 3	24 6	33 3
	159	410 8			9 6	24 8	33 4
	158	435 3		6 9	9 6	25 0	33 2
	157	458 7		7 1	9 7	25 1	34 5
				6 8	9 5	24 8	33 7
Mean of all measurements				6 5	9 4	24 8	33 7

Table V —Pt′

No	Voltage	Method	V_1	V_2	V_3	V_4
198	242 3	acc pot	6 5	11 5	23 8	33 8
197	259 0		6 9	11 5	24 1	35 2
196	273 8		6 3	11 4	24 0	35 7
193	335 9		6 7	11 5	24 1	34 9
192	356 7		6 6	11 4	25 0	35 1
201	400 0		6 7	11 9	25 7	34 2
200	422 9		6 7	12 0	25 3	35 1
199	443 9		6 6	12 3	26 1	34 2
			6 6	11 7	24 8	34 8

Table VI Magnesium Oxide

No	Voltage	Method	V_1	V_2	V_3	V_4	V_5
107	202 2	acc pot	6 8		17 6	22 8	
106	222 7		7 8		17 3	22 7	34 6
105	243 6		6 9		17 9	22 8	33 8
98	261 0			11 5	17 8	22 7	34 2
104	280 6		7 0	11 5	16 7	23 0	33 4
100	300 6		6 6		17 9	22 4	33 3
109	319 3		6 9		17 4	22 6	
101	339 9		6 5	12 2		22 7	33 6
102	368 5		6 3	11 9	17 1	22 8	33 8
110	388 5			11 7	17 8	23 0	
103	415 0				17 7	22 8	
111	456 4		7 1	11 6	17 3	22 7	33 9
			6 9	11 7	17 5	22 7	33 8

Table VII —Calcium Oxide

Target	No	Voltage	Method.	V_1	V_2	V_3	V_4	V_5
I	42	105.0	var field		13.0			36.1
	47	138.9			15.1			38.4
	43	170.3			13.8			
	40	200.8			13.0			35.9
	46	232.2			13.5			
	44	267.2			13.4			35.1
	41	322.9			13.0			36.1
	48	362.0			13.6			35.0
	45	413.9			12.5			34.7
					13.4			35.9
II	80	143.0	acc pot	9.1	13.8		29.0	37.1
	81	170.4		9.7	14.0		29.0	36.3
	82	204.0		9.5	13.8	20.6		36.5
	83	227.0		9.8	13.9	19.3	28.9	36.4
	79	245.9		9.2	14.1		29.2	36.3
	86	316.2		9.6	13.9	19.7	29.2	36.8
	87	343.3		9.6	13.7	19.8	29.5	36.7
	88	370.4		9.4	13.9	20.9	28.5	36.5
	89	392.6		9.0	14.0	20.8	29.1	36.5
	91	460.6		9.2	13.8	19.8	29.4	36.8
	90	472.1		9.1	13.9	19.2	29.0	36.8
	92	481.5		9.3	13.9	19.5	29.2	37.1
	93	504.2		9.3	13.8	19.8	29.3	36.9
				9.4	13.8	19.9	29.1	36.0
III	214	314.1	acc pot	9.9	14.2		29.9	37.5
	213	335.0		9.6	14.2		29.9	37.4
	212	354.7		9.9	14.2		30.4	37.5
				9.8	14.2		30.1	37.5
IV	246	244.1	acc pot 81°	9.7	13.9		29.7	36.3
	245		99°	9.1	14.3		29.6	37.0
	244		137°	9.8	14.1	20.6	29.8	37.3
	247	467.3	74°		13.8		30.0	36.5
	248		99°		14.3		29.3	37.8
	249		137°		14.4	20.5	29.9	37.9
				9.5	14.1	20.5	29.7	37.1
Mean of all measurements				9.4	13.8	20.0	29.4	36.7

Table VIII —Strontium Oxide

Target	No	Voltage	Method	V_1	V_2	V_3	V_4	V_5
I	65	268 0	acc pot	6 4	9 7	13 9	25 6	31 6
	66	306 0			9 7	13 3		32 1
	67	336 0		7 4	10 1	13 7		31 7
	68	360 0		7 5	9 9	13 1	24 6	31 4
	69	380 4		7 3	9 6	13 1	24 7	31 6
	70	404 4		7 6	9 8	12 8	25 3	31 4
	71	439 9		7 8	9 9	13 1		31 7
				7 3	9 8	13 3	25 1	31 6
II	74	153 9	acc pot		9 7	13 4	24 1	
	72	467 2		7 2	8 9	12 8	25 3	30 7
	73	490 3			9 1	12 4	25 7	30 5
				7 2	9 2	12 9	25 0	30 6
III	76	239 0	acc pot	6 8	9 7	13 4	24 5	31 7
	75	273 9			9 3	13 5		31 5
	78	286 0		7 3	9 5	12 7	25 3	31 4
	77	313 8		7 5	9 9	13 0		31 3
				7 2	9 6	13 2	24 9	31 5
IV	224	331 2	acc pot		9 3	13 6	24 0	32 5
		352 2			9 5	13 8	24 8	32 5
					9 4	13 7	24 4	34 5
Mean of all measurements				7 3	9 6	13 2	24 9	31 6

Table IX —Barium Oxide

Target	No	Voltage	Method	V_1	V_2	V_3	V_4
I	61	94 0	acc pot		17 0	25 2	
	62	125 9		10 1	18 1	24 8	
	54	216 3		10 3			
	55	262 8		10 4	16 6	25 0	
	51	269 2		10 5	16 2	24 2	32 7
	56	282 8		10 1	16 2	24 6	32 4
	57	308 1		10 6	16 8	25 8	32 7
	58	347 3		10 6	17 1	25 5	33 2
	59	376 1		10 5	16 5	25 5	32 8
	60	414 8		10 6	16 4	25 5	
				10 4	16 7	25 1	32 7
II	219	328 0		11 4		26 5	
	218	391 9		11 5	17 3	26 1	
				11 4	17 3	26 3	
Mean of all measurements				10 6	16 8	25 3	32 7

It may seem strange to take a simple mean of all the values in the vicinity of 25 volts for gold. Several of the curves for the first target give fairly definite evidence of two maxima in this region. The corresponding maxima for the second target, however, have not been separated, although there is a considerable spreading of the individual values, and a separation of these values into two groups, with respect to their magnitude, would be very arbitrary. This is the reason why I have treated this part of the curves as a single maximum.

In many of the cases where several targets of the same substance have been tested it will be found that the mean values for the different targets do not show such a close agreement among themselves as would be expected from the magnitude of the individual deviations within each group. Hence there would seem to be a systematic difference in these cases. It is fairly certain that the position of these maxima is influenced to a certain extent by conditions not controlled in the experiments, the nature of which remains unknown. In some cases, the temperature of the heated target may be of some importance, although several experiments in which this factor was varied failed to reveal any influence of this kind. The changes in relative intensity and the disappearance of some of the maxima should probably be connected with the same change in conditions, which is responsible for the shift in position. Under these circumstances one might be inclined to regard the mean of the average positions of the maximum for each separate target as the best value to represent this position. I have chosen, however, to use the simple mean of all determinations. The difference is usually not very large; where the number of measurements is the same for the different groups, the two methods obviously lead to the same result. The mean positions of the maxima thus calculated, together with the error in these mean values obtained in the usual way are summarized in Table X.

Table X

Copper	3.4±0.11	6.9±0.10	12.3±0.15	25.5±0.31	34.5±0.31
Silver	4.6±0.06	7.4±0.08	24.8±0.26	—	—
Gold	7.3±0.07	10.1±0.29	25.9±0.21	35.2±0.19	—
Platinum	6.5±0.09	9.4±0.08	24.8±0.16	33.7±0.14	—
Pt′	6.6±0.06	11.7±0.12	24.8±0.30	34.8±0.23	—
Magnesium oxide	6.9±0.10	11.7±0.11	17.5±0.11	22.7±0.05	33.8±0.13
Calcium oxide	9.4±0.07	13.8±0.07	20.0±0.17	29.4±0.10	36.7±0.13
Strontium oxide	7.3±0.13	9.6±0.08	13.2±0.11	24.9±0.17	31.6±0.12
Barium oxide	10.6±0.14	16.8±0.19	25.3±0.20	32.7±0.14	—

The data of this table are shown graphically in fig. 11, where each value is represented by a pointed, vertical wedge. The height of the wedge should give a rough idea of the relative importance of the corresponding maximum for each particular substance, i.e., the weight given to the corresponding value. This was determined by the product of the number of curves showing this maximum, and a second weight factor from 0.5 to 1.0, to take account of the shape of the maximum in the curves (whether there was a real maximum or merely an outstanding change of slope). In order that this figure should give at least a rough idea of the relative accuracy in the different values, the "Halbwertsbreite" of the wedges was made equal to the calculated mean errors from Table X. The shape of the wedges has, of course, very little to do with the shape of the actual maxima in the curves. For the sake of brevity I shall use the term "(energy) loss spectrum" for a representation like those in fig. 11.

Discussion

The smallest values recorded are those for the first maximum in the case of copper and silver. There follows, for all the metals tested, a prominent

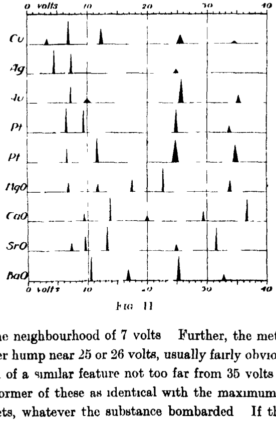

FIG. 11

maximum in the neighbourhood of 7 volts. Further, the metals will be seen to give a broader hump near 25 or 26 volts, usually fairly obvious, and a rather faint indication of a similar feature not too far from 35 volts. I am inclined to regard the former of these as identical with the maximum always present with cold targets, whatever the substance bombarded. If this maximum is attributed to some common foreign substance, the possibility of a hump in this part of the loss spectrum characteristic of the metal itself should not be excluded The behaviour of the curves for gold may have some significance in this connection, but the question requires further experiments The loss spectrum for Pt′ bears a close resemblance to that for platinum, and there is no reason why this target should have differed essentially from the ordinary platinum ones The prominent platinum maximum at 9 4 volts, however appears replaced by an equally sharp one at 11 7 volts This is certainly not an accidental shift The possibility* cannot be entirely excluded, that this last maximum is due to copper, although it does not seem very likely that the adjustment was so bad that the scattering from the copper leads to the foil was included in the measured emission to a considerable extent Also, these leads should have been at a comparatively low temperature in the experiments

As regards the loss spectra for the four different oxides tested, the possibility of the appearance of features pertaining to the backing substance must not be overlooked since the deposits were sometimes thin and did not cover the entire surface of the strips Both the position and the general shape of the first maximum in the case of magnesium oxide and calcium oxide are in agreement with the view that these maxima belong to the platinum support The same is probably true for the first and second maximum in the loss spectrum for strontium oxide although the value for the former one is rather high The second maximum for magnesium oxide coincides exactly with the strongest one in the loss spectrum for Pt′ The peaks near 25 volts for strontium oxide and barium oxide are probably not related to the one common to the metal targets, although they fall in the same region

It is difficult to trace any relations between the different loss spectra as shown in fig 11 Although the series of substances studied—elements from the first and second column of the periodic table—was chosen partly with the view of looking for such regularities, there is, of course, no binding reason why a relationship should be expected As regards the metals, however, the gap between 13 and 25 volts should be observed With the oxides there would seem to be some evidence of sequences in the loss spectra Thus the values CaO 13 8 SrO 13 2, BaO 10 6, and CaO 36 7, SrO 31 6, BaO 25 3, for the two strongest maxima in each case, show a similar trend , to the first series the fairly prominent maximum at 17 5 for magnesium oxide could perhaps be added at the top The less important peaks CaO 29 4, SrO 24 9, BaO 16 8 (to which MgO 33 8 may indicate a prolongation at the upper end) form a sequence with a similar trend I have no theoretical explanation to offer for this behaviour of the maxima in the curves, and it is, of course, possible that it is only a matter of chance, to which no significance should be attached I think, however, that this particular feature is sufficiently striking in fig 11, and perhaps still more in the curves, to justify mentioning at the present state of things

---

* Prof. O W Richardson has very kindly suggested this possibility to me

Interpretation

It does not seem possible to give a detailed quantitative interpretation of the experimental results at present As to the nature of the phenomenon, the following conclusions may be drawn The effect is not one of diffraction of electron waves of the usual character, which is related to the crystal structure of the target This is shown by its independence of bombarding voltage, orientation of the target and scattering angle It is also difficult to imagine that the often complicated structure of the experimental distribution curves could simply represent the variation of the probability for one single kind of ionisation The several maxima in the distribution curve for the secondary electrons proper, which would be expected on this view have not been observed also, a probability curve of this kind could hardly show such a remarkable independence of voltage and scattering angle In fact, I believe that the constant position of the maxima measured in terms of energy from the reflected peak constitutes definite proof that their appearance is accompanied by definite energy changes taking place in the bombarded atoms at the surface of the targets The values obtained should thus represent a kind of critical potentials for the substances in question Such potentials, secured by a modification of the well-known method of Franck and Hertz, have recently been published by H B Wahlin* for the vapours of copper and silver His curves show a great number of small breaks for potentials in the region from 1 to 11 volts, some of which are not too far from the few values for targets of these metals listed in Table X but these breaks are in no way outstanding ones and it is very doubtful if any correlation exists From spectroscopic data, the values for the resonance potential, $1S - 2P_{1\;2}$, and the first ionisation potential, 1S, should be for copper, 3 80 3 77 and 7 69, for silver 3 76, 3 65 and 7 54, for gold, 5 08, 4 61 and 9 25, all in volts † On the whole it would seem that the two first maxima obtained reproduce, to some extent, the general trend of these values—the resonance doublet could scarcely be expected to be resolved - although there are very large individual deviations (for instance gold) The spectroscopically determined values, however, correspond to the free atoms in the gaseous state, and though there may have been some metal vapour present of a very low pressure at the temperatures of the bombarded targets, the greater part of the scattering must have taken place in the solid substance, where the conditions probably were rather different from those governing the reactions of free atoms Brown and Whiddington,* using oxide coated targets, obtained lines which they ascribed to oxygen The strong maxima at 13 8 volts for calcium oxide and 13 2 volts for strontium oxide are fairly close to the ionisation potential 13 56 volts for atomic oxygen, but the corresponding maximum in the case of barium oxide is too far removed to make this interpretation appear likely to be correct

---

* 'Phys Rev' vol 31, p 155 (1928) vol 32 p 277 (1928)

† Franck and Jordan, 'Anregung von Quantensprüngen durch Stösse," p 127, Berlin (1926)

Maxima in the distribution curves, which result from the excitation of free atoms, should be expected to be very sharp The greater width of the maxima found, as compared with the width of the peak due to reflected electrons, could be accounted for by the fact that the regions for which energy changes take place in solids are often quite broad Small changes in energy, suffered by the scattered electron along its short path in the target, would produce the same result In the case of ionizing collisions the energy lost should vary from a lower limit upwards, depending on the amount of kinetic energy with which the liberated electron escapes, hence the maximum may appear shifted to a higher voltage value than the actual ionizing potential An accurate knowledge of the energy distribution for the slow-moving secondary electrons formed, and particularly of the position of its maximum, would make it possible to correct for this shift With this object, I have spent much time trying to measure the low velocity end of the distribution curves for different targets The influence of the magnetic field due to the heating current, which prevented measurements in this region in the earlier work, was satisfactorily removed by the construction of the new target holder, but owing to the effect of space charge, necessarily present for bombarding currents of this magnitude, the behaviour of the tube was sometimes erratic When conditions were steady, curves very similar to those for cold targets were obtained The position of the maximum in these curves--plotted against energy after recalculation--often exhibited changes for the same substance much greater than those in the curves for the scattered electrons Apart from the deformation of the curve probably produced by the space charge, the distribution of the electrons escaping from the surface could scarcely be expected to be identical with the initial one for the secondary electrons at the moment they leave the parent atom, since subsequent collisions on their way out is likely to change this In view of this uncertainty, no attempt has been made to apply a correction of the kind mentioned to the data in Table X

---

* 'Leeds Phil Lit Soc Proc,' vol 1, p 162 (1927)

Recently E Rupp* has published some interesting results on the absorption and reflection suffered by comparatively slow-moving electrons in thin films of a number of different elements Characteristic maxima were found in the curves, which were very similar for the two kinds of phenomena under investigation They are regarded as indications of characteristic absorption frequencies for the electron waves analogous to the characteristic frequencies in the corresponding case of optical dispersion The general shape of these maxima is often similar to that for the peaks found in the present research but for the few elements which have been tested in both respects, the positions of the maxima are different In spite of this it would seem likely that there is a relation between the two effects

It would be a matter of great interest if a characteristic spectrum of radiation, related to the energy losses found, could be obtained by subjecting solid targets to electron bombardment Such a spectrum should occur in the region from the visible down to the far ultra-violet In the case of metals, a survey of existing experimental data by different investigators has recently led me to conclude, that there is no appreciable amount of such radiation emitted for bombarding voltages of the magnitude here considered, and that the return of the atoms to the normal state must therefore involve some kind of a radiationless process † For the oxides things may possibly be different Whilst thus the prospects do not look entirely hopeful for a fresh attempt to find characteristic radiations to correlate with the maxima here found, it is possible that previous shortcomings could be due to a failure to hit some essential condition, such as, perhaps, heating the target, in the experiments hitherto performed It appears to me a matter of some importance to re-investigate this point and I am hoping to be able to try some experiments of this kind presently

Summary

An apparatus is described by means of which the velocity distribution of an initially homogeneous beam of electrons can be obtained after scattering from the surface of targets of different substances, kept at incandescence

---

* 'Z Physik,' vol 58 p 145 (1929)

† *Loc cit*

The distribution with respect to energy among the scattered electrons has a sharp peak, corresponding to truly reflected electrons, and several small maxima for slightly lower values of the energy, which form the principal object of the present investigation These maxima are characteristic of the substance forming the target, and their position with respect to the reflected peak remains constant for the wide range of bombarding voltages tested Using a modified form of the same apparatus in which the target and electron gun can be rotated, it has been proved that these maxima are also independent of the angle of scattering

Tables are given containing the positions of such maxima measured for different targets

In discussing these results it is pointed out that the maxima show the characteristics which they should possess, if they result from inelastic collisions with the target atoms involving definite energy changes, such as excitation and ionization of the latter ones No definite conclusion concerning their classification has, however, so far been arrived at, from a comparison of the values obtained with existing spectroscopic data for the gaseous state In this connexion the demand for investigations on the radiation from heated solids, bombarded by electrons, is emphasized

The Effect of a Nucleus Spin on the Optical Spectra —II

By J Hargreaves, B A, Clare College, Cambridge

(Communicated by R H Fowler, F R S —Received December 21, 1929)

Introduction

In a recent paper* the author has considered the effect of a nuclear spin of half a quantum on the optical spectra of an atom with a central field The investigation had special reference to cæsium, the hyperfine structure of which has been examined by Jackson,† but the results obtained were not in very good agreement with the experimental observations In the former paper it was stated that the method could be extended to the case of an atom with a nuclear spin of i_n quanta (where $2i_n$ is an integer), but that the investigation of such a case would be difficult when $i_n > \frac{1}{2}$, owing to the large number of wave-functions required by the method used to describe any state of the atom It has been found, however, that the work is not so arduous as was anticipated, and in the present paper a general method of solving the problem is developed, and applied to the cases $i_n = 1, 1\frac{1}{2}, 4\frac{1}{2}$ The first two cases are, as yet, of little practical interest, but are sufficiently simple to make a general solution possible On the other hand, the case of $i_n = 4\frac{1}{2}$ has practical application to bismuth, the hyperfine structure of which has been investigated in two papers by Back and Goudsmidt ‡ In the second of these, which deals with the Zeeman effect, it is shown conclusively that the hyperfine structure is due to a spin of $4\frac{1}{2}$ quanta It has been found too difficult in the present work to obtain a general solution of the multiplet levels of bismuth, but it has been possible to calculate the intensities of the components of the lines $p_{\frac{3}{2}} \to s_{\frac{1}{2}}$, and $p_{\frac{1}{2}} \to s_{\frac{1}{2}}$, the former of which has been examined by Back and Goudsmidt, and the results obtained are in fair agreement with theirs There is, of course, the usual lacuna regarding the S levels, and we have to make special assumptions to obtain these In addition the P → S transitions for $i_n = 1$ and $i_n = 1\frac{1}{2}$ are calculated In all cases we treat the problem as that of one electron in a central field

Since the present work was completed a paper has appeared by Hill § in which he gives a general formula for the nuclear spin multiplet intensities He obtains a result which agrees with our former result for $i_n = \frac{1}{2}$, and his formula gives the same intensities as the calculations described here for bismuth His treatment of the problem is purely kinematical, without reference to multiple wave-functions or energy levels He points out that the assumption we made in I that the interaction energy of the nuclear and electron magnets is negligible is none too justifiable As far as the present writer can see his objection is valid The problem is, however, so far as the intensities are concerned, a kinematical one, and independent of the Hamiltonian The method we use provides a convenient way of finding the multiple wave functions The problem is actually the one of finding a set of $4i_n + 2$ unperturbed wave-functions which give the same total intensities as the unresolved wave-functions The present treatment gives in addition the increment energies due to the interaction of the nuclear spin and orbital momentum We can find the increments due to the interaction of the two spins, by averaging the corresponding part of the Hamiltonian over the unperturbed system of wave functions This is really a separate problem, and involves some lengthy calculations, and will therefore be dealt with elsewhere

---

* 'Roy Soc Proc,' A, vol 124, p 568 (1928) Referred to later as I

† Roy Soc Proc, A, vol 121, p 432 (1928)

‡ 'Z Physik,' vol 43, p 321 (1927), and vol 47, p 174 (1928)

§ 'Proc Nat Acad Sci,' October, 1929

It is thought that the present treatment of the problem will not be without interest, in so far as it enables one to deal with the dynamical as distinct from the kinematical properties of the problem, and in particular enables one to calculate the energy levels

As in I a quantum number f is assigned to each level This is representative of the total angular momentum of the atom (including nuclear spin), and this mechanical interpretation is easily verified for any particular case by the method described in I It is also easily verified that f cannot change by more than unity, as is evident from other considerations

§ 1 *Calculation of the Spin Matrices*—We use the same notation as in I, σ_x σ_y, σ being the spin variables of the series electron and ρ_x, ρ_y, ρ_z those of the nucleus The Hamiltonian is the same as that in I (equation (13)) Our first problem is to calculate matrices which we may take to represent the σ's and ρ's at any instant of time, that is matrices which satisfy the necessary "vertauschungs" and commutative relations, and have the correct characteristic values We must also impose the condition that they should be Hermitian The matrices for σ_x, σ_y, σ_z will be similar to those used in I, except that we shall have to extend them to contain the same number of rows and columns as the ρ's The angular momentum of the nucleus about any axis will have quantised values differing by h, and having $\pm i_n h$ as maximum and minimum respectively, and therefore each of the ρ's will have as characteristic values the numbers*

$$\pm 2i_n, \quad \pm(2i_n - 2), \quad \pm(2i_n - 4), \quad \ldots, \quad \pm 1 \text{ or } 0$$

We shall consider first the case $i_n = 1$ and from this and the results for $i_n = \frac{1}{2}$ we shall be able to construct the matrices for any value of i_n by induction.

In order to do this we consider the single quantum of spin denoted by $i_n = 1$ to be made up of two equal spins of half a quantum each and represented by variables ρ_x', ρ_y', ρ_z' and ρ_x'', ρ_y'', ρ_z''. We have in addition σ_x, σ_y, σ_z for the electron spin. The three spins interact to give us 8 $(= 2^3)$ different wave-functions $\psi(x, y, z, \sigma_z, \rho_z', \rho_z'')$ denoted by ψ_r $(r = 1, 2, \ldots, 8)$, where

$$\left.\begin{array}{ll}
\psi_1 = \psi(x, y, z, 1, 1, 1) & \psi_2 = \psi(x, y, z, -1, 1, 1) \\
\psi_3 = \psi(x, y, z, 1, -1, 1) & \psi_4 = \psi(x, y, z, -1, -1, 1) \\
\psi_5 = \psi(x, y, z, 1, 1, -1), & \psi_6 = \psi(x, y, z, -1, 1, -1) \\
\psi_7 = \psi(x, y, z, 1, -1, -1), & \psi_8 = \psi(x, y, z, -1, -1, -1)
\end{array}\right\} \qquad (1)$$

For the case of electron spin alone the matrices for σ_x, σ_y, σ_z may be taken to be

$$\sigma_x = \begin{pmatrix} 0, & 1 \\ 1, & 0 \end{pmatrix} \qquad \sigma_y = \begin{pmatrix} 0, & -i \\ i, & 0 \end{pmatrix} \qquad \sigma_z = \begin{pmatrix} 1, & 0 \\ 0, & -1 \end{pmatrix}$$

from which we obtain the result of the operation of any of the σ's on ψ. We can apply this to the present case, associating for this purpose ψ_1 with ψ_2, ψ_3 with ψ_4, etc. (i.e., we associate wave functions in pairs for which $\sigma_z = \pm 1$ and in which ρ_z' has the same value and also ρ_z''). In the same way we can use the above matrices to calculate the operation of any of the ρ''s or ρ'''s on ψ. For the purpose of operating with a ρ' we associate ψ_1 with ψ_3, ψ_2 with ψ_4, etc., and for a ρ'', ψ_1 with ψ_5, ψ_2 with ψ_6, etc. We thus find the result of any operation of the form

$$(\sigma\psi)_r, \quad (\rho'\psi)_r, \quad (\rho''\psi)_r \qquad r = 1, 2, \ldots, 8$$

Actually in our problem we are concerned only with operators of the forms σ, $\rho' + \rho''$, and in this case it is easily seen that all the ψ's are not independent. In fact we can combine either of the two characteristic values of σ_z (± 1) with any of the three characteristic values of $\rho_z' + \rho_z''$ (i.e., ± 2, 0) giving six wave-functions. It is clear from (1) that when $\rho_z' + \rho_z''$ is taken for an independent variable in ψ in place of the two variables ρ_z', ρ_z'', then $\psi_3 = \psi_5$

---

* The angular momentum is $\frac{1}{2}h\rho$

and $\psi_4 = \psi_6$, and this is verified by the calculations just described Now the functions ψ_r $(r = 1, 2, \quad 8)$ must satisfy the normalising relation

$$\int \sum_{r=1}^{8} |\psi_r|^2 \, dt = 1,$$

i e ,

$$\int \{ |\psi_1|^2 + |\psi_2|^2 + 2|\psi_3|^2 + 2|\psi_4|^2 + |\psi_7|^2 + |\psi_8|^2 \} \, d\tau = 1$$

If, therefore, we rename the wave functions thus

$$\psi_1 = u_1, \quad \psi_2 = u_2, \quad 2^{\frac{1}{2}}\psi_3 = u_3, \quad 2^{\frac{1}{2}}\psi_4 = u_4, \quad \psi_7 = u_5, \quad \psi_8 = u_6,$$

the functions u satisfy the usual normalising relation

$$\int \sum_{r=1}^{6} |u_r|^2 \, d\tau = 1$$

If now we find as a result of the above calculations that

$$[(\rho' + \rho'')\,\psi]_s = a_{s\,1}\,\psi_1 + a_{s\,2}\,\psi_2 + a_{s\,3}\,\psi_3 + a_{s\,4}\,\psi_4 + a_{s\,7}\,\psi_7 + a_{s\,8}\,\psi_8,$$
$$s = 1, 2, 3, 4, 7, 8,$$

we are able to write down the matrix representation of $\rho' + \rho''$ regarded as an operator on the ψ s, the sth row being formed by the coefficients in the above expression We require, however, to know its representation regarded as an operator in the u s, and therefore have to transform the above equation to one containing u s It is found that this is merely equivalent to the process of making the corresponding matrices Hermitian It is easier to generalise our matrices from the non-Hermitian type so we shall write these down first They are found to be

$$\sigma_x = \begin{Bmatrix} 0 & 1 & 0 & 0 & 0 & 0 \\ 1 & 0 & 0 & 0 & 0 & 0 \\ 0 & 0 & 0 & 1 & 0 & 0 \\ 0 & 0 & 1 & 0 & 0 & 0 \\ 0 & 0 & 0 & 0 & 0 & 1 \\ 0 & 0 & 0 & 0 & 1 & 0 \end{Bmatrix} \qquad \sigma_y = \begin{Bmatrix} 0 & -i & 0 & 0 & 0 & 0 \\ i & 0 & 0 & 0 & 0 & 0 \\ 0 & 0 & 0 & -i & 0 & 0 \\ 0 & 0 & i & 0 & 0 & 0 \\ 0 & 0 & 0 & 0 & 0 & -i \\ 0 & 0 & 0 & 0 & i & 0 \end{Bmatrix}$$

$$\sigma_z = \begin{Bmatrix} 1 & 0 & 0 & 0 & 0 & 0 \\ 0 & -1 & 0 & 0 & 0 & 0 \\ 0 & 0 & 1 & 0 & 0 & 0 \\ 0 & 0 & 0 & -1 & 0 & 0 \\ 0 & 0 & 0 & 0 & 1 & 0 \\ 0 & 0 & 0 & 0 & 0 & -1 \end{Bmatrix},$$

$$\rho_x = \begin{Bmatrix} 0 & 0 & 2 & 0 & 0 & 0 \\ 0 & 0 & 0 & 2 & 0 & 0 \\ 1 & 0 & 0 & 0 & 1 & 0 \\ 0 & 1 & 0 & 0 & 0 & 1 \\ 0 & 0 & 2 & 0 & 0 & 0 \\ 0 & 0 & 0 & 2 & 0 & 0 \end{Bmatrix} \qquad \rho_y = \begin{Bmatrix} 0 & 0 & -2i & 0 & 0 & 0 \\ 0 & 0 & 0 & -2i & 0 & 0 \\ i & 0 & 0 & 0 & -i & 0 \\ 0 & i & 0 & 0 & 0 & -i \\ 0 & 0 & 2i & 0 & 0 & 0 \\ 0 & 0 & 0 & 2i & 0 & 0 \end{Bmatrix}$$

$$\rho = \begin{Bmatrix} 2 & 0 & 0 & 0 & 0 & 0 \\ 0 & 2 & 0 & 0 & 0 & 0 \\ 0 & 0 & 0 & 0 & 0 & 0 \\ 0 & 0 & 0 & 0 & 0 & 0 \\ 0 & 0 & 0 & 0 & 2 & 0 \\ 0 & 0 & 0 & 0 & 0 & 2 \end{Bmatrix}$$

The ρ's are made Hermitian by the trivial canonical transformation which consists of multiplying the third and fourth rows and dividing the third and fourth columns by $2^{\frac{1}{2}}$ Such a transformation leaves diagonal matrices unchanged The result is that all the coefficients in ρ_x and ρ_y are $2^{\frac{1}{2}}$ This is the result we obtain by the equivalent process of formation

Now by comparing the above matrices with those representative of the case $i_n = \frac{1}{2}$ (as given in I) we are able easily to deduce those for the general value of i_n (we shall then have to make them Hermitian) The σ's are sufficiently obvious In ρ_x there are two diagonal sets of terms commencing with the third place in the first row and the third place in the first column In the first diagonal the elements are $2i_n$, $2i_n$, $2i_n - 1$, $2i_n - 1$, 1, 1, and in the second diagonal the elements are the same but in the reverse order In ρ_y these two sets of terms are multiplied by $-i$ and $+i$ respectively ρ_z consists of the leading diagonal filled with the terms $2i_n$, $2i_n$ $(2i_n - 2)$, $(2i_n - 2)$, $-(2i_n - 2)$, $-2i_n$, $-2i_n$ These are made Hermitian by multiplying the rows in succession by

$$1,\ 1,\ (2i_n - 1)^{\frac{1}{2}},\ (2i_n - 1)^{\frac{1}{2}},\ [(2i_n - 1)2]^{\frac{1}{2}},\ [(2i_n - 1)\,2]^{\frac{1}{2}}$$

and dividing the columns by the same quantities The resulting matrices for ρ_x, ρ_y have then the same formation as before with coefficients

$$(2i_n)^{\frac{1}{2}},\ (2i_n)^{\frac{1}{2}},\ [(2i_n - 1)\ \ 2]^{\frac{1}{2}},\ [(2i_n - 1)\ \ 2]^{\frac{1}{2}}\quad ,\ [2\ \ (2i_n - 1)]^{\frac{1}{2}},\ (2i_n)^{\frac{1}{2}},\ (2i_n)^{\frac{1}{2}}$$

ρ_z is, of course, unchanged

In the general problem then there are $4i_n + 2$ wave functions, and therefore (with certain exceptions, which we shall find) each level splits up into $4i_n + 2$ separate levels as indicated in I

If $f(\sigma_x, \quad , \rho_z)$ is any rational algebraic function of the operators $\sigma_x, \quad , \rho_z$ and it is found (from the matrices for the σ's and ρ's) that

$$f(\sigma_x, \quad , \rho_z) = [a_{r\,s}]$$

then

$$(f\psi)_r = a_{r\,1}\psi_1 + a_{r\,2}\psi_2 + \qquad + a_{r\,q}\psi_q, \tag{2}$$

where

$$q = 4i_n + 2$$

§ 2 *The Wave Equations* —The general wave equations may be written in the form (see I),

$$\Delta W\psi = \left\{\frac{Z\mu_0 e}{2mcr^3}(\boldsymbol{\sigma}\mathbf{M}) + \frac{\mu e}{mcr^3}(\boldsymbol{\rho}\mathbf{M})\right\}\psi \tag{3}$$

M is the orbital angular momentum vector ($\mathbf{M}_x$, $\mathbf{M}_y$, $\mathbf{M}_z$) where

$$\mathbf{M}_x = yp_z - zp_y = -ih\left(y\frac{\partial}{\partial z} - z\frac{\partial}{\partial y}\right) = -ih\kappa_x, \text{ etc}$$

We consider the $(2s-1)$th and $(2s)$th components of this equation The first term on the right hand side of (2) gives terms in the component equations which are exactly the same as the corresponding terms in the equations for ψ_α, ψ_β in I with $2s - 1$ and $2s$ written for α, β respectively

We obtain the second set of terms from the results of § 1 The $(2s-1)$th component is obtained from the $(2s-1)$th rows of ρ_x, ρ_y ρ_z and the $(2s)$th component from the $(2s)$th rows It is seen from § 1 that the $(2s-1)$th rows are made up as follows —

(i) ρ_x has a term $\{(s-1)(2i_n - s + 2)\}^{\frac{1}{2}}$ in the $(2s-3)$th column (when $2s - 3 \geqslant 1$) and $\{(2i_n - s + 1)s\}^{\frac{1}{2}}$ in the $(2s+1)$th column

(ii) ρ_y has terms $i\{(s-1)(2i_n - s + 2)\}^{\frac{1}{2}}$ and $-i\{(2i_n - s + 1)s\}^{\frac{1}{2}}$ in the $(2s-3)$th and $(2s+1)$th columns

(iii) ρ_z has a term $(2i_n - 2s + 2)$ in the $(2s-1)$th column

The $(2s)$th rows are made up as follows —

(i)′ p_x has terms $\{(s-1)(2i_n - s + 2)\}^{\frac{1}{2}}$ and $\{(2i_n - s + 1)s\}^{\frac{1}{2}}$ in the $(2s-2)$th and $(2s+2)$th columns respectively

(ii)′ ρ_y has terms $i\{(s-1)(2i_n - s + 2)\}^{\frac{1}{2}}$ and $-i\{(2i_n - s + 1)s\}^{\frac{1}{2}}$ in the $(2s-2)$th and $(2s+2)$th columns respectively (iii)′ ρ has a term $(2i_n - 2s + 2)$ in the $(2s)$th column

Applying these results to (3), using (2), we can write down the $(2s-1)$th and $(2s)$th components of the wave equation Thus, for example, using (i)

$$(\rho_x\psi)_{2s-1} = \{(s-1)(2i_n - s + 2)\}^{\frac{1}{2}}\,\psi_{2s-3} + \{(2i_n - s + 1)\,s\}^{\frac{1}{2}}\,\psi_{2s+1}$$

The $(2s-1)$th and $(2s)$th equations ($s = 1, 2, \quad , 2i_n + 1$) are

$$\begin{aligned}\Delta W\psi_{2s-1} = &-\frac{iZ\mu_0 eh}{2mcr^3}\left[(\kappa_x - i\kappa_y)\,\psi_{2s} + \kappa_z\psi_{2s-1}\right]\\ &-\frac{i\mu eh}{mcr^3}\left[\{(2i_n - s + 1)\,s\}^{\frac{1}{2}}(\kappa_x - i\kappa_y)\,\psi_{2s+1}\right.\\ &+\{(s-1)(2i_n - s + 2)\}^{\frac{1}{2}}(\kappa_x + i\kappa_y)\,\psi_{2s-3}\\ &\left.+(2i_n - 2s + 2)\,\kappa_z\psi_{2s-1}\right],\end{aligned}\tag{4 1}$$

$$\begin{aligned}\Delta W\psi_{2s} = &-\frac{iZ\mu_0 eh}{2mcr^3}\left[(\kappa_x + i\kappa_y)\,\psi_{2s-1} - \kappa_z\psi_{2s}\right]\\ &-\frac{i\mu eh}{mcr^3}\left[\{(2i_n - s + 1)\,s\}^{\frac{1}{2}}(\kappa_x - i\kappa_y)\,\psi_{2s+2}\right.\\ &+\{(s-1)(2i_n - s + 2)\}^{\frac{1}{2}}(\kappa_x + i\kappa_y)\,\psi_{2s-2}\\ &\left.+(2i_n - 2s + 2)\,\kappa_z\psi_{2s}\right]\end{aligned}\tag{4 2}$$

As in I we now try for solutions of the form

$$\psi_s = \sum_{k\,u} a^{(s)}_{k\,u}\,P_{n\,k\,u}\exp\{-\,i\,(W_0 + W_1 + \Delta W_s(k, u))\,t/h\}\tag{5}$$

We substitute in (4 1) and (4 2), multiply each equation by $\overline{P}_{n\,k\,u}$, and integrate over all space, obtaining

$$\begin{aligned}\Delta W_{2s-1}\,a^{(2s-1)}_{k\,u} = {}&\beta_1\left[u a^{(2s-1)}_{k\,u} - (k + u + 1)\,a^{(2s)}_{k\,u+1}\right]\\ &+\beta_2\left[(2i_n - 2s + 2)\,u a^{(2s-1)}_{k\,u}\right.\\ &-\{(2i_n - s + 1)s\}^{\frac{1}{2}}(k + u + 1)\,a^{(2s+1)}_{k\,u+1}\\ &\left.-\{(s-1)(2i_n - s + 2)\}^{\frac{1}{2}}(k - u + 1)\,a^{(2s-3)}_{k\,u-1}\right],\end{aligned}\tag{6 1}$$

$$\begin{aligned}\Delta W_{2s}\,a^{(2s)}_{k\,u} = {}&\beta_1\left[-u a^{(2s)}_{k,u} - (k - u + 1)\,a^{(2s-1)}_{k\,u-1}\right]\\ &+\beta_2\left[(2i_n - 2s + 2)\,u a^{(2s)}_{k\,u}\right.\\ &-\{(2i_n - s + 1)\,s\}^{\frac{1}{2}}(k + u + 1)\,a^{(2s+2)}_{k\,u+1}\\ &\left.-\{(s-1)(2i_n - s + 2)\}^{\frac{1}{2}}(k - u + 1)\,a^{(2s-2)}_{k\,u-1}\right]\end{aligned}\tag{6 2}$$

We now write $u + s - 1$ and $u + s$ in place of u in these equations and suppose that

$$\Delta W_{2s-1}(k, u + s - 1) = \Delta W_{2s}(k, u + s) = \Delta$$

(say) In this way we obtain equations in which a's with the same upper suffixes have the same lower suffixes, and we get solutions of the wave equations which consist of one finite term, the others being small We shall abbreviate by writing a_1, a_2, a_3, etc , for $a^{(1)}_{k\,u}$, $a^{(2)}_{k\,u+1}$, $a^{(3)}_{k\,u+1}$, etc , since there is no longer any ambiguity about the lower suffixes The equations (6 1) and (6 2) become

$$\begin{aligned}\Delta a_{2s-1} = {}& \beta_1 [(u + s - 1)\, a_{2s-1} - (k + u + s)\, a_{2s}] \\ & + \beta_2 [(2i_n - 2s + 2)(u + s - 1)\, a_{2s-1} - \{(2i_n - s + 1) s\}^{\frac{1}{2}} (k + u + s)\, a_{2s+1} \\ & \qquad - \{(s - 1)(2i_n - s + 2)\}^{\frac{1}{2}} (k - u - s + 2)\, a_{2s-3}] \qquad (7\,1)\end{aligned}$$

$$\begin{aligned}\Delta a_{2s} = {}& \beta_1 [-(u + s)\, a_{2s} - (k - u - s + 1)\, a_{2s-1}] \\ & + \beta_2 [(2i_n - 2s + 2)(u + s)\, a_{2s} - \{(2i_n - s + 1) s\}^{\frac{1}{2}} (k + u + s + 1)\, a_{2s+2} \\ & \qquad - \{(s - 1)(2i_n - s + 2)\}^{\frac{1}{2}} (k - u - s + 1)\, a_{2s-2}] \qquad (7\,2)\end{aligned}$$

There are $2i_n + 1$ pairs of equations of this type, homogeneous in the $4i_n + 2$ constants a, so that we can eliminate the constants, and obtain an equation in Δ of the $(4i_n + 2)$th degree

When $\beta_2 = 0$ any pair of equations gives the Darwin solution for electron spin, viz ,

$$\Delta = \beta_1 k, \qquad (-k + u + s - 1)\, a'_{2s-1} = (k + u + s)\, a'_{2s} \qquad (8\,1)$$

$$\Delta = -\beta_1 (k + 1), \quad a'_{2s-1} = a'_{2s} \qquad (8\,2)$$

For $\beta_2 \neq 0$ but $\beta_2 \ll \beta_1$ we try first

$$\Delta = \beta_1 k + \delta \qquad a_s = a_s' + \varepsilon_s$$

where δ, ε_s are small compared with $\beta_1 k$ and a_s' respectively Substituting in (7 1) and (7 2) and subtracting we obtain an equation independent of the ε's viz ,

$$\begin{aligned}&\{\delta - (2i_n - 2s + 2)(u + s - 1)\beta_2\}\, a_{2s-1} - \{\delta - (2i_n - 2s + 2)(u + s)\beta_2\}\, a_{2s} \\ &\quad + \{(2i_n - s + 1) s\}^{\frac{1}{2}} \{(k + u + s)\, a_{2s+1} - (k + u + s + 1)\, a_{2s+2}\}\beta_2 \\ &\quad + \{(s - 1)(2i_n - s + 2)\}^{\frac{1}{2}} \{(k - u - s + 2) a_{2s-3} - (k - u - s + 1)\, a_{2s+2}\}\beta_2 = 0 \qquad (9)\end{aligned}$$

Writing

$$\frac{a_{2s-1}}{k + u + s} = -\frac{a_{2s}}{(k - u - s + 1)} = \frac{a_{2s-1} - a_{2s}}{2k + 1} = \mathrm{A}_s, \qquad (10)$$

and

$$\delta (2k + 1)/\beta_2 k = \zeta, \qquad (11)$$

equation (9) becomes

$$\begin{aligned}&2\{(s - 1)(2i_n - s + 2)\}^{\frac{1}{2}} (k - u - s + 2)\, \mathrm{A}_{s-1} \\ &\qquad + \{\zeta - (2i_n - 2s + 2)(2u + 2s - 1)\}\, \mathrm{A}_s \\ &\qquad + 2\{(2i_n - s + 1) s\}^{\frac{1}{2}} (k + u + s + 1)\, \mathrm{A}_{s+1} = 0, \qquad (12)\end{aligned}$$

where $s = 1, 2, \quad 2i_n + 1$ By eliminating the A's we obtain a $(2i_n + 1)$-rowed determinantal equation in ζ, and the a's obtained are sufficient to describe the state of the atom

In a similar way, by writing

$$\Delta = -\beta_1 (k + 1) + \delta' \qquad a_s = a_s' + \varepsilon_s',$$

we obtain the levels into which the nuclear spin doublet level $j = k - \frac{1}{2}$ is split up by the nuclear spin Using (8 2) we obtain equations corresponding to (12) (11), (10) viz,

$$2\{(s-1)(2i_n - s + 2)\}^{\frac{1}{2}} \mathrm{B}_{s-1} + \{\zeta' - (2i_n - 2s + 2)(2u + 2s - 1)\} \mathrm{B}_s + 2\{(2i_n - s + 1)s\}^{\frac{1}{2}} (k + u + s) \mathrm{B}_{s+1} = 0, \tag{13}$$

where

$$a_{2s-1} = a_{2s} = \mathrm{B}_s \tag{14}$$

$$\delta' (2k + 1)/\beta_2 (k + 1) = \zeta' \tag{15}$$

It is seen at once that equation (13) is the same as (12) with $(k - 1)$ written in place of k, and so the splitting of the lower one of the two electron spin doublet levels is deducible from the splitting of the level immediately below it

§ 3 *Calculation of the Wave Functions* —The algebraic solution of equations (12) and (13) for any numerical value of i_n would be very irksome when i_n is at all large For $i_n = 1, 1\frac{1}{2}$ we get three and four rowed determinants respectively and the work is comparatively simple The levels for the general value of k in these two cases have been found, and are given later The case of $i_n = 4\frac{1}{2}$ has only been dealt with for the value $k = 1$, i e, the P levels The work here is fairly easy owing to the fact that there are only six P levels (In I it was shown that each electron spin fine structure level splits up into $2i_n + 1$ or $2j + 1$ levels, whichever is the less) The occurrence of these six levels only is well brought out in the solution of the equations $\mathrm{P}_{n\,k\,u}$, which contains as a factor the associated Legendre function $\mathrm{P}_k^u(\cos\theta)$, is only different from zero when $|u| \leqslant k$, and so any $a_{k\,u}^{(r)}$ is only different from zero when $|u| \leqslant k$ Now the P levels are determined by the coefficients $a_{1\,u}^{(1)}$, $a_{1\,u+1}^{(2)}$, $a_{1\,u+1}^{(3)}$, $a_{1\,u+2}^{(4)}$, $\quad$, $a_{1\,u+9}^{(19)}$, $a_{1\,u+10}^{(20)}$, and so, in any solution u can only have values 1, 0, −1, −2, $\quad$, −11 The maximum number of a's which exist for any of these values of u is six, and so there exist only a small number of A's or B's for any u The determinants for ζ and ζ' are therefore reduced considerably Equation (12) for $i_n = 4\frac{1}{2}$ and $k = 1$ is

$$2\{(s-1)(11-s)\}^{\frac{1}{2}} (3 - u - s) \mathrm{A}_{s-1} + \{\zeta - (11 - 2s)(2u + 2s - 1)\} \mathrm{A}_s + 2\{(10 - s)s\}^{\frac{1}{2}} (u + s + 2) \mathrm{A}_{s+1} = 0 \qquad (s = 1, 2, \quad, 10) \tag{16}$$

When $u = 1$ it is seen that the coefficient of A_1 in the second equation is zero, and on this account we can obtain a solution of the equations in which only A_1 is different from zero, and referring to (10) this makes only a_1 different from zero, as required by the above considerations The corresponding root in ζ is given by the equation for $s = 1$, viz ,

$$(\zeta - 9\ 3)\,A_1 = 0 \quad \text{or} \quad \zeta = 27$$

In the case of $u = 0$ we see that the equation for $s = 3$ has a zero coefficient for A_2 and so we can get a solution in which only A_1 and A_2 differ from zero, and therefore (using (10)) in which only a_1 a_2, a_3 differ from zero In the general case $u = -t$, since the $(t+3)$th equation has a zero coefficient for A_{t+2}, while the $(t-2)$th equation has a zero coefficient for A_{t-1}, we can get a solution in which all the A s are zero except A_{t-1}, A_t, A_{t+1}, A_{t+2} , again, using (10) it is seen that only $a_{2t-2}, a_{2t-1}, \quad , a_{2t+3}$ are different from zero We get a corresponding four-rowed determinantal equation for ζ, viz

$$\begin{vmatrix} \zeta + 3(13-2t), & 2(11-t)\ , & 0 \ , & 0 \\ 6(t-1)\ , & \zeta + (11-2t) & 4(10-t)\ , & 0 \\ 0\ , & 4t\ , & \zeta - (9-2t), & 0 \\ 0\ , & 0\ , & 2(t+1)\ , & \zeta - 3(7-2t) \end{vmatrix} = 0$$

which gives the roots $\zeta = 27,\ 3,\ -17,\ -33$

For $u = -t = 1, 0, -1, -9, -10, -11$ only certain of these roots are relevant These cases may be dealt with separately, as we have done with $u = 1, 0$, or they may be derived quite straightforwardly with the help of (10) It is found that for the four roots the respective permissible ranges of u are 1 to -11, 0 to -10, -1 to -9 and -2 to -8, respectively

The four $p_{3/2}$ levels are therefore given by

$$\Delta = \beta_1 \lambda + \delta, \qquad \delta = 9\beta_2, \qquad \beta_2, -17\beta_2/3, -11\beta_2 \tag{17}$$

In a similar way, with the help of (13) it is found that the two $p_{1/2}$ levels are given by $\zeta' = 9, -11$ or

$$\Delta = -\beta_1(\lambda + 1) + \delta', \qquad \delta' = 6\beta_2, \ -22\beta_2/3 \tag{18}$$

As observed above we may deduce the $d_{3/2}$ levels from those for $p_{3/2}$

For the cases $i_n = 1, 1\frac{1}{2}$, there are in general three and four hyperfine structure levels respectively These are reduced in the $p_{1/2}$ levels to two This is clearly given by the non applicability of certain of the algebraic solutions obtained for $k = 1$

§ 4 *Empirical Adjustment* — The equations (4·1) and (4·2) need some additional terms before they will give the ζ-levels correctly. It is clear that the adjustment will not come from the addition of the spin interaction energy. This only results in a shift of the levels. The additional terms will be those which would ensue from an exact relativistic treatment of the problem, and will be similar to those given in I for $i_n = \frac{1}{2}$. It is not difficult to give equations containing these terms, provided we assume that they are of the same form as the additional terms required by the relativistic treatment of electron spin. We have to make solutions which preclude the possibility of transitions in which f changes by more than 1. In this way provided we make the extra terms of the same special form as in I, containing two consecutive wave-functions we are able to obtain a unique adjustment. The corrected equations thus obtained are

$$\begin{aligned}\Delta W \psi_{2s-1} = {} & -\frac{iZ\mu_0 eh}{2mcr^3}\Big[(\kappa_x - i\kappa_y)\psi_{2s} + \kappa_z \psi_{2s-1} - ir\frac{\partial}{\partial r}\psi_{2s-1}\Big] \\ & - \frac{i\mu eh}{mcr^3}\Big[\{(2i_n - s + 1)s\}^{\frac{1}{2}}(\kappa_x - i\kappa_y)\psi_{2s+1} \\ & + \{(s-1)(2i_n - s + 2)\}^{\frac{1}{2}}(\kappa_x + i\kappa_y)\psi_{2s-3} + (2i_n - 2s + 2)\kappa_z\psi_{2s-1} \\ & - (2i_n - 2s + 2)\, ir\frac{\partial}{\partial r}\psi_{2s-1} - 2\{(s-1)(2i_n - s + 2)\}^{\frac{1}{2}}\, ir\frac{\partial}{\partial r}\psi_{2s-2}\Big]\end{aligned} \tag{4·1$'$}$$

$$\begin{aligned}\Delta W \psi_{2s} = {} & -\frac{iZ\mu_0 eh}{2mcr^3}\Big[(\kappa_x + i\kappa_y)\psi_{2s-1} - \kappa_z\psi_{2s} - ir\frac{\partial}{\partial r}\psi_{2s}\Big] \\ & - \frac{i\mu eh}{mcr^3}\Big[\{(2i_n - s + 1)s\}^{\frac{1}{2}}(\kappa_x - i\kappa_y)\psi_{2s+2} \\ & + \{(s-1)(2i_n - s + 2)\}^{\frac{1}{2}}(\kappa_x + i\kappa_y)\psi_{2s-2} + (2i_n - 2s + 2)\kappa_z\psi_{2s} \\ & + (2i_n - 2s + 2)\, ir\frac{\partial}{\partial r}\psi_{2s} - 2\{s(2i_n - s + 1)\}^{\frac{1}{2}}\, ir\frac{\partial}{\partial r}\psi_{2s+1}\Big]\end{aligned} \tag{4·2$'$}$$

The procedure is then the same as in I and the roots for $k = 0$ are found to be

$$\Delta = \beta_{1\,0} + 2i_n\beta_{2\,0}, \qquad \beta_{1\,0} - 2(i_n + 1)\beta_{2\,0}$$

where

$$\begin{aligned}\beta_{1\,0} &= -\frac{Z\mu_0 eh}{2mc}\int_0^\infty \frac{1}{r} f_{n\,0}(r)\frac{d}{dr}\left\{\frac{1}{r}f_{n\,0}(r)\right\}dr \\ &= \frac{Z\mu_0 eh}{2mc}\left[\tfrac{1}{2}\left(\frac{1}{r}f_{n\,0}(r)\right)^2\right]_{r=0}\end{aligned}$$

$$\beta_{2\,0} = \frac{\mu eh}{mc}\left[\tfrac{1}{2}\left(\frac{1}{r}f_{n\,0}\right)^2\right]_{r=0},$$

where $f_{n\,k}(r)$ is the part of the wave function depending on r For the first root n may have values from zero to $-(2i_n+1)$ and for the other -1 to $-2i_n$ The additions leave the solutions for $k > 0$ unchanged

§ 5 The solutions obtained must be normalised in the usual way, the extension of (33), I, for this purpose being

$$a^{(1)\,2}_{k\,u}(k+u)!\,(k-u)! + (a^{(2)\,2}_{k\,u+1} + a^{(3)\,2}_{k\,u+1})(k+u+1)!\,(k-u-1)!$$
$$+ \dots + a^{(4i_n+2)\,2}_{k\,u+2i_n+1}(k+u+2i_n+1)!\,(k-u-2i_n-1)! = 1 \quad (19)$$

We also obtain relations similar to (44) I, for the intensities of transitions from a state determined by k, u with coefficients a, to one with coefficients a'

$$\begin{pmatrix} k \to k-1 \\ u \quad\; u-1 \end{pmatrix} = [a_1 a_1'(k+u)!\,(k-u)!$$
$$+ (a_2a_2' + a_3a_3')(k+u+1)!\,(k-u-1)!$$
$$+ \dots + a_{4i_n+2}\,a'_{4i_n+2}(k+u+2i_n+1)!\,(k-u-2i_n-1)!]^2 \quad (20\ 1)$$

$$\begin{pmatrix} k \to k-1 \\ u \quad\;\; u \end{pmatrix} = 4 \times \text{similar expression} \quad (20\ 2)$$

$$\begin{pmatrix} k \to k-1 \\ u \quad\; u+1 \end{pmatrix} = \text{similar expression} \quad (20\ 3)$$

The expressions on the right differ only by their k, u suffixes which are determined by the left-hand sides, and are unambiguous The total intensity of any line of the hyperfine structure is found by summing these intensities over all possible values of u for the k, j, and f of the line

The quantum number f has been assigned arbitrarily, but it clearly represents the total angular momentum of the system This can easily be verified in any particular case

§ 6 *Results* —(i) $i_n = 1$ The doublet level $j = k + \frac{1}{2}$ splits up into three levels given by

$$\Delta = \beta_1 k + \delta,$$
$$\delta = 2k\beta_2, \quad -4k\beta_2/(2k+1) \quad -2k(2k+3)\beta_2/(2k+1)$$

for which $f = k + \frac{3}{2}$, $k + \frac{1}{2}$, $k - \frac{1}{2}$ respectively, while the level $j = k - \frac{1}{2}$ splits up into three levels,

$$\Delta = -\beta_1(k+1) + \delta',$$

$$\delta' = 2(k+1)(2k-1)\beta_2/(2k+1), \quad -4(k+1)\beta_2/(2k+1), \quad -2(k+1)\beta_2$$

$$f = k + \tfrac{1}{2}, \quad k - \tfrac{1}{2}, \; k - \tfrac{3}{2}, \quad \text{respectively}$$

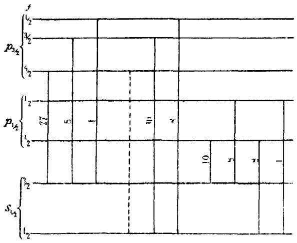

FIG 1 $i_n = 1$

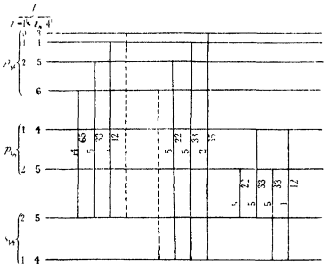

FIG 2 $i_n = 1\frac{1}{2}, 4\frac{1}{2}$

(The figures on the left indicate the intensities for $i_n = 1\frac{1}{2}$, those on the right for $i_n = 4\frac{1}{2}$.)

(ii) $i_n = 1\frac{1}{2}$

For $j = k + \frac{1}{2}$, $\Delta = \beta_1 k + \delta$,

$$\delta = 3k\beta_2,\quad k(2k-5)\beta_2/(2k+1),\quad -k(2k+9)\beta_2/(2k+1),\quad -3k(2k+3)\beta_2/(2k+1),$$

$f = k + 2$, $k + 1$, k, $k - 1$, respectively

For $j = k - \frac{1}{2}$, $\Delta = -\beta_1 (k+1) + \delta'$,

$$\delta' = 3(2k-1)(k+1)\beta_2/(2k+1), \quad (2k-7)(k+1)\beta_2/(2k+1)$$
$$-(2k+7)(k+1)\beta_2/(2k+1), \quad -3(k+1)\beta_2,$$

$f = k-2, \quad k-1, \quad k, \quad k+1,$ respectively

(iii) $i_n = 4\frac{1}{2}$

For $k = 1$, $j = \frac{3}{2}$, $\Delta = \beta_1 + \delta$, $\delta = 9\beta_2, \ \beta_2, \ -17\beta_2/3, \ -11\beta_2$,

$f = 6, 5, 4, 3$ respectively,

$k = 1$, $j = \frac{1}{2}$, $\Delta = -2\beta_1 + \delta'$, $\delta' = 6\beta_2, \ -22\beta_2/3$

$f = 5, 4,$ respectively

It is seen that the ratios of the energy differences of the four $p_{3/2}$ levels are 6 : 5 : 4 which agree with the observations of Back and Goudsmidt It would seem, therefore, that the spin interaction energy is in this case negligible in comparison with the interaction energy of the nuclear spin and the orbital momentum It is hoped to investigate this point further however

The intensity ratios of the lines of the multiplets P → S for $i_n = 1$ are given in fig 1 and for $i_n = 1\frac{1}{2}$, $4\frac{1}{2}$ in fig 2 It is seen that the sum intensities of $p_{3/2} \to s_{1/2}$ and $p_{1/2} \to s_{1/2}$ bear the ratio 2 : 1, forming a useful check on the work

The Effect of Water Vapour on Diffusion Coefficients and Mobilities of Ions in Air

By Prof J J Nolan and T E Nevin, University College, Dublin

(Communicated by A W Conway, F R S — Received January 16 1930)

Introduction

Determinations of the coefficient of diffusion of positive and negative ions were first made by Townsend Measurements have since been carried out by Franck and Westphal and Salles using Townsend's method The results for air are given in Table I

Table I

Gas	D_+	D	Ionising agent	Observer *
Dry air	0·028	0·043	X rays	Townsend
,,	0·029	0·045		Franck and Westphal
,	0·032	0·043	Radioactive substance	Townsend
	0·032	0·043		Salles
Moist air	0·032	0·035	X rays	Townsend
	0·036	0·041	Radioactive substance	

* Townsend, 'Phil Trans A, vol 193, p 129 (1899) and vol 195 p 259 (1900) Franck and Westphal Verh D Phys Ges vol 11 pp 146 276 (1909) Salles, Ann Physique,' vol 2 p 273 (1914)

In spite of the elaborate apparatus used by the later observers their results are little if at all more accurate than those of Townsend

The mobility, K, and the coefficient of diffusion, D, are connected by the relation $K/D = Ne/P$, where N is the number of molecules per cm ^{3} at pressure P and the temperature of the gas, and e is the charge on the ion It has been shown by Millikan and his collaborators† that the charge is one electron, so that the above results may be used to calculate the mobility The value obtained for negative ions in dry air is 1·77 cm per second per volt per centimetre, which, though in approximate agreement with that obtained by Zeleny‡ and others, differs considerably from the latest result, 2·15 of Tyndall and Grindley §

The present work was undertaken to examine the effect of water vapour on the diffusion coefficient, on parallel lines to Tyndall and Grindley's work on the mobility, and to test the relation between the mobility and the diffusion coefficient above mentioned It was hoped also with the improved methods of measurement now available to increase the accuracy of the observations

---

† 'Phil Mag,' vol 21, p 753 (1911) and Phys Rev,' vol 15 p 157 (1920)

‡ 'Phil Trans,' A, vol 195, p 193 (1900)

§ 'Roy Soc Proc,' A, vol 110, p 342 (1926)

Details of Apparatus

In his first paper (*loc cit*) Townsend gave the theory of the diffusion of ions from a stream of gas to the wall of a cylindrical tube through which it is passing Those of one sign which emerge are driven by a suitably directed field to a collecting electrode If the ratio of the currents to the electrodes after the gas has passed through tubes of lengths z_1 and z_2, respectively is c_1/c_2 then

$$\frac{c_1}{c_2} = \frac{0.1952 \exp(-7.313\pi \mathrm{D} z_1/2\mathrm{Q}) + 0.0243 \exp(-44.56\pi \mathrm{D} z_1/2\mathrm{Q})}{0.1952 \exp(-7.313\pi \mathrm{D} z_2/2\mathrm{Q}) + 0.0243 \exp(-44.56\pi \mathrm{D} z_2/2\mathrm{Q})},$$

where D is the diffusion coefficient of ions of the sign collected and Q is the volume of gas passing through the tubes in unit time From the graph

$$y = \frac{0.1952 \exp(-x) + 0.0243 \exp(-44.56x/7.313)}{0.1952 \exp(-xz_2/z_1) + 0.0243 \exp(-44.56xz_2/7.313z_1)}$$

where $y = c_1/c_2$ and $x = 7.313\pi \mathrm{D} z_1/2\mathrm{Q}$, the value of x corresponding to the experimentally determined value of y can be obtained and D calculated

To get sufficiently large electrometer readings, Townsend found it necessary to use two sets of 24 tubes, 4 cm and 0.5 cm long respectively The tubes in each set were arranged on the circumference of a circle 2 cm in diameter so that the ionised gas on entering the tubes divided into 24 equal streams The bore of the tubes was 1 mm In the present work it has been found possible to reduce the number of tubes in each set to one, while a simple method of producing a circulation of air in a closed system has made it a comparatively simple process to bring the gas to any desired humidity

The method of producing the circulation is shown in fig 1 The bottle of mercury P is connected to a 500 cm ^{3} graduated cylinder Q by a length of pressure tubing The cylinder is closed by a rubber stopper through which pass two tubes S and T and a short piece of thick walled capillary tubing to which the pressure tubing is attached This capillary in conjunction with a screw clip on the tubing controls the rate at which the mercury flows from P to Q, a second clip can be used to cut off the flow completely At the end of a reading the mercury is returned to P by placing it below the level of Q and inverting the latter The tube S extends above the level of the mercury in the inverted cylinder in order to prevent it entering the apparatus

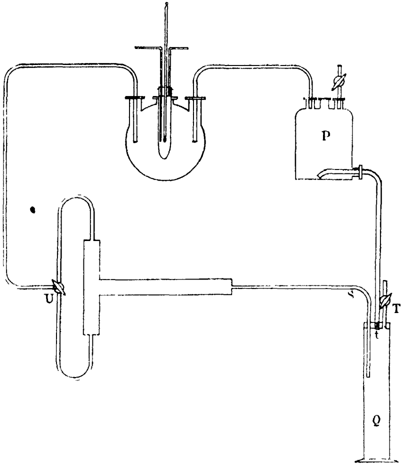

FIG 1

The diffusion apparatus is shown in fig 2 It consists of three brass tubes, A and B, each 15 cm long, and C, 60 cm long, 3 6 cm diameter, which slide for a distance 5 cm into the brass junction T The diffusion tubes are of steel with a bore of 1 mm, circular to 0 5 per cent The longer tube, 4 cm long, is mounted in an axial hole in a brass cylinder K_1, 4 cm long and the shorter, 1 cm long, in a cylinder K_2, 1 cm long The cylinders screw into brass rings 1 cm long soldered in position in A with their centres 2 5 cm and 1 cm from the ends respectively The joints between the cylinders and the rings are made gas-tight by vacuum grease smeared on the threads of the screw The electrode E_1 lies in the axis of the tube symmetrically between the diffusion tubes It is supported by a rod M_1 insulated by a grooved ebonite

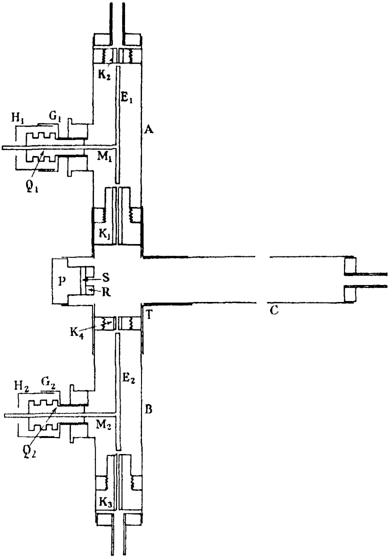

FIG 2

plug Q_1 provided with the usual guard ring arrangement The plug is protected from light and dust and screened from electrostatic disturbances by a short tube H_1 sliding into an extension on the guard ring G_1 The tube B contains two diffusion tubes mounted in a similar manner to those in A A and B are mounted in T so that the ionised gas can be made to pass through the longer diffusion tube in A or the shorter in B by turning the three-way tap U, fig 1

The tube C is packed with cotton wool to remove nuclei and large ions produced by the splashing of the mercury when it enters the graduated cylinder The source of ionisation S is a deposit of polonium on bismuth mounted on a brass plug P which slides into the fourth limb of T It is covered by a brass disc R through a hole in which an approximately parallel beam of α rays emerges This ensures that all the ions reaching the diffusion tubes have approximately the same age In order to prevent contamination of the apparatus by volatilisation of the polonium the source is covered with a film obtained by evaporating a 1 per cent solution of collodion

The apparatus is raised to a potential of ± 80 volts and the currents are measured by a Lindemann electrometer used at sensitivities of 75–120 divisions per volt

Humidity Control and Measurement

In the beginning sulphuric acid solutions of known strengths were employed to obtain air of definite humidity, the strength of the acid being obtained from the density and the vapour pressure from tables * A thermal hygrometer of the pattern devised by Tyndall and Chattock was used as an independent method of measuring the vapour pressure The sulphuric acid solution was run from one aspirator bottle to a second, the air in the latter being drawn through the apparatus into the first The acid was then passed back into the first bottle After this had been repeated a few times it was assumed that the air in the apparatus was in equilibrium with the acid The arrangement proved unsatisfactory On altering the strength of the acid the humidity did not change appreciably and the vapour pressure calculated from the strength of the solution did not agree with the value given by the hygrometer It was found that the vapour pressure in the apparatus was really controlled by the moisture in the cotton wool filter The substitution of glass wool effected only a slight improvement

The method was abandoned, and, as some doubt was felt about the accuracy of the thermal hygrometer, a dew point instrument enclosed in a glass bulb was substituted The cotton wool filter was then found to give a very convenient method of varying the humidity During the time required for a set of observations the vapour pressure remained constant to 0 1 mm From day to day, however, as the temperature of the surroundings varied, the vapour pressure, after passing a current of air through the apparatus to bring the enclosed air into equilibrium with the cotton wool, varied within limits of 1 mm each way about a mean. Varying the vapour pressure in this manner, the change in the diffusion coefficient for small changes in the vapour pressure could be examined. By passing a current of air through the apparatus and warming the filter the amount of water in the cotton wool could be decreased enabling readings to be taken over a new range of vapour pressures.

---

* Wilson, 'J Ind Eng Chem,' vol 13, p 326 (1921)

Even after prolonged heating of the filter in a current of dry air the pressure of water vapour in the apparatus was still 1.5 mm. A wide glass tube about 150 cm. long was connected in a horizontal position between the filter and the diffusion apparatus. It contained a layer of sulphuric acid along the bottom. After passing a current of air over the surface of the acid for some hours the vapour pressure was still 1.2 mm. As it was thought that the diffusion of water vapour through the rubber tubing used to connect the bottle of mercury P to the hygrometer might be responsible for the lack of drying, a second tube of acid was interposed between the hygrometer and the bottle. This proved completely successful; with a suitable solution of acid in the tubes there was no sign of condensation on the silver thimble at −26° which was the lowest temperature that could be reached. In view of this experience the dryness of a gas which has been in contact with rubber tubing after drying is open to suspicion.

The range of vapour pressures 0.1 mm. to 1.2 mm. was covered by means of sulphuric acid solutions, the vapour pressure being calculated. The dew point hygrometer was not used below −14° C. on account of the difficulty of judging the first sign of deposition of dew. Some readings at vapour pressures above 1.2 mm. were also obtained with sulphuric acid solutions, the observed and calculated vapour pressures generally agreeing to within 0.1 mm.

Experimental Procedure

On account of the limited volume of mercury in P, not more than 300 cm.^{3} of air could be passed through the diffusion tubes without interrupting the flow to return the mercury from Q to P. Because of the fall in level of the mercury in P the rate of flow was different at the beginning and end of a reading. A special procedure in taking observations was therefore necessary. The three-way tap was turned so that the gas stream passed through either A or B, the electrometer being connected to the corresponding electrode. When the volume of mercury in Q was about 135 cm.^{3} the electrometer was unearthed. As the needle passed over a division of the eyepiece scale chosen so that the volume was about 150 cm ^{3} a stop-watch was started and stopped again when the volume was about 250 cm ^{3} and the needle again passing over a division A second observer measured the exact time taken for the 100 cm ^{3} of mercury to flow into Q In this way the electrometer readings could be accurately taken and the average value of Q was always the same The electrometer scale was carefully calibrated before or after each set of observations

Corrections

(*a*) Allowance for any difference in the density of ionisation at the entrances to the two diffusion tubes when the gas was passing through, or for any difference in the capacities of A and B was made as follows —The apparatus was set up so that the ionised gas could pass through either of the short tubes K_2 or K_4, fig 2, and the currents to the electrodes were measured The ratio of the currents C_A/C_B was found to be 0·990 Before calculating y the readings at B were multiplied by this factor

(*b*) The head under which the mercury runs into the graduated cylinder changes about 2 per cent from beginning to end of the time in which an electrometer observation is being taken A correction to Townsend's formula must be applied to allow for this variation If the rate of flow at the beginning of an observation extending over T seconds be Q_1, and at the end Q_2, then

$$Q = Q_1 - (Q_1 - Q_2)t/T$$

The number of ions entering the tube of length z_1 being n per second and the number leaving in the same time being n_1 Townsend has shown that

$$n_1 = 4n\{0{\cdot}1952 \exp(-7{\cdot}313\pi Dz_1/2Q) + 0{\cdot}0243 \exp(-44{\cdot}56\pi Dz_1/2Q) + \quad\}$$

The number leaving in T seconds is

$$N_1 = 4n\left\{0{\cdot}1952\int_0^T \exp(-7{\cdot}313\pi Dz_1/2Q)\,dt \right.$$
$$\left. + 0{\cdot}0243\int_0^T \exp(-44{\cdot}56\pi Dz_1/2Q)\,dt\right\}$$

If the change in Q is small, an approximate value of the integral suffices and we get

$$N_1 = 4nT\,[0{\cdot}1952 \exp(-7{\cdot}313\pi Dz_1/2Q)\{1 - 7{\cdot}313\pi Dz_1(Q_1 - Q_2)/4Q_1^2\}$$
$$+ 0{\cdot}0243 \exp(-44{\cdot}56\pi Dz_1/2Q)],$$

and finally

$$y = \frac{N_1}{N_2} = \frac{0{\cdot}1952 \exp(-x\{1 - x(Q_1 - Q_2)/2Q_1\}) + 0{\cdot}0243 \exp(-44{\cdot}56x/7{\cdot}313)}{0{\cdot}1952 \exp(-xz_2/z_1\{1 - xz_2/z_1\ (Q_1 - Q_2)/2Q_1\}) + 0{\cdot}0243 \exp(-44{\cdot}56xz_2/7{\cdot}313z_1)}$$

Putting $(Q_1 - Q_2)/2Q_1$ equal to a we get approximately

$$y\{1 + ax(1 - z_2/z_1)\} = \frac{0{\cdot}1952 \exp(-x + 0{\cdot}0243) \exp(-44{\cdot}56\,x/7{\cdot}313)}{0{\cdot}1952 \exp(-xz_2/z_1 + 0{\cdot}0243) \exp(-44{\cdot}56x\,z_2/7{\cdot}313z_1)}$$

From Townsend's graph an approximate value of x can be obtained and the factor $1 + ax(1 - z_2/z_1)$ calculated so $y\{1 + ax(1 - z_2/z_1)\}$ gives a more exact value of x which may be used to calculate D

By finding the time taken by the mercury to rise from 125 cm^3 to 175 cm^3 and from 225 cm^3 to 275 cm^3 approximate values of Q_1 and Q_2 are obtained The correction is about 2 per cent

(*c*) The effects of recombination in the fine tubes and of self-repulsion of the ions due to the inequality of D_+ and D_- have been discussed by Townsend* He has shown that they can be made negligible by using fine bore tubing and a low density of ionisation The corrections have been neglected in the present work, the former being about 0·4 per cent and the latter about 0·06 per cent

(*d*) The values have been reduced to 15° and 76 cm pressure on the assumption that the diffusion coefficient is proportional to the absolute temperature and inversely proportional to the pressure

Results

The results for ions of both signs have been plotted against the vapour pressure in fig 3 The corresponding mobilities calculated from the formula $K/D = 40{\cdot}3$ can be read off by means of the scale attached to the right hand side of the figure The probable error in the individual determinations is 1–3 per cent, the smaller accuracy being associated with the high values for negative and low values for positive ions The error in the vapour pressures above 1·2 mm lies between 1 and 2 per cent For the vapour pressures below this value which have been calculated from the strength of sulphuric acid solutions it is unknown, but in view of the precautions taken to ensure equilibrium between the solution and the air in the apparatus it is probably small The value of Q lay between 2·4 and 2·7 cm^3 per second and the age of the ions was therefore about 0·2 second The air was ordinary room air which, after bubbling through concentrated sulphuric acid, was filtered through glass wool before entering the apparatus The character of the results was not affected by changing the cotton wool filter or replacing it by glass wool

The variation of the diffusion coefficient is of a totally different character to what might have been expected from Tyndall and Grindley's mobility observations The fluctuations which occur are far outside the limits of

---

* *Loc cit* (1900)

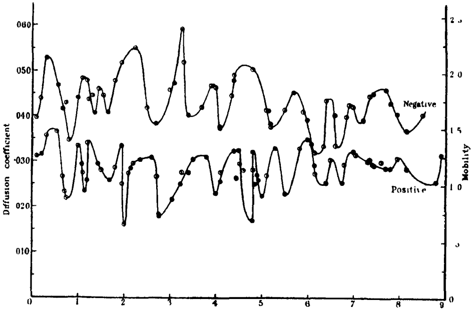

Fig 3

experimental error The mobility appears to oscillate between certain stable values At certain parts of the curve the change from a high to a low value or conversely takes place gradually, but at other parts the transition takes place for such a small alteration in the vapour pressure that it appears to be nearly discontinuous

With regard to the question of how far the results at any particular vapour pressure can be repeated, it may be pointed out that on the ascending and descending parts of the curve the variation is rapid, and it is difficult to reproduce exactly the same conditions As far as this can be done the results are repeatable At the maxima and minima of the curve where the variation is less rapid it is easier to repeat the results Two typical examples of the agreement are given in Table II

The air was dried by replacing the tubes of sulphuric acid by tubes containing a layer of phosphorus pentoxide over which the air passed The results quoted represent six completely independent sets of observations Other examples of the agreement might be quoted but the above are typical In

Table II

Vapour pressure	Date	D_+	D_-
Dry air	March 24, 1929	—	0 0435
,,	March 25, 1929	0 0279	0 0449
,,	March 27 1929	0 0276	0 0443
11 1 mm	October 19, 1928	0 0330	0 0364
,,	October 22, 1928	0 0343	0 0342
,,	October 23, 1928	0 0340	0 0372

particular the very low value of 0 0185 obtained for positive ions at a vapour pressure of 2 75 mm could be repeated within 3 per cent after an interval of several months The results plotted were not obtained by a progressive alteration of the vapour pressure in any one direction but were taken more or less at random along the curve Furthermore the result of every set of observations, with the exception of four obtained when using the cotton wool as a humidity control, has been plotted A considerable change of humidity occurred while these four sets of observations were being taken and they have therefore been discarded Taking everything into account there can hardly be any doubt that the phenomenon is genuine

It was decided to see whether under suitable conditions the mobility would vary in a manner similar to the diffusion coefficient In view of the probable presence of groups of ions having different mobilities it is to be noted that the mobility values deduced from the diffusion coefficient are mean mobilities and not the mobility of a predominant group of ions, so it is the mean mobility which is of importance for the present purpose The experiments are described in the following section

Measurement of Mobility

The slope, i/V, of the initial straight part of the curve connecting the current and voltage in a uniformly ionised gas is proportional to $(K_+ + K_-)/\alpha^{1/2}$ where α is the recombination coefficient between ions of opposite sign and K_+ and K_- the mobilities of positive and negative ions respectively Measurements of this slope should give a rapid and simple qualitative verification of the results above

The air between two parallel plates 2 5 cm apart was ionised by α-rays from a polonium source attached to one of them The apparatus was mounted on an iron plate through which the leads emerged and covered by a bell jar The air in the enclosed space was brought to a definite humidity by dishes of sulphuric acid The relation between current and voltage was linear with voltages up to 4 between the plates The slope, i/V, and the sum of the mobilities of positive and negative ions obtained by adding the ordinates of the curve in fig 3 are exhibited as functions of the vapour pressure in fig 4,

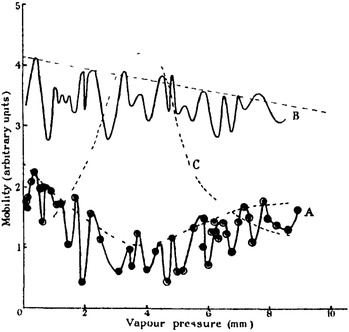

FIG 4—A, Variation of slope, i/V, of current-voltage curve between two parallel plates B, Variation of sum of mobilities obtained by adding ordinates of fig 3 C, Variation of recombination coefficient obtained by dividing the square of the ordinates of the dotted curve B by the square of the ordinates of the dotted curve A

curves A and B respectively The agreement in the positions of the maxima and minima of both curves is very satisfactory It is probable that the quantitative agreement between the curves would have been improved if more points had been taken on A, but the curve is sufficient to show that the type of variation previously found for the diffusion coefficient exists also for the mobility In any case as the recombination coefficient probably depends on the vapour pressure, and as there are differences in the experimental conditions in the two cases which will be pointed out later, we cannot expect exact quantitative agreement between the two curves The results have only been plotted up to a vapour pressure of 9 5 mm but observations have been made up to 15 mm They show that the oscillations persist up to this vapour pressure

Rutherford-Franck Alternating Field Method *— In view of this confirmation of the results of the diffusion coefficient measurements it was judged advisable to carry out observations using the alternating field method to examine the discrepancy between these results and those of Tyndall and Grindley The apparatus was of the type described by Nolan † The ions were caught by a brass plate 8 cm diameter surrounded by a guard ring 13 cm diameter A sheet of gauze 8 cm diameter was attached to a brass ring of the same dimensions as the guard ring Care was taken to ensure that the gauze was flat and its lower surface flush with the ring The ring was kept at a distance of 2 55 cm above the guard ring by three ebonite pillars The source of ionisation was a deposit of polonium on bismuth which rested on the upper surface of the gauze At a distance of 5 cm above the gauze was a parallel plate and between it and the gauze a potential difference of 40 volts was maintained The alternating field was obtained from the secondary of a transformer one terminal of which was connected to the gauze, and the other through a battery of 80 volts to the guard ring and to earth This battery was connected so that the ions not caught by the plate in the advancing phase were driven back to the gauze when the field was reversed The apparatus was enclosed in a brass box which could be made airtight and the humidity was varied by dishes of sulphuric acid solution placed on the bottom of the box The alternating voltage was increased in steps of 20 volts for the negative and 40 volts for the positive between each electrometer reading The observations were plotted and a smooth curve drawn through the points The intersection of this curve with the voltage axis was taken as the critical voltage No attempt was made to examine the curve for groups of ions‡ and the mobility deduced must be considered a mean value

The results corrected for the effect of the bias on the critical voltage and reduced to 15° and 76 cm pressure are shown in fig 5 The results for negative ions confirm the observations of Tyndall and Grindley on the variation of the negative mobility with vapour pressure, the general agreement being very satisfactory The mobility in air dried for 3 days in contact with phosphorus pentoxide in a sealed vessel is 2 26 cm per second per volt per centimetre, which is higher than the result, 2 15, they obtained in air dried to the maximum extent their apparatus permitted The results in moist air are slightly lower

---

* Rutherford, 'Proc Camb Phil Soc,' vol 9, p 401 (1898), Franck, 'Ann Physik,' vol 21, p 972 (1906)

† Nolan, 'Phys Rev,' vol 44, p 16 (1924)

‡ Nolan, 'Proc R Irish Acad,' vol. 35, p 38 (1920), and vol 36, p 74 (1923), Nolan and Harris *ibid*, vol. 36, p 31 (1922)

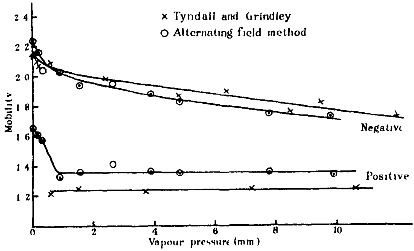

FIG 5

than theirs, but the difference is within the limits of experimental error in the determination of the constants involved in calculating the mobility The mean value of the positive mobility above 0 8 mm is 1 36 which is higher than the result 1 22 obtained by Tyndall, Starr and Powell,* though it is in agreement with the value generally accepted The results confirm their observation that over a wide range water vapour has no effect on the positive mobility Below a vapour pressure of 0 8 mm the positive mobility rises rapidly its value in dry air being 1 65 This high value cannot be due to the fact that the initial ions have only partly been transformed into final ions since the rate of transformation is more rapid in dry than in moist air and the ions in moist air are apparently fully aged Values of this order have repeatedly been obtained in this laboratory in dry air by the alternating field method The age of the ions in these experiments lay between 0 1 and 0 2 second

That the measurements of the diffusion coefficient are correct seems hardly open to question since results of the same character have been obtained by a widely different method The difference between these results and those obtained by Tyndall and Grindley's and the alternating field method cannot be attributed to ageing effects of the type hitherto known, as the ages are of the same order, 0 2 second, in all cases The only point of similarity in the current-voltage and diffusion experiments is that the field in which the measurements are made is very small in both cases It is zero in the diffusion apparatus as the voltage applied serves only to collect the ions which have not diffused to the walls of the fine tubes, and in the mobility estimations by the current-voltage method its greatest value is 1 6 volt per centimetre In most mobility measurements the fields used have been of the order 100–200 volt per centimetre or even higher It therefore seemed possible that the effect of water vapour on the ordinary small ion might be very different from its effect in fields of the order generally used Accordingly attempts were made to measure mobilities in fields of different strengths, using the method of surface ionisation due to Rutherford and Child

---

* 'Roy Soc Proc,' A, vol 121, p 172 (1928)

Rutherford-Child Method *—If the ionisation between two parallel plates d cm apart is confined to the surface of one of them the current density is given by

$$i = \frac{9E^2}{32\pi d}k,$$

where E is the field between the plates and k the mobility of the ions which are driven across the space by the field

The apparatus is shown in fig 6 An α-ray source consisting of a deposit

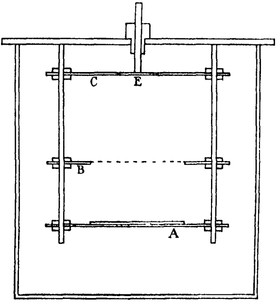

FIG 6

---

* Rutherford, 'Phil Mag,' vol 2, p 210 (1901), Child, 'Phys Rev,' vol 12, pp 65, 135 (1901)

of polonium on a bismuth disc 6 cm diameter is mounted on a brass plate A at a distance of 3 5 cm from a sheet of fine gauze which is stretched across an opening 6 cm wide in a brass ring B The α-rays produce a layer of ionisation in which the intensity falls to zero at a distance of 4 mm above the gauze An electrode E, 2 5 cm diameter, surrounded by a guard ring C from which it is separated by a gap 0 4 mm wide, is mounted parallel to B at a distance of 4 cm The three plates are mounted on three screwed brass rods attached to a heavy brass base A and B are connected together and insulated from the supports by ebonite washers The electrode is adjusted to lie in the plane of the guard ring It is supported by a rod passing through the base from which it is insulated by an ebonite plug The apparatus was enclosed in a copper box which could be made air-tight and the humidity was varied by sulphuric acid solutions placed in a dish on the bottom The capacity of the apparatus and the Lindemann electrometer to which it was connected was 15 8 cm

The current was measured with voltages up to 4 applied between B and C, so that the highest field was 1 volt per centimetre The curve connecting i and E^2 was a straight line through the origin Some of the results for the mobilities of positive and negative ions are shown in fig 7 The three maxima occur at the same vapour pressures as the first three maxima for the diffusion coefficient and the results therefore confirm the existence of the periodic variation of the mobility with the vapour pressure in low fields The time taken by the ions to cross from B to C depends on the voltage, the minimum age which corresponds to the highest field used being 3 seconds

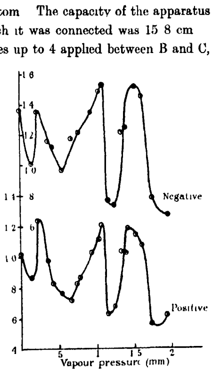

Fig 7

Experiments were also made with a distance of 3 2 cm between source and gauze and 2 cm between B and C As the strength of the polonium source had decreased somewhat it was necessary to use a thick layer of ionisation to get the linear relation between i and E^2 to hold up to sufficiently high field strengths On account of the thickness of the layer it was not possible to obtain absolute values of the mobility The highest voltage used was 4, the corresponding value of the field being 2 volts per centimetre On plotting the relation between i and E^2 the current readings for values of E^2 between 0 and 2, *i e*, for fields between 0 and 1 4 volts per centimetre were much larger than would be expected and fluctuated considerably with the vapour pressure The large values of the current were attributed to the diffusion of ions to the electrode on account of the larger density of ionisation and the reduced distance between the plates The points for values of E^2 between 2 and 4, *i e*, for fields between 1 4 and 2 volts per centimetre lay on a straight line which did not pass through the origin This linear relation between i and E^2 broke down when voltages higher than 4 were applied Probably if a stronger source of ionisation had been available the relation would have held over a wider range The slope of the straight part of the curve was taken as a measure of the mobility The results are shown in fig 8 The oscillations have almost completely disappeared, the points for ions of both signs lying on smooth curves It appears therefore that in fields up to about 1 volt per centimetre the mobility varies periodically with the vapour pressure, but that when the field is increased to 1 4 volts per centimetre the periodic variation disappears and

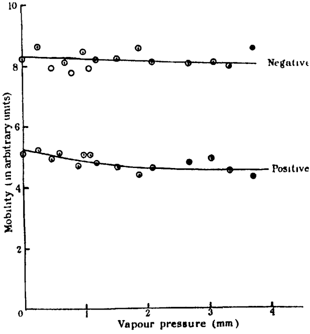

Fig 8

in higher fields the mobility varies in the manner observed by Tyndall and Grindley

Discussion

The variation of the negative mobility in air with the humidity has been examined by Tyndall and Grindley, Erikson, Griffiths and Awbery and Zeleny * They are all agreed that the negative mobility gradually decreases as the water vapour content is increased Tyndall, Starr and Powell (*loc cit*) found that water vapour had no effect on the mobility of the positive ion, while Zeleny found that it produced a slight increase in mobility The agreement between Tyndall, Starr and Powell's results and those obtained by the alternating field method has already been discussed

It is difficult to compare the diffusion measurements with those of other workers Townsend† and Franck and Westphal (*loc cit*) believed that there was a real difference between the diffusion coefficients of positive ions produced by X-rays and those produced by α- and β-rays They attributed the difference to the production of doubly charged ions by X rays On the other hand, Millikan and his co-workers, using the oil drop method, were unable to find any evidence of the production in air of positive ions with double charges by X-rays, while Salles, using a method of measuring k/D devised by Langevin, found that the positive ions produced by γ-rays, which presumably should have the same effect as X-rays, were singly charged If we compare the results given in Table II, which have been obtained in the present work, for ions produced by α-rays with those given in Table I for ions produced by X-rays the agreement is fairly satisfactory In dry air the values obtained in the present work are $D_+ = 0\ 0277$ and $D_- = 0\ 0439$, while Townsend's values are $D_+ = 0\ 028$ and $D_- = 0\ 043$ In moist air the values are $D_+ = 0\ 0348$, $D_- = 0\ 0373$ and $D_+ = 0\ 032$ and $D_- = 0\ 035$ respectively Bearing in mind the vagueness of the terms " dry " and " moist " the results are sufficient to show that under certain conditions the diffusion coefficients of positive ions produced by α-rays and X-rays are identical The differences in Townsend's and Franck and Westphal's work are probably due to differences in the state of drying and the purity of the gas The experiments of the latter workers in which they believed they produced a separation of positive ions bearing double charges by allowing the ionised gas to pass through sheets of wire gauze before the diffusion coefficient was measured, may be explained on the assumption that they were dealing with a mixture of ions of different mobilities. The lighter ions would naturally diffuse to the gauze in larger numbers than the heavier resulting in a low value for the diffusion coefficient of the ions which passed through.

---

* Tyndall and Grindley, *loc cit*, Erikson, 'Phys Rev,' vol. 30, p 791 (1928), Griffiths and Awbery, 'Proc Phys Soc,' vol 41, p 240 (1929), Zeleny, 'Phys Rev,' vol 34, p 310 (1929)

† 'Roy Soc Proc,' A, vol 80, p 207 (1908), and vol 81, p 464 (1908)

Likewise, the rapid changes in the value of the diffusion coefficient with small changes in the humidity cannot be ascribed to the presence of doubly charged ions at certain vapour pressures as precisely similar changes in the mobility have been observed under certain conditions. It has already been suggested that the ordinary small ion may possess very different properties in weak fields to those it possesses in the higher fields ordinarily used in mobility measurements. This hypothesis seems to be confirmed by the results obtained by the Rutherford-Child method. In view of the fact that the measuring fields used by other workers vary from 1400 volts per centimetre in Erikson's work down to about 3 volts per centimetre in Zeleny's, while the periodic variation disappears at about 1.4 volts per centimetre, it is not surprising that previous workers have not observed this effect.

Comparing the results obtained at the lower values of the field at an age of about 2.5 second with the results obtained by the diffusion method at an age of 0.2 second, it is clear that in the former case the oscillations are more highly developed. The values for the negative mobility vary between 1.5 and 0.8 cm. per second per volt per centimetre, and for the positive between 1.2 and 0.6. The corresponding variations in the values deduced from the diffusion measurements are from 2 to 1.5 cm. per second per volt per centimetre and from 1.4 to 0.9. Apart from the absolute values, if the results for the Rutherford-Child apparatus for positive and negative ions are plotted from the same origin the curves overlap considerably, so there can be no doubt that the negative mobility is lowered by increasing the age. This raises the question whether the phenomenon is completely developed at the shorter age used in the diffusion measurements. An answer to this would necessitate measurements of the diffusion coefficient at a greater age. The apparatus in its present form is not suited for this work.

The humidity has been varied by changing the moisture content of cotton wool and also by means of sulphuric acid solutions so that the phenomenon is independent of the precise method of humidity control. As a result of plotting the diffusion coefficient against the relative humidity it has been established that there is no relation between these two quantities. In fact the oscillations seem to be independent of the form of the apparatus and of all experimental conditions except the field and possibly the age of the ions

The mobility corresponding to the peaks of the negative curve is of the order 2 cm per second per volt per centimetre and if a straight line be drawn through the peak values its slope is roughly the same as that of Tyndall and Grindley's curve Similarly the mobility corresponding to the peaks of the positive curve is about 1 3 These facts seem to mean that we are dealing with ordinary positive and negative ions at the maxima of the curves The minima must then be due to the formation of a loose outer cluster of water-molecules round the ion At vapour pressures corresponding to the maxima this cluster must become unstable and break up The reason for the successive growth and shedding of this cluster is not clear, but the presence of some such process seems to be the logical inference to be drawn from the presence of the maxima and minima The electric field must either prevent the formation of the loose cluster or make it unstable at all vapour pressures, though here again the mechanism of the action is not plain

From the relation already given for the slope of the initial part of the current-voltage curve between two parallel plates in an ionised gas we find that the recombination coefficient is proportional to $(k_+ + k_-)^2/(i/V)^2$ The variation of the sum of the mobilities and the slope i/V of this curve have already been discussed In view of the significance we have attached to the peaks, dotted curves have been drawn through the maxima of the two curves A and B, fig 3 These dotted curves show the variation of $k_+ + k_-$ and i/V respectively in an electric field of a strength sufficient to destroy the oscillations The ratio of the square of the ordinates of B to the square of the ordinates of A, which we have seen is proportional to the recombination coefficient, is shown in C In the absence of an electric field we shall have a series of oscillations superposed on this The curve shows that the recombination coefficient has a maximum value, about four times its value in dry air, at a vapour pressure of 4 mm The existence of this maximum is supported by the fact that the currents in the diffusion apparatus are considerably smaller between 3 and 5 mm, than at higher and lower vapour pressures Since recombination must play a large part in reducing the density of ionisation in the space between A and B, fig 2, this observation supports the idea that there is a maximum value of the recombination coefficient about 4 mm pressure When a more accurate investigation of the recombination coefficient is made it may be found that the variation shown by Curve C, fig 4, is not quantitatively accurate, but that a considerable variation exists there can be no doubt

Application to Atmospheric Electricity

The potential gradient in the atmosphere near the ground is, in many places, of the order 1 volt per centimetre Considerable variations in atmospheric conductivity may therefore be expected to occur in such places owing to the changes of ionic mobility with small changes in humidity As the atmosphere is probably not very homogeneous from the point of view of water vapour content, it is possible that abrupt changes of conductivity may occur in space as well as in time Even in places where the potential gradient exceeds the critical value, the ionic content of the air, in so far as it is controlled by recombination between small ions, will vary considerably with variation in humidity

Summary

The variation of the diffusion coefficient of ions in air with the water vapour content has been examined by Townsend's method

The diffusion coefficient of ions of both signs exhibits a periodic variation with the vapour pressure

This result has been confirmed by determinations of the variation of the sum of the mobilities of positive and negative ions, derived from conductivity observations in weak fields

Further confirmation has been obtained by determination of the positive and negative mobilities separately, in weak fields, by the Rutherford-Child method By the same method, it has been shown that an increase in the field-strength from 1 to 1 4 volts per centimetre causes the periodic variation to disappear

The Rutherford-Franck alternating-field method gives results in agreement with those of other observers

Apart from periodic variations, it has been shown that the ionic recombination coefficient varies considerably with humidity The maximum value is at about 4 mm vapour pressure

One of us (T E N) is indebted to the Ministry of Education, Irish Free State, for a research grant

Measurements on the Ranges of α-Particles

By G. I. HARPER and E. SALAMAN, Newnham College, Cambridge

(Communicated by Sir Ernest Rutherford, P.R.S.—Received January 21, 1930.)

Introduction

Measurements of the stopping power of a gas relative to air, which will be defined as the ratio of the range of an α-particle in air to the range in the gas, have been made by T. S. Taylor and van der Merwe,[*] the former using a scintillation method for α-particles from radium C′ and polonium, the latter a Wilson chamber method for polonium only. These two methods did not give accurate results, owing, in both cases, to the difficulty in determining the range to a high degree of precision. Experiments have recently been carried out by Joliot and Onoda[†] to obtain an accurate Bragg curve for the α-particles from polonium in hydrogen, and by Onoda[‡] in oxygen. Estimating the extrapolated range as defined by Henderson,[§] they have then calculated the stopping powers of these gases using the value of the range in air given by I. Curie.[||]

In the experiments to be described, the extrapolated ranges have been measured for α-particles from radium C′, thorium C, thorium C′ and polonium in air, oxygen, nitrogen, argon and hydrogen, only the portion of the Bragg curve from the maximum to the end of the range being experimentally determined. In obtaining this portion of the Bragg curve the distance of the source from the ionisation chamber was varied, the pressure being kept constant during one set of observations.

Apparatus

The apparatus employed is shown to scale in fig. 1. It consists of a brass cylinder about 50 cm. long, at one end of which is the ionisation chamber I, resembling that used by Geiger[¶] in his determination of the range of α-particles from radium C′. The parallel plate electrodes P_1, P_2 and P_3 are placed perpendicular to the path of the rays. P_1 is a brass disc connected to a quadrant electrometer of sensitivity 800 divisions per volt, P_2 a wire grid charged to a potential sufficient to give saturation and P_3 a second wire grid, earthed, and

---

[*] Taylor, 'Phil. Mag.,' vol. 26, p. 402 (1913); v. d. Merwe, 'Phil. Mag.,' vol. 45, p. 379 (1923).

[†] 'J. Physique,' vol. 9, p. 175 (1928).

[‡] 'J. Physique,' vol. 9, p. 185 (1928).

[§] 'Phil. Mag.,' vol. 42, p. 538 (1921).

[||] 'Ann. Physique,' vol. 3, p. 299 (1925).

[¶] H. Geiger, 'Z. Physik,' vol. 8, p. 45 (1921).

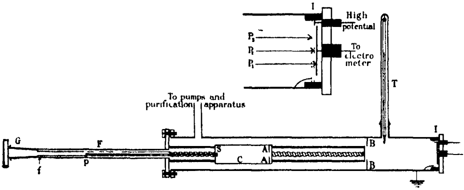

FIG 1

serving as a shield to prevent ions produced on the left of P_2 from entering the ionisation chamber Ebonite insulation is used, the wire grids being held in position by ebonite rings The separation of the electrodes P_1 and P_2 and also of P_2 and P_3 is 2 mm , and as the greatest air pressures were about 17 cm the ionisation was measured over a fraction of less than 0 005 of the range The ionisation chamber has a diameter of 4 cm and the beam of α-rays is stopped down so that the entire beam enters the chamber at all distances of approach used in the measurements The maximum difference in length of the paths of the particles before entering the ionisation chamber due to the spreading of the beam is less than the experimental error The source of α-particles S and the slit A limiting the beam are mounted on a carriage sliding on rails The carriage is moved by a screwed rod rotated by a ground glass joint G at the end of the glass tube F attached to the cylinder as shown A brass rod *p* rigidly attached to the carriage extends into F to indicate the position of the source The distance from the end of this pointer to a fixed mark *f* on the tube F was measured by a travelling microscope. A thermometer T measured the temperature inside the chamber, which could be exhausted to a pressure of 0 001 mm The pressure of the gas was measured by a wide bore mercury manometer, the mercury levels being read by a cathetometer The pressure was measured to an accuracy of 0 01 cm and the temperature to 0 1° C The pressures used were so chosen that the end portions of the ranges could be examined in the ionisation chamber and were thus different for α-particles of different ranges At the pressures used the α-particles from a source of activity equivalent to 1 mgm of radium gave a maximum ionisation current of the order of 200 divisions per minute.

Gases

The air used was dried by passing slowly over calcium chloride and phosphorus pentoxide. Hydrogen was obtained from a cylinder and was further purified by bubbling through concentrated sulphuric acid and by passing over charcoal cooled in liquid air. Oxygen was obtained by heating potassium permanganate, the gas being passed through a tube containing glass wool and then over caustic potash and phosphorus pentoxide. Cylinder nitrogen and argon were employed and were dried by passing over phosphorus pentoxide. The argon was 99 per cent pure, the impurities being oxygen and nitrogen. It was calculated that in no case could impurities be present in sufficient quantity to affect appreciably the value of the range as measured.

Corrections for Decay of Sources

In the case of radium C′ correction for the decay was made using the tables from "Radioaktivitat" by Meyer and Schweidler. The decay of the thorium (B + C) sources used was corrected for taking the half value period as 10.6 hours.

Results

A specimen curve is given in fig. 2 which shows long and short range α particles from thorium (C′ + C″) in hydrogen. A list of the ranges obtained is given in Table I. The extrapolated ranges R_m were reduced to a pressure of 76 cm of mercury and a temperature of 15° C by the relation

$$R = R_m \times p/76 \times 288/(273 + t)$$

where p denotes the pressure used and t the temperature. In each case the value given is the mean of at least two or three determinations. The greatest deviation of any single value from the mean was less than 0.3 per cent.

Table I

Source	Air	Oxygen	Nitrogen	Argon	Hydrogen
	cm	cm	cm	cm	cm
ThC′	8.61	8.10	8.67	8.99	40.88
RaC′	6.94	6.55	6.98	7.27	32.74
ThC	4.72	4.46	4.75	5.00	21.61
Po	3.87	3.64	3.89	4.17	17.29

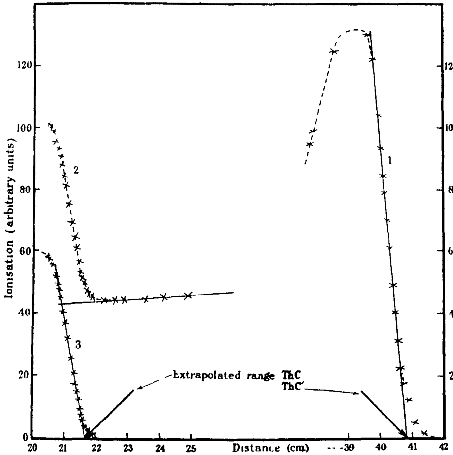

Fig 2—Curve 1 ThC′ α particles in Hydrogen Curve 2 (ThC + ThC′) α particles in Hydrogen Curve 3 ThC α particles in Hydrogen

Allowing for the errors which might have been made in measurement and especially also in the drawing of the straight line portions of the curves, these values can be taken as correct to about 1 part in 500

Some of the values obtained by other workers are given in Table II

While the results for polonium agree very well with those of Curie, Joliot and Onoda, and Onoda, the ranges in air found for thorium C′, radium C′ and thorium C are all smaller than the values hitherto obtained The deviation is greatest for the particles from thorium C, and in this case it seems to be definitely outside the range of experimental error We cannot suggest any satisfactory explanation for this discrepancy in the case of thorium C It

Table II

Observer *	Source	Air	Oxygen.	Hydrogen
		cm	cm	cm
Henderson	ThC′	8 616	–	—
Geiger	ThC	8 617	—	—
Henderson	RaC	6 953	—	-
Geiger	RaC′	6 971	—	—
Curie and Behounek	RaC′	6 96	—	—
Henderson	ThC	4 778	—	—
Geiger	ThC	4 783	—	-
Geiger	Po	3 925	-	—
Curie	Po	3 87	—	
Joliot and Onoda	Po	—	—	17 30
Onoda	Po	—	3 63	—

* Curie and Behounek, J Physique,' vol 7, p 125 (1926), and *loc cit*

may be noted, however, that Rosenblum† has found that the α-particles consist of four groups with different initial velocities, the main group being that of second greatest velocity To make sure that the differences in the values were not due to some difference in the conditions of the various experiments, tests were made on the long and short range thorium particles to find if the values could be affected by any of the following alterations, viz —

1 The depth of the ionisation chamber P_1 P_2 approximately halved
2 A second screen B inserted
3 Using the maximum and minimum possible pressures
4 Placing a mica screen in front of the source (Geiger used a mica screen in all his measurements except in the case of radium C′)

Further experiments were then made by varying the pressure and keeping the distance constant The results obtained were in all cases unchanged In case 4, it was found that the stopping power of the mica did not change sufficiently with velocity for this to affect the results The slopes of the straight line portions of the curves for thorium C′, radium C′ and thorium C were compared with those of Henderson's curves and were found to be practically identical Thus we were unable to find the cause of the discrepancy between other observers' values and ours

---

† S Rosenblum, 'C R,' vol 188, p 1401 (1929)

Velocity Considerations

The ranges obtained may be considered in relation to the initial velocities of the α-particles as measured by Briggs and Laurence * Assuming the law

$$V^3 = \lambda R,$$

where V is the velocity and R the range, the ranges can be calculated from the velocities by taking the data for radium C′ as a basis of comparison For the accuracy required in the values of the velocities, the differences between the values of Briggs and Laurence are negligible The agreement of the observed ranges with the values calculated from the velocities is by no means exact as can be seen from fig 3 In fig 3 the differences between the observed ranges and the calculated ranges are plotted against the latter, the ranges of radium C′ being taken as unity The difference curve appears to be of the same general form in each case, having a maximum negative value for short range thorium C′ α particles

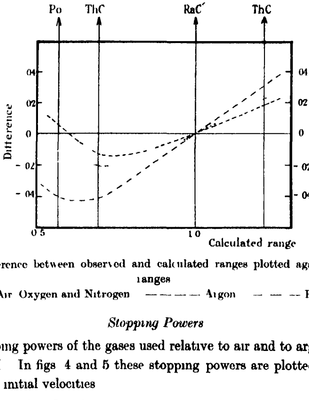

Fig 3—Difference between observed and calculated ranges plotted against calculated ranges

Air Oxygen and Nitrogen ———— Argon — — — Hydrogen

Stopping Powers

The stopping powers of the gases used relative to air and to argon are given in Table III In figs 4 and 5 these stopping powers are plotted against the cubes of the initial velocities

---

* Briggs, 'Roy Soc Proc,' A, vol 114 p 341 (1927) Laurence, 'Roy Soc Proc A, vol 122, p 543 (1929)

Table III

Stopping power = range in air/range in gas

Source	Air	Oxygen	Nitrogen	Argon	Hydrogen
ThC′	1	1 060	0 993	0 958	0 211
RaC′	1	1 058	0 994	0 954	0 214
ThC	1	1 059	0 993	0 940	0 218
Po	1	1 062	0 993	0 929	0 224

Stopping power = range in argon/range in gas

Source	Air	Oxygen	Nitrogen	Argon	Hydrogen
ThC′	1 044	1 110	1 037	1	0 220
RaC′	1 047	1 110	1 042	1	0 222
ThC	1 059	1 121	1 053	1	0 231
Po	1 076	1 145	1 071	1	0 241

Table IV gives the values obtained by other workers

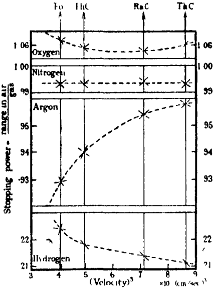

FIG 4

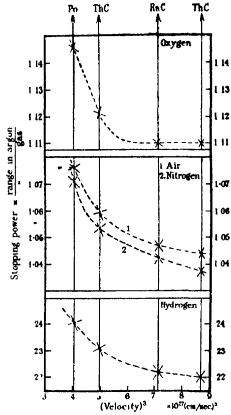

FIG 5

Table IV

Stopping power = range in air/range in gas

Observer	Source	Air	Oxygen	Nitrogen	Argon	Hydrogen
Taylor	RaC′	1	1 11	—	—	0 224
Taylor	Po	1	1 10		—	0 224
van der Merwe	Po	1	1 06	0 99	—	0 26
Joliot and Onoda	Po	—	—	—	—	0 223
Onoda	Po	—	1 066		—	—

From fig 5 it would appear that the stopping power relative to argon varies in the same way for all the gases examined

Gurney, Gibson and Gardiner and Gibson and Eyring* have measured the stopping powers of certain gases relative to air for different small portions of the ranges Their experiments give the distance δx travelled by the α-particles in the gases used for a definite small decrease δE in the energy Thus the stopping power σ of a gas relative to air is expressed as

$$\sigma = \frac{\delta x_{\text{air}}}{\delta E} \Big/ \frac{\delta x_{\text{gas}}}{\delta E}$$

Whence

$$\frac{\delta x_{\text{gas}}}{\delta E} = \frac{\delta x_{\text{air}}}{\delta E} \quad \frac{1}{\sigma}$$

Assuming that extrapolated ranges R correspond to equal absorptions of energy E, this equation can be integrated —

$$\int_0^E \frac{\delta x_{\text{gas}}}{\delta E} dE = \int_0^E \frac{\delta x_{\text{air}}}{\sigma \, \delta E} dE$$

Therefore

$$R_{\text{gas}} = \int_0^{R \text{ gas}} dx = \int_0^{R \text{air}} \frac{dx}{\sigma}$$

Hence by integrating the curves of $1/\sigma$ plotted against distance in air, the range in a gas can be calculated, assuming the values we have obtained in the case of air This can only be done for the cases of hydrogen and argon and the values found are given in Table V together with the experimental results The agreement is as good as can be expected from the data available

---

* Gurney, 'Roy Soc Proc ' A, vol 107, p 340 (1925), Gibson and Gardiner, 'Phys Rev ,' vol 30, p 543 (1927), Gibson and Eyring 'Phys Rev ' vol 30, p 553 (1927)

Table V

Source	Argon		Hydrogen	
	Observed	Calculated	Observed	Calculated
	cm	cm	cm	cm
ThC	8.99	9.16	40.88	40.76
RaC	7.27	7.44	32.74	32.72
ThC	5.00	5.10	21.61	21.44
Po	4.17	4.19	17.29	17.24

Gaunt's Theory of the Stopping Power of Hydrogen

The stopping power of hydrogen atoms for α particles has been calculated according to the new quantum mechanics by Gaunt* who obtains the formula

$$-\frac{dT}{dx} = \frac{4\pi NE^2\varepsilon^2}{\mu v^2}\log\frac{\gamma'\mu v^3}{2\pi\omega' E\varepsilon}$$

where $-dT/dx$ is the rate of loss of energy for an α-particle of charge E and velocity v, N is the number of atoms per cubic centimetre and μ and ε are the mass and charge of an electron, ω' is the frequency of the head of the Lyman series and γ' is a constant equal to 1.02 This formula is the same as those previously obtained by Bohr and by Fowler† except in the value of the constant γ' Gaunt considers that this equation will have the same *form* in the case of hydrogen molecules but that there is no reason to suppose that the constant γ' which is given in a very complicated way, will have the same value as for hydrogen atoms By integration of this equation the range R is obtained as a function of the initial velocity v_0 --

$$\int_0^R dx = -\frac{m\mu}{4\pi NE^2\varepsilon^2}\int_{v_0}^{0}\frac{v^3\,dv}{\log(\gamma'\mu v^3/2\pi\omega' E\varepsilon)},$$

where m is the mass of the α-particle On making the substitution

$$u = -\tfrac{1}{3}\log\frac{\gamma'\mu v^3}{2\pi\omega' E\varepsilon},$$

this equation reduces to

$$R = \frac{m\mu}{12\pi NE^2\varepsilon^2(\gamma'\mu/2\pi\omega' E\varepsilon)^{4/3}}\int_{\infty}^{-\frac{1}{3}\log(\gamma'\mu v_0^3/2\pi\omega' E\varepsilon)}\frac{e^{-4u}\,du}{u},$$

---

* 'Proc Camb Phil Soc,' vol 23, p 732 (1927)

† Bohr, 'Phil Mag' vol 44 p 10 (1913), Fowler, 'Proc Camb Phil Soc' vol 22 p 793 (1925)

which can be evaluated The ranges R for different values of v_0 were calculated using the values of the constants given in the ‘ Physical Review Supplement,’ July, 1929, and the value 1 02 for γ' (or 3 10 10^{-16} for the value of the ratio of γ' to ω') In order to compare the theoretical values for monatomic hydrogen with the observed values for molecular hydrogen, the calculated ranges were halved and are plotted in fig 6 (Gaunt, in his calculations, uses the same value of γ'/ω' as for atomic hydrogen although ω' should be proportional to the ionisation potential) Clearly this modification of the formula does not give the correct values of the ranges in molecular hydrogen

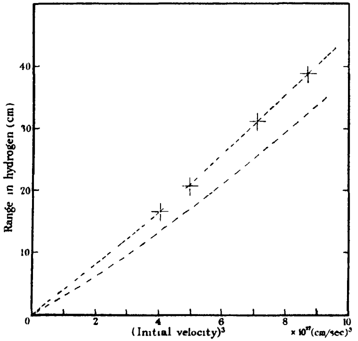

Fig 6

— — — Theoretical curve $\gamma'/\omega = 3\ 10\ \ 10^{-16}$
— - - - Theoretical curve $\gamma'/\omega' - 1\ 20\ \ 10^{-16}$
+ + + Experimental values

Assuming the form of the equation to be correct, the value of γ'/ω' was calculated from the known initial velocity and range of radium C′ and was found to be (1 20 ± 0 02) × 10^{-16} Using this value of γ'/ω', a new theoretical curve was calculated and is shown in the upper curve of fig 6 The experimental values lie on this curve with an accuracy well within the limits of experimental error In his paper, Gaunt calculates the value of $(V_0{}^4 - V^4)/X$, where V_0 and V are the velocities at the ends of a short interval of length X, and compares the result with Gurney's experimental value (*loc cit*) for the mean velocity 1 98 × 10^9 cm per second Gurney's experimental value is 5 4 × 10^{35}, Gaunt's calculated value, 6 16 × 10^{35}, and the calculated value using our value of γ'/ω', 5 39 × 10^{35} The theory of Gaunt for hydrogen atoms can therefore be extended to the case of molecular hydrogen if a new value of the ratio of γ' to ω' equal to (1 20 ± 0 02) × 10^{-16} is used The calculated values of both stopping powers and ranges agree with the observed values within the limits of experimental error

γ' may be calculated by assuming a value for the ionisation potential of molecular hydrogen Gaunt's theory gives no indication as to which value of this quantity should be used, and there are considerable variations in the values obtained both theoretically and experimentally Assuming the value 15 3 volts obtained from the spectroscopic data of the International Critical Tables, we deduce the value 0 446 for γ', but whatever value of the ionisation potential is adopted, the value of γ' obtained is much less than the value for atomic hydrogen Thus although the expression for the rate of loss of energy remains of the same form in molecular hydrogen, γ' and ω' both alter Had γ' remained unaltered, then the rate of loss of energy would have been the same in molecular hydrogen as in atomic hydrogen except for the difference brought about by their different ionisation potentials, but since γ' is less, it appears that the processes controlling the rate of loss of energy of an α-particle are less effective in molecular hydrogen

Summary

The ranges of α-particles of different initial velocities have been measured in certain gases and the stopping powers of these gases obtained The gases used were air, oxygen, nitrogen, argon and hydrogen The results for polonium are in agreement with those of Curie, Joliot and Onoda, and Onoda In the case of argon and hydrogen the ranges agree with those calculated from the stopping powers obtained by Gurney The relation between ranges and initial velocities is discussed Finally, it is shown that the theory of Gaunt for the stopping power of hydrogen atoms can be extended to the case of molecular hydrogen

In conclusion we wish to express our thanks to Sir Ernest Rutherford for his interest throughout this work, and to Dr Chadwick for his advice and help We further wish to thank Dr Chadwick and Mr Crowe for the preparation of the radioactive sources

The Effect of Rotation upon the Lift and Moment of a Joukowski Aerofoil

By W G Bickley, D Sc , City and Guilds (Engineering) College

(Communicated by G I Taylor, F R S —Received December 20, 1929)

1 *Introduction*

In a recent paper* the author has given a number of general formulæ concerning two dimensional hydrodynamics, including the working out in some detail of a solution of the problem of a rotating cylinder by a method outlined by him some years ago † It was suggested by Prof G I Taylor that the application of these methods and results to the Joukowski and other aerofoil sections would be interesting, and perhaps useful, and the present paper is an account of the results obtained

The solution of the main problem, that of the effect of rotation upon the lift and moment coefficient, necessitated the examination of the force and moment due to fluid pressure acting upon a cylinder in the most general case (the motion of the cylinder being considered as compounded of a translation and a rotation, with circulation about the cylinder superimposed), and the author's solution has been recently published ‡

2 *Summary of Results*

The results to be obtained may be briefly summarised for the benefit of those who may not wish to follow their detailed deduction

The effect of ordinarily occurring thickness is shown to be small, and neglecting it we find, as the effect of the rotation —

(*a*) An increase in the Joukowski circulation, Γ, of amount

$$\delta\Gamma = \tfrac{1}{4}\pi\omega c^2, \qquad \text{(Equation 5 43, } \textit{infra}\text{)}$$

where ω is the angular velocity, and c the chord of the aerofoil

---

* 'Phil Trans ,' A, vol 228, p 235 (1929) Referred to in the text as T D P

† 'Phil Mag ,' vol 35, p 500 (1918)

‡ 'Roy Soc Proc ,' A, vol 124, p 296 (1929) Referred to in the text as H C See also H Glauert 'Aeronautical Research Committee, R & M 1215' and H Lamb, *ibid* , 1218 (1929)

(*b*) A change in the lift coefficient, k_L, of amount

$$\delta k_L = \frac{\pi}{4}\frac{\omega c}{U}\cos^2\gamma \qquad \text{(Equation 6 35, } \textit{infra}\text{)}$$

$$= \frac{\pi}{4}\frac{\omega c}{U} \qquad \text{(when } \gamma \text{ is small),}$$

U being the velocity of (the hydrodynamic centre of) the aerofoil and γ the angle of incidence

(*c*) A small drag, producing a change in the drag coefficient, k_D, of amount

$$\delta k_D = \frac{\pi}{8}\frac{\omega c}{U}\sin 2\gamma \qquad \text{(Equation 6 38, } \textit{infra}\text{)}$$

(*d*) A change in the moment coefficient (about the leading edge), k_m, of amount

$$\delta k_m = \frac{\pi}{8}\frac{\omega c}{U}\cos\gamma \qquad \text{(Equation 6 47 } \textit{infra}\text{)}$$

$$= -\frac{\pi}{8}\frac{\omega c}{U} \qquad \text{(when } \gamma \text{ is small)}$$

While the work was in progress, H Glauert was applying the method of trigonometric series to the " thin " aerofoil, and his paper* contains indications of the possible usefulness of the knowledge, and an extension to the case of finite span The above results all agree (when γ is small) with his Considering the generality of Glauert's " skeleton " section, and its possible divergences from the circular arc skeleton of the Joukowski section, together with the smallness of the effects of thickness found below, it would seem evident that the above formulæ apply to any ordinary aerofoil section with sufficient accuracy, so that a detailed examination of other sections given by mathematical formulæ would scarcely seem to be worth while—at any rate from the point of view of practical aerodynamics

3 *The Transformation*

In Joukowski's original transformation, the aerofoil section and the region outside it in one plane (our z-plane) are transformed into a circle and the region outside it in another plane† (our τ-plane), by the formula

$$z = \frac{c}{4}\left(\tau + \frac{1}{\tau}\right) \qquad (3\ 1)$$

as shown in the figure, the points at infinity corresponding $dz/d\tau$ has zeroes where $\tau = \pm 1$ Any circle through these points (A and B) in the τ-plane is transformed into a circular arc of chord c in the z-plane (dotted curves), any

---

* ' Aeronautical Research Committee, R & M ,' 1216 (1929)

† Though on account of an elegant geometrical construction these planes are usually superposed The transformation is then $z = \tau + c^2/\tau$ and $4c$ is the chord It has been thought desirable to modify this as above for the present purpose

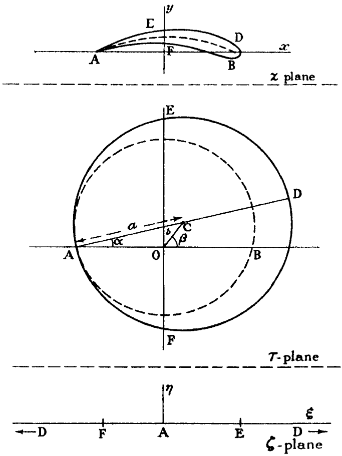

circle touching one of these at the point $\tau = -1$, and surrounding it, such as AEDFA, is transformed into a curve having a cusp at $z = -\frac{1}{2}c$, and a blunt leading edge, surrounding the corresponding circular arc To use the methods of T D P, we must transform the circle into the real axis of the ζ-plane Taking $\zeta = 0$ to correspond to $\tau = -1$, the formula is

$$\zeta = i\,\frac{\tau + 1}{\tau - \mu} \tag{3 21}$$

or

$$\tau = \frac{\mu\zeta + i}{\zeta - i} \tag{3 22}$$

where μ is the value of τ at the point D diametrically opposite $\tau = -1$. If the centre, C, of the circle is at $\tau = be^{i\beta}$ (where b is small, usually < 0.1, so that its square will frequently be neglected) we shall have

$$\mu = 1 + 2be^{i\beta} \tag{3.23}$$

Also if in the τ plane, $AC = a$ and $\angle DAB = \alpha$,

$$1 + \mu = 2ae^{i\alpha} \tag{3.24}$$

It is easy to show that the angle subtended by the circular arc at its centre is 4α, and that the camber is $\frac{1}{2}\tan\alpha$, and that the maximum breadth of the section is, approximately, $3\sqrt{3}/4 \; b\cos\beta \; c$.

Combining (3.1) and (3.22) we get the required transformation,

$$z = \frac{c}{4}\left(\frac{\mu\zeta + i}{\zeta - i} + \frac{\zeta - i}{\mu\zeta + i}\right) \tag{3.31}$$

whence

$$\frac{dz}{d\zeta} = -\frac{i(1+\mu)c}{4}\left\{\frac{1}{(\zeta - i)^2} - \frac{1}{(\mu\zeta + i)^2}\right\}, \tag{3.32}$$

By the substitution $\zeta = \tan\frac{1}{2}t$ (*cf* T. D. P., *passim*) we obtain

$$z = \frac{c}{4}\left\{\frac{(\mu - 1)e^{it} + (\mu + 1)}{2e^{it}} + \frac{2e^{it}}{(\mu - 1)e^{it} + (\mu + 1)}\right\}, \tag{3.33}$$

and if $t = r + is$, $s = 0$ is the boundary, while $s = \text{const}$ and $r = \text{const}$ are respectively stream-lines and equi-potentials for circulation round the section. As $s \to \infty$, $e^{it} \to 0$, so we can write

$$z = -\frac{c}{4}\left\{\frac{\mu + 1}{4}e^{-it} - \frac{\mu - 1}{2} + \frac{2}{(\mu + 1)}\sum_{n=0}^{\infty}\left(\frac{\mu - 1}{\mu + 1}\right)^n e^{i(n+1)t}\right\} \tag{3.34}$$

the series certainly converging if $s \nless 0$, this simplifies calculations for plotting the profile, stream-lines and equipotentials. It also shows that the "hydrodynamic centre" (*cf* H. C.) is the point

$$z = \frac{c}{4}\frac{\mu - 1}{2} = \tfrac{1}{4}cbe^{i\beta}$$

In the more usual form of the transformation, with the z- and τ-planes superposed (and a relation between the units necessitated by the geometrical construction), this coincides with the centre of the circle AEDF. The convenience of using such a point of reference, especially as one about which to take moments, has been realised by writers on aerodynamics,* but not, apparently, other properties of the hydrodynamic centre

The area enclosed by the profile is†

$$A = \tfrac{1}{2}c \int_{-\infty}^{\infty} \bar{z} \frac{dz}{d\zeta} d\zeta \tag{3 41}$$

Using (3 31) and (3 32) and evaluating the integral by residues, we find

$$A = \frac{\pi c^2}{16}(1 + \mu)(1 + \bar{\mu}) \left\{ \tfrac{1}{4} - \frac{1}{(\mu + \bar{\mu})^2} \right\} \tag{3 42}$$

$$= \frac{\pi c^2}{16}(1 + 2b \cos \beta + b^2) \left\{ 1 - \frac{1}{(1 + 2b \cos \beta)^2} \right\} \tag{3 43}$$

$$= \frac{\pi c^2}{4} b \cos \beta, \tag{3 44}$$

where, in the last, higher powers of b are neglected

4 *Circulation and Streaming*

The methods of T D P give us the solutions for circulation round, flow past, and translatory motion, in the forms —

(*a*) Circulation, Γ,

$$w_\Gamma = \phi_1 + \iota\psi_1 = \frac{\iota\Gamma}{2\pi} \log \frac{\zeta + \iota}{\zeta - \iota} \tag{4 1}$$

(*b*) Stream, coming from infinity in the direction $-\gamma$ (the negative sign being taken so that γ can be taken as the angle of incidence) and undisturbed velocity U

$$w_U = \phi_U + \iota\psi_U = \frac{U\iota c}{4} \left\{ \frac{(1 + \mu)e^{\iota\gamma}}{\zeta - \iota} - \frac{(1 + \bar{\mu})e^{-\iota\gamma}}{\zeta + \iota} \right\} \tag{4 2}$$

(*c*) Translation with velocity U in direction $-\gamma$, in fluid undisturbed at infinity

$$w_U' = w_U - Uze^{\iota\gamma}$$

$$= -\frac{Uc}{4} \left\{ \mu e^{\iota\gamma} + \frac{\iota(1 + \bar{\mu})e^{-\iota\gamma}}{\zeta + \iota} + \frac{(\zeta - \iota)e^{\iota\gamma}}{\mu\zeta + \iota} \right\} \tag{4 3}$$

in which the first term in brackets, being constant, may be omitted

---

* *Cf* Glauert, 'Aerofoil and Airscrew Theory' (Cambridge, 1929), p 85, where, unless the fact that the planes are superposed is borne in mind, there may be some confusion

† Bars denote, consistently, conjugate complex quantities

The impulse in translatory motion per unit length, including the momentum of fluid the profile would enclose, is $2\pi\rho \times$ the coefficient of $1/z$ in the expansion of w_U' valid near $z = \infty$. Now when z is large, $\zeta = \iota\{1 + (1 + \mu)c/4z \quad \}$ so that

$$w_U' = \frac{Uc}{4}\left\{\mu\iota\;{}^{\gamma} - \frac{(1 + \mu)(1 + \bar{\mu})e^{-\iota\gamma}c}{4z} + \frac{e^{\iota\gamma}c}{4z} + \quad \right\}$$

whence the impulse, *not* including the momentum of enclosed fluid, is

$$\begin{aligned} I_U &= \frac{\pi\rho Uc^2}{8}\left\{\frac{(1 + \mu)(1 + \mu)e^{-\iota\gamma}}{4} - e^{\iota\gamma}\right\} - \rho AUe^{-\iota\gamma} \\ &= \frac{\pi\rho Uc^2}{16}\left\{\frac{(1 + \mu)(1 + \mu)}{4}\left(1 + \frac{4}{(\mu + \bar{\mu})^2}\right)e^{-\iota\gamma} - 2e^{\iota\gamma}\right\} \end{aligned} \tag{4.4}$$

on using the value of A from (3.42). If m_x and m_y are the inertia coefficients,

$$I_U = m_x U\cos\gamma - \iota m_y U\sin\gamma,$$

so that

$$\left.\begin{aligned} m_x &= \frac{\pi\rho c^2}{16}\left\{\frac{(1 + \mu)(1 + \bar{\mu})}{4}\left(1 + \frac{4}{(\mu + \bar{\mu})^2}\right) - 2\right\} \\ &\quad - \tfrac{1}{4}\pi\rho c^2 b^2\cos^2\beta \end{aligned}\right\} \tag{4.51}$$

$$\left.\begin{aligned} m_y &= \frac{\pi\rho c^2}{16}\left\{\frac{(1 + \mu)(1 + \bar{\mu})}{4}\left(1 + \frac{4}{(\mu + \bar{\mu})^2}\right) + 2\right\} \\ &\quad \tfrac{1}{4}\pi\rho c^2(1 + b^2\cos^2\beta \quad) \end{aligned}\right\} \tag{4.53}$$

and

$$m_y - m_x = \tfrac{1}{4}\pi\rho c^2 \tag{4.53}$$

exactly, for *all* Joukowski aerofoils having the same chord.

The Joukowski condition that the velocity at the trailing edge is finite is equivalent to the condition that $dw/d\zeta = 0$ when $\zeta = 0$, where $w = w_1 + w_U'$, i.e.,

$$w = \frac{\iota\Gamma}{2\pi}\log\frac{\zeta + \iota}{\zeta - \iota} - \frac{Uc}{4}\left\{\frac{\iota(1 + \bar{\mu})e^{-\iota\gamma}}{\zeta + \iota} + \frac{(\zeta - \iota)e^{\iota\gamma}}{\mu\zeta + \iota}\right\}$$

$$\frac{dw}{d\zeta} = \frac{\iota\Gamma}{\pi(\zeta^2 + 1)} + \frac{Uc}{4}\left\{\frac{\iota(1 + \bar{\mu})e^{-\iota\gamma}}{(\zeta + \iota)^2} - \frac{\iota(1 + \mu)e^{\iota\gamma}}{(\mu\zeta + \iota)^2}\right\},$$

and so the condition is

$$\frac{\Gamma}{\pi} - \frac{\iota Uc}{4}\{(1 + \bar{\mu})e^{-\iota\gamma} - (1 + \mu)e^{\iota\gamma}\} = 0,$$

or since $1 + \mu = 2ae^{\iota\alpha}$ and $1 + \bar{\mu} = 2ae^{-\iota\alpha}$

$$\Gamma = \pi Ua\sin(\alpha + \gamma) \tag{4.6}$$

The resultant force per unit length, is

$$X + iY = i\rho\Gamma U e^{-i\gamma}$$
$$= \pi\rho U^2 ca e^{-i\gamma} \sin(\alpha + \gamma), \tag{4.71}$$

which is perpendicular to the direction of motion; it is a lift,

$$L = \pi\rho U^2 ca \sin(\alpha + \gamma) \tag{4.72}$$

and the lift coefficient is

$$k_L = \pi a \sin(\alpha + \gamma) \tag{4.73}$$
$$\simeq \pi(\alpha + \gamma)$$

The moment about the hydrodynamic centre is

$$M_c = (m_y - m_x) U^2 \sin\gamma \cos\gamma$$
$$= \tfrac{1}{8}\pi\rho c^2 U^2 \sin 2\gamma \tag{4.81}$$

About the leading edge [taken, with an error of order b^2, as the point $(c/2, 0)$] the moment is

$$M = M_c - L\frac{c}{2}\{\cos\gamma - \tfrac{1}{2}b\cos(\beta + \gamma)\}$$
$$= -\tfrac{1}{8}\pi\rho U^2 c^2 \{\sin 2\gamma + 2b(1 + \cos^2\gamma)\sin\beta$$
$$+ b\sin 2\gamma\cos\beta - b^2 \sin 2(\beta + \gamma)\}, \tag{4.82}$$

where we have used the identity $a\sin(\alpha + \gamma) = \sin\gamma + b\sin(\beta + \gamma)$. If we neglect b^2, and take γ as not being very large, so that we can put $\cos^2\gamma = 1$ and also neglect $b\sin^2\gamma$, we get the moment coefficient about the leading edge in the form

$$k_m = -\tfrac{1}{8}\pi\{\sin 2\gamma + 4b\sin\beta\} \tag{4.83}$$
$$\simeq -\tfrac{1}{8}\pi(2\gamma + 4\alpha) \tag{4.84}$$

(since $b\sin\beta = a\sin\alpha \simeq \alpha$)

$$= k_{m0} - \tfrac{1}{4}k_L, \tag{4.85}$$

k_{m0} being the moment coefficient at zero lift, i.e., when $\gamma = -\alpha$.

5. *Rotation*

For the velocity potential stream function when the profile rotates about an axis through $z = z_0$ with angular velocity ω, we require a function of ζ finite and continuous in the upper half-plane, the imaginary part of which reduces, on the real axis, to $\frac{1}{2}i\omega\,|z - z_0|^2$. We naturally take, according to the results of the previous paper (H. C.), the point z_0 as the hydrodynamic centre, $z_0 = \frac{1}{8}c\,(\mu - 1)$.

Now, on the boundary (where ζ is *real*),

$$|z - z_0|^2 = (z - z_0)(\bar{z} - \bar{z}_0) = \frac{c^2}{16}\left\{\frac{\mu\zeta + i}{\zeta - i} + \frac{\zeta - i}{\mu\zeta + i} - \frac{\mu - 1}{2}\right\}\left\{\frac{\bar{\mu}\zeta - i}{\zeta + i} + \frac{\zeta + i}{\bar{\mu}\zeta - i} - \frac{\bar{\mu} - 1}{2}\right\} \qquad (5.11)$$

This may be split into partial fractions, giving

$$\frac{c^2}{16}\left\{\frac{(\mu - 1)(\bar{\mu} - 1)}{4} + \frac{\mathrm{K}}{\zeta - i} + \frac{\bar{\mathrm{K}}}{\zeta + i} + \frac{\mathrm{L}}{\mu\zeta + i} + \frac{\bar{\mathrm{L}}}{\bar{\mu}\zeta - i}\right\}, \qquad (5.12)$$

and we easily find

$$\left.\begin{aligned} \mathrm{K} &= 2i\,\frac{\mu + 1}{\bar{\mu} - 1}, \qquad \bar{\mathrm{K}} = -2i\,\frac{\mu + 1}{\mu - 1} \\ \mathrm{L} &= i\,\frac{\mu + 1}{\mu}\left\{\frac{(\mu + 1)(\bar{\mu} + 1)}{2\,(\mu - 1)} + \frac{\mu - 1}{\mu + \bar{\mu}}\right\} \\ \bar{\mathrm{L}} &= -i\,\frac{\bar{\mu} + 1}{\bar{\mu}}\left\{\frac{(\mu + 1)(\bar{\mu} + 1)}{2\,(\bar{\mu} - 1)} + \frac{\bar{\mu} - 1}{\mu + \bar{\mu}}\right\} \end{aligned}\right\} \qquad (5.13)$$

Now because (5.12) is purely real, the real part of

$$\frac{c^2}{16}\left\{\frac{\bar{\mathrm{K}}}{\zeta + i} + \frac{\mathrm{L}}{\mu\zeta + i}\right\}$$

will differ from $\frac{1}{2}\{z - z_0\}^2$ by a constant on the boundary and it is evidently finite and continuous in the upper half-plane. We may thus take*

$$w_\omega = \phi_\omega + i\psi_\omega = \frac{i\omega c^2}{16}\left\{\frac{\bar{\mathrm{K}}}{\zeta + i} + \frac{\mathrm{L}}{\mu\zeta + i}\right\} \qquad (5.21)$$

Also, on the boundary (but not elsewhere)

$$(\phi_\omega) = w_\omega - \tfrac{1}{2}i\,\omega\,|z - z_0|^2$$
$$= \frac{i\omega c^2}{32}\left\{\frac{\bar{\mathrm{K}}}{\zeta + i} - \frac{\mathrm{K}}{\zeta - i} + \frac{\mathrm{L}}{\mu\zeta + i} - \frac{\bar{\mathrm{L}}}{\bar{\mu}\zeta - i}\right\}, \qquad (5.22)$$

---

* The procedure, and equation (5.434), at T. D. P., also give this result.

from which we find the impulse

$$I_\omega = -\iota\rho \oint (\phi_\omega)\, dz = \iota\rho \int_{-\infty}^{\infty} (\phi_\omega) \frac{dz}{d\zeta}\, d\zeta \tag{5 31}$$

$$= -\frac{\pi\rho\omega c^3}{64}\left\{\frac{(1+\mu)\bar{K}}{4} - \frac{K}{\mu+1} + \frac{\mu L}{\mu+1} - \frac{\bar{\mu}(1+\mu)\bar{L}}{(\mu+\bar{\mu})^2}\right\} \tag{5 32}$$

$$= -\frac{\iota\pi\rho\omega c^3}{64}\left[\frac{\mu-1}{\mu+\bar{\mu}}\left\{2+\frac{(1+\mu)(1+\bar{\mu})}{2(\mu+\bar{\mu})}\right\} + \frac{(\bar{\mu}-1)(\mu+1)(\bar{\mu}+1)}{(\mu+\bar{\mu})^3}\right] \tag{5 33}$$

$$= \frac{\pi\rho\omega c^3}{32}(2b\cos\beta + \iota b\sin\beta) \tag{5 34}$$

neglecting higher powers of b

For the Joukowski circulation we must have as before $dw/d\zeta = 0$ when $\zeta = 0$, but with $w = w_\Gamma + w_\omega$, i e ,

$$\frac{\Gamma}{\pi} + \frac{\iota\omega c^2}{16}\{\bar{K} + \mu L\} = 0 \tag{5 41}$$

or

$$\Gamma = \frac{\pi\omega c^2}{16}\left\{(\mu+1)(\bar{\mu}+1) - \frac{(\mu-1)(\bar{\mu}-1)(\mu+\bar{\mu}+2)}{2(\mu+\bar{\mu})}\right\} \tag{5 42}$$

$$= \tfrac{1}{4}\pi\omega c^2\left\{1 + 2b\cos\beta + b^2 - \frac{b^2(1+b\cos\beta)}{(1+2b\cos\beta)}\right\}$$

$$= \tfrac{1}{4}\pi\omega c^2\left\{1 + 2b\cos\beta + \frac{b^3\cos\beta}{(1+2b\cos\beta)}\right\} \tag{5 43}$$

This can be taken as $\frac{1}{4}\pi\omega c^2$ with a small error, or as $\frac{1}{4}\pi\omega c^2(1 + 2b\cos\beta)$ with a *very* small error It is noteworthy that the value, $\frac{1}{4}\pi\omega c^2$, was deduced by Glauert (*loc cit*) for a *thin* aerofoil of *any* section of small camber We see here that it is a good approximation for *any* Joukowski aerofoil of reasonably small thickness, it would thus seem to be a reasonable approximation for any ordinary aerofoil section

6 *Flight in a Curved Path*

We have now obtained all the necessary material for building up the results for flight in a curved path If U and γ refer to the motion of the hydrodynamic centre,* and ω is the angular velocity, equations (4 6) and (5 43) give for the total circulation

$$\Gamma = \pi U c a \sin(\alpha + \gamma) + \tfrac{1}{4}\pi\omega c^2(1 + 2b\cos\beta \quad) \tag{6 1}$$

---

* This defines γ Glauert shows that the appropriate value of γ varies with the reference point, and it is convenient to have a standard reference point *not* arbitrarily chosen

The total impulse is

$$I = I_U + I_\omega = m_x U \cos\gamma - i m_y U \sin\gamma + I_\omega \tag{6.2}$$

where I_ω is given by (5.33).

The resultant force [*cf.* H. C., equation (4.3)] is

$$X + iY = i\rho\Gamma U e^{-i\gamma} - i\omega I \tag{6.31}$$

If L′ is the lift, and D′ the drag,

$$X + iY = ie^{-i\gamma}(L' + iD')$$

or

$$L' + iD' = \rho\Gamma U - \omega I e^{i\gamma} \tag{6.32}$$

Neglecting b^2 and higher powers, we find

$$L' = \pi\rho c\left\{U^2 a \sin(\alpha + \gamma) + \tfrac{1}{4}c\omega U(\cos^2\gamma + 2b\cos\beta) - \frac{b\omega^2c^2}{32}(2\cos\beta\sin\gamma + \sin\beta\cos\gamma)\right\} \tag{6.33}$$

and the lift coefficient

$$k_L' = \pi a \sin(\alpha + \gamma) + \frac{\pi}{4}\frac{\omega c}{U}(\cos^2\gamma + 2b\cos\beta) - \frac{\pi b}{32}\left(\frac{\omega c}{U}\right)^2(2\cos\beta\sin\gamma + \sin\beta\cos\gamma) \tag{6.34}$$

Now in ordinary flight in a curved path, $\omega c/U$ is equal to c/r, r being the radius of curvature of the path of the hydrodynamic centre; $\omega c/U$ will be small, and its square multiplied by the small quantity b is negligible. Thus we have

$$\delta k_L = k_L' - k_L = \frac{\pi}{4}\frac{\omega c}{U}(\cos^2\gamma + 2b\cos\beta) \tag{6.35}$$

If we neglect b altogether, and restrict ourselves to small angles of incidence,

$$\delta k_L = \frac{\pi}{4}\frac{\omega c}{U} \tag{6.36}$$

which agrees with Glauert's result.*

D′ is small; again neglecting the product of b and $(\omega c/U)^2$, we have

$$D' = \tfrac{1}{4}\pi\rho\omega c^2 U \sin\gamma\cos\gamma, \tag{6.37}$$

$$k_D' = \frac{\pi}{8}\frac{\omega c}{U}\sin 2\gamma \tag{6.38}$$

---

* *Loc. cit.* The approximate formulæ for small angles used in the course of Glauert's work make it impossible for him to find the small effect of γ shown by the $\cos^2\gamma$ in (6.35).

Using the formula (5 32)* of H C, the moment of the pressures about the hydrodynamic centre is

$$\mathrm{M}_c' = \mathfrak{R}\iota \mathrm{U}e^{\iota\gamma}\mathrm{I} \qquad (6\ 41)$$

$$= (m_y - m_x)\,\mathrm{U}^2 \sin\gamma\cos\gamma + \mathfrak{R}\iota \mathrm{U}e^{\iota\gamma}\mathrm{I}_\omega \qquad (6\ 42)$$

$$= \tfrac{1}{8}\pi\rho c^2\mathrm{U}^2 \sin 2\gamma + \frac{\pi\rho\omega c^3 \mathrm{U}b}{64\,(1+2b\cos\beta)}\left\{\left(2 + \frac{a^2}{1+2b\cos\beta}\right)\cos(\beta+\gamma) + \frac{a^2}{(1+2b\cos\beta)^2}\sin(\beta+\gamma)\right\}$$

$$= \tfrac{1}{8}\pi\rho c^2\mathrm{U}^2 \sin 2\gamma + \frac{\pi\rho\omega c^3 \mathrm{U}b}{32}(2\cos\beta\cos\gamma - \sin\beta\sin\gamma), \qquad (6\ 43)$$

neglecting higher powers of b The moment about the leading edge [again taken as $(c/2, 0)$] is

$$\mathrm{M}' = \mathrm{M}_c' - \tfrac{1}{2}\mathrm{L}'c\{\cos\gamma - \tfrac{1}{2}b\cos(\beta+\gamma)\} - \tfrac{1}{2}\mathrm{D}'c\{\sin\gamma - \tfrac{1}{2}b\sin(\beta+\gamma)\} \qquad (6\ 44)$$

so that

$$k_m' = k_{mc}' - \tfrac{1}{2}k_\mathrm{L}'\{\cos\gamma - \tfrac{1}{2}b\cos(\beta+\gamma)\} - \tfrac{1}{2}k_\mathrm{D}'\{\sin\gamma - \tfrac{1}{2}b\sin(\beta+\gamma)\} \qquad (6\ 45)$$

or, neglecting b^2 and $b\,(\omega c/\mathrm{U})^2$,

$$k_m' = k_m - \frac{\pi}{8}\frac{\omega c}{\mathrm{U}}\cos\gamma - \frac{\pi b}{32}\frac{\omega c}{\mathrm{U}}(4\cos\beta\cos\gamma + \sin\beta\sin\gamma), \qquad (6\ 46)$$

so that

$$\delta k_m = k_m' - k_m$$

$$- \frac{\pi}{8}\frac{\omega c}{\mathrm{U}}\cos\gamma - \frac{\pi b}{32}\frac{\omega c}{\mathrm{U}}(4\cos\beta\cos\gamma + \sin\beta\sin\gamma) \qquad (6\ 47)$$

and with γ small,

$$\delta k_m = -\frac{\pi}{8}\frac{\omega c}{\mathrm{U}} - \frac{\pi b}{32}\frac{\omega c}{\mathrm{U}}(4\cos\beta + \gamma\sin\beta) \qquad (6\ 48)$$

The term $-\frac{1}{8}\pi\omega c/\mathrm{U}$ agrees with Glauert's result, expressed in our notation by

$$k_m' = k_{m0} - \tfrac{1}{4}k_\mathrm{L}' - \frac{\pi}{16}\frac{\omega c}{\mathrm{U}}, \qquad (6\ 49)$$

which differs by the last term from the (approximate) relation (4 85) usually adopted for translatory motion

In conclusion, the author would like to thank Prof G I Taylor for suggesting the problem, and for his continued interest in the work, and also Prof H Levy for various suggestions

---

* It is much regretted that by an oversight the formula for I in H C did not include a term in ω, so that the work following (5 32) there is incomplete, and some statements—especially that the moment about the hydrodynamic centre is independent of ω—are in error The author wishes to thank Dr Lamb for pointing this out

On the Spectrum of Bromine in Different Stages of Ionisation

By SURESH CHANDRA DEB, M Sc, Research Scholar, Allahabad University

(Communicated by M Saha, F R S —Received December 30, 1929)

The spectra of elements belonging to the halogen group have been investigated by many workers during recent years in their successive stages of ionisation *

Systematic classification of bromine lines has not yet been done, though there is plenty of experimental work In the arc spectrum Turner (*loc cit*) got only the fundamental lines For the spark spectrum, Bloch† has separated the groups belonging to the different stages of ionisation from λ 2200 Å to λ 6000 Å , though he did not attempt any classification

Spectral investigation has now proceeded so far that it is possible to locate almost exactly lines belonging to different transitions of any element in any stage of ionisation First of all we have the Pauli-Heisenberg Russell-Hund theory which enables us to calculate the types of spectral lines arising from any electronic configuration Secondly we have the arithmetic progression rule discovered by Hertz‡ for the X ray region and applied by Millikan and Bowen§ with conspicuous success for locating the spectra of stripped atoms containing only one or two valency electrons This law has been extended by Saha and Kichlu, and simultaneously by Mack, Laporte and Lang, and Gibbs and White|| also to complex spectra Lastly, we have the " horizontal

---

* The following complete classifications may be mentioned —

F—de Bruin 'K Akad Ams Proc ' vol 30 p 947 (1927)

F--Dingle 'Roy Soc Proc ,' A vol 113 p 323 (1927)

F++- Millikan and Bowen 'Phys Rev ' vol 23, p 11 (1924) and vol 29 p 231 (1927)

F++—Dingle 'Roy Soc Proc ' A vol 122 p 144 (1929)

Cl- Turner 'Phys Rev ' vol 27 p 397 (1926)

Cl -Majumdar 'Roy Soc Proc ' A vol 123 p 60 (1929)

Cl—Kiess and de Bruin 'Bur Stand J Res ' vol 2 p 1117 (1929)

Cl++—Bowen, 'Phys Rev ' vol 31 p 35 (1928)

Cl++—Majumdar and Chandra Deb, 'Ind J Phys ,' vol. 3, pt 3 (1929)

Also a partial classification of Cl+ by Paschen 'Ann Physik,' vol 71 p 792 (1923)

† 'Ann Physique ' vol 7, p 205 (1927)

‡ 'Z Physik,' vol 3, p 19 (1920)

§ 'Phys Rev ,' vol 24, p 209 (1924) and subsequent paper

|| Saha and Kichlu, 'Ind J Physics ' vol 2, pt I (1928) , Mack, Laporte and Lang, 'Phys Rev ' vol 31, p 1124 (1928) Gibbs and White, 'Phys Rev ,' vol 29, p 359 (1927)

comparison method ' due to Saha and Majumdar,* which enables us to locate lines with almost arithmetic certainty and helps us to make a complete survey of lines belonging to definite transitions of any element

To illustrate the use of these rules let us consider the spectra of following groups of elements -

Table I

x	0	1	2	3	4	5	6
I	Ga	Ge	As	Se	Br	Kr	Rb
II	Ge^{+}	As^{+}	Se^{+}	Br^{+}	Kr^{+}	Rb^{+}	Sr^{+}
III	As^{++}	Se^{++}	Br^{++}	Kr^{++}	Rb^{++}	Sr^{++}	Y^{++}
IV	Se^{+++}	Br^{+++}	Kr^{+++}	Rb^{+++}	Sr^{+++}	Y^{+++}	Zr^{+++}
V	Br$^{+\mathrm{iv}}$	Kr$^{+\mathrm{iv}}$	Rb$^{+\mathrm{iv}}$	Sr$^{+\mathrm{iv}}$	Y$^{+\mathrm{iv}}$	Zr$^{+\mathrm{iv}}$	La$^{+\mathrm{iv}}$

These groups of elements have the electronic composition $(2K\ 8L\ 18M\ 2N_1)x'N_2$ x' varying from 1 in Ga to 6 in Kr x' represents their normal state In their excited states they have the composition $(2K\ 8L\ 18M\ 2N_1)\ xN_2\ O_1\ O_2$ etc , x now varying from 0 to 6 as we pass from Ga to Rb (The same holds from groups II to V also) The light electron runs through the unfilled levels O_1, O_2, etc , as graphically denoted in the following general diagram †

$$\begin{array}{lcccc}
2K\ 8L\ 18M\ 2N_1 & N_2 & N_3 & N_4 & \\
 & x & 1 & & \\
 & O_1 & O_2 & O_3 & O_4 \\
 & 1 & 1 & 1 & \\
 & & P_1 & P_2 & P_3 \\
 & & 1 & 1 & 1 \\
 & & & Q_1 & Q_2 \\
 & & & 1 &
\end{array}$$

Location of Lines due to different Transitions

(1) Transition $\begin{array}{c} N_2 \leftarrow N_3 \\ \uparrow \\ O_1 \end{array}$

---

[*] 'Ind J Physics,' vol 3, pt I (1928) See also Gibbs and White Proc Nat Acad Sci ,' vol 14 (1928)

[†] We are following the notation used in the Allahabad Laboratory, as this seems to present, at least to us, marked advantages over the system which has been proposed by Russell, Shenstone and Turner (' Phys Rev ,' vol 33, p 900 (1929)) There is no essential distinction in principle between the two systems, ours is graphical, while the other is symbolical We have found that, with our graphical system, we can locate lines and assign transitions much more quickly than by using the other system

In most cases, these lines for the groups of elements considered in Table I lie in the Schumann region They are excluded from our discussions

(2) Transition N_2 $(O_1 \leftarrow O_2)$

For many of the elements in Table I the lines due to this transition are known They are shown in Chart 1 (pp 200–1) and plotted in fig 1

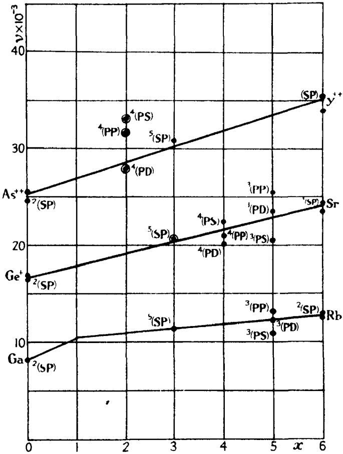

FIG 1 —Transition $xN_2 (O_1 \leftarrow O_2)$

In this Chart the most important lines are noted The reference has been given under the line

The diagram shows the validity of the two empirical rules, viz, of the arithmetic progression law, and the horizontal comparison method The extreme elements (Ga and Rb) have simple doublet spectra, and there are only two lines corresponding to the transition $O_1 \leftarrow O_2$ We plot the lines $^2S_{1/2}$— $^2P_{3/2}$ due to Ge$^+$ and Sr$^+$ at the extreme ends, and draw a line through

Chart 1 —Transition xN_2 $(O_1 \leftarrow O_2)$

$x \rightarrow$	0	1	2	3	4	5	6
(1)	—	$^3P_2 - {}^3D_3$	$^4P_3 - {}^4D_4$	—	$^4P_3 - {}^4D_4$	$^3P_2 - {}^3D_3$	—
(2)	$^2S_1 - {}^2P_2$	$^3P_2 - {}^3\overline{P}_2$	$^4P_3 - {}^4\overline{P}_3$	$^5S - {}^5P_3$	$^4P_3 - {}^4\overline{P}_3$	$^3P_2 - {}^3\overline{P}_2$	$^2S_1 - {}^2P_2$
(3)	—	$^3P_2 - {}^3S_1$	$^4P_3 - {}^4S_2$	—	$^4P_3 - {}^4S_2$	$^3P_2 - {}^3S_1$	—
I	Ga	Ge	As	Se	Br	Kr	Rb.
(1)	—	—	11551	—	12085	12322	—
(2)	8373	—	10074	11431	—	13151	12817
	—	—	10749		—	11193	—
	Fowler, 'Report,' p. 158		Meggers and De Bruin 'B S J Res vol 3 p 773 (1929)	Fowler Report, p 171	Kiess and de Bruin in course of publication	Gremmer Zs f Phys,' vol 54, p 222 (1929)	Fowler, Report, p 104
II	Ge+	As+	Se+	Br+	Kr+	Rb+	Sr+
(1)	—	—	—	—	20078	23553	—
	16963	—	—	211820	21094	25370	24517
(3)	—	—	—	—	22295	20732	—
				S Chandra Deb (this paper)	P K. Kichlu, 'Roy Soc. Proc.,' vol. 120, p. 643 (1928)	R Majumdar, 'Naturwissenschaften,' p 198 (1929).	Fowler, Report, p. 132

III	As^{++}	Se^{++}	Br^{++}	Kr^{++}	Rb^{++}	Sr^{++}	Y^{++}
(1)	—	23979	28063	—	—	—	—
(2)	25487	27482	31497	30800	—	—	35487
(3)	—	28210	33096	—	—	—	—
	Lang 'Phys Rev,' vol 32 (1928)	D K. Bhattacharyya, 'Nature,' June, 1929	S Chandra Deb (this paper)	D P Acharyya (*unpublished*)			Bowen and Millikan, 'Phys Rev,' vol. 28, p 923 (1926)
IV	Se^{+3}	Br^{+3}	Kr^{+3}	Rb^{+3}	Sr^{+3}	Y^{+3}	Zr^{+3}
(1)	—	36675	—	—	—	—	—
(2)	34080	40130	—	—	—	—	46201
(3)	—	42247	—	—	—	—	—
		S Chandra Deb (this paper)					Bowen and Millikan, 'Phys Rev,' vol. 28, p 923 (1926).

them (thick lines in the diagram) Then it is found that the most important lines due to the intermediate elements (As^+ to Rb^+) lie on this line, and the other groups lie scattered about this line in a regular order implying an exact correspondence between similar groups of elements having iso-electronic structure Thus let us take the spectra of Kr, Rb^+ and Sr^{++} Both in Kr and Rb^+, the $^3(PD)$ lines lie on the line, while $^3(PS)$ lie below, and $^3(\bar{P}P)$ above the line The classification of the lines of Sr^{++} is not known But from analogy, we can predict that $^3(PD)$ will be on the line, $^3(PS)$ will be below the line, and $^3(\bar{P}P)$ above the line I have always taken advantage of this correspondence in order to locate the different groups

The two empirical laws hold not only for the transition ($O_1 \leftarrow O_2$) but, as has been shown by Dr Majumdar, also for the transition ($O_2 \leftarrow O_3$) The available data relating to this transition for the elements in Table I are collected in Chart 2 and plotted in fig 2

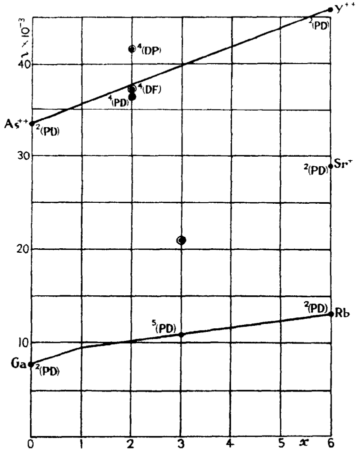

FIG 2 —Transition xN_2 ($O_2 \leftarrow O_1$)

Chart 2 —Transition xN_2 ($O_2 \leftarrow O_3$)

$x \rightarrow$	0	1	2	3	4	5	6
— (1) (2) (3)	$^2P_3 - {}^2D_3$	$^3P_3 - {}^3D_3$ $^3S_1 - {}^3P_2$ $^3D_3 - {}^3F_4$	$^4P_3 - {}^4D_4$ $^4D_4 - {}^4F_5$ $^4D_4 - {}^4P_3$	$^5P_3 - {}^5D_4$	$^4P_3 - {}^4D_4$ $^4D_4 - {}^4F_5$ $^4P_3 - {}^4D_4$	$^3P_2 - {}^3D_3$ $^3D_3 - {}^3F_4$ $^3S_1 - {}^3P_2$	$^2P_2 - {}^2D_3$
I	Ga.	Ge	As	Se	Br	Kr	Rb
(1) (2) (3)	— [7621] — Calculated from Paschen and Gotze	— — —	— [10947] — Calculated	— — —	— — —	— — —	— 13121 — Fowler, Report, p 104
II	Ge$^+$	As$^+$	Se$^+$	Br$^-$	Kr$^+$	Rb$^+$	Sr$^+$
(1) (2) (3)	— — —	— — —	— — —	— 21179 — S Chandra Deb	— — —	— — —	— 28855 — Fowler, 'Report,' p 132
III	As^{++}	Se^{++}	Br^{++}	Kr^{++}	Rb^{+-}	Sr^{++}	Y^{++}
(1) (2) (3)	— 33525 — Lang, 'Phys. Rev,' vol. 32, p. 738 (1928)	— — —	36233 37340 41796 S Chandra Deb	— — —	— — —	— — —	— 45623 — Bowen and Millikan, 'Phys Rev,' vol 28, p 323 (1926)

Spectrum of Br^+

With the aid of these guiding principles, I have tried to classify the spectrum of bromine in its different stages of ionisation In Br itself no data is yet available In Br^+ I made use of Bloch's data and obtained the quintet terms due to $(O_1 \leftarrow O_2)$ transitions They fall exactly in the predicted places and are shown in Table II I have also obtained lines due to $(O_2 \leftarrow O_3)$ $(O_2 - P_1)$ and $(N_3 \leftarrow O_2)$ transitions They are shown in Table II

Ionisation Potential of Br^+

From Table II we see that

$$O_1 - O_2 = 21182 \text{ taking the line } ({}^5S_2 - {}^5P_3)$$

$$O_2 - P_1 = 20930 \text{ taking the line } ({}^5P_3 - {}^5S_2),$$

therefore

$$O_1 - P_1 = 42112$$

Let $O_1 = 4N/(2 + \sigma)^2$, and $P_1 - 4N/(3 + \sigma)^2$ Then from a table of Rydberg-sequences (Fowler's 'Report')

$$O_1 = 82128 \quad \text{and} \quad P_1 = 40016$$

From this we have

$$O_2 = 60946$$

Taking $O_2 = 4N/(2 + \pi)^2$, we get $N_2 = 4N/(1 + \pi)^2 = 154888$, which gives the ionisation potential of Br^+ to be 19 1 volts

The value is actually higher than the actual ionisation potential of Br^+, as the fundamental terms arising from the $4N_2$ combination is ^3P This will form the larger Rydberg sequence of ^3P arising from $3N_2O_2$ But we have not got the triplet terms, but only quintets Hence the value of the ionisation potential obtained here is larger than the actual value

Spectrum of Br^{++}

The Quartet Group due to the Transition $2N_2(O_1 \leftarrow O_2)$ —From fig 1 it is at once seen that the lines due to the transition $2N_2\,(O_1 \leftarrow O_2)$, viz , $^4(P_3D_4)$, $^4(P_3\overline{P}_3)$ and $^4(P_3S_2)$ are located as ν 28000, ν 31500 and ν 33000 respectively A strong set of lines in this region is given by Bloch, and from consideration of intensity, the following lines were identified, ν 28063 as $^4P_3 - {}^4D_4$, ν 31497 as $^4P_3 - {}^4P_3$ and ν 33096 as $^4P_3 - {}^4S_2$ The prediction turned out to be completely successful and the following multiplets were obtained

Table II

$3N_2O_1$ \ $3N_2O_2$		$3N_2O_2$	10 7	17	21	42	$3N_2P_1$	$2N\ N_3$	29 2	30 5	35 6	39 9
	$b\,^5S_2$	$f\,^5D_0$	$f\,^5D_1$	$f\,^5D_2$	$f\,^5D_3$	$f\,^5D_4$	$e\,^5S_2$	$c\,^5D_0$	$c\,^5D_1$	$c\,^5D_2$	$c\,^5D_3$	$c\,^5D_4$
$d\,^5P_1$	(10) 20970 3	(1) 21301 0	(1) 21310 7	(1) 21328 3	—	—	(4) 21143 8	(0) 20813 4	(2) 20784 2	(8) 20755 0	—	—
62												
$d\,^5P_2$	(3) 21034 1	—	(10) 21249 2	(3) 21266 1	(4) 21287 1	—	(10) 21079 6	—	(3) 20848 0	(6) 20817 1	(15) 20781 5	—
150												
$d\,^5P_3$	(8) 21182 0	—	—	*	(2) 21137 5	(6) 21179 5	(10) 20930 0	—	—	(10) 20970 2	(10) 20930 0	(20) 20890 1

Table III —Br^{++} Transition $2N_2\,(O_1 \leftarrow O_2)$

$2N_2O_1$ / $2N_2O_2$	516	838		1138		1283	
	$b\,^4P_1$	$b\,^4P_2$	$b\,^4P_3$	$b\,^2P_1$	$b\,^2P_2$	$b\,^2D_2$	$b\,^2D_3$
$d\,^4D_1$	(7) 27764 5	(0) 27246 2	—	—	—	—	—
332							
$d\,^4D_2$	—	(2) 27576 2	(2) 26739 3	—	—	—	—
576							
$d\,^4D_3$	—	(7) 28153 7	(2) 27315 0	—	—	—	—
748							
$d\,^4D_4$	—	—	(10) 28063 2	—	—	—	—
$d\,^2D_2$	—	—	—	(4) 28769 6	(2) 27631 7	(3) 26989 4	—
1366							
$d\,^2D_3$	—	—	—	—	(6) 28998 7	(4) 28353 9	(8) 27069 2
$d\,^4P_1$	(6) 31608 9						—
472							
$d\,^4P_2$	(5) 32083 6	(7) 31562 4		—	—	—	—
773							
$d\,^4P_3$	—	(5) 32335 0	(8) 31497 7	—	—		—
$d\,^2P_1$	—		—	(2) 32352 6	(4) 31214 1	(5) 30573 5	—
1171							
$d\,^2P_2$				—	(3) 32383 6	(4) 31744 0	(5) 30461 3
$d\,^4S_2$	(5) 34456 3	(2) 33034 1	(10) 33096 9	—		—	—

The Doublet Group —For the identification of the doublet group, we are guided by Mr D K Bhattacharyya's observation that in the case of S^+ (which has the same electronic structure as Br^{++}) the ^{2}(PD) group will be situated just below $^4(P\bar{P})$ and $^2(P\bar{P})$ group near ^{4}(PS) groups It was not difficult to identify the other groups once the correct difference has been obtained The doublet group is also included in Table III

Lines Due to the Transition $2N_2\,(O_2 \leftarrow O_3)$ —These are identified from examination of fig 2 and there shown by ⊙ The group of lines due to this transition is shown in Table IV

Table IV —Br^{++} Transition $2N_2(O_2 \leftarrow O_3)$

		267	477	808		720		114	359	584		1186		469	607		980
$2N_2O_3$ \ $2N_2O_2$	$f\,^4F_2$	$f\,^4F_3$	$f\,^4F_4$	$f\,^4F$	$f\,^2F_3$	$f\,^2F_4$	$f\,^4D_1$	$f\,^4D_2$	$f\,^4D_3$	$f\,^4D_4$	$f\,^2D_3$	$f\,^2D_2$	$f\,^4D_1$	$f\,^4P_2$	$f\,^4P_3$	$f\,^2P_1$	$f\,^2P_2$
$d\,^4D_1$	—	—	—	—	—	—	(0) 40277 1	—	—	—	—	—	—	—	—	—	—
332																	
$d\,^4D_2$	(5) 37106 2	(2) 37377 1	—	—	—	—	39945 2	(1) 40057 4	—	—	—	—	(0) 42044 6	—	—	—	—
576																	
$d\,^4D_3$	(1) 36532 5	—	(3) 37281 9	—	—	—	—	(1) 39476 8	(1) 39835 2	(5) 40423 3	—	—	—	(2) 41932 1	(1) 42538 6	—	—
748																	
$d\,^4D_4$	—	(3) 36056 8	(1) 36532 5	(4) 37340 5	—	—	—	—	(4) 39084 7	(6) 39671 7	—	—	—	—	(2) 41796 2	—	—
$d\,^2D_2$	—	—	—	—	(2) 37669 7	—	—	—	—	—	(3) 39911 4	—	—	—	—	(0) 41965 5	(1) 42969 4
1366																	
$d\,^2D_3$	—	—	—	—	(1) 36309 5	(3) 37029 4	—	—	—	—	(2) 38549 8	(3) 39734 5	—	—	—	—	—
$d\,^4P_1$	(4) 33595 8	—	—	—	—	—	(2) 36424 3	(2) 36540 2	—	—	—	—	(4) 38533 8	(2) 39004 0	—	—	—
472																	
$d\,^4P_2$	—	(8) 33391 2	—	—	—	—	(2) 35952 0	(1) 36064 4	(2) 36424 3	—	—	—	(6) 38064 9	(4) 38532 0	(1) 39139 1	—	—
774																	
$d\,^4P_3$	(1) 32352 6	32618 1	(10) 33096 9	—	—	—	—	—	(3) 35651 7	(4) 36233 2	—	—	—	—	(6) 38361 9	—	—
$d\,^2P_1$	—	—	—	—	—	—	—	—	—	—	(2) 36329 0	—	—	—	—	(5) 38405 0	(2) 39382 6
1171																	
$d\,^2P_2$	—	—	—	—	(5) 32722 3	—	—	—	—	—	(2) 35157 5	(3) 36345 0	—	—	—	(2) 37230 8	(3) 38211 9
$d\,^4S_1$	—	—	—	—	—	—	—	(6) 33692 0	(5) 34049 6	—	—	—	—	—	(5) 36767 8	—	—

Lines Due to Transition $2N_2(N_3 \leftarrow O_2)$ —These lines would be fairly strong and would be comparable in intensity to the $(O_1 \leftarrow O_2)$ lines Our analysis of the spectrum of Cl^{++} enabled me to predict that the group would be found between ν 16000 and ν 28000 I obtained a multiplet from Bloch's data, but all of the expected multiplets could not be obtained as the data did not extend beyond λ 5000 So I undertook an experimental investigation of the spectrum of Br^{++} in this region and obtained a number of new lines shown in the general Table X The ^{4}(DF), ^{4}(PF) and ^{4}(DD) groups are entirely new and some of the lines of ^{4}(PD) and ^{4}(PP) groups are partially identified from my data

Experimental Arrangements

The spectrum was obtained by passing a condensed discharge through a spectrum tube of special design which has been described by Dr K Majumdar ('Roy Soc Proc,' vol 125, p 62, 1929) in his work on the arc spectrum of chlorine The diagram is not reproduced here as my tube differed very little from Dr Majumdar's The electrodes were of nickel, as this metal was found to be the best material for withstanding the effects of bromine gas The bromine used was Kahlbaum's extra pure B in Majumdar's figure was replaced by a bromine bulb The tube length between the stopcock S and the discharge tube was about 3 feet, hence there was little probability of bromine getting contaminated by the grease in the stopcock The condenser was made of thick glass plates separated by tin foils and immersed in kerosine oil Capacity was about 0 01 microfarad A pressure of about 3 mm of mercury was maintained in the discharge tube

The spectrum was formed by a plane transmission grating with a glass lens having a dispersion of about 25 Å per millimetre at the region under investigation (λ 4000–λ 7500) several photographs were taken on Kodak panchromatic and dicyanine plates with the exposure of about 3 hours Neon comparison lines were used for measurement, and the order of accuracy was found to be about 0 1 Å for fairly strong lines About 230 lines were measured of which 60 were entirely new

Identification of other Groups

For the identification of the groups due to other transitions we worked out the ν values of the different energy levels, with the aid of a Rydberg formula Let us take the following structure diagram The approximate energy values

Table V —Br^{++} Transition $2N_2(N_3 \leftarrow O_2)$

$2N_2N_3$ / $2N_2O_2$	$c\,^4F_2$	28 $c\,^4F_3$	43 $c\,^4F_4$	79 $c\,^4F_5$	$c\,^2F_3$	114 $c\,^2F_4$	$c\,^4D_1$	37 $c\,^4D_2$	119 $c\,^4D_3$	285 $c\,^4D_4$	$c\,^2D_2$	786 $c\,^2D_3$	$c\,^4P_1$	203 $c\,^4P_2$	464 $c\,^4P_3$	$c\,^2P_1$	958 $c\,^2P_2$
$d\,^4D_1$	(4) 16589 4	—	—	—	—	—	(2) 19952 6	20009 8	—	—	—	—	(3) 22577 7	(2) 22780 7	—	—	—
332																	
$d\,^4D_2$	(2) 16917 7	(2) 16945 2	—	—	—	—	—	(3) 20338 7	(1) 20460 1	—	—	—	—	(2) 23122 8	(2) 23580 2	—	—
576																	
$d\,^4D_3$	—	(1) 17521 3	(3) 17564 3	—	—	—	—	(1) 20917 3	(2) 21036 3	(1) 21326 1	—	—	—	(2) 23694 6	(3) 24158 [illegible]	—	—
748																	
$d\,^4D_4$	—	(0) 18272 3	(2) 18314 5	(5) 18393 9	—	—	—	—	(3) 21784 [illegible]	(7) 22072 2	—	—	—	—	(4) 24904 1	—	—
$d\,^2D_2$	—	—	—	—	(1) 16061 3	—	—	—	—	—	(1) 20632 9	—	—	—	—	(2) 24285 4	(3) 25243 3
1366																	
$d\,^2D_3$	—	—	—	—	(3) 17425 7	(2) 17539 2	—	—	—	—	(1) 21997 4	(2) 22782 3	—	—	—	—	—
$d\,^4P_1$	(3) 20428 7	—	—	—	—	—	(3) 23795 8	(3) 23854 2	—	—	—	—	(4) 26426 1	(0) 26629 [illegible]	—	—	—
472																	
$d\,^4P_2$	(2) 20902 9	(7) 20930 6	—	—	—	—	—	(3) 24324 1	(3) 24445 0	—	—	—	(3) 26898 3	(6) 27101 8	(1) 27562 6	—	—
774																	
$d\,^4P_3$	—	(4) 21706 9	(6) 21750 3	—	—	—	—	(2) 25100 9	(1) 25218 0	(3) 25511 0	—	—	—	(2) 27871 2	(5) 28338 1	—	—
$d\,^2P_1$	—	—	—	—	—	—	—	—	—	—	—	—	—	—	—	(3) 27866 3	(2) 28821 3
1171																	
$d\,^2P_2$	—	—	—	—	(1) 20813 [illegible]	—	—	—	—	—	(1) 25381 2	(4) 26169 6	—	—	—	(2) 29037 8	(7) 29995 0
$d\,^4S_2$	(0) 23275 4	—	—	—	—	—	—	—	—	—	—	—	(3) 29263 7	—	—	—	—

of the levels are indicated below these levels, and were obtained in the way explained below —

N_2	N_3		
209600	126000		
O_1	O_2	O_3	
130000	98200	64300	
	P_1	P_2	P_3
	70700	56700	44100

We have from the tables —

$$O_1 - O_2 = 31497 \text{ taking the line } {}^4(P_3D_4)$$

$$O_2 - O_3 = 36233 \text{ taking the line } {}^4(P_3D_4)$$

and

$$N_3 - O_2 = 28338 \text{ taking the line } {}^4(P_3P_3)$$

Hence

$$N_3 - O_3 = 64571$$

Let us suppose that

$$\nu_{N_3} = 9N/(2 + \delta)^2,$$

then

$$\nu_{O_3} = 9N/(3 + \delta)^2$$

therefore

$$9N\,[1/(2 + \delta)^2 - 1/(3 + \delta)^2] = 64571$$

We find from reference to tables of Rydberg terms given in Fowler's ' Report,' p 82, that roughly

$$N_3 = 126000$$

and

$$O_3 = 64300$$

Hence

$$O_2 = 98200$$

$$O_1 = 130000$$

Taking $\nu_{O_1} = 9N/(2 + s)^2$ and $\nu_{P_1} = 9N/(3 + s)^2$ we get ν_{P_1} from the above-mentioned table (after proper calculations) to be 70700 Similarly we worked out the values of ν_{P_2}, ν_{P_3}, , which are shown in the diagram above

From these values we find that the lines $2N_2(O_2 \leftarrow P_1)$ would lie in the range (27000–32000) There is a large group of unidentified lines in this region, and with the help of known $2N_2O_2$ differences, I easily identified the multiplets They are shown in Table VI

Table VI – Br^{++} Transition $2N_2 (O_2 \leftarrow P_1)$

$2N_2P_1$ \ $2N_2O_2$		798	901	778		990	
	$e\,^4P_1$	$e\,^4P_2$	$e\,^4P_3$	$e\,^2P_1$	$e\,^2P_2$	$e\,^2D_2$	$e\,^2D_3$
$d\,^4D_1$		(10) 32519 1	--				
332							
$d\,^4D_2$	(7) 31387 1	(1) 32186 6	33083 4				
576							
$d\,^4D_3$		(6) 31608 9	32507 1				
748							
$d\,^4D_4$			(10) 31759 2				
$d\,^2D_2$		–	–	(2) 32331 7	-	(4) 33866 8	(3) 34856 7
1366							
$d\,^2D_3$	—			–	(4) 31744 0	—	(1) 33492 5
$d\,^4P_1$	(2) 27871 2	(0) 28672 1	–				
472							
$d\,^4P_2$	(1) 27401 4	(2) 28202 8	(1) 29104 9				
773							
$d\,^4P_3$			(7) 28330 4				
$d\,^2P_1$		-		(3) 28749 6	(5) 29528 4	(4) 30284 5	
1171							
$d\,^2P_2$	-	–	—	(2) 27576 2	(4) 28353 9	(6) 29113 3	(6) 30103 1
$d\,^4S_2$	(1) 25029 3	(4) 25824 8	(2) 26727 9				

It is also clear that no other group of lines in the region investigated by Bloch can be assigned to Br^{++}

Ionisation Potential of Br^{++}

We can make a provisional estimate of the ionisation potential of Br^{++}

Taking $O_2 = 9N/(2 + p)^2$, and $N_2 = 9N(1 + p)^2$, we get $N_2 = 209600$, which is equivalent to 25 9 volts

The value can, of course, be regarded only as approximate The resonance lines are expected at about λ 1250

Spectrum of Br^{+++}

By applying the method of "horizontal comparison" we see that lines due to the $(O_1 \leftarrow O_2)$ of Br^{+++} spectrum would be located (see fig 1) at about ν 37000 A strong group of lines in this region are ascribed by Bloch to Br^{+++} I could easily classify these lines into multiplets arising from transition $(O_1 \leftarrow O_2)$ and they are shown in Table VII below No other group has been obtained Intercombinations have been obtained in this case

Table VII Br^{+++} Transition $(O_1 \leftarrow O_2)$

N_2O_1 N_2O_2		$^3P_0$	$^3P_1$	$^3P_2$	$^1P_1$
			506	1093	933
$^3D_1$		(1) 32368 2	(0) 32874 8	(2) 33965 7	—
	1193				
$^3D_2$		—	(1) 34065	(2) 35158	(2) 36094 8
	1517				
$^3D_3$				(3) 36675 2	—
$^1D_2$		–	(2) 35863	(2) 36958	—
$^3P_0$			(1) 38066	-	(4) 40090 6
	364				
$^3P_1$		—	(4) 38429	(4) 39523	(1) 40453
	607				
$^3P_2$		—	39035 7	40130 8	—
	1114				
$^1P_1$		(4) 39644	—	(1) 41244	(3) 42177
	1003				
$^3S_1$		(2) 40649	(1) 41155	(2) 42247	—

Spectrum of Br^{+IV}

Br V atoms form an iso electric system with Ge II, As III and Se IV atoms The spectra of these are known, and are classified by various workers (shown in Chart 1), from which we at once see that the two doublet lines arising from the combination ${}^2S_{1/2} - {}^2P_{1/2\ 3/2}$ due to the transition $(O_1 \leftarrow O_2)$ would be situated at about ν 40000 The difference between them would be of the same order as the difference terms $({}^3P_0 - {}^1P_1)$ of O_1 in Br^{+++} spectrum This difference is 2532 in wave-numbers (*vide* Table VII) The lines could be easily identified and are shown below

Table VIII —Br^{+IV}

$2N_1O_1$ \ $2N_1O_2$	${}^2S_1$	N_3 ${}^2D_2$	${}^2D_3$
${}^2P_1$	(2) 41018 2	(1) 33511 7	
2572			
${}^2P_2$	(3) 43590 1	(4) 36084 2	(4) 35440 9

Table IX —Classified Lines of Br^+

λ.	Int	ν_{vac}	Quintet combinations
4686 61	1	21328 3	$d\,{}^5P_1 - f\,{}^5D_2$
4691 24	1	21310 7	$d\,{}^5P_1 - f\,{}^5D_1$
4693 30	1	21301 1	$d\,{}^5P_1 - f\,{}^5D_0$
4696 43	4	21287 1	$d\,{}^5P_2 - f\,{}^5D_3$
4701 00	3	21266 1	$d\,{}^5P_2 - f\,{}^5D_2$
4704 86	10	21249 2	$d\,{}^5P_2 - f\,{}^5D_1$
4719 77	8	21182 0	$b\,{}^5S_1 - d\,{}^5P_2$
4720 30	6	21179 5	$d\,{}^5P_3 - f\,{}^5D_4$
4728 24	4	21143 8	$d\,{}^5P_1 - e\,{}^5S_2$
4728 79	2	21137 5	$d\,{}^5P_3 - f\,{}^5D_3$
4742 70	10	21079 6	$d\,{}^5P_2 - e\,{}^5S_2$
4752 95	3	21034 1	$d\,{}^5S_2 - d\,{}^5P_3$
4767 10	10	20970 3	$\begin{Bmatrix} b\,{}^5S_2 - d\,{}^5P_1 \\ c\,{}^5D_2 - d\,{}^5P_3 \end{Bmatrix}$
4776 42	10	20930 0	$\begin{Bmatrix} d\,{}^5P_3 - e\,{}^5S_2 \\ c\,{}^5D_3 - d\,{}^5P_3 \end{Bmatrix}$
4785 50	20	20890 1	$c\,{}^5D_4 - d\,{}^5P_3$
4795 23	3	20848 0	$c\,{}^5D_1 - d\,{}^5P_2$
4803 21	0	20813 4	$c\,{}^5D_0 - d\,{}^5P_1$
4802 24	6	20817 2	$c\,{}^5D_3 - d\,{}^5P_2$
4810 04	2	20784 2	$c\,{}^5D_1 - d\,{}^5P_1$
4810 71	15	20781 5	$c\,{}^5D_2 - d\,{}^5P_2$
4816 72	8	20755 0	$c\,{}^5D_2 - d\,{}^5P_1$

Table X —Classified Lines of Br^{++}

λ	Int	ν_{vac}	Combinations	
			Quartets	Doublets
2326 56	1	42969 4		$d\,^2D_2 - f\,^2P_2$
2350 26	1	42538 6	$d\,^4D_3 - f\,^4P_2$	
2377 70	0	42044 6	$d\,^4D_2 - f\,^4P_1$	
2381 15	0	41985 5		$d\,^2D_2 - f\,^2P_1$
2384 12	2	41932 1	$d\,^4D_2 - f\,^4P_2$	
2391 86	2	41796 2	$d\,^4D_4 - f\,^4P_2$	
2473 18	5	40423 3	$d\,^4D_3 - f\,^4D_4$	
2482 15	0	40277 0	$d\,^4D_1 - f\,^4D_1$	
2495 62	1	40057 4	$d\,^4D_2 - f\,^4D_2$	
2502 74		39945 2	$d\,^4D_2 \quad f\,^4D_1$	
2504 92	3	39911 4		$d\ D_2 - f\,^2D_2$
2509 66	1	39835 2	$d\,^4D_3 - f\,^4D_3$	
2516 05	3	39734 5		$d\,^2D_3 - f\,^2D_4$
2520 27	6	39671 7	$d\,^4D_4 \quad f\,^4D_4$	
2532 43	1	39476 8	$d\,^4D_3 - f\,^4D_2$	
2538 68	2	39382 6		$d\,^2P_1 - f\,^2P_2$
2554 26	1	39139 1	$d\,^4P_2 \quad f\,^4P_1$	
2557 82	4	39084 7	$d\,^4D_4 - f\,^4D_3$	
2563 19	2	39004 0	$d\,^4P_1 - f\,^4P_2$	
2592 34	2	38549 8		$d\,^2D_3 - f\,^2D_2$
2594 45	4	38533 7	$d\,^4P_1 - f\,^4P_1$	
2594 40	4	38532 0	$d\,^4P_2 - f\,^4P_2$	
2603 15	5	38405 0		$d\,^2P_1 - f\,^2P_1$
2606 18	6	38361 9	$d\,^4P_3 - f\,^4P_3$	
2616 21	3	38211 9		$d\,^2P_2 \quad f\,^2P_2$
2626 49	6	38064 9	$d\,^4P_2 - f\,^4P_1$	
2653 91	2	37669 7		$d\,^2D_2 - f\,^2F_3$
2674 89	2	37377 1	$d\,^4D_2 \quad f\,^4F_3$	
2677 34	4	37340 5	$d\,^4D_4 - f\,^4F_5$	
2681 53	3	37281 9	$d\,^4D_3 - f\,^4F_4$	
2685 25	3	37230 8		$d\,^2P_2 - f\,^2P_1$
2694 23	5	37106 2	$d\,^4D_2 - f\,^4F_2$	
2699 85	3	37029 4		$d\,^2D_3 - f\,^2F_4$
2719 03	5	36767 8	$d\,^4S_2 - f\,^4P_2$	
2735 85	2	36542 2	$d\,^4P_1 - f\,^4D_2$	
2736 52	1	36532 5	$d\,^4D_4 - f\,^4F_4$ $d\,^4D_3 - f\,^4F_2$	
2744 79	2	36424 3	$d\,^4P_2 - f\,^4D_3$ $d\,^4P_1 \quad f\,^4D_1$	
2750 60	3	36345 9		$d\,^2P_2 - f\,^2D_3$
2751 99	2	36329 0		$d\,^2P_1 - f\,^2D_2$
2753 31	1	36309 5		$d\,^2D_3 - f\,^2F_3$
2759 11	4	36233 2	$d\,^4P_3 - f\,^4D_4$	
2772 00	1	36064 4	$d\,^4P_2 - f\,^4D_2$	
2772 62	3	36056 8	$d\,^4D_4 - f\,^4F_3$	
2780 73	2	35952 0	$d\,^4P_2 - f\,^4D_1$	
2804 12	3	35651 7	$d\,^4P_3 - f\,^4D_3$	
2842 69	2	35157 5		$d\,^2P_2 - f\,^2D_2$
2868 19	3	34856 7		$d\,^2D_2 - e\,^2D_3$
2901 42	5	34456 3	$b\,^4P_1 - d\,^4S_2$	
2936 06	5	34049 6	$d\,^4S_2 - f\,^4D_2$	
2946 17	2	33934 1	$b\,^4P_2 - d\,^4S_2$	
2951 92	4	33866 8		$d\,^2D_2 - e\,^2D_2$
2967 23	6	33692 0	$d\,^4S_2 - f\,^4D_2$	
2975 70	4	33595 8	$d\,^4P_1 - f\,^4F_2$	
2984 9	1	33492 5		$d\,^2D_2 - e\,^2D_2$
2993 93	8	33391 1	$d\,^4P_2 - f\,^4F_3$	

Table X—(continued)

λ	Int	ν_{vac}	Combinations	
			Quartets	Doublets
3020.65	10	33096.9	$d\,{}^4P_3 - f\,{}^4F_4$ $b\,{}^4P_1 - d\,{}^4S_2$	
3021.22	—	33083.4	$d\,{}^4D_2 - f\,{}^4P_3$	
3036.56	5	32722.8		$d\,{}^2P_2 - f\,{}^2F_3$
3064.27		32618.1	$d\,{}^4P_3 - f\,{}^4F_4$	
3074.38	10	32519.1	$d\,{}^4D_1 - e\,{}^4P_2$	
3075.27	—	32507.1	$d\,{}^4D_3 \quad e\,{}^4P_3$	
3076.86	1	32492.3		$d\,{}^2D_3 - e\,{}^2D_3$
3087.11	3	32383.6		$b\,{}^2P_2 \quad d\,{}^2D_2$
3089.70	2	32352.6	$d\,{}^4P_3 - f\,{}^4F_2$	
3091.87	3	32335.0	$b\,{}^4P_3 - d\,{}^4P_2$	
3092.20	2	32331.7		$d\ D_2 \quad e\,{}^2P_1$
3106.03	1	32186.6	$d\,{}^4D_2 - e\,{}^4P_2$	
3116.04	5	32083.6	$b\,{}^4P_2 - d\,{}^4P_1$	
3147.81	8	31759.2	$d\,{}^4D_4 - e\,{}^4P_3$	
3149.35	4	31744.0		$b\,{}^2D_2 \quad d\,{}^2P_2$ $d\,{}^2D_3 - e\,{}^2P_1$
3162.74	6	31608.9	$b\,{}^4P_1 - d\,{}^4P_1$ $d\,{}^4D_3 \quad e\,{}^4P_2$	
3169.49	7	31562.4	$b\,{}^4P_2 - d\,{}^4P_2$	
3174.08	8	31497.7	$b\,{}^4P_3 - d\,{}^4P_3$	
3185.10	7	31387.1	$d\,{}^4D_2 - e\,{}^4P_1$	
3202.84	4	31214.1		$b\ P_2 - d\,{}^2P_1$
3269.93	3	30573.3		$b\,{}^2D_2 \quad d\,{}^2P_1$
3282.09	3	30461.3		$b\,{}^2D_3 - d\,{}^2P_2$
3301.13	4	30284.3		$d\,{}^2P_1 - e\,{}^2D$
3321.03	6	30103.1		$d\,{}^2P_2 - e\,{}^2D_3$
3333.07	7	29995.0		$d\,{}^2P_2 - f\,{}^2P_2$
3385.32	3	29528.4		$d\,{}^2P_1 - e\,{}^2P_2$
3416.17	3	28263.7	$e\,{}^4P_1 - d\,{}^4S_2$	
3433.93	6	29113.3		$d\,{}^2P_2 - e\,{}^2D_2$
3434.93	1	29104.9	$d\,{}^4P_2 - e\,{}^4P_3$	
3442.99	2	29037.8		$c\ P_1 \quad d\,{}^2P_2$
3447.56	6	28998.7		$b\,{}^2P_2 - d\,{}^2D_3$
3468.73	2	28821.3		$c\,{}^2P_2 - d\,{}^2P_1$
3474.90	4	28769.6		$b\,{}^2P_1 \quad d\,{}^2D_2$
3477.48	3	28749.6		$d\,{}^2P_1 - e\,{}^2P_1$
3488.07	0	28672.1	$d\,{}^4P_1 - e\,{}^4P_2$	
3526.00	4	28354.9		$d\,{}^2P \quad e\,{}^2P_2$
3526.03	4	28353.9		$b\,{}^2D_2 - d\,{}^2D_3$
3527.98	4	28338.1	$c\,{}^4P_3 - d\,{}^4P_3$	
3528.83	7	28330.4	$d\,{}^4P_3 \quad e\,{}^4P_3$	
3544.86	2	28202.8	$d\,{}^4P_2 - e\,{}^4P_2$	
3551.08	7	28153.7	$b\,{}^4P_2 - d\,{}^4D_3$	
3562.43	10	28063.2	$b\,{}^4P_3 - d\,{}^4D_4$	
3587.08	2	27871.2	$b\,{}^4P_1 - e\,{}^4P_1$ $c\,{}^4P_2 - d\,{}^4P_3$	
3587.65	3	27866.0		$c\ P_1 - d\,{}^2P_1$
3600.71	7	27764.5	$b\,{}^4P_1 - d\,{}^4D_1$	
3618.26	2	27631.7		$b\,{}^2P_2 - d\,{}^2D_2$
3625.32	2	27576.2	$b\,{}^4P_2 - d\,{}^4D_2$	$d\,{}^2P_2 - e\,{}^2P_1$
3627.13	1	27562.6	$c\,{}^4P_2 - d\,{}^4P_2$	
3648.41	1	27401.4	$d\,{}^4P_2 - e\,{}^4P_1$	
3660.05	2	27315.0	$b\,{}^4P_3 - d\,{}^4D_3$	
3669.20	0	27246.2	$b\,{}^4P_2 - d\,{}^4D_1$	
3688.86	6	27101.8	$c\,{}^4P_3 - d\,{}^4P_2$	

Table X —(continued)

λ	Int	ν_{vac}	Combinations	
			Quartets	Doublets
3693 47	8	27069 2		$b\,^2D_3 - d\,^2D_2$
3704 03	3	26989 4		$b\,^2D_2 - d\,^2D_2$
3716 74	3	26898 3	$c\,^4P_1 - d\,^4P_2$	
3738 85	2	26739 3	$b\,^4P_3 - d\,^4D_2$	
3740 41	2	26727 9	$d\,^4S_2 - e\,^4P_3$	
3754 18	0	26629 2	$c\,^4P_2 - d\,^4P_1$	
3783 03	2	26425 9	$c\,^4P_1 - d\,^4P_1$	
3820 25	4	26169 6		$c\,^2D_3 \quad d\,^2P_2$
3871 21	4	25824 8	$d\,^4S_2 - e\,^4P_2$	
3918 83	3	25511 0	$c\,^4D_4 - d\,^4P_3$	
3960 47	3	25243 3		$c\,^2P_2 - d\,^2D_2$
3964 32	1	25218 0	$c\,^4D_3 - d\,^4P_3$	
3982 80	2	25100 9	$c\,^4D_2 \quad d\,^4P_3$	
3994 05	1	25029 3	$d\,^4S_2 - e\,^4P_1$	
4014 32	6	24904 1	$c\,^4P_3 - d\,^4D_4$	
4089 73	3	24445 0	$c\,^4D_3 - d\,^4P_2$	
4110 00	3	24324 1	$c\,^4D_2 - d\,^4P_2$	
4116 65	2	24285 4		$c\,^2P_1 - d\,^2D_2$
4138 38	3	24158 2	$c\,^4P_3 \quad d\,^4D_3$	
4190 82	3	23854 2	$c\,^4D_2 - d\,^4P_1$	
4201 35	3	23795 8	$c\,^4D_1 - d\,^4P_1$	
4219 21	2	23694 6	$c\,^4P_2 \quad d\,^4D_1$	
4239 74	2	23580 2	$c\,^4P_3 - d\,^4D_2$	
4295 37	0	23280 1	$c\,^4F_2 \quad d\,^4S_2$	
*4223 65	2	23122 6	$c\,^4P_2 - d\,^4D_3$	
4386 69	2	22780 7	$c\,^4P_2 - d\,^4D_1$	
4388 05	2	22782 3		$c\,^2D_3 - d\,^2D_3$
4428 09	3	22577 7	$c\,^4P_1 - d\,^4D_1$	
4529 49	7	22072 2	$c\,^4D_4 - d\,^4D_4$	
4544 87	1	21997 4		$c\,^2D_2 - d\,^2D_3$
*4589 21	3	21784 2	$c\,^4D_3 - d\,^2D_4$	
4596 63	6	21750 3	$c\,^4F_4 - d\,^4P_3$	
4605 66	4	21706 9	$c\,^4F_3 - d\,^4P_3$	
*4686 4	1	21326 3	$c\,^4D_4 - d\,^4D_3$	
*4751 34	2	21036 3	$c\,^4D_3 - d\,^4D_1$	
4776 42	7	20930 6	$c\,^4F_3 \quad d\,^4P_2$	
*4779 4	1	20917 3	$c\,^4D_2 - d\,^4D_1$	
*4782 5	2	20902 9	$c\,^4F_2 - d\,^4P_2$	
4803 2	1	20813 7		$c\,^2F_3 - d\,^2P_2$
4845 3	1	20632-9		$c\,^2D_2 - d\,^2D_2$
*4886 2	1	20460 1	$c\,^4D_3 - d\,^4D_2$	
*4892 68	3	20428 7	$c\,^4F_2 - d\,^4P_1$	
4915 52	2	20338 7	$c\,^4D_2 - d\,^4D_2$	
4996 3	1	20009 8	$c\,^4D_2 - d\,^4D_1$	
5010 73	2	19952 4	$c\,^4D_1 - d\,^4D_1$	
5435 11	5	18393 9	$c\,^4F_5 - d\,^4D_4$	
*5458 2	2	18314 5	$c\,^4F_4 - d\,^4D_4$	
*5471 3	0	18272 3	$c\,^4F_3 \quad d\,^4D_4$	
5692 12	3	17564 3	$c\,^4F_4 - d\,^4D_3$	
*5700 1	2	17539 2		$c\,^2F_4 - d\,^2D_3$
*5705 6	1	17521 7	$c\,^4F_3 - d\,^4D_1$	
5337 13	3	17425 7		$c\,^2F_3 - d\,^2D_2$
*5899 8	2	16945 2	$c\,^4F_3 - d\,^4D_2$	
5909 46	2	16917 7	$c\,^4F_2 - d\,^4D_2$	
6023 98	4	16589 4	$c\,^4F_2 - d\,^4D_1$	
*6224 4	1	16061 3		$c\,^2F_3 - d\,^2D_2$

All the lines above wave length λ4223 65 are from my measurements and those marked with an asterisk are new lines obtained by me

Table XI —Classified Lines of Br^{+++}

λ	Int	ν_{vac}	Combinations		
			Triplets	Singlets	Inter combinations
2366 37	2	42247 4	$^3P_0 \quad ^3S_1$		
2370 20	3	42177 6		$^1P - ^1P_1$	
2423 95	1	41244 1			$^3P_2 - ^1P_1$
2429 17	1	41155 1			$^3P_1 - ^1S_0$
2453 95	2	40649 0	$^3P_0 - ^3S_1$		
2471 30	1	40453 1			$^1P_1 - ^3P_1$
2491 12	4	40130 8	$^3P_2 \quad ^3D_2$		
2493 50	4	40090 6			$^1P_1 - ^3P_0$
2521 84	5	39644 0			$^3P_0 - ^1P_1$
2529 48	4	39523 4	$^3P_2 \quad ^3P_1$		
2601 54	4	38428 8	$^3P_1 - ^3P_1$		
2626 13	1	38066 1	$^3P_1 - ^3P_0$		
2705 04	2	36958 3			$^3P_2 - ^1D_2$
2725 97	3	36675 2	$^3P - ^3D_1$		
2769 71	2	36094 8			$^1P_1 - ^3D_2$
2787 60	2	35862 8			$^3P_1 - ^1D_2$
2843 69	2	35157 9	$^3P - ^3D$		
2934 73	1	34065 5	$^3P_1 - ^3D_2$		
2943 33	2	33965 7	$^3P_2 \quad ^3D_1$		
3041 09	0	32874 8	$^3P_1 - ^3D_1$		
3088 64	1	32368 2	$^3P_0 - ^3D_1$		

Table XII —List of Series Lines of Br^{+IV}

λ.	Int	ν_{vac}	Transition
			$2N_1 (O_1 \leftarrow O_2)$
2437 20	2	41018 2	$^2S_1 - ^2P_1$
2293 41	3	43590 1	$^2S_2 - ^2P_2$
			$2N_1 (N_3 \leftarrow O_2)$
2770 52	4	36084 2	$^2D_2 - ^2P_2$
2820 83	4	35440 9	$^2D_3 - ^2P_2$
2983 24	1	33511 7	$^2D_2 - ^2P_1$

Summary

The lines of bromine in the different stages of ionisation (from Br^{+} to Br^{+IV}) have been classified by using the data of L and E Bloch and those given in Kayser's "Handbuch der Spectroscopie" Additional data have been obtained by the author in the region λ 4200 to λ 7500, and assigned to Br^{++} Rough values of the ionisation potentials of Br^{+} and Br^{++} have been obtained They are 19 1 and 25 7 volts respectively The classification illustrates in a very convincing way the utility of the extension of the irregular doublet law, and the horitzontal comparison method of Saha and Majumdar

In conclusion I wish to express my sincere thanks to Prof Meghnad Saha, D Sc, F R S, for his advice and guidance in this work

The Kinetics of the Oxidation of Gaseous Benzene

R Fort and C N Hinshelwood, F R S

(Received January 28, 1930)

Introduction

The comparatively few exothermic gaseous oxidation reactions which have been investigated kinetically nearly all exhibit interesting peculiarities of behaviour connected with the existence of the " chain " mechanism The oxidation of hydrocarbons is an example to which considerable attention is at present being given The rate of oxidation is sometimes retarded by an increase in the surface of the containing vessel—a fact which points directly to the existence of reaction chains —and the relation between the rate and the concentrations of the gases is often a remarkable one Thus ethylene is oxidised at a speed which is relatively little affected by the oxygen concentration but depends upon a high power of the ethylene concentration * Similar relations hold good for acetylene † It seemed, therefore, of interest to study the oxidation of gaseous benzene, partly to ascertain what would be the behaviour of a hydrocarbon of a quite different kind of structure, and partly because benzene is a substance of inherent chemical importance

The results indicate that the oxidation of benzene is a homogeneous reaction in which chains play a part, though not so important a part as, for example, in the combination of hydrogen and oxygen Kinetically the reaction resembles the oxidation of ethylene in many respects In particular, rapid oxidation both of benzene and ethylene is markedly favoured by a high concentration of the hydrocarbon, and, other things being equal, by a high ratio of hydrocarbon to oxygen From this it appears that the primary product of oxidation gives rise to chains by reacting with more hydrocarbon, but not so readily by reacting with oxygen

This result, which may be of some general significance, suggests that it would be interesting to investigate the oxidation of a substance already containing oxygen in its molecule The oxidation of methyl alcohol vapour is therefore being studied

---

* Thompson and Hinshelwood, ' Roy Soc Proc ,' A, vol 125, p 277 (1929)

† Kistiakowsky and Lenher, ' Nature,' vol 124, p 761 (1929)

Method of Experiment

The method of experiment was similar to that which has already been described in connection with previous investigations.* Vapour from a small bulb containing pure liquid benzene and pure oxygen from a gas-holder were admitted at known pressures to a vessel of porcelain or silica, provided with a mercury manometer, and maintained by an electric furnace at a carefully controlled temperature in the neighbourhood of 500° C., where the reaction velocity is conveniently measurable. The change of pressure at different times was then observed. When desirable, samples of the reaction products were withdrawn into gas holders and transferred for analysis to a "Bone and Wheeler" apparatus.

The Products of Oxidation

The final products consist principally of steam and carbon monoxide with a smaller proportion of carbon dioxide. In the light of Bone's researches† on oxidation of aliphatic hydrocarbons the great preponderance of carbon monoxide over the dioxide suggests strongly that the last stage of the reaction is the decomposition of formic acid, which at these temperatures decomposes more rapidly than it is oxidised. (Direct oxidation of carbon monoxide is slow.) This decomposition of formic acid is also the final stage in the oxidation of ethylene and acetylene.

In Table I (p. 220) it is to be noted that the proportion of carbon monoxide is somewhat, but not greatly, decreased by using a greater ratio of oxygen to benzene. Little or no decomposition occurred in the unpacked bulbs when the benzene was heated without oxygen, but the small amounts of "residue" are probably methane formed by a complex series of side decompositions. Small amounts of condensation products were observed, but no carbon. The possible intermediate stages of the oxidation will be referred to later, but it may be said here that hydroxylation of the double bonds may be assumed to occur, followed by rapid further oxidation of the open chain unsaturated compounds so produced to a substance like glyoxal. The remaining stages would then be analogous to the oxidation of acetylene:‡

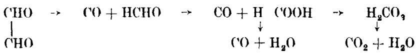

$$\begin{array}{ccccccc} \mathrm{CHO} & \rightarrow & \mathrm{CO}+\mathrm{HCHO} & \rightarrow & \mathrm{CO}+\mathrm{H\ COOH} & \rightarrow & \mathrm{H_2CO_3} \\ | & & & & \downarrow & & \downarrow \\ \mathrm{CHO} & & & & \mathrm{CO}+\mathrm{H_2O} & & \mathrm{CO_2}+\mathrm{H_2O} \end{array}$$

---

* 'J. Chem. Soc.,' vol. 125, p. 393 (1924); 'Roy. Soc. Proc.,' A, vol. 111, p. 245 (1926); vol. 118, p. 170 (1928).

† 'Flame and Combustion in Gases,' Bone and Townend (1927).

‡ Bone and Andrew, 'J. Chem. Soc.,' vol. 87, p. 1232 (1905).

Table I —Analysis of the Final Products of Oxidation of Benzene

Per cent	(a) ' Normal " reaction					(b) Abnormal ' reaction in packed bulb.	
	C_6H_6 100 mm O_2 450 mm 527° C Porcelain bulb	C_6H_6 100 mm O_2 450 mm 527° C Silica bulb	C_6H_6 100 mm O_2 450 mm 507° C Silica bulb	C_6H_6 100 mm O_2 300 mm 527° C Porcelain bulb	C_6H_6 100 mm O_2 300 mm 527° C Silica bulb	C_6H_6 100 mm O_2 300 mm 567 C	C_6H_6 100 mm. O_2 300 mm 567° C
CO_2	34 6	32 8	35 6	31 7	24 8	54 3	42 5
O_2	4 7	4 4	6 8	4 7	4 3	18 2	7 7
CO	57 6	59 5	55 1	60 3	66 5	16 3	45 6
Residue (CH_4, etc)	3 1	3 4	2 5	3 4	4 3	11 2 In this experiment some benzene decomposed before the oxygen was added	4 2

Course of the Reaction

When the benzene and oxygen are admitted to the reaction vessel the pressure changes only very slowly at first, but after an apparent period of induction it rises rapidly The behaviour is shown by the following typical examples

Table II

527° C_6H_6 100 mm O_2 447 mm		527° C_6H_6 100 mm O_2 305 mm	
Time	Increase of pressure in mm	Time	Increase of pressure in mm
′ ′			
0 0	0	0 0	0
0 41	1	1 35	2
1 13	2	5 17	4
2 0	3	8 11	11
2 37	4	9 36	23
3 0	5	9 56	30
3 30	8	10 36	43
3 52	12	10 56	51
4 17	17	11 58	71
4 46	27	12 45	83
5 4	37	13 36	96
5 20	47	14 42	108
5 50	67	16 12	118
6 26	87	18 0	125
7 20	117	20 32	130
8 23	132	25 10	131
9 34	147	∞	132
12 5	159		
14 6	165		
∞	171		

The existence of the “induction period is not so much due to an initial inhibition of the oxidation as to the fact that the first oxygenated products are formed without any pressure increase, and only the subsequent stages of the reaction are shown on the manometer This was shown in the following way

100 mm benzene vapour mixed with 250 mm oxygen and 250 mm nitrogen were admitted to the reaction vessel at 517° and allowed to react until the pressure had increased by 4 per cent of the total change expected The products were withdrawn through a U-tube cooled in solid carbon dioxide to remove benzene, and analysed The percentages found were referred back by means of the nitrogen percentage to millimetres in the reaction vessel

11 4 per cent of the original oxygen had disappeared, and carbon monoxide and dioxide had been formed to an extent accounting for about 60 per cent of this oxygen The formation with decrease of pressure, of some intermediate product containing oxygen therefore compensated largely for the increase due to the production of the oxides of carbon This may also explain the phenolic-smell which was often observed, but since the partial pressure of this intermediate substance was estimated not to exceed about 5 mm at normal temperature, investigation of its nature was deferred Further experiments for its identification are being made with a different form of apparatus In the meantime it suffices from the kinetic point of view to know that there is primary oxidation to a product which is possibly phenolic but which does not accumulate, being rapidly oxidised further by a mechanism resembling the oxidation of ethylene and acetylene

Influence of the Concentrations on the Rate of Oxidation

For a given ratio of benzene to oxygen the rate of oxidation increases in a remarkable manner with the pressure The length of the ' induction period " is however, less influenced than the subsequent stages It will be enough to give some typical figures referring to the central stages of the reaction In all the following tables t_{10}, t_{20}, etc , represent the times required for the pressure to increase by 10, 20 per cent , etc of the total increase corresponding to complete reaction

Pressure of benzene	Pressure of oxygen	$t_{60} - t_{20}$
mm	mm	minutes
100	300	5 5
75	225	9 6
50	150	38 4

The order of reaction," calculated in the usual way from these figures varies from 3 to over 4 This does not mean that each primary act of chemical change depends upon the collision of three or four molecules, since the order is not constant and is also improbably high for a simple gaseous reaction

The explanation is probably that we are dealing with a chain reaction, and the " high order " depends upon the product of several probabilities in the following way The primary act initiating the chain may depend on the square of the pressure, and the probability that the chain shall be continued varies with the pressure again according to a complex law

The concentration of benzene is much more important than that of oxygen Its influence is shown by some of the curves in the figure Many series of experiments were made The considerable amount of numerical data are difficult to reproduce, and only summaries will be given The method of summarising will first be illustrated by an example Curves are plotted for all the experiments in the series The times required for the reaction to reach certain definite stages are then tabulated as follows

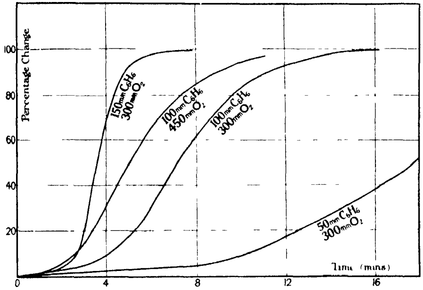

Initial oxygen pressure constant = 300 mm

Initial pressure of benzene	Total pressure increase at completion	Time in minutes for the intervals			
		0-20 per cent	20-40 per cent	40-60 per cent	60-80 per cent
mm	mm				
150	136	5 0	0 55	0 50	0 85
100	128	8 1	2 35	2 10	3 65
50	83	12 4	5 25	5 30	9 45

Taking all the intervals for the 150 mm experiment as unity the following table of relative values is drawn up —

Relative benzene pressure	Relative times				Average excluding 0–20 per cent	Relative reciprocal of average time
	0–20 per cent	20–40 per cent	40–60 per cent	60–80 per cent		
3	1	1	1	1	1	10 4
2	1 62	4 27	4 20	4 30	4 25	2 45
1	2 48	9 55	10 60	11 1	10 4	1

It will be observed that, after the first, the ratios for each interval are nearly enough the same for them to be averaged A threefold change in pressure thus produces a tenfold change in the time except for the first interval, in which only a 2 5-fold change is produced These experiments were made in a porcelain bulb A second series made in a silica bulb at the same temperature, 527°, yielded almost identical results

Initial oxygen pressure = 300 mm

Initial pressure of benzene, mm	150	125	100	75	50
Relative reciprocal times for interval 0–10 per cent	3 9	3 9	2 6	1 2	1
Relative reciprocal times for average of later intervals	10 2	5 7	3 1	2 3	1 0

The influence of oxygen is a little more complicated, and depends upon the benzene pressure With 100 mm benzene at 527° the following results were obtained -

Pressure of oxygen, mm	450	400	300	250	200
Relative reciprocal times for average of intervals 20–40 per cent, etc	0 79	0 61	0 45	0 61	1 00

Thus at first addition of more oxygen has virtually a retarding influence, which, however, is later followed by an accelerating influence Since the rate of reaction is very sensitive to the benzene concentration, the initial retardation by oxygen is probably to be regarded as a function of the reduction in the ratio C_6H_6/O_2 rather than of the absolute increase in the oxygen For practical reasons the highest pressure of oxygen in the above series was only 4 5 times that of the benzene With 50 mm benzene and ratios up to 10 it could be shown that there was a steady increase of rate with oxygen pressure at the higher ratios

Pressure of oxygen in mm	500	400	300	200	100
Relative reciprocal times	9 5	5 2	4 0	1 6	1

The influence of oxygen pressure on the "induction period" was much smaller than the above

These results suggest that as in the oxidation of ethylene the primary oxidation product gives rise to chains if it encounters more hydrocarbon, but to non-chain oxidation if it reacts further with oxygen

Influence of the Surface of the Vessel and the Presence of Foreign Gases

The rate of reaction is nearly the same in porcelain and in silica bulbs, and also in a silica bulb filled with cylindrical tubes with a surface several times greater

Percentage change	2 5	5	10	20	40	60	80
Time in porcelain bulb (minutes)	2 7	4 2	5 9	7 6	9 75	11 65	14 3
,, silica bulb	2 8	4 4	6 2	8 1	10 4	12 7	16 2
,, tube packed silica bulb	1 9	3 8	5 4	7 5	10 15	12 4	15 6

The "induction period" is somewhat shortened by the packing, but otherwise the surface has very little influence Thus we may conclude that the part played by the walls in breaking chains is a small one, and that therefore the chains are probably short

When a silica bulb was used which was completely filled with small spheres of silica possessing a very large surface indeed, an abnormal reaction predominated The results were erratic, there was decomposition of the benzene the proportion of carbon dioxide was increased (Table I), and the total rate of reaction was decreased, temperatures about 40° higher having to be employed to obtain rates comparable with those found in the other bulbs

The influence of foreign gases on the rate of combination of hydrogen and oxygen is very marked indeed In the reaction of ethylene and oxygen their influence is very much smaller With benzene and oxygen the addition of an equal volume of nitrogen or argon caused an acceleration of about 20 per cent only

Influence of Temperature

Except for the induction period all parts of the curve are affected by temperature to the same extent Therefore the times required for the change to proceed from 20 to 80 per cent are typical of the whole curve For 100 mm C_6H_6 and 300 mm O_2 we find -

Temperature	t_{0-10}	t_{20-80}
°C		
547	3 8	1 50
537	4 1	2 87
527	7 1	5 00
517	9 8	10 3
507	16 3	18 6

When log t_{20-80} is plotted against $1/T_{abs}$ the values lie fairly accurately on a straight line, the slope of which corresponds to a "heat of activation" of 81,000 calories The t_{0-10} values give 51,000 calories only For the corresponding experiments with 100 mm benzene and 450 mm of oxygen the values are 82,000 calories and 50,000 calories respectively With 75 mm benzene and 225 of oxygen the t_{20-80} line is curved, corresponding to a value of the "heat of activation" roughly equal to that for the other curves at higher temperatures and falling markedly at lower temperatures

These values of E, the heat of activation, are illuminating A bimolecular or termolecular reaction which could proceed at the speed of the benzene oxidation in the same region of temperature would not have a heat of activation greater than about 50,000 calories, unless it depended on a chain mechanism* The E corresponding to the induction period is actually of this order of magnitude The much greater value corresponding to the later stages can arise in two ways Either it represents the true heat of activation, the acquiring of which at the necessary rate by the molecules becomes possible owing to the existence of chains of great length, or it is only an apparent value, expressing the fact that not only the primary rate of reaction increases with temperatures, but also the chain length This latter factor may vary from a number of causes, including the existence of "secondary" activation as postulated by Semenov† From the small influence of the surface on the rate of reaction it seems probable that the chains are not of great length Thus the second hypothesis is to be preferred, namely that the abnormal temperature coefficient of the main stages of the reaction depends upon a variable chain length

---

* Hinshelwood, 'Kinetics of Chemical Change in Gaseous Systems,' 2nd ed, chap 3 (1929)

† 'Z Phys Chem,' B, vol 2, p 161 (1929)

Summary

The oxidation of gaseous benzene is a predominantly homogeneous reaction The first products are formed without pressure increase, and then oxidised further, by a mechanism rather closely resembling the oxidation of ethylene or acetylene, probably to glyoxal, formaldehyde and formic acid The final products are steam and carbon monoxide with a smaller proportion of carbon dioxide

The rate of reaction varies according to a high power of the benzene concentration , and a high ratio of benzene to oxygen favours rapid oxidation Over a certain range, increase in the oxygen concentration may retard the reaction, though in another range the rate increases with the oxygen concentration

It appears probable that comparatively short reaction chains are propagated, the variation in the length of which gives rise to the abnormal influence of temperature and pressure on the velocity From the much greater sensitiveness of the rate to benzene concentration than to oxygen concentration it is concluded that chains are propagated more readily when the initial oxygenated product encounters another molecule of hydrocarbon than when it is oxidised further by oxygen These results are analogous to those found in the oxidation of ethylene, and have suggested the investigation of the oxidation of a substance such as methyl alcohol, already containing oxygen in its molecule

The Conductivity of Thiocyanates in Methyl Alcohol

By AUGUSTA UNMACK (Ramsay Memorial Fellow), D M MURRAY-RUST, and
SIR HAROLD HARTLEY, F R S

(Received February 5, 1930)

This investigation is a continuation of the work of Frazer and Hartley* on the conductivity of uni-univalent salts in methyl alcohol, which dealt mainly with the halides and nitrates of the alkali metals The thiocyanates are a particularly important class of salts in the investigation of non aqueous solutions, as the thiocyanates of the alkali metals are soluble in a number of solvents, while many of the corresponding salts of other acids are too sparingly soluble to admit of investigation They thus afford an opportunity of comparing the behaviour of ions of the alkali metals in various solvents and of determining their mobilities The thiocyanates of many of the divalent metals are soluble also, but their preparation in an anhydrous condition is much more difficult

Since the publication of Frazer and Hartley's paper Onsager has modified the Debye Huckel theory of the conductivity of electrolytes by taking into account the Brownian motion of the ions, thereby bringing it into much closer agreement with experimental results In water the agreement is good both for uni-univalent and di-univalent electrolytes, and Onsager used Frazer and Hartley's results to show how well his equation represented the behaviour of uni-univalent electrolytes in methyl alcohol † In this solvent, however, there are systematic deviations between the calculated and observed values of the conductivities, which indicate that association between the ions increases with the atomic number of the alkali metal This has been confirmed by the results described in this paper and an explanation is discussed later

The results we have obtained with univalent cations are in general agreement with Onsager's theory, and with the exception of lithium they confirm the values for the mobilities of the ions found by Frazer and Hartley The thiocyanates of the divalent metals show much greater deviations from theory and it is clear that a considerable amount of association occurs even in very dilute solutions of the alkali earth metals, while the thiocyanates of zinc and cadmium behave as weak electrolytes in methyl alcohol

---

* 'Roy Soc Proc ,' A, vol 109, p 351 (1925)

† 'Trans Faraday Soc ,' vol 23, p 341 (1927)

Preparation of Materials and Solutions

Methyl Alcohol.—This was prepared as described by Hartley and Raikes*, the water content, determined by viscosity measurements, was usually less than 0.05 per cent.

Salts. The thiocyanates of the alkali metals were prepared from the carbonate or from a solution of the hydroxide by boiling with a solution of ammonium thiocyanate, the divalent thiocyanates were prepared from the carbonates either by this method or by treating them with a dilute solution of thiocyanic acid. This was freshly prepared before use by distilling a mixture of 60 grams of potassium thiocyanate in 100 c.c. of water and 250 c.c. of a 25 per cent solution of phosphoric acid (sp. gr. = 1.15) in hydrogen under a pressure of about 20 mms. As some of the thiocyanates show signs of decomposition when heated in air, all the salts were dried to constant weight out of contact with air.

Lithium thiocyanate was prepared from pure lithium carbonate, the concentrated aqueous solution being allowed to crystallise in an evacuated desiccator over phosphorus pentoxide. It was dried to constant weight in nitrogen at 110° C. in a Richards bottling apparatus.

Sodium thiocyanate, prepared from the carbonate, was recrystallised either from methyl alcohol or from acetone and dried in nitrogen at 110° C.

Potassium thiocyanate was prepared from a B.D.H. sample by recrystallisation from ethyl alcohol and was dried to constant weight at 110° C. in nitrogen.

Rubidium Thiocyanate.—A solution of rubidium hydroxide was prepared by treating a solution of the chloride with excess of silver oxide. The solution was filtered and boiled with a solution of ammonium thiocyanate. The rubidium thiocyanate was recrystallised from ethyl alcohol and dried in an evacuated desiccator over phosphorus pentoxide.

Caesium thiocyanate was prepared from the carbonate, recrystallised from methyl alcohol and dried in nitrogen at 110° C.

Ammonium thiocyanate was prepared from a B.D.H. sample by recrystallisation from ethyl alcohol and was dried in an evacuated desiccator containing phosphorus pentoxide and caustic potash.

Barium, strontium and zinc thiocyanates were prepared from the carbonates and dried in nitrogen at 110° C.

Calcium, magnesium and cadmium thiocyanates decompose on heating and were dried to constant weight *in vacuo* over phosphorus pentoxide. It was not found possible to obtain anhydrous samples of calcium and magnesium thiocyanates by this method The salts were analysed when constant weight was reached and were found to have the compositions $Ca(CNS)_2\ 2H_2O$ and $Mg(CNS)_2\ 4H_2O$, and samples of this composition were used for making the solutions The amount of water added to the solvent by this procedure is negligible in dilute solutions

---

* 'Trans. Chem. Soc.,' p. 524 (1925).

All solutions were made up by weight, the concentration being checked by titration with silver nitrate after each series of measurements in order to make sure that no decomposition had taken place

Measurement of Conductivity

The experimental procedure was the same as that described by Frazer (*loc cit*), except for the modifications in the measurement of resistance described by Murray-Rust and Hartley* successive additions of salt solution were made to a known weight of solvent contained in a cell of the pattern described by Hartley and Barrett † The resistance was determined after each addition

Experimental Results

The following table gives the values of the equivalent conductivity at various concentrations The values of the concentration in gram equivalents per litre were calculated by assuming the density of the dilute solutions to be the same as that of the pure solvent, $D^{25^\circ}_{4^\circ} = 0\ 7861$ The cell constant, determined by measuring the conductivity of aqueous solutions of potassium chloride at 18° C, was $0\ 03411_7$ The solvent correction was applied by subtracting the specific conductivity of the solvent from that of the solution in each case

Different samples of salt were generally used for the various series of measurements as shown in the first column of the table, if the method of drying differed from that described above, it is mentioned This column also gives the mean values of Λ_0 and x for those salts which obey the relation

$$\Lambda_c = \Lambda_0 - x\sqrt{c}$$

Column 2 gives the specific conductivity of the solvent in reciprocal megohms, column 3, the value of $c \times 10^4$ where c is the concentration in gram equivalents per litre, column 4, the value of $100\sqrt{c}$, column 5, the observed equivalent conductivity, Λ_c, column 6, the difference, D, between the observed value of Λ_c and that calculated from the given values of Λ_0 and x

---

* 'Roy Soc Proc,' A vol 126, p 84 (1929)

† 'Trans Chem Soc,' p 789 (1913)

	k	$c \times 10^4$	$100\sqrt{c}$	Λ_c	D
Lithium thiocyanate— Sample I	0.061	0.7783	0.882	99.54	−0.03
		1.4668	1.211	98.67	−0.06
		2.6917	1.641	97.55	−0.10
		4.5650	2.137	96.19	−0.21
		6.3715	2.524	95.33	−0.09
		8.8561	2.976	94.33	+0.06
Sample I	0.044	0.9030	0.950	99.21	−0.19
		1.8978	1.378	98.20	−0.11
		3.5180	1.876	96.93	−0.11
		6.3082	2.512	95.30	−0.14
		8.8482	2.975	94.18	−0.04
		11.7015	3.421	93.03	−0.11
Sample II (Dried over P_2O_5. Concentration determined by titration.)	0.044	1.8375	1.350	98.47	+0.09
		3.2358	1.799	97.31	+0.06
		6.5968	2.568	95.37	+0.09
		11.2383	3.352	93.48	+0.16
		15.3451	3.917	92.17	+0.28
Addition of 0.22 per cent. water		15.312	3.913	91.85	—
$\Lambda_0 = 101.8$					
$x = 253$					
Sodium thiocyanate— Sample I	0.042	1.5894	1.261	103.80	+0.02
		3.2950	1.815	102.31	−0.06
		5.4567	2.336	100.90	−0.14
		8.7215	2.953	99.37	−0.10
		11.8988	3.449	98.20	−0.01
		16.4174	4.052	96.67	0.00
Sample II	0.058	1.4595	1.208	103.95	+0.03
		3.1130	1.764	102.51	+0.01
		5.6004	2.367	100.95	−0.01
		8.9475	2.991	99.34	−0.03
		12.3223	3.510	98.03	−0.02
		17.7114	4.208	96.45	+0.18
Sample I (recrystallised)	0.058	1.7222	1.312	103.80	+0.14
		3.3886	1.841	102.40	+0.09
$\Lambda_0 = 107.0$		5.9312	2.435	100.88	+0.09
$x = 255$		9.6128	3.100	99.12	+0.03
		13.0618	3.607	97.84	+0.04
		17.6156	4.197	96.70	+0.40
Potassium thiocyanate— Sample I	0.085	1.2218	1.105	111.45	−0.10
		2.5435	1.595	110.24	+0.02
		4.9292	2.220	108.57	+0.08
		7.7231	2.779	107.05	+0.03
		11.9297	3.454	105.23	+0.03
Sample II	0.110	1.4001	1.183	111.23	−0.11
		2.4813	1.575	110.20	−0.08
		4.2057	2.051	108.95	−0.04
		6.2455	2.499	107.75	−0.03
		8.5185	2.919	106.73	−0.08
		11.6718	3.416	105.37	+0.06

	k	$c \times 10^4$	$100\sqrt{c}$	Λ_c	D
Potassium thiocyanate—(contd)—					
Sample I	0 043	0 7519	0 867	112 14	−0 05
(Dried over P_2O_5 *in vacuo*)		1 4376	1 199	111 28	−0 01
		3 2796	1 811	109 65	+0 01
$\Lambda_0 = 114\ 5_5$		5 3577	2 315	108 30	+0 02
$x = 268$		7 1821	2 680	107 29	0 00
		9 3760	3 062	106 27	+0 01
Rubidium thiocyanate —					
Sample I	0 040	0 7821	0 884	115 75	−0 10
		1 5829	1 254	114 82	−0 03
		2 9200	1 709	113 57	−0 05
		4 9107	2 216	112 16	−0 08
		6 8124	2 610	111 12	−0 06
		9 3435	3 057	109 80	−0 17
Addition of 0 5 per cent water		9 298	3 049	108 43	—
Sample I	0 033	0 5516	0 743	116 05	−0 19
		1 6248	1 275	114 72	−0 07
		3 6980	1 923	113 09	−0 03
		5 3534	2 314	112 07	+0 09
		7 3676	2 714	111 04	+0 14
		10 4866	3 238	109 63	+0 15
Sample II	0 033	1 2723	1 128	115 37	+0 18
		2 5190	1 587	114 09	+0 14
$\Lambda_0 = 118\ 2_5$		4 8700	2 207	112 35	+0 08
		7 8074	2 794	110 68	0 00
$x = 271$		10 5690	3 251	109 50	−0 06
		14 7656	3 843	107 83	+0 01
Caesium thiocyanate—					
Sample I	0 042	0 8002	0 895	120 42	−0 06
		1 5848	1 259	119 30	−0 07
		2 9875	1 729	117 94	0 00
		4 5641	2 137	116 64	−0 06
		6 3271	2 515	115 48	−0 07
		8 9478	2 991	114 07	−0 04
Sample II	0 027	0 7423	0 862	120 46	−0 09
		1 4094	1 187	119 59	0 00
		2 5006	1 581	118 43	+0 04
$\Lambda_0 = 123\ 2$		5 0435	2 246	116 46	+0 09
		6 5427	2 558	115 44	+0 02
$x = 304$		8 6794	2 946	114 33	+0 09
Ammonium thiocyanate—					
Sample I	0 034	1 7786	1 334	115 11	+0 13
		3 4966	1 870	113 57	+0 09
		6 8062	2 609	111 50	+0 08
		10 1065	3 179	109 93	+0 10
		12 6320	3 540	108 90	+0 08
Sample II	0 036	1 1032	1 050	115 70	−0 08
		2 5651	1 601	114 15	−0 08
$\Lambda_0 = 118\ 7$		5 2049	2 281	112 30	−0 04
		8 4952	2 914	110 39	−0 18
$x = 279$		11 3791	3 373	109 23	−0 06

	k	$c \times 10^4$	$100\sqrt{c}$	Λ_c	D
Calcium thiocyanate—					
Sample I	0 053	2 310	1 520	100 80	—
(Dried in nitrogen at 110° Slight		3 889	1 972	94 68	—
decomposition, concentration		6 815	2 611	87 11	-
determined by titration)		10 890	3 300	80 39	
		15 015	3 875	75 66	-
		21 924	4 682	70 22	—
Sample II	0 031	1 4771	1 215	105 42	—
($Ca(CNS)_2 \, 2H_2O$)		2 7974	1 673	98 87	-
		5 5787	2 362	90 11	
		8 6437	2 940	83 92	-
		12 0245	3 468	79 06	-
		17 3611	4 167	73 69	- -
Addition of 0 15 per cent water		17 335	4 164	74 53	-
Λ_0 = 122 (approx)					
Strontium thiocyanate—					
Sample I	0 038	1 2921	1 137	110 80	—
		2 4556	1 567	106 34	- -
		4 1672	2 041	101 53	
		7 2635	2 695	95 44	—
		9 7491	3 122	91 76	
		12 5050	3 536	88 56	-
Sample II	0 091	0 9291	0 964	112 28	
		1 7331	1 317	108 71	- -
		3 3746	1 837	103 47	
Λ_0 = 122 (approx)		5 4434	2 333	98 54	—
		7 3494	2 711	95 13	
		10 0699	3 173	91 31	
Barium thiocyanate—					
Sample I	0 041	1 1832	1 088	113 55	—
		2 3519	1 534	109 52	-
		5 0062	2 237	103 29	—
		7 5311	2 744	99 20	
		10 2397	3 200	96 68	-
Sample I (recrystallised)	0 053	0 4948	0 703	116 46	
		1 1073	1 052	113 72	
		2 0649	1 437	110 32	
		3 6637	1 914	106 15	-
		4 9569	2 226	103 47	- -
		7 1208	2 668	99 86	
Sample II	0 058	0 4982	0 662	116 45	- -
		1 2752	1 129	112 92	
		2 7190	1 649	108 49	-
		5 0545	2 248	103 19	
Λ_0 = 122 5 (approx)		6 0691	2 464	101 47	-
		8 7769	2 963	97 56	—
Magnesium thiocyanate—					
Sample I	0 053	1 1127	1 055	98 82	-
		2 2530	1 501	89 86	
		4 8601	2 205	78 73	—
		8 5749	2 928	70 48	—
		11 5557	3 399	66 34	—
		16 2163	4 027	61 90	-

	k	$c \times 10^4$	$100\sqrt{c}$	Λ_c	D
Magnesium thiocyanate—(contd)—					
Sample II	0 036	1 2657	1 125	97 39	—
		2 5610	1 600	88 04	—
		4 5200	2 126	79 79	—
		8 0839	2 843	71 31	—
		11 2283	3 351	66 71	—
		15 6541	3 957	62 37	—
Addition of 0 20 per cent. water		15 622	3 952	65 16	—
Sample II	0 036	0 6115	0 782	104 91	—
		1 3220	1 150	96 86	—
Addition of 0 14 per cent water		1 320	1 149	98 25	—
Λ_0 = 120 (approx)					
Zinc thiocyanate—					
Sample I	0 058	1 4199	1 191	41 98	—
		2 9069	1 705	35 64	—
		4 9707	2 230	30 84	—
		7 8864	2 808	26 81	—
Sample I	0 058	0 9929	0 996	45 07	—
		2 0682	1 438	38 65	—
		4 2604	2 064	32 22	—
		6 9430	2 635	27 91	—
		9 6795	3 111	25 08	—
		14 4147	3 797	21 93	—
Sample II	0 030	1 3966	1 182	41 48	—
		3 0128	1 736	34 67	—
		5 9951	2 449	28 57	—
		10 3333	3 215	23 96	—
		13 9048	3 729	21 63	—
		20 3800	4 514	18 88	—
Cadmium thiocyanate—					
Sample I	0 051	1 7318	1 316	41 52	—
		2 9344	1 713	38 21	—
		5 2568	2 293	34 13	—
		9 0844	3 014	29 91	—
		13 9498	3 735	26 53	—
		18 7087	4 325	24 26	—
Sample II	0 029	2 4201	1 556	39 27	—
		4 7556	2 181	34 82	—
		7 5638	2 750	31 34	—
		11 3343	3 367	28 20	—
		16 2049	4 025	25 41	—
		23 2071	4 817	22 65	—

Discussion of Results

Uni-univalent Salts—The results plotted in fig 1 show that the fall in the equivalent conductivity is proportional to $\sqrt{c}$ in accordance with theory Table II gives the values of Λ_0, and of "x" the observed slope of the conductivity curve, and also of the theoretical slope calculated from Onsager's

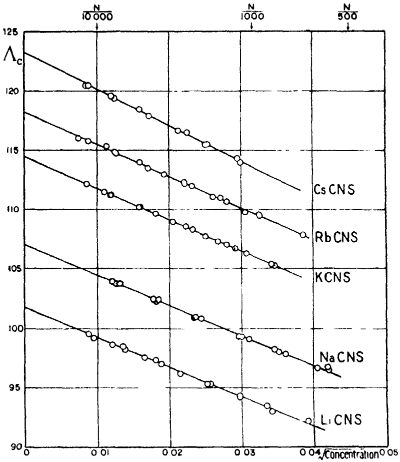

FIG 1

equation, which for uni-univalent electrolytes in methyl alcohol at 25° C reduces to the form

$$\Lambda_c = \Lambda_0 - (0\ 957\ \Lambda_0 + 158\ 1)\sqrt{c}$$

The last column of the table (p 236) gives the values of Δ the percentage deviation of the observed values from theory, $\Delta = \frac{x_{\text{obsd}} - x_{\text{calc}}}{x_{\text{calc}}} \times 100$

The values for the chlorides and nitrates found by Frazer and Hartley are included in the table for purposes of comparison It will be seen that in each series the value of "x" for the lithium salt is slightly less than the theoretical value, and that the difference between the observed and calculated values of

Table II

Salt	Λ_0	x_{obsd}	x_{calc}	Δ	Salt	Λ_0	x_{obsd}	x_{calc}	Δ
LiCNS	101 8	253	255	− 1	KCl	105 0	261	258	+ 1
NaCNS	107 0	255	260	− 2	RbCl	108 6	281	262	+ 7
KCNS	114 5	268	268	0	CsCl	113 6	293	267	+10
RbCNS	118 2	271	271	0					
CsCNS	123 2	304	276	+10	$LiNO_3$	100 2	250	254	− 2
NH_4CNS	118 7	279	271	+ 3	$NaNO_3$	106 4	288	260	+ 1
					KNO_3	114 5	345	268	+29
LiCl	90 9	224	245	− 9	$RbNO_3$	118 1	355	273	+30
NaCl	96 9	230	250	− 8	$CsNO_3$	122 9	379	276	+37

the slope increases with the atomic number of the metal, showing a greater tendency to ionic association in the case of the heavier cations

Both Bjerrum and Fajans have suggested reasons for ionic association such as we probably have to deal with there Bjerrum* has pointed out that if the radii of the solvated cations and anions are less than a certain limit, the probability of association to form aggregates which contribute nothing to the conductivity of the solution is greatly increased Fajans† from a more chemical standpoint has emphasised the increasing tendency to form complexes in the case of small cations and large anions, since these conditions are most favourable for the deformation by the cation of the electron orbits of the anion until a co-valent linkage is produced In the series of salts of the alkali metals such as we are considering, it is easy to decide which of these two causes is operative, as on the Bjerrum hypothesis the fast moving caesium ion should show the greatest amount of association, while on the Fajans' theory it should be the lithium ion, since in the unsolvated condition this is the smallest of the ions of the alkali metals In all three series of salts the lithium ion appears to be the least associated, leading to the conclusion that in dilute solutions of methyl alcohol the size of the solvated ion is the factor which determines the ionic association, in accordance with Bjerrum's view It is only fair to add, however, that in some other solvents the reverse behaviour is found to exist, showing that either mechanism can be operative according to the nature of the solvent The relative importance of the two effects may also alter with change of concentration Güntelberg‡ has shown that in 0 1 N solutions of chlorides of the alkali metals in water, lithium chloride has the smallest activity coefficient indicating the greatest ionic interaction

---

* 'K. Danske Vid Selsk,' Mat fys, vol 7, No 9 (1926)

† 'Z Physik,' vol. 23, p 1 (1924)

‡ 'Z Phys Chem,' vol 123, p 199 (1926)

The Mobility of the Thiocyanate Ion —Values of l_0 for the thiocyanate ion are given in Table III, the mobilities of the ions of the alkali metals being taken from the results of Frazer and Hartley and that of the ammonium ion from measurements by us of ammonium perchlorate and nitrate which will be published shortly

Table III

—	LiCNS	NaCNS	KCNS	RbCNS	CsCNS	NH_4CNS
Λ_0	101 8	107 0	114 5	118 2_5	123 2	118 7
l_0 (cation)	39 6	45 7	53 8	57 4	62 3	57 9
l_0 CNS−	62 2	6[illegible] 3	60 7	60 8_5	60 9	60 8

The value of l_0 obtained from lithium thiocyanate is clearly too high and is omitted from the calculation of the mean value Lithium thiocyanate is extremely hygroscopic and therefore difficult to dry, and it is possible that slight decomposition took place during drying The mean value of the mobility of the CNS′ ion calculated from the other results is 60 9

Di-univalent Salts —The results for these salts are shown in fig 2 The salts fall into two groups the thiocyanates of barium, strontium calcium and magnesium, which are largely dissociated in dilute solution, and the thiocyanates of cadmium and zinc, which are weak electrolytes The conductivity curves for the first group approximate to straight lines in dilute solutions and their slopes in this range are compared in Table IV with those calculated from the Onsager equation, which for di-univalent salts in methyl alcohol at 25° C reduces to the form

$$\Lambda_c = \Lambda_0 - \left\{3\ 064 \frac{\Lambda_0/(l_1^0 + \Lambda_0)}{1 + \sqrt{\tfrac{2}{3}\Lambda_0/(l_1^0 + \Lambda_0)}} \quad \Lambda_0 + 168\right\} \sqrt{3c},$$

where l_1^0 is the mobility of the univalent ion

Table IV

Salt	Λ_0	l_0 (cation)	x_{obsd}	x_{calc}
$Mg(CNS)_2$	120	59	2000	545
$Ca(CNS)_2$	122	61	1400	550
$Sr(CNS)_2$	122	61	980	550
$Ba(CNS)_2$	122 5	61 5	850	552

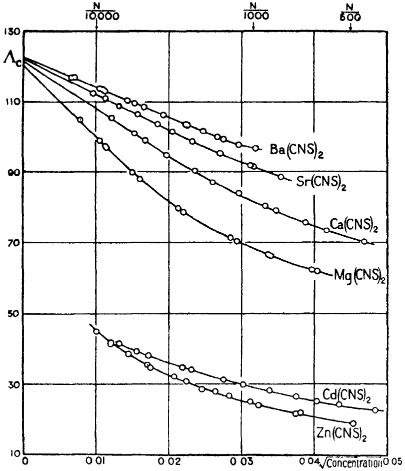

Fig 2

The slopes are all much greater than the theoretical values, indicating that there is a considerable tendency to association, which decreases with increase of atomic number of the metal Table IV includes also approximate values for Λ_0 for these salts and for the mobilities of the alkali earth metals obtained from them, which agree within the limits of error with those found from the investigation of other salts The small number of experimental points in the short range of concentration over which the linear relation is obeyed makes the extrapolation uncertain, and in the case of calcium and magnesium thiocyanates it must be remembered that the solutions were made up with the hydrated salt There is a possibility too that the results are complicated by alcoholysis since the measurements of Bjerrum and Zechmeister* indicate that the first dissociation constant of magnesium methylate in methyl alcohol is 10^{-4}, so that the second dissociation constant must be much smaller Also Murray-Rust and Hartley (*loc cit*) have shown that thiocyanic acid has a dissociation constant of $0\ 45 \times 10^{-4}$ in ethyl alcohol, and by analogy with other acids it is probably weak also in methyl alcohol Nevertheless it is clear that the presence of the double charge on the divalent ion greatly increases the tendency to association in methyl alcohol

The Change in Conductivity Produced by Small Quantities of Water

Small quantities of water were added to the cell at the conclusion of an experiment with a few of the salts, and Table V gives the resulting change in conductivity

Table V

Salt	c	Per cent water	Λ_c before water addition	Λ_c (corrected for dilution and viscosity change due to water)	Λ_c after water addition
LiCNS	0 001534	0 22	92 17	91 16	91 85
RbCNS	0 000934	0 50	109 80	107 06	108 43
$Mg(CNS)_2$	0 000132 0 001565	0 14 0 20	96 86 62 37	96 18 61 65	98 25 65 16
$Ca(CNS)_2$	0 001736	0 15	73 69	73 14	74 53

The addition of 0 1 per cent of water increases the viscosity by 0 4 per cent and should therefore lower the conductivity by this amount if no other changes took place By comparing the values of Λ_c in column 5, which are corrected for the dilution and the change in viscosity on addition of water, with the observed values in the last column, it will be seen that the small quantities of water lower the conductivity of the uni-univalent salts though to a lesser extent than would be accounted for by the change in viscosity With the two di-univalent salts, however, the conductivity is raised considerably, indicating that the degree of association is diminished by the presence of a small amount of water

---

* 'Ber Deutsch Chem Ges,' vol. 56, p 894 (1923)

Summary

1 The conductivity in methyl alcohol at 25° C of solutions of the thiocyanates of six univalent and six di valent cations has been measured over a range of concentration from 0 0001 N to 0 002 N

2 The results for the univalent cations, like those of Frazer and Hartley, are in good agreement with the Debye-Hückel-Onsager theory and indicate that in the series of the alkali metals the tendency to ionic association in dilute methyl alcohol solution increases with increasing atomic number

3 The mobility of the thiocyanate ion is found to be 60 9

We wish to express our thanks to the Government Grants Committee of the Royal Society, and to the Directors of Imperial Chemical Industries Ltd for grants which defrayed the cost of part of the apparatus used in this investigation

---

Discussion on Catalytic Reactions at High Pressures

(March 20, 1930)

Prof G T **Morgan** The study of catalytic reactions under high pressure began with the systematic development of organic chemistry and more especially in connection with the preparation of intermediates required in the production of synthetic colouring matters

The General Use of Pressure in Chemical Synthesis

Pressure is employed as an aid to chemical reactions for one or both of the following reasons —

1 Pressure diminishes the volatility of chemical reagents, thus retaining them in the liquid phase even when the chemical reactions involved take place at temperatures above the boiling points of these reagents under atmospheric conditions

2 Pressure brings about a greater concentration of gaseous reagents, thus facilitating their interaction, especially in those cases where chemical change is accompanied by a decrease in volume of the gaseous phase Chemical processes conducted under pressure are usually accelerated by raising the temperature but by employing a catalyst it is often possible to avoid unduly high

temperatures The present survey refers exclusively to pressure reactions facilitated by catalysts

I *Catalytic Pressure Reactions with Volatile Liquids*

A familiar example of this type of reaction is the hydrolysis of fats and oils to glycerol and fatty acids by water under pressure Water alone will effect this hydrolysis, but at the high temperature required the fatty acids are partially decomposed The addition of about 3 per cent of a base, calcium hydroxide, magnesia or zinc oxide facilitates the change catalytically so that it occurs at much lower temperatures, such as 170° under a pressure of 8 atmospheres In this example the volatile reagent is water which acquires more intense chemical properties at high temperatures

The two following examples of general reactions relate to the production of coal tar intermediates

1 *Alkylation of Aromatic Amines*—The alkylation of aromatic bases is both of scientific interest and of industrial importance An outstanding example is the manufacture of dimethylaniline by heating aniline with methyl alcohol in the presence of a small amount of sulphuric acid This operation is conducted in large autoclaves at 230°, the pressure developed being 30 to 40 atmospheres

In this example both reagents may be regarded as volatile, although the high pressure attained is due mainly to methyl alcohol and to a gaseous by-product, dimethyl ether

A more recent procedure patented by Knoll & Co (D R -P 250,236) brings out clearly the catalytic nature of this process Aniline (93 parts), methyl alcohol (96 parts), and 1 part of iodine are heated under pressure at 230° when a practically quantitative yield of dimethylaniline is obtained

The reaction is a fairly general one, methyl alcohol may be replaced by other alcohols and aniline by other aromatic primary bases

$$C_6H_5\ NH_2 + (x+2)CH_3\ OH \xrightarrow[{[I_2]}]{[H_2SO_4]} C_6H_5N(CH_3)_2 + xCH_3\ OH + 2H_2O$$

2 *Interconversion of Naphthols and Naphthylamines*—When heated at 200° under pressure (50–60 atmospheres) with ammonia in presence of zinc or calcium chloride, β-naphthol is converted into β-naphthylamine (about 70 per cent yield) This catalytic process is not entirely satisfactory and has been superseded by another method of wider application which is named

after its discoverer—the Bucherer reaction * The catalyst in this process is ammonium or sodium bisulphite and the reaction is clearly reversible, for it can be employed either in converting naphthols into naphthylamines or conversely in transforming the latter into the former A high concentration of ammonia favours the production of amines whereas the presence of excess of water leads to the reverse change of amine into naphthol

$$\mathrm{R\ OH} + (x+1)\mathrm{NH_3} + y\mathrm{H_2O} \xrightleftharpoons{[\mathrm{NaHSO_3}]} \mathrm{R\ NH_2} + x\mathrm{NH_3} + (y+1)\mathrm{H_2O}$$

The temperatures and pressures required vary somewhat with the nature of the aromatic radical R The conversion of β naphthol into β-naphthylamine requires a temperature of 150° with a pressure of approximately 5 to 6 atmospheres (D R P 117,471), and the yield is 85 per cent

In the foregoing examples the catalysts are of electrolytic character and recall Prof Armstrong's theory of "reversed electrolysis," a generalisation which postulates the intervention of an electrolyte in chemical interactions between two pure substances

These examples also support the explanation of catalysis based on the transitory formation of intermediate compounds In this connection the bisulphite reaction is noteworthy, for it is applicable generally to those phenols (resorcinol and the naphthols) which can function readily in their tautomeric ketonic forms and to those amines (the naphthylamines and benzenoid metadiamines) which can behave as ketimines With these tautomeric modifications the bisulphites unite to form additive compounds $\mathrm{HO\ R''\ SO_3NH_4}$ and $\mathrm{NH_2\ R''\ SO_3Na}$, whereupon exhaustive amination of the former or hydroxylation of the latter yields the corresponding amine or phenol respectively

II *Concentration of the Gaseous Phase*

The commercial exploitation of the foregoing and other high pressure reactions led to considerable improvements in the technique of autoclaves and other pressure vessels, and it is not surprising to find that colour-producing firms skilled in the use of these appliances were among the first to experiment with high pressure catalysis as applied to inorganic reactions

Ammonia Synthesis —Quantitative experiments on the thermal dissociation of ammonia and on its synthesis from hydrogen and nitrogen were made by

---

* 'J Pr Chem.,' vol. 69, p 47 (1904), and vol. 71, p 433 (1905)

Haber and van Oordt, who calculated the equilibrium percentage of ammonia over a range of temperatures under atmospheric pressure [*]

Nernst and Jost redetermined the ammonia equilibrium constant up to pressures of 75 atmospheres [†]

Subsequently Haber obtained confirmatory results under even higher pressures, and in collaboration with Le Rossignol the research assumed an industrial aspect [‡] In 1908 the Badische Anilin und Soda Fabrik became actively interested in the problem of synthetic ammonia, and having received a report from Haber and Le Rossignol in 1909 they commenced to develop the process on a considerable scale [§] Reference should, however, be made to the pioneering work of Ramsay and Young (1884) and of Le Chatelier (1901), the former studied the decomposition of ammonia by heat under ordinary pressure, whereas the latter experimented on the synthesis of ammonia under high pressures (1901, Fr Pat 313,950) Perman caused these gases to combine under ordinary pressure in presence of catalysts, and he indicated the following metals as furnishing catalytic materials iron, cobalt, nickel, palladium and copper [||]

In 1918, E B Maxted pointed out from theoretical considerations that although the ammonia concentration decreased at first with rise of temperature, yet at about 1200° an inversion point was reached beyond which the concentration increased with considerable rapidity This deduction, which was proved experimentally, had not, however, led to any large production of terrestrial ammonia, although it accounted for the presence of ammonia in the sun's atmosphere as revealed by the solar spectrum (A Fowler and C C L Gregory, 'Roy Soc Proc,' A, vol 94, p 470 (1918))

Hinshelwood, in 1925, studied the kinetics of the thermal decomposition of ammonia in quartz vessels and on platinum and tungsten wires

Owing to the circumstances of the war, the utilisation of atmospheric nitrogen through the ammonia synthesis under pressure and in presence of catalysts had been worked out independently of the German workers by a group of investigators in this country whose efforts had culminated in the Billingham process

A voluminous literature has also appeared on the subject of catalysts for ammonia, including many patents, the indications of which are often somewhat vague Owing to this lack of definite information on the technical side the publications of the Fixed Nitrogen Research Laboratory, Washington, are of considerable interest *

---

[*] 'Z Anorg Chem,' vol 43, p 111 (1905), and vol 44, p 341 (1905)

[†] 'Z Elektrochem,' vol. 13, p 521 (1907), vol 14, p 373 (1908), 'Z Anorg Chem,' vol 57, p 414 (1908)

[‡] 'Z Elektrochem,' vol. 19, p 53 (1913)

[§] Haber, 'Chemiker Zeit,' p 742 (1914), and Bosch, *ibid*, p 721 (1920)

[||] 'Roy Soc Proc,' A, vol 76, p 167 (1905)

Methanol Synthesis —Although Sabatier and Senderens had contemplated the possibility of combining carbon monoxide and hydrogen to produce formaldehyde, yet their own catalytic experiments on these reacting gases carried out under ordinary pressure had led to methane In 1913, however, the Badische Anilin und Soda Fabrik, with the experience of high pressure technique gained in the successful industrial synthesis of ammonia, arrived at a more promising result through experiments carried out at high temperatures and pressures in presence of catalysts (Eng Pat 20,488, D R-P 293,787) In these specifications the patentees claimed the manufacture of easily liquefiable hydrocarbons and oxygenated organic compounds by passing a mixture of carbon monoxide and hydrogen over a heated catalytic reagent under high pressure This high pressure was defined as a pressure exceeding 5 atmospheres The catalytic agents mentioned were cerium, chromium, cobalt, manganese, molybdenum, osmium, palladium, titanium, zinc and their oxides or other compounds In their first example they cited the use of asbestos impregnated with cobalt or osmium oxide and caustic soda, whereas in the second example a suitable carrier such as pumice or diatomaceous earth was successively soaked in potassium carbonate and zinc nitrate

The oxygenated products consisted of alcohols, ketones (such as acetone), aldehydes (such as formaldehyde) and acids (such as acetic acid and homologues) Ten years later the production of methyl alcohol by the B A S F had already reached a manufacturing scale

Meanwhile G Patart had, in 1921, taken up the study of methanol production, and in his first patent (Fr Pat 540,543) he described a process for the synthetic production of alcohols, aldehydes and organic acids by submitting mixtures of hydrogen and oxides of carbon or equivalent gases to the action of appropriate catalytic agents at 300° to 600° under pressures of 5 to 300 kilograms per square centimetre (about 5 to 300 atmospheres) He suggested nickel, silver, copper, iron or other metals known as catalytic agents in hydrogenation or oxidation The oxides or salts of these metals are also mentioned The oxygenated products of these catalyses were, however, not specified In February, 1925, Patart published an account of the industrial synthesis of methyl alcohol by catalysis under pressure in which he indicated the following oxides as suitable catalysts for methanol V_2O_3, Cr_2O_3, ZnO Favourable results were also obtained by addition of copper to these oxides Moreover, the chromates, manganates, vanadates, molybdates and tungstates of metals promoting catalytic hydrogenation or oxidation gave after careful reduction active catalysts furnishing very pure methyl alcohol

---

* Larson, 'Ind Eng Chem,' vol. 16, p 1002 (1924), Ernst, Reed, Edwards, *ibid*, vol 17, p 775 (1925), Larson and Brooks, *ibid*, vol. 18, p 1305 (1926), Almquist and Crittenden, *ibid*, vol 18, p 1307 (1926), Almquist and Black, 'J Amer Chem Soc,' vol. 48, p 2814 (1926) See also Ammoniak, Ullmann's "Enzyklopädie der Technischen Chemie," 2nd ed., 1928

In 1923–24, Franz Fischer and Tropsch published the results of their researches on the hydrogenation of carbon monoxide under pressure (150 atmospheres) and at high temperatures (400° to 450°), using an alkalised iron catalyst These investigators, who employed iron turnings impregnated with potassium carbonate, made a detailed examination of the product and found that it contained alcohols, aldehydes, ketones and aliphatic acids with small quantities of hydrocarbons The products separated into two layers, the oily one being termed 'synthol' and suggested as a substitute for motor spirit *

Reference should be made to a suggestive result obtained by E Lush in 1922, who working with carbon monoxide and hydrogen at 300–400° under 10 atmospheres pressure with a contact mass containing nickel (4 parts), copper (1 part) and alumina (5 parts) obtained in addition to methane, formaldehyde and its polymerides (Eng Pat 180,016)

When work on catalytic reactions under high pressures was begun at Teddington in January 1926, the patent specifications of the I G and B A S F and the published researches of G Patart and Audibert in France and Franz Fischer in Germany, were the main sources of information on this subject The immediate objective was the acquirement of the technique of high pressure research, and for this purpose a study of the methanol synthesis was initiated A preliminary account of the early experiments was communicated to the Society of Chemical Industry in 1928 †

Methanol —With a catalyst prepared either from normal zinc chromate, ZnO, CrO_3, or from the basic salt, 3ZnO, CrO_3, working at 420° under a pressure of 200 atmospheres at a rate per hour of 2000 litres of gas (N T P) through 60 c c of catalyst, the hourly output of organic products is about twice the catalyst volume The liquid obtained is homogeneous, it contains 95 per cent of methyl alcohol, 1 per cent of higher alcohols and 4 per cent of water

---

* 'Brennstoff Chem,' vol 4, p 276 (1923), and vol. 5, pp 201, 217 (1924)

† 'J Soc Chem Ind,' vol 47, p 117T (1928)

The quantitative aspect of methanol synthesis will be discussed by Prof Bone, who has investigated the compressibilities of the reacting gases

Higher Alcohols —The addition of alkaline substances to the zinc chromate catalyst favours the formation of higher alcohols The liquid products from such a mixed catalyst separate into two portions owing to the presence of partially miscible alcohols and esters which form an oily layer on the aqueous methyl alcohol

Ethanol—Catalysts containing cobalt were employed under ordinary pressure by F Fischer and Tropsch in the production of complex liquid hydrocarbons, a fact which suggested that this metal might be equally efficacious in uniting together carbon atoms in reactions under pressure Accordingly, to the methanol catalyst, zinc chromate, were added varying proportions of cobalt chromate with the result that, although methyl alcohol remained the predominant constituent, yet higher alcohols, including ethyl alcohol, were produced in appreciable quantities together with small amounts of aldehydes

In these syntheses the chromate may be replaced by manganate The catalyst containing cobalt shows a marked tendency to become overheated, and this overheating is associated with the formation of methane and water, a reaction which is more exothermic than the formation of methanol from carbon monoxide and hydrogen This local overheating has been largely overcome by improved temperature control in our latest plant, but nevertheless the formation of methane always accompanies the production of ethyl alcohol

Aldehydes and Higher Alcohols —By the use of mixed cobalt catalysts also containing copper, zinc, chromium or manganese, the following alcohols have been identified in addition to methyl and ethyl alcohols *n*-propyl, *n*-butyl, and *iso*butyl So far all the alcohols detected are primary alcohols

Aldehydic products have also been identified as follows formaldehyde, acetaldehyde, propaldehyde, and *n*-butaldehyde There is also indirect evidence of the presence of aldehydals, R $CH(OX)_2$, the ortho-ethers of the aldehydes

It should, moreover, be mentioned that H Dreyfus claims the production of ketene by operating with a mixture of hydrogen and carbon monoxide containing the latter in excess (Eng Pat 262,364)

Acids —Our more recent results confirm the presence of aliphatic acids, and notably of propionic acid with smaller proportions of formic, acetic and *n*-butyric acids

Hypotheses concerning the Mechanism of Methanol Syntheses

As a result of their work with alkalised iron F Fischer and Tropsch suggested that the oxygenated products were formed by the synthesis of methyl alcohol followed by the direct addition of carbon monoxide to this alcohol, with production of acetic acid from which acetone is formed by loss of carbon dioxide This scheme accounts for the presence of acids, ketones and higher alcohols *

Zinc formate on heating decomposes into zinc carbonate formaldehyde, methyl formate and methyl alcohol Under the conditions of the methanol synthesis, zinc formate might play the part of an unstable intermediate compound which is continually being regenerated and decomposed

$$
\begin{aligned}
&\mathrm{ZnO + H_2O + CO = Zn(HCO_2)_2}\\
&\mathrm{Zn(HCO_2)_2 = ZnCO_3 + H\;CHO}\\
&\mathrm{ZnCO_3 + CO + H_2 = Zn(HCO_2)_2}\\
&\mathrm{H\;CHO + H_2 = CH_3\;OH}
\end{aligned}
$$

Higher Aldehydes and Alcohols by repeated Aldolisation and Hydrogenation

$$
\begin{aligned}
&\mathrm{2H\;CHO = H_2C(OH)\;CHO}\\
&\mathrm{H_2\;C(OH)\;CHO + H_2 = CH_3\;CHO + H_2O}\\
&\mathrm{CH_3\;CHO + H_2 = CH_3\;CH_2\;OH}\\
&\mathrm{H\;CHO + CH_3\;CHO = H_2C(OH)\;CH_2\;CHO}\\
&\mathrm{H_2C(OH)\;CH_2\;CHO + H_2 = CH_3\;CH_2\;CHO + H_2O}\\
&\mathrm{CH_3\;CH_2\;CHO + H_2 = CH_3\;CH_2\;CH_2\;OH}\\
&\mathrm{2CH_3\;CHO = CH_3\;CH(OH)\;CH_2\;CHO}\\
&\mathrm{CH_3\;CH\,(OH)\;CH_2\;CHO + H_2 = CH_3\;CH_2\;CH_2\;CHO + H_2O}\\
&\mathrm{CH_3\;CH_2\;CH_2\;CHO + H_2 = CH_3\;[CH_2]_2\;CH_2\;OH}
\end{aligned}
$$

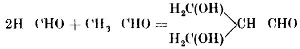

$$\mathrm{2H\;CHO + CH_3\;CHO = \begin{matrix}H_2C(OH)\\ H_2C(OH)\end{matrix}\!\!>\!CH\;CHO}$$

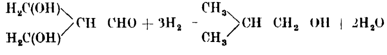

$$\mathrm{\begin{matrix}H_2C(OH)\\ H_2C(OH)\end{matrix}\!\!>\!CH\;CHO + 3H_2 = \begin{matrix}CH_3\\ CH_3\end{matrix}\!\!>\!CH\;CH_2\;OH + 2H_2O}$$

This sequence continues to yield still higher alcohols The aldolisation hypothesis accounts for the products hitherto isolated, but it also postulates the transitory existence of intermediate hydroxyaldehydes and glycols which have not so far been detected These substances may, however, be transformed by dehydration into unsaturated aldehydes and alcohols which would speedily undergo hydrogenation to saturated aldehydes and alcohols If substantiated by further experiment, this aldolisation hypothesis brings the syntheses of homologous alcohols by high pressure catalysis into line with the transformations following on photosynthesis which take place through the agency of living organisms (bacteria, yeasts, moulds and the green plant) With more efficacious catalysts and less elevated temperatures one may anticipate that this analogy will become increasingly closer

---

* 'Ind Eng Chem,' vol 17, p 576 (1925)

III *High Pressure Catalyses involving Liquids and Solids*

The hydrogenation of finely divided coal made into a paste with low temperature tar or other tar as carried out by the Bergius process under 200 atmospheres, is an example of high pressure catalysis since the process is facilitated by addition to the paste of bog iron ore (hydrated ferric oxide) This pasty mass is driven through three bombs arranged in series , the first is maintained at 468° and the other two at 470° Hydrogen is taken up and the end product is a black viscous oil containing saturated hydrocarbons largely aromatic with small amounts of phenolic substances

The tars from low temperature carbonisation contain from 10 to 15 per cent of petroleum soluble crystallisable phenols, and the problem of disposing of these substances would be simplified considerably if they could be converted into hydrocarbons suitable for liquid fuels This conversion is effected according to English Patent No 247,586 of the I G Farbenindustrie Aktiengesellschaft by passing tar in a hydrogen atmosphere over a contact mass containing molybdenum compounds heated at about 500° and under a pressure of 200 atmospheres The product consists of colourless saturated hydrocarbons boiling almost wholly below 350° and to the extent of 30 to 50 per cent below 150°

A much simpler example of this type of catalytic process is the hydrogenation of naphthalene in the liquid state at 180 to 200°, under 15 atmospheres pressure in the presence of nickel The reduction goes in two well-marked stages tetrahydronaphthalene (tetraline) being the intermediate and decahydronaphthalene (decaline) the final product Another interesting and simple example of high pressure catalysis in heterogeneous systems has recently been patented by the I G Farbenindustrie Aktiengesellschaft (Eng Pat 307,223), whereby benzene and its homologues and certain derivatives are converted into the corresponding carboxylic acids by heating at 100° with carbon dioxide under 50 atmospheres in the presence of anhydrous aluminium chloride

As illustrated by the specimens displayed, these uses of pressure in the synthesis of liquid and solid carbon compounds are capable of considerable extension The condensations involved are catalytic reactions, and the chemical nature of the products varies considerably with the catalyst employed

The examples mentioned in the foregoing brief review do not afford experimental evidence for any general theory of catalysis In the case of catalysts soluble in the reagents, the hypotheses of electrolytic interaction and of intermediate compounds offer some explanation of the mechanism of chemical change, but in the case of contact masses the texture of these materials plays a more important part and suggests a close relation between adsorptive power and catalytic activity

More light on these points will probably arise in the subsequent discussion

Prof W A Bone It is only three years ago that the work in the High Pressure Gas Research Laboratories under my direction at the Imperial College, South Kensington, was extended so as to include catalytic reactions, and the new equipment installed there for the purpose was specially designed for investigating the fundamental aspects, both chemical and physical, of the subject Up to the present we have mostly worked upon the catalytic interactions of carbonic oxide and hydrogen mixtures, and more particularly upon the production of methyl alcohol (" methanol ") from them

On first surveying the field of catalytic reactions, what impressed us most was the fact that, save in regard to the comparatively simple case of ammonia synthesis—the thermodynamical aspect of which had been worked out first of all by Haber and Le Rossignol (1907)* and later by Larson and Dodge (1924)†—very few (if any) well-established experimental data for equilibria conditions in gaseous catalytic reactions at high pressures were available It also seemed that little reliance could be placed on mere theoretical calculations owing to uncertainties, not only in the various physical constants entering into them, but also concerning the rôle of pressure itself, which may not always be merely to effect an increase in the density of the medium, and, therefore, in the concentration of the reactants While it may be that theoretical calculations indicate in a general way the respective influences of temperature and pressure in a reversible catalytic interaction, it is only from well-conducted laboratory experiments that precise knowledge will arise

---

* 'Ber Deut Chem,' vol 40, p 2144 (1907)

† 'Jour Amer Chem Soc,' vol 46, p 367 (1924)

In order that such experiments shall be capable of giving reliable results it is necessary that the apparatus employed shall be designed, not merely to withstand the pressure and temperatures concerned (which may be of the order of from 300 to 500 atmospheres and from 300° to 500° C.) and to be handled with safety, but also to permit of accurate pressure and temperature readings being made, to respond readily to comparatively small changes therein, and to enable the chemical state of the gaseous phase in the reaction zone being ascertained precisely at any moment. Also, in equilibria experiments by any static method it is particularly important to keep all the reactants homogeneously in the zone of reaction, so that special precautions must be taken for preventing the segregation or condensation of any one of them outside the zone. In designing our apparatus and methods we have kept these objectives continuously in mind.

As one of the best examples of the influence of pressure in catalytic reactions, I would specially invite attention to the possible changes inducible by various catalysts in systems initially containing carbonic oxide and hydrogen. Without discussing the theory of intermediate products which Prof. Morgan has put forward it may be stated that, according to the catalyst and the temperature selected, one or other (or even all simultaneously) of the following changes may be induced :—

(1) Production of formaldehyde $CO + H_2 \rightleftarrows H_2{:}C{:}O \pm 13.5$
(2) Production of methyl alcohol $CO + 2H_2 \rightleftarrows CH_3OH \pm 22.8$
(3) Production of methane $CO + 3H_2 \rightleftarrows CH_4 + H_2O \pm 55.2$

Without troubling at the moment to discuss whether or no these three reactions form a natural interdependent sequence or are independent of each other, we know in fact that by selecting a suitable catalyst and temperature we may effect the formation of any desired one of the three products to the practical exclusion of the others. Thus, if our object were to produce formaldehyde, for instance, we should use preferably a copper catalyst, at a temperature of from 300° to 400°; if it were to produce methyl alcohol, we should use a reduced basic zinc chromate catalyst at a temperature of from 300° to 350° C.; but if it were to produce methane, we could do so almost exclusively by using a reduced nickel catalyst at a temperature of from 150° to 200° C. And in all such cases we should work at fairly high pressures.

With regard to the production of methane, we have found that if a mixture of carbonic oxide with three times its own volume of hydrogen be passed at a rate of 30 cubic feet per hour, at a pressure of 150 atmospheres, over 100 grams of a reduced nickel catalyst at a temperature of 280° C, there results a 95 per cent conversion into methane and steam So that, after cooling the resulting gas and removing any carbon dioxide, it contains approximately 95 per cent of methane, 4 per cent of hydrogen, and 1 per cent only of carbonic oxide Indeed, we have prepared in this way all the methane used in our research laboratories, afterwards purifying it by condensation at the temperature of liquid air and subsequent evaporation of the liquid Incidentally, we have also found that a mixture of one volume of carbon dioxide with four volumes of hydrogen may be used with equally good results

We may next consider more particularly the synthetic production of methyl alcohol As already stated by Prof Morgan in opening this discussion, the production of alcohols, aldehydes and acids by the interaction of carbonic oxide and hydrogen mixtures suitably catalysed at pressures up to 300 atmospheres and at temperatures between 300° and 600° C, has been studied experimentally by a number of investigators, whom he has mentioned Unfortunately no satisfactory equilibria data in regard to the methyl alocohol synthesis had resulted from their work In 1926–27, however, K K Kelly* and independently Audibert and Raineau,† deduced the one from free energy data and the others from Nernst's heat theorem—the following theoretical values for the equilibrium constants, at various temperatures these being (I think) the first published data on the subject —

$$K_p = \frac{P_{MeOH}}{P_{CO} \times P^2_{H_2}}$$

Temperature °C	K$_p$ calculated by	
	Kelly	Audibert and Raineau
227	3.16	5.75×10^{-2}
327	3.85×10	3.20×10^{-4}
427	1.54×10^{-3}	7.55×10^{-6}
400	1.18×10^{-2}	$6.9 \quad 10^{-5}$

The first published experimental K$_p$ values for the system $CO + 2H_2 \rightleftarrows CH_3OH$ in contact with a basic zinc chromate catalyst at 400° C (under which conditions methyl alcohol is practically the sole synthetic product) were the following —

---

* 'Ind and Eng Chem,' vol 18, p 78 (1926)

† *Ibid*, vol 20, p 1105 (1927)

Observers	Pressure atmospheres	K_p found
Audibert and Raineau	150	1 92 × 10^{-5}
Lewes and Frolich	204	1 80 × 10^{-5}
Brown and Galloway	180	1 62 to 1 98 × 10^{-5}*

It will be seen that, although agreeing well amongst themselves, these results did not agree with either of the foregoing calculated figures, for according to Kelly's calculations K_p at 400° should be 1 18 × 10^{-3}, and according to Audibert and Raineau it should be 6 9 × 10^{-5}

The experiments just referred to seem to be open to the criticism that in each case the equilibrium has been approached from one side only This is an important consideration when it is realised that towards the end, change in such a system is apt to become very slow Indeed, in our experience no equilibrium determined at such high pressure can be considered satisfactory unless approaches are made to the equilibrium from *both* sides

Such was the unsatisfactory state of affairs when the matter was taken up by Drs D M Newitt, B J Byrne and H W Strong in our laboratories three years ago, and, in order to ensure accuracy in the determinations of K_p, it was decided to employ two independent experimental methods, namely, a "static" and a "flow" method, respectively, and in each case to approach the equilibrium from both sides, *i e*, from both the synthesis and decomposition of methyl alcohol As the experimental methods and results have already been published by the Society, readers are referred to the original paper† for details thereof Suffice it here to say that, using a suitably reduced $3ZnO\ Cr_2O_3$ catalyst to which 0 5 per cent copper nitrate had been added, a temperature range from 280° to 338° C, and pressures between 60 and 100 atmospheres—conditions under which a mixture of one volume of carbonic oxide and two volumes of hydrogen was found to produce methyl alcohol to the practical exclusion of other products—and at each experimental temperature approaching the equilibrium from *both* sides by each of the two methods referred to, practically identical results for the equilibrium conditions at each temperature were obtained Two examples may be given By the "static" method the value of K_p at 320° C was found to be 6.7×10^{-5} when equilibrium was approached from the excess methyl alcohol side, and 6.4×10^{-5} when approached from the other side, at 338° C the two experimental values were 4.3×10^{-5} and 4.6×10^{-5}, respectively—and by interpolation the value at 330° C would be 5.5×10^{-5} By the "flow" method the experimental value at 330° C was 5.2×10^{-5}

---

* 'Ind and Eng Chem,' vol 20, p 960 (1928)

† 'Proc Roy Soc,' A, 123, p 236 (1929)

The results as a whole showed the following linear relationship between the free energy and absolute temperature —

$$\Delta F = 70.5T - 30,500$$

From the results as a whole the following K_p values were calculated for every 20° C over the range 260° to 380°, which is the most practicable for the synthesis of a substantially pure methyl alcohol from a $CO + 2H_2$ mixture

Temperature	K_p	Temperature	K_p
° C		° C	
260	1.2×10^{-3}	340	2.9×10^{-5}
280	4.5×10^{-4}	360	1.3×10^{-5}
300	1.6×10^{-4}	380	6.3×10^{-6}
320	6.7×10^{-5}		

It may be observed that these values are all considerably lower than any corresponding values either calculated or experimentally obtained by previous workers Thus, for example, taking 200 atmospheres as a practical working pressure and 600° K (327° C) as temperature, according to the determinations of Newitt and his collaborators the partial pressure of the three components of the equilibrium mixture $CO + 2H_2 \rightleftarrows CH_3OH$ would be

$$CO = 54.5, \quad H_2 = 109.0, \quad \text{and} \quad CH_3OH = 36.5 \text{ atmospheres}$$

Whereas, from Audibert and Raineau's calculated K_p for 600° K and 200 atmospheres pressure, we should expect

$$CO = 39.0, \quad H_2 = 78.0 \quad \text{and} \quad CH_3OH = 83.0 \text{ atmospheres,}$$

and from Kelly's calculated K_p,

$$CO = 10.4, \quad H_2 = 20.8, \quad \text{and} \quad CH_3OH = 168.2 \text{ atmospheres}$$

The correct determination of K_p values in such a system is of considerable commercial as well as scientific interest, inasmuch as such values are the best criteria of the efficiency of a catalyst at a given temperature For example, if by using a given catalyst at a given temperature a quantitative yield of methyl alcohol near to that of the equilibrium proportion predicted by the experimental K_p values at such temperature were readily obtained, clearly there would be no particular object in searching for a more active catalyst

Another point which should be dealt with is that in the paper by Dr Newitt and his collaborators a *caveat* was lodged about corrections which should be applied to their observed experimental pressure values on account of deviations of their equilibria mixtures from the gas laws, but which at the time of its publication had not been actually determined

Hitherto it has been customary, in dealing with such equilibria conditions, to apply the ordinary mass action law on the assumption that the equilibrium mixture is behaving as an ideal gas, but whereas at ordinary pressures such an assumption introduces no appreciable error, at high pressures it is not the case

Experiments are now in progress in our laboratories with the object of determining the isotherms of the $x\mathrm{CH_3OH} + y(\mathrm{CO} + 2\mathrm{H_2})$ equilibria mixtures found by Dr Newitt and his collaborators, but they are not yet sufficiently advanced to enable us to say what are the precise corrections which must be applied to their K_p values So far as we have gone, however, it would appear that at about 100 atmospheres the proper correction to their K_p values should be of the order of *minus* 2 per cent, and that at higher pressures it will be still greater This point is mentioned because it reveals a serious gap in our knowledge in respect of the compressibilities of equilibria mixtures at high pressures and temperatures which must be filled up before such experimental K_p values can be finally accepted We are making it part of the business of our laboratories to determine such compressibilities

In cases such as the interactions of carbonic oxide and hydrogen in contact with various catalysts at suitable temperatures and high pressures, where more than one product is possible and/or more complex changes may be superposed on the initial one, the question of selecting a suitable catalyst and temperature range to produce a given result is of prime importance Unfortunately so little is known about the inner mechanism of catalytic reactions in general that our view of the matter is still largely empirical, we know that by substituting one catalyst for another, or by adding some other constituent to those already in use, in certain cases the result is profoundly affected Thus the addition of an alkaline oxide to the $3\mathrm{ZnO}$ $\mathrm{Cr_2O_3}$ catalyst used in the methyl alcohol synthesis induces the formation of higher alcohols, while by using an iron-alkaline catalyst with water gas at 400° under pressure, F Fischer obtained the product (synthol) containing some 40 individual compounds In our experiments we have naturally sought to work under conditions most favourable to the formation of one particular product, principally with a view to the exact determination of equilibria conditions The systematic exploration of the mechanism of the catalyst is one of the outstanding problems of the subject at present unsolved

Mr C N HINSHELWOOD There are several ways in which the study of reactions at high pressures may yield theoretical information beyond that which can be discovered at ordinary pressures

It would be interesting to make experiments on the actual rates of high-pressure catalytic reactions, because the relation between rate and the pressure of the reacting substances at the very low pressures employed by Langmuir is often quite different from that which holds at ordinary pressures A further comparison with the relationships holding at high pressures may yield important information about the mechanism of the "adsorption" process and the structure of catalytic surfaces

Another interesting point is that very many of the reactions which can be investigated in a theoretically interesting way at ordinary pressures are decompositions proceeding almost to completion At high pressures the reverse reactions could be measured, and a useful correlation of the kinetic and thermodynamic aspects of the problem achieved

Mr M P APPLEBEY I do not think I need to make many comments on what has been said by previous speakers, but I should like to second what Prof Bone has said about the necessity for knowing more about the physical properties of gases and mixtures of gases at high pressures As has been shown by the data resulting from Dr Larsen's work in the Dupont Laboratory, it is very necessary that we should know far more than we do about these physical properties before we can attempt to foretell the behaviour of gases under equilibrium conditions at high pressures Another point I might mention in that connection is that it is almost impossible to apply Nernst's heat theorem to any of these reactions relating to organic substances, for the lack of really accurate thermo-chemical data

On Prof Morgan's interesting introduction I want to make only one comment We are extremely interested in the results he has obtained in the methanol reaction, but I think I ought to say that in our experience we have never succeeded in obtaining, with any catalyst whatsoever, more than a mere trace of ethyl alcohol

Although there is no essential difference between the mechanism of catalytic reactions under high pressure and at atmospheric pressures, it will be very useful to discuss catalysis on this occasion, because I think that the work which has been done during the last four or five years on the ammonia catalyst has led to a much fuller understanding of the behaviour of a catalyst The ammonia catalyst used industrially is essentially metallic iron Many other substances have been proposed as catalysts, and almost every element in the periodic table has been patented at one time or another, but iron is the one substance which is used on a large scale for the ammonia catalysis There are one or two well established facts about the iron catalyst in the ammonia synthesis which are very illuminating The first is that pure iron is quite an active catalyst, but its activity falls off very rapidly indeed , the addition of quite small percentages of magnesia or alumina, however, makes the activity of the iron practically permanent We have had iron catalysts working unchanged in a converter for as long as a year Alumina is a very active promoter and prevents the decline of the activity of the iron Potash also acts as a promoter, but the reason for its activity is very far from understood Fortunately, we do know why alumina acts as a promoter, and I think it is the one example of promoter action which we do know something fundamental about This promoter action of alumina is evidenced by another very important and interesting fact about the technical ammonia catalyst—a fact which was discovered quite a number of years ago, but was not understood until lately—namely, that the iron catalyst is much more active if it is formed by the reduction of magnetic oxide of iron (Fe_3O_4) than if it is introduced as metal or as ferric oxide (Fe_2O_3) These facts have been explained by Wyckoff and Crittenden as being due to the isomorphism of Fe_3O_4 or $Fe(FeO_2)_2$ with iron spinel, $Fe(AlO_2)_2$ The reason why alumina acts as a promoter in the iron catalyst prepared from Fe_3O_4 is that the two elements become intimately mixed owing to this isomorphism The alumina is uniformly disseminated through the iron catalyst, and when reduction of the catalyst takes place, barriers of alumina are formed, which prevent the growth and coalescence of the multitudes of tiny iron crystals on which the activity of the catalyst depends The real cause of the loss of activity of the pure iron catalyst is the growth of the crystals and the coalescence of the small active particles This beautiful theory is to me a very satisfactory explanation both of the action of alumina as a promoter and of the experimentally observed fact that a really active iron catalyst is best prepared from Fe_3O_4

Another point of great importance about the iron catalyst is that it is poisoned by very small quantities of oxygen or oxygen compounds The fact that the amount required to poison the iron catalyst is extremely small indicates that the number of active centres on the surface of the iron is probably very small Very few of the total number of atoms of iron present are active catalytically, and very few atoms of oxygen are necessary to poison them This is in line with Prof Taylor's views on the reaction of solid catalysts, and it forms a very good example

In my view the function of a catalyst is essentially, as Mr Hinshelwood has shown very clearly, to lower the energy of activation of the reacting substance I do not remember Mr Hinshelwood's figure, but I think he has shown that in the decomposition of nitrous oxide the homogeneous uncatalysed reaction requires about twice as much activation energy as the same reaction in the presence of a catalyst The same thing, I think, is shown in the decomposition of ammonia The catalyst seems to me essentially a thing which makes the reacting substance reactive by picking up a smaller amount of energy than it requires to make it reactive in the absence of a catalyst A calculation we made recently, based on Dr Rideal's determinations on the activation potential of nitrogen, gives a very good idea of the work the catalyst does We found that the total amount of energy necessary in industrial practice to fix a given amount of nitrogen by the use of a catalyst was about one quarter of the amount of energy required to activate the same amount of nitrogen electrically That is a very clear indication both of the activity of the catalyst and also of the superiority of catalytic processes over other processes such as the arc process It has also been shown by others than nitrogen adsorbed on a surface of active iron has an ionisation potential much below the normal value

Incidentally, we may note that it is the nitrogen which must be activated, hydrogen is not enough We have made experiments on the activation of hydrogen by passing it over heated tungsten which is known to be an activating agent, and mixing the hydrogen immediately afterwards with nitrogen, but in those experiments no ammonia was formed That is not surprising, because the energy of activation of hydrogen is much less than that of nitrogen

Accordingly, I suggest that we must picture the iron atoms as in some way entangling themselves with the nitrogen so as to loosen the bonds between the atoms of the nitrogen molecule That comes very near to the conception of alternate formation and decomposition of iron nitride I should like to mention some recent work in this connection which seems to be really fundamental Many people have looked for iron nitride as an intermediate in ammonia synthesis, but until recently without any success Recently, however, Mittasch and Frankenburger have published the results of some very fruitful experiments carried out in the research laboratories at Oppau They have shown that the reason why other workers did not identify iron nitride is that the number of active centres in iron is very small, and therefore the amount of iron nitride is very small They have also succeeded in making iron extremely active by volatilising iron wires and condensing the vapour on cooled surfaces along with suitable diluents which prevent the re crystallisation and coalescence of the active iron particles Such active iron has been shown by Mittasch to absorb both hydrogen and nitrogen The amount of hydrogen absorbed is one atom to one atom of iron but the amount of nitrogen absorbed is not stated Also tungsten, which is known to catalyse the decomposition of ammonia, has been produced in this active form by similar methods It is found that at a temperature of 300° approximately this tungsten decomposes ammonia with no change of volume and with the formation of hydrogen as the gaseous product, the NH being presumably attached to the tungsten thus

$$nW + NH_3 = W_nNH + H_2$$

At higher temperatures the tungsten gives off nitrogen and hydrogen in equal volumes

Dr A M J F Michels In referring to high pressures I should like to define the ranges of pressure as we have done as the result of the technique used in Amsterdam In general we refer to pressures up to 2500 atmospheres as low, pressures between 2500 and 10,000 atmospheres are regarded as medium, and pressures above 10,000 atmospheres are regarded as high Prof Morgan has pointed out two influences which high pressures would be expected to have on chemical reactions, but I feel certain that if the definition I have given of "high" pressures is adopted one of these influences must be extended, and three more must be considered The influence in the direction of increased concentration, which Prof Morgan has mentioned I should prefer to consider in terms of the increased number of collisions, as it is certain that at appreciable pressures the ordinary law of mass is a rather rough approximation, and at really high pressures does not apply at all What must replace it can only be determined from experimental results on isotherms and compressibilities of mixtures, as discussed by Prof Bone Another influence is the induced or increased polarity when the molecules are forced together, and in some cases the change from the non polar to the polar form of a molecule For example, it appears from some work of Kirkwood that at moderate pressures the non-polar form of CO_2 changes to the polar form For this investigation we shall have to deal with the measurement of the dielectric constant. For any chemical reaction to occur, the molecules must possess a certain minimum energy, which is in general available as kinetic energy. By compressing the molecules a certain amount of potential energy is stored, which may result in the reaction occurring with a lower kinetic energy, *i.e.*, at a lower temperature. It might be, for instance, that an exothermic reaction which will not normally take place at a low temperature could be made to do so by the application of a sufficiently high pressure. If the potential energy is very high there may be an appreciable distortion of the molecules and a resultant change in the vibrational and rotational specific heats and in some optical properties, although the last will be rather difficult to measure. From a purely thermodynamic point of view it is easy to show that the entropy is decreased by increasing pressure, the total decrease being given by $\int \alpha dp$, where α is the temperature coefficient of expansion. At $T = 0$, α is zero and the entropy is independent of the pressure. Therefore, the difference between the entropy at a given temperature and zero temperature will decrease with increasing pressure and consequently the specific heat at constant volume must also decrease. Lewis has suggested that it may be that at $p = \infty$, $c_V = 0$. The decrease in specific heat will not only be expected for the vibrational and rotational specific heats, but also for the translational specific heat, in accordance with modern quantum statistics. If however the specific heat is changed, the heat production of a chemical reaction and therefore the equilibrium, will also be expected to change. It follows then, that the measurement of the specific heat and the temperature coefficient are of interest to high pressure chemistry. Finally, all the facts pointed out are influencing the free energy, the well-known ψ function and the thermodynamic potential. Application of the Gibbs' principle of equilibrium to chemical reactions with the help of these functions has led to the law of mass and the law of Van T Hoff, but in the deduction of these laws assumptions are made which no longer hold at high pressures.

It is hoped that the high pressure research which is being carried out at Amsterdam may contribute to the advancement of high pressure chemistry along these lines. In the first range of pressure—up to 2500 atmospheres—we have a pressure balance that will give a maximum reproducibility of the order of 1 in 500,000, and have worked out a differential method of calibrating this instrument in absolute units, *i.e.*, KG/cM^2. In this range there are no longer any technical difficulties to be expected, and measurements on the effect of pressure on the following physical constants are being carried out:—isotherms of gases, compressibilities of liquids and solids, viscosity of liquids and solids solubility of gases in liquids, dielectric constants, refraction index, specific heats, electrical resistance of metals Some of the results have been published already, and others will follow shortly

For the second range of pressure -from 2500 to 10 000 atmospheres- the preparatory work is finished, and the final work will be started as soon as there are trained men available

For the third range we are doing preliminary work consisting mainly of the examination of materials to stand really high pressures We have been able already to reach pressures of 35 000 atmospheres

Dr E K RIDEAL The question of the adsorption of the gases has been mentioned by Mr Appleby as a possible characteristic of catalytic behaviour but that cannot be the only criterion He mentioned the work of Mittasch for example who volatilised iron wire and produced very active iron which iron absorbed both hydrogen and nitrogen We can get exactly similar results with platinum wire , one atom of platinum, on deposition on glass will occlude or absorb or combine at liquid air temperature with one molecule of nitrogen and also with approximately one molecule of hydrogen Iron and platinum are, however, very different in respect to their catalytic activities in commercial synthesis So that that is not the only criterion in determining the behaviour of catalysts Reference has been made by Mr Hinshelwood to the measurement of the rate of catalytic reactions, and to the problem of making some of the catalytic surfaces reproducible, and I think that one of the important things we have to consider is how far we can make catalytic surfaces reproducible either by building up a surface from volatilised metallic atoms or by disintegration of a macrocrystalline solid We know, of course, that there is a phenomena termed "activation " If we take a piece of ordinary copper and oxidise and reduce it several times it becomes more and more active What has happened to it on oxidation and reduction ? One can see, at any rate, by examining it under the microscope, that the surface has been broken up into smaller and smaller pieces and that is associated with an enormous increase in the catalytic activity The question which arises is whether there are changes other than increase in the specific surface and specific " edge length " that one can associate with that change in catalytic activity and which might give us a quantitative measure of the catalytic activity and also indicate the lines on which to proceed in order to get an effective catalyst There are two pieces of work which have led to some rather interesting results in that connection The first concerns the study of the oxidation of copper If we oxidise it at high pressures with oxygen we obtain a gradual oxidation following a very simple law The oxide film increases so that the square of the thickness goes up proportionately with time But if we lower the oxygen pressure we find that at a certain critical pressure this law breaks down In other words, there must be a pressure below which the so called diffusion law does not hold In the oxidation of copper at low pressures with oxygen we find that when we have a very active copper from the catalytic point of view this critical pressure is very high, and there exists a rough proportionality between the activity and this pressure The conclusion can be drawn that in an active copper catalyst the surface is broken up into a number of minute cracks—which are supposed to occur in a great number of solids—and that when the gas hits the surface the molecules of gas flow along the surface and run down into the cracks, and possibly the more cracks there are the greater is the pressure necessary to obtain the saturation of the copper surface That seems to confirm in a general way the action of aluminium oxide as a promoter in an iron catalyst One can also find some evidence for this sort of phenomenon in the study of the heats of adsorption Originally the heats of adsorption of gases on metals was studied as a criterion of catalytic activity by Taylor, and he obtained some very interesting curves If we plot the heat of adsorption against the quantity adsorbed he obtained the first portion of the curve rising, and later a falling off Taylor suggested that the rise in the initial portion was due to adsorption on a very active patch We have been doing some more experiments on the heats of adsorption, using a modified type of calorimeter, and the interesting point about the results is that when we take an active catalyst the quantity of gas that goes into solution during the time interval necessary to measure the heat of adsorption is relatively great, and if one corrects for the quantities of gas going into solution in the metal one finds that the heat of adsorption is independent of the quantity adsorbed One gets a series of straight lines, depending on the specific activity of the catalyst The heat of adsorption of hydrogen on a catalyst which is very active is something like 10 000 calories, and in the case of inactive copper it is about 12,000 So that the problem is now more definite These active patches are not distinguished by a very high heat of adsorption, but the whole character of the metal has been changed It looks as though we have potential energy stored up in an active catalyst which is not present in an inactive one

We have found that the rising portion of the curve obtained is entirely due to solution, and the rate of solution of many gases is extremely rapid I think that is a factor we may have to consider in the process of catalysis, especially at high pressures

Mr S J Green Chemists up to the present have been guided in their work on catalysis by the older theories, as, for example, the theory of chemical constitution, and the deductions from the laws of thermodynamics, as applied to the chemical reaction, and these theories have been supplemented by theories of catalysis—particularly the adsorption theory and the chemical "intermediate compound" theory—to enable us to understand the effect that a catalytic agent may have in aiding the usual type of chemical change None of these theories provides any guidance to those of us who are more interested in the practical applications of catalysis, in finding the catalyst we want for any particular reaction, and, having found it, to discover what course the reaction takes in producing the final product Alcohol, and many other substances, may undergo a number of changes, the nature of which depends purely and simply on the catalysts with which the substances are brought into contact I would like to suggest that modern physics could provide the key, and that we may find it as soon as physicists are less occupied with their own problems, or as soon as we as chemists apply modern physical methods It is now many years since Ehrlich and, later, Fischer, suggested the "lock and key" analogy to explain the action of enzymes, especially the highly specific action of these catalysts' At that time this analogy could only remain a mental picture of the mechanism, without any practical significance Now, with the means available of exploring surface and molecular structure, some advance would seem well within the practical range If a chemical action occurs in contact with a surface which would not happen under the same conditions if that surface were absent, then there must be some relation between the surface and the molecules in which it induces a change I would suggest that a structural relation exists, on the lock and key analogy, as best explaining the specific action of catalytic surfaces, and also that this structural relation is capable of elucidation by X-ray methods The practical point I have in mind is this Thoria, zirconia and alumina have many actions in common, and, of course, some differences It would seem to be worth investigating whether the actions in common cannot be associated with features of their surfaces in common—the ultimate molecular structure of their surfaces The differences, of course, would also be instructive, and possibly could be correlated with the differences in their catalytic action Likewise, thoria is well known to exert very different actions according to the method by which it is prepared The voluminous form, made by ignition of the nitrate, for example, is comparatively inert Could not the difference in the action of the two forms be associated with some difference in their surface structures ? I suggest that perhaps our best hope of answering the two difficult questions in regard to catalysis – how to find our catalyst, and having found it, how does it act ? lies in closer co operation between chemists and physicists between shall we say, Prof Morgan and Prof Bragg

It is worth considering the results that have been achieved already in correlating surface structure and catalytic action Frolich Davidson and Fenske last year* studied the decomposition of methanol at ordinary pressure in contact with catalysts known to promote its formation at higher pressures namely, copper reduced from its oxide at a low temperature zinc oxide and mixtures of these two substances In the first place, copper and zinc oxide were shown to maintain their characteristic crystal structure in the catalytic form—both when pure and when mixed The only apparent surface change produced by the mixing was in the " unit cell size " of the copper and zinc oxide that is, the distances apart of the atoms of copper and the atoms of zinc were each altered by the presence of the other in a way that is only partially understood by metallurgists At the same time, pure copper induced decomposition of methanol mainly to methyl formate and formaldehyde, while zinc oxide promoted decomposition to carbon monoxide The significant fact emerged from the work of these three investigators on mixtures of copper and zinc oxide that an exact parallelism existed between firstly the variation of the copper lattice and the percentage of methyl formate (and formaldehyde) in the decomposition products, and secondly, between the variation of the zinc oxide lattice and the percentage decomposition of methanol to carbon monoxide, that is to say, the percentage of formaldehyde and methyl formate varied in a manner closely connected with the variation of the copper lattice, and likewise the percentage of carbon monoxide in the products of decomposition varied with the variation of the zinc oxide lattice That seems extremely significant, and I should like to suggest that our next theory of catalysis will correlate surface structure and chemical action in some such way I would commend this line of approach to Prof Bone and Mr Hinshelwood, both of whom have made so many interesting observations on surface action

A question for Dr Newitt In connection with his work on the methanol equilibrium to which Prof Bone has referred, did he observe the formation of di-methyl-ether when methanol or carbon monoxide and hydrogen were maintained in contact for considerable periods with the catalyst he was using ? I suggest that correction for di-methyl-ether formation would possibly raise his figures more nearly to those obtained by Audibert and Raineau

---

* 'Ind Eng Chem ,' Feb , 1929, p 109

Dr F A FREETH At the beginning of the preamble which Prof Morgan has prepared there is a statement which, to put it plainly, is not true It is stated that Pressure diminishes the volatility of chemical reagent, thus retaining them in the liquid phase " That is true only at quite small pressures, and if you have a liquid in contact with a gas, above the critical point and increase the pressure reasonably, the whole thing will go into the homogeneous phase

Prof MORGAN I appreciate the point, but I said in my opening remarks that this was the older use of pressure I quite realise that this older method has to some extent been superseded by the new one, and I only meant that the statement applied within certain comparatively narrow limits, and when all the reagents were "in the liquid phase under atmospheric conditions

The PRESIDENT Why is it that only a little of the iron, and not the whole surface acts in the fixation of nitrogen ?

Mr M P APPLEBEY I think we can only say that we know nothing about it I always thought it was a question of the irregularity of the surface

The PRESIDENT Whether it is a plain surface, or broken up ?

Mr APPLEBEY If the surface is plain, I imagine the atoms are interlocked and are not free to make these combinations with the nitrogen, but if the surface is irregular you have particular atoms active, and I have always considered that those particular atoms which stand up make the actual contact

Mr C N HINSHELWOOD There are two facts about chemical reactions of this kind which are important The first is that we have to supply energy to the molecule before it can re-arrange itself, the second is that catalytic actions are very sensitive to the actual structure of the surface It is probable that when the molecules are adsorbed on the surface, there is distortion, depending on the spacing, and the greater the distortion the greater is the potential energy stored up, therefore, the less the energy which has to be supplied to break the molecule up or cause it to be re arranged

Prof F G DONNAN In connection with what Mr Hinshelwood has said I should like to remind you of a very interesting series of investigations on rates of reaction the kinetics of hydrogenation of various substances carried out by Mr E S Lush, which showed that the velocity is proportional very accurately to the square root of the hydrogen pressure About 17 years ago Mr Shaw, of Liverpool I think we were the first to do it carried out under my direction a research on the velocity of the reduction of oleic acid and other substances—but oleic acid especially by hydrogen under pressure in the presence of a nickel catalyst, and it was pointed out by Mr Lush that that had shown that the velocity was accurately proportional to the square root That is interesting, because it is known that the solubility or absorption of hydrogen in metals is proportional to the square root of the pressure It is quite clear that the active substance is atomic hydrogen

Mr A C EGERTON One part of my own work seems to indicate something of the sort mentioned by Mr Hinshelwood When an anti knock for instance a lead compound, is present as vapour it will combine with oxygen and produce an active chain breaker but as soon as it conglomerates, so that the particles become bigger, it becomes less and less active As a single molecule it is active, but when spread out on a layer or molecules all the bonds between the various molecules get mutually satisfied and it is no longer active

Dr MAXTED With regard to the velocity of hydrogenation it is true that under some conditions it is proportional to the square root of the pressure but I think that under other conditions it is directly proportional to the pressure, and under certain other conditions it is not directly proportional either to the square root or to the pressure but to something between the two

Prof DONNAN The conditions of the experiments carried out by Mr Lush and by Mr Shaw were quite different, except that they both used nickel as the catalyst and the law held accurately in both cases It also held at high pressures

The PRESIDENT Do you think that is a universal law ?

Prof DONNAN Well, there was considerable variation in the conditions, including the pressures applied in those two cases and the results agreed very closely

The PRESIDENT The work was done a long time ago ?

Prof DONNAN Mr Shaw's work was done 17 years ago but I think it was done quite as accurately as it would be done to-day The work of Mr Lush was done three or four years ago, and I do not think the technique has changed much since then

Dr E F **Armstrong*** It is perhaps appropriate to call attention to and emphasise the detailed explanation given of the action of catalyst promoters as well as of catalyst poisons in a series of papers published together with Dr T P Hilditch in the 'Proceedings' from 1919 to 1925 Any general theory to explain the action of promoters was found undesirable The increased activity in presence of the promoter may be ascribed in some cases to causes which are essentially chemical rather than physical, in others it has been shown that a simple mechanical explanation, the development of greater surface, is most in harmony with the observed facts Nearly 30 years' close association with catalysts of very varied nature both in the laboratory and on the large industrial scale, has convinced me that the development and maintenance of the maximum of active surface is the one essential fact connected with their activity Impurities present either during manufacture or introduced with the materials which are to interact, errors in mechanical and physical treatment during the preparation of the catalyst, have the effect of reducing surface and therefore lessening activity The subsequent course of the catalytic reaction depends on the concentration of the reactants at the surface, on the removal of the products of action from the surface and other obvious factors In reactions involving a gas, pressure increases the concentration of gas in the active system at the surface of the catalyst, so that the rate of action is proportional to the pressure, except in certain abnormal instances ('Proceedings,' A, vol 100, p 240 (1921))

As an example of the mechanical increase of surface by promoters it has been shown ('Proceedings,' A, vol 103, p 586 (1923)) that alumina in particular and certain other metallic oxides stimulate the action of unsupported nickel, owing to the action of the non-reducible oxide in separating the nickel particles and preventing them from coalescing

Increased catalytic activity due to chemical causes is illustrated by the effect of adding copper to a nickel catalyst ('Proceedings,' A, vol 102, p 27 (1922)) Very active catalysts are obtained only when the two metals are precipitated together in the same complex carbonate molecule Such a compound is reduced to metal by hydrogen at 180° C, whereas nickel compounds alone require a temperature above 300° C, a possible explanation being that the reduction of the copper salt is strongly exothermic, so that sufficient local heat is produced to reduce the nickel salt. Unless there is this close proximity—which is effected by nothing short of combination in the same molecule—the nickel is not reduced at 180°.

---

* Contributed in writing after the discussion

The finely divided nickel so obtained at the lower reducing temperature is more active than that prepared at a higher temperature, but it is in no way equal in activity to nickel adequately distributed on a support. In this connection reference may be made (‘Proceedings,’ A, vol. 103, p. 594 (1923)) to the fact that in acid extracted Kieselguhr, the removal of the original metallic constituents causes the nickel oxide to penetrate too far into the siliceous structure, with the result that it is less accessible to reduction and to contact with oil and hydrogen. Deposition on the guhr of a layer of oxide, such as alumina, fills up these inaccessible parts of the diatom structure and causes the superimposed layer of nickel oxide to be placed in a more favourable position for contact action.

In industry a close study of the means of increasing and maintaining the surface of each individual catalyst is requisite—there is no mystery attached to the problem until the question is asked why does the reaction go in a particular manner, as evidenced by the multiplicity of substances to which ethyl alcohol gives rise in presence of different catalysts within the same range of temperature and general conditions.

SIR RICHARD THRELFALL, F.R.S.: I have worked for a good many years on this subject, and every theory I have put forward I have been able to destroy, and I have never met anybody who was in any better position.

The PRESIDENT: I think Sir Richard has ended the discussion more or less on the right note. The great interest in this subject is due to the fact that we know so little about it, and obviously we shall require the combined efforts of the physicists and the chemists, including those engaged in the works, if we are to arrive at a solution of these extraordinarily important questions. Ten years ago we knew nothing of catalytic reactions, but we are now beginning to get some idea and to realise the importance of these things. I should like to express thanks to those who have taken part in this discussion, which has been exceedingly interesting.

The Origin and Nature of Coals and Chars

By HENRY E. ARMSTRONG, F.R.S.

(Received March 15, 1930.)

Prof. Bone and his co-workers have now reached a stage in their *systematic* study of the coal substance—their results are so remarkable and significant—that it may be to the advantage of further inquiry to consider very briefly the evidence we have of the *process* involved in the formation of coals. The inquiry has too long been left in the unassisted hands of the geologist and palæo-botanist, and only benefit can accrue to it if the outlook be not only widened but made precise.

The problem of the nature of coal has been in my thoughts since early in the '70's, when I grasped the meaning of Pasteur's most remarkable demonstration that moist sterilised sawdust is not oxidised by exposure to oxygen—that ordinary vegetable decay is the outcome of bacterial action.

At about the same time, I read the Rev. Charles Kingsley's book, 'At Last," a description of his voyage to the West Indies, of Trinidad, in particular. He calls special attention to the way in which fallen trees decay in the forest—the wood rapidly rotting away, only the outer bark remaining. I was able to verify this myself years later, in north-west Canada: entering the forest and straying from the path, on attempting to climb over what appeared to be a solid tree trunk one fell in through the shell of bark which alone remained.

From the early '80's onwards I had many opportunities of studying the oils obtained on carbonising coals at low temperatures. Nothing is more striking than the large proportion of phenolic (benzenoid) compounds, cresols in particular, present in these distillates. The temperatures at which they are produced are so low, relatively, that these compounds cannot well be otherwise than "precontained" in the coal. It has long been known that a certain proportion of mellitic acid, $C_6(CO_2H)_6$, can be obtained by oxidation of charcoal; it was clear, therefore, that highly complex benzene derivatives could be formed during the change into coal, as such compounds are not known to occur in wood, although these contain phenolic derivatives.

Geologists generally have regarded coal as mainly the decayed remains of an arboreal and swamp vegetation, and they have supposed that resinous spores are often an important constituent. Prof. Huxley, in particular, in his celebrated lecture on Coal (1870, 'Collected Essays,' vol. 8), lays great stress on the importance of these latter and supposes them to be the origin of the yellow material in coals He speaks of anthracite coals as consisting of "carbonised substance" without the yellow material Huxley's picture of the changes effected is a simple one—

> "The mixed heap of spores, leaves and stems in the coal forest would be persistently searched by the long-continued action of air and rain, the leaves and stems would gradually be reduced to little but their carbon, in other words, to the condition of mineral charcoal in which we find them, while the spores and sporangia remained as a comparatively unaltered and compact residuum"

Leaves and stems, under natural conditions, are not reduced to little but their carbon" inevitably, the carbon also goes until nothing organic is left

If coal were but modified wood, how then had the wood been preserved and changed into coal? The only explanation in accordance with observation seemed to be that the "raw material" had at least been collected under water away from oxygen Coal could not well be the outcome of a mere oxidation process, whatever the nature of the change Further light was thrown upon the problem when it was shown that, if 'cellulosic" material were heated to a by no means high temperature, in a closed vessel, it was converted into a coal-like substance After all, charcoal is so prepared Even more striking is the production of a black char in the modern process of cracking" petroleum hydrocarbons under high pressure, especially as the char is obtained even from light distilled hydrocarbons

The organic chemist can but reflect upon carbon itself My speculations on carbon have been carried so far that I have even questioned the existence of elementary carbon in more than one form, that of the diamond, particularly in two Essays written for the Managers of the Royal Institution upon the work of Sir James Dewar Even graphite always contains a small proportion of hydrogen— though scarcely enough perhaps to permit of our assuming that it is a hydrocarbon As a matter of fact, at present, we know very little of the chemistry of the elementary substance carbon Maybe the amorphous carbons are but incompletely crystallised graphite Largely on optical grounds, I have gone so far as to suggest that graphite and other black carbons may be composed of two distinct forms of atomic carbon—a view to which Prof Bone's observations lend no little support A question of importance to be considered will be, whether chars be actually or merely potentially benzenoid, the absence of naphthalene and anthracene derivatives from the oxidation products is very remarkable

As long as the deposit be not of excessive thickness, it may be possible to assume that a coal has been produced *in situ* and is mainly of arboreal origin. This becomes impossible when the seam is of the excessive thickness of some of the Australian deposits, such as the Morwell Brown Coal. As perhaps at Valdarno, the glacial plough may have forced down great masses of surrounding vegetation (Wellingtonia ?) into a natural cavity. The extent to which peat was the original material laid down has also to be considered, this, apparently, may grow to a considerable thickness

Shales have to be explained as well as coals. Unlike most coals, these contain a large admixture of earthy matter. Their composition, too, must be different from that of the average coal—as they often yield a high percentage of paraffin wax on distillation, a substance rarely present in more than small amount in low temperature tars. The origin of shales is probably not far to seek. When sea-water plankton is examined it is usually rich in unicellular organisms each of which contains a big fat globule. The raw material of the shales may well have been fat bearing diatoms, algæ and similar organisms growing in swamp pools. Some coals the highly bituminous are conceivably mixtures of arboreal and peaty vegetation with such "algal" growths built up in marshy pools. The Kimmeridge beds present a remarkable alternation of thin layers of limestone with clay-shales rich in organic matter. I am not aware of any evidence of arboreal growth in the series. The deposits need a far closer examination with the aid of the chemist

Finally, we have to think of vegetable humus formed within the soil - as a material on the way to coal, carbonaceous materials, such as sugar, we know are easily condensed and carbonised, there is evidence that such products are in part benzenoid. The true anthracites are, perhaps, formed from peat alone

This last year, for the first time, I had the opportunity of inspecting a deposit of lignite, at Valdarno, in Tuscany, of such a character as to leave no doubt in my mind that the original material was wood pure and simple. Evidently, at some time, a great forest had been swept down into the lake—not gradually but suddenly, as the deposit was not mixed with earthy material. The woods were to be seen in various stages of transformation—the walnut in places was still wood whilst the oak was coal. I there and then made up my mind *finally* that coal was no mere residue but an organically re wrought "condensed" material, largely a synthetic artefact—a natural Bakelite ! The conception had long been floating in my mind. I put this conclusion on record in the account I gave of my visit. Bakelite, now so largely used as an insulator, is a material formed by condensing, as it is termed, phenol and its homologues with formic aldehyde. In this material, many molecules of a simple benzenoid are linked together by means of formaldehydrol, $CH_2(OH_2)$—the links being single carbon atoms carrying little hydrogen; even this is for the most part removed from chars. The striking results obtained by Prof. Bone and his colleagues all serve to support such a view. It is clear that the work opens up a great future, one that will need systematic and long continued study in many directions. At present, discussion may best be limited to the broad conclusions now set forth.

The Optical Rotatory Power of Quartz on either side of an Infra-Red Absorption Band

By T. M. Lowry, F.R.S., and C. P. Snow.

(Received December 13, 1929.)

Drude's equation for natural optical rotations depends on the existence of "ions" of characteristic frequency, of which each type contributes a partial rotation to the total rotatory power of the medium. There is nothing in the equation to limit the range of these frequencies, but in discussing the rotatory power of quartz (the only substance for which sufficient data were then available), Drude himself concluded that "the kinds of ions whose natural periods lie in the infra-red are inactive" ('Physical Optics,' 1907, translation, p. 413). An alternative view was put forward by R. W. Wood, who concluded that a "spurious" anomaly could be produced in colourless media by the combined influence of an infra red and an ultra violet absorption band ('Physical Optics,' 1919 edition, p. 492); and C. E. Wood and Nicholas* have applied the same theory in the hope of deducing the configuration of the molecule from the sign of an infra-red term of which the existence is not yet established by experiment. Experiments on these lines have, however, already been made by Ingersol,† who found that the rotatory powers of a series of typical compounds decreased progressively in the infra-red region, right up to the limit of transparency of the medium This experimental result is in agreement with the conclusions of Kuhn (private communication, *cf* 'Z Phys Chem,' B, vol 4, p 14 (1929), who anticipates that *all* rotations will *diminish* asymptotically to zero in the infra-red, but it is directly opposed to the theoretical deductions of the authors cited above, whose diagrams represent the rotations as *increasing* asymptotically to $\pm\ \infty$ on approaching a characteristic frequency in the infra-red Moreover, since the rotatory powers of limonene and pinene decrease progressively, even when passing through a region which includes three absorption bands, it is clear that the phenomenon discovered by Cotton* in coloured organic compounds is not reproduced in these infra-red bands

---

* 'J. Chem. Soc.,' p. 1671 (1928).

† 'Phys. Rev.,' vol. 9, p. 257 (1917).

In the case of quartz, the evidence hitherto available is somewhat contradictory Thus, although Drude's equation for the rotatory power of quartz did not include an infra-red term, the increased number of arbitrary constants which was required to represent the more accurate measurements published in 1912 ('Phil Trans,' A, vol 212, p 261) was provided by assigning a small value to the infra-red term which Drude had supposed to be non-existent The characteristic frequencies which Drude had deduced from the published data for the refraction and selective reflection of quartz were, however, retained for all the terms, and no attempt was then made to derive them directly from measurements of optical rotation This limitation was finally removed when it became necessary to find a new equation to express the much more accurate and extensive measurements which were published in 1927 † It then appeared that the rotatory dispersion of quartz could be expressed over a very wide range of wave lengths by means of *two ultra-violet terms and a small constant term* This constant term, of which the theoretical significance is still open to question, was, however, less than 1 per cent of the rotation in the yellow and less than 0 1 per cent of the rotation in the ultra violet at 2300 A U The rotations observed in the ultra-violet have since been extended as far as 1854 A U by Duclaux and Jeantet,‡ with the help of a plate of quartz with a wider range of transparency than the crystal from which the rods of our long column had been cut, but it appears probable that these additional data could be covered by a small modification of the two ultra-violet terms, and it is unlikely that the small constant term, which has replaced the hypothetical infra-red term of the earlier equation, would be modified to any marked extent in this process It is therefore, an exiguous task to extract from the existing experimental data any valid evidence of the existence of an optically-active infra-red term, and it is impossible to derive from them any information as to the characteristic frequency of such a term, even if its existence should be admitted The object of the present experiments, therefore was to extend both the accuracy and the range of the observations in the infra red region to the extreme limit of the greatly improved experimental methods that are now available and thus to secure, if possible a clear answer to this much-debated question As a result we have obtained convincing proof of the optical-inactivity of one infra-red absorption band, and indirect evidence that the activity of the others, if it exists at all, is too insignificant to be demonstrated experimentally, at least until some novel method of investigation is discovered which will make it possible to measure rotations in a region which is now inaccessible to experimental work

---

* 'C R.,' vol. 120, p 1044 (1895), 'Ann. Chim. Phys,' vol 8, p 347 (1896)

† Lowry and Coode Adams, 'Phil. Trans,' A, vol. 226, p 391 (1927)

‡ 'J Physique,' vol 7, p 200 (1926).

Table I Rotatory Power of Quartz in the Infra-red
First series 18000 to 28000 A U

Wave length	Total rotation	Rotation per millimetre		
		Observed	Calculated	Difference
18000	1023	2 061	2 059	+0 002
18100	1012	2 038	2 035	+0 003
18200	1000	2 014	2 011	+0 003
18300	987	1 988	1 987	+0 001
18400	976	1 966	1 963	+0 003
18500	964	1 940	1 939	+0 001
18600	953	1 919	1 916	+0 003
18700	943	1 898	1 893	+0 005
18800	931	1 876	1 870	+0 006
18900	917	1 848	1 848	±
19000	907	1 827	1 826	+0 001
19100	895	1 803	1 805	−0 002
19200	888	1 789	1 785	+0 004
19300	879	1 771	1 765	+0 006
19400	868	1 748	1 745	+0 003
19500	858	1 728	1 726	+0 002
19600	849	1 711	1 707	+0 004
19700	840	1 693	1 688	+0 005
19800	829	1 670	1 669	+0 001
19000	816	1 647	1 650	−0 003
20000	811	1 633	1 631	+0 002
20100	800	1 612	1 612	±
20200	793	1 598	1 594	+0 004
20300	786	1 582	1 576	+0 006
20400	776	1 562	1 559	+0 003
20500	766	1 544	1 542	+0 002
20600	757	1 527	1 525	+0 003
20700	750	1 510	1 508	+0 002

Table I—(continued)

Wave length	Total rotation	Rotation per millimetre		
		Observed	Calculated	Difference
	°			
20800	742	1 494	1 492	+0 002
20900	735	1 480	1 476	+0 004
21000	725	1 461	1 460	+0 001
21100	720	1 450	1 444	+0 006
21200	710	1 429	1 428	+0 001
21300	703	1 417	1 413	+0 004
21400	695	1 400	1 398	+0 002
21500	685	1 381	1 383	−0 002
21600	681	1 373	1 368	+0 005
21700	673	1 356	1 353	+0 003
21800	668	1 346	1 338	+0 008
21900	659	1 327	1 324	+0 003
22000	651	1 312	1 310	+0 002
22100	645	1 299	1 296	+0 003
22200	637	1 284	1 282	+0 002
22300	630	1 268	1 269	−0 001
22400	624	1 258	1 257	+0 001
22500	620	1 250	1 245	+0 005
22600	617	1 243	1 233	+0 010
22700	609	1 226	1 221	+0 005
22800	602	1 213	1 209	+0 004
22900	595	1 199	1 197	+0 002
23000	590	1 188	1 185	+0 003
23100	582	1 173	1 173	±
23200	576	1 160	1 161	−0 001
23300	573	1 155	1 149	+0 006
23400	567	1 142	1 137	+0 005
23500	559	1 127	1 126	+0 001
23600	556	1 120	1 115	+0 005
23700	548	1 104	1 104	±
23800	546	1 099	1 093	+0 006
23900	540	1 087	1 082	+0 005
24000	533	1 074	1 072	+0 002
24100	529	1 068	1 062	+0 006
24200	526	1 060	1 052	+0 008
24300	523	1 054	1 042	+0 012
24400	515	1 036	1 032	+0 004
24500	509	1 025	1 022	+0 003
24600	504	1 016	1 012	+0 004
24700	498	1 003	1 002	+0 001
24800	495	0 998	0 992	+0 006
24900	490	0 987	0 983	+0 004
25000	484	0 977	0 974	+0 003
25100	481	0 968	0 965	+0 003
25200	476	0 959	0 956	+0 003
25300	472	0 951	0 947	+0 004
25400	468	0 942	0 938	+0 004
25500	461	0 929	0 929	±
25600	458	0 922	0 920	+0 002
25700	453	0 913	0 911	+0 002
25800	449	0 905	0 902	+0 003
25900	446	0 898	0 893	+0 005
26000	441	0 888	0 883	+0 005
26100	438	0 883	0 875	+0 008
26200	433	0 872	0 867	+0 005

Table I (continued)

Wave length	Total rotation	Rotation per millimetre		
		Observed	Calculated	Difference
	°			
26300	427	0·860	0·859	+0·001
26400	425	0·856	0·851	+0·005
26500	421	0·848	0·843	+0·005
26600	418	0·842	0·835	+0·007
26700	413	0·831	0·827	+0·004
26800	410	0·825	0·819	+0·006
26900	403	0·813	0·811	+0·002
27000	401	0·806	0·803	+0·006
27100	397	0·800	0·796	+0·004
27200	393	0·793	0·789	+0·004
27300	391	0·787	0·782	+0·005
27400	387	0·779	0·775	+0·004
27500	384	0·774	0·768	+0·006
27600	380	0·765	0·761	+0·004
27700	377	0·760	0·754	+0·006
27800	373	0·752	0·747	+0·005
27900	370	0·746	0·740	+0·006

Table II Rotatory Power of Quartz in the Infra-red

Second series 31800 to 32100 Å U

Wave length	Total rotation	Rotation per millimetre		
		Observed	Calculated	Difference
31800	267	0·537	0·528	+0·009
31900	262	0·529	0·522	+0·007
32000	260	0·525	0·516	+0·009
32100	257	0·520	0·510	+0·010

Experimental

The column of quartz was the same as that used in the earlier experiments.* In the meanwhile, however, the column had been taken down, in order to test the transparency of the separate rods to ultra-violet light of wave-length less than 2250 Å U, and had been reassembled with the rods in optical contact. The rotation at 19·995° C (corr) of the whole column for light of wave-length 5460·742 was then found to be $n\pi + 78·93°$, as compared with the value $70\pi + 78·96°$ at 20°, recorded previously.

---

* Lowry and Coode-Adams, *loc cit*

The earlier work covering the range from 13000 to 25170 Å U depended on determining the wave-lengths at which the rotatory power of the column of quartz is an integral multiple of 90° as indicated by observations of maxima and minima when the radiation from a Nernst glower was passed through the quartz column between crossed or parallel Nicol prisms In extending the readings to longer wave lengths, however, it was desired to use a method which would be independent, not only of the varying slope of the emission-curve, but also of minor irregularities in that curve

The instrument used for this purpose was the grating spectrometer described by Snow and Taylor * The gas tubes were replaced by a simple polarimeter, reading by means of a vernier to 0 1° On account of the greater length of this instrument the source of radiation had to be moved back about 40 cms, but a parallel beam was made to pass through the quartz column (in exactly the same way as it had passed through the gas-tubes) with the help of a concave mirror with the Nernst glower at its focus Since intensity of radiation rather than high spectroscopic purity was required, the width of the slit by which radiation is admitted to the grating was increased from 0 2 mm to over 1 0 mm For the same reason the galvanometer was kept at its maximum sensitivity (10^{-11} amps per deflection of 1 mm, with the scale at 1 metre distance)

Readings were taken at intervals of 100 Å U At each wave-length, the angle was observed through which the analyser had to be rotated in order to give a maximum deflection The accuracy of the method depends on the following factors —

(i) The adjustment of polariser and analyser to give a maximum deflection with no quartz in the path of the beam

(ii) Setting up the quartz column between the polariser and analyser with the help of a reflecting eye-piece, to give the correct rotation for mercury green light

(iii) A constant sensitivity of the galvanometer, since, if this varies from minute to minute, readings for different positions of the analyser cannot be compared In order to avoid errors from this source the readings for each setting of the analyser were compared with those for an arbitrarily chosen setting for the same wave-length, in this way any variation in intensity was at once detected

(iv) The magnitude of the galvanometer-deflections at each wave-length In practice, the maximum deflection varied from 100 mm at 21000 Å U to 10 mm at 27900 Å U

---

* 'Roy Soc Proc,' A, vol. 124, p 442 (1929)

The readings are in two series. The first series (Table I) covers the range from 18000 Å U up to 28000 Å U, where the close proximity of an absorption band made it impossible to proceed further, even when working at night and with the galvanometer at its maximum sensitivity The second series (Table II) depends on the existence of a narrow " window " on the other side of this absorption band, where the quartz was sufficiently transparent, over a range of 300 Å U only, to transmit enough radiation to deflect the galvanometer through about 10 mm when the analyser was set to the most favourable position for transmission Beyond this point further readings were impossible, since the transparency of the quartz was even less than at the maximum of absorption at about 30000 Å U Since the rotatory power of quartz has already fallen to 0 5° per millimetre at 32000 Å U, accurate readings in this region can only be obtained by making use of a long column, the usual device of reducing the length of the column, in order to compensate for its growing opacity, is therefore of no great value, and in our opinion further progress in the direction of longer wave lengths is absolutely barred, so long as we are limited to the methods of measurement that have been used hitherto

The accuracy claimed for the observations is about ± 5°, corresponding to an uncertainty of ± 0 01° in the rotation per millimetre, but a comparison of the observed rotations in Table I with these calculated (as before) from the formula

$$\alpha = \frac{9\ 5639}{\lambda^2 - 0\ 0127493} - \frac{2\ 3113}{\lambda^2 - 0\ 000974} - 0\ 1905$$

shows that this is approximately the *maximum* deviation, and that individual groups of readings are actually consistent within about 1°, since the systematic error is almost constant at + 0 003 ± 0 001 over the range from 18000 to 28000 Å U Thus the average deviation in successive groups of 10 readings is as follows —

Wave length	Average difference	Wave length	Average difference
μ	° per mm	μ	° per mm
1 8 to 1 89	+0 0027	2 4 to 2 49	+0 0050
1 9 to 1 99	+0 0021	2 5 to 2 59	+0 0029
2 0 to 2 09	+0 0028	2 6 to 2 69	+0 0048
2 1 to 2 19	+0 0031	2 7 to 2 79	+0 0050
2 2 to 2 29	+0 0033	3 18 to 3 21*	+0 009
2 3 to 2 39	+0 0030		

* Four readings only

The observations set out in Tables I and II give no indication of a Cotton effect in the neighbourhood of the absorption band at 30000 Å U, and provide conclusive evidence that this band is optically-inactive It is more difficult to decide whether the rotatory power of quartz in the region of transparency from 28000 to 1850 Å U is influenced by the more intense absorption bands which are known to exist at 8 5, 9 0 and 20 7 μ, and on which Drude based his use of an infra-red term, with $\lambda_0^2 = 78\ 22$, in calculations of the refractive indices of quartz The deviations from the 1927 equation as now disclosed are as follows —

Wave length	Deviation	Infra red term
Å U		
6707	−0 0008	[−0 173]
18000	+0 003	[−0 179]
27000	+0 005	[−0 189]
32000	+0 009	[−0 197]

It is noteworthy that, although the rotation per millimetre has decreased from 202° to 2263 Å U, to 0 52° at 32000 Å U, so that the small constant finally contributes 36 per cent instead of only 0 1 per cent of the total rotation, the deviations shown above are still within the limits of acknowledged experimental error and therefore serve to confirm the essential accuracy of the formula

The partial rotations due to the infra-red term of the 1912 equation, as shown in the last column of the preceding table, increase from −0 172 at zero wave-length to −0 197 at 32000 Å U, whereas the constant term of the 1927 equation amounts to −0 1905° per millimetre throughout Since the infra-red term is negative, and becomes more important as the wave-length is increased, its effect is to *depress* the calculated rotation to a growing extent in the infra-red On the other hand, the deviations set out above, if they have any real significance, increase from +0 003° per millimetre at 18000 Å U to +0 009° per millimetre at 32000 Å U, showing that the calculated values are already decreasing rather too rapidly The introduction of an infra-red term in place of a constant would therefore increase, and not diminish, the deviations In these circumstances, any further readjustment of the 1927 equation can very well wait until the deviations in the far ultra-violet, disclosed by the work of Duclaux and Jeantot, have been confirmed by a new series of precise measurements in the difficult region of the spectrum between 2250 and 1850 Å U

Study of Electrolytic Dissociation by the Raman Effect
I.—*Nitric Acid.**

By I. RAMAKRISHNA RAO, M.A., Ph.D., Bezwada Research Fellow, Andhra University.

(Communicated by O. W. Richardson, F.R.S.—Received January 29, 1930.)

[PLATE 3.]

1. *Introduction.*

In a recent discovery Raman† found that when monochromatic light of frequency ν is incident upon a substance, the scattered light contains not only light of the original frequency ν but also light of modified frequency ν_1, and the difference in frequency between the two corresponds to an infra red characteristic frequency ν_0 of the molecules constituting the substance. Thus a new field of work has been opened up, in which the infra-red characteristic frequencies of molecules can be determined with as much precision as is possible in the visible and ultra-violet regions of the spectrum. The present investigation has shown a further possibility of the new discovery. On studying the Raman effect in solutions of nitric acid at different concentrations, the author was able to trace the progress in the electrolytic dissociation of the acid by measuring the changes in the intensities of the Raman lines due to the undissociated molecules and of the ions. Thus the method not only gives direct evidence of the phenomenon of dissociation, but enables the determination of its amount as accurately as is possible in the measurement of intensities of spectral lines.

The only defect of the method lies in the fact that it cannot be extended to those electrolytes that do not show any Raman lines. The purpose of the present communication is to describe the results with nitric acid.

2. *Experimental Method.*

By far the best method of studying the Raman effect is that suggested by Wood,‡ for it not only gives a greater amount of scattered light, but the exact collimation, which is important for getting the largest amount of scattered light into the spectrograph, is made much easier. In the present investigation, Wood's arrangement is used with slight modifications in the experimental tube containing the liquid to be studied The form of the tube adopted is represented in fig 1 It consists of a glass tube one end of which is bent into a horn with an opening at the top At the other end is attached a narrower glass tube whose axis exactly coincides with the axis of the wider tube, and which has a clear glass bulb blown at its end The bulb is so made that there are no irregularities in its surface such that a distant light source is seen perfectly undistorted through it A small glass bead is melted on to the sloping wall of the horn as nearly along the axis of the tube as possible Leaving the central portion of the tube equal in length to the length of the mercury arc, the front portion of the bulb, and the glass bead, the whole of the apparatus is blackened with black enamel The tube is surrounded by a water jacket made of glass for circulation of cold water

---

* A preliminary note of this was given in 'Nature,' vol. 124, p. 762 (1929).

† 'Ind. J. Phys.,' vol. 2, p. 387 (1928).

‡ 'Phil. Mag.,' vol. 6, p. 729 (1928).

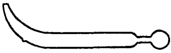
FIG 1

The mercury arc, specially constructed by the Hewittic Electric Company for work with the Raman effect, is placed above this tube containing the liquid and as near to it as possible The arc is run on 200 volts at a current of 3 amperes The horn, drawn at one end of the apparatus, enabled all background illumination to be eliminated The narrow glass tube between the glass bulb and the wider tube prevented stray light from the walls of the apparatus from entering the spectrograph The glass bulb not only eliminated the use of any cement for attaching a glass plate to the end of the tube in its place, but it formed a liquid lens to focus the scattered light on to the slit of the spectrograph Thus the use of an additional lens, which absorbs part of the scattered light, is avoided

To use the spectrograph to the best advantage, the glass bead melted on to the sloping wall of the horn along the axis of the tube is essential The scattered light being very feeble, the focussing on the slit of the spectrograph is difficult without it The glass bead is illuminated by a diffuse electric lamp placed near it, and the spectrograph is now adjusted so that the point image of the bead as formed by the lens of the glass bulb is on the slit The inclination of the spectrograph is so changed that, on placing the eye at the position where the spectrum is formed, the whole field of view of the camera appears illuminated The best position of the spectrograph is that in which the intensity of the light from the bead as seen through the camera is a maximum

To get the largest amount of light from the mercury arc into the scattering substance, two aluminium reflectors are used, one above the arc and the other below the tube containing the liquid under investigation With Hilger s constant deviation glass spectrograph, an exposure of 3 hours with Ilford iso-zenith plates enabled even the faint Raman lines in nitric acid to be recorded clearly For accurate measurement of the wave-lengths of the lines, a copper arc is used for the comparison spectrum and the measurements are made with a micrometer reading to 0 01 mm The wave-lengths are calculated by the usual Hartmann s interpolation formula

It is not found necessary to distil the liquids in vacuum so long as there are no fluorescent impurities and they are comparatively free from dust The only effect of small traces of dust is to increase the intensity of the unmodified lines in the scattered light which come out very dark in the negative

3 *Results*

Table 1 contains the results of measurements of the Raman lines with concentrated nitric acid (65 per cent acid) In the first column are given the wave-lengths of the exciting mercury lines The second column contains the wave-lengths of the Raman lines corresponding to these original lines, and their approximate relative intensities are indicated in brackets The wave-numbers of these two sets of lines are given in columns 3 and 4 The fifth column represents in wave-numbers the differences between the exciting lines and the corresponding Raman lines, and the reciprocals of these differences giving the infra-red characteristic wave-lengths of nitric acid are given in column 6

Table 1

λ_{Hg}	λ_R	ν_{Hg}	ν_R	$\Delta\nu$	λ_{IR}
Å I	Å I	cm^{-1}	cm^{-1}	cm^{-1}	μ
4046 6	4226 0 (0)	24705	23656	1049	9 53
4046 6	4273 0 (0)	24705	23396	1309	7 64
4358 6	4483 3 (1)	22937	22299	638	15 67
4358 6	4492 8 (2)	22937	22252	685	14 60
4358 6	4548 3 (4)	22937	21980	957	10 45
4358 6	4566 8 (12)	22937	21891	1046	9 56
4358 6	4580 3 (0)	22937	21827	1110	9 00
4358 6	4620 3 (13)	22937	21638	1299	7 69
4046 6	4649 2 (00)	24705	21603	3202	3 12
4046 6	4675 0 (00)	24705	21384	3321	3 01
4046 6	4698 3 (5)	24705	21278	3427	2 92
4046 6	4720 2 (1) to 4745 6	24705	21180 to 21066	3525 to 3639	2 83 to 2 75

From spectra taken with $NaNO_3$, NH_4NO_3, and KNO_3 solutions the Raman lines corresponding to the NO_3^- ion are identified as those with wave-number differences of 638, 685 and 1016 cm $^{-1}$ corresponding to infra-red absorptions at 15 67, 14 60 and 9 56 μ respectively The one at 9 56 μ is the most intense of the three, both in HNO_3 and in the solutions of the nitrates, and of identically the same wave-length in all of them The three lines with wave-number differences of 3202, 3427 and the band 3439 to 3525 belong to water Thus the rest of the Raman lines with differences 957, 1110 1299 and 3321 cm $^{-1}$ must belong to the undissociated nitric acid molecule, as there is no other molecule present in the liquid

4 *Electrolytic Dissociation in Nitric Acid*

Plate 3 shows the Raman spectra taken with various concentrations of nitric acid in water Fig 1 in the Plate is with pure concentrated nitric acid containing 65 per cent acid, and figs 2 to 7 correspond to 58 5, 48, 39, 29 2 19 5 and 9 7 per cent concentrations of the acid respectively Fig 8 is the spectrum for pure redistilled water

These spectra are taken with exactly equal exposures of 3 hours each The amount of light from the mercury arc incident on the liquid is kept constant by keeping the distance between the tube containing the solution and the mercury arc exactly the same for all of them The aluminium reflectors are also in the same position for all the exposures By regulating the flow of cold water through the jacket surrounding the experimental tube, the temperature of the solutions was maintained the same for all of them within a variation of 2° C The average current through the mercury arc was 3 amperes with a variation of not more than 0 2 ampere The voltage drop between the terminals of the arc was 140 volts with a maximum variation of 3 volts on either side Thus, on an average the energy consumption of the arc could not have varied from one exposure to another by more than 4 or 5 per cent

Thus all the spectra are taken under identical conditions as far as practicable Any variations in the intensities of the Raman lines must be due to the dilutions themselves and not to any other circumstances It is clear from figs 1 to 7 that the Raman line at 4566 8 Å U found in nitric acid and nitrates increases in intensity with increasing dilution of the acid, while the line at 4620 3 Å U, which is absent in the nitrates and which must therefore be due to the excitation of the undissociated HNO_3 molecule, diminishes in intensity These changes indicate clearly that, while the number of NO_3^- ions, giving rise to the Raman line at 4566 8 Å U, increases with increasing dilution, the number of undissociated HNO_3 molecules, giving rise to the line at 4620 3 Å U diminishes with increasing dilution of the acid This is clear evidence of the electrolytic dissociation of nitric acid

To get an idea of the intensity variations with acid concentration of these two lines, the intensity records of the different spectra taken with a **Moll's** microphotometer are represented in fig 2 The horizontal line at the top of

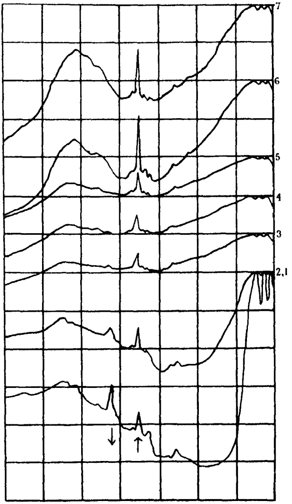

FIG 2 —Microphotometric Intensity Curves of Raman Spectra, taken with diminishing concentration of nitric acid

each curve along which the number of the curve is marked represents the zero line for that curve, which corresponds to complete blackening of the photographic plate The intensity changes indicated above in the actual spectra of the two Raman lines are very clearly demonstrated by these intensity curves

The maxima marked with downward arrows correspond to the undissociated HNO_3 molecule, and their intensity diminishes so rapidly that they almost disappear in the fourth curve corresponding to a concentration of 39 per cent The maxima denoted by the upward arrows are for the NO_3^- lines and they very rapidly increase in intensity up to 39 per cent concentration They then diminish again showing that, whereas for the first few dilutions the dissociation increases much more rapidly than the diminution in concentration, resulting in a larger number of NO_3^- ions, after a certain stage, the increase in dissociation becomes less in proportion to diminution in concentration of the ions Thus the curves indicate that the intensity of the nitrate lines increases at first and then diminishes again

In the curves 3 to 5 the intensity maxima have reached very nearly the zero line In these three curves even the continuous spectrum, which is also present in the direct mercury arc, is very prominent The unmodified lines of the mercury arc spectrum are also very intense in these spectra showing thereby that the classical scattering also increases very much with the dilution of the acid

Though the author has used the same nitric acid and the same redistilled water, neither of which shows a conspicuous continuous spectrum, in the scattered light, as is seen from figs 1 and 8 of Plate 3, this continuous spectrum increases in intensity in the same way as the Raman lines corresponding to the nitrate ion An explanation of this obviously seems to be that the intensity of the classical scattering also increases with increasing ionisation of the acid But Venkateswaran,* working with nitric acid at various concentrations distilled *in vacuo* and using sunlight, found no such anomalous changes in intensity He found that the intensity of the scattered light increased with increasing concentration of the acid without any reversal, such as is found in this investigation With a view to finding the behaviour of other acids in this respect, the author worked with sulphuric and acetic acids also Even in these cases, the continuous spectrum becomes more prominent with increasing dilution In fact, in the case of sulphuric acid, the continuous spectrum is so strong that the Raman lines are completely masked by it for intermediate dilutions Further work is necessary to find the cause of the variation of the intensity of this continuous spectrum

---

* Venkateswaran, 'Ind J Phys,' vol 1 p 239 (1926)

5 *Estimation of the amount of Dissociation from the Intensities and Comparison with Conductivity Data*

The relative intensities of the Raman line at 4566 8 Å U in the spectra with the various concentrations of nitric acid are given in Table II They are estimated from the deflections in the microphotometer records given in fig 2 The intensity due to the continuous spectrum is eliminated from each of them But the intensity of this being a large proportion (in some cases 75 per cent) of the total intensity, the values are uncertain to a range of as much as 10 to 15 per cent Thus the table gives the intensities of the Raman lines exclusive of that of the continuous spectrum only approximately With elimination of the continuous spectrum, whose origin is now unknown, it may be possible to measure the intensities of the Raman lines very accurately

Table II —Relation between Concentration and Degree of Dissociation

Con centration per cent c	Int I	$\dfrac{I/c}{I_{65}/c_{65}}$	Con centration per cent c	Molecular con ductivities Λ in cm $^{-1}$ ohm^{-1}	Viscosity η in g cm $^{-1}$ sec $^{-1}$	Λ/Λ_{65}	$\dfrac{\Lambda\ \eta}{\Lambda_{65}\ \eta_{65}}$
65 0	0 52	1 0	65 0	32 5	0 0201	1 00	1 00
58 5	0 63	1 3	62 0	36 4	0 0199	1 12	1 11
—	—	—	55 8	47 1	0 0193	1 45	1 39
48 0	1 19	3 1	49 6	61 1	0 0183	1 88	1 72
39 0	1 52	4 9	37 2	103 4	0 0149	3 18	2 36
29 2	1 75	7 5	31 0	133 1	0 0133	4 10	2 72
19 5	1 97	12 6	24 8	169 3	0 0121	5 21	3 14
9 7	1 46	18 8	12 4	257 0	0 0106	7 91	4 17
—		—	6 2	307 1	0 0103	9 45	4 84

The first column in the table gives the concentration of the acid in grams per 100 grams of solution The second column contains the relative intensity of the Raman line at 4566 8 Å U If N_c is the number of free NO_3^- ions present in the solution, and I_c is the intensity of the Raman line at concentration c,

$$N_c = k\ \ I_c,$$

where k is a constant, since the intensity is proportional to the number of emitters present, the emitters here being the free nitrate ions The degree of dissociation α is given by the ratio

$$\frac{N_c/c}{N_\infty/c_\infty} - \frac{I_c/c}{I_\infty/c_\infty}$$

where N_∞ is the number of free ions present and I_∞ is the intensity of the Raman line at concentration c_∞, corresponding to infinite dilution, since here the dissociation is supposed to be complete, the degree of dissociation being unity But as there is no knowledge of the intensity at large dilutions in the above data, and as only the relative values of the dissociation are aimed at in this communication, the values relative to the dissociation at 65 per cent concentration are given in column 3 of the above table

If the amount of dissociation were the same for all concentrations, the number of free nitrate ions present in the solution should diminish in proportion to dilution, and the intensity of the Raman line due to the NO_3^- ions should also diminish in proportion Thus the numbers in the third column, giving the ratio of the intensity to concentration, ought to be constant But the large increase in this value shows how rapidly the dissociation of nitric acid increases with increasing dilution

The results of electrolytic conductivity by Kohlrausch are given in the other columns of Table II The fourth gives the concentration in grams per 100 grams of solution The molecular conductivities Λ* and the viscosities η† of the solutions at each concentration are given in the next two columns If Λ_c is the molecular conductivity at concentration c, and Λ_∞ that at infinite dilution, the degree of dissociation according to Kohlrausch's law, that the mobility of ions is independent of concentration, is given by Λ_c/Λ_∞ Even at small concentrations this law is supposed not to hold good So its applicability at higher concentrations such as those used in this work is still less Another formula for the degree of dissociation at moderate concentrations in terms of the molecular conductivity is

$$\alpha = \frac{\Lambda_c}{\Lambda_\infty} \frac{\eta_c}{\eta_0}$$

where η_c and η_0 are the viscosities of the solutions at concentrations c and 0 respectively In Table II the degree of dissociation calculated according to the two above formulæ are given in columns 7 and 8

Fig 3 gives the curves indicating the relation between the concentration and the relative amount of dissociation The steeper curve is from the intensity measurements of the Raman line for the nitrate ion The middle curve is that according to Kohlrausch's formula and the lowest corresponds to the

---

* Landolt and others, 'Physikalisch Chemisch Tabellen,' 5th ed, vol 2, p 1074

† Ditto, First Supplement, p 86 The values given in the table are extrapolated from the actual values

Fig 8

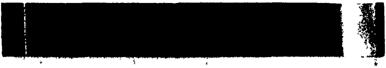

Water

Fig 7

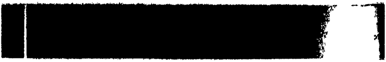

9.7 per cent acid

Fig 6

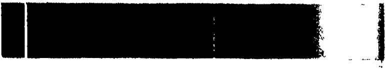

19.5 per cent acid

Fig 5

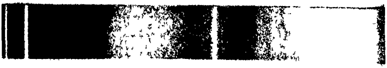

29.2 per cent acid

Fig 4

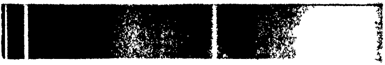

39 per cent acid

Fig 3

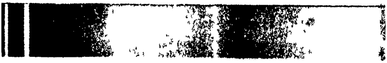

48 per cent acid

Fig 2

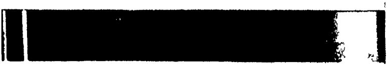

58.5 per cent acid

Fig 1

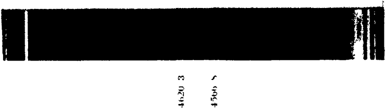

65 per cent acid

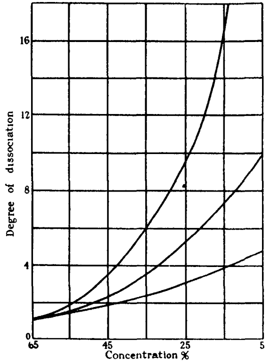

Fig 3—Relation between Concentration of Nitric Acid and Degree of Dissociation The lowest is from viscosity conductivity formula The middle curve from Kohlrausch's conductivity formula and the uppermost from measurements of Raman lines for the nitrate ion

dissociation calculated from the viscosity formula The disagreement between the three is very striking

6 *Discussion*

To investigate the cause of the discrepancy it is necessary to see how far the various methods give the actual degree of dissociation Of these methods one is from osmotic pressure measurements The osmotic pressure can be either directly determined or calculated from the lowering of freezing point of the solutions The second and more common method is that from conductivity measurements There are several other methods which are more indirect All these are known to be inapplicable for determination of the degree of dissociation at high concentrations Even at low concentrations there is no knowledge as to how far the values calculated represent the so called "true degree of dissociation" which is the ratio of the number of molecules dissociated to the total number of molecules All of them entail a certain number of assumptions whose validity even at moderate dilutions is questioned In osmotic pressure measurements, the values calculated may be approximately correct over the range where Henry's law of solutions is applicable, and it is well known that this range is limited to very high dilutions Thus at higher concentrations this method does not give even approximate values of the true degree of dissociation

Even in the case of electrolytic conductivity measurements Kohlrausch's law, that the mobility of ions is independent of concentration, applies only for very high dilutions At higher concentrations the viscosity formula given before is suggested But how far this gives the actual degree of dissociation is not definitely understood even at moderate concentrations Much more so is it uncertain at concentrations of the order of one normal and above Hence there is, up till now, no method known whereby the true degree of dissociation can be determined at high or moderate concentrations Thus the two lower curves given in fig 3 cannot represent the degree of dissociation even approximately

The Raman effect on the other hand gives a direct method of determining the actual number of ions produced irrespective of concentration The intensity of the Raman line being directly proportional to the number of free ions present, and being independent of either their mobility or their concentration, the intensity ratios directly give the ratios of the degree of dissociation at different dilutions Thus this seems to be the only method by which the true degree of dissociation can be determined This explains the discrepancy between the three curves in fig 3

A study of the effect at higher dilutions will enable the decision as to how far the various methods give the dissociation correctly even at those dilutions It will also decide between the theories of complete dissociation and progressive dissociation at intermediate concentrations in the case of strong electrolytes

Further work with nitric acid at larger range of concentrations and with other electrolytes is in progress With these data it may be possible to throw new light on the prevalent theories of electrolytic dissociation

Summary

1 A modified form of apparatus, adopted by the author for the study of the Raman effect, is briefly described

2 Ten Raman lines are observed with nitric acid, four of which correspond

to undissociated HNO_3 molecules, three to NO_3^- ions and found in common with nitrates, and three to pure water

3 In Raman spectra taken with different concentrations of nitric acid, the lines corresponding to the HNO_3 molecule diminish in intensity very rapidly with increasing dilution, whereas the NO_3^- lines increase in intensity, showing thereby that with increasing dilution the number of free nitrate ions increases, which is clear evidence of electrolytic dissociation

4 Microphotometric records are taken for measurement of the intensities, and from the intensities of the Raman lines due to the nitrate ions for the different concentrations the relative amounts of dissociation are calculated

5 The degree of dissociation found from the above is compared with that determined from conductivity measurements in nitric acid, and the general form of the curve obtained by plotting the dissociation against the concentration is found to be roughly the same in both cases The causes of such differences as are found are discussed

In conclusion, the author has great pleasure in thanking Prof O W Richardson F R S, for the interest he has taken during the course of this work which was carried out in the Physics Research Laboratories at King's College London

The Splitting Strength of Mica

By J W OBREIMOFF, Fellow of the Physics and Technics Institute, Leningrad

(Communicated by P Kapitza, F R S —Received February 1, 1930)

(PLATE 4)

Two well-ground and polished plane glass plates if put together, adhere This phenomenon is called optical contact and is very much used in the manufacture of optical instruments, since the boundary between the two glass surfaces shows practically no reflection of light, when the gap between the two glass surfaces is exceedingly small in comparison with the wave-length of visible light An analogous phenomenon can be easily observed in mica Two freshly split mica foils if put together adhere again with an appreciable force It is interesting to see if the restoration is perfect, *i e* , if we need to apply the same force to split two mica sheets placed in optical contact as to split a fresh one

In the present work it will be shown that the splitting strength is a constant for mica , that we can determine a surface energy of mica which is independent of the shape of the mica sheets chosen and that mica placed in optical contact is totally restored A description will also be given of some electrical phenomena obtained by splitting mica in a high vacuum It appears that the cleavage surface of mica is covered with electrical charges , further, that the strength of mica in a high vacuum is more than in air and is also a fairly well-defined constant The present observations are connected with the well-known work of A Joffé[*] on the tensile strength of rock salt In the case of rock salt the surface was either dissolved to avoid the effect of imperfections of the surface or the surface action was avoided altogether as in the experiment with the rock salt sphere [*]

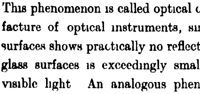

FIG 1

§ 1 Let us apply to a thick mica sheet a bending moment M sufficient to strip off a thin lamina Let us suppose the split sheet to be rectangular, of breadth *b* and thickness *h* This moment M will be in equilibrium with the molecular forces sticking the two parts of mica together at a point O. Under the influence of the moment M the stripped flake of mica will assume a circular shape, and if we assume the deflections to be small we can approximately represent them by a parabola

---

[*] Joffé, ' Physics of Crystals,' pp 62–64

$$y = x^2/2\rho, \tag{1}$$

where y is the gap between the two freshly split mica surfaces, x the corresponding abscissa measured from the point O to the left, ρ the radius of curvature.

From the elementary theory of elasticity

$$1/\rho = 3\mathrm{M}/\mathrm{E}bh^3, \tag{2}$$

where b is the breadth of the mica sheet, h the thickness of the stripped flake, E, Young's modulus.

If for a constant moment M the cleavage proceeds to a depth dx, the work done by the moment M will be equal to $d\mathrm{A} = \mathrm{M}d\phi$ where ϕ is the angle between the tangent at the point of application of the moment M and the x axis. The work per unit area should then be equal to

$$\frac{1}{b}\frac{d\mathrm{A}}{dx} = \frac{\mathrm{E}h^3}{3\rho^2}, \tag{3}$$

since $d\phi = dx/\rho$.

It may easily be shown that half of this work is stored in the energy of the bent mica lamina,* and the remaining work divided by 2 gives the surface energy of each of the two fresh surfaces. So the surface energy per square centimetre becomes

$$\mathrm{Q} = \tfrac{1}{12}\frac{\mathrm{E}h^3}{\rho^2} = \tfrac{1}{3}\frac{\mathrm{E}h^3y^2}{x^4}. \tag{4}$$

The first question will be whether mica has any consistent tensile strength at all. As a test we will choose the constancy of the work done by splitting different mica specimens rather than the constancy of the splitting moment M, since it is rather difficult to deduce from the experimentally obtained moment M the real splitting force without knowledge of the mechanism of the

---

* The energy of the bent lamina of length dx equals

$$\int_0^\phi \mathrm{M}d\phi = \tfrac{1}{6}\frac{\mathrm{E}h^3b\phi^2}{dx} = \tfrac{1}{6}\frac{\mathrm{E}h^3dx}{\rho 2},$$

then

$$\mathrm{M} = \tfrac{1}{3}\frac{\mathrm{E}h^3b}{\rho} = \tfrac{1}{3}\frac{\mathrm{E}h^3b\phi}{dx} \quad \phi = y' = \frac{dx}{\rho}$$

splitting. We might expect Q to be a constant for all our mica specimens; E is also a constant, and we will assume for it the value 20,000 kg per square millimetre taken from Landolt Bornstein tables. If, then, we make all our measurements for a given y (as, for example, by measuring the interference fringes), we have two variables only, x and h, related by the expression

$$x = (Ey^2/3Q)^{1/4}h^{3/4} \tag{5}$$

If such a relation really obtains for different specimens, we can deduce from it the work Q.

§ 2. The experiments were made with a specially chosen mica specimen (muscovite) from the White Sea (Chupa), these specimens being kindly placed at my disposal by Prof. Loewinson Lessing. From a sheet 0·2–0·5 mm thick by means of a Gillette blade I cut rectangular pieces about 20 × 50 mm area ($b = 20$ mm). These pieces were then split by means of a glass wedge finely ground with emery, the greatest care being taken to have the edge slightly rounded to prevent scratching and cutting. The split foils were from 0·1 mm to 0·2 mm thick, the thickness being measured after the experiment by means of double refraction. It is evident that the split foils can be assumed thin in comparison with the remaining part.

Although the splitting wedge does not exercise a bending moment, but a bending force, we can still use all the formulæ (1)–(4), since at the vicinity of the point O the stress due to the glass wedge will be a bending moment

$$M = Fl$$

where l is the distance between the edge of the wedge and the point O, and F is the force exercised by the wedge on the mica.

As a matter of control it was proved first that the thin stripped foil has actually a parabolic shape in the vicinity of the point O. This was measured many times with the aid of the interference fringes (Newton rings) in the air gap between the two mica surfaces. The light to produce the interference fringes was thrown on the mica from above through a vertical illuminator fixed on the tube of the microscope. The green mercury line ($\lambda = 5460$ A) was chosen for illumination. The distance between the fringes of order n, taking values of n equal to the square of a whole number, was measured by means of a Zeiss travelling metallurgical microscope.

If the shape of the strip is parabolic these fringes must be equidistant. In Table I is given the result of such an experiment.

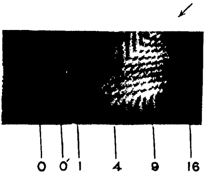

Fig 2

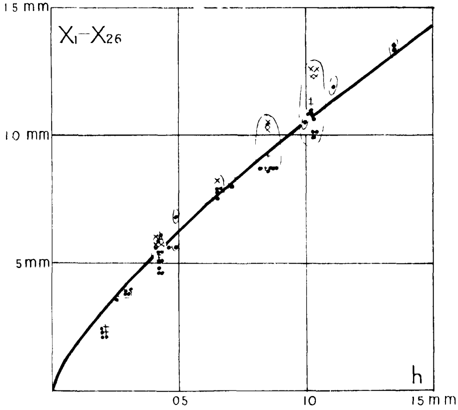

Fig 3

Table I Thickness h of the strip $= 0.110$ mm $\lambda = 5.46 \times 10^{-5}$ cm

n	O	1	4	9	16	25	36
	mm	mm	mm	mm	mm	mm	mm
Division on the travelling microscope	27.51	27.37	27.09	26.79	26.50	26.21	25.90
Difference	0.14	0.28	0.30	0.29	0.29	0.31	

Mean difference 0.30 mm

We take the fringe of order O' to be the place which appears to the eye to give no more reflection. Table I shows that this place is where the air gap between the two mica surfaces is equal to $\lambda/8$. It seems to be more reasonable to obtain the position of the point O by extrapolation of the measurements of the fringes of number 1, 4, 9, etc.

The parabolic shape of the bent strip was also proved several times by measuring the distance between successive interference fringes. In such a case one shows clearly that the shape is parabolic and that the discrepancies in Table I arise from errors of measurement.

The photograph of fig. 2 (Plate 1) is reproduced to show the picture of the fringes. There are marked the 1st, 4th and 9th fringes, also what we call the fringe of order O' and the true position of the point O obtained by extrapolation. Attention is drawn also to a fir shaped interference pattern marked by an arrow. It is very often observed and results from the light reflected from very thin mica strips connecting the two cleavage surfaces of mica. These thin strips occur very often and are a common source of trouble in our experiments.

The parabolic shape of the foil proved, we turn to the determination of the quantity Q. On fig. 3 are given by dots the results of the experiments on different mica samples. The thickness h in millimetres are plotted on the axis of abscissæ and the distance between the 1st and the 26th interference fringe (in millimetres) on the axis of ordinates. The points occurring from one strip for different positions of the splitting wedge are surrounded by a closed curve. If several experiments gave the same value of $x_1 - x_{26}$ for the same foil, the corresponding dots are laid on a horizontal line close to each other. The continuous curve is of the type

$$x = \mathrm{k}h^{\frac{3}{4}}$$

laid through the experimental points. From it we obtain for Q the very high value

$$Q = 1500 \text{ erg/cm}^2 \qquad (6)$$

As fig. 3 (Plate 4) shows, the points do not lie very well on the curve, but it seems to me rather surprising that they can be connected with a curve at all and are not distributed at random. If we remember the many different causes which can disturb the experiment such as imperfection of the crystal, "fir-shaped" strips, defects of mica near corner made in cutting it with the Gillette blade, and the simple method of splitting used to measure the cleavage strength, it is rather surprising that any consistent result is obtained.

§ 3. If we pull our glass wedge away the two mica sheets stick together without any pressure put on them. The crosses on fig. 3 belong to an experiment similar to those described in the previous paragraph, but made with mica split in air and then restored by pulling the wedge away. The skew crosses (×) belong to the movement of the wedge backwards and the upright crosses (+) to the movement of the splitting wedge forwards again on the old path. We see that in the majority of cases the skew crosses lie above the upright crosses and above the dots, i.e., the mica, once split and then restored, appears to be less strong than a fresh one. In a few cases the crosses fall between the dots, but never below. It is evident that many causes may reduce the strength of mica after splitting (particles of dust, scratches, etc.). Only in a few cases can this be avoided and then after putting the split parts together the mica is completely restored. It is curious to notice that the splitting moment, M, of mica is not a constant, being the smaller, the thinner the mica sheet.

§ 4. If split in darkness, mica becomes slightly luminescent (triboluminescense). This is due to electric discharges between the mica surfaces through the air. If we split them under an air pressure of 1.0–0.1 mm mercury the glow spreads to all the air in the vessel and is similar to the glow of a Geissler tube. In a high vacuum (10^{-4}–10^{-5} mm mercury) the glass of the vessel fluoresces like an X-ray bulb. The light is feeble and can be observed only after the eye has rested about 3 minutes in darkness. It is, however, bright enough to be visible when the light in the room is sufficient to make visible the contours of the glass vessel and the mica itself, and bright enough then to illumine the surrounding objects. After splitting mica in high vacuum, the inner surfaces of the glass vessel and of the mica itself are covered with electrical charges. If we lower, then, the vacuum to about 0.1 mm we obtain a splash of light in the gas At the same time the strength of mica in a high vacuum is greater than in air at an atmospheric pressure or 0 1 mm

On fig 4 is shown schematically the arrangement of the apparatus Mica is fastened by means of metallic clips to a metallic platform The glass wedge is

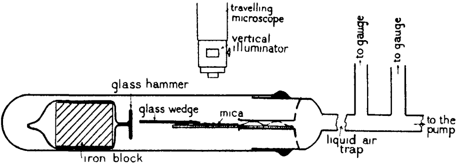

FIG 4

driven in by means of gentle strokes of a glass hammer provided with an iron block and put in motion by means of an electromagnet For the experiments in a very high vacuum (1 10^{-6} mm) all the apparatus was made from glass and an ionisation gauge used for measuring pressure (the connection being made in the latter case before the liquid air trap) On fig 5 are shown two parallel sets of measurements for mica, in air at atmospheric pressure (upper curve) and in high vacuum (lower curve) The curves are analogous to those of fig 3 On the axis of abscissæ is plotted the thickness of the foils and on the axis of ordinates the distance, l between the splitting wedge (0 48 mm thick) and the boundary O The observed points are interpolated by straight lines (instead of curves of the type $y = kx^{\frac{1}{2}}$) Fig 5 shows that the ratio of the ordinates of the two lines is nearly 1 9, which gives from (4) for the surface energy of mica split *in vacuo* the extremely high value

$$20{,}000 \text{ erg/cm}^2$$

The strength of mica *in vacuo* is independent of the pressure over a range between 10^{-6} and 10^{-2} mm of mercury, but there is a curious time phenomenon If the splitting wedge is kept still, the boundary of the split proceeds sometimes silently and uniformly and sometimes with a brusque jump accompanied with a cracking sound At atmospheric pressure also the split boundary does not arrive at its final position immediately but needs for it from 10–15 seconds In the intermediate pressure range between one atmosphere and high vacuum, the time of attainment of the final position of the boundary is longer than at atmospheric pressure At 20 mm pressure it is no less than 15 minutes, and

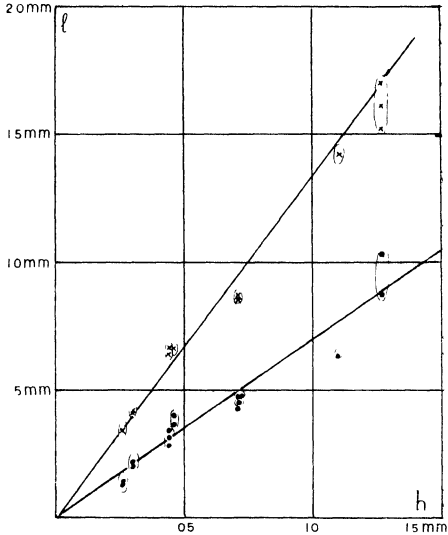

Fig 5

at 0 2 mm pressure no less than 4 days Thus a long time is required to measure the strength of mica under different pressures

§ 5 If we are starting in our high vacuum experiments with a mica specimen prepared in air, it will not assume at once its high strength, the boundary must move in the fresh mica to a depth of about 1 mm before the mica obtains its full strength Fig 6 illustrates such an experiment On the axis of the abscissæ is plotted the position of the boundary *O*, and on the axis of ordinates the distance between the splitting wedge and boundary corresponding to *l*

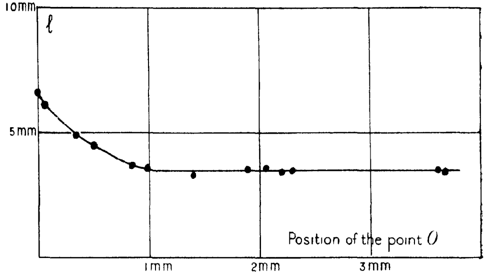

FIG 6.—Thickness of the foil 0·043 mm., thickness of the splitting wedge, 0·48 mm.

on the fig 5. It shows that the splitting strength increases to a depth of 1 mm., then becoming constant. If now we pull our wedge back, the two split foils stick together again, but their strength is perceptibly less than that of fresh mica and approaches that of mica in air.

§ 6. All the phenomena described can be qualitatively explained by the structure as given for muscovite by G. Wulff.* Following him the cleavage plane of muscovite consists of potassium ions lying on the corners of an equilateral triangular grating, the sides being equal to 5 A. A direct measurement of the electrical charge is impossible. By covering mica with silver, connecting them with an electrometer, and splitting in high vacuum we really can prove the existence of high potentials (up to 1000 v.), but a true measurement of the charge is impossible since in splitting the mica the electrical discharge makes the space a conductor. Actually, when splitting mica between the charged parallel plates of a condenser in a high vacuum it is possible to observe that the charge of the plates of the condenser is lost every time.

It seems not hopeless to apply the same method of direct measurement of cleavage to study the phenomena of absorption of different gases on mica and of cleavage in other crystals.

I am very indebted to Mr. W. J. Voleiko for his kind assistance in the work and his valuable help in constructing all the apparatus used.

---

* 'Trans. Inst. Econ. Mineral. Metall.,' No. 25, 1926, Moscow.

The Mobility of Ions in Air

J L HAMSHERE, M Sc , Instructor in Physics, University of Saskatchewan

(Communicated by Sir Joseph Thomson, F R S —Received February 6, 1930)

Introduction

In a previous paper* I have described an experimental method of measuring ion mobilities in a gas, which yields accurate values for both upper and lower limits of a distribution range, and from which one can also derive a curve showing the general shape of the distribution band, with a calculable resolving power It was found that negative ions in dry air at normal pressures had mobilities ranging from 2 15 to 1 45 cm per second per volt per centimetre, while the distribution band showed a peak value about 1 8 and a sharp upper limit at 2 15 There was also some reason to believe that in the presence of water vapour the band was narrowed, the faster ions being eliminated in the manner found by other observers, and the slower ions remaining comparatively unaffected

In the experiments here described, an improved form of the apparatus is used to study in greater detail the effect of water and other vapours on the mobility distribution, for positive and negative ions in air

Experimental Method

The general principle of the experiment has already been described in detail (*loc cit*), and will only be briefly recapitulated here

Ions are formed by alpha-rays from a polonium source near a plate C (fig 3), and subjected to a square-wave alternating field (± X′) maintained between C and a metal gauze B , those ions which reach the gauze are caught in a second alternating field (± X), and may reach the plate A which is connected to an electrometer The fields X and X′ are made as nearly equal as possible, to minimise interpenetration of the fields near the gauze, and are synchronised so that their cycles have the form shown in fig 1

The ions pass through the gauze from C towards A only when both fields are in " advance " phase, *i e* , between P and Q in fig 1 If T is the time of one complete cycle, and the advance phases PR, QR, occupy times aT, bT, respectively, it can be shown (*loc cit*) that the theoretical current curve for ions of a single mobility k is of the form given in fig 2, the current is zero when $d/(\mathrm{XT})$ is greater than bk, and reaches a final value when $d/(\mathrm{XT})$ becomes less

---

* 'Proc Camb Phil. Soc ,' vol 25, p 205 (1929)

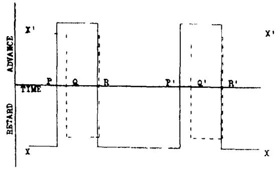

FIG 1 —Alternating Field Cycles
$\mathrm{PP'} = \mathrm{T}$ $\mathrm{PQ} = a\mathrm{T}$, $\mathrm{PR} = b\mathrm{T}$

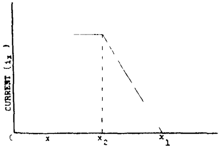

FIG 2 —Theoretical Current Curve for Unique Mobility (K)
$x = d/\mathrm{XT}$, $x_1 = b\mathrm{K}$, $x_2 = (b - a)\,\mathrm{K}$

than $(b - a)k$, d being the distance from the gauze B to the electrometer plate A Between these limits the current is given by the equation

$$i = i_0\,(b - d/k\mathrm{XT}),$$

where i_0 is the total current available, that is, the current which reaches A if both fields are held permanently in advance phase

If we put the experimental variable $d/(\mathrm{XT})$ equal to x, the equation may conveniently be written

$$i = i_0\,(b - x/k) \tag{1}$$

The maximum value reached by the experimental current will be ai_0

The general equation for the current in the case of a continuous distribution of mobility is obtained by integrating (1) with respect to k If the total current due to ions having mobility between k and $(k + \delta k)$ is written $f(k)\delta k$, we obtain

$$i_x = a\int_{k=x/(b-a)}^{k=k_1} f(k)\,dk + \int_{k=x/b}^{k=x/(b-a)} (b - x/k)\,f(k)\,dk, \tag{2}$$

where k_1 is the highest mobility present

We can further show, by differentiating (2) with respect to x, that the gradient of the experimental curve will give the mobility distribution, subject to the limitations of a finite resolving power For a high resolving power the differential reduces to

$$\frac{di_x}{dx} = \frac{a}{b} f(k), \quad \text{where } k = x/b \tag{3}$$

The resolving power of the apparatus can be calculated from the usual condition, that the overlap of two curves corresponding to mobilities k, $k + \delta k$, shall equal half their apparent range, this gives

$$R = k/\delta k = 2b/a \tag{4}$$

The experimental procedure is to keep d and X constant, and to vary the frequency (1/T) of the field cycle The upper and lower limits of the mobility range are then directly obtained from the zero and maximum points of the current frequency curve which give

$$k_1 = x_1/b \qquad k_2 = x_2/(b - a) \tag{5}$$

The derived curve, $-di_x/dx = f(k)$ can be made to show the mobility distribution directly by taking as ordinate the mean value $k' = x/(b - \frac{1}{2}a)$ If k_1' and k_2' are the limits given by this curve, the true limits may be obtained, corrected for resolving power, on putting

$$k_1 = k_1'(1 - 1/R) \qquad k_2 = k_2'(1 + 1/R) \tag{6}$$

Apparatus

The apparatus used in these experiments was similar in most respects to that previously described, but differed from it in the design of the measuring condenser, and in the adoption of a synchronous speed control for the commutator

The brass case of the old measuring condenser was replaced by a glass cover standing on a heavy brass base plate, a circular ledge was cut in the plate, as shown in fig 3, to fit accurately inside the glass, which was ground on to it, the joint being made gastight with hard wax on the outside All the electrical leads and the gas inlet pass through the base plate, the electrometer lead through a central ebonite plug, and the four field connections through two double plugs, one of which is shown in the figure The surface of ebonite inside the chamber was reduced to a minimum

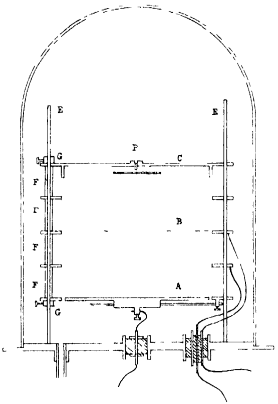

Fig 3 —Detail of Measuring Condenser

The plate and guard ring system is supported on three glass rods E, which pass through carefully aligned holes in each ring, the distance pieces FF are lengths of glass tubing which fit over the rods, and are accurately ground to the required length Small set-screw collars G serve to clamp the assembly firmly together The electrometer plate A is supported from its guard ring by two horizontal rods of quartz, the rods are threaded through short pieces of brass tube soldered to A and through small clamps soldered to the guard ring The quartz rods are not in contact with the underside of A, and so, although the air gap between plate and guard ring is only 1 mm wide, the effective length of quartz insulation is about 2 cm at each end of the rod

The gauze B is soldered as before to its guard ring, stretched as tight as possible and flattened by clamping in a vice The polonium coated wire P is mounted in a vertical position at the centre of the upper plate C, with a shield of thin brass just below it A small brass rim at the edge of C prevents the alpha-particles from travelling right out to the walls of the vessel, thus the ions available for experiment are those formed in the annular space between the shield and the rim

The electrical system is shown diagrammatically in fig 4 The potential of the gauze B with respect to earth is controlled through the three-way key K_{123} In the K_1 position the commutator S is short-circuited and B has the constant potential V, in the K_2 position, with the single key K_4 open, B has the constant potential U, and with K_4 also closed the commutator comes into play, giving a potential U at "break" and approximately V at "make" (The resistance R is of the order of a megohm) In K_3 position the gauze is earthed The connections for the plate C, through the commutator S′, are exactly similar, except that the potential of C is alternated with respect to the gauze B, not to earth The voltages U, V, and U′, V′, are read on a D C voltmeter whose connections are not shown in the diagram

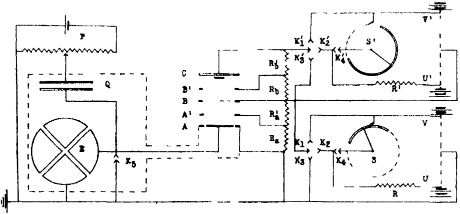

Fig 4 —Diagram of Electrical Connections

Guard rings A′, B′, are inserted between the plates to ensure a more uniform field, and the potentials of these are obtained by connecting AB and BC through high resistances and tapping off these, as shown in the diagram During "break" phase of the commutator these resistances are in series with the short-circuiting resistances R, R′, and so the actual potential of B, for example, will be, not U but $U(R_A + R_A')/(R + R_A + R_A')$, and similarly for C and the intermediate guard rings In order to have the retard field equal to the advance field strength it is therefore necessary to make U greater than V in the inverse ratio The resistances used were Dubilier grid leaks, of the order 1 megohm for R and 5 megohms for R_A and R_A', thus the correction for U is about 10 per cent This was verified by direct checks on the plate and guard ring potentials with an electrostatic voltmeter, which were repeated at regular intervals during the work, to guard against degeneration of the resistances

The two commutators were built up on a single shaft in the way described in the earlier paper, and some additional smoothness of running was obtained by mounting them on ball-bearings Chain drives were substituted for belts to avoid slip errors, Meccano sprocket wheels and chain were used and ran very well at all the speeds required, and a set of the wheels mounted on a single shaft gave a conveniently quick change of gear ratio between commutator and driving motor The measured values of a and b for the new commutator were 0 025 and 0 370, the resolving power being therefore, by equation (4), $R = 30$

It was found essential for accurate work to have a reliable control for the commutator speed, to check temporary fluctuations too small to be controlled by the observer Various types of synchronous control were tried, the method finally adopted being the following a four-pole Rayleigh impulse motor is run in series with an electrically maintained tuning fork, with which it is then synchronous, in the usual way, this motor is not sufficiently powerful to drive the commutator, but acts as a very efficient governor when coupled to the main driving motor, with a chain drive The main motor is illuminated by a flickering neon lamp whose circuit is interrupted by the same fork the procedure then is to set the fork at the frequency required, and adjust the motor resistances till it is seen stroboscopically to fall into step with the fork, after which the Rayleigh motor will keep it steady The fork frequencies and the various gear ratios being known, it is possible quickly to obtain any particular commutator speed required, and so to work by regular steps up and down a current frequency curve, interpolating values where they are needed

The experiments were made on dry air, or on air which was first dried and then mixed with measured proportions of water and other vapours The method generally used was to pump out the system to 1 or 2 mm pressure, and refill very slowly with air drawn through a drying chain consisting of a glass wool filter, strong H_2SO_4, and long tubes of $CaCl_2$ and P_2O The apparatus was pumped out and refilled to atmospheric pressure several times before each run, and when changing from one vapour to another an intermediate run was taken in dry air, the pumping out being repeated until "normal" curves were obtained.

Experimental Results

1. *Dry Air*.—Results with negative ions in dry air at atmospheric pressure confirm those obtained with the earlier apparatus as can be seen in fig. 5;

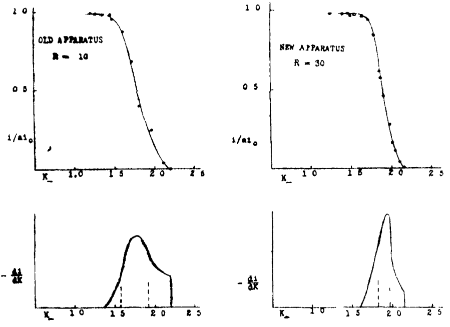

FIG. 5.—Negative Ions in Dry Air. Above: experimental curves; below: derived distributional curves.

the first curve is reproduced from my previous paper, and was taken with a resolving power 10; the second curve shows a narrower band, as might be expected from the higher resolving power and the more accurate speed control of the commutator. There still remains, however, definite evidence of a distribution of mobility over a range which exceeds any possible experimental error; the results of a series of runs made with different field strengths and plate distances are as follows, k_1 and k_2 being the upper and lower limits of the distribution band, corrected for resolving power according to equations (6), and k_0 the uncorrected peak value

$$k_1 = 2.1 \pm 0.05 \qquad k_0 = 1.8 \pm 0.1 \qquad k_2 = 1.6 \pm 0.1$$

No ions were found to have mobilities outside these limits.

Curves of the same general nature were also obtained with positive ions;

a typical distribution band in dry air is shown in the first graph of fig 6 The mean values obtained are

$$k_1 = 1\ 35 \pm 0\ 05 \qquad k_0 = 1\ 1 \pm 0\ 1 \qquad k_2 = 0\ 78 \pm 0\ 05$$

The relative breadth of the band appears to be about double that of the negative ions

Several attempts were made to detect the "young" ions of mobility 1 9, found by Erickson and Tyndall and Grindley,* but these were all unsuccessful Runs were taken at 100 mm pressure, with field strengths and plate distances which gave the ions reaching the electrometer an age of the order 0 015 second If the number of collisions made is regarded as the ageing factor, this is equivalent to an age of 0 002 second at atmospheric pressure, about one tenth of the mean life of Erickson's initial ions No trace was found of any mobility higher than 1 4, and similar negative results were obtained in moist air

Tyndall, Starr and Powell† report erratic results under somewhat similar experimental conditions , they suggest that this is due to some highly active impurity, possibly a product of the alpha-ray source, which accumulates in a closed vessel This impurity" has not yet been identified, but it appears to be the only satisfactory explanation

2 *Water Vapour in Air*

In order to experiment with known proportions of water vapour the apparatus was first exhausted, and distilled water evaporated into it to the full vapour pressure The water flask was then shut off, and dry air added to atmospheric pressure , the concentration is then, say, 14/760, measured in partial pressures If this mixture is again partially exhausted, to a pressure p, and refilled to atmospheric pressure with more dry air, the concentration is then reduced to $(14 \times p)/(760)^2$ In order to work also at relative concentrations higher than that given by saturation at 760 mm , water was first evaporated in, to pressure 14 mm , and air added to give a total pressure p, less than 760 , the concentration is then $14/p$, and the results can be co-ordinated to those obtained at other pressures by multiplying the measured mobilities by $p/760$

Results obtained are shown in the graphs, fig 6 The derived distribution curves alone are given, since they bring out more clearly the points under discussion , the experimental curves on which they are based are of the same order of accuracy as those in fig 5, and could be repeated at will

---

* Erickson, 'Phys Rev ,' vol 20, p 117 (1922), and vol 33 p 403 (1929) , Tyndall and Grindley, 'Roy Soc Proc ,' A, vol 110, p 351 (1926)

† 'Roy Soc Proc ,' A, vol 121, p 172 (1928)

It can be seen that the water vapour causes a marked narrowing of the negative ion band, which is almost entirely due to the disappearance of the faster ions There is also, however, a shift of the band as a whole, in the direction of lower mobility, which is more clearly shown in the higher concentrations , the initial narrowing of the band occurs for small traces of water vapour, and is apparently superposed on the " normal " displacement of the whole band

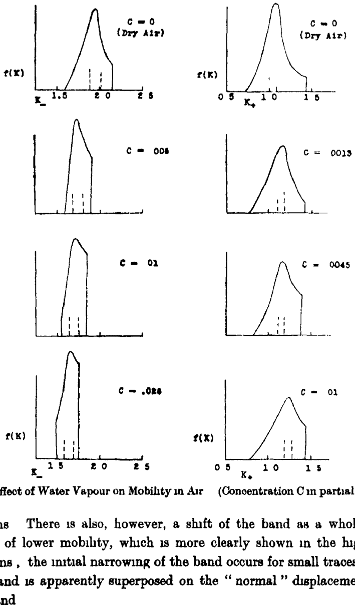

FIG 6 —Effect of Water Vapour on Mobility in Air (Concentration C in partial pressures)

When these results are compared with those obtained with other vapours, described below, it appears that water vapour can be correlated to the other strongly polar gases if we work over a sufficiently wide range of concentrations

This can be shown very clearly if we plot the reciprocal mobilities, $1/k_1$, $1/k_2$, as functions of concentration, as in fig 9 The lower limit of the distribution band, k_2, obeys Blanc's reciprocal law at all concentrations, while the upper limit, k_1, and the peak value k_0 after the "abnormal" initial drop, also follow the linear law

The effect of traces of water vapour on the width of the band suggests that the curves obtained in normally dry air might be further widened if the air is more thoroughly dried To test this point, open dishes containing P_2O_5 were placed inside the condenser vessel, which was filled with dry air in the usual way and then sealed up Runs were taken at intervals extending over a total time of 10 days, without any perceptible change either in the mobility limits or in the shape of the distribution curve

The only effect of water vapour on the positive ion curves is a slight broadening of the peak, and shift in the direction of increased mobility, which is barely within limits of experimental error

3 *Methyl Alcohol in Air*

The effect of the aliphatic alcohols on mobility in air has been systematically studied by Tyndall and Phillips,* using an experimental method in which the mobility is obtained from the peak of an experimental curve of unknown resolving power They find an abnormal initial drop for small traces of vapour in the case of negative ions, followed by the normal linear (reciprocal) decrease for higher concentrations It seemed of interest to repeat some of these observations with the present experimental method, in view of the results obtained with water vapour

The various concentrations were obtained in the same manner as for water vapour, and the runs were all made at atmospheric pressure The results are shown in the graphs of fig 7, and the reciprocals of the upper and lower limits of the band are plotted against concentration in fig 9

The whole curve for the negative ions undergoes the abnormal initial decrease in mobility found by Tyndall and Phillips, without change of breadth There is, however, a broadening of the peak, and the lower limit, k_2, becomes more sharply defined There is good agreement with the results of Tyndall and Phillips, if we take their value of k to correspond to my upper limit k_1

For positive ions the upper limit k_1 is affected "normally," but there is an abnormal initial *increase* in k_2, the slower ions completely disappear in the presence of the smallest trace of the vapour, leaving a narrow band which then follows the reciprocal law for higher concentrations The agreement

---

* 'Roy Soc Proc,' A, vol 111, p 577 (1926)

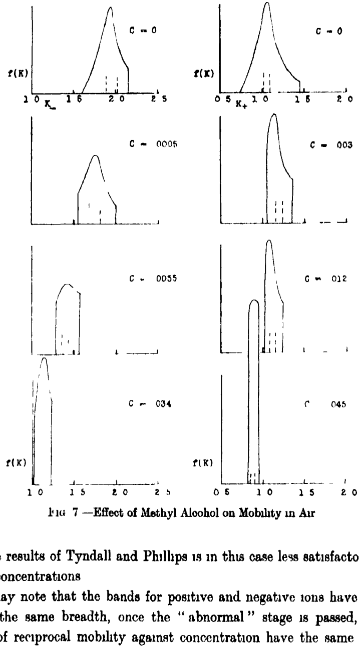

FIG 7 —Effect of Methyl Alcohol on Mobility in Air

with the results of Tyndall and Phillips is in this case less satisfactory at the higher concentrations

We may note that the bands for positive and negative ions have approximately the same breadth, once the "abnormal" stage is passed, and the graphs of reciprocal mobility against concentration have the same gradient

4 *Ethyl Ether in Air*

The second vapour used was ethyl ether, which was evaporated into the vessel in the same way, to give known concentrations Results are shown in fig 8 The only effect on the negative ion is the sharpening of the lower limit of the band, there is no initial abnormality, and the band is unchanged in breadth

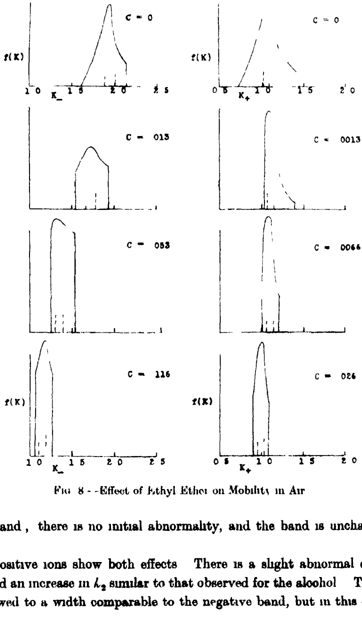

Fig 8—Effect of Ethyl Ether on Mobility in Air

The positive ions show both effects There is a slight abnormal decrease in k_1, and an increase in k_2 similar to that observed for the alcohol The band is narrowed to a width comparable to the negative band, but in this case the concentration curves, fig 9, have different slopes, the positive ions being apparently more strongly affected by the vapour than are the negative ions

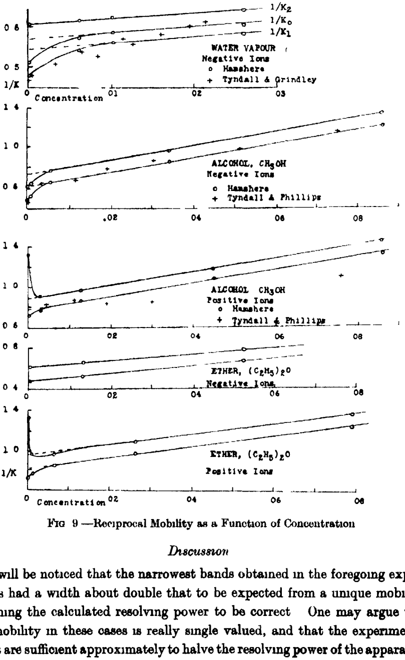

FIG 9 —Reciprocal Mobility as a Function of Concentration

Discussion

It will be noticed that the narrowest bands obtained in the foregoing experiments had a width about double that to be expected from a unique mobility, assuming the calculated resolving power to be correct One may argue that the mobility in these cases is really single valued, and that the experimental errors are sufficient approximately to halve the resolving power of the apparatus, in the absence of independent evidence this point cannot be decided, but even if we make this somewhat drastic "correction" there remains the much wider band in dry air. For example, if we correct the data for negative ions in dry air previously given, assuming a resolving power of 15 instead of 30, we are still left with a distribution between approximate limits 2·05 and 1·7.*

As was pointed out in the previous paper, a distribution of this range is sufficient to account for the experimental discrepancies continually found between measurements made by different observers, some using methods which measure the highest mobility, others the peak (mean) value. That these discrepancies are real has been confirmed by Schilling.†

Since narrow bands are obtained in some circumstances, there does not seem to be any way of accounting for the wider bands in terms of diffusion.

The results in the presence of the vapours tried show that the actual nature of the ions must vary in a very complex way; before one can reach any satisfactory theory it will be necessary to extend the experiments to a number of representative gases and vapours, and in particular to investigate the effect of thorough purification of the gas, in an apparatus which can be baked out.

There are, however, a few points which may be noted here. First, in the widest range found, for positive ions in dry air, the mobilities vary over a range which, expressed as the ratio of highest to lowest mobility, is 1·35/0·78 = 1·7; for negative ions the ratio is 1·3. Theoretical calculations of ion mobility, based on classical gas-kinetic theory, make it seem probable that the size of the ion can affect its mobility in two ways; through the mean free path, which varies inversely as the cross-section, and through a factor depending on the relative masses of the ion and the gas molecule. This mass factor in any theory based on the assumption of elastic collisions takes as a first approximation the form $\{(m + m_1)/m_1\}^{\frac{1}{2}}$, where m is the mass of the gas molecule and m_1 that of the ion (*e.g.*, the theories of Langevin, J. J. Thomson, and Loeb‡). So if the mass of the ion varies from that of a single molecule to a large cluster, its effect on the mobility can only vary in the ratio of $\sqrt{2}$ to 1 In the more rigorous expressions derived by J J Thomson and by Lenard* the mass factor varies over a range of the same order

---

* Zeleny ('Phys. Rev.,' vol. 34, p. 310 (1929)) has recently repeated his original air stream experiment, and finds in slightly moist air a distribution band whose mean range, corrected for diffusion and resolving power, is from 1·03 to 1·48 for positive ions, with a peak at 1·24, and for negative ions, 1·68 to 2·18, with peak at 2·00.

† 'Ann. Physik,' vol. 83, p. 23 (1927).

‡ Langevin, 'Ann. Chim.,' vol. 5, p. 245 (1905); Thomson, 'Phil. Mag.,' vol. 47, p. 337 (1924); Loeb, 'Phil. Mag.,' vol. 48, p. 446 (1924).

Thus the observed variation in mobility is sufficiently small to be explained, at least for the negative ions, by a variation in the ionic mass alone If the variation in the radius is also taken into account, the two effects reinforce each other, and the possible range of mobility is increased In any case, the range observed is of the order to be expected on the assumption of an ion which may vary considerably in size without changing in its electrical properties

To explain the width of the band we must also postulate some degree of permanence in the individual ions, a labile cluster of the type suggested by Loeb†, in which the cluster is so loosely bound as to be little more than an increase in the gas density in the neighbourhood of the charged nucleus would change its effective mass many times during its experimental "life," and by relatively small fractions, so that we should expect it to have a statistical mean mobility which would be for all experimental purposes unique

On the other hand, these experiments afford no evidence for the discrete groups of ions of different mobility, found by Nolan ‡, there may, of course, be such groups within the range found, the mobilities being too close together to be resolved by the apparatus, but the groups also found by Nolan which lie outside this band were never observed

It appears to the writer that small traces of gaseous impurity, such as water vapour, ebonite, tap grease, etc, play a very important part both in the formation of the ions, particularly in the capture of electrons to form negative ions, and in their structure The distribution found in air may be regarded as the maximum range obtainable in an " impure " gas, in which the nuclei may have any molecular mass, attempts to purify the gas may be expected slightly to alter the distribution of mobility within this range, without affecting its actual width until we reach a very high degree of physical purity, at which stage the negative ions may remain free electrons

The " abnormal " effect of small traces of active impurities has been investigated by several observers, notably Loeb, and Tyndall and Phillips (*loc cit*), the assumption being that the mobility in each mixture was unique If the results of the present experiments are accepted as showing a distribution over a finite range, the work of these observers must be regarded as applying either to the highest mobility present, as in Loeb's experimental method, or to some intermediate value

---

* Thomson, 'Proc Phys Soc,' vol 27, p 94 (1914), Lenard, 'Ann Physik,' vol 61, pp 349, 665 (1920)

† 'Phys Rev,' vol 32, p 81 (1928)

‡ *Ibid* vol 24, p 16 (1924)

The "selective cluster" theory of Loeb may be modified to account, at least qualitatively, for the present results The strongly polar molecules of the added gas or vapour will be attracted to the charged nucleus with greater forces than the original gas molecules, the result being what we may regard as an effective concentration in the neighbourhood of the ion which is higher than the measured average concentration in the whole gas This is sufficient to account for an abnormal shift of the whole distribution band, as found for negative ions in the alcohol-air mixtures But for a shift of the upper limit only, as found in water vapour, we must also assume a definite clustering in which the faster (presumably smaller) ions are eliminated altogether, and all the ions formed have the maximum size (minimum mobility) characteristic of the gas Further increases in the relative density of the added vapour then affect the mobility in the "normal" way, by modifying the dielectric constant and density of the gas as a whole

The converse effect found for positive ions in both the ether and alcohol mixtures points to an inhibitory effect which may be pictured as a protective cluster, comparatively permanent, of "impurity" molecules, which prevents the formation of the larger (slower) clusters There is an interesting analogy here to the suggestion of Mahoney,* that water vapour, and possibly other "impurities," increase the life of the young positive ions by inhibiting the formation of the larger final ion At present, however, we have insufficient evidence to justify further speculation in this direction

Summary

The experimental method for measuring gas ion mobilities, described in a previous paper, has been improved in accuracy and resolving power, and applied to examine the effect of water vapour, methyl alcohol, and ethyl ether, on positive and negative ion mobilities in air

The finite distribution band previously found is confirmed in dry air As water vapour is added the negative ion band is first narrowed, and then shifted in the normal way for gas mixtures Positive ions are comparatively little affected

In the alcohol vapour the whole negative band is abnormally shifted, without change of breadth The positive ion band is abnormally narrowed by the disappearance of the slower ions

---

* 'Phys Rev,' vol. 33, p 217 (1929)

In the ether vapour the negative ions are very slightly affected, and the positive band shows both effects

An attempt is made to interpret these results in the light of a modified cluster theory

These experiments were made at the Cavendish Laboratory I gladly take this opportunity to express my indebtedness to Sir J J Thomson for suggesting the problems and for his interest and advice

The Kinetics of the Heterogeneous Thermal Decomposition of Methyl Formate

By E W R STEACIE, Physical Chemistry Laboratory, McGill University, Montreal

(Communicated by A S Eve, F R S —Received February 7, 1930)

Introduction

In investigating the rates of chemical reactions, gaseous systems are to be preferred on account of their simplicity The investigation of the thermal decomposition of organic compounds in the gaseous state possesses the added advantage that there is only one reactant The present investigation deals with the thermal decomposition of gaseous methyl formate

Apparatus

The apparatus was essentially the same as that which has been employed by Hinshelwood and his co-workers in a large number of investigations *

A silica reaction bulb was contained in an electric furnace of a type which has been previously described † This was connected to a glass capillary manometer by capillary tubing and a De Khotinsky seal Connection was also made through stopcocks to a reservoir of methyl formate or to the pumping system All the connecting tubing between the methyl formate reservoir and the furnace, including the manometer, was wound with nichrome wire and was kept at a temperature of about 60° C (*i e*, about 30° above the boiling point of methyl formate) At this temperature the De Khotinsky seal did not soften sufficiently to be troublesome

---

* ' Roy Soc Proc, A, vol. 111, p 245 (1926), vol 113, p 221 (1927), vol 114, p 84 (1927), etc.

† Steacie and Johnson, ' Roy Soc Proc,' A, vol. 112, p 542 (1926)

The volume of the reaction bulb was about 50 c c and that of the dead space outside the furnace about 1 0 c c Hence the gas not in the reaction vessel was only about 2 per cent of the total amount and could be neglected without serious error

Temperatures were measured with a constant-volume nitrogen thermometer which had been checked at the freezing and boiling points of water and at the boiling point of sulphur

Two samples of methyl formate were used The first was obtained from the Eastman Kodak Company It was distilled from phosphorus pentoxide three times to remove water and was then fractionated four times The second sample was prepared from methyl alcohol and formic acid* and was then dried and fractionated as before The two samples had identical boiling points and there was no detectable difference in their behaviour during the course of the investigation

Experimental Procedure

Before making an experiment the reaction vessel was evacuated thoroughly by means of two mercury condensation pumps in series The furnace was brought to the desired temperature and the heating element surrounding the manometer was switched on The tap leading to the methyl formate supply was opened, methyl formate vapour entered the apparatus, the tap was quickly closed again and the pressure and time were immediately read Subsequent pressure readings were taken from time to time until the reaction had reached completion The course of the reaction was followed by the rate at which the pressure increased

The analysis of the products and the mechanism of the reaction will be discussed later It may be mentioned here that the main reaction consists of the decomposition of methyl formate into methyl alcohol and carbon monoxide, involving the doubling of the initial pressure

The Effect of Surface

After a series of experiments had been made, the reaction vessel was disconnected, powdered silica made from the same tubing was added, and the vessel was sealed on again After the addition of the powdered silica the reaction velocity was about 29 times greater than before at all temperatures A sample of the same silica powder was examined microscopically using a micrometer eyepiece, and its surface was estimated The total surface of the silica after the addition of the powder to the reaction vessel was calculated to be about 25 9 times greater than before Considering the approximate nature of the estimation of the surface, this corresponds with the increased reaction rate within the experimental error It may be concluded, therefore, that the reaction takes place entirely at the surface of the silica The complete heterogeneity of the reaction is further confirmed by the fact that the temperature coefficient was unaltered by the addition of powdered silica and is satisfactorily expressed by the Arrhenius equation

---

* Perkin, 'J Chem. Soc,' vol. 45, p 489 (1884), Young and Thomas, *ibid*, vol 63, p 1191 (1893)

The Course of the Reaction

The products of the thermal decomposition of methyl formate have been the subject of two previous investigations The rate of the reaction, however, was not included in either of these

Hurd* points out that since formates possess the functional grouping of aldehydes it is possible that they will decompose in the same manner, viz,

$$HCOOCH_3 = CO + CH_3OH$$

Muller and Peytral† studied the decomposition of methyl formate vapour when passed through platinum tubes at 1150° C From the analysis of the products they concluded that the reaction probably occurred in stages, methyl formate first giving formaldehyde,

$$HCOOCH_3 = 2HCHO,$$

which was then followed by the decomposition of the formaldehyde in the manner found by Bone and Smith,‡

$$HCHO = CO + H_2$$

The gaseous products of the reaction were carbon monoxide 53 per cent, hydrogen 43 1 per cent, methane 1 5 per cent, carbon dioxide 1 8 per cent Formaldehyde was also isolated together with a small amount of methyl alcohol which, they suggest, results from the hydrogenation of the formaldehdye

The results of the present investigation are at variance with the above explanation As will be shown later, the reaction apparently consists of a

---

* 'Pyrolysis of Carbon Compounds,' New York, 1929, p 524

† Muller and Peytral, 'C R,' vol. 179, p 831 (1924), Peytral, 'Bull. Soc Chim.,' vol. 37, p 562 (1925)

‡ 'J Chem. Soc,' vol 87, p 910 (1905)

rapid decomposition involving the doubling of the initial pressure, followed by a slow secondary reaction This fact, taken in conjunction with the results of the analysis of the products, indicates that the reaction proceeds thus

$$HCOOCH_3 = CH_3OH + CO$$

The alcohol then decomposes in stages*

$$CH_3OH = HCHO + H_2$$

$$HCHO = CO + H_2$$

It has been shown by Bone and Smith (*loc cit*) that in the decomposition of formaldehyde at low temperatures some condensation products are formed, together with carbon monoxide, hydrogen, and some methane and carbon dioxide This is in agreement with the results of the present investigation, since small amounts of carbon dioxide and methane are formed and the final pressure never reached four times the initial pressure, presumably due to condensation of some of the products in the later stages of the reaction

The Analysis of the Products of the Reaction

Gaseous Products —The gaseous products of the reaction were analysed in a small form of Hempel apparatus, samples of about 5 c c being used

In the early stages of the reaction the gaseous products consisted entirely of carbon monoxide This result was independent of the temperature or pressure at which the reaction was carried out When the reaction had proceeded to such an extent that the ratio of the pressure to the initial pressure had reached about 1 7, hydrogen appeared as a product together with small

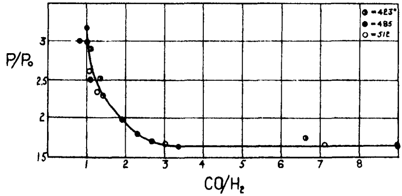

Fig 1 —The Gaseous Products of the Reaction.

---

* Nef, 'Ann D Chem Ges,' vol 318, p 191 (1901), Bone and Davies 'J Chem Soc,' vol. 105, p 1691 (1914)

amounts of carbon dioxide and methane As the reaction progressed further the proportion of hydrogen in the products increased rapidly Finally, when the ratio of pressure to initial pressure reached about 3 0 the amount of hydrogen became equal to that of carbon monoxide

In fig 1 the carbon monoxide-hydrogen ratio is plotted against the ratio of pressure to initial pressure It will be seen that within the experimental error the CO/H_2 ratio is independent of the temperature Some sample analyses follow --

			per cent
I—			
Temperature = 485° C	CO		62 9
	H_2		33 0
Initial pressure = 35 9 cms	CO_2		2 4
	CH_4		2 3
Sample taken when $P/P_0 = 2$ 0	CO/H_2	=	1 90
II —			
Temperature = 485° C	CO		90 1
	H_2		9 8
Initial pressure = 22 5 cms	CO_2		0 0
	CH_4		0 0
Sample taken when $P/P_0 = 1$ 63	CO/H_2	=	9 19
III —			
Temperature = 423° C	CO		45 4
	H_2		41 8
Initial pressure = 17 2 cms	CO_2		6 2
	CH_4		6 8
Sample taken when $P/P_0 = 2$ 91	CO/H_2	=	1 08

Other Products — On account of the very small amounts of products which were available, only qualitative tests were carried out for methyl alcohol and formaldehyde The products were withdrawn from the reaction vessel into an evacuated tube The condensable products were then removed by means of a U-tube surrounded by solid carbon dioxide and acetone The condensed material was washed out later with a few drops of water and tested colorimetrically

The test which was used for formaldehyde was the phenyl hydrazine hydrochloride method described by Schryver *

---

* 'Roy Soc Proc,' B, vol 82, p 226 (1909)

If formaldehyde were absent, the solution was examined for methyl alcohol by the oxidation of the methyl alcohol to formaldehyde by means of a hot copper wire dipped into the solution, and the subsequent test for formaldehyde by the method of Schryver

In the early stages of the reaction no formaldehyde could be detected in the products but very definite tests for methyl alcohol were obtained In the later stages of the reaction formaldehyde was easily detectable

The results obtained for the rate of decomposition, together with the analyses of the products, definitely indicate that the course of the reaction is that previously mentioned, viz ,

$$HCOOCH_3 = CH_3OH + CO$$
$$CH_3OH = HCHO + H_2$$
$$HCHO = H_2 + CO$$

At any rate there seems to be no doubt that the primary reaction under investigation is the decomposition of methyl formate into methyl alcohol and carbon monoxide, involving the doubling of the initial pressure

The Velocity of the Reaction

Correction for the Slow Secondary Reaction —As mentioned above, the main reaction is apparently followed by slow secondary changes The first requisite for the interpretation of the experimental results is the disentanglement of the main reaction from the slow later reactions

In fig 2, curve A, the ratio of the pressure to the initial pressure is plotted

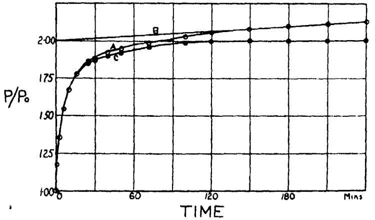

FIG 2 —Correction for Secondary Reaction Temperature, 423° C Initial Pressure, 23 20 cm.

against time for a typical experiment It will be seen that the pressure increases rapidly at first and appears to be about to reach equilibrium at double the initial pressure Instead of this, however, a very slow, practically linear, increase in pressure takes place in the later stages of the reaction If this linear portion of the curve is extrapolated back to zero time, it intersects the P/P_0 axis at a value of 2 0 This line, B, represents approximately the rate of increase in pressure due to the secondary reaction At any time the distance between B and the ordinate $P/P_0 = 2\ 0$ represents the increase in pressure due to the secondary reaction, which must be subtracted from the value of P/P_0 in curve A to give the true rate of the primary reaction Curve C is constructed from the difference between A and B in this way Except in the later stages of the reaction this correction is almost negligible, so that no appreciable error is introduced by its approximate nature All the experimental results described in the succeeding sections have been corrected in this way In no case is the correction large except towards the end of the reaction

The Dynamics of the Reaction —It has been shown by Hinshelwood and Prichard* that in a heterogeneous unimolecular reaction if the reacting gas is only slightly adsorbed, while one of the products of the reaction is strongly adsorbed, the rate of the reaction will be given by the equation

$$\frac{dx}{dt} = \frac{K(a-x)}{1+bx},$$

where a is the original concentration of the reactant, x the amount transformed at time t, K the velocity constant, and b is a constant which depends on the degree of adsorption of the product This equation satisfactorily expresses the rate of thermal decomposition of methyl formate On integration we obtain

$$K = \frac{1+ab}{t} \log \frac{a}{a-x} - \frac{bx}{t}$$

As Hinshelwood and Prichard point out, the applicability of this equation may be tested as follows

Let $1/t \ \log a/a - x = K_m$, and $x/t = v$

The above equation then becomes

$$K = (1 + ab)\,K_m - bv,$$

or

$$v = (a + 1/b)\,K_m - K/b$$

---

* 'J Chem Soc,' vol 127, p 327 (1925)

Hence K_m should be a linear function of v. The linearity of the expression will be a test of the form of the equation The values of the constants will

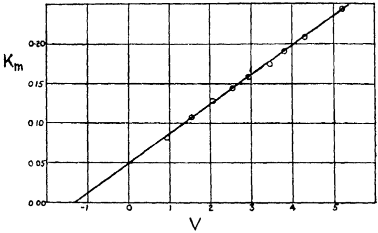

FIG 3 —Temperature, 423° C Initial Pressure, 23 20 cm

only affect the slope and the intercepts on the axes Fig 3 is an example of the agreement of the experimental results with the form of the above equation The slope of the line in fig 3 is equal to $a + 1/b$ and the intercept on the v axis gives the value of $-K/b$ The complete data for two runs are given in Tables I and II The constancy of the figures in the last column of each table proves the applicability of the equation

Table I —Powdered silica added to bulb Temperature $=$ 423° C Initial pressure $= a =$ 23 20 cms

Time	x	v	K_m	$v+1\ 35$	$(v+1\ 35)/K_m = a+1/b$
mins	cms				
0 5	2 60	5 20	0 244	6 55	26 8
1 0	4 31	4 31	0 207	5 66	27 4
1 5	5 69	3 78	0 190	5 13	27 0
2 0	6 90	3 45	0 174	4 80	27 5
3 0	8 82	2 94	0 159	4 29	27 0
4 0	10 11	2 53	0 143	3 88	27 2
6 0	12 43	2 07	0 127	3 42	27 0
10 0	15 18	1 52	0 106	2 87	27 1
20 0	18 50	0 98	0 080	2 28	27 5
				Mean	27 2

Slope $= a + 1/b = 27\ 2$ Intercept $= -K/b = -1\ 35$ Whence $K = 0\ 338$ $b = 0\ 250$

Table II—No powdered silica added Temperature = 512° C Initial pressure = a = 14 01 cms

Time	x	v	K_m	$v + 1\ 35$	$(v+1\ 35)/K_m = a+1/b$
mins	cms				
0 5	2 30	4 60	0 350	5 63	16 1
1 0	3 50	3 50	0 286	4 53	15 8
3 0	6 16	2 05	0 193	3 08	15 9
5 0	7 82	1 56	0 163	2 59	15 9
8 0	9 28	1 16	0 136	2 19	16 1
13 0	10 93	0 84	0 115	1 87	16 3
20 0	12 21	0 61	0 102	1 64	16 1
31 0	13 10	0 42	0 089	1 45	16 3
				Mean	16 1

Slope = 16 1 Intercept = − 1 03 K = 0 491 b = 0 476

The variation of " b "—In any one experiment the above equation fits the experimental results with practically perfect accuracy At constant temperature, however, b varies decidedly with the initial pressure of the reactant In fig 4, K_m is plotted against v for experiments at four different initial pressures The data from fig 4 are summarised in Table III

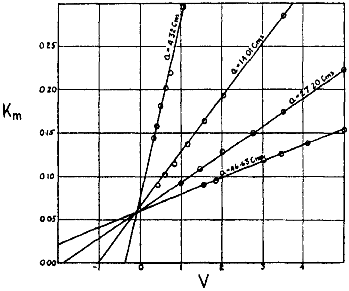

Fig 4—Temperature, 512° C. Various Pressures

Table III -- Temperature = 512° C

a	Slope	Intercept	b	K	ab
4 32	4 95	−0 34	1 54	0 525	6 68
14 01	16 1	−1 03	0 476	0 491	6 63
27 20	31 1	−1 90	0 256	0 486	6 95
46 63	54 5	−3 51	0 127	0 445	5 93

The product ab is thus practically constant In other words, b is inversely proportional to a The data from a series of experiments at a different temperature are given in Table IV

Table IV - Temperature = 485° C

a	Slope	Intercept	b	K	ab
9 70	12 6	−0 270	0 345	0 0690	3 34
14 41	19 3	−0 261	0 240	0 0628	3 46
25 92	32 0	−0 340	0 164	0 0558	4 25
35 40	45 0	−0 690	0 104	0 0698	3 68

The same variation of b with the initial pressure is shown here It should be emphasised that since b is the reciprocal of the difference between two quantities of similar magnitude, small experimental errors will be very greatly magnified in calculating the value of b Consequently more than approximate constancy of the product ab cannot be expected The most significant point is that there is no steady drift in the product ab with changing pressure

The above equation may be modified so as to include the variation of b with the initial pressure If we replace b by a new constant c such that $c = ab$, we have

$$\frac{dx}{dt} = \frac{K(a - x)}{1 + cx/a}$$

On integration this gives

$$K = \frac{1 + c}{t} \quad \log \frac{a}{a - x} - \frac{cx}{at}$$

The Effect of Temperature—The effect of temperature on the constant c is shown in Table V.

Table V

Empty bulb		Powdered silica added	
Temperature °C	c (average)	Temperature °C	c (average)
457	4 04	368	3 81
485	3 68	423	5 80
512	6 55	457	4 12
550	5 12	485	6 03
		393	4 46

If there is any variation in the value of c with changing temperature, it is very small compared with the variation in K, the velocity constant The extreme variation in the value of K for the conditions given in the above table is about 67-fold Hence, considering the magnification of errors in the calculation of the constant, we may regard c as independent of the temperature

The Order of the Reaction

If the equation

$$K = \frac{1 + ab}{t} \log \frac{a}{a - x} - \frac{bx}{t}$$

holds for the reaction velocity, then the time to 1/2 value will be given by

$$T = \{(1 + ab) \log 2 - \tfrac{1}{2}ab\}/K$$

As shown above, b varies inversely as the initial concentration and must be replaced by c/a The expression for the half-life then becomes

$$T = \{(1 + c) \log 2 - \tfrac{1}{2}c\}/K$$

Hence T is independent of the initial concentration and the reaction should be kinetically of the first order.

In order to reduce the effect of the retardation to a minimum the time for the reaction to proceed 15 per cent has been used instead of the time to 1/2 value As may be seen from Tables VI and VII, the time for the reaction to proceed 15 per cent is independent of the pressure within the experimental error

Table VI

No powdered silica added				$\frac{\text{Surface}}{\text{Volume}} = 3\ 3\ \text{cms}^{-1}$			
550° C		512° C		485° C		457 C	
Pressure	T	Pressure	T	Pressure	T	Pressure	T
cms	secs	cms	secs	cms	secs	cms	secs
6 05	8 2	4 32	27	9 70	135	7 65	303
10 71	7 2	14 01	28	14 41	133	25 37	309
16 22	8 8	27 20	33	25 92	139	40 81	298
35 57	7 8	46 63	31	35 40	124	—	—
Mean	8 0	—	29 7	—	133	—	303

Table VII

Powdered silica in bulb				$\frac{\text{Surface}}{\text{Volume}} = 86\ 5\ \text{cms}^{-1}$			
457° C		423° C		393° C		368° C	
Pressure	T	Pressure	T	Pressure	T	Pressure	T
cms	secs	cms	secs	cms	secs	cms	secs
8 11	5 5	5 92	22	9 65	101	6 82	705
9 81	5 0	6 86	26	20 59	100	16 20	742
32 76	5 5	22 92	26	40 18	104	25 37	728
—	—	23 20	28	—	--	40 55	738
Mean	5 3	—	25 5	—	101 6	—	728

The Temperature Coefficient and the Heat of Activation

The temperature coefficient of the reaction can also be obtained from the results given in Tables VI and VII In fig 5 the logarithm of the time to 15 per cent completion is plotted against the reciprocal of the absolute temperature The linearity of the curves shows the applicability of the Arrhenius equation,

$$\frac{d \log \text{K}}{d\text{T}} = \text{E}/\text{RT}^2,$$

or

$$\frac{d \log 1/t}{d\text{T}} = \text{E}/\text{RT}^2,$$

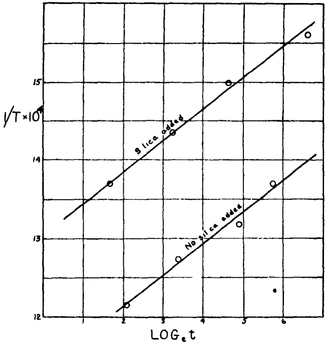

FIG 5

where t is the time to 15 per cent completion, T is the absolute temperature and E is the heat of activation The value of E, the heat of activation, calculated from the slope of the lines in fig 5, is —

Empty bulb	E = 49,000 cal per gram mol
Silica added	E = 47,500 ,,
Mean	48,700

The Retardation of the Reaction by the Products

Since the rate of the reaction is given by the equation

$$dx/dt = \frac{K(a-x)}{1+cx/a},$$

one of the products must be adsorbed so strongly that the free space is inversely proportional to the pressure of the product * In an attempt to confirm this the effect of various added gases on the rate of the reaction was determined

A series of experiments at 393° C were made with methyl formate alone The effect of added carbon dioxide, methane, carbon monoxide, hydrogen, and water vapour was then investigated Some experiments were also carried

* Hinshelwood and Prichard, *loc cit*

out in the presence of the products of a former experiment which had been allowed to go to completion None of these additions produced any alteration in the rate of reaction, as may be seen from Table VIII

Table VIII —The Effect of added Gases on the Time for the Reaction to go to 15 per cent completion at 393° C

Initial pressure of methyl formate	Added gas	Pressure of added gas	Time to 15 per cent completion
cms		cms	seconds
9 65	None	—	101
20 59	,,	—	100
40 18	,,	—	104
25 10	Carbon dioxide	5 02	102
10 45	,,	45 27	98
20 17	Methane	10 11	101
20 99	,,	43 33	104
19 87	Carbon monoxide	9 86	97
21 31	,,	41 04	101
21 12	Hydrogen	5 95	112
17 84	,,	25 01	102
19 03	,,	42 78	104
6 03	Water vapour	2 51	106
36 71	,,	1 71	99
20 01	Products of former reaction	15 65	101
29 84	,,	29 66	104
39 33	,,	44 00	102

It appeared therefore that the retardation must be due to some product formed in the early stages of the reaction and decomposed before the reaction had reached completion The effect of added formaldehyde and methyl alcohol was therefore investigated

Formaldehyde —Formaldehyde was prepared by heating paraformaldehyde A small amount of decomposition of the formaldehyde occurred at 393° C for which a correction was applied The results are summarised below

Initial pressure of methyl formate	Pressure of added formaldehyde	Time to 15 per cent. completion
20 51	1 62	101
19 87	6 71	107
20 43	14 24	104
20 86	20 15	108
7 02	20 08	107

There thus seems to be a very small retarding effect due to the addition of formaldehyde It is not, however, much larger than the experimental error

Methyl Alcohol—At 393° C there was also some decomposition of methyl alcohol for which a correction had to be applied This correction was considerably larger than that with formaldehyde and consequently introduced some uncertainty into the calculation of the reaction velocity The alcohol was found to have a retarding effect which was independent of the absolute concentration, but was dependent on the ratio of the concentration of methyl alcohol to that of methyl formate The effect is summarised in Table IX

Table IX —The Retarding Effect of Methyl Alcohol

$\frac{(CH_3OH)}{(HCOOCH_3)}$	Rate expressed as per cent decomposed in 100 seconds	Rate calculated
0 00	14 9	14 9
0 58	9 0	4 16
0 75	7 0	3 35
0 88	6 8	3 02
1 18	6 0	2 37
2 09	4 1	1 44

The figures given in the last column are calculated from the expression

$$\text{Rate} = \frac{14\ 9}{1 + cx/a} = \frac{14\ 9}{1 + 4\ 46\,(CH_3OH)/(HCOOCH_3)}$$

While the retarding effect of the alcohol is considerable, it is very much less than the calculated amount In order to bring the observed and calculated values into line, it would be necessary to lower the observed value of the constant *c* from 4 46 to about 1 2, which is quite outside the experimental error

In any case, if the alcohol were the cause of the retarding effect the rate of reaction should be expressed by

$$\frac{dx}{dt} = \frac{K(a-x)}{1 + bx}$$

Instead of this, the observed behaviour is expressed by

$$\frac{dx}{dt} = \frac{K(a-x)}{1 + cx/a}$$

It seems probable, therefore, that the retarding effect is caused, not by methyl alcohol itself, but by some product present in small amount which arises from the decomposition of the alcohol.

The Addition of the Products of the Reaction —In order to prove that the peculiar retarding effect really existed and was not an apparent effect due to some error in the interpretation of the mechanism of the reaction, some experiments were carried out in which the reaction was allowed to proceed for a short time and more methyl formate was then added For example, in one experiment the initial pressure of methyl formate was 12 02 cms When the reaction had proceeded for 120 seconds the ratio of pressure to initial pressure was 1 17 By calculation, therefore, the partial pressure of methyl formate remaining was 9 96 cms, and that of the products 4 12 cms From the results of other experiments it was calculated that if the reaction had proceeded further the time required for 15 per cent of the remaining methyl formate to decompose would have been 151 seconds When the reaction had reached this stage methyl formate sufficient to increase the pressure by 15 71 cms was added The total concentration of methyl formate present was then $15\ 71 + 9\ 96 = 25\ 67$ cms The time taken for 15 per cent of this to decompose was 153 seconds

Apparently, then, the time for the reaction to proceed, say, 15 per cent, is in no way dependent on the relative quantities of reactant and products, or on the initial pressure of the reactant The retarding effect presumably depends merely on how far the reaction has proceeded, *i e*, on the ratio x/a The conclusions previously reached regarding the dynamics of the reaction are therefore confirmed

The retarding effect in other examples was similar in every way to the above The effect of the products increased with time, *i e*, with x/a, until the ratio P/P_0 had reached about 1 7 After this the retarding effect of the products decreased with time, and after the ratio P/P_0 had passed 2 0 the products exerted no retarding effect

It might be thought at first sight that the retarding effect is caused by some product, present in small amount, which arises by a zero order decomposition of methyl formate If this were so its concentration would be dependent only on the duration of the reaction, and therefore in the early stages of the reaction roughly proportional to x/a This, however, is quite impossible since the zero order decomposition of methyl formate would mean very strong adsorption of the reactant, while the observed rate of reaction corresponds to a very small adsorption of the methyl formate

Summary

The thermal decomposition of gaseous methyl formate has been investigated in silica vessels from 368° C to 550° C The decomposition is entirely heterogeneous and is retarded by the products of the reaction The rate of the reaction is expressed by

$$-\frac{d}{dt}(\mathrm{HCOOCH_3}) = \frac{\mathrm{K}(\mathrm{HCOOCH_3})}{1+c(\mathrm{CH_3OH})/a},$$

where c is a constant, and a is the initial concentration of methyl formate The temperature coefficient of the reaction is in agreement with the Arrhenius equation The heat of activation is 48,700 calories per gram molecule

---

The Spectra of Trebly-ionised Oxygen (O IV) and Trebly-ionised Nitrogen (N IV)

By L J Freeman, Ph D , D I C , Imperial College of Science and Technology, South Kensington

(Communicated by A Fowler, F R S —Received February 25, 1930)

(1) The Spectrum of Trebly-ionised Oxygen (O IV)

Introductory

The spectrum of trebly-ionised oxygen has been investigated in the extreme ultra-violet by Bowen,* who has identified five of the deepest doublet terms, namely $2p\,^2\mathrm{P}$, $2p'\,^2\mathrm{S}$, $2p'\,^2\mathrm{P}$, $2p'\,^2\mathrm{D}$ and $2p^3\,^2\mathrm{P}$ A list of 76 lines in the near ultra-violet, attributed to O IV, was given by Mihul,† but no classifications were made

The present paper deals mainly with the identification of the $3s\,^2\mathrm{S}$, $3p\,^2\mathrm{P}$, $3d\,^2\mathrm{D}$ terms of the doublet system, and of the $3s'$, $3p'$ and $3d'$ terms of the quartet system from their combinations occurring in the visible and near ultra-violet regions The spectrum has been photographed on various instruments from λ 7000 to λ 1250 by using strongly condensed discharges in vacuum tubes containing oxygen The detection of some of the fainter multiplets was greatly facilitated by the prediction of their positions by extrapolation from corresponding multiplets in C II* and N III† As the region investigated is rich in lines of O II and O III, there are many instances of O IV lines being masked by lines of O II and O III

---

* 'Phys. Rev ,' vol 29, p 237 (1927)

† 'Thesis, University of Nancy,' Paris (1927)

Predicted Terms

The predicted terms of O IV are shown in Table I, the notation adopted being similar to that used by Fowler and others in recent papers‡

Table I —Predicted Terms of O IV

1_1	2_1	2_2	3_1	3_2	3_3	Adopted prefix	Terms			
2	2	1				$2p$	^2P			
2	2		1			$3s$	^2S			
2	2			1		$3p$	^2P			
2	2				1	$3d$	^2D			
2	1	2				$2p$	^2S	^2P	^2D	^4P
2	1	1	1			$3s$	^4P			
2	1	1		1		$3p'$	^4S	^4P	^4D	
2	1	1			1	$3d'$	^4P	^4D	^4F	
2		3				$2p^3$	^2P	^2D	^4S	

Doublets

The $2p^3\,{}^2D$ term was identified by its combinations with $2p'\,{}^2P$ and $2p'\,{}^2D$, the former giving a very strong diffuse doublet with inverted satellite at λ 1343 A principal pair and a diffuse pair with satellite, having a common separation of 87 wave-number units, served to identify the $3s\,{}^2S$, $3p\,{}^2P$ $3d\,{}^2D$ terms which also were found to combine with some of the deepest terms giving lines in the extreme ultra-violet In Table II are collected the doublet combinations observed, including those given by Bowen The term values are based on Bowen's estimate of 623500 for $2p\,{}^2P_1$

---

* A. Fowler and E W H Selwyn, 'Roy Soc Proc,' A, vol. 118, p 34 (1928)

† L. J Freeman, 'Roy Soc Proc,' A, vol 121, p 318 (1928)

‡ A Fowler, 'Roy Soc Proc,' A, vol 117, p 317 (1928), vol 123, p 422 (1929)

Table II —Doublet Combinations in O IV

		$2p\ {}^2P_1$ 623500†	387	$2p\ {}^2P_2$ 623113†	$2p^3\ {}^2D_3$ 368342	−27	$2p^3\ {}^2D_2$ 368315	$2p^3\ {}^2P_{1\ 2}$ 334476†	$3p\ {}^2P_1$ 233240 6	87 0	$3p\ {}^2P_2$ 233153 6
$2p'\ {}^2D_3$	496563 6†			126549 4 (6)*	128234 (1)‡			162093 (1)*	263435 (0)‡		
	−12 9										
$2p\ {}^2D_2$	496550 7†	126949 3 (6)*									
$2p'\ {}^2S_1$	459132†	164368 (4)*	387	163981 (4)*				124656 (1)*			
$2p'\ {}^2P_1$	443018†	180484 (5)*	391	180093 (4)*			74701 2 (5)	108546 (2)*			
	246	244		247			244 3	240			
$2p'\ {}^2P_2$	442772†	180728 (4)*	388	180340 (5)*	74429 7 (6)	— 27 2	74456 9 (3)	108306 (3)*			
$3s\ {}^2S_1$	265787 0	357513 (1)*							32546 3 (4)	87 1	32633 4 (6)
$3d\ {}^2D_2$	203868 2	419041 (1)*							29372 4 (3)	86 9	29285 5 (1)
	16 6										16 5
$3d\ {}^2D_3$	203851 6										29302 0 (4)

* Observed and classified by Bowen.
† Bowen's term values
‡ λ by Bowen.

Quartets

Of the quartet terms, only those of principal quantum number 3 have been identified—from combinations among themselves Their combinations with terms of principal quantum number 2 or 4 would occur far down in the Schumann region, probably below λ 1300

The term values are based upon the value 269000 for $3s'\,{}^4P$, derived by extrapolation of $\sqrt{T/R}$ for C II and N III Thus

Values of $\sqrt{T/R}$ *for* $3s'\,{}^4P$

C II	Diff	N III	Diff (assumed)	O IV (assumed)
0 869	*0 349*	1 218	*(0 349)*	(1 567)

The quartet combinations observed are given in Table III, and the term values are collected in Table IV Table V is a list of lines of O IV and includes the list previously published by Bowen The disruptive discharge necessary to produce the O IV spectrum is very favourable also to the appearance of impurity lines, so that it is unsafe to ascribe faint lines to O IV unless they can be classified Actually there are very few lines in the region considered which could possibly be ascribed to O IV and which have not been classified The most outstanding are λ 2921, λ 2916 and λ 2450, λ 2449 These, by analogy with corresponding lines in the spectrum of N III, have been provisionally classified as $4p\,{}^2P - 5s\,{}^2S$ and $4f\,{}^2F - 5g\,{}^2G$ respectively

Wave-numbers enclosed in brackets have been calculated from multiplet structures

Table III —Quartet Combinations in O IV

	$3s'\,{}^4P_3$ 269000 0	*246 9*	$3s'\,{}^4P_2$ 269246 9	*135 1*	$3s'\,{}^4P_1$ 269382 0
$3p'\,{}^4P_3$ = 229159 2	39840 8 (8)	*246 9*	40087 7 (7)		
129 1	*129 2*		*129 1*		
$3p'\,{}^4P_2$ = 229288 3	39711 6 (7)	*247 0*	39958 6 (4)	*135 1*	40093 7 (7)
94 5			*94 5*		*94 5*
$3p'\,{}^4P_1$ = 229382 8			39864 1 (7)	*135 1*	39999 2 (3)
$3p'\,{}^4D_4$ = 239471 1	29528 9 (6)				
209 7	*209 6*				
$3p'\,{}^4D_3$ = 239680 8	29319 3 (2)	*246 8*	*29566 1 (4)		
135 5	*135 4*		*135 3*		
$3p'\,{}^4D_2$ = 239816 3	29183 9 (0)	*246 9*	29430 8 (2)	*135 3*	*29566 1 (4)
78 8					
$3p'\,{}^4D_1$ = 239895 1			†[29351 8]		‡[29486 7]
$3p'\,{}^4S_2$ = 233752 7	35247 5 (6)	*246 7*	35494 2 (4)	*135 1*	35629 3 (3)

* Used twice † O III line at 29353 4 ‡ O II line at 29487 83

Table III—(continued)

	$3p'\,^4D_4$ 239471 1	*209 7*	$3p'\,^4D_3$ 239680 8	*135 5*	$3p'\,^4D_2$ 239816 3	*78 8*	$3p'\,^4D_1$ 239895 1
$3d'\,^4F_5$ = 212717 7	*26753 4 (4)						
154 1	*154 2*						
$3d'\,^4F_4$ = 212871 8	26599 2 (0)	*209 8*	26809 0 (3)				
112 4			*112 4*				
$3d'\,^4F_3$ = 212984 2	[26480 9]		26696 6 (0)	*135 6*	*26832 2 (2)		
78 8					*78 8*		
$3d'\,^4F_2$ = 213063 0			[26617 8]		*26753 4 (4)	*78 8*	*26832 2 (2)
$3d'\,^4D_4$ = 208323 9	31147 2 (3)		[31356 9]				
64 6							
$3d\,^4D_3$ = 208388 5	[31082 6]		31292 3 (1)		[31427 8]		
46 7			*46 7*				
$3d\,^4D_2$ = 208435 2			31245 6 (1)	*135 4*	31381 0 (0)	*78 3*	31459 3 (0)
28 9							*28 9*
$3d\,^4D_1$ = 208464 1					[31352 2]		31430 4 (0)

* Used twice

	$3p\,^4P_3$ 229159 2	*129 1*	$3p\,^4P_2$ 229288 3	*94 5*	$3p'\,^4P_1$ 229382 8
$3d'\,^4D_4$ = 208323 9	20835 1 (5)				
64 6	*64 1*				
$3d'\,^4D_3$ = 208388 5	20771 0 (1)	*128 7*	20899 7 (4)		
46 7			*47 1*		
$3d'\,^4D_2$ = 208435 2	[20724 0]		20852 6 (2)	*94 6*	20947 2 (2)
28 9					*28 5*
$3d'\,^4D_1$ = 208464 1			[20824 1]		20918 7 (2)

	$3d'\,^4P_3$ 204136 0	*−113 4*	$3d'\,^4P_2$ 204022 6	*−79 2*	$3d\,^4P_1$ 203943 4
$3p'\,^4S_2$ = 233752 7	29616 8 (3)		*[29730 1]		29809 3 (2)
$3p'\,^4P_3$ = 229159 2	25023 2 (2)	*−113 7*	25136 9 (1)		
129 1					
$3p'\,^4P_2$ = 229288 3	[25152 2]		[25265 6]		[25344 8]
94 5					
$3p'\,^4P_1$ = 229382 8			25359 8 (0)		[25439 4]
$3p'\,^4D_4$ = 239471 1	35335 2 (2)				
209 7	*209 5*				
$3p'\,^4D_3$ = 239680 8	35544 7 (0)	*−113 3*	35658 0 (1)		
135 5					
$3p'\,^4D_2$ = 239816 3	[35680 3]		[35793 7]		[35872 9]
78 8					
$3p'\,^4D_1$ = 239895 1			[35872 5]		[35951 7]

* Masked by O III line at 29732 17

Table IV —Quartet Terms of O IV

$3s'\,^4P_1$	269382 0		$3d'\,^4F_2$	213063 0	
		135 1			*78 8*
P_2	269246 9		F_3	212984 2	
		246 9			*112 4*
P_3	269000 0		F_4	212871 8	
					154 1
			F_5	212717 7	
$3p'\,^4D_1$	239895 1				
		78 8			
D_2	239816 3		$3d'\,^4D_1$	208464 1	
		135 5			*28 9*
D_3	239680 8		D_2	208435 2	
		209 7			*46 7*
D_4	239471 1		D_3	208388 5	
					64 6
			D_4	208323 9	
$3p'\,^4S_2$	233752 7				
			$3d'\,^4P_3$	204136 0	
$3p'\,^4P_1$	229382 8				*−113 4*
		94 5	P_2	204022 6	
P_2	229288 3				*− 79 2*
		129 1	P_1	203943 4	
P_3	229159 2				

Table V Lines of O IV

λ	ν	Classification	
	[20724 0]	$3p'\,^4P_3$ −	$3d'\,^4D_2$
4813 07 (1)	20771 0	P_3	D_3
	[20824 1]	P_2	D_1
4798 25 (5)	20835 1	P_3	D_4
4794 22 (2)	20852 6	P_2	D_2
4783 43 (4)	20899 7	P_2	D_3
4779 09 (2)	20918 7	P_1	D_1
4772 57 (2)	20947 2	P_1	D_2
3995 17 (2)	25023 2	$3p'\,^4P_3$ −	$3d'\,^4P_3$
3977 10 (1)	25136 9	P_3	P_2
	[25152 2]	P_2	P_3
	[25265 6]	P_2	P_2
	[25344 8]	P_2	P
3942 14 (0)	25359 8	P_1	P_2
	[25439 4]	P	P
	[26486 9]	$3p\,^4D_4$ −	$3d'\,^4F_3$
3758 45 (0)	26599 2	D_4	F_4
	[26617 8]	D_3	F_2
3744 73 (0)	26696 6	D_3	F_3
3736 78 (4)	26753 4	$D_{4,\,2}$	$F_{5,\,2}$
3729 03 (3)	26809 0	D_3	F_4
3725 81 (2)	26832 2	$D_{2,\,1}$	$F_{3,\,2}$
3425 57 (0)	29183 9	$3s\,^4P_3 - 3p\,^4D_2$	
3413 68 (1)	29285 5	$3p\,^2P_2$ −	$3d\,^2D_2$
*3411 76 (4)	29302 0	$^2P_2$	$^2D_3$
3409 75 (2)	29319 3	$^4P_3$	$^4D_3$
	[29351 8]	$^4P_2$	$^4D_1$
*3403 58 (3)	29372 4	$^2P_1$	$^2D_2$
3396 83 (2)	29430 8	$^4P_2$	$^4D_2$
	[29486 7]	$^4P_1$	$^4D_1$
*3385 55 (6)	29528 9	$^4P_3$	$^4D_4$
*3381 28 (4)	29566 1	$^4P_2$	$^4D_3$
3375 50 (3)	29616 8	$3p'\,^4S_2$ −	$3d'\,^4P_3$
	[29730 1]	S_2	P_2
3353 70 (2)	29809 3	S_2	P_1
	[31082 6]	$3p'\,^4D_4$ −	$3d'\,^4D_3$
3209 64 (3)	31147 2	D_4	D_4
3199 53 (1)	31245 6	D_3	D_2
3194 75 (1)	31292 3	D_3	D_3
	[31352 2]	D_2	D_1
	[31356 9]	D_3	D_4
3185 72 (0)	31381 0	D_2	D_2
	[31427 8]	D_2	D_3
3180 72 (0)	31430 4	D_1	D_1
3177 80 (0)	31459 3	D_1	D_2
3071 66 (4)	32546 3	$3s\,^2S_1$ −	$3p\,^2P_1$
*3063 46 (6)	32633 4	S_1	P_2
2921 40 (3)	34219 0	$4p\,^2P_2$ −	$5s\,^2S_1$?
2016 25 (2)	34280 6	P_1	S_1 ?

* λ by Bowen

Table V—(continued)

λ	ν	Classification	λ	ν	Classification
2836 25 (6)	35247 5	$3s'\,{}^4P_3 - 3p'\,{}^4S_2$	λvac		
2829 18 (2)	35335 6	$3p\,{}^4D_4 - 3d'\,{}^4P_3$	1343 55 (7)	74429 7	$2p'\,{}^2P_2 - 2p^3\,{}^2D_3$
2816 53 (4)	35494 2	P_2 S_2	1343 06 (4)	74456 9	P_2 D_2
	[35544 8]	D_3 P_3	1338 66 (6)	74701 2	P_1 D_2
2805 85 (3)	35829 3	P_1 S_2	†923 31 (3)	108306	$2p\,{}^2P_2$ $2p^3\,{}^2P_{1,2}$
2803 60 (2)	35657 9	D_2 P_2	†921 27 (2)	108546	P_1 $P_{1,2}$
	[35793 7]	D_3 P_2	†802 21 (1)	124656	$2p\,{}^2S_1 - 2p^3\,{}^2P_{1,2}$
	[35872 5]	D_1 P_2	†790 205 (6)	126549 4	$2p\,{}^2P_2 - 2p'\,{}^2D_{2,3}$
	[35872 9]	D_2 P_1	†787 716 (6)	126949 3	P_1 D_2
	[35951 7]	D_1 P_1	*779 82 (1)	128234	$2p\,{}^2D - 2p^3\,{}^2D$
			†625 848 (4)	159783	$2p'\,{}^4P_3 - 2p^3\,{}^4S_2$
2517 40 (7)	39711 6	$3s'\,{}^4P_3 - 3p'\,{}^4P_3$	†625 126 (4)	159968	P_2 S_2
2509 23 (8)	39840 8	P_3 P_2	†624 609 (3)	160100	P_1 S_2
2507 77 (7)	39864 1	P_2 P_1	†616 93 (1)	162093	$2p\,{}^2D - 2p^3\,{}^2P$
2501 84 (4)	39958 6	P_2 P_2	†609 828 (4)	163981	$2p\,{}^2P_2 - 2p'\,{}^2S_1$
2499 30 (3)	39999 2	P_1 P_1	†608 390 (4)	164368	P_1 S_1
2493 78 (7)	40087 7	P_2 P_3	†555 270 (4)	180093	$2p\,P - 2p'\,{}^2P_1$
2493 40 (7)	40093 7	P_1 P_2	†554 507 (5)	180340	P_2 P_2
			†554 066 (5)	180484	P_1 P_1
*2450 06 (10)	40802 9	$4f\,{}^2F_4 - 5g\,{}^2G_4$	†553 318 (4)	180728	P_1 P_2
*2449 36 (8)	40814 6	F_3 G_4	*379 6 (0)	263436	$3p\,P - 2p'\,{}^2D$
			†279 7 (1)	357513	$2p\,P - 3s\,{}^2S$
			†238 6 (1)	419041	$2p\,P - 3d\,{}^2D$

* λ by Bowen
† λ and classification by Bowen

(2) THE SPECTRUM OF TREBLY-IONISED NITROGEN (N IV)

Nothing has previously been published on the spectrum of N IV except an identification of a PP′ group by Millikan and Bowen * The predicted terms shown in the table are similar to those of the arc spectra of the alkaline earths - mostly simple singlet and triplet terms The extrapolated values given have been derived by application of the irregular doublet law to the terms of Be I, B II, and C III.

In order to distinguish N IV lines from those of N III, spectra have been photographed with various intensities of discharge, the lines ascribed to N IV being those which were found to require a stronger discharge for their development than neighbouring N III lines

Only the $3s\,{}^3S$, $3p\,{}^3P$, $3d\,{}^3D$ terms have been identified with certainty, the S and P terms combining to give a triplet at λ 3484, and the P and D terms giving a group at λ 7123 A very strong, easily excited line at λ 1718 may be the resonance line $2s\,{}^1S_0 - 2p\,{}^3P_1$ As has been pointed out before,† its position accords well with the result obtained by extrapolation from the resonance lines of B II and C III The only other prominent lines of N IV in the region investigated (λ 900–λ 7600) form a triplet at λ 2646 which is almost certainly the combination $4f\,^3F - 5g\,^3G$, expected to occur approximately at $16N/4^2 - 16/N5^2 = 39500$ (λ 2530)

---

* 'Phys Rev,' vol. 26, p 154 (1925)

† 'Roy Soc Proc,' A, vol. 121, p. 339 (1928)

It is of interest to note that the SP triplet at λ 3478 occurs very strongly in the spectra of some high-excitation Wolf-Rayet stars * notably B D 35° 4001 37° 3821 and 36° 3987 It is probable therefore that the spectra of these stars would also show the PD group at λ 7123, but no observations appear to have been made in this region

Predicted Terms of N IV

1_1	2_1	2_2	3_1	3_2	3_3	Prefix	Terms and extrapolated values	
2	2					$2s$	$\underline{^1S\ (606000)}$	
2	1	1				$2p$	^1P (478000)	$\underline{^3P\ (545000)}$
2	1		1			$3s$	^1S (226000)	$\underline{^3S\ (239000)}$
2	1			1		$3p$	^1P (202000)	$\underline{^3P\ (211000)}$
2	1				1	$3d$	^1D (189000)	^3D (198000)
						$4f$	^1F ( )	$\underline{^3F\ (111000)}$
						$5g$	^1G ( )	$\underline{^3G\ (71000)}$
2		2				$2p$	^1S ( ) ^1D ( )	$\underline{^3P\ (131000)}$

Terms involved in observed combinations are underlined

	$3p\,^3P_2$ 210261 7	*35 4*	$3p\,^3P_1$ 210297 1	*15 8*	$3p\,^3P_0$ 210212 9
$3s\,^3S_1$ = 239000 0	28738 3 (7)	*35 4*	28702 9 (5)	*15 8*	28687 1 (3)
$3d\,^3D_3$ = 196226 7	14035 0 (5)				
8 6	*8 1*				
$3d\,^3D_2$ = 196235 3	14026 9 (1)	*34 9*	14061 8 (3)		
3 5			*3 5*		
$3d\,^3D_1$ = 196238 8	(14022 9)		14058 3 (1)	*15 8*	14074 1 (1)

---

* 'Pub Dom Ast Obs, vol 2 No 16 "The O type Stars" by J S Plaskett

Lines of N IV

λ	ν	Classification.
7127 21 (1)	14026 9	$3p\,^3P_2 - 3d\,^3D_3$
7123 10 (5)	14035 0	$P_2 - D_2$
7111 28 (1)	14058 3	$P_1 - D_1$
7109 48 (3)	14061 8	$P_1 - D_2$
7103 28 (1)	14074 1	$P_0 - D_1$
*3484 90 (3)	28687 1	$3s\,^3S_1 - 3p\,^3P_0$
*3482 98 (5)	28702 9	$S_1 - P_1$
*3478 69 (7)	28738 3	$S_1 - P_2$
2646 89 (8)	37768 9	$4f\,^3F_4 - 5g\,^3G_5$
2646 10 (7)	37780 1	$F_3 - G_4$
2645 57 (7)	37787 7	$F_2 - G_3$
λ_{vac}		
1718 60 (10)	58186 9	$2s\,^1S_0 - 2p\,^3P_1$?
†924 31	108188 8	$2p\,^3P_2 - 2p'\,^3P_1$
†923 68	108262 6	$P_1 - P_0$
†923 18	108321 2	$P_2 - P_2$
†922 57	108392 9	$P_0 - P_1$
†922 02	108457 5	$P_1 \quad P_2$

* λ by Fowler, 'M N R A S ' vol 81, p 189 (1921)

† λ and classification by Millikan and Bowen

Summary

About 50 lines in the spectrum of trebly-ionised oxygen (O IV) have been newly classified All the doublet and quartet terms of principal quantum number 3 have been identified

In the spectrum of trebly-ionised nitrogen (N IV), combinations of the $3p\,^3P$ term with $3s\,^3S$ and $3d\,^3D$ have been observed Provisional classifications have been given for four other lines

The author wishes to express his thanks to Prof Fowler for his helpful criticism and advice, and to Mr W E Pretty for access to his oxygen plates.

The Group Properties of Dirac's Operators

By G TEMPLE, Ph D, 1851 Exhibition Research Student Trinity College, Cambridge.

(Communicated by A S Eddington F R S—Received March 1, 1930)

§ 1 *Introduction*

The wave equation for the spinning electron devised by Dirac[*] has the form

$$\{\alpha\partial/\partial x + \beta\partial/\partial y + \gamma\partial/\partial z + \delta\partial/\partial(ict) + 2\pi imc/h\}\,\psi = 0$$

in free space, the symbol ψ standing for an ordered set of four wave functions $(\psi_1, \psi_2, \psi_3, \psi_4)$, operated on by the matrices α, β, γ, δ These matrices satisfy the equations

$$\alpha^2 = 1, \quad \beta^2 = 1 \qquad\qquad \alpha\beta + \beta\alpha = 0$$

which will be referred to as "Dirac's equations"

A particular set of matrices satisfying these conditions was constructed by Dirac and some of their properties were developed by him Eddington,[†] however, has obtained all such sets of four-point matrices and has investigated their properties by a symmetrical method An obvious generalisation of these researches is to remove the restriction that the matrices should be four-point matrices, and to study the properties common to all sets of matrices satisfying Dirac's equations A further extension of this work is indicated by Eddington's observation that most of these properties still persist when α, β, γ and δ are taken to be any set of operators satisfying Dirac's equations, and ψ is a corresponding operand This interpretation seems to mark the limit to which the above process of generalisation can be extended

The object of this paper is to develop the fundamental properties of such sets of operators We consider first their "internal properties" It is shown that they generate groups of order 32, all of which are equivalent to one another, and from which sets of 16 linearly independent operators may be chosen (the other 16 operators differing from the first 16 only in sign) The law of transformation of the operand ψ is then deduced from the invariance of the wave-equation This leads to the determination of the "external properties" of the operators, *i e*, the determination of all invariants, 4-vectors and 6-vectors which are quadratic in ψ

---

[*] 'Roy Soc Proc,' A, vol 117, p 614 (1928)

[†] *Ibid*, A, vol 121, p 524 (1928)

§ 2 *Definitions, Axioms and Fundamental Theorems*

In the place of the ordered set of four wave-functions used by Dirac and the set of matrices operating upon them, we introduce two fundamental types of entities—wave-numbers and wave-operators—whose natures are only restricted by the following axioms

Wave-numbers, denoted by small Greek letters, ψ, ϕ, , can be combined in pairs to form " products " (ψ, ϕ) and (ϕ, ψ), which are ordinary complex numbers and functions of x, y, z, t In this paper no relation is assumed between the products (ψ, ϕ) and (ϕ, ψ), although further researches may be facilitated by the assumption that they are conjugate complex numbers

Wave-operators, denoted by capitals, A, B, , can be combined with one another or with wave-numbers The product of the wave-operator A and the wave-number ψ is written $A\psi$ and is another wave-number The sum or product of two wave-operators is another wave operator, and the ordinary axioms of algebra apply except the commutative law of multiplication

To any wave-operator A there corresponds an adjoint operator A†, with the property that

$$(A\psi, \phi) = (\psi, A^\dagger\phi)$$

for all pairs of wave numbers ψ and ϕ Since

$$(AB\psi, \phi) = (B\psi, A^\dagger\phi) = (\psi, B^\dagger A^\dagger\phi)$$

it is clear that

$$(AB)^\dagger = B^\dagger A^\dagger$$

Two types of operators are of especial importance- Hermitian operators for which $A^\dagger = A$, and alternating or skew operators for which, $A^\dagger = - A$ The product of two Hermitian operators is Hermitian or skew accordingly as they commute or anti-commute The last axiom required is that if A is any operator and

$$(A\psi, \psi) \equiv (\psi, A\psi) = 0,$$

for all wave-numbers ψ, then $A = 0$

The preceding axioms are proved to be consistent by the fact that they are true when the following interpretations are adopted —A wave-number ψ is an ordered set of n numbers $(\psi_1, \psi_2, \quad \psi_n)$, A wave operator is a matrix with n rows and columns , the products (ψ, ϕ), $\chi = A\psi$ and AB are respectively given by

$$(\psi, \phi) = \Sigma\, \psi_n\phi_n^*, \quad \chi_m = \sum_n A_{mn}\psi_n, \quad (AB)_{mn} = \sum_k A_{mk}B_{kn} ,$$

the adjoint of a matrix has its usual meaning,

$$A_{mn}\dagger = A_{nm}^{*},$$

using asterisks to denote the conjugate complex number

No particular interpretation of wave-numbers and wave-operators is used in the following sections of this paper The axioms given above are made the sole basis of the analysis

§ 3 *Perpendicular Sets of Operators and the Groups they generate*

Any ordered set of four Hermitian wave-operators, A_1, A_2, A_3, A_4, will be called a "perpendicular set" if every pair of operators satisfies Dirac's equations,

$$\begin{aligned} \tfrac{1}{2}(A_m A_n + A_n A_m) &= 1 \text{ if } m = n, \\ &= 0 \text{ if } m \neq n \end{aligned}$$

By multiplying together any number of wave-operators from a perpendicular set and arranging the factors of the product in any order, there is obtained another wave-operator The number of distinct operators which can be formed in this way is 32 (including the operators $+1$ and -1) These 32 operators form a group which will be called the group (A) generated by the perpendicular set (A_1, A_2, A_3, A_4) The other 28 operators not included in the perpendicular set will be denoted by $(A_5, A_6, \quad A_{32})$

An Hermitian invariant of the group (A) will have the form $(S\psi, \psi)$ (where S is an Hermitian operator), and will satisfy the equations

$$(S\psi, \psi) = (SA_n\psi, A_n\psi) = (A_n\dagger SA_n\psi, \psi),$$

for all values of n Now, it is clear that $A_n\dagger A_n = 1$, for all values of n, since $A_n\dagger$ is obtained from A_n by reversing the order of its factors derived from the original perpendicular set Hence

$$S = A_n\dagger SA_n,$$

and

$$A_n S = SA_n,$$

or S commutes with all the operators of the group (A), and must therefore be $+1$ or -1 Hence the only Hermitian invariant of (A) is (ψ, ψ) and the group (A) is therefore transitive

Let (B_1, B_2, B_3, B_4) form another perpendicular set generating a group (B) Let the other operators of (B), $(B_5, B_6 \quad B_{32})$ be numbered in such a way that B_n, $(n > 4)$, is formed from the set $(B_1, \quad B_4)$ in the same way that A_n, $(n > 4)$, was formed from the set $(A_1, \quad A_4)$ Then, it is obvious that if the product $A_r A_s = A_t$ then the product $B_r B_s = B_t$. Hence the groups (A) and (B) are isomorphic

Now, let

$$P = \sum_{(r)} B_r{\dagger} A_r, \qquad (r = 1, 2, \ldots 32)$$

Then

$$B_s{\dagger} P A_s = \sum_{(r)} (B_s{\dagger} B_r{\dagger})(A_r A_s)$$

$$= \sum_{t} B_t{\dagger} A_t = P,$$

Hence

$$B_s P = P A_s$$

and

$$B_s = P A_s P^{-1}$$

This equation shows that any perpendicular set (together with the operators of the group it generates) may be obtained from any other perpendicular set (and the operators of the associated group) by a canonical transformation, *i e*, any two groups, such as (A) and (B) are equivalent

§ 4 *A Classification of the Operators of a Group generated by a Perpendicular Set*

It is easily verified that, apart from the unit operators ± 1, each of the operators of a group generated by a perpendicular set commutes with 16 operators and anti-commutes with the other 16 It may also be shown that if R and S are two commuting operators of the group, distinct from one another and from ± 1, then the only operators which commute with both R and S are the eight following ± (1, R, S, RS)

For, if T is any other operator which commutes with both R and S, the 16 operators

$$\pm (1, R, S, RS, T, RT, ST, RST)$$

all commute with one another If X is any other operator of the group, the other 16 operators are

$$\pm (X, RX, SX, RSX, TX, RTX, STX, RSTX)$$

It is clear that X must anti-commute with R, S, and T, otherwise, these operators would commute with every operator of the group It may now be verified that it is impossible to select from the above operators four operators which anti-commute with one another Hence such an operator as T does not exist

Now suppose that R and S both anti-commute with Z and Y Then R, S must both commute with XY Hence

$$XY = \pm (1 \text{ or } R \text{ or } S \text{ or } RS),$$

and

$$Y = \pm (X \text{ or } RX \text{ or } SX \text{ or } RSX)$$

Hence there are only eight operators which anti commute with both R and S

To classify the operators, let c (R) denote those commuting with R and let a (R) denote those anti-commuting with R, while c (R S), a (R, S) denote those commuting, or anti-commuting with both R and S Then the scheme of classification may be represented diagrammatically as

c (R)		a (R)	
c (R, S)	b	a (R S)	d

c (S)		a (S)	
c (R, S)	d	a (R S)	b

b and d denote the sets of operators (of eight members each) common to c (R) and a (S), a (R) and c (S) respectively

§ 5 *The Linear Independence of the Operators generated by a Perpendicular Set*

The operators of a group generated by a perpendicular set evidently form 16 pairs the members of which differ only in sign By selecting one operator from each pair we obtain a set of 16 operators which may be called a ' fundamental set " It will now be proved that the operators of a fundamental set are all linearly independent

If possible, let there be an effective linear relation, $H_1 = 0$, connecting some or all, of the 16 operators in question H_1 must contain at least one operator say R, distinct from the unit operators ± 1 Hence we may deduce a further effective linear relation,

$$H_2 = RH_1 + H_1R,$$

which can involve only those operators which commute with R H_2 must involve the unit operator and at least one other operator distinct from R, say S Hence we may deduce a third effective linear relation,

$$H_3 = SH_2 + H_2S,$$

which can involve only those operators which commute with both R and S H_3 must contain S Hence by the theorem of § 4,

$$H_3 = l + mR + nS + pRS,$$

where l, m, n, and p are ordinary numbers and $n \neq 0$

Let X be any operator which anti-commutes with both R and RS Then

$$0 = H_4 = XH_3 + H_3X = 2lX + 2nXS,$$

whence

$$l = \pm nS, \qquad (X^2 = \pm 1)$$

This is impossible unless $n = 0 = l$, in contradiction with the fact that $n \neq 0$ Hence no effective linear relation can connect the operators of a fundamental set

This result is especially important when the wave operators are interpreted, in the usual manner, as matrices of four rows and four columns In this particular case it follows that *any* matrix of this type can be expressed as a linear function of the 16 matrices of a fundamental set

§ 6 *Complete Perpendicular Sets*

We have already defined, in § 3, the group (A) generated by the perpendicular set of operators (A_1, A_2, A_3, A_4) It is clear that all the operators which are linear functions of the operators of the group (A) also form a group (of infinite order) which will be called the extended group of (A) or (A′)

Eddington's "coupling theorem" now presents itself as a corollary to the solution of the following problem —What operators of the extended group (A′) anti-commute with (A_1, A_2, A_3, A_4)? It is found that the only such operators are numerical multiples of the operator

$$E = A_1A_2A_3A_4$$

Since

$$E\dagger = A_4A_3A_2A_1 = A_1A_2A_3A_4 = E,$$

and

$$E^2 = E\dagger E = 1,$$

this operator is Hermitian and unitary The five operators (A_1, A_2, A_3, A_4, E) may be called a "complete perpendicular set"

It is an obvious corollary that the operators (A_1E, A_2E, A_3E, A_4E) all anti-commute with one another But since

$$(A_1E)\dagger = E\dagger A_1\dagger = EA_1 = -A_1E,$$

these operators are not Hermitian but alternating Hence they do not, strictly speaking, form a perpendicular set, with the definition of § 3

§ 7 *The Invariance of the Wave Equation*

The wave-equation may be written as

$$W\psi \equiv \sum_n p_n A_n \psi + (2\pi i mc/h)\psi = 0,$$

where (A_1, A_2, A_3, A_4) are a perpendicular set of operators and $p_n = \partial/\partial x_n$, (x_1, x_2, x_3, x_4) being written for (x, y, z, ict) Any two sets of quantum operators $(p_1, \quad p_4)$ and $(p_1', \quad p_4')$, which may be used in this wave equation, are connected by a relation of the form

$$p_m' = \sum_n \Lambda_{mn} p_n,$$

which is equivalent to a Lorentz transformation connecting the variables (x, y, z, t) and (x', y', z', t') Any two wave numbers ψ and ψ' are connected by a relation of the form

$$\psi' = L\psi,$$

L being a wave-operator The coefficients Λ_{mn} constitute a matrix Λ which must satisfy the condition

$$\Lambda^\dagger \Lambda = 1$$

The wave equation in the accented variables and wave-number is

$$W'\psi' \equiv \sum_n p_n' A_n \psi' + (2\pi i mc/h)\psi' = 0$$

In general, this equation will be inconsistent with the original equation $W\psi = 0$ But we shall show that to any matrix Λ, there corresponds as wave-operator L, such that each of the wave-equations implies the other, *i e* , the wave-equation is invariant under the transformations specified by Λ and L

Now

$$W'\psi' = \sum_n p_n B_n L\psi + (2\pi i mc/h) L\psi,$$

where

$$B_n = \sum_m A_m \Lambda_{mn}$$

Hence the wave-operator L must be chosen so that

$$W' = LW,$$

i e ,

$$B_n L = LA_n$$

It may be shown, as in Dirac's paper (*loc cit*), that the four operators (B_1, B_2, B_3, B_4) form a perpendicular set Hence we may conclude at once, using the theorem and notation of § 3, that

$$L = l \sum_r B_r^\dagger A_r, \qquad (r = 1, 2, \quad 32)$$

l being an ordinary number

It is possible to choose l so that the operator L is unitary, *i e* , so that $L^\dagger L = 1$ For, since

$$B_n L = LA_n \qquad (n = 1, 2, 3, 4)$$

it follows that

$$L^{\dagger}B_n = A_n L^{\dagger} \quad \text{(the operators } A_n \text{ and } B_n \text{ being Hermitian)},$$

whence

$$L^{\dagger}L = L^{\dagger}B_n\, B_n L = A_n\, L^{\dagger}LA_n$$

Since $L^{\dagger}L$ commutes with (A_1, A_2, A_3, A_4) it must be an ordinary number Hence l may be chosen to make this number unity This is supposed to be done throughout the remainder of this section

Since

$$(L\psi, L\psi) = (L^{\dagger}L\psi, \psi) = (\psi, \psi),$$

it follows that (ψ, ψ) is an invariant under the transformation $\psi' = L\psi$, and that $L^{\dagger}L = 1$ is the necessary condition for this invariance It has now been shown that to any transformation matrix Λ there corresponds one and only one operator L which leaves invariant the equation $W\psi = 0$ and the quantity (ψ, ψ) Hence if L corresponds to Λ and P to Π, PL must correspond to $\Pi\Lambda$ But the transformations Λ, Π, form a group (Γ) Hence the transformation L, P, must also form a group (G), and this group must be isomorphic with the group (Γ)

The infinitesimal transformations of the group (G) are easily found directly or deduced from the finite transformations found above A typical infinitesimal transformation of the group (Γ) is

$$(\Gamma_{mn}) \qquad \begin{aligned} x_m' &= x_m + ex_n, \\ x_n' &= x_n - ex_m \end{aligned} \qquad x_p' = x_p, \quad \text{if } p \neq m \text{ or } n$$

The corresponding infinitesimal transformation of the group (G) is

$$(G_{mn}) \qquad \psi' = \psi + \tfrac{1}{2}eA_mA_n\psi$$

§ 8 *Quadratic Invariants*

The results of the preceding sections will now be applied to determine all the invariants, 4-vectors and 6-vectors of the group (Γ) with components of the form $(T\psi, \psi)$, T being an operator of the extended group (A′) defined in § 6 It is, of course, sufficient to consider the infinitesimal transformations of the groups (Γ) and (G) noted at the end of the last section

On applying these transformations to $(T\psi, \psi)$ we find that

$$\begin{aligned} (T\psi', \psi') &= (T\psi + \tfrac{1}{2}eTA_mA_n\psi,\ \psi + \tfrac{1}{2}eA_mA_n\psi) \\ &= (T\psi, \psi) + \tfrac{1}{2}e\,(TA_m^{\dagger}A_n\psi, \psi) + \tfrac{1}{2}e\,(T\psi, A_mA_n\psi) + \\ &= (T\psi, \psi) + \tfrac{1}{2}e\,([TA_mA_n + A_nA_mT]\,\psi, \psi) + \dots \end{aligned}$$

Now, if $(T\psi, \psi)$ is invariant, the term in e must vanish, *i e*,

$$TA_mA_n + A_nA_mT = 0$$

Hence T commutes with the six operators of the form A_mA_n $(m \neq n)$, and must therefore have the form

$$T = a + bE, \qquad (E = A_1A_2A_3A_4),$$

where a, b are ordinary numbers Hence the number of linearly independent invariants is two and they may be taken to be

$$(\psi, \psi) \quad \text{and} \quad (E\psi, \psi)$$

§ 9 4-*Vectors*

Let the components of a 4-vector be $(\xi_1, \xi_2, \xi_3, \xi_4)$, where

$$\xi_n = (T_n\psi, \psi)$$

T_n being an operator of the group (A′) The ξ's transform according to the same law as the x's, and the application of the infinitesimal transformations (Γ_{mn}) and (G_{mn}) leads to the equations,

$$T_mA_mA_n + A_nA_mT_m = 2T_n, \qquad (m \neq n)$$
$$T_pA_mA_n + A_nA_mT_p = 0, \qquad \text{if } p \neq m \text{ or } n$$

These equations have the general solution

$$T_n = aA_n + bA_nE$$

Hence there are only two linearly independent 4 vectors, which may be taken to have the components

$$(A_n\psi, \psi) \quad \text{and} \quad (A_n\psi, E\psi), \qquad (n = 1, 2, 3, 4)$$

§ 10 6-*Vectors*

Let the components of a 6-vector be $(\eta_{23}, \eta_{31}, \eta_{12}, \eta_{14}, \eta_{24}, \eta_{34})$ where

$$\eta_{mn} = (T_{mn}\psi, \psi),$$

T_n being an operator of the group (A′) The transformation of the 6-vector, corresponding to the infinitesimal transformation (Γ_{mn}), is expressed by the equations

$$\eta'_{mn} = \eta_{mn},$$
$$\eta'_{pq} = \eta_{pq}, \qquad \text{if neither } p \text{ nor } q \text{ equals } m \text{ or } n,$$
$$\left.\begin{aligned}\eta'_{mp} &= \eta_{mp} + e\eta_{np},\\ \eta'_{np} &= \eta_{np} - e\eta_{mp},\end{aligned}\right\} \text{if } p \neq m \text{ or } n$$

These relations lead to the following equations for the operators T_{mn}, viz —

$$T_{mn}A_mA_n + A_nA_mT_{mn} = 0,$$
$$T_{pq}A_mA_n + A_nA_mT_{pq} = 0,$$

and

$$T_{mp}A_mA_n + A_nA_mT_{mp} = 2T_{np}$$

These equations have the general solution

$$T_{mn} = aA_mA_n + bA_mA_nE$$

Hence there are only two linearly independent 6-vectors which may be taken to have the components

$$(A_nA_m\psi,\ \psi) = (A_m\psi,\ A_n^{\dagger}\psi)$$
$$(EA_mA_n^{\dagger}\psi,\ \psi) = (A_p\psi,\ A_q^{\dagger}\psi),$$

corresponding to $(x_m,\ \iota_n)$

§ 11 *Conclusion*

In conclusion, I must express my gratitude to Prof Eddington for the encouragement and advice which he has given me in the course of this investigation

The Operational Wave Equation and the Energy Levels of the Hydrogen Atom

By G. Temple, Ph.D., 1851 Exhibition Research Student, Trinity College, Cambridge

(Communicated by A. S. Eddington, F.R.S.—Received March 19, 1930.)

§ 1. *Introduction*

The operational wave equation used in this paper is a generalisation of the linear wave equation introduced by Dirac. The generalisation consists in replacing Dirac's matrices by any four linear operators (A_1, A_2, A_3, A_4), which satisfy Dirac's conditions,

$$\tfrac{1}{2}(A_m A_n + A_n A_m) \;=\; \begin{array}{l} 0 \text{ if } m \neq n \\ 1 \text{ if } m = n \end{array} \qquad (1.1)$$

The operational wave equation for free space is therefore

$$W\psi \equiv \sum_{n=1}^{4} p_n A_n \psi + \iota m_0 c \psi = 0, \qquad (1.2)$$

p_n being the quantum operator $-\iota\hbar\,\partial/\partial x_n$.*

The fundamental properties of a set of wave operators (A_n), satisfying the conditions of perpendicularity and normality (1.1), have been discussed in a previous paper† by the author. The object of this paper is to obtain the energy-levels of hydrogen-like atoms by the use of the operational wave equation for a purely electrostatic field, the four wave operators being restricted only by the conditions (1.1).

Using real co-ordinates x_1, x_2, x_3, $t = -\iota x_4/c$, the wave equation for a field of potential V may be written as

$$W\psi \equiv \{p_1 A_1 + p_2 A_2 + p_3 A_3 + c^{-1}(p_0 + eV)\,\iota A_4 + \iota m_0 c\}\,\psi = 0,$$

p_1, p_2, p_3 being the momentum operators and p_0 the energy operator. In manipulating this equation it is convenient to treat A_1, A_2, A_3 as the Cartesian components of a vector **A**, and to divide the operator W into two parts,

$$W = W_s + W_t,$$

where

$$W_s = \mathbf{p} \cdot \mathbf{A}, \qquad (1.3)$$

and

$$W_t = c^{-1}(p_0 + eV)\,\iota A_4 + \iota m_0 c \qquad (1.4)$$

---

* $\hbar = h/(2\pi)$, where h is Planck's constant.

† 'Roy. Soc. Proc.,' A, vol. 127, p. 339 (1930).

§ 2 *General Principles*

The possibility of obtaining a "solution" of the operational wave equation depends upon the existence of operators X such that $X\psi = a\psi$ for any ψ satisfying the wave equation a being a numerical constant characterising ψ Operators such as X may be said to be "reducible" for ψ to the eigen value a A set of operators which are all reducible for ψ must evidently be commutable The eigen values of ψ for such a set of operators provide a numerical representation of ψ and the primary question is to examine how far ψ is determined by these eigen values

From this point of view the wave equation $W\psi = 0$ signifies that W is reducible, and has eigen value 0, and all other reducible operators for ψ must commute with W

Since the wave equation is linear in the p's we are primarily interested in reducible operators which also have this property For a free electron the p's themselves (being commutable with W and with each other) form a set of reducible operators which are restricted only by the equation

$$\mathbf{p}^2 - c^{-2}\mathbf{p}_0^2 + m_0^2 c^2 = 0 \tag{2 1}$$

The eigen values of the p's are limited only by a similar relation, and the complete solution of the problem is contained in the statements

The presence of an electromagnetic potential in W which does not commute with the p's renders the discovery of a set of reducible operators more difficult. It is clear that there cannot be more than four independent reducible operators (C_1 C_2, C_3, C_4) linear in the p's Any other operator R, linear in the p's, will be a linear function of the C's, say

$$R = R_0 + \sum_{n=1}^{4} R_n C_n, \quad = \sum_{n=0}^{4} R_n C_n, \tag{2 2}$$

if $C_0 = 1$, the coefficients (R_0 R_4) being functions of the variables x and the operators A, and, if R is reducible, these coefficients will be constants

To prove this, we note that R must commute with the operator W of the wave equation Now

$$W = \sum_{k=1}^{4} A_k (p_k + G_k) + \iota m_0 c,$$

G_k being proportional to the 4-vector potential of the field Hence

$$WR - RW = \sum_{n=1}^{4} (WR_n - R_n W) C_n,$$

and

$$WR_n - R_n W = \sum^{4} (A_k R_n - R_n A_k)(p_k + G_k) + \sum^{4} A_k (p_k R_n - R_n p_k)$$

The last term is independent of the p's and the first term is a linear function of the C's, unless R_n commutes with A_1, A_2, A_3 and A_4. Hence $WR - RW$ is expressed as a quadratic function of the C's. For the quadratic terms to vanish R_n must depend only on the variables x, and for the linear terms to vanish R_n must reduce to a constant, r_n, say,

Hence

$$R\psi = (r_0 + r_n a_n)\,\psi,$$

where a_1, a_2, a_3, a_4 are the eigen values for the operators C_1, C_2, C_3, C_4. It follows that if two distinct ψ's, say ξ and η, have the same eigen values (a_1, a_2, a_3, a_4) for the operators (C_1, C_2, C_3, C_4), they will have the same eigen value for any other reducible operator R linear in the p's. The same conclusion persists if R is a polynomial in the p's. For, in this case, R will be a polynomial in the C's also, say $R = f(C_1, C_2, C_3, C_4)$, and both ξ and η will still have the same eigen value for R, namely $f(a_1, a_2, a_3, a_4)$. It follows that unless ψ is determined by the reducible operators C_1, C_2, C_3, C_4, no other reducible operator will give any further help in its determination.

The first stage in the solution of the problem of this paper is the discovery of four reducible operators linear in the p's (§ 3). This virtually solves the problem. Following the methods of Dirac* and Pidduck† we determine the relation connecting these operators by transforming the wave equation to polar co-ordinates (§ 4), and replacing it by a second order equation for an ordinary numerical (*i e*, not operational) function of the variables (§§ 5 and 6). Finally, we identify the inner quantum numbers (§ 7).

§ 3 *The Reducible Operators*

In constructing a set of reducible operators we are guided by the results of earlier quantum theories in which such a set was provided by the x_3-component of the angular momentum operator, the square of the total angular momentum operator, the total energy operator and the Hamiltonian operator.

We introduce the spin operators,

$$S_1 = -\iota A_2 A_3, \qquad S_2 = -\iota A_3 A_1, \qquad S_3 = -\iota A_1 A_2, \tag{3 1}$$

with the properties

$$S_1^2 = S_2^2 = S_3^2 = 1, \tag{3 2}$$

$$S_2 S_3 = A_2 A_3 = \iota S_1 = -S_3 S_2, \text{ etc}, \tag{3 3}$$

and

$$S_n = S_n\dagger, \qquad (n = 1, 2, 3)$$

---

* 'Roy Soc Proc,' A, vol 117, p 610

† 'J Lond Math Soc,' vol 4, p 163 (1929)

These spin operators may be treated as the Cartesian components of a spin-vector **S**.

Although neither the spin momentum operator, $\frac{1}{2}\mathfrak{h}\mathbf{S}$, nor the orbital momentum operator, $\mathbf{m} = \mathbf{x}_\wedge \mathbf{p}$, commutes with W, the total momentum operator, $\mathbf{M} = \mathbf{m} + \frac{1}{2}\mathfrak{h}\mathbf{S}$, has the required property. Since

$$\mathbf{M}_\wedge \mathbf{M} = \iota\mathfrak{h}\mathbf{M}, \tag{3·4}$$

the components of **M** do not commute with one another, but they all commute with

$$\mathrm{L} = \mathbf{M} \cdot \mathbf{M} = \mathrm{M}_1^2 + \mathrm{M}_2^2 + \mathrm{M}_3^2, \tag{3·5}$$

and this operator commutes with W. Hence M_3, L and W form a commuting set of operators, M_3 and W being linear functions of (p_1, p_2, p_3), and L being quadratic. A distinctive feature of the linear wave equation is the existence of a further operator which commutes with M_3 and W, and, like them, is a *linear* function of (p_1, p_2, p_3).

To obtain this operator we expand L in terms of **m**.

Since

$$\mathrm{L} = m^2 + \mathfrak{h}\, \mathbf{m} \cdot \mathbf{S} + \tfrac{3}{4}\mathfrak{h}^2,$$

and

$$(\mathbf{m} \cdot \mathbf{S})^2 = m^2 - \mathfrak{h}\, \mathbf{m} \cdot \mathbf{S}, \quad \text{(from equations (3·2) and (3·3))},$$

it follows that

$$\mathrm{L} + \tfrac{1}{4}h^2 = \{(\mathbf{m} \cdot \mathbf{S}) + \mathfrak{h}\}^2.$$

We write $\mathrm{N} = \mathbf{m} \cdot \mathbf{S}$ for brevity.

The operator $(\mathrm{N} + \mathfrak{h})$ commutes with W_i and anti-commutes with W_4. Hence the operator $\mathrm{A}_4(\mathrm{N} + \mathfrak{h})$ commutes with W. It also commutes with the components of **M**, and satisfies the equation

$$\{\mathrm{A}_4(\mathrm{N} + \mathfrak{h})\}^2 = \mathrm{L} + \tfrac{1}{4}\mathfrak{h}^2 \tag{3·6}$$

It is clear that we may take W to be one of the reducible operators and that a further reducible operator is the energy operator p_0, whose eigen value is the energy, ε, of the system.

Hence we have found a set of four reducible operators, all linear in the p's, namely,

$$\mathrm{M}_3 = m_3 + \tfrac{1}{2}\mathfrak{h}\mathrm{S}_3, \qquad \mathrm{Q} = \mathrm{A}_4\{(\mathbf{m} \cdot \mathbf{S}) + \mathfrak{h}\}, \qquad p_0 \text{ and W}$$

The eigen values of ψ for these operators are taken to be

$$u\mathfrak{h}, \qquad \mu\mathfrak{h}, \qquad \varepsilon \text{ and } 0 \tag{3·7}$$

It is shown in §§ 4 and 5 that these eigen values are connected by the well-known relation (5 9),

$$\frac{\varepsilon}{\varepsilon_0} = \left\{1 + \frac{\alpha^2 Z^2}{[n' + (\mu^2 - \alpha^2 Z^2)^{\frac{1}{2}}]^2}\right\}^{-\frac{1}{2}},$$

where $\varepsilon_0 = m_0 c^2$, n' is an integer or zero and α is the fine structure constant

§ 4 *The Transformation of the Wave Equation to Polar Co-ordinates*

The object of this transformation is to obtain an equation for ψ which shall involve only its derivative with respect to the radial co-ordinate r The transformation consists essentially in replacing the Cartesian components of **A** by its components in spherical polar co-ordinates The wave equation thus obtained, say, $W_r\psi = 0$, is then further simplified by applying a canonical transformation to W_r,

$$\Omega = TW_rT^{-1}, \tag{4 1}$$

and introducing a new wave-function,

$$\phi = T\psi, \tag{4 2}$$

so that

$$\Omega\phi = 0 \tag{4 3}$$

Let R_1, R_2, R_3 be the components of **A** in spherical polar co-ordinates (r, θ, ϕ) If the equations of transformation are

$$R_m = \sum_n \Lambda_{mn} A_n,$$

the coefficients Λ_{mn} must satisfy the conditions that

$$\sum_m \Lambda_{mn}\Lambda_{mp} = \begin{array}{l} 0 \text{ if } n \neq p, \\ 1 \text{ if } n = p \end{array}$$

Hence

$$\tfrac{1}{2}(R_m R_p + R_p R_m) = \begin{array}{l} 0 \text{ if } m \neq p, \\ 1 \text{ if } m = p \end{array}$$

It is clear that

$$R_m A_4 + A_4 R_m = 0, \qquad (m = 1, 2, 3),$$

so that the operators (R_1, R_2, R_3, A_4) form a perpendicular set

In order to replace (A_1, A_2, A_3) by (R_1, R_2, R_3) we note that

$$rR_1 = x_1A_1 + x_2A_2 + x_3A_3$$

Hence, since

$$W_s = \mathbf{p} \quad \mathbf{A}, \qquad (1\ 3),$$

$$rR_1W_s = (\mathbf{x} \quad \mathbf{p}) + i\,(\mathbf{m} \,.\, \mathbf{S})$$

Therefore

$$R_1W_s = -\,i\mathfrak{h}\,\partial/\partial r + ir^{-1}(A_4Q - \mathfrak{h})$$

Hence the wave equation is equivalent to

$$-\iota\mathfrak{h}\left\{\frac{\partial}{\partial r}+\frac{1}{r}\right\}\psi+\frac{\iota}{r}A_4Q\psi+R_1W_\iota\psi=0,$$

or

$$-\iota\mathfrak{h}\left\{\frac{\partial}{\partial r}+\frac{1-\mu A_4}{r}\right\}\psi+R_1W_\iota\psi=0, \qquad (4\ 4)$$

since

$$Q\psi=\mu\mathfrak{h}\psi, \qquad (3\ 7)$$

The wave equation, $W_r\psi=0$, (4 4), may be further simplified by the use of a theorem proved in a previous paper,[*] namely, that since the two sets[†] of operators (R_1, R_2, R_3, A_4) and (E, A_2, A_3, A_4) are each perpendicular, there exists an operator T such that

$$R_1=T^{-1}ET,\quad R_2=T^{-1}A_2T,\quad R_3=T^{-1}A_3T,\quad A_4=T^{-1}A_4T, \qquad (4\ 5)$$

and

$$T\dagger T=1 \qquad (4\ 6)$$

Hence, applying to W this canonical transformation, we have (4 1)

$$\Omega=TW_rT^{-1}=-\iota\mathfrak{h}\left\{\frac{\partial}{\partial r}+\frac{1-\mu A_4}{r}\right\}+\frac{\iota}{c}(\varepsilon+eV)EA_4+\iota m_0cE,$$

so that the simplified wave equation is, (4 3),

$$\Omega\phi\equiv-\iota\mathfrak{h}\left\{\frac{\partial}{\partial r}+\frac{1-\mu A_4}{r}\right\}\phi+\frac{\iota}{c}(\varepsilon+eV)EA_4\phi+\iota m_0cE\phi=0 \qquad (4\ 7)$$

§ 5 *The Formal Solution of the Wave Equation*, $\Omega\phi=0$

Although the wave equation (4 7) involves the wave operators E and A_4, it may still be solved by the usual methods of analysis We rewrite the equation as

$$\left.\begin{aligned}&\partial\phi/\partial r+F\phi+r^{-1}(G+1)\phi=0,\\ &F=-EA_4\varepsilon/\mathfrak{h}c-Em_0c/\mathfrak{h},\\ &G=-\mu A_4-EA_4Ze^2/\mathfrak{h}c,\end{aligned}\right\} \qquad (5\ 1)$$

where … and … since

$$V=Ze^2/r,$$

Z being the effective nuclear number

'Roy Soc Proc,' A, vol. 127, p 339

[†] In the second set of operators E may be replaced by any operator perpendicular to A_2, A_3, A_4, *e.g.*, by A_1 ($E=A_1A_2A_3A_4$)

It is convenient to note here various properties of the operators F and G In the first place, we find that

$$\left.\begin{aligned} &\mathrm{F}^2 = \lambda^2 \quad \text{and} \quad \mathrm{G}^2 = g^2, \\ \text{where} \qquad &\lambda = (\varepsilon_0{}^2 - \varepsilon^2)^{\frac{1}{2}}/\hbar c, \\ \text{and} \qquad &g = (\mu^2 - \alpha^2 \mathrm{Z}^2)^{\frac{1}{2}}, \end{aligned}\right\} \tag{5 2}$$

α being the fine structure constant, $2\pi e^2/hc$ In quantised orbits $\varepsilon < \varepsilon_0$ (the rest energy), and μ^2 is never less than 1 (see § 7) Hence the expressions under the root sign are positive, and we shall agree to take the positive value of the square root

Secondly,

$$\left.\begin{aligned} &\mathrm{FG} + \mathrm{GF} = -2\delta, \\ \text{where} \qquad &\delta = \varepsilon \mathrm{Z}\alpha/\hbar c \end{aligned}\right\} \tag{5 3}$$

Thirdly, it is clear from equation (5 2) that the eigen values of F and G are $\pm\lambda$ and $\pm g$ respectively Also, it follows from equation (5 3) that, if χ is an eigen function of F with eigen value $\pm\lambda$, then $(\mathrm{G} \pm \delta/\lambda)\chi$ is also an eigen function of F with eigen value $\pm\lambda$

Returning to the differential equation (5 1), we first determine the leading term in the asymptotic expansion of ϕ This term is the solution of the equation

$$\partial\phi/\partial r + \mathrm{F}\phi = 0,$$

whence

$$\partial^2\phi/\partial r^2 = \mathrm{F}^2\phi = \lambda^2\phi \quad (\text{from (5 2)})$$

Therefore

$$\phi \sim \phi_0 \exp(\pm\lambda r),$$

ϕ_0 being independent of r Accordingly we take

$$\left.\begin{aligned} &x = 2\lambda r \\ \text{as a new variable, and} \qquad &\xi = \phi \quad \exp \lambda r \end{aligned}\right\} \tag{5 4}$$

as a new function The equation for ξ is

$$\xi' + \tfrac{1}{2}(\lambda^{-1}\mathrm{F} - 1)\xi + x^{-1}(\mathrm{G} + 1) = 0,$$

using accents to denote differentiation with respect to x

We now assume that this equation possesses a formal solution of the type

$$\xi = x^{\rho} \sum_{n=0}^{\infty} \xi_n \, x^n, \tag{5 5}$$

n being an integer or zero, and ξ_n an operator independent of x The indicial equation is

$$(1 + \mathrm{G})\,\xi_0 + \rho\xi_0 = 0,$$

and the recurrence relation is

$$(\mathrm{G} + \rho + n + 2)\,\xi_{n+1} = -\tfrac{1}{2}(\lambda^{-1}\mathrm{F} = 1)\,\xi_n, \quad (n = 0, 1, 2, \quad)$$

Hence $(\rho + 1) = \pm\, g$, and, to obtain a solution which is finite when $x = 0$, we choose the upper sign, i e ,

$$\rho = g - 1 \tag{5.6}$$

The recurrence relation now becomes

$$(\mathrm{G} + g + n + 1)\,\xi_{n+1} = -\tfrac{1}{2}(\lambda^{-1}\mathrm{F} - 1)\xi_n, \quad (n = 0, 1, 2, \quad) \tag{5.7}$$

Now $\phi = \exp(-\tfrac{1}{2}x)\ \xi$, and, anticipating the results of the next section, we may say that the series for ξ must terminate if ϕ is to remain finite as $x \to \infty$ If the last coefficient is ξ_n , it follows that

$$\mathrm{F}\xi_n = \lambda\xi_n$$

But

$$\begin{aligned} -\tfrac{1}{2}(\lambda - {}^{1}\mathrm{F} - 1)\,\xi_{n-1} &= (\mathrm{G} + g + n')\,\xi_n \\ &= (\mathrm{G} + \delta/\lambda)\,\xi_n + (g + n' - \delta/\lambda)\,\xi_n \end{aligned}$$

On multiplying both sides by $(\lambda - {}^{1}\mathrm{F} + 1)$ we find from (5.2) that

$$\delta/\lambda - g = n', \tag{5.8}$$

whence we obtain Sommerfeld's result that

$$\frac{\varepsilon}{\varepsilon_0} = \left\{1 + \frac{\alpha^2 Z^2}{[n' + (\mu^2 - \alpha^2 Z^2)^{\frac{1}{2}}]^2}\right\}^{-\frac{1}{2}} \tag{5.9}$$

§ 6 *Introduction of Laguerre Polynomials*

In this section we shall show that the first order wave equation for the wave function ϕ (5.1) may be replaced by a second order equation for an ordinary function *f*, the wave operators having been eliminated

Since by equation (5.7),

$$(\mathrm{G} + g + n)\,\xi_n = -\tfrac{1}{2}(\lambda^{-1}\mathrm{F} - 1)\,\xi_{n-1}, \quad (n = 1, 2 \quad) \tag{6.1}$$

it follows that

$$(\mathrm{F} + \lambda)(\mathrm{G} + g + n)\,\xi_n = 0,$$

i e $(\mathrm{G} + g + n)\,\xi_n$ is an eigen function of F with eigen value $-\,\lambda$ for all values of $n > 0$ The simplest way of satisfying this condition is to take any eigen function of F with eigen value $-\,\lambda$, say η, and to write

$$(\mathrm{G} + g + n)\,\xi_n = c_n\eta,$$

c_n being an ordinary number

It now follows that

$$(\mathrm{G}-g-n)(\mathrm{G}+g+n)\,\xi_n=c_n(\mathrm{G}-g-n)\,\eta,$$

or

$$(n^2+2ng)\,\xi_n=c_n(g+n-\mathrm{G})\,\eta$$

Hence

$$\xi_n=a_n(g+n-\mathrm{G})\,\eta, \tag{6 2}$$

where a_n is an ordinary number, and

$$\sum_{n=0}^{\infty}\xi_n x^n=(g-\mathrm{G})\,\eta\ \sum_{n=0}^{\infty}a_n x^n+\eta\ \frac{\partial}{\partial x}\sum_{n=0}^{\infty}a_n x^n \tag{6 3}$$

This is the genesis of Pidduck's transformation (*loc cit*) We write

$$f(x)=\sum_{n=0}^{\infty}a_n x^n,$$

and

$$\xi=x^{g-1}f(x)\ \ (g-\mathrm{G})\,\eta+x^g f'(x)\,\eta \tag{6 4}$$

The equation for $f(x)$ is easily found to be

$$\eta x f''+\eta\{(2g+1)-x\}f'+\eta\{\lambda^{-1}\delta-g\}f=0$$

If we write

$$\left.\begin{aligned}q&=2g\\ p&=\lambda^{-1}\delta-g\end{aligned}\right\}, \tag{6 5}$$

and

so that

$$xf''+(q+1-x)\,f'+pf=0, \tag{6 6}$$

it will be recognised that $\phi\ (=\exp(-\frac{1}{2}x)\ \ \xi)$ will remain finite at infinity only if p is zero or a positive integer This is the condition (5 8) anticipated in the previous section

If p is zero or a positive integer, $f(x)$ will be a multiple of Laguerre's polynomial $\mathrm{L}_p{}^q(x)$ The expressions for ξ and ϕ may be simplified by the use of the reduction formula,

$$x\frac{d\mathrm{L}_p{}^q(x)}{dx}=p\mathrm{L}_p{}^q(x)-(p+q)\,\mathrm{L}_{p-1}^q(x) \tag{6 7}$$

We find that

$$\phi=e^{-\frac{1}{2}x}x^{g-1}\{\mathrm{L}_p{}^q(x)\ \ (p+g-\mathrm{G})'\eta-(p+q)\,\mathrm{L}_{p-1}^q(x)\ \ \eta\}, \tag{6 8}$$

where

$$g=(\mu^2-\alpha^2\mathrm{Z}^2)^{\frac{1}{2}},\quad q=2g,\qquad p \text{ is } 0,\ 1,\ 2\quad ,$$

and η is any solution of the equation

$$(\mathrm{F}+\lambda)\,\eta=0,$$

F being the operator $-(\mathrm{EA}_4\varepsilon+\mathrm{E}\varepsilon_0)/\mathfrak{h}c$, and λ being $(\varepsilon_0{}^2-\varepsilon^2)^{\frac{1}{2}}/\mathfrak{h}c$

This result and that obtained in the last section (5 9) contain the solution of the problem of determining the wave functions and energy levels of hydrogen-like atoms It only remains to identify the quantum number μ

§ 7 *The Nature of the Quantum Number* μ

In this section it is shown that the quantum number μ is a non-vanishing integer and that it is simply related to the serial quantum number l of non-relativistic quantum theory

The operators m_3, $\frac{1}{2}\mathfrak{h}\mathrm{S}_3$ and M_3 all commute with one another Let $m\mathfrak{h}$, $s\mathfrak{h}$ and $u\mathfrak{h}$ be a simultaneous set of eigen values Then it is clear that

$$u = m + s, \tag{7 1}$$

and

$$s = \pm \tfrac{1}{2} \tag{7 2}$$

But $m_3 \equiv \dfrac{h}{2\pi i}\ \dfrac{\partial}{\partial\phi}$, whence it follows that the eigen functions of m_3 will contain the factor $\exp(im\phi)$ and will be single-valued functions of the co-ordinate ϕ only if m is an integer or zero Hence the eigen values of M_3, *i e*, the quantum numbers u, are all half odd integers

Now let ψ be a simultaneous eigen function of M_3, Q and W with eigen values $u\mathfrak{h}$, $\mu\mathfrak{h}$, and 0 Since

$$\mathrm{M}_3(\mathrm{M}_1 + i\mathrm{M}_2) - (\mathrm{M}_1 + i\mathrm{M}_2)\,\mathrm{M}_3 = \mathfrak{h}\,(\mathrm{M}_1 + i\mathrm{M}_2),$$

it follows that, unless $(\mathrm{M}_1 + i\mathrm{M}_2)\,\psi$ equals zero, it is also an eigen function of M_3 with eigen value $(u + 1)$ Also, since

$$\begin{aligned}(\mathrm{M}_1 - i\mathrm{M}_2)(\mathrm{M}_1 + i\mathrm{M}_2) &= \mathbf{M}\quad\mathbf{M} - \mathrm{M}_3{}^2 - \mathfrak{h}\mathrm{M}_3\\ &= \mathrm{Q}^2 - \tfrac{1}{4}\mathfrak{h}^2 - \mathrm{M}_3{}^2 - \mathfrak{h}\mathrm{M}_3,\end{aligned}$$

it follows that if χ is the eigen function of M_3 which gives the eigen value, u, its greatest value, $u_{\max}$, then

$$(\mathrm{M}_1 + i\mathrm{M}_2)\,\chi = 0,$$

and

$$\mathrm{Q}^2\chi = (\mathrm{M}_3 + \tfrac{1}{2}\mathfrak{h})^2\chi$$

Hence

$$\left.\begin{aligned} u_{\max} &= |\,\mu\,| - \tfrac{1}{2},\\ u_{\min} &= -|\,\mu\,| + \tfrac{1}{2}\end{aligned}\right\} \tag{7 3}$$

and, similarly,

The quantum numbers of M_3 evidently form an arithmetical progression of half odd integers, symmetrically distributed about zero Hence the number of u's, *i e*, $2\,|\,\mu\,|$, is an even integer Hence μ is a non-vanishing integer

To obtain the relation between μ and l, we form a second order equation for the wave function ϕ Since

$$\left(\frac{\partial}{\partial r} + \mathrm{F} + \frac{1+\mathrm{G}}{r}\right)\phi = 0, \qquad \text{(equation (5 1))},$$

it follows that

$$\left(\frac{\partial}{\partial r} - \mathrm{F} + \frac{1-\mathrm{G}}{r}\right)\left(\frac{\partial}{\partial r} + \mathrm{F} + \frac{1+\mathrm{G}}{r}\right)\phi = 0$$

In virtue of the relations established in equations (5 2) and (5 3), this reduces to

$$\left(\frac{\partial^2}{\partial r^2} + \frac{2}{r}\frac{\partial}{\partial r} - \frac{\mathrm{G}+g^2}{r^2} - \lambda^2 + \frac{2\delta}{r}\right)\phi = 0,$$

whence

$$\left(\frac{\partial^2}{\partial r^2} + \frac{2}{r}\frac{\partial}{\partial r} - \frac{g^2-g}{r^2} - \lambda^2 + \frac{2\delta}{r}\right)(\mathrm{G}-g)\,\phi = 0$$

This reduces again to the non-relativistic wave equation, if we put

$$\varepsilon = \mathrm{H} + \varepsilon_0, \tag{7 4}$$

and make $c \to \infty$

Then,

$$g \to |\mu|, \quad \lambda^2 \to (8\pi^2 m/h^2)\,\mathrm{H}, \quad \text{and} \quad 2\delta \to (8\pi^2 m/h^2)\;Ze^2$$

Hence the equation becomes

$$\left\{\frac{\partial}{\partial r^2} + \frac{2}{r}\frac{\partial}{\partial r} - \frac{\mu^2-|\mu|}{r^2} + \frac{8\pi^2 m}{h^2}\left(\mathrm{H} + \frac{Ze^2}{r^2}\right)\right\}(\mathrm{G}-g)\,\phi = 0 \tag{7 5}$$

A comparison of this with Schrodinger's equation shows that

$$\mu^2 - |\mu| = l(l+1)$$

Hence, since l is never negative,

$$\left.\begin{aligned} l &= |\mu| - 1, \quad \text{if } \mu > 0 \\ l &= |\mu|, \qquad\;\; \text{if } \mu < 0 \end{aligned}\right\} \tag{7 6}$$

Now if n is the total quantum number, *i e*,

$$n = n' + |\mu|, \tag{7 7}$$

the possible values of l are $0, 1, 2, \quad (n-1)$ Hence the possible values of μ are $-(n-1), -(n-2), \quad -2, -1, 1, 2, \quad (n-1), n$

Even when c is taken as finite the same conclusion persists, since μ—necessarily a continuous function of c—cannot vary *per saltem* Hence it must retain the same integral values

§ 8 *Conclusion*

The usual approximation to ε, obtained from the exact equation (5 9) by retaining powers of α up to the fourth only, is

$$\frac{\varepsilon - \varepsilon_0}{h} = \frac{RZ^2}{n^2} + \frac{R\alpha^2Z^4}{n^4}\left\{\frac{n}{|\mu|} - \frac{3}{4}\right\}, \tag{8 1}$$

where Ryberg's constant $R = \varepsilon_0\alpha^2/2h = 2\pi^2 m_0 e^4/h^3$ From this equation and the relation between $|\mu|$ and l, the fine structure of the spectrum of hydrogen-like atoms is easily deduced

It must be emphasised in conclusion that the wave operators A_1, A_2, A_3, A_4 occurring in the wave equation have remained unidentified throughout the whole of the investigation together with the wave function ψ

The author hopes to discuss, in a subsequent paper, the anomalous Zeeman effect, the selection rules and the intensities of spectral lines

In conclusion, I must express my gratitude to Prof Eddington for his interest in this work and for many valuable suggestions

---

The Raman Spectra of some Organic Halogen Compounds

By S Bhagavantam and S Venkateswaran

(Communicated by Sir Venkata Raman, F R S —Received February 3, 1930)

1 *Introduction*

The Raman spectra of organic compounds have recently been the subject of investigation in many laboratories As yet, however, only a few organic halogen compounds have received attention * It was considered that a detailed investigation of several compounds of this class would throw light on fundamental questions concerning the Raman effect Some 17 halogen derivatives of the aliphatic and aromatic hydrocarbons were accordingly investigated by the authors and the results are described in this paper The experimental arrangements are those recommended by R W Wood † The accompanying tables show the analysis of the Raman lines Under the column

---

* Pringsheim and Rosen, 'Z Physik,' vol. 50, p 741 (1928), see also Bonino and Brüll, 'Gazz Chim. Ital.,' vol. 59, p 643 (1929)

† 'Phil Mag,' vol 6, p 729 (1928)

$\Delta\nu$ are given the differences between the wave-numbers of Raman lines and the exciting lines of the mercury spectrum λ A U 3650 1, 3654 8, 3663 3, 4046 6, 4077 8, 4339 2, 4347 5, 4358 3, 5460 7, 5769 5, and 5790 5 represented by the letters *a*, *b*, *c*, *d*, *e*, *f*, *g*, *h*, *k*, *l* and *m* respectively Those Raman lines which happen to coincide with the incident lines of the mercury spectrum are not included in the tables

2 *Discussion of Results*

Before discussing the question whether any, and if so which, of the Raman lines may be regarded as characteristic of the halogen atoms in these compounds, we may consider those to which a different origin may be definitely assigned Among these, the group of lines which appears at about $\Delta\nu$ 2950 wave numbers is the most prominent, and has been assigned by various investigators to the aliphatic C-H vibration As in most of the other aliphatic compounds in the halides also, the lines of this group are more or less equally spaced (the constant spacing being about 40 cm $^{-1}$), and show a distinct tendency to broadening in the higher members But there is one significant fact which deserves emphasis, viz , that in the simple derivatives like $CHCl_3$ and $CHBr_3$ which contain only a single hydrogen atom, the multiple structure seems to disappear completely, only one line corresponding to a shift of 3020 cm $^{-1}$ appearing in this region This frequency is also much higher than the mean value 2950 generally attributed to the vibration of aliphatic C–H In CH_2Cl_2 the line is double (2930 and 2988), while in methane itself in the gaseous state it shows three distinct components corresponding to $\Delta\nu$ 2915, 3022, and 3072 respectively * The origin of the fine structure of this aliphatic C–H band has not been clearly understood, but the above observations seem to suggest that the structure depends to some extent on the number of the CH bands present in the molecule and on the complexity of the latter

The Raman line corresponding to a shift of 1440 wave-numbers also appears to be connected with the vibration of the hydrogen atom in the aliphatics, since it is invariably present in all the aliphatic compounds where the 3 μ band appears Whether the fact that the former frequency is roughly half of the latter, is in any way significant cannot be answered until the dynamics of the different modes of vibrations of the molecule have been actually worked out

We now come to the frequencies characteristic of the halogen atoms Tables I, II, III and IV give the analysis of the Raman spectra of CH_2Cl_2, $CHCl_3$,

---

* Dickinson, Dillon and Rasetti, 'Phys Rev ' vol 34, p 582 (1929)

$CHBr_3$ and CCl_4 which are the simplest of the compounds studied by us A prominent feature of their spectra is the occurrence of several Raman lines very close to the exciting line which is evidently due to the large mass of the halogen atoms From the fact that these low frequencies are very much smaller than in the case of the infra-red frequencies of most of the ordinary types of vibrations, there has recently been a tendency to conclude that they must be of the nature of differential frequencies, i e , can be explained as differences between two others which lie in the near infra-red Thus Langer* explains the presence of Raman lines corresponding to $\Delta\nu$ 215, 314 and 459 in CCl_4 as due to differences between certain observed infra-red absorption

Table I —Methylene Chloride,* CH_2Cl_2

I	ν_1	$\Delta\nu$	I	ν_1	$\Delta\nu$	I	ν_1	$\Delta\nu$
0	24985	*d* + 280	8	24001	*d* − 704	1*b*	22200	*h* − 738
2	24417	*d* − 288	0*d*	23964	*d* − 741	0*d*	21771	*d* − 2934
2	24397	*a* − 2992	0*d*	23277	*d* − 1428	10	21716	*d* − 2989
1	24361	*b* − 2993	1	23221	*h* + 283	1*d*	21515	*h* − 1423
1	24305	*c* − 2985	8	22650	*h* − 288	0	20068	*f* − 2971
0	24233	*e* − 283	0	22266	*h* − 672	0	20013	*h* − 2925
0	24028	*d* − 677	10	22234	*h* − 704	2*s*	19951	*h* − 2987

$\Delta\nu$ 288 (6), 675 (0) 704 (10), 739 (1*b*), 1425 (1*b*), 2930 (0), 2988 (8)

* The Raman spectrum of this liquid has been studied by Pringsheim and Rosen who report only the three strong frequencies (*loc cit*)

[Note —In the tables that follow the abbreviations used are given below —*s* = sharp, *d* = diffuse, *b* = broad, ν_1 = wave number of the Raman line, I = intensity]

Table II —Chloroform,* $CHCl_3$

I	ν_1	$\Delta\nu$	I	ν_1	$\Delta\nu$	I	ν_1	$\Delta\nu$
0	25371	*d* + 666	0	23758	*e* − 758	8	22270	*h* − 668
3	25070	*d* + 365	1*d*	23603	*h* + 665	3	22172	*h* − 766
3	24965	*d* + 260	2*d*	23486	*d* − 1219	1*d*	21721	*h* − 1217
4*d*	24445	*d* − 260	3	23303	*h* + 365	4*d*	21684	*d* − 3021
3*d*	24370	*a* − 3019	0	23254	*d* − 1451	2	21497	*h* − 1441
1	24273	*c* − 3017	4	23199	*h* + 261	2*d*	19921	*h* − 3017
2	24255	*e* − 261	0	22731	*g* − 264	1*d*	18572	*k* + 264
3*d*	24148	*e* − 368	6	22676	*h* − 262	3*d*	18049	*k* − 259
6	24037	*d* − 668	0	22633	*g* − 362	2	17945	*k* − 363
3*d*	23944	*d* − 761	7	22568	*h* − 370			
2*d*	23847	*e* − 669	1	22324	*g* − 671			

$\Delta\nu$ 261 (4), 367 (5); 669 (4), 762 (3*d*), 1218 (2*d*), 1441 (1), 3019 (3*d*)

* This liquid has been studied by several investigators and the results are in good agreement.

---

* 'Nature,' vol 123, p 345 (1929)

Table III —Bromoform,* $CHBr_3$

I	ν_1	$\Delta\nu$	I	ν_1	$\Delta\nu$	I	ν_1	$\Delta\nu$
0	27613	$a + 224$	0	26732	$a - 657$	2	23159	$h + 221$
0	27509	$c + 155$	1	24930	$d + 225$	2	23094	$h + 156$
0	27239	$a - 150$	1	24859	$d + 154$	3	22784	$h - 154$
0	27198	$b - 156$	2	24553	$d - 152$	3	22714	$h - 224$
0	27132	$\left\{\begin{matrix} c - 158 \\ b - 222 \end{matrix}\right\}$	2	24486	$d - 219$	2	22398	$h - 540$
			0	24370	$a - 3019$	2*d*	22280	$h - 658$
0	27065	$c - 225$	2	24168	$d - 537$	0	21796	$h - 1142$
0	26847	$a - 542$	1*d*	24048	$d - 657$	0	21684	$d - 3021$
						0	21501	$h - 1437$

$\Delta\nu$ 154 (2), 223 (2), 540 (2), 657 (1*d*), 1142 (0) 1437 (0) 3020 (0)

* The Raman spectrum of this liquid has been studied by Ganesan and Venkateswaran, 'Ind J Phys, vol 4, p 195 (1929)

Table IV —Carbon Tetrachloride,* CCl_4

I	ν_1	$\Delta\nu$	I	ν_1	$\Delta\nu$	I	ν_1	$\Delta\nu$
0	27139	$b - 215$	4	24492	$d - 213$	0	22778	$g - 217$
2	27076	$a - 313$	4	24391	$d - 314$	5	22718	$h - 220$
0	27042	$b - 312$	0	24299	$e - 217$	0	22679	$g - 316$
3	26929	$a - 460$	5	24247	$d - 458$	7	22623	$h - 315$
0	26896	$b - 458$	0	24207	$e - 309$	0	22535	$g - 460$
0	26830	$c - 460$	0	24056	$e - 460$	8	22480	$h - 458$
1	26625	$a - 764$	2*d*	23943	$d - 762$	2	22177	$h - 761$
1	26597	$a - 792$	2*d*	23914	$d - 791$	2	22149	$h - 789$
0	25162	$d + 457$	1	23393	$h + 455$	0	21403	$h - 1535$
1	25017	$d + 312$	2	23248	$h + 310$			
2	24920	$d + 215$	3	23154	$h + 216$			

$\Delta\nu$ 216 (4) 313 (5), 459 (5), 791 (2), 762 (2*d*), 1535 (0)

* This liquid has been investigated by several others and the results are in good agreement

values, and is of opinion that such long wave-lengths cannot be due to fundamental oscillations His arguments, however, are not convincing, especially in view of the fact that Marvin* has quite as successfully explained the occurrence of short wave lengths in infra-red absorption as due to summational combinations of the long waves as revealed by the Raman spectra, taking the latter as truly representative of fundamental oscillations in the molecule

The case of carbon tetrachloride is a system of the AX_4 type which has nine degrees of freedom if we neglect rotation and translation of the molecule as a whole It is shown by Dennison,† in the particular case of methane, that such a system, if it is perfectly tetrahedral in nature, is degenerate and gives four fundamental vibrations, any slight departure resulting in new and slightly different fundamentals coming in From the work on light scattering it is, however, definitely known that these compounds *do* show a small anisotropy which implies an asymmetry In view of this the number of frequencies actually observed in the Raman spectrum of carbon-tetrachloride, namely, six, is not too large, and there is no *a priori* reason for assuming that they have a combinational origin In fact, a rough calculation on the basis of the well-known discussions of Dennison on the vibrations of the CH_4 molecules shows that such small frequencies can directly be attributed to some of the modes of vibration of the molecule

---

* 'Phys Rev,' vol 33, p 952 (1929)

† 'Astrophys J,' vol 62, p 84 (1925)

Considering the simple case of a diatomic molecule, Van Vleck* has given good reasons for believing that the most intense scattered lines correspond to $\Delta v = 0$ representing simple Rayleigh scattering while those corresponding to $\Delta v = \pm 1$ represent the strongest Raman lines and come next in intensity, where v stands for the vibrational quantum number Less intense still are the Raman lines $\Delta v = \pm 2$, which are ordinarily too weak to detect experimentally Similarly, in the case of polyatomic molecules, the occurrence of Raman lines whose displacements are either harmonics of a fundamental vibration frequency or combinations of two different fundamentals is to be admitted, if at all, only as an exception In fact, it is suggested by Van Vleck that in the case of carbondioxide the two prominent frequency shifts $\Delta\nu$ 1284 and 1392, which do not correspond to any observed infra-red absorption lines, are really the fundamentals

The available data regarding the Raman spectra of a large number of compounds reveal definitely that the presence of combinational frequencies or overtones seems to be very rare *if they occur at all*, which is in agreement with the above views This is supported by the fact that some of the small frequencies of CCl_4 persist more or less unchanged in the other chlorides also as may be seen from the tables As already mentioned in an earlier part of this section, the presence of such low frequencies, which are more numerous in the case of the halogen compounds (especially in the earlier members) than in other compounds of comparable complexity, affords further support for our view †

---

* 'Proc Nat Acad Sci,' vol 15, p 754 (1929)

† In the more complex cases, we clearly realise that even if the masses of any of the individual component atoms is not large, we might still get very low vibrational frequencies due to oscillations of groups, rather than individual atoms, *e g*, pentane shows a Raman frequency as small as 143 cm $^{-1}$ (see Ganesan and Venkateswaran, 'Ind J Phys,' vol 4, p 195 (1929))

We would also like in this connection to draw attention to some of the inorganic chlorides and bromides studied by Dauret† where *all* the Raman frequencies occur *only* in the region we are discussing The continual shifting of the Raman lines towards the exciting line, as we go from the lighter to the heavier atoms, as is evidenced, for example, by the transition from the trichlorides to the tribromides, or from the trichlorides of the various elements of widely varying masses, may also be emphasised as supporting the view suggested Thus it seems fairly clear that in general a combinational or overtone frequency, if it comes at all, does so with far too feeble an intensity to be detected experimentally

Tables V to XVII give the analysis of the Raman lines in the more complex halogen compounds studied The general features such as the occurrence of

Table V —Ethylene Chloride,* $C_2H_4Cl_2$

I	ν_1	$\Delta\nu$	I	ν_1	$\Delta\nu$	I	ν_1	$\Delta\nu$
0	24465	$a - 2923$	0	23342	$e - 1174$	0*b*	21789	$d - 2916$
4	24426	$\left\{\begin{matrix} a - 2963 \\ d - 279 \end{matrix}\right\}$	1	23272	$d - 1433$	10	21743	$d \quad 2962$
			1	23244	$h + 306$	2*d*	21697	$d - 3008$
4*b*	24393	$\left\{\begin{matrix} a - 2996 \\ d - 312 \end{matrix}\right\}$	0	23204	$h + 266$	2	21632	$\left\{\begin{matrix} h \quad 1306 \\ e - 2884 \end{matrix}\right\}$
			1	22665	$h - 273$			
0*d*	24300	$d - 405$	8	22634	$h - 304$	2	21549	$e \quad 2967$
0*d*	24224	$e - 292$	0	22555	$h - 383$	2*d*	21503	$\left\{\begin{matrix} e - 3013 \\ h \quad 1435 \end{matrix}\right\}$
8	24051	$d - 654$	1	22525	$h - 413$			
0	24027	$d - 678$	10	22282	$h - 656$	0	20103	$h - 2835$
8*d*	23952	$d - 753$	0	22261	$h - 677$	0	20067	$h - 2871$
0	23854	$e - 662$	10*b*	22183	$h - 755$	0	20016	$h - 2922$
1	23762	$\left\{\begin{matrix} e - 754 \\ d - 943 \end{matrix}\right\}$	1	21994	$h - 944$	2	19978	$h - 2960$
			0	21882	$h - 1156$	0	19937	$h - 3001$
0	23553	$d - 1152$	0	21851	$d - 2854$			
1	23397	$d - 1308$	0	21827	$d - 2878$			

$\Delta\nu$ 273 (1), 304 (5) 383 (0), 409 (1) 655 (8) 677 (0) 754 (8*d*) 943 (1), 1154 (0), 1307 (1), 1434 (1), 2845 (0), 2874 (0), 2920 (0), 2963 (8), 3004 (1)

* Bonino and Brüll have investigated this liquid (*loc cit*)

Table VI —Hexachlorethane Dissolved in Carbon Tetrachloride,* C_2Cl_6

I	ν_1	$\Delta\nu$	I	ν_1	$\Delta\nu$	I	ν_1	$\Delta\nu$
0*d*	24360	$d - 345$	1	23845	$d - 860$	0	22562	$g - 433$
2	24271	$d - 434$	0	23375	$h + 437$	2	22505	$h - 433$
0	24082	$e - 434$	0	22593	$h - 345$	1*d*	22079	$h - 859$

$\Delta\nu$: 345 (0) 434 (2), 860 (1)

* The Raman lines due to CCl_4 are omitted The choice of the solvent is not quite satisfactory in that there is a possibility of some of the Raman lines characteristic of the two compounds coinciding

† Thesis presented to the University of Paris (1929)

Table VII —Propyl Chloride, C_3H_7 Cl

I.	ν_1	$\Delta\nu$	I	ν_1	$\Delta\nu$	I	ν_1	$\Delta\nu$
0*d*	24418	*a* — 2971	1	22765	*h* — 173	1	21890	*h* — 1048 *d* — 2815
0	24373	*b* 2981	0	22688	*h* — 250	2	21816	*d* — 2889
0	24102	*d* — 603	0	22632	*h* — 306	3*b*	21746	*d* — 2959
1	24042	*d* 663	1	22564	*h* — 374	0	21559	*e* — 2957
1*d*	23974	*d* — 731	0	22342	*h* — 596	1	21478	*h* — 1460
0	23908	*d* — 797	2	22272	*h* — 666	2	20069	*h* — 2869
0	23682	*d* 1023	2*d*	22200	*h* — 738	1*d*	19977	*h* — 2961
0*b*	23226	*d* — 1479	1	22139	*h* — 799			
1	22830	*h* — 108						

$\Delta\nu$ 108 (1), 173 (1), 250 (0), 306 (0), 374 (1), 600 (0), 665 (2), 735 (2*d*), 798 (1), 1031 (0), 1469 (1), 2815 (0) 2879 (2), 2959 (3*b*)

Table VIII —Isopropyl Chloride,* $(CH_3)_2$ CHCl

I	ν_1	$\Delta\nu$	I	ν_1	$\Delta\nu$	I	ν_1	$\Delta\nu$
0	24471	*a* — 2918	0*d*	23361	*e* — 1155	4	21776	*h* — 1162 *d* — 2929
0	24432	*a* — 2957	0*d*	23253	*d* — 1452 *e* — 1263	2	21748	*d* — 2957
0	24389	*b* - 2956	0*d*	22832	*h* — 106	2*b*	21717	*d* — 2988
0	24360	*a* — 3029 *d* — 345	0*d*	22771	*h* — 167	0	21675	*h* — 1263
0	24303	*d* — 402	1*b*	22595	*h* — 343	0	21639	*e* — 2877
0	24277	*d* - 428	0	22549	*h* — 389	0	21601	*e* — 2915
0	24178	*e* — 338	1	22511	*h* — 427	0	21567	*e* — 2949
2	24088	*d* — 617	0	22475	*h* — 463	0	21516	*e* — 3000
0*d*	23884	*e* - 632	4	22321	*h* - 617	1	21486	*h* — 1452
0	23816	*d* — 889	2	22050	*h* — 888	0	20113	*h* — 2825
0	23762	*d* — 943	0	21972	*h* — 966	1	20070	*h* — 2868
0*d*	23699	*d* — 1006	0*b*	21916	*h* — 1022	1	20026	*h* — 2912
0	23640	*d* - 1065	2	21873	*h* — 1065 *d* — 2832	1	20002	*h* — 2936
0*d*	23540	*d* — 1165	2	21836	*d* — 2869	0	19959	*h* — 2989
0*d*	23437	*d* — 1268 *e* — 1079	4	21789	*d* — 2916	0	19929	*h* — 3019

$\Delta\nu$ 106 (0*d*), 167 (0*d*), 344 (1), 395 (0), 428 (1), 463 (0), 617 (4), 889 (2), 954 (0), 1014 (0*b*), 1065 (1), 1163 (2), 1265 (0), 1452 (0), 2828 (2), 2869 (2), 2915 (3), 2932 (2), 2957 (2), 2992 (2), 3024 (0)

* The Raman line corresponding to a frequency shift 750 cm $^{-1}$ is very weak in the scattered spectrum of this liquid and hence could not be measured accurately

Table IX —Isobutyl Chloride, $(CH_3)_2$ CH CH_2Cl

I	ν_1	$\Delta\nu$	I	ν_1	$\Delta\nu$	I	ν_1	$\Delta\nu$
1*b*	24411	*a* − 2978	1	23242	*d* − 1463	2	21978	*h* − 960
0	24178	*e* − 338 *d* − 527	0	22781	*h* − 157	6*b*	21806	*d* − 2899
			0	22700	*h* − 238	0*b*	21727	*d* − 2978
0	24091	*e* − 425	1	22597	*h* − 341	1	21615	*e* − 2909 *h* − 1323
2	24009	*d* − 696	1	22505	*h* − 433			
3*b*	23969	*d* − 736	0	22410	*h* − 528	1	21539	*e* 2977
1	23893	*d* − 812	0	22350	*f* − 689	2	21473	*h* − 1465
0	23837	*d* − 868	0	22297	*g* − 698	1	20064	*h* − 2874
1*b*	23753	*d* − 952	3	22242	*h* − 696	0	20020	*h* 2918
0*d*	23598	*d* − 1107	4	22199	*h* 739	1*b*	19975	*h* − 2963
0	23475	*d* − 1230	2	22120	*h* − 818			
0	23384	*d* − 1321	0	22061	*h* − 867			

$\Delta\nu$ 157 (0), 238 (0), 340 (1), 433 (1), 528 (0) 696 (3) 738 (4), 815 (1), 867 (0) 956 (2), 1107 (0), 1230 (0) 1322 (0), 1464 (2), 2874 (5), 2918 (0) 2977 (5)

Table X —Allyl Chloride,* CH_2 CH CH_2Cl

I	ν_1	$\Delta\nu$	I	ν_1	$\Delta\nu$	I	ν_1	$\Delta\nu$
2*b*	24422	*a* − 2967	3	23289	*d* − 1416	6	21676	*d* − 3029 *h* − 1262
2*b*	24389	*d* − 316	0	22680	*g* − 315			
2*b*	24363	*a* − 3026	2	22638	*h* − 300	2	21631	*h* − 1307
2	24297	*d* − 408	4	22519	*h* − 419	2	21604	*h* − 1334
2	24265	*c* − 3025	0*b*	22417	*h* − 521	3*b*	21520	*h* − 1418
1	24191	*d* − 514	5	22342	*h* − 596	0	21345	*g* − 1650
3	24109	*d* − 596	6*b*	22196	*h* − 742	6	21293	*h* − 1645
6*b*	23965	*d* − 740	2	21994	*h* − 944	0	21241	*h* − 1697
3	23768	*d* − 937	1	21816	*d* − 2889 *h* − 1122	1*b*	20063	*h* − 2875
0*b*	23592	*d* − 1113				1*b*	19976	*h* − 2962
3	23497	*d* − 1208	6	21737	*d* − 2968 *h* − 1201	1*b*	19897	*h* − 3041
3	23438	*d* − 1267						
3	23403	*d* − 1302						

$\Delta\nu$ 310 (2), 413 (4), 517 (0), 596 (4), 741 (6*b*), 940 (3), 1117 (0), 1204 (3), 1264 (3) 1304 (3), 1334 (2), 1417 (3), 1647 (6), 1697 (0), 2882 (1), 2966 (3), 3027 (3)

---

* Petrikaln and Hochberg have studied the Raman spectrum of this liquid Some of the frequencies have, however, been overlooked by these authors, 'Z Phys Chem,' vol 4 p 299 (1929)

Table XI —Ethylene Bromide, $C_2H_4Br_2$,

I	ν_1	$\Delta\nu$	I	ν_1	$\Delta\nu$	I.	ν_1	$\Delta\nu$
0	24608	*d* − 97	0*b*	22769	*h* − 169	2	20115	*h* − 2823
0	24419	*a* − 2970	0*d*	22451	*h* − 487	0	20023	*h* − 2915
0	24377	*a* − 3012	0	22362	*h* − 556	0*b*	19967	*h* − 2971
0	24358	*a* − 3031	0	22349	*h* − 589	0	19926	*h* − 3012
0	24233	*d* − 472			*g* − 646	0*b*	18129	*k* − 179
0	24117	*d* − 588	5	22278	*h* − 660	0	17739	*k* − 569
3*d*	24044	*d* − 661	0*b*	21876	*d* − 2820	0	17703	*k* − 605
0	23848	*e* − 668	1	21725	*d* − 2980	0	17647	*k* − 661
1	23446	*d* − 1259	0	21703	*d* − 3002			
0	23255	*e* − 1261	2	21680	*d* − 3025			
1	22838	*h* − 100			*h* − 1258			

$\Delta\nu$ 99 (1) 174 (0*b*), 480 (0*d*), 556 (0), 589 (0), 661 (4), 1259 (1), 2826 (1), 2915 (0), 2971 (1), 3008 (0), 3028 (0)

Table XII Ethyl Bromide, C_2H_5Br

I	ν_1	$\Delta\nu$	I	ν_1	$\Delta\nu$	I	ν_1	$\Delta\nu$
0*b*	24604	*d* − 101	1	22783	*h* − 155	1	21741	*d* − 2964
0*b*	24564	*d* − 141	0	22722	*h* − 216	0	20118	*h* − 2820
1*b*	24465	*a* − 2923	2	22377	*h* − 561	1	20067	*h* − 2871
1*b*	24421	*a* − 2968	0	22305	*h* − 633	1	20017	*h* − 2921
1*b*	24373	*b* − 2980	1	21826	*d* 2879	0	19978	*h* − 2960
1	22836	*h* − 102	2	21779	*d* − 2926	0	17748	*k* − 560

$\Delta\nu$ 102 (1), 148 (1), 216 (0), 560 (2), 633 (0), 2820 (0), 2875 (1), 2923 (2), 2964 (1)

Table XIII —Propyl Bromide, C_3H_7Br

I	ν_1	$\Delta\nu$	I	ν_1	$\Delta\nu$	I	ν_1	$\Delta\nu$
0	24420	*a* − 2869	0	23593	*d* − 1112	1	22154	*h* 4
		d − 285	1	23482	*e* − 1034	0	22090	*h* − 848
0	24376	*b* − 2977	0	23416	*e* − 1100	0	22036	*h* − 902
		d − 329	1	23252	*d* − 1453	0	21951	*g* − 1044
0	24295	*d* − 410	0	22882	*h* − 106	1	21905	*h* − 1033
0	24200	*e* − 316	0	22762	*h* − 176	2*b*	21812	*d* − 2893
2*d*	24057	*d* − 648	0	22702	*h* 236			*h* − 1126
0*b*	23933	*d* − 772	0	22660	*h* − 278	2*b*	21752	*d* − 2953
0	23858	*d* − 847	1	22619	*h* − 319	0	21538	*e* − 2978
0*b*	23809	*d* − 896	1	22520	*h* − 409	1	21485	*h* − 1453
0	23745	*e* − 771	0*d*	22423	*g* − 572	1*b*	20053	*h* − 2885
1	23672	*d* − 1033	3	22369	*h* − 569	1*b*	19983	*h* − 2955
		e − 844	2*d*	22286	*h* − 652			
0	23618	*e* − 898	0	22203	*g* − 792			

$\Delta\nu$ 106 (0) 176 (0), 236 (0), 278 (0), 319 (1) 409 (1), 569 (3) 650 (2*d*), 780 (1), 847 (0) 899 (0), 1034 (1), 1113 (0), 1453 (1), 2889 (2*b*), 2954 (2*b*)

Table XIV —Isobutyl Bromide, $(CH_3)_2\ CH\ CH_2Br$

I	ν_1	$\Delta\nu$	I	ν_1	$\Delta\nu$	I	ν_1	$\Delta\nu$
2	24463	*a* — 2926	4	22635	*h* — 303	4*b*	21787	*h* — 1151 *d* — 2918
3*b*	24425	*a* — 2964	0*b*	22512	*g* — 483	4*b*	21740	*d* — 2965
3*b*	24400	*a* — 2989	1	22467	*h* — 471	2*b*	21703	*d* — 3002 *h* — 1235
0	24232	*d* — 473	4	22420	*h* — 518	0	21661	*e* — 2855
0	24209	*e* — 307	0	22370	*g* — 625	0*b*	21619	*h* — 1319
1	24184	*d* — 521	0	22338	*g* — 657 *h* — 600	0	21592	*e* — 2924
0	24109	*d* — 596	3	22313	*h* — 625	0*b*	21548	*e* — 2968
1	24080	*d* — 625	4	22284	*h* — 654	2*b*	21486	*h* — 1452
2*d*	24052	*d* — 653	2	22128	*h* — 811	1	20069	*h* — 2869
1	23892	*d* — 813	0	22100	*h* — 838	0*b*	20023	*h* — 2915
0	23864	*d* — 841	1*b*	21980	*h* — 958	0*b*	19974	*h* — 2964
0	23585	*d* — 1120	0	21925	*f* — 1114	0	19939	*h* — 2999
1	23561	*d* — 1144	3	21831	*h* — 1107 *d* — 2874			
0*b*	23462	*d* — 1243						
0*b*	23392	*d* — 1313						
0	22688	*g* — 307						

$\Delta\nu$ 305 (4), 472 (1), 519 (3), 598 (0), 625 (3), 654 (4), 812 (2), 840 (0), 958 (1), 1113 (0), 1147 (2), 1239 (0), 1316 (0*b*), 1452 (2*b*), 2866 (2), 2920 (2), 2965 (4), 3000 (2)

Table XV —Allyl Bromide, $CH_2\ CH\ CH_2Br$

I	ν_1	$\Delta\nu$	I	ν_1	$\Delta\nu$	I	ν_1	$\Delta\nu$
2*d*	24165	*d* — 540	1	22679	*h* — 259	0	21882	*d* — 2823
3	24013	*d* — 692	1	22533	*h* — 405	1	21730	*d* — 2975 *h* — 1208
0	23750	*d* — 955	1	22408	*h* — 530	0	21617	*h* — 1321
1*b*	23496	*d* — 1209	1	22250	*h* — 688	0*d*	21520	*h* — 1418
0*d*	23404	*d* — 1301	0	22129	*h* — 809	1	21297	*h* — 1641
0*d*	23294	*d* — 1411	0	21992	*h* — 946			

$\Delta\nu$ 259 (1), 405 (1) 535 (2), 690 (3), 809 (0), 950 (0), 1208 (1*b*), 1301 (0), 1321 (0), 1415 (0*d*), 1641 (1), 2823 (0), 2975 (0)

Table XVI —Chlorobenzene, C_6H_5Cl [*]

I	ν_1	$\Delta\nu$	I	ν_1	$\Delta\nu$	I	ν_1	$\Delta\nu$
3	24897	*d* + 192	2	23583	*d* − 1122	10	21936	*h* − 1002
0	24404	*d* − 301	3*b*	23544	*d* − 1161	8	21915	*h* − 1023 *g* − 1080
8	24318	*e* − 198 *a* − 3071	3	23513	*e* − 1003	8	21851	*h* − 1087
10	24286	*d* − 419 *b* − 3068	1	23491	*e* − 1025	3	21814	*h* − 1124
10	24225	*a* − 3164 *c* − 3065 *e* − 291	2*b*	23430	*e* − 1086	4*d*	21778	*h* 1160
0*b*	24186	*b* − 3168	0	23383	*e* − 1133	10*b*	21638	*d* 3067
0*d*	24122	*c* − 3168	2*d*	23355	*h* + 417	0	21555	*h* − 1383
6	24091	*e* − 425 *d* − 614	1*d*	23230	*h* + 292	2	21537	*d* − 3168
8	24003	*d* − 702	5*b*	23126	*d* − 1579	6	21449	*e* − 3067
0	23967	*d* − 738	6	22740	*f* − 299 *h* − 198	0	21411	*g* − 1584
0	23865	*d* − 840	2	22639	*h* − 299	8	21352	*e* − 3164 *h* − 1586
1	23810	*e* − 706	8	22518	*h* − 420	0*d*	19983	*f* − 3056
0*d*	23768	*e* − 748	6	22322	*h* − 616	0*d*	19928	*g* − 3067
10	23702	*d* − 1003	8	22234	*h* − 704	6	19875	*h* − 3063
8	23682	*d* − 1023	0*d*	22196	*h* − 742	0	19778	*h* − 3160
10	23623	*d* − 1082	0*d*	22161	*g* − 834	1	18490	*k* + 191
			1	22105	*h* − 833	1	18107	*k* − 201
			1	22030	*f* − 1009	1	17882	*k* − 426
			2	21991	*g* − 1004	0	17682	*k* − 626
			1	21969	*g* − 1026			

$\Delta\nu$ 198 (5), 299 (2), 420 (8), 615 (6), 704 (8), 742 (0*d*) 836 (1), 1004 (10), 1023 (6) 1084 (6), 1123 (3), 1160 (4), 1383 (0), 1583 (6), 3067 (10), 3168 (1)

[*] Several investigators have studied the Raman spectrum of this liquid but many new frequencies have been recorded in this paper

Table XVII —Bromobenzene,[*] C_6H_5Br

I	ν_1	$\Delta\nu$	I	ν_1	$\Delta\nu$	I	ν_1	$\Delta\nu$
0	24386	*d* − 319	0	23338	*d* − 1367	0	21750	*h* − 1188
0	24285	*b* − 3069	0*d*	23255	*h* + 317	1*b*	21643	*d* − 3062
0	24229	*c* − 3061	0*d*	22761	*h* − 177	1*d*	21348	*h* − 1590
0	24200	*e* − 316	0	22699	*h* − 239	0	19893	*h* − 3045
0*b*	24090	*d* − 615	0	22607	*h* − 331	1	18123	*k* − 185
0*b*	24032	*d* 673	1	21936	*h* − 1002	0	18069	*k* − 239
1	23703	*d* − 1002	0	21912	*h* − 1026	0*d*	17708	*k* − 600
0	23679	*d* − 1026	0	21859	*h* − 1079			

$\Delta\nu$ 181 (1), 239 (0), 317 (0) 607 (0*b*), 673 (0*b*) 1026 (0) 1079 (0) 1188 (0), 1367 (0), 1590 (1*d*), 3060 (1)

[*] This liquid has been studied by Dadieu and Kohlrausch, 'Sitz Ber K Akad Wien,' vol 138, p 335 (1929), and Fujioka, 'Inst Phys Chem Res' (Japan) vol 2, p 205 (1929) and the results are in good agreement,

low frequency shifts characteristic of the earlier members already noticed continue to appear in these compounds A comparison of the frequency shifts in the chlorine and the corresponding bromine compounds shows that they are invariably shifted farther away from the exciting line in the case of the former This is obviously due to the large difference in the masses of the chlorine and bromine atoms The prominent frequencies of the chlorine compounds range about the mean values Δν 750, 660, 320 and 250, whereas in the bromine compounds we get Δν 660, 550, 230 and 160 There is thus seen a one-to-one correspondence between the characteristic frequencies of the two classes of compounds This is particularly conspicuous in the case of $CHCl_3$ and $CHBr_3$ as may be seen in the figure

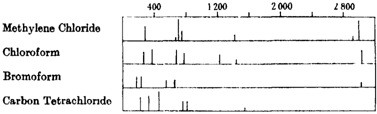

On an examination of the tables it is also found that the frequency 750 cm $^{-1}$ appears prominently in all the chlorine compounds except in isopropyl chloride, where it is very weak, and it seems reasonable to attribute it to the C-Cl bond The frequency 660 cm $^{-1}$ plays a similar part in all the bromine compounds But when we attempt to calculate from the known dissociation constants for these bonds on the basis of the formula used by Dadieu and Kohlrausch (which has been applied with fair success to the calculation of the Raman frequencies of several types of chemical bonds*), the frequencies for the C Cl and C-Br bonds come out as 832 and 693 respectively These are somewhat higher than the experimental values mentioned above, and the reason for this discrepancy is not clear It is probably due to the simple assumptions underlying Dadieu and Kohlrausch's method of calculation not being applicable to cases where one of the vibrating atoms is of very large mass It must, however, be pointed out in this connection that the discrepancy in the case of the heavier atom, viz, bromine, does not seem to be greater than in the case of chlorine Whatever might be the reason for the failure of the theoretical formula, it seems fairly clear that the frequencies above mentioned, viz, Δν 750 and Δν 660, are really characteristic of the C-Cl and C-Br bonds since they respectively appear without any exception in all the chlorine and bromine compounds studied by us, and in most of these liquids with some prominence

There is one interesting fact connected with the Raman lines corresponding to the above frequencies ($\Delta\nu$ 750 for chlorine derivatives and $\Delta\nu$ 660 for bromine derivatives) which distinguishes them from the other Raman lines appearing in our spectrograms, viz, they are somewhat diffuse As has already been pointed out by one of us,† this is particularly conspicuous in the case of CCl_4, $CHCl_3$ and $CHBr_3$ Whether the diffuseness of this Raman line is really due to the occurrence of two very close lines due to a small difference in frequency of oscillation of the two isotopes of the chlorine and bromine atoms is more than we can say, since the dispersion of our instrument was not sufficiently large to be capable of resolving the lines if they occur

---

* Dadieu and Kohlrausch, 'Sitz Ber K Akad Wien,' vol 138, p 419 (1929), see also Venkateswaran and Bhagavantam, "The Raman spectra of some aldehydes" (in course of publication)

We shall now discuss briefly the characteristic features of the Raman spectra of chloro- and bromobenzene, which are the only aromatic compounds studied in this paper In the scattered spectrum of the former a Raman line corresponding to $\Delta\nu$ 3168 is observed which is of special significance in view of the fact that such high frequencies are rare As might be expected, these two compounds show several Raman lines corresponding to low frequency shifts The general phenomenon mentioned already regarding the shift of the Raman lines of the chloro-derivatives farther away from the incident line than in the corresponding bromo-derivatives is also observed here Chlorobenzene shows two prominent Raman lines corresponding to $\Delta\nu$ 1084 and 1123 which are absent in benzene

The Raman line corresponding to $\Delta\nu$ 1000 which is very prominent in benzene continues to appear in both these compounds, in addition to which a new frequency $\Delta\nu$ 1025 is present This doubling seems to be characteristic of substitution, as data on other substituted benzene derivatives also show the same phenomenon The intensity of this new component, namely, $\Delta\nu$ 1025, varies with the nature of the substitution Its significance is discussed by the authors in another paper

3 *Summary*

Results of a study of Raman spectra of 17 halogen derivatives of the aliphatic and aromatic hydrocarbons are reported It is suggested that combinational or overtone frequencies may occur in the Raman spectra, if they do so at all, only under exceptional conditions, and that the frequency shifts usually observed are to be interpreted as primarily due to the fundamental oscillations in the molecules The occurrence of several small frequency shifts in all the substances studied with a more or less one to-one similarity in the corresponding chlorine and bromine derivatives is taken as evidence supporting the above view The band at about 3 3 μ characteristic of the aliphatic C-H linkage, which usually consists of several components in the higher members, gives place to a single line in chloroform and bromoform

---

† Ganesan and Venkateswaran, *loc cit*

From a comparison of the data it appears that the Raman line corresponding to Δν 750 can be ascribed to a vibration in the C-Cl bond, whereas the one corresponding to Δν 660 can be ascribed to the C-Br bond The diffuse nature characterising the Raman lines shifted by the above frequencies, which is particularly conspicuous in $CHCl_3$, CCl_4, and $CHBr_3$ may be due to an unresolved structure arising from the presence of isotopes in chlorine and bromine

In conclusion, the authors desire to express their best thanks to Prof Sir C V Raman, F R S , and Mr K S Krishnan for their kind interest in the work The investigation was carried out in the laboratory of the Indian Association for the Cultivation of Science

---

The Liberation of Electrons from Metal Surfaces by Positive Ions
Part I —Experimental

By M L E OLIPHANT, Ph D, Exhibition of 1851 Senior Research Student, Trinity College, Cambridge

(Communicated by Sir Ernest Rutherford, F R S —Received February 27, 1930)

Modern theories* of the glow and arc discharges require that electrons should be set free from the cathode surface as a result of the bombardment by positive ions The conditions in the neighbourhood of the negative electrode are exceedingly complex, and it is only by systematic examination of each reaction which we believe to be present, isolated from the disturbing effects of the others, that we can hope for a complete understanding of this important region This paper describes some experiments which have been carried out in an endeavour to explain the precise nature of the reaction between the positive ions and the surface of the conductor

The literature of this subject is fairly extensive, and many of the experiments have been very carefully thought out * It seems to be quite definitely established that ions of velocity greater than about 100 volts set free electrons from metal surfaces which are not rigorously freed from gas Most of the experiments have been carried out with alkali ions from thermionic sources, and owing to the abnormally low ionisation potentials of the alkalis the results are scarcely applicable to the case of discharges in ordinary gas We are not concerned with the liberation of electrons by very fast canal rays or alpha particles, but with the effect produced by positive ions of less than about 1000 volts energy Penning† has established by a series of experiments that neon ions of as little as 7 volts energy, drifting up against a metal surface, are able to set free electrons from it

---

* *Cf* Compton and Morse, ' Phys. Rev ,' vol. 30, p 305 (1927)

The present experiments were carried out with helium ions, except in one or two special instances, for three reasons Firstly, the part played by the ionisation potential will probably appear very clearly with a gas of such high ionising energy, secondly, it will not be adsorbed appreciably at the surface of the conductor, and after neutralisation will escape again in the atomic condition, while thirdly, it can be continually and easily purified by passing over activated charcoal cooled in liquid air

Two methods of examining the emitted electrons have been employed The most careful experiments have been carried out by a retarding potential method, but these results have been confirmed by experiments using magnetic analysis of the velocity distribution

Apparatus

The production of a homogeneous beam of gas ions is by no means as simple as in the case of the alkali ions, for a thermionic source does not exist, but a method has been developed, based on the Langmuir " probe " theory, which yields a beam surprisingly " monochromatic " in character and of fair intensity

It is known from the work of Langmuir and Mott Smith,‡ that a negatively charged electrode in a strongly ionised gas becomes surrounded by a sheath of positive ions, whose space charge neutralises the potential of the electrode at points outside the sheath Every positive ion which crosses the outer boundary of this dark sheath must eventually reach the electrode, unless it makes a collision in its passage across the space, or the electrode is so small that the random ion velocities are able to cause it merely to perform an orbit about the probe If the ionised gas is the positive column of a glow discharge or a low voltage arc, the random velocities of the ions will be only of the order of a few volts, so that after traversing the sheath the greater number will strike the electrode with the energy corresponding to its potential relative to the surrounding gas The abnormally long free paths of ions in most gases support the probability that there is little loss of energy by the ions in traversing a sheath which is not too many gas kinetic free paths in thickness If the electrode is perforated in such a way that the field is not seriously distorted, that is, so that the diameter of the perforations is small compared with the sheath thickness, ions will travel through with a velocity determined only by the potential applied These facts have been utilised in the method employed for producing a beam of He$^+$ ions

---

* ' Handbuch d Physik,' vol 24, p 171, *et seq*

† Penning, ' K Akad Wet Amsterdam, Proc ,' vol 31, p 14 (1927), ' Physica, vol 8, p 13 (1928)

‡ Langmuir and Mott-Smith, ' Gen. Elec Rev ,' vol. 27, p 449 (1924)

Helium gas was admitted to the bulb O, fig 1, through a fine leak, passing on the way over activated charcoal cooled in liquid air An arc of 50 400

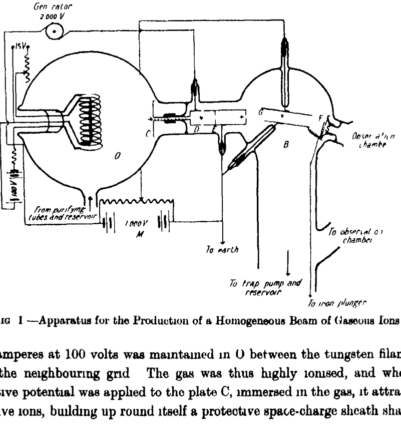

FIG 1 —Apparatus for the Production of a Homogeneous Beam of Gaseous Ions

milliamperes at 100 volts was maintained in O between the tungsten filament and the neighbouring grid The gas was thus highly ionised, and when a negative potential was applied to the plate C, immersed in the gas, it attracted positive ions, building up round itself a protective space-charge sheath sharply defined as a dark space about 1 cm thick Between the edge of the dark space and C the ions were accelerated by the full potential of C relative to the gas around it, that is, practically the potential of this electrode relative to the anode of the arc Some few of these ions entered the hole in the centre of the electrode Of these the larger portion collided with the walls of the canal, 3 mm in diameter and 5 cm long, but a few travelled right through. Between D and E these ions were subjected to a reversed field, due to the potential between the anode of the arc and C applied in the opposite direction, but diminished by a battery of small storage cells M In this way a beam of ions was obtained whose energy was independent of the high potential from the generator applied to C in order to collect them from the glowing gas It was not possible to vary the " pulling out " potential in order to change the energy of the beam of ions A potential of at least 1500 volts was required on C as at lower potentials the thickness of the positive ion space charge sheath was so small that the hole in the centre of the electrode caused a serious disturbance of the field, and a resultant decrease in the intensity of the beam obtained

Earlier experiments had shown that the beam of ions issuing from E was accompanied by large numbers of excited metastable atoms, which possessed high energies and were able to set free electrons from a metal surface which they struck * For this reason the beam of ions was deflected away from the direct path followed by the neutral atoms, by an electric field across the plates G The beam could be located upon the willemite covered surface of the shutter F, which served to close the slit S, and which was operated magnetically through an iron plunger The well-defined nature of the spot of fluorescence on the screen F, produced by the impact of the beam, afforded a good criterion of its homogeneity

(*a*) *Retarding Potential Apparatus* For this method of analysis the beam was allowed to enter the bulb D, fig 2, and fall upon a target T, by lowering the shutter F The target was in the form of a pill box, and contained a tungsten filament which enabled it to be heated to a temperature of about 1200° C The box was so constructed that no electrons from the filament were able to escape from it The target was carried on a long ground glass joint, cooled by a stream of water flowing through a coil of metal tubing cemented to the outer sleeve In this way the whole of the glass portions of the apparatus, right up to W, could be baked out at 550° C The bulb was covered with a conducting film of platinum, deposited in a vacuum by evaporation from a heated wire, contact being made by wires sealed through the wall of the bulb A variable retarding or accelerating potential could be

---

* Oliphant, 'Roy Soc Proc,' A, vol 124, p 228 (1929)

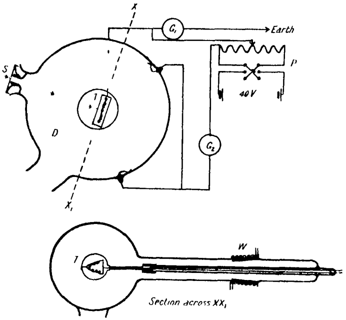

Fig 2 —Retarding Potential Effects

applied between the target and bulb by means of a potentiometer P The current to the target and the collecting sphere, *i e*, the total positive ion current entering the system through the slit S, was measured by the galvanometer G_1, and varied up to 45 microamperes The secondary electron, or reflected positive ion current from the target, was measured by the more sensitive galvanometer G_2, connected between the collecting sphere and the target

(*b*) *Magnetic Analysis*--For this method of observation the beam, after passing through the slit behind the shutter, was directed upon the target T, fig 3, which was inclined at an angle of 45° to the beam, and which could be heated to about 1200° C by radiation from a coiled tungsten filament inside the " pill box " attached to the opposite face Electrons set free from this target were bent into a semicircle by the field of a pair of Helmholtz coils the beam being defined by the usual slit system The final slit was 0 25 mm wide and 4 mm long, and below it was fastened the Faraday cylinder Z, insulated with quartz, and surrounded by an insulated guard ring Q, the whole being enclosed in a shielding box U The complete system of target, slit system and shielding box was cut and folded from a single sheet of molybdenum, to eliminate contact potentials, and the Faraday box was rolled from the same piece All joints were lapped and spot welded The analysing apparatus was

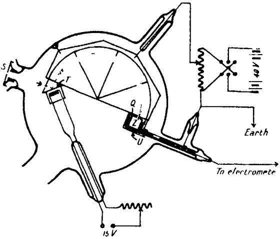

FIG 3 —Apparatus for Analysis of Secondary Electrons by Magnetic Bending

suspended within a glass bulb by two stout tungsten wires sealed into the walls

The apparatus was evacuated through a large liquid air trap of low resistance, by a four stage Gaede diffusion pump, which returned the helium gas to the reservoir The pressure on this side of the canal was maintained at less than 4×10^{-5} mm with a pressure of 0 01 mm in O, fig 1 An auxiliary pumping system allowed the whole apparatus, reservoir and Gaede pump, to be evacuated and the glass parts baked out till the residual pressure was not greater than 10^{-6} mm as measured by an ionisation gauge The system was separated from the exhausting pump and gas inlet by mercury cut-offs, barometrically operated The helium used was purified by fractionating 10 times from charcoal in liquid air, slight traces of hydrogen being removed by electrolysing a trace of oxygen from the glass wall of a discharge tube into the glowing gas, after a method described by Taylor *

The whole apparatus was of pyrex glass with tungsten seals, the metal parts molybdenum or nickel, with the exception of the canal and the coating on the collecting sphere, which were of platinum The ground joints at W, fig 2, and those on the steel Gaede pump, were lubricated with a grease of very low vapour pressure †

---

* 'Roy Soc Proc,' A, vol 123, p 252 (1929)

† Burch, 'Roy Soc Proc,' A, vol. 123, p 271 (1929)

The system of electrical connections used is shown in the figures, and does not call for comment

Results

(*a*) *The Variation of the Total Electron Emission with the Energy of the Positive Ions*—The number of electrons set free by each positive ion which struck a molybdenum target is plotted in fig 4 for a series of energies from 80 to 1000 volts, for a cold and for a red hot surface In the case of the cold target the points do not lie on a smooth curve, although they give a fairly accurate idea of its general shape The emission was reasonably constant at energies below about 200 volts, but beyond this point it increased approximately linearly with the energy up to 1000 volts When the target had been heated for some time at a bright red heat, and was maintained red hot during the measurements, the curve obtained was very much smoother, and was reproducible The emission did not now begin to increase till a potential of about 500 volts was reached, when it increased gradually, assuming an approximately linear form beyond 800 volts, but curving over again beyond 1000 volts The emissions were also smaller than with a cold target

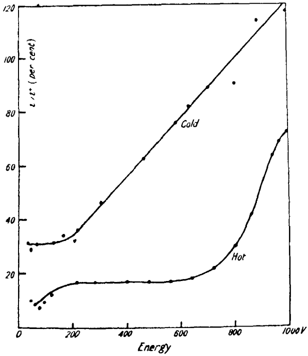

Fig 4

If the electron emission from a hot target is plotted against the velocity rather than the energy of the helium ions, the curve obtained is even more striking, fig 5 The rate of increase of emission at a velocity of about 2 × 10^7 cms per second is extraordinarily sharp

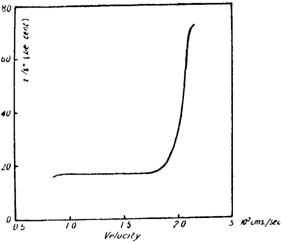

FIG 5

(b) *The Effect of Variation of the Angle of Incidence of the Bombarding Ions* — The measurements which we have described were carried out with normal incidence of the ions upon the target The apparatus is so constructed that the angle of incidence could be varied by rotating the ground joint which carried the target

The secondary emission was found to increase with the angle of incidence of the ions * The results of a series of measurements with a nickel target are graphically depicted in fig 6 A very good straight line is obtained from all the measurements so far made, if the total emission is plotted against the cosine of the angle of incidence, for a hot or for a gas-covered surface The emission is therefore proportional to $(1 - \cos \theta)$ This law was found to hold for a molybdenum surface polished to a good mirror, or for a nickel surface polished very roughly with fine emery paper It was not possible to carry the measurements to very glancing angles, owing to the finite width of the beam of ions, which caused some of them to miss the target at angles of incidence greater than about 60°

---

* This increase of electron emission with angle of incidence has been observed by Saxen, 'Ann Physik,' vol. 38, p 319 (1912), in the case of relatively fast canal rays

(c) *The Velocity Distribution of the Secondary Electrons*.—The energy distribution of the secondary electrons was determined both by the retarding potential method and by the magnetic deflection method of analysis. A large number of curves have been obtained under very varying conditions of the target surface, and for a large range of energy of the incident ions. The magnetic method fails for velocities below about 2·8 volts, probably on account of uncompensated magnetic fields, or to contact potential differences due to different gas-conditions of the target and slits. Contact potentials between the target and the collecting sphere in the retarding potential apparatus were eliminated by heating the target to about 1200° C., at which temperature the thermionic electron emission from the large area could be detected on a sensitive galvanometer, and determining the potential difference which would just prevent emission. The correction for contact potential was usually of the order of 0·4 volt, the collecting sphere being negative with respect to the target. The same correction was determined experimentally for a cold target by illuminating strongly with light from an arc and using the photoelectric characteristic, or by observation of the known velocity distribution of the

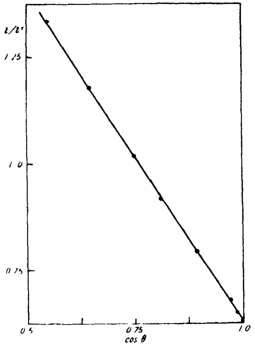

FIG. 6.

electrons liberated by the impact of metastable atoms of helium formed in the canal of the discharge tube * The magnetic apparatus was calibrated absolutely by calculation from the dimensions of the box and the Helmholtz coils, a check being obtained by determining the current required to neutralise the earth's known horizontal component The earth's field was neutralised by suitable pairs of coils, the residual field over the box being less than ½ per cent of the normal intensity

With a cold target, or one which had not been strongly heated for some time, the velocity distribution curve was very like that found for the electrons liberated by metastable atoms of helium † Typical curves for a molybdenum target are given in fig 7 The form of the energy distribution appeared to be practically independent of the velocity of the impacting ions in the range from 120 to 1000 volts

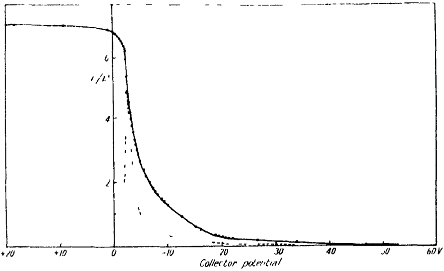

FIG 7 —Retarding Potential Curve for the Electrons set free from a gas covered surface of Mo by He⁺ ions of 400 volts energy The dotted curve is the velocity distribution derived from it

After long continued heat treatment of the target, and purification of the helium, the velocity distribution curve changed its character The total number of electrons ejected was smaller than for a gas-covered surface, but the relative number possessing the higher energies increased considerably (fig 8) The curve was no longer smooth, but exhibited a number of maxima,

---

* *Loc cit*, p 13, footnote

† *Loc cit.*

the most prominent, and most consistent in occurrence, being at 2 5, 6 8, 17 0 and 20 volts There was a very sharp cut-off at approximately 20 2 volts, while the retarding potential curve revealed a low velocity cut-off, almost as pronounced, at 2 3 volts The position of these maxima, as well as of the upper and lower limits, did not differ by more than a fraction of a volt for the three materials for which they have been obtained, Ni, Mo and W There is some evidence of their presence with a platinum target, but Al, Cu and Ag gave a smooth curve of the type obtained with gas-covered Ni or Mo These materials are very difficult to outgas thoroughly without melting them Molybdenum, however, gave by far the most consistent results of any material tested, and the results obtained for this metal are given in the graphs in this paper

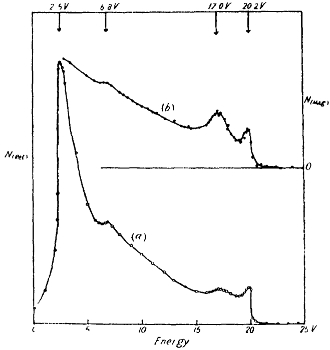

FIG 8—Velocity Distribution Curve for thie Electrons liberated from gas free Mo by He$^+$ ions of 400 volts energy (a) Retarding Potential Method (b) Magnetic Analysis.

It was not possible to retain liquid air on the trap between the diffusion pump and the apparatus overnight, so that when starting a run in the mornings a certain amount of mercury vapour was always found to have diffused over into the discharge chamber O, fig 1. This was soon swept away if the apparatus was heated to about 200° C and the helium allowed to circulate for 15 minutes or so, and its removal could be followed by observation of the spectrum from the arc If an experiment was carried out with the composite beam of He$^+$ + Hg$^+$ + the velocity distribution of the secondary electrons was found to be very much changed The number of electrons possessing energies in the neighbourhood of zero increased enormously relative to the higher velocities, while the total emission produced was much smaller than for pure helium ions A distinct change of slope in the velocity distribution curve was found at very nearly 6 volts, if the target were well degassed (fig 9) A trace of impurity which could only just be detected spectroscopically, completely destroyed the clear-cut character of the distribution curve produced by He$^+$ ions Indeed, it was only after purification had been carried out for several hours after the spectroscopic disappearance of impurities that the curve assumed its final form as shown in fig 8

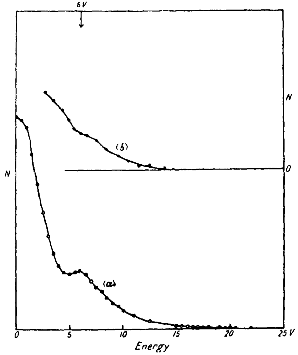

Fig 9—Energy Distribution for the Electrons set free from hot Mo by He$^+$ + Hg$^+$ + Hg^{++} + (a) Retarding Potential Method (b) Magnetic Analysis

The intensity of the 20-volt maximum increased with the velocity of the ions With an accelerating potential of 200 volts it was just noticeable, while at 400 volts it was very pronounced and exceedingly sharp, fig 10 At potentials greater than about 700 volts the maximum began to spread, mainly

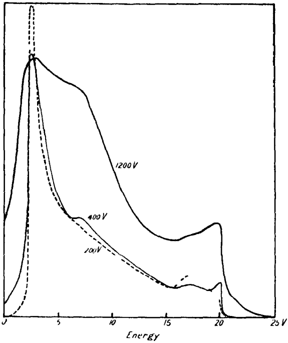

FIG 10—Energy Distribution of the Electrons liberated from degassed Mo by He$^+$ ions of various energies (Retarding Potential Method)

towards the low velocity side, till at 1200 volts the curve had assumed the shape plotted in the graph The lower energy portion of the distribution curve did not undergo any radical change with the energy of the bombarding ions below 1500 volts, but above this it began to spread, becoming very diffuse at 5000 volts

Experiments with Alkali Ions

It is shown in the second portion of this paper that the emission of secondary electrons is profoundly influenced by the relative values of the ionisation potential of the atom from which the bombarding ion originated, and the work function of the struck surface The cases which we have so far considered were such that the ionising energy was far greater than the work function of the surfaces, and it is desirable to have results obtained when this position is reversed For this reason some experimental curves are given which show the velocity distribution among the electrons ejected from various surfaces by singly charged potassium ions from a thermionic source The apparatus used has already been described,* and the retarding potential curves given in fig 2 were obtained at the same time as the experimental results given in that paper

It is apparent that even at 600 volts energy K^+ ions are able to set free considerable numbers of electrons with energies greater than 5 volts, from platinum or nickel surfaces There appears to be a greater relative number of low velocity electrons from an aluminium surface than from nickel or platinum, whose work functions are considerably higher An untreated surface of any metal, freshly introduced into the apparatus, always gives a much greater emission than a cleaner one, but the relative number of the high velocity electrons is small Surface factors which increase the magnitude of the emission always tend to decrease the relative number of the electrons with higher energies This is also true of the electron emission produced by He^+

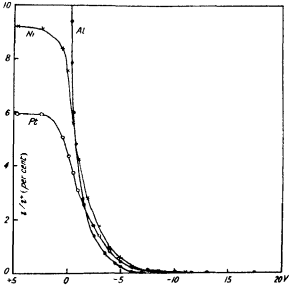

Fig 11 —Retarding Potential Curves for the Electrons set free from various metals by K^+ ions of 600 volts energy

The maximum of the velocity distribution curve, for the electrons liberated by the impact of low velocity alkali ions, always occurs in the neighbourhood of zero energy There is a greater probability that an electron will possess just sufficient energy to escape from the surface than that it should escape with any considerable velocity (The fact that a collecting potential of a volt or so is required in order to collect the total emission on the bulb is probably due to the contact differences of potential which exist between the bulb and the target, and to the uncompensated magnetic field of the earth) The general form of the energy distribution did not change much with the energy of the ions, a slow increase in the relative number of higher velocity electrons taking place as the energy increased, but the curves remained exponential to the volt axis

---

* Oliphant, 'Proc Camb Phil Soc,' vol 24, p 451 (1928)

Conclusion

A theoretical discussion of the process of neutralisation of positive ions at metal surfaces is given in the second part of this paper, and the experimental results here presented satisfactorily explained, at least qualitatively Further experiments are needed before a satisfactory attempt can be made to apply these results to the problems of the cathode region of the electrical discharge through gases, and some of these are at present being carried out with the collaboration of Mr P B Moon.

I wish to express my thanks to Prof Sir Ernest Rutherford for his encouragement and help

The Liberation of Electrons from Metal Surfaces by Positive Ions
Part II —*Theoretical*.

By M L E Oliphant, Trinity College, and P B Moon, Sidney Sussex College, Cambridge

(Communicated by Sir Ernest Rutherford, P R S —Received February 27, 1930)

Introduction

In this paper we propose to consider the process of electron capture by positive ions at a metal surface, and the emission of electrons which occurs as a secondary phenomenon The discussion which we venture to give is admittedly crude, and it is to be hoped that an adequate theoretical treatment of the problem will not be long delayed

As a preliminary we shall discuss some aspects of present knowledge regarding electrical conditions near metal surfaces Recent experiments of Compton and van Voorhis* suggest that positive ions capture an electron from a metal before making thermal contact with the surface, so we require to know the nature of the electric field at some distance from the mechanical boundary We shall proceed to some calculations on the probability of neutralisation, basing our work on the supposition that neutralisation is due to auto-electronic emission under the influence of the electrostatic field of the approaching positive ion † We shall then discuss the phenomenon from the viewpoint of the transition of an electron through a potential barrier between two states of equal energy, and attempt to apply the results obtained to an explanation of the mechanism of secondary electron emission

1 --*Electrical Conditions near a Metallic Surface*

(1) According to the theory of metallic conduction developed by Sommerfeld,‡ the free electrons have at ordinary temperatures an energy distribution not appreciably different from that at absolute zero, which is given by

$$n(\varepsilon)\, d\varepsilon = \frac{4\pi (2m)^{\frac{3}{2}}}{h^3}\, \varepsilon^{\frac{1}{2}} d\varepsilon, \tag{1}$$

---

* Compton and van Voorhis, ' Proc Nat Acad Sci ,' vol 13, p 336 (1927), van Voorhis, ' Phys Rev ,' vol 30, p 318 (1927)

† The suggestion that electron emission is due to electrostatic attraction was made by Holst and Oosterhuis, ' Physica,' vol 1, p 82 (1921), and by Dauvillier, ' J Physique, vol 7, p 369 (1926)

‡ Sommerfeld, ' Z Physik,' vol. 47, p 1 (1928)

up to a maximum value, μ, of ε such that

$$\mu = \frac{h^2}{8m}\left(\frac{3n_0}{\pi}\right)^{2/3} \tag{2}$$

Here $n(\varepsilon)\,d\varepsilon$ is the number of electrons per cubic centimetre having kinetic energies between ε and $\varepsilon + d\varepsilon$, n_0 the total number of free electrons per cubic centimetre, m the mass of an electron, and h Planck's constant.

In order that the electrons shall not escape from the metal their potential energy in the interior, relative to that in free space, must be negative and numerically not less than μ. The statistical theory is not concerned with the mechanism responsible for this potential barrier, nor does it either predict or deny that the height of the barrier should exceed μ by a finite amount—the "work function," here denoted by ϕ and, unless otherwise stated, measured in ergs. From the point of view of the Sommerfeld theory, the existence of a work-function is a purely experimental fact, due to the particular mechanism responsible for the potential barrier. Frenkel,* however, has obtained, on the basis of the virial equation, the relation $\phi = \frac{1}{5}\mu$. Experimental values of $\mu + \phi$ are most definite in the case of nickel, for which the total potential difference is about 18 volts, corresponding on Frenkel's theory to $\phi = 3$ volts. Actually $\phi = 4 \cdot 3$ volts.

(2) *The "Image-force" Hypothesis*.—In calculations on the passage of electrons through the barrier it is usual to assume either that the potential jump is perfectly sudden or, as a second approximation, that it is entirely due to the "image-attraction" on the escaping electron, this attraction being assumed to cease suddenly at a distance x_0 from the surface such that

$$\int_{\infty}^{x_0} \frac{e^2}{4x^2}\,dx = \text{total potential difference} = \mu + \phi$$

It is almost certain that the image-force hypothesis is physically correct at comparatively large distances (*e g*, greater than 2×10^{-7} cms) from the surface, it is in excellent agreement with the observed lack of saturation of thermionic emission as the accelerating field increases.† However, in order to account for a potential jump of the order of 20 volts, x_0 must be about 2×10^{-9} cms, and it is clear that at such distances the structure of the surface (lattice spacing about 2×10^{-8} cms) will be of fundamental importance, and that the image force hypothesis would appear to become invalid. It should be mentioned, however, that experiments on electron diffraction show that electrons much faster than those here considered react not with one but with many points of the crystal lattice. We are here considering electrons whose de Broglie wave-lengths are larger than the lattice spacing, and they should react with even more atoms, while diffraction effects will not be of great importance. It is thus possible that the structure of the surface is not so important as might at first sight appear. For simplicity it will be necessary to ignore the structure in most of the following discussion.

---

* Frenkel, 'Z Physik,' vol 49, p 39 (1928)

† *E g*, Pforte, 'Z Physik,' vol 49, p 333 (1928), de Bruyne, 'Roy Soc Proc,' A, vol. 120, p 423 (1928)

The validity of the image-force hypothesis must also be very seriously limited by the high velocity of the escaping electron; for the response of the other electrons to the repulsion of the electron considered cannot be instantaneous. Kronig* calculates the "time of relaxation" of the metallic electrons to be of the order of 10^{-14} seconds, during which time a 1-volt electron will travel about 6×10^{-7} cms. It will thus be seen that the attractive force on the electron will lag behind the equilibrium value postulated by the simple theory, and that this lag will be serious at distances from the surface of 10^{-7} cms and below, *i.e.*, just the distances at which the image attraction would begin to have an appreciable value.

Again, the image-force is an *attraction* towards the surface for both electrons and positive ions; it cannot be the only force acting, for a positive ion (*e.g.*, of cæsium) can remain in equilibrium outside the metal surface while an electron will be absorbed into the metal. At small distances from the surface, therefore, an electron will be attracted by the metal while a positive ion is repelled.† A probable explanation of this is discussed below.

(3) *Electron Densities near Metal Surfaces.* It is important to realise that a large part of the potential barrier which binds the electrons to the metal may be regarded as a space charge effect.‡ For if no barrier existed, electrons from the metal would begin to escape into the surrounding space with kinetic energies between 0 and μ, and so would establish outside the surface a negative space charge which would greatly limit the rate of escape. That is to say, a potential barrier would automatically build up whose height would approach μ. Once this barrier were formed, the rate of escape of electrons would remain small and such as to maintain the barrier. This, of course, is the classical space-charge argument; it may not apply strictly to the present case, for

---

* Kronig, 'Roy. Soc. Proc.,' A, vol. 124, p. 409 (1929).

† This fact can be utilised to explain very satisfactorily the form of the scattering of positive ions from metal surfaces.

‡ Frenkel, 'Z. Physik,' vol. 51, p. 232 (1928).

the scale of the phenomenon is less than the wave-length of the electron waves concerned

It should be emphasised that it is not legitimate to superimpose, at any one point of space the image force upon the forces due to space charge, for the two hypotheses are alternative approximations to a full consideration of the mutual interaction of the electrons concerned We are interested in the electrical forces acting on one particular electron (or positive ion, as the case may be) which is under the influence of the other charges (mobile electrons and fixed positive lattice) which constitute the metal Let us call this electron B In order to solve the problem exactly we should require the initial positions and velocities of all particles concerned we should then write down the equation of motion of each particle, including B*, each equation would involve the instantaneous position of every other particle Solving these simultaneous equations, and using the known initial conditions, we could in theory obtain the position of each particle including B and the forces acting on it, at any time in the history of the system This is a hopeless task but in two particular cases we can obtain reasonable approximations to the forces acting on B

(*a*) If the particles are very close together, we may treat the system as a continuous massive electric fluid—*i e*, we may apply the space-charge treatment—and obtain the potential at any point Note that in doing so we have allowed for the effect of B on the rest of the system, for B is now represented by a portion of the fluid

(*b*) If B is in an isolated position at some distance from the main system of particles, we may proceed as follows We divide the interactions of the particles into three parts —

(i) The mutual interaction of all particles except B
(ii) The polarising effect of B on the rest of the system
(iii) The effect of the remainder of the system on B

We observe that if B were absent there would be no field at the point in question, since the point is outside the cloud of particles and the metal has no net charge We conclude that the only field acting on B is due to that portion of (iii) which is a consequence of (ii), and as an approximate method of calculation we apply the macroscopic law that the metal surface remains equipotential, finally arriving at the " image force " law

---

* For simplicity we here consider classical particle mechanics

We may thus regard part of the potential barrier near to the surface, and having a height approaching μ, as due to space charge , the portion which occurs furthest from the surface is to be regarded as due to image force, and the intermediate portion is not calculable, but may be derived by extrapolation of data from both main regions Roughly speaking, that portion up to a height μ may be taken as space-charge effect, and the remaining ϕ as due to image force

Numerical calculations based on the space-charge theory are open to grave suspicion, for the neglect of the structure of the surface and of the discrete nature of the electron is, despite the considerations put forward above on p 390, a very serious defect We have, however, little doubt as to the fundamental soundness of the idea , it is in good qualitative agreement with the present belief that positive ions, but not electrons, can remain in equilibrium outside a metal surface, for the space-charge force is an attraction for electrons and a repulsion for positive ions, while the image force is an attraction for both (see fig 1)

Calculation shows that the space-charge field varies very rapidly with distance from the surface, nearly the whole space-charge effect taking place within 10^{-8} cm of the surface * That is to say, the first part of the potential

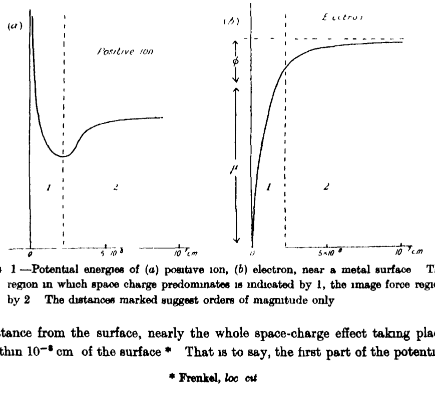

FIG 1 —Potential energies of (a) positive ion, (b) electron, near a metal surface The region in which space charge predominates is indicated by 1, the image force region by 2 The distances marked suggest orders of magnitude only

---

* Frenkel, *loc cit*

barrier rises more sharply than if the whole barrier obeyed the image-force law This is of importance for our subsequent calculations

2 —*Neutralisation of Positive Ions through Autoelectronic Emission*

The electric field at a metal surface due to a positive ion at a distance of 10^{-7} cms from the surface reaches the large value of 3×10^7 volts per centimetre , it is clear that the autoelectronic emission under the influence of this field will be large and may be sufficient to provide a mechanism for neutralisation of the ion We give an outline of calculations which lead to the conclusion that one electron will, on the average, be extracted by the field before the ion has approached nearer the surface than two atom diameters, so that the ion has a large probability of becoming neutralised before actually reaching the surface Two formulæ for calculating autoelectronic emission are available That of Fowler and Nordheim* is based on the assumption of a perfectly sharp potential barrier which becomes narrowed, but not decreased in height, by the external field They obtain for the current density due to a field F the value

$$\frac{e^3}{2\pi h} \; \frac{\mu^{\frac{1}{2}} F^2}{(\phi + \mu)\, \phi^{\frac{1}{2}}} \; e^{\frac{4\kappa\phi^{\frac{3}{2}}}{3Fe}}, \tag{3}$$

where

$$\kappa^2 = 8\pi^2 m/h^2$$

Nordheim† finds that if the potential barrier has the form calculated on the pure image-force hypothesis, so that the barrier is lowered as well as narrowed by the field, then the exponent in (3) becomes

$$-\frac{4}{3}\frac{\kappa\phi^{\frac{3}{2}}}{Fe}\;V,$$

where V is a function of $e\sqrt{F}/\phi$, lying between 0 and 1, which is tabulated in his paper $V \rightarrow 1$ as $F \rightarrow 0$, so that for weak fields the two expressions are in agreement When $e\sqrt{F}/\phi = 1$, i e , when the external field has lowered the height of the potential hump from $\mu + \phi$ to μ, $V = 0$, we shall assume that for greater fields the exponent remains zero, and shall thus underestimate the current A conservative estimate is desirable and the underestimation will not be serious, for the following reasons —

(1) There will be no *discontinuity* of the emission at this critical point ‡

---

* Fowler and Nordheim, 'Roy Soc Proc ,' A, vol 119, p 173 (1928)

† Nordheim, 'Roy Soc Proc ,' A, vol. 121, p 626 (1928)

‡ Fowler, 'Roy Soc Proc ,' A, vol 122, p 36 (1928)

(2) The space-charge theory indicates that the inner part of the potential barrier—from 0 to μ—rises very suddenly, so that increase of the field beyond the critical point will not greatly decrease the height of the potential barrier

(3) Nordheim's formula will tend to overestimate the emission for strong fields owing to his assumption that the potential barrier does not commence until the electron has travelled a small distance (about 2×10^{-9} cm) from the surface

(4) We shall not need to consider fields greatly in excess of the critical value

The discussion of §1 indicates that the Nordheim formula is more likely to be correct than that of Fowler and Nordheim, but we first sketch the calculations based on the latter formula, which is more easily handled We find that in ordinary cases neutralisation will not take place until the ion is so close that the two formulæ differ greatly, though in exceptional cases the simpler calculation will be of importance The calculations are extended to closer distances of approach on the basis of the Nordheim formula

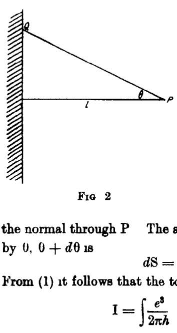

Fig 2

(*a*) *Calculations on Fowler - Nordheim Theory*—The field at a point Q on a metal surface, due to a positive ion at P (fig 2) is

$$F = 2e \cos^3 \theta / l^2, \tag{4}$$

where l is the distance of the ion from the surface and θ is the angle between PQ and the normal through P The area of an annular element of the surface defined by θ, $\theta + d\theta$ is

$$dS = 2\pi l^2 \tan \theta \quad \sec^2 \theta \quad d\theta \tag{5}$$

From (1) it follows that the total electron current from the surface is

$$I = \int \frac{e^3}{2\pi h} \; \frac{\mu^{\frac{1}{2}}}{(\phi + \mu)\,\phi^{\frac{1}{2}}} \,.\, F^2 \,.\, e^{-\frac{4\kappa\phi^{\frac{3}{2}}}{3Fe}} \,.\, dS, \tag{6}$$

the integral being taken over the surface of the metal

Substituting the values of F and dS from (4) and (5), putting

$$\sec^3 \theta = x, \quad 4e^4 \mu^{\frac{1}{2}}/3h\,(\phi + \mu)\,\phi^{\frac{1}{2}} = C, \quad 2\kappa\phi^{\frac{3}{2}}/3e^2 = a$$

we get

$$I = \frac{Ce}{l^2} \int_1^\infty x^{-\frac{1}{2}}\, e^{al^2x}\, dx$$

The total charge extracted by the ion as it moves with velocity v normal to the surface from infinity to a distance l_0 will be

$$\int I\, dt = \int_{l_0}^{\infty} \frac{I\, dl}{v} = \frac{Ce}{v}\int_{l_0}^{\infty}\int_{1}^{\infty} l^{-2} x^{-\frac{7}{3}} e^{-al^2x}\, dl\; dx$$

and the number of *electrons* emitted will be

$$N = \frac{C}{v}\int_{l}^{\infty}\int_{1}^{\infty} l^{-2} x^{-\frac{7}{3}} e^{-al^2x}\, dl\; dx \tag{7}$$

Exact integration in finite terms is impossible, in order to perform the x integration we integrate by parts repeatedly and obtain an asymptotic series, retaining the first term only we get an upper limit The approximation is good if $al^2 \gg \frac{7}{3}$, it will fail completely when $al^2 < 1$ Numerical values show that the failure occurs at $l = 6 \times 10^{-8}$ cm for the case of a sodium surface and at 3×10^{-8} cm for nickel or tungsten

To this approximation we get

$$N = \frac{C}{v}\int_{l}^{\infty} \frac{1}{al^2}\, e^{-al^2}\, dl$$

or, putting $l^2 = y$,

$$N = \frac{C}{2a}\int_{l}^{\infty} y^{-\frac{3}{2}}\, e^{-ay}\, dy \tag{8}$$

We obtain an upper limit to this integral by the same method as before, the limits of applicability being almost identical

The final result is

$$N = C l_0^{-3} e^{-al_0^2}/2a^2 \tag{9}$$

If ϕ and μ are expressed in volts, then

$$C = 6.62\, \mu^{\frac{1}{2}}/(\phi + \mu)\, \phi^{\frac{1}{2}} \quad \text{and} \quad a = 2.53 \times 10^{14} \phi$$

Take now a favourable case, that of a 10-volt potassium ion ($v = 6.5 \times 10^5$ cms per second) approaching a surface whose work function is 2.5 volts If we put $\mu = 5$ volts (the final expression is very insensitive to variations in μ), and take the smallest allowable value of l_0, viz, 6×10^{-8} cms, we get $N = 0.35$, which shows that even in this case the theory breaks down before neutralisation becomes highly probable When v is smaller, i e, for very heavy ions of low energy, and in particular for oblique incidence, equation (9) will, of course, become applicable

(*b*) *Calculation on Nordheim Image force Formula* —As indicated earlier the calculation falls into two parts, according to whether the field of the ion is or is not sufficient to reduce the work function below zero over any part of the surface If the normal work function is 4 5 volts (Ni, Mo, W) the critical distance of the ion from the surface is 4×10^{-8} cms , while for a work function of 2 volts the critical distance is 10^{-7} cms By approximate integration, taking care to overestimate the emission, we can show that, except in the case of very slow ions, it is unlikely that an electron will be extracted before the critical distance has been reached We therefore need to consider the case where the exponent in the emission formula vanishes over part of the surface It is easy in this case to obtain upper and lower limits to the emission which are sufficient for our purpose For we can (*a*) overestimate the emission by assuming the exponent to be zero over the whole surface, and (*b*) underestimate the emission by neglecting that part of the surface over which the exponent is not zero

Consider as before a positive ion at a distance l from a metal surface (fig 2) The exponent in the emission formula will be zero for all parts of the surface for which $e\sqrt{\mathrm{F}}/\phi > 1$ Since the field F is $2e \cos^3 \theta/l^2$ it follows that the exponent is zero for values of $\sec\theta$ less than $\sqrt[3]{2}\,(e^2/\phi l)^{\frac{2}{3}}$ We now calculate the total autoelectronic current, assuming the current density to be

$$\frac{e^3}{2\pi h}\,\frac{\mu^{\frac{1}{2}}}{(\phi+\mu)\,\phi^{\frac{1}{2}}}\quad \mathrm{F}^2 \tag{10}$$

To obtain the upper limit we integrate over the whole surface , for the lower limit we integrate over that part of the surface for which θ is less than

$$\sec^{-1}\sqrt[3]{2}\;(e^2/\phi l)^{\frac{2}{3}}$$

We have as in (6) $\mathrm{F} = 2e/l^2 \sec^3\theta$, area of elementary ring

$$= 2\pi l^2 \sec^2\theta \quad \tan\theta \quad d\theta$$

Hence

$$\begin{aligned}
\text{current I} &= \int \frac{e^3}{2\pi h}\frac{\mu^{\frac{1}{2}}}{(\phi+\mu)\,\phi^{\frac{1}{2}}}\quad \frac{4e^2}{l^4\sec^6\theta}\quad 2\pi l^2\sec^2\theta \quad \tan\theta \quad d\theta, \\
&= \frac{4e^5}{l^2 h}\quad \frac{\mu^{\frac{1}{2}}}{(\phi+\mu)\,\phi^{\frac{1}{2}}}\int\frac{\tan\theta}{\sec^4\theta}\;d\theta, \\
&= \frac{4e^5}{l^2 h}\quad \frac{\mu^{\frac{1}{2}}}{(\phi+\mu)\,\phi^{\frac{1}{2}}}\int y^{-5}\,dy, \quad \text{where } y = \sec\theta, \\
&= \frac{e^5}{l^2 h}\quad \frac{\mu^{\frac{1}{2}}}{(\phi+\mu)\,\phi^{\frac{1}{2}}}\Big[y^{-4}\Big]_{y_1}^{y_2}
\end{aligned} \tag{11}$$

The limits of integration are in the case of our upper limit, 1 and ∞ , for our lower limit they become 1 and $\sqrt[3]{}/2\,(e^2/\phi l)^{\frac{1}{2}}$ To obtain the number of electrons emitted per second we divide by e and thus get

$$\left.\begin{array}{r}\text{Number of electrons}\\ \text{emitted per second}\end{array}\right\} = \frac{e^4}{l^2h}\,\frac{\mu^{\frac{1}{2}}}{(\phi+\mu)\,\phi^{\frac{1}{2}}} \quad \text{(upper limit)}$$

$$= \frac{e^4}{l^2h}\,\frac{\mu^{\frac{1}{2}}}{(\phi+\mu)\,\phi^{\frac{1}{2}}}\left[1-\frac{1}{2^{\frac{1}{2}}}\left(\frac{\phi l}{l^2}\right)\right] \quad \text{(lower limit)} \qquad (12)$$

Numerical values calculated from equations (12) are shown graphically in fig 3, the upper and lower limits to the emission at various distances being

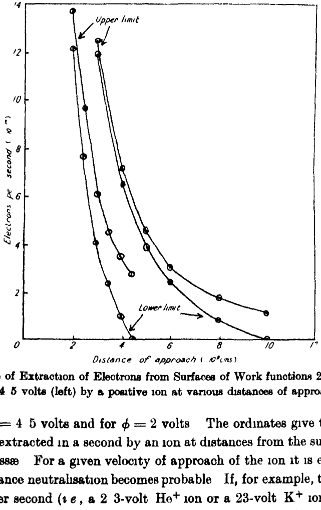

Fig 3 —Rate of Extraction of Electrons from Surfaces of Work functions 2 volts (right) and 4 5 volts (left) by a positive ion at various distances of approach

given for $\phi = 4\ 5$ volts and for $\phi = 2$ volts The ordinates give the number of electrons extracted in a second by an ion at distances from the surface given by the abscissæ For a given velocity of approach of the ion it is easy to find at what distance neutralisation becomes probable If, for example, the velocity is 10^6 cm per second (*i e*, a 2 3-volt He$^+$ ion or a 23-volt K$^+$ ion) then the number of squares below the appropriate graph gives the number of electrons emitted. For $\phi = 4.5$ volts we see from the lower limit graph that the emission will amount to one electron by the time the ion has approached to a distance of 3.6×10^{-8} cm. Since this is a lower limit we conclude that neutralisation is quite likely at an even greater distance from the surface, but the numerical integration referred to above shows that it will probably not occur at a greater distance than 4.0×10^{-8} cms. The calculations therefore give a quite well-defined position at which neutralisation becomes probable. It must, of course, be remembered that the emission of electrons will be to some extent a random process, so we must not conclude that every ion will become neutralised at or near this position, or even before reaching the surface. The only conclusion which we draw is that on this view of the mechanism of neutralisation it is probable that most slow ions will be neutralised before reaching the surface.

3.—*The Neutralisation of a Positive Ion at a Metal Surface, considered as a Transition of an Electron between States of Equal Energy.*

The autoelectronic mechanism considered above provides an approximate method of calculating the probability that an electron shall pass from a metal surface to an ion in its neighbourhood, but ignores the difference in potential energy (ionisation potential) of different kinds of ion. A treatment which is physically more correct, though less suited to approximate calculation, is to regard the process as the transition through the potential barrier of an electron of given energy, from the metal to a state of equal energy associated with the ion.

Consider the way in which the energy of an electron varies between a metal surface and an ion near the surface; that is, let us map out the field by a curve which represents at every point the energy required to remove an electron to infinity. As before, we idealise the metal surface to a true plane. Then for a positive ion at a considerable distance from the surface the possible energies of an electron lie on a Coulomb curve, with an abrupt ending at the ground level energy of the neutral atom (fig. 4A). Between any possible position of an electron associated with the ion, and the similar state in the metal, there exists a potential barrier. Unless the ion approaches very closely to the surface the height of the barrier will be greater than μ, the maximum kinetic energy of the electrons in the metal, so that classically no electron could leave the metal and reach the ion. According to wave-mechanical conceptions, however, there is a finite probability that an electron with a given energy in the metal will make a transition through the potential barrier to a state of

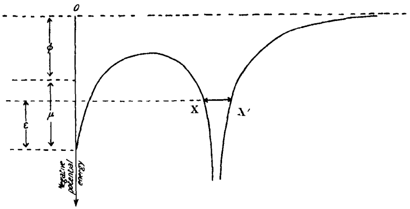

FIG 4A

equal energy X, associated with the ion The chance that an electron in any small energy range will make the transition will depend upon several factors

(1) The relative abundance of electrons of that particular energy in the metal,

(2) The width (and height) of the potential barrier,

(3) The existence of a more or less stable state of equal energy in the ion

The first two factors appear quite naturally, but the significance of (3) is a little less clear It is quite possible that transitions do take place for electrons whose energy does not correspond with that of a stationary state in the ion but in this case the electron wave-packet will not fit exactly between X and X′, and consequently it is reflected back to the metal at once, from the outer barrier at X′ On the other hand, if X is a characteristic energy level of the atom, the electron will almost certainly be captured and remain with the ion A transition back to the metal after a finite time will probably be ruled out by the re-establishment of the degenerate Fermi distribution of energies, which would allow no vacant "phase-cell" within that range in the metal Since the energy levels have a finite "width" the probability of capture will fall off very rapidly but not infinitely rapidly, for energies on either side of the characteristic value, while the perturbation of the ion-field by the surface will possibly serve to make the levels neither so sharp nor of exactly the same energy as those associated with the free atom

(*a*) The probability that the potential barrier is penetrated depends only on the kinetic energy of an electron, while the energy level in the ion to which it will go depends upon the total energy, *i e*, upon the sum of the negative potential energy and the positive kinetic energy The high energy levels associated with the ion are those which extend farthest from it, so that effectively the "width" of the barrier is smallest for the electrons in the metal which have greatest kinetic energy These electrons are just those which are most abundant, so that every condition tends to increase the probability that it is one of these electrons which makes the transition across the barrier from the metal to the ion We should expect, then, that the ion would capture an electron into the nearest stationary energy level corresponding to an energy of $V_i - \phi$

This conclusion receives considerable support from some experiments described by one of us * Helium ions which collide with an outgassed surface of platinum or nickel at a glancing angle escape largely as neutral atoms in the metastable state The ionisation potential of helium is 24 6 volts, and ϕ for outgassed platinum in contact with a rare gas is 4 77 volts † The helium ions would capture electrons most easily into the 24 6 — 4 77 = 19 83 volt level, and the nearest lower *stable* state is at 19 77 volts, the metastable $2\,^3S$ level for helium The difference of 0 06 volt may be no greater than the "width" of the perturbed energy level

Exact calculation of this type of transition involves considerable mathematical difficulty, and we have been unable to obtain a solution to the problem In the strong field calculations we ignored completely the ionisation energy of the ion, which means that the probability of neutralisation which we obtain is independent of the kind of ion involved However, the theories are agreed in asserting that there exists a probability that a positive ion whose ionisation energy is greater than the work function of a metal surface can capture an electron while at some distance from the conductor, to give an excited atom

(*b*) If the ion is moving very quickly it may penetrate very closely to the surface before being neutralised For very close distances of approach the electron energy diagram becomes of the form shown in fig 4B

We have given reasons for assuming that the field of the ion will not lower the potential barrier at the surface of the metal much below a height μ, but an increased field, owing to close approach of the ion, will render it very narrow Electrons in the metal with energy μ can now reach the ion without penetrating any barrier Effectively, then, the ion is inside the region of action of the work function ϕ If the ion penetrates completely through the potential barrier and into the lattice itself before neutralisation takes place, the conditions of capture become analogous to those for electron capture by ions in free space That is to say, an electron of zero energy will probably be captured

---

* Oliphant, 'Roy Soc Proc,' A, vol. 124, p 228 (1929)

† Compton and Van Voorhis, *loc cit*

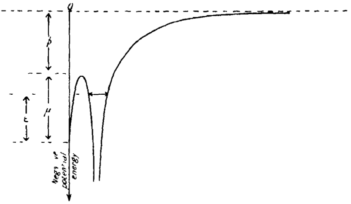

Fig 4B

at first into an extreme outer level of the atom, corresponding to the ionisation potential V_i * In both these cases there now exists, however, a much greater probability of capture of a lower energy electron into an energy state in the atom less than $V_i - \phi$, owing to the extreme narrowness or to complete penetration of the potential barrier

(c) If the ionisation potential of the ion atom is less than the work function of the surface, there are no electrons in the metal of kinetic energy great enough to occupy any of the available energy levels of the ion Also, if the ion should capture an electron, the transition back to the metal would be very probable for there are vacant phase cells of energy greater than μ This is in accord with an observation of ours, that positive ions of the alkali metals, when fired upon hot, gas-free surfaces of high work function, largely escape again as positive ions (It is well known, of course, that a hot metal surface will ionise the alkali metals by removing electrons from atoms which collide with it)

4 *The Emission of Secondary Electrons*

(*a*) *Emission due to the Potential Energy of the Ions* —In the preceding paragraphs we have shown that there is a finite probability that a positive ion approaching a metal surface will capture an electron from the metal before making contact, and give an excited atom This excited atom, of potential energy $V_i - \phi$, will collide with the surface after a very short interval of time (after 10^{-12} seconds if it were neutralised at 10^{-7} cms from the surface, and possessed a velocity of only 10^5 cms per second, of the order of thermal velocities) It is improbable, therefore, that the excited atom will lose its potential energy by radiating However, after reaching the metal, or the electron atmosphere just outside it, it will be very likely to hand over its energy to an electron in a collision of the second kind If the electron then possesses a total energy greater than the height of the potential barrier, it will be able to escape from the metal, the energy with which it is ejected being given by

---

* *Cf* Seeliger, 'Phys Z,' vol 30, p 329 (1929)

$$V_e = (V_i - \phi + \varepsilon) - (\mu + \phi),$$

i e , will lie within the limits defined by ε, i e ,

$$\left.\begin{aligned} V_{e\,(\min)} &= V_i - \mu - 2\phi \\ V_{e\,(\max)} &= V_i - 2\phi \end{aligned}\right\} \tag{13}$$

and

Thus, in the absence of straggling, we would expect a sharp cut off at both the low velocity and high velocity limits of the energy of emission Of course the low velocity limit would only be observed when $V_i > \mu + 2\phi$ i e , in practice, > about 20 volts The probability of the collision of the second kind will fall off rapidly as the energy which has to be dissipated as kinetic energy of the electron increases, so that a distinct maximum in the number emitted would be expected in the neighbourhood of the minimum energy This is off-set by the preponderance of electrons with negative potential energy in the neighbourhood of ϕ in the metal and particularly in the electron space-charge just outside the surface, so that a considerable number may still be observed in the neighbourhood of the maximum energy

We have seen that the ion may penetrate through the potential barrier before it captures an electron, and in that case would form a transient excited atom of energy V_i This excited atom would at once react with a second electron, giving a normal atom and an electron with considerable energy In the absence of straggling the limits of the energy with which the electron could escape from the metal would be given by

$$\left.\begin{aligned} V_{e\,(\min)} &= V_i - \mu - \phi \\ V_{e\,(\max)} &= V_i - \phi \end{aligned}\right\} \tag{14}$$

In a system as closely packed with free and bound electrons as the interior of a metal, we might expect that the probability of a three body collision, in which two electrons react simultaneously with the ion, would be large For instance, reaction with two electrons of energy μ in the metal might lead to an ejected electron of energy $V_i + \mu - \phi$, considerably greater than the maximum given by equation (14)

Comparison with Experiment These predictions may be compared with the results, given in the preceding paper, for the energy distribution among the electrons liberated from clean molybdenum surfaces by He^+ ions of low velocity Here $V_i = 24$ 6 volts, $\mu = 13$ 5 volts,* $\phi = 4$ 3 volts Thus for ions which capture electrons before reaching the surface the energy limits are $V_{e(\min)} = 2$ 5 volts, $V_{e(\max)} = 16$ 0 volts (equation (13)) The experimental curves show a very sharp cut-off at 2 3 volts (fig 8, Part I), and in accordance with theory, a maximum number of electrons emitted with about 2 5 volts energy A rather flat peak also occurs in the velocity distribution curves at between 15 and 17 volts, corresponding with the predicted maximum energy In some previous experiments, one of us† has shown that excited metastable helium atoms set free electrons from a metal surface the energy limits being very sharply defined by equation (13) The very sharp cut off at low velocities seems to indicate the absence of serious straggling

Ions which penetrate the barrier before neutralisation would give by (14), $V_{e(\min)} = 6$ 8 volts $V_{e(\max)} = 20$ 3 volts The maximum energy agrees very well with the sharp upper limit in the experimental curves in fig 9, Part I, and as would be expected, the relative number of these electrons increases with the energy of the incident ions *i e*, with the chance of penetration of the barrier Also for energies beyond about 500 volts some of the ejected electrons escape only after considerable straggling in the surface layers of the metal, and the high energy maximum becomes much more diffuse on the low velocity side A noticeable peak is found at about the predicted 6 8 volts, but the position of this subsidiary minimum energy in the curve is rendered somewhat uncertain by the proximity of the very pronounced 2 5 volt peak The sharpness of the high energy cut-off at about 20 volts, and the complete absence of evidence for the presence of higher velocity electrons, renders it improbable that a three-body collision, as suggested above, can play any considerable part in the neutralisation of ions which penetrate through the potential barrier

The distribution curve found for the electrons set free from nickel by He^+ ions is very similar to that for molybdenum, as would be expected from the practical identity of the work functions and the values of μ * The qualitative theory which we have put forward is therefore able to account satisfactorily for the energy distribution among the electrons set free from gas-free surfaces of Mo or Ni If every encounter of an ion with a conducting surface led to the production of an electron moving in some random direction the maximum efficiency of the process of emission would probably be somewhat greater than 50 per cent, on account of the scattering back of some electrons projected into the metal Actually some ions penetrate into the metal, and straggling and absorption would lead to a considerably smaller emission Experiment shows (*cf* Part I) that below about 500 volts the emission remains sensibly constant at about 20 per cent, rising rapidly to about 70 per cent at 1000 volts ion-energy The efficiency over this range is thus of the right order of magnitude

---

* Obtained from equation (2), by assuming 4 free electrons for each atom in the solid

† Oliphant, *loc cit*

(*b*) *The Emission due to the Kinetic Energy of the Ions* The number of electrons set free by a positive ion is not independent of the energy of impact of the ion upon the surface, as we have just had occasion to mention Above 1000 volts the emission increases slowly to about 90 per cent at 5000 volts At the same time the sharp upper and lower limits to the velocity spectrum of the ejected electrons begin to disappear and in particular many electrons are emitted with zero energy (*cf* fig 11, Part I) This would indicate either an increased straggling due to the electrons being produced at greater depths in the metal, or else the growth of a different emission phenomenon which begins to mask that which is preponderant at lower velocities

It is possible to obtain information about that part of the emission which is due only to the kinetic energy of the ions, by employing ions for which $V_i < 2\phi$, or even $V_i < \phi$, so that the possibility of liberation of electrons by the potential energy is ruled out These ions, when fired upon a conductor also set free electrons, but with a much smaller efficiency than He^+ ions With gas-free surfaces the emission is less than 1 per cent of the ion current at bombarding energies of a few hundred volts,† but some of the electrons possess energies corresponding to several volts

The retarding potential curve for the electrons set free by alkali ions is exponential to the volt-axis (see fig 11, Part I) If the curve is plotted semi-logarithmically a straight line is obtained, fig 5 The velocity distribution is therefore Gaussian, or a very close approximation thereto We can find a

---

* The value of μ, calculated on the assumption of 3 free electrons per atom for Ni, is 12 8 volts (Fowler, 'Statistical Mechanics," p 548 (1929)) and this agrees with the value of $\mu + \phi$ required by electron diffraction experiments

† Oliphant, 'Proc Camb Phil Soc,' vol 24, p 451 (1928)

" temperature " for the electrons from the slope of the curve by the relation*

$$e/kT = 11{,}600/T = \text{slope},$$

if natural logarithms are used The temperatures derived vary from 10,000° for an Al target, to 66,000° for Pt, using 600-volt potassium ions

If we assume with Kapitza† that the emission is thermionic and due to local heating at the spots struck by the ions, the temperature of the electrons must be identical with the mean temperature of the spots This would mean that temperatures are obtained by this process which are of a totally different order from any others reached in the laboratory, except perhaps in the electric spark at high pressures Thermal evaporation would then account for the " sputtering " action of the ions ‡ It is significant that Al, a good conductor of heat, gives a temperature of 10,000°, while Pt, a bad conductor, gives 66,000° Nickel, which is intermediate in properties, gives 30,000° This is the order in which these metals sputter when used as cathode in a glow discharge

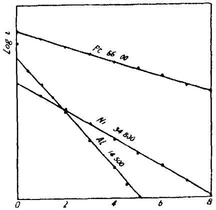

Fig 5

In conclusion, we should like to record our thanks to Prof Sir Ernest Rutherford for his encouragement and help, and to Mr R H Fowler for helpful suggestions throughout, and in particular for integrating for us the expression based on the Fowler-Nordheim theory of autoelectronic emission One of us (P B M) is indebted to the Department of Scientific and Industrial Research for a maintenance grant

Summary

(1) A critical account is given of present theories regarding the electrical conditions at metal surfaces The origin and form of the surface potential barrier are discussed, and reasons given for regarding the major part of this barrier as due to " space-charge " rather than to " image-attraction "

(2) Calculations of the autoelectronic emission from a metal surface under the intense electric field of an approaching positive ion show that slow ions

---

* Langmuir and Mott-Smith, ' Gen Elec Rev ,' vol 27, p 449 (1924)

† Kapitza, ' Phil Mag ,' vol 45, p 989 (1923)

‡ *Cf* Hippel, ' Ann Physik,' vol 81, p 1043 (1926), and vol 86, p 1006 (1928)

will probably capture an electron in this manner while still several atom-diameters from the surface, though faster ions have an increasing chance of reaching the metal before capturing an electron We suggest a more direct treatment of the process regarding neutralisation as due to the transition of an electron through the potential barrier to a state of nearly equal energy associated with the ion

(3) The electron will presumably be captured into one of the " outer orbits " of the atom If, as appears most probable, this neutralising electron possessed while in the metal the maximum energy allowed at low temperatures by the Fermi distribution, then the potential energy of the system thus formed will be $V_i - \phi$ where V_i is the ionisation potential of the atom and ϕ the electronic work function of the surface If $V_i > 2\phi$ the excited atom possesses enough energy to set free, by some quantised process, a second electron from the metal In the case of an ion which penetrates the surface before neutralisation, it is sufficient that $V_i > \phi$ in order that secondary emission by this process should be possible For an atom whose ionisation potential is less than ϕ electron emission cannot be due to a simple quantised mechanism alone, but must involve some more complex process, such as local heating, in which a portion of the kinetic energy of the approaching ion is utilised

(4) The above ideas are found to provide a satisfactory basis for the interpretation of the experimental results In particular, the theory is in good agreement with the observed energy distribution of secondary electrons produced by ions of various kinds and at various velocities

The Effect of a Nuclear Spin on the Optical Spectra—III

By J Hargreaves, Clare College, Cambridge

(Communicated by R H Fowler, F R S—Received March 12, 1930)

In two recent papers* the author has discussed the effect of a nuclear spin on the optical spectra by the method of multiple wave-functions In these papers the interaction energy of the nuclear and electron spins was not taken into account, as has been pointed out by Hill † By its omission the equations were simplified considerably, without affecting the intensity ratios of the lines of the multiplet The problem of finding the relative intensities is a purely kinematical one, depending as it does, to the first approximation, on the unperturbed wave-functions In the papers cited we used the interaction energy of the nuclear spin and orbital momentum to find the $4i_n + 2$ wave functions (i_n being the number of quanta of nuclear spin) which must replace the two wave-functions necessary to describe the electron spin fine structure In order to describe the multiple energy levels correctly we must calculate the interaction energy of the two spins in addition to the energy increments already calculated in I and II This is the first purpose of the present paper, and the work is carried out for the cases $i_n = \frac{1}{2}, 1, 1\frac{1}{2}, 4\frac{1}{2}$ It is found that in the case of the $p_{\frac{1}{2}}$ levels the interaction energy of the two spins is equal to that of the nuclear spin and orbital momentum, while for the $p_{3/2}$ levels the ratio is $-\frac{1}{5}$ It is further found that the energy levels of the S terms are correctly given in I and II

As regards comparison with Jackson's results in the case of cæsium, it would seen that, the separation of the p-levels being very small in comparison with that of the S-level, he has been able to observe the multiplet structure of the lines due to the separation of the S level only If we make this assumption it will be seen on reference to I that our results agree quite well with his observations

A simple description is also given of the hyperfine structure of the Zeeman effect (in strong fields, so that the Zeeman effect is of greater order than that of the nuclear spin, but less than the doublet structure), and the energy levels of the multiplets calculated Results are found which agree very well with

---

* 'Roy Soc Proc,' A, vol 124, p 568 (1929), and vol. 127, p 141 (1930) Quoted as I and II respectively

† 'Proc Nat Acad Sci,' vol 15, p 779 (1929)

Back and Goudsmidt's observations for bismuth, and confirm the assumption they made of the 'cosine' law for the interaction energy Further, the agreement confirms the validity of the empirical equations given in I and II

It should be noted that the present method only enables one to calculate the energy levels in the case of an atom with one electron in the outer shell, or, in the case of atoms (such as bismuth) with more than one, the multiplet energy levels for those states in which the total spin angular momentum is $\frac{1}{2}h$ Thus we are enabled to apply the present method to the $p_{1/2}$, $p_{3/2}$ levels of bismuth

Some recent papers have appeared on hyperfine structure White has published accounts of the hyperfine structure of praseodymium,* thallium,† and given an interpretation of the hyperfine structure‡ of various atoms We cannot, however, apply the present methods to these atoms, which are of a complicated multiplet structure Goudsmidt and Bucher§ have calculated the separations for various cases by assuming the "cosine" law They do not, however, give the absolute values of the separations, this paper is in part a justification of their assumptions

§ 1 The interaction energy Hamiltonian of the nuclear and electron magnets in the notation used in the papers I and II is

$$\mathrm{H}' = -\mu\mu_0 r^{-3}\{(\boldsymbol{\sigma}\ \boldsymbol{\rho}) - 3(\boldsymbol{\sigma}\ \mathbf{1})(\boldsymbol{\rho}\ \mathbf{1})\} \tag{1}$$

where **1** denotes the vector $(x/r,\ y/r,\ z/r)$ To find the energy increments we have, in accordance with the usual perturbation theory, to average H′ over the undisturbed wave-functions, *i e*, the wave-functions found in I and II In other words, we have to find the diagonal elements of H′ in the matrix scheme in which the unperturbed Hamiltonian is a diagonal matrix If ψ_r $(r = 1, 2, \quad)$ are the unperturbed wave-functions of any hyperfine structure level the interaction energy due to H′ for that level is

$$\sum_{r=1}^{4i+2} \int \overline{\psi}_r (\mathrm{H}'\psi)_r \, d\tau \Big/ \sum_r \int \bar{\psi}_r \psi_r \, d\tau \tag{2}$$

The part of this expression depending on r is

$$\int^1 \{f_{n\,k}(r)\}^2 r^2 \, dr \Big/ \int \{f_{n,\,k}(r)\}^2 r^2 \, dr$$

---

* 'Phys Rev,' vol 34, p 1397 (1929)

† 'Proc Nat Acad Sci.,' vol. 16, p 68 (1930)

‡ 'Phys Rev,' vol 34, p 1404 (1929)

§ *Ibid*, vol 34, p 1501 (1929)

Noting that $\mu_0 = eh/2mc$, $\mu\mu_0$ times the integral is $\frac{1}{2}\beta_2$ as defined in I (24), so that if we write

$$\mathrm{E} = (\boldsymbol{\sigma}\ \boldsymbol{\rho}) - 3(\boldsymbol{\sigma}\ \mathbf{1})(\boldsymbol{\rho}\ \mathbf{1}) \tag{3}$$

the expression (2) is

$$-\tfrac{1}{2}\beta_2 \sum_r \int \bar{\psi}_r (\mathrm{E}\psi)_r\, d\tau \Big/ \sum_r \int \bar{\psi}_r \psi_r\, d\tau \tag{2 1}$$

where the ψ's now refer to the part of the wave function depending on θ and ϕ. The complete solutions for these have been given for the different levels in I and II. Thus

$$\left.\begin{aligned} \psi_{2r-1} &= a_{2r-1}\, \mathrm{P}_k^{u+r-1}(\cos\theta)\, e^{i(u+r-1)\phi} \\ \psi_{2r} &= a_{2r}\, \mathrm{P}_k^{u+r}(\cos\theta)\, e^{i(u+r)\phi} \quad (r = 1, 2, \ldots 2i_n + 1) \end{aligned}\right\} \tag{4}$$

The denominator of the expression (2 1) is

$$\frac{4\pi}{2k+1} \sum_r \{a_{2r-1}^2 (k+u+r-1)!/(k-u-r+1)! + a_{2r}^2 (k+u+r)!/(k-u-r)!\}$$

(using I (20)) and this is equal to

$$4\pi/(2k+1)$$

by the normalisation relation II (19). The expression (2 1) for the energy increments therefore reduces to

$$\frac{(2k+1)\beta_2}{8\pi} \sum_r \int \bar{\psi}_r (\mathrm{E}\psi)_r \sin\theta\, d\theta\, d\phi \tag{2 2}$$

The calculation of the operation $(\mathrm{E}\psi)_r$ for a particular value of r and i_n is tedious though some simplifications can be made

$$\left.\begin{aligned} (\boldsymbol{\sigma}\ \mathbf{1}) &= (\sigma_x \cos\phi + \sigma_y \sin\phi)\sin\theta + \sigma_z \cos\theta \\ &= (\alpha e^{i\phi} + \alpha' e^{-i\phi})\sin\theta + \sigma_z \cos\theta \\ \text{where}\qquad \alpha &= \tfrac{1}{2}(\sigma_x - i\sigma_y), \qquad \alpha' = \tfrac{1}{2}(\sigma_x + i\sigma_y) \\ \text{and}\qquad (\boldsymbol{\rho}\ \mathbf{1}) &= (\beta e^{i\phi} + \beta' e^{-i\phi})\sin\theta + \rho_z \cos\theta \\ \beta &= \tfrac{1}{2}(\rho_x - i\rho_y), \qquad \beta' = \tfrac{1}{2}(\rho_x + i\rho_y) \end{aligned}\right\} \tag{5}$$

α, α', β, β' are easily calculated from the matrices for the σ's and ρ's as given in II. They are very simple consisting, in fact, of matrices in which only one diagonal is filled.

The operator $(\boldsymbol{\sigma}\ \mathbf{1})(\boldsymbol{\rho}\ \mathbf{1})$ is then given by

$$\begin{aligned} (\boldsymbol{\sigma}\ \mathbf{1})(\boldsymbol{\rho}\ \mathbf{1}) &= (\alpha\beta e^{2i\phi} + \alpha'\beta' e^{-2i\phi} + \alpha\beta' + \alpha'\beta)\sin^2\theta \\ &\quad + [(\beta\sigma_z + \alpha\rho_z)e^{i\phi} + (\beta'\sigma_z + \alpha'\rho_z)e^{-i\phi}]\sin\theta\cos\theta + (\sigma_z\rho_z)\cos^2\theta \end{aligned} \tag{6}$$

The operator ($\boldsymbol{\sigma p}$) and the operators in the brackets ( ) on the right-hand side of the above equation are then easily calculated by the simple multiplication of matrices. It is found that the result of the operation $\bar{\psi}_r\,(\mathrm{E}\psi)_r$ does not contain ϕ and so the result of integration with respect to ϕ is simply 2π.

It would be very long and tedious to calculate the energy increments for general values of k and u in the case of $i_n = 4\frac{1}{2}$, as there are in general 20 wave functions, but fortunately this is unnecessary, owing to the fact that the system is degenerate. For each value of k there are $2k + 2i_n + 2$ sets of solutions in which $-(k + 2i_n + 1) \leqslant u \leqslant k$, and for which the energy is the same. This degeneracy persists also for the energy increments under present consideration. Accordingly we need only make the calculations for one particular value of u. Further, in the case in which we are interested for bismuth, viz, $k = 1$, the eigen functions are all simple trigonometrical functions of θ.

In the case of $i_n = \frac{1}{2}$, however, it is sufficiently easy to calculate the energy increments for general values of k and u and this we shall accordingly do. We easily find with the aid of (5) and (6) and the calculation of α, β, etc that the expression (2 2) is

$$\frac{(2k+1)}{4}\sum_r\int\bar{\psi}_r^{1}\,(\mathrm{E}\psi)_r\sin\theta\,d\theta-\frac{(2k+1)}{4}f(k,u), \tag{2 3}$$

where

$$\left.\begin{aligned}(k,u) &= a_1^2\,(p_{k,u}-3q_{k,u})+a_4^2\,(p_{k,u+2}-3q_{k,u+2})\\ &\quad-(a_2+a_3)^2\,(p_{k,u+1}-q_{k,u+1})-6a_1\,dr_{k,u}-6a_1\,(a_2+a_3)\,s_{k,u}\\ &\quad+6a_4\,(a_2+a_3)\,s_{k,u+1}\\ p_{k,u} &= \int_0^\pi(\mathrm{P}_k^u)^2\sin\theta\,d\theta\qquad q_{k,u}=\int_0^\pi\cos^2\theta\,(\mathrm{P}_k^u)^2\sin\theta\,d\theta\\ r_{k,u} &= \int_0^\pi\mathrm{P}_k^u\,\mathrm{P}_k^{u+2}\sin^3\theta\,d\theta,\quad s_{k,u}=\int_0^\pi\sin\theta\cos\theta\,\mathrm{P}_k^u\,\mathrm{P}_k^{u+1}\sin\theta\,d\theta\end{aligned}\right\} \tag{7}$$

The integrals $p_{k,u}$, $q_{k,u}$, $r_{k,u}$, $s_{k,u}$ are evaluated in the following section.

§ 2 The function $\mathrm{P}_n^m(\cos\theta)$ used in the solutions (4) are defined as

$$\mathrm{P}_n^m(x)=(n-m)!\;(1-x^2)^{m/2}\frac{d^{n+m}}{dx^{n+m}}[(x^2-1)^n]/2^n\,n! \tag{8}$$

With this definition it is easily proved that

$$\mathrm{P}_n^{-m}=(-1)^m\,\mathrm{P}_n^m$$

Accordingly we can write

$$\mathrm{P}_n^m(x)=(-1)^m\,(n+m)!\;(1-x^2)^{-m/2}\frac{d^{n-m}}{dx^{n-m}}[(x^2-1)^n]/2^n\,n! \tag{8 1}$$

Therefore

$$\int_{-1}^{1} x^2 \mathrm{P}_n^m(x)\,\mathrm{P}_n^m(x)\,dx$$
$$= \frac{(-1)^m (n-m)!\,(n+m)!}{2^{2n}(n!)^2}\int_{-1}^{1} x^2 \frac{d^{n-m}}{dx^{n-m}}[(x^2-1)^n]\frac{d^{n+m}}{dx^{n+m}}[(x^2-1)^n]\,dx$$

The integral on the right is equal to

$$-\int_{-1}^{1} \frac{d^{n-m-1}}{dx^{n-m-1}}(x^2-1)^n \frac{d}{dx}\left[x^2 \frac{d^{n+m}}{dx^{n+m}}(x^2-1^n)\right]dx ,$$
$$= (-1)^{n-m}\int_{-1}^{1}(x^2-1)^n \frac{d^{n-m}}{dx^{n-m}}\left[x^2\frac{d^{n+m}}{dx^{n+m}}(x^2-1)^n\right]dx$$

integrating $n-m$ times by parts Working this out we find that

$$q_{n,m} = (n-m)!\,(n+m)!\,(4n^2-4m^2+4n-2)/(2n-1)(2n+1)(2n+3)$$

We may calculate $r_{n,m}$ and $s_{n,m}$ in a similar way and find that

$$r_{n,m} = -4(n-m)!\,(n+m+2)!/(2n-1)(2n+1)(2n+3)$$
$$s_{n,m} = (n-m)!\,(n+m+1)!\,2(2m+1)/(2n-1)(2n+1)(2n+3),$$

$p_{n,m}$ is a well-known integral, and is given in I (20)

§ 3 In the case $i_n = \frac{1}{2}$ there are four hyperfine structure levels, and the constants a_1, a_2, a_3, a_4 for each of the levels are given in I (34), (the constants are there called a, b, c, d), as well as the energy increments due to the interaction of nuclear spin and orbital momentum Making the calculations involved in (2 3) and (7) we find that the energy increments of the four levels are given (in order of magnitude) by —

$$\left.\begin{aligned}
\Delta W &= \beta_1 k - 2\beta_2 k(k+1)/(2k+1)\\
\Delta W &= \beta_1 k + 2\beta_2 k(k+1)/(2k+3)\\
\Delta W &= -\beta_1(k+1) - 2\beta_2 k(k+1)/(2k-1)\\
\Delta W &= -\beta_1(k+1) + 2\beta_2 k(k+1)/(2k+1)
\end{aligned}\right\} \qquad (9)$$

In particular the $p_{3/2}$ and $p_{1/2}$ separations are $\frac{32}{15}\beta_2$ and $\frac{16}{3}\beta_2$

The particular cases $k = 1$, $i_n = 1, 1\frac{1}{2}, 4\frac{1}{2}$, can be dealt with fairly shortly if we make the calculations for $u = -2$, for example In this case only the five functions ψ_2 to ψ_6 for $i_n = 1$, and the six functions ψ_2 to ψ_7 for $i_n = 1\frac{1}{2}$, $4\frac{1}{2}$ The Legendre functions concerned are P_1^{-1}, P_1^0, P_1^1 which are simply $-\sin\theta$, $\cos\theta$, $\sin\theta$, respectively The calculations are too long to reproduce here in detail, and we shall therefore give only the results. As stated earlier, for the $p_{\frac{1}{2}}$ level the nuclear and electron spin energy is equal to the nuclear spin and orbital momentum energy, while for the $p_{3/2}$ levels it is $-\frac{1}{5}$. We find then the following energy levels :-

(i) $i_n = 1$. The $p_{3/2}$ levels are given by

$$\Delta W = \beta_1 + 8\beta_2/5, \quad \beta_1 - 16\beta_2/5, \quad \beta_1 - 8\beta_2/3 \tag{10.1}$$

and the $p_{1/2}$ levels by

$$\Delta W = -2\beta_1 + 8\beta_2/3, \quad -2\beta_1 - 16\beta_2/3 \tag{10.2}$$

(ii) $i_n = 1\frac{1}{2}$

$$\Delta W = \beta_1 + 12\beta_2/5, \quad \beta_1 - 4\beta_2/5, \quad \beta_1 - 44\beta_2/5, \quad \beta_1 - 4\beta_2/5 \tag{11.1}$$

$$\Delta W = -2\beta_1 + 4\beta_2, \quad -2\beta_1 - 20\beta_2/3 \tag{11.2}$$

(iii) $i_n = 1\frac{1}{2}$

$$\Delta W = \beta_1 + 36\beta_2/5, \quad \beta_1 + 4\beta_2/5, \quad \beta_1 - 68\beta_2/15, \quad \beta_1 - 14\beta_2/5 \tag{12.1}$$

$$\Delta W = -2\beta_1 + 12\beta_2, \quad -2\beta_1 - 14\beta_2/3 \tag{12.2}$$

It will be seen that in all cases the cosine law for the total interaction energy is obeyed and in particular that the separations of $p_{3/2}$ on (iii) are in the ratio 6 : 5 : 4 as observed by Goudsmidt and Back.

It is necessary now to consider the effect of the nuclear and electron spin interaction of the s terms. It will be seen that this is zero. In the solution for $k = 0$ for all values of i_n, and for some valid value of u only two wave-functions exist. Suppose we choose the value of u which makes ψ_{2s} and ψ_{2s+1} only different from zero.

The relevant Legendre function P_0^0 is equal to unity, so that the ψ_r s referred to in (2.2) are all zero except ψ_{2s} and ψ_{2s+1}, which are equal to a_{2s} and a_{2s+1} respectively. It is found that in this case only the operations of $(\alpha\beta' + \alpha'\beta)$ and $(\sigma_z\rho_x)$ on the right-hand side of (6) give non-zero results. In fact we find that

$$\Sigma\psi_r(E\psi)_r = [(2i_n - 2r)a^2_{2s+1} - (2i_n - 2s + 2)a^2_{2s} - 2\{s(2i_n - s + 1)\}^{\frac{1}{2}} a_{2s}a_{2s+1}](1 - 3\cos^2\theta)$$

The integral (2) therefore contains $\int_0^\pi (1 - 3\cos^2\theta)\sin\theta\, d\theta$, and the average energy density of the nuclear and electron spin interaction over a sphere with centre at the nucleus is zero. The total interaction energy is therefore zero, although the part of the integral in (2) with respect to r is not in this case convergent. The S-levels are therefore correctly given in I and II.

§ 4. In dealing with the hyperfine structure of the Zeeman effect we first find solutions of the wave equations neglecting nuclear spin, and then take the latter as a perturbation. In doing this we may neglect the energy of the nuclear magnet in the external magnetic field. We start with equations II (4), neglecting μ, but including the effect of a uniform magnetic field **H**. The course of the work follows that in I as far as equations (25) except that we now use $4i_n + 2$ ψ's instead of four. We get $2i_n + 1$ pairs of equations similar to I (25.1) and (25.2)

$$\Delta W_{2s-1}\, a_{k,u}^{(2s-1)} = \beta_1 [u a_{k\,u}^{(2s-1)} - (k + u + 1)\, a_{k\,u+1}^{(2s)}] + (u + 1)\,\omega a_{k\,u}^{(2s-1)}$$

$$\Delta W_{2s}\, a_{k\,u}^{(2s)} = \beta_1 [- u a_{k\,u}^{(2s)} - (k - u + 1)\, a_{k\,u-1}^{(2s-1)}] + (u - 1)\,\omega a_{k\,u}^{(2s)}$$

where $\omega = \mu_0 \mathbf{H}$ and $s = 1, 2 \ldots 2i_n + 1$. It is seen that by writing $u + 1$ for u in (12.2) we obtain solutions in which only two of the constants a are different from zero. We get Darwin's pair of solutions $2i_n + 1$ times denoting a $(2i_n + 1)$-fold degeneracy.

(i) $\Delta W = \beta_1 k + \omega (u + \frac{1}{2})(k + 1)/(k + \frac{1}{2})$

$$\psi_{2s-1} = a_{2s-1} f_{n\,k}(r)\, P_k^u e^{iu\phi}, \quad \psi_{2s} = a_{2s} f_{n\,k}(r)\, P_k^{u+1} e^{i(u+1)\phi}$$

$$a_{2s} = -[(k - u)/(k + u + 1)]\, a_{2s-1},$$

$$a_{2s-1}{}^2 = (k + u + 1)/(2k + 1)(k + u)!\,(k - u)!$$

(ii) $\Delta W = -\beta_1 (k + 1) + \omega (u + \frac{1}{2})\, k/(k + \frac{1}{2})$

$$a_{2s} = -a_{2s-1}, \quad a_{2s-1}{}^2 = (k - u)/(2k + 1)(k + u)!\,(k - u)!$$

In both (i) and (ii) only ψ_{2s}, ψ_{2s-1} are different from zero and there are $2i_n + 1$ sets of solutions in each case, i.e., $s = 1, 2 \ldots (2i_n + 1)$. u has the usual range of values, viz., $-k - 1 \leqslant u \leqslant k$.

We find the additional energy due to μ by averaging the relevant part of the Hamiltonian over the unperturbed system represented by (i) and (ii). The empirical terms in II are ineffective except for $k = 0$ when they become the dominant terms. For $k \neq 0$ the additional terms in the Hamiltonian are

$$F = \frac{\mu e}{mcr^3}(\boldsymbol{\rho} \cdot \mathbf{M}) - \frac{\mu\mu_0}{r^3}\{(\boldsymbol{\sigma} \cdot \boldsymbol{\rho}) - 3(\boldsymbol{\sigma} \cdot \mathbf{1})(\boldsymbol{\rho} \cdot \mathbf{1})\} = F_1 - F_2 \quad (13)$$

(say). F_1 represents the second set of terms in the equations II (4.1′) and (4.2′). The increment energy for any of the solutions (i) or (ii) is

$$\delta = \delta_1 - \delta_2$$

where

$$\delta_t = \sum_r \int \overline{\psi_r}\, (F_t \psi)_r\, d\tau \Big/ \sum_r \int \overline{\psi_r}\, \psi_r\, d\tau \quad (t = 1, 2) \qquad (14)$$

F_1 involves the operators $\kappa_x \pm i\kappa_y$, κ_z as defined in I (16)

$$\iint P_k^u e^{-iu\phi} (\kappa_x \pm i\kappa_y) P_k^u e^{iu\phi} \sin\theta \, d\theta \, d\phi$$
$$= -i (k \mp u) \iint P_k^u e^{-iu\phi} P_k^{u\pm 1} e^{i(u\pm 1)\phi} \sin\theta \, d\theta \, d\phi = 0$$

by I (19) The relevant part of F_1 is therefore

$$-\frac{i\mu eh}{mcr^3}(2i_n - 2s + 2)\kappa_z$$

Using I (19) and (20) we find the values of δ_1 in the solutions (i) and (ii) are

$$\text{(i)}' \quad \delta_1 = (2i_n - 2s + 2)\beta_2 k (2u + 1)/(2k + 1)$$
$$\text{(ii)}' \quad \delta_1 = (2i_n - 2s + 2)\beta_2 (k + 1)(2u + 1)/(2k + 1)$$

The evaluation of δ_2 involves similar work to that described in the earlier part of the paper, but having calculated the relevant matrices is much simpler as we have now only two ψ's We find that

$$\text{(i)}'' \quad \delta_2 = (2i_n - 2s + 2)\beta_2 k (2u + 1)/(2k + 1)(2k + 3)$$
$$\text{(ii)}'' \quad \delta_2 = -(2i_n - 2s + 2)\beta_2 (k + 1)(2u + 1)/(2k - 1)(2k + 1)$$

It is seen that δ_2 is equal to $\delta_1/(2k + 3)$ and $\delta_1/(2k - 1)$ respectively, the same relation as holds for the ratios of the interactions of the nuclear spin with the electron spin and orbital momentum in the absence of an external field There fore the values of δ are —

$$\text{(i)}''' \quad \delta = 2(2i_n - 2s + 2)\beta_2 k (k + 1)(2u + 1)/(2k + 1)(2k + 3)$$
$$\text{(ii)}''' \quad \delta = 2(2i_n - 2s + 2)\beta_2 k (k + 1)(2u + 1)/(2k - 1)(2k + 1)$$

In the case of the S-levels the unperturbed solutions (neglecting μ) are found to be

$$\text{(iii)} \quad \Delta W = \beta_{1,0} + \omega$$
$$\psi_{2s-1} = \frac{1}{r} f_{n,0}(r), \text{ all other } \psi\text{'s being zero}$$
$$\text{(iv)} \quad \Delta W = \beta_{1,0} - \omega$$
$$\psi_{2s} = \frac{1}{r} f_{n,0}(r), \text{ all other } \psi\text{'s being zero}$$

The first terms in ΔW are due to the empirical terms in the wave equations, and were found in I and II, the second terms are simply the second term in (i) with $u = 0, -1$ respectively The relevant perturbation terms are now the empirical terms, the value of δ being given by (14), with F_1 replaced by F, the part of the Hamiltonian representing the empirical terms In the operations $(F\psi)_{2s-1}$, $(F\psi)_{2s}$ we need only retain terms containing ψ_{2s-1}, ψ_{2s} respectively, since there is only one ψ in any unperturbed solution Hence

$$(F\psi)_{2s-1} = -(2i_n - 2s + 2)\,\frac{\mu e h}{m c r^3}\, r\,\frac{\partial \psi_{2s-1}}{\partial r}$$

$$(F\psi)_{2s} = +(2i_n - 2s + 2)\,\frac{\mu e h}{m c r^3}\, r\,\frac{\partial \psi_{2s}}{\partial r}$$

Using I § (6), we find that for solutions (iii) and (iv)

$$(\text{iii})' \quad \delta = -(2i_n - 2s + 2)\,\beta_{2\,0}$$

$$(\text{iv}) \quad \delta = +(2i_n - 2s + 2)\,\beta_{2\,0}$$

respectively Each level is therefore split up into $2i_n + 1$ nuclear spin levels to each of which belong two (or, for the S-levels, one) wave functions ψ_{2s-1}, ψ_{2s} ($s = 1, 2 \ldots 2i_n + 1$) The intensity of a transition from a k-level to a $(k-1)$-level depends on $\sum_r \psi_r \psi_r'$ and we see, therefore, that the only possible transitions are between corresponding levels (*i e*, with the same value of s) Further, the wave functions are the same for all s in (i) to (iv), so that the intensities of the transitions are the same Therefore each line in the Zeeman effect is split up by the nuclear spin into $2i_n + 1$ lines of equal intensity Moreover, the difference between consecutive values of δ in any (k, u) level is seen to be constant, and so there is a constant frequency difference between the nuclear spin multiplet lines

The line $p_{3/2} \to s$ ($i_n = 4\frac{1}{2}$) has been observed for bismuth in detail by Back and Goudsmidt According to our calculations for the $p_{3/2}$ level

$$k = 1,\ u = 1, 0, -1, -2 \qquad \delta = 4\,(11 - 2s)\,\beta_2\,(2u + 1)/15$$

and for the s-level

$$k = 0,\ u = 0, -1, \quad \delta = \mp\,(11 - 2s)\,\beta_{2\,0}$$

respectively

For the two parallel components ($u = 0, -1$ to $u = 0, -1$) the energy difference between consecutive lines of the nuclear spin multiplets is in each case

$$8\beta_2/15 + 2\beta_{2\,0}. \tag{15}$$

For the perpendicular components $u = 1, -2$ to $u = 0, -1$, it is

$$8\beta_2/5 + 2\beta_{2\,0}, \tag{16}$$

and for the perpendicular components $u = 0, -1$ to $u = -1, 0$

$$8\beta_2/15 - 2\beta_{2\,0} \tag{17}$$

The separation of the S levels is by II, § 4, $20\beta_{2\,0}$, and the total separation of the $p_{3/2}$ levels is by (12·1) $16\beta_2$. The experimental results cited show these quantities (subject to a constant factor) to be 0·830 and 0·605 respectively. The separations (15), (16), (17) should therefore be 0·1032, 0·1435, 0·0628. These values agree very well with observations, and with the deductions of Back and Goudsmidt based on the classical quantum theory and the assumption of the "cosine" law.

As regards the hyperfine structure of cæsium, if we assume that the doublets observed by Jackson were due to the doubling of the S-level, and that he was unable to observe the separations due to the doubling of the $p_{3/2}$ and $p_{1/2}$ levels, we must suppose (see I, fig. 3) that the lines he observed were the two strongest of $p_{3/2} \rightarrow s_{1/2}$ and $p_{1/2} \rightarrow s_{1/2}$. If we do this for the lines $1s \rightarrow 2^2p_{3/2}$ and $1s \rightarrow 2^2p_{1/2}$, which he examined, we deduce that the separation of the $p_{3/2}$ levels, viz., $35\beta_2/15$, is equal to 0·021 cm^{-1}. The electron spin doublet separation of the p-levels, viz., $3\beta_1$, is 550 cm^{-1}. Hence

$$32\beta_2/45\beta_1 = 0\cdot021/550.$$

If, therefore, we suppose the magnetic moment of the nucleus to be $CZeh/2m'c$ (see I), we find that C is approximately 6·5. We deduce, therefore, that the ratio of magnetic moment to mechanical moment in the nucleus is approximately $6\cdot5Ze/m'c$.

Added Note.—While the present work was being written up a paper appeared by Fermi,* in which he obtains the s, $p_{1/2}$, and $p_{3/2}$ multiplet levels. The results are identical with the ones obtained in the present paper, a different notation being used.

---

* Fermi, 'Z. Physik,' vol. 60, p. 320 (1929).

The Crystal Structure of the Normal Paraffins at Temperatures Ranging from that of Liquid Air to the Melting Points

By ALEX MULLER

(Communicated by Sir William Bragg, F.R.S.—Received March 12, 1930.)

[PLATES 5, 6.]

Introduction

The aim of this paper is to give a survey of the structures of the normal paraffins at temperatures ranging from that of liquid air to those in the neighbourhood of the melting points. The paper divides naturally into two parts, one dealing with the thermal expansion, i.e., with the gradual and continuous increase of the lattice dimensions with increasing temperature; the other with the discontinuous structural changes which occur under certain conditions when the substances are subjected to temperature changes.

Chemical Material

The chemical material was partly that already used in previous work and partly new material. Most of the substances were synthesised in the Davy-Faraday Laboratory. Some of the preparations such as hexane and pentane were bought and carefully purified. The writer is again very much indebted to his colleagues, Dr. H. S. Gilchrist and Mr. E. L. Holmes, who were kind enough to do all the chemical work for him.

Experimental

The following method for mounting the samples on the X-ray spectrometer was found to be very convenient. Thin-walled glass tubes of, say, ½ to 1½ mms. diameter were partly filled with the substances and then sealed off at both ends. In this form the samples could be kept indefinitely and handled with ease. These glass tubes were made to fit closely into small metal holders and could then be centred accurately on the spectrometer. During the exposure they were rotated. The cooling of these samples was quite a simple matter. For the liquid air investigation the sample holder had the shape of a small cup supported by a stem. The glass tubes were made to fit into a narrow central hole in the stem. The liquid air was conducted through a small glass funnel which ended very close to the sample and near the point where the X-rays struck the substance The liquid air flowed along the glass tube into the cup and overflowed or evaporated there By this method it was possible to keep substances like butane and pentane frozen The film holder which surrounded the sample was made into a camera sufficiently air-tight to prevent moisture from entering it No traces of ice lines could be detected on the photographs Work at higher temperatures was done with the same apparatus except for a few minor alterations The cup shaped holder was replaced by a small cylindrical one and a small platinum heating coil which surrounded the sample closely was put immediately below the point where the X-rays struck the glass tube Any of the samples investigated here could be kept in a liquid state by sending a small current through the coil The surface which separated the solid from the liquid phase inside a sample tube could be shifted up and down and the solid or liquid portion could be brought into the path of the X-rays at will

The X ray tube with copper anticathode $\lambda = 1\ 539$ A U was run by an induction coil with a Wehnelt interrupter and the radiation was filtered by nickel foil

1 *Thermal Expansion*

Before giving an account of the expansion measurements it is necessary to recall a few facts about the structure of these hydrocarbons $C_{29}H_{60}$ has been previously determined from X-ray measurements on a single crystal * In the present work there was no necessity to procure single crystals Powder photographs, examples of which are given at the end of this paper, showed at once that a whole series of these substances have identical structures, *i e*, the chain molecules although different in length are arranged in exactly the same manner throughout the series It will be shown in the second part of this paper that under certain conditions some of these paraffins can form a second structure different from the one mentioned above It should be remembered that the expansion measurements treated in this section have been carried out on the first, or "normal" structure, *i e*, on the one corresponding to $C_{29}H_{60}$

A few words may be said about the way the figures for the expansion were obtained from the photographs The plan was to find the linear expansion in the direction of the three crystallographic axes First it was necessary to identify the reflections on the films The size of the lattice being known, the usual difficulty did not arise There were three reflections which could always be obtained with comparatively short exposures, namely, the 110, 200 and 020

---

* 'Roy Soc Proc,' A, vol 120, p 437 (1928)

The first was the strongest, the two others were weaker. The two last reflections were usually the most clearly defined of the three. The spacings corresponding to them gave at once half the length of the two main axes *a* and *b* in the basal plane of the crystals. The following table gives the numerical data of the lengths of these two axes as obtained from different substances at different temperatures. With regard to the temperature it will be noted that no figures are given in the table. No attempt is made in this preliminary paper to obtain a high degree of accuracy.

Table I

Number of C atoms	Liquid air temperature		Room temperature		Few degrees C below melting point	
	$a/2$	$b/2$	$a/2$	$b/2$	$a/2$	$b/2$
11	3.59	2.46	-		-	
15	3.59	2.47		—	—	
17	3.595	2.445			3.83	2.51
18	—	-	—		3.84	2.50
19	3.58	2.44	3.70	2.49	3.86	2.485
20	-	—	—		3.88	2.50
23	3.60	2.45	—		—	-
24	3.62	2.45	3.73	2.49	3.80	2.51
29	—	—	3.70	2.47	3.79	2.49
30	—		3.74	2.48	—	

The figures show clearly that the lengths of both axes increases considerably with increasing temperature. We take the figures $a/2$ and $b/2$ for different paraffins at liquid air temperature. They are identical within the limits of experimental error, i.e. ½ to 1 per cent. The average for $a/2$ and $b/2$ at liquid air temperature is –

$$a/2 = 3.593 \pm 0.004 \text{ Å U}$$

$$b/2 = 2.453 \pm 0.004 \text{ Å U}$$

The relative errors of the averages are thus only a few thousandths. (The absolute values should be correct within, say, ½ per cent.) In the following table the linear expansions of the *a* and the *b* axis have been calculated with the aid of the figures in the previous table.

Table II

Number of C atoms	Melting points	Temperature range	Δ_a in per cent	Δ_b in per cent	Δ_a/Δ_b
	°C				
17	22	Liquid air—near melting point	6.74	2.32	2.9
18	28	— ,,	6.87	1.91	3.6
19	31	— room temperature	2.98	1.51	2.0
19		near melting point	7.57	1.30	5.8
20	38	—	7.99	1.91	4.2
24	54	—room temperature	3.81	1.51	2.5
24		near melting point	5.76	2.34	2.5
29	64	,, —room temperature	3.14	0.77	4.1
29		near melting point	5.48	1.51	3.6
30	66	— room temperature	4.01	1.10	3.5

a_l = length of a axis at liquid air temperature

b_l = length of b axis at liquid air temperature

a_t = length of a axis at temperature t

b_t = length of b axis at temperature t

$$\Delta_a = 100\,(a_t - a_l)/a_l \qquad \Delta_b = 100\,(b_t - b_l)/b_l$$

The table shows that the percentage expansions of the a axes are considerably larger than the corresponding ones of the b axes. The average of the figures in the last column of the table gives

$$(\Delta_a/\Delta_b)_{\mathrm{av}} = 3.5 \pm 0.35$$

In order to get sufficiently accurate data for the change in length of the c axes it was found necessary to adopt the usual method for mounting the powder samples in which the substances are spread into thin layers on flat glass surfaces. The photographs obtained with the glass tube samples did as a rule show the long spacings corresponding to the c axes, but the definition of the lines was not good enough to allow measurements of small changes. The photographs obtained from these thin layers show very sharp lines and changes of the order of 1 per cent could have been detected in the distance of two symmetrical reflections on the films.

The photographs showed no appreciable displacement of the long spacing reflections when taken at different temperatures. In other words the expansion of the c axis was found to be much smaller than that of the a or b axes, and not to exceed one-tenth of the expansion of the a axis. A reproduction of a photograph which shows this very clearly is given at the end of this paper. The figures obtained in this section will be discussed later on.

II *The Structural Changes with Temperature*

This second section deals with the discontinuous changes in the structures which take place when some of the substances are subjected to temperature alterations The fact that such changes can easily be detected by X ray methods has been shown in an earlier investigation on the paraffins * It was noted that these changes were reversible Each of the two crystalline forms which the substances could assume were stable over a certain range of temperatures and the substance could be made to change from one form into the other by altering the temperature

In this section of the paper an attempt is made to follow up the earlier investigation by a more detailed study of the phenomena The substances which are dealt with in this section range from C_5H_{12} pentane to $C_{30}H_{62}$ triacontane

The lower members of the series being liquids at room temperature had to be kept frozen during the X ray exposure These samples were kept in those thin walled glass tubes mentioned at the beginning The higher members of the series were either used in the same way or in the form of thin layers on glass

The following table gives the data for the long spacings,' i e those spacings which depend essentially upon the length of the carbon chain in each individual substance

Table III

N	Even numbers		N	Odd numbers	
	d_1	d		d_1	d_2
6	-	8 55	5	—	7 35
8	—	11 0	7	—	10 0
10	—	13 4	9	—	12 8
16	—	20 9	11	15 9	—
18	25 3	23 3	15	21 0	—
20	27 4	25 4	17	23 6	—
24	32 6	—	19	26 2	—
26	35 2	—	21	28 7	—
30	40 0	—	23	31 0	—
—	—	—	29	38 8	—

The figures of Table III are plotted in fig 1

---

* 'J Chem Soc,' vol 127 p 599 (1925)

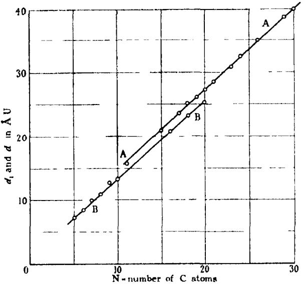

Fig 1

The spacings d_1 and d_2 are plotted against the number N of carbon atoms in the chains. Above N = 20 the spacings of both the odd and the even numbered substances lie within the limits of experimental error on one straight line AA. The increase of the spacing per carbon atom is 1·25 Å U. In the neighbourhood of N = 20 the odd and even numbered substances begin to differ in their behaviour. From both $C_{20}H_{42}$ and $C_{18}H_{38}$ two sets of spacings can be obtained. If the substances are kept near their melting points longer spacings appear which lie on AA. At lower temperatures another set appears, and the spacings now lie on the line BB. Further cooling no longer produces any change and the two spacings still persist at liquid air temperature. $C_{16}H_{34}$ gives only one spacing on the lower line, and the same thing is for the still lower members of the even series down to C_6H_{14}. The odd members of the series behave in a different way. $C_{19}H_{40}$ gives only one spacing and no change is found when the substance is cooled down to liquid air temperature. The spacing of $C_{19}H_{40}$ lies on the upper line AA. The same holds for C_{17}, C_{15} and C_{11}. At C_9H_{20} a change takes place, and the long spacings of the members of the odd series from N = 9 downwards approach the straight line BB. This is so far as the long spacings are concerned. The structural changes which both C_{20} and C_{18} can undergo are shown not only by the appearance of the two sets of long spacings but also in the general appearance of the powder photographs.

Particularly when "glass tube samples" are used the two structures give quite different patterns on the photographs Those on which the longer spacings appear show the features characteristic of the normal form, and similarly, those on which the shorter spacings appear are almost indistinguishable from each other except for the long spacing lines This second characteristic pattern is not only found with $C_{20}H_{42}$ and $C_{18}H_{38}$ but also with lower members of the even series and can be traced down to C_8H_{18} Structures which show this second characteristic pattern will from now on be called "second form" in contradistinction to the "normal form" Reproductions showing the difference between the two patterns will be found at the end of this paper The three strongest lines of the second structure have the spacings 4 56, 3 79, 3 58 Å U ($C_{20}H_{42}$ at room temperature)

With regard to the appearance of the second form it may be mentioned that on rare occasions faint traces were found on photographs of $C_{24}H_{50}$ of a line which did not belong to the normal structure This line coincided with the strongest line of the second form It is therefore not unlikely that traces of the second form may coexist with the normal form The writer has not been able to find the exact conditions under which this phenomenon occurs

An attempt was further made to explore the finer details of the changes in the crystal structure in the immediate neighbourhood of the melting point A very fine pencil of X-rays had to be used for getting a clear separation of the lines and the temperatures had to be changed in small steps A sample was first completely melted The photograph obtained at this stage was the well known broad ring characteristic of the liquid state The temperature was then lowered a very little The X rays beam was made to strike the spot where the solid and the liquid phase met The photograph obtained under these circumstances was rather striking The broad ring had vanished and a very well-defined sharp ring appeared which had the appearance of a normal crystal reflection The striking fact was that no other reflection of anything like the same order of intensity could be found on the photographs At a slightly lower temperature more lines appeared, but this line remained without showing any appreciable change in definition or position, and was found to coincide with the 110 reflection of the normal structure The various stages through which the structures went are shown in the reproductions The sharp single reflection was found to appear with both even and odd numbered substances

Discussion

The data in the first part of this paper show that the hydrocarbons are strongly anisotropic The average coefficient of expansion between the temperature of liquid air and the melting points of all the substances investigated is 6 8 per cent in the direction of the *a* axes and 1 9 per cent for the *b* axes The average ratio of the two is 3 5 ± 0 35, *i e*, the coefficient of expansion of the *a* axis is about three to four times as large as the one of the *b* axis Compared with these expansions of the two axes in the basal plane the expansion in the direction of the third long axis of the higher members of the series is very small In the photograph which is shown at the end of the paper there is no displacement detectable in the long spacing reflections at liquid air temperature and at room temperature This photograph was obtained from $C_{19}H_{40}$ The above facts are illustrated in fig 2

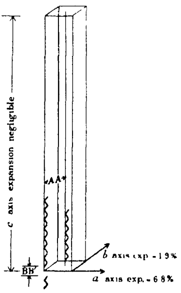

FIG 2

In this diagram is shown a zig zag line indicating the position of the chain molecules in the unit cell The distances and arrangement of the chains in the crystals and the structure of the chain itself have been discussed in detail in the previous paper on $C_{20}H_{60}$ (*loc cit*)

The expansion data show that the chain axes move apart from each other as the temperature increases *i e*, the distance AA' becomes larger when the crystal is heated The expansion of the length of the *c* axis depends upon two factors One is the moving apart of the end groups, *i e*, the increase of BB' with temperature The second is the expansion of the chain molecule itself The expansion or possible contraction of BB' is unlikely to differ in magnitude from the lateral change in distance of the chain axes If, therefore, it is found that the total expansion of the *c* axis is negligible compared with this lateral expansion, the conclusion is that the molecule itself has a negligible expansion in the direction of its axis This simply indicates that the forces which hold the atoms together in the molecule are different in magnitude from those which keep the molecules apart from each other The chemical conception of the entity of the molecule is thus confirmed for the solid state This in itself is not surprising, but the fact that the investigation is now brought within the range of numerical treatment opens interesting possibilities By increasing the accuracy of the measurements it will undoubtedly be feasible to obtain the expansion of the chain itself and so to compare the intramolecular with the intermolecular cohesion

The expansion ratio 3 5 of the *a* and *b* axis confirms what has been found in the structure investigation of the paraffins, namely, that the chain molecule has no radial symmetry about the chain axis

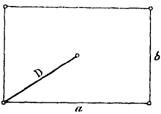

Fig 3

It is interesting to see how the distance of nearest approach of two adjacent chain axes alters when the temperature is raised This distance *D* is shown in fig 3

Take the measurements for $C_{19}H_{40}$ which melts at 31° C

Temperature		D
		Å U
Liquid air		4 35
Room temperature		4 5
Near melting point	Solid	4 6
	Molten	4 6

The last figure refers to the substance in the liquid state when the temperature is not far from the melting point The X-ray reflection on the photograph is a broad ring, and the spacing corresponding to this ring cannot be calculated with the same degree of accuracy as those which appear when the substance is in the solid state It seems, however, that there is no appreciable discontinuity in the figures By measuring the width of the ring it is therefore possible to get an approximate measure of the distance of nearest approach of the chain axes when the substance is a liquid

Rings of this nature have been obtained by several investigators, the interest of the above figures lies in the fact that they suggest a more definite interpretation of the significance of this ring than has been obtained hitherto

A few words may be said about the rather unexpected phenomenon of the single sharp reflection which appeared when the substances were investigated in the immediate proximity of the melting point The phenomenon will have to be studied in more detail before a definite explanation can be given It is perhaps not out of place, however, to discuss the subject to some extent

The first of the following diagrams represents a cross-section through the unit cell of a "normal" paraffin crystal The chain axes, which are supposed to stand perpendicular to the plane of the paper, intersect this plane in points which are surrounded by small ellipses in the drawing These ellipses represent the cross-sections through the chain molecules There are two sets of these ellipses present, their major axes are placed symmetrically with regard to the *a* axis of the crystal The positions of the molecules indicated in fig 4 have to be regarded as average positions at a given temperature

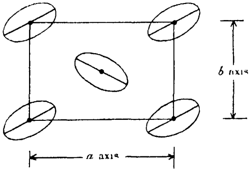

Fig 4

Apart from a change in proportions the above arrangement is found to exist until the temperature reaches very nearly the melting point

At this juncture the arrangement of the molecules in the crystal seems to alter The X-ray photographs change their appearance The 200 reflection becomes very faint compared with 110 line, and seems to disappear completely when the photograph is taken at a slightly higher temperature Yet the 110 line does not alter appreciably in sharpness and only disappears when the substance turns into the liquid state The broad ring which then appears has a distinctly different spacing, 4 6 Å U compared with 4 2 Å U of the 110 reflection

A photograph with a single sharp reflection would be obtained from a layer structure, *i e*, from an arrangement in which groups of molecules are placed in equidistant layers Each group would have to contain a sufficiently large number of molecules to give sharp reflections The groups themselves taken as a whole could be oriented at random The question arises as to whether the normal structure can be transformed into a layer structure in a simple way This seems to be so The oscillations of the molecules round their chain axes, one possible mode of thermal agitation, must increase as the temperature rises These oscillations may become so strong that some of the first set of molecules turn into positions occupied by the other set, and *vice versa* The step from such an arrangement to one where groups of molecules are arranged in layers is then easily made This is illustrated in fig 5

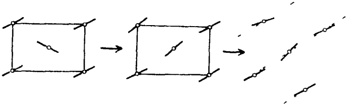

FIG 5

Without the knowledge of the nature of the intermolecular forces it is obviously impossible to see why just this layer arrangement should have a certain stability Further investigation will show whether the explanation of this sharp single line is correct If this is so, then observations taken in the neighbourhood of the melting points are of particular interest, for they are likely to reveal the strongest bonds between the molecules

The following part of the discussion will deal with the abrupt changes in the structures of some of the paraffins The essential facts have already been given in an earlier part of this paper The experiments show that there is a marked difference in the behaviour of the odd and even numbered substances This general observation is hardly surprising, for it has been shown in a previous note* that such differences may almost be regarded as geometrical consequences of the zig zag chain structure The interest lies in the manner in which these differences reveal themselves A qualitative explanation can easily be found

Supposing first we deal with paraffin crystals which contain very long chains. The influence of the groups at the ends of these chains upon their mutual arrangement must then be very small, and the chains will arrange themselves in their own typical fashion Both odd and even numbered substances will practically have the same structure, as is shown in the case of the paraffins which have more than 20 carbon atoms But supposing the chains become shorter The discontinuity in the structure of the chains at their ends, or in other words the end groups, will then increase their relative influence At a certain chain length they may become preponderant and a complete change in the crystal structure may be the result It is here that we expect to see a difference in the behaviour of the odd and the even numbered substances The orientation of the end groups relative to each other being different in the odd and the even series there is no reason why these groups should act alike This is what actually happens The change of the structure in the even series occurs in the neighbourhood of $N = 20$ in the odd series between $N = 9$ and N 11

---

* 'Roy Soc Proc,' A, vol 124, p 317 (1929)

The fact that a small temperature change is capable of disturbing the balance of the internal forces is worth noticing It is here that an external electric or magnetic field may have the power of influencing this balance in a similar way

A problem the complete solution of which has been postponed is the determination of the structure of the second form The powder photographs suggest that the cross section of the unit cell of this form is no longer rectangular From the three strongest reflections a cross section can be calculated The result is shown in fig 6 in correct proportions

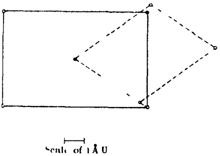

FIG 6

The figure in full lines represents the cross-section of the normal structure The figure in dotted lines refers to the other The transformation of the normal section into the second one is easily obtained by a small distortion It is, however, not unlikely that the base of the second form is a multiple of that which corresponds to the cross section in the diagram In this case the molecules of second structure would have to be oriented in alternate directions

The figures given in Table III show that the long spacings of the second form are shorter than the corresponding spacings of the normal form The reason for this may either be a shortening of the molecule itself which would involve an alteration of the chain structure, or it may be a tilt of the normal chain relative to the base of the unit cell, or it may be the result of a re arrangement of the end groups accompanied by a contraction in the direction of the chain axes, or, of course, a combination of these changes A change in the chain structure itself is, however, not likely to occur A further investigation will decide which of the explanations is the correct one

Summary

1 The structures of a number of normal paraffins ranging from C_5H_{12} to $C_{30}H_{62}$ have been investigated by means of X-rays at liquid air temperature room temperature, and in the neighbourhood of the melting points

2 It is observed that the higher members of the paraffin series crystallise in the so-called normal form which has been described in an earlier paper irrespective whether their carbon content is an even or an odd number This normal form is found to be stable between the melting points and liquid air temperature

3 The linear expansion within these temperature limits has been investigated, and it is shown that the coefficient of expansion of the *a* axes is three to four times larger than the one of the *b* axes The coefficient of expansion of the *c* axes is very much smaller than the one of either the *a* or the *b* axes It was, in fact, too small to be measured in the present experiments

4 Differences in the behaviour of the even and the odd members begin to show when the carbon content of the substances decreases $C_{20}H_{42}$ and $C_{18}H_{38}$* both exist in two alternative structures Within a small range of temperatures near the melting points the normal form is found to be stable for either substance At lower temperatures a second crystal structure appears The change from one form into the other is reversible for $C_{20}H_{42}$ and $C_{18}H_{38}$ The change from the normal form into another one occurs also in the series of the odd members The transition takes place between $C_{11}H_{24}$ and C_9H_{20}

5 Observations taken in the immediate neighbourhood of the melting point indicate that these substances tend to form layer structures

6 The conclusions drawn from the experiments are given in the last section of the paper

The writer wishes to express his best thanks to Sir William Bragg for the friendly interest which he has taken in this work, also to Dr H S Gilchrist

---

* *Note added in proof*—The missing $C_{22}H_{46}$ has been investigated by the writer since this paper was sent in C_{22} behaves like C_{18} and C_{20}, *i e* it shows the two forms

and Mr E L Holmes for their unfailing and enthusiastic help He feels also much obliged to the managers of the Royal Institution for the opportunities given to him for carrying out this work at the Davy-Faraday Laboratory

EXPLANATION OF PLATES 5, 6

The X ray photographs 1–5 and 9–15 in the table are taken with "glass tube" samples of normal paraffins Radiation copper rays and Ni filler Film radius, 3 79 cms (1 mm = 1 510) Reproduction natural size

No 1 $C_{30}H_{62}$ room temperature
No 2 $C_{29}H_{60}$ room temperature
No 3 $C_{24}H_{50}$ liquid air temperature
No 4 $C_{17}H_{36}$ room temperature near melting point
No 5 $C_{17}H_{36}$ liquid air temperature
No 9 $C_{29}H_{60}$ liquid
No 10 $C_{29}H_{60}$ near melting point
No 11 $C_{20}H_{42}$ near melting point (normal form)
No 12 $C_{20}H_{42}$ second form
No 13 $C_{20}H_{42}$ liquid air temperature
No 14 $C_{6}H_{14}$ liquid air temperature
No 15 $C_{5}H_{12}$ liquid air temperature
No 6 $C_{19}H_{40}$ same distance and radiation as before, but substance spread into thin layer on glass Top, liquid air temperature bottom, room temperature
No 7 Enlargement of No 6
No 8 Photograph taken on plate at 15 00 cms distance Copper radiation Top, $C_{30}H_{62}$ room temperature middle, $C_{20}H_{42}$ second *form*, *bottom* $C_{20}H_4$ normal form Substances spread into layer on glass plate (by melting)

1

2

3

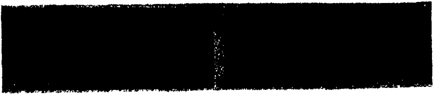

4

5

6

7

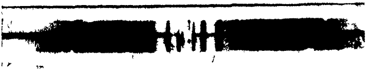

8

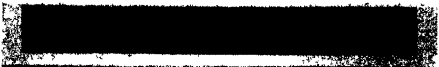

9

10

11

12

13

14

15

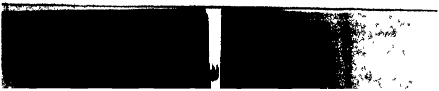

The Behaviour of a Single Crystal of Antimony subjected to Alternating Torsional Stresses

By H J Gough M B E , D Sc , Ph D , and H L Cox, B A , National Physical Laboratory

(Communicated by Sir Thomas Stanton, F R S —Received January 15, 1930)

[Plates 7–11]

Previous experiments on the failure by fatigue of single crystals of aluminium, iron and zinc, representing the face-centred cubic, the body-centred cubic, and the close packed hexagonal lattices, respectively, have shown that failure of metallic single crystals tends to occur by slip on the plane of greatest atomic density in the direction of greatest (linear) atomic density The results obtained with iron seemed to indicate that of the two factors, the linear density is the more important In all three lattices, however, the *line* of greatest density lay in the *plane* of greatest density, so that slip in the direction of the line of greatest density could always occur on the plane of greatest density and definite differentiation between the two factors was not possible The structure of antimony (and also of bismuth), however, is such that the planes of maximum density do not contain any of the lines of maximum density, so that if the type of the slip plane were determined, definite evidence of the relative importance of the two factors would be obtained The present experiment was designed to yield this evidence , but in so far as the results are inconclusive, it is hoped to obtain further evidence by a similar experiment on a single crystal of bismuth

Lattice Structure —The lattice structure of antimony as determined by A Ogg (' Phil Mag ,' vol 42, p 163 (1921)) and by James and Tunstall (' Phil Mag ,' vol 40, p 233 (1920)) is a lattice of trigonal symmetry composed of two similar face-centred rhombohedral lattices, similarly orientated, displaced relative to each other along the longest diagonal of the rhombohedron (the axis of trigonal symmetry) The angle between any pair of edges of the rhombohedron is 86° 58′ and the atoms are spaced along these edges at points 6 18 Å * apart The ratio of the lengths into which the lattice points of either constituent lattice divide the long diagonals of the other lattice is given as 0 412 0 588 by Ogg and as 0 389 0 611 by James and Tunstall For the purpose of the present report the exact value of this ratio is of little importance, but where some value has to be inserted (*e g*, in fig 1) the value 0 4 0 6 has for convenience been assumed

---

* A Ogg : James and Tunstall give 6 20 Å

Fig 1 shows three views of a model of the lattice structure of antimony which was constructed for the purpose of the present research The model was made in the form of a vertical hexagonal prism, about the trigonal axis of symmetry as axis, truncated at the top by three planes parallel to the rhombohedral faces Fig 1 (*a*) shows an elevation of the model with one (horizontal) diagonal of a rhombohedral face in the plane of the paper, fig 1 (*b*) an elevation with a pair of rhombohedral edges in this plane, fig 1 (*c*) is a plan of the model, the trigonal axis being perpendicular to the plane of the paper In all three diagrams the full black dots represent the atoms on the outside planes of the model and the open dots the atoms visible within the model, in order not to confuse the diagrams the internal horizontal supporting wires are omitted in figs 1 (*a*) and 1 (*b*) On figs 1 (*a*) and (*b*) are indicated the traces of such of the principal crystallographic planes as are perpendicular to the plane of each diagram Figs 1 (*d*), (*e*), (*f*), (*g*), (*h*) and (*k*) show the arrangement of atoms on the principal crystallographic planes together with the principal

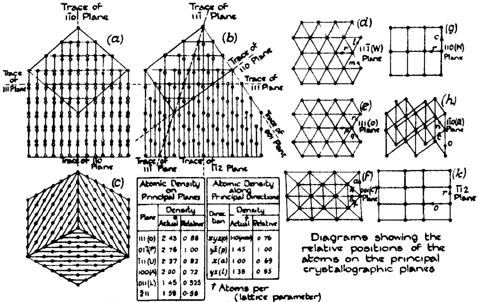

Atomic Density on Principal Planes

Plane	Density Actual*	Density Relative
111 (O)	2 43	0 88
$01\bar{1}$ (P)	2 76	1 00
$\bar{1}11$ (U)	2 27	0 82
100 (A)	2 00	0 72
011 (L)	1 45	0 525
$\bar{2}11$	1 59	0·58

* Atoms per (lattice parameter)²

Atomic Density along Principal Directions

Direction	Density Actual†	Density Relative
xyz (o)	1 10 (max)	0 76
$y\bar{z}$ (p)	1 45	1 00
x (a)	1 00	0 69
yz (l)	1 38	0 95

† Atoms per (lattice parameter)

Diagrams showing the relative positions of the atoms on the principal crystallographic planes

FIG 1—Diagrammatic Representation of the Structure of Antimony Rhombohedral Lattice (face centred) —Angle 86° 58′, Parameter 6 18 Å, with Interlaced Lattice displaced along Trigonal Axis

atomic directions contained by these planes The densities of the atoms on the principal planes and along the principal directions are also given in fig 1

Conventions and Symbols —The lattice structure of antimony is very nearly cubic, and for this reason the Millerian indices of the crystallographic planes have been referred to the rhombohedral edges as, in the case of the cubic structures, they are usually referred to the cube edges , but with this notation, planes, which in the cubic system would be of the *same* type, may in the present system be of *different* types, and, in particular, *the atomic densities on two such planes may not be the same* (*cf* Table I) Another important difference between the rhombohedral and the cubic systems is that in the rhombohedral lattice *the principal lines of atoms are not in general perpendicular to the principal atomic planes*

Fig 2 is a stereographic projection of the lattice of antimony in which the long diagonal of the rhombohedron (the axis of trigonal symmetry) is taken as the pole of the diagram This particular mode of projection is considered to be preferable to any other since, besides showing the true trigonal symmetry of the structure, it differentiates fairly clearly between planes of different atomic densities (*cf* Table I) Since the principal lines of atoms are not represented by the normals to the principal planes, these lines cannot conveniently

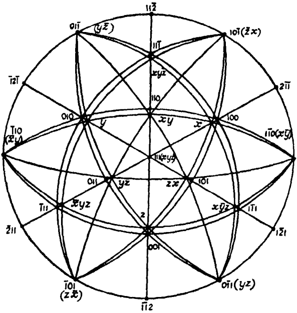

Fig 2 —Stereographic Projection of Rhombohedral Lattice Rhombohedral Angle (Antimony) = 86° 58′.

be denoted by the Millerian indices of the planes perpendicular to them, a supplementary notation must therefore be introduced For this purpose the rhombohedral lattice may be supposed to be obtained from the cubic lattice by a process of extension in the direction of one of the diagonals of the cube, this process of extension causes the principal lines of atoms to separate from the normals to the principal planes The principal lines of atoms might therefore be denoted by the indices of the planes with the normals to which they coalesce in the cubic structure, but these indices are already in use for the normals to the planes themselves These indices, therefore, when they refer to a line of atoms, are rewritten, x and $\bar{x}$ being substituted for 1 and $\bar{1}$ in the first place of the Millerian form, y and $\bar{y}$ for 1 and $\bar{1}$ in the second place, and z and $\bar{z}$ for 1 and $\bar{1}$ in the third, all zeroes being disregarded, each set is then, for convenience, rearranged in cyclical order Thus x denotes the line of intersection of the planes 010 and 001, $y\bar{z}$ the line of intersection of the planes 100 and 011, etc

In addition to the Millerian notation, it is convenient, for the purpose of stress analysis, etc, to denote each of the principal planes and lines by a separate letter, capital letters being used for the planes and the corresponding small letters for the lines of atoms with which the normals to each plane coalesce in the cubic structure In Tables I and II, where the second column shows the letter chosen to represent each plane and direction, this convention has been adopted

In Table I, the principal planes of the antimony structure are grouped in classes in terms of the density of atoms on the planes, and the atomic density on the planes of each group is listed together with the principal lines of atoms contained by each plane

It will be seen that the planes of highest atomic density are the $01\bar{1}$, $\bar{1}01$ and $1\bar{1}0$ planes, and that these planes are of a different type from the planes 011, 101 and 110, which have a much lower atomic density, that the plane next in atomic density to the $01\bar{1}$, $\bar{1}01$ and $1\bar{1}0$ planes is the 111 plane, and that this plane is of a different type from the $\bar{1}11$, $1\bar{1}1$ and $11\bar{1}$ planes, which again have a somewhat lower atomic density

In Table II the densities of atoms along the principal atomic directions are tabulated, together with the letters designating these directions The directions of highest (linear) atomic density are the *p*, *q*, *r* directions and the next in order are the *l*, *m*, *n* directions.

Table I

Millerian indices of plane	Designation	Contained directions	Density (atoms per lattice parameter)[2]	Relative density
111	O	*p*, *q*, *r*	2 43	0 88
$01\bar{1}$	P	*o*, *a*, *l*	2 76	1 00
$\bar{1}01$	Q	*o*, *b*, *m*		
$1\bar{1}0$	R	*o*, *c*, *n*		
$\bar{1}11$	U	*p*, *m*, *n*	2 27	0 82
$1\bar{1}1$	V	*q*, *n*, *l*		
$11\bar{1}$	W	*r*, *l*, *m*		
100	A	*p*, *l*, *b*, *c*	2 00	0 72
010	B	*q*, *m*, *c*, *a*		
001	C	*r*, *n*, *a*, *b*		
011	L	*p*, *a*	1 45	0 52_5
101	M	*q*, *b*		
110	N	*r*, *c*		
$2\bar{1}\bar{1}$	—	*o*, *p*	1 59	0 58
$\bar{1}2\bar{1}$	—	*o* *q*		
$\bar{1}\bar{1}2$	—	*o*, *r*		

Table II

Amended Millerian indices of line	Designation	Density (atoms per lattice parameter)	Relative density
xyz	*o*	1 10 (mean)	0 76
$y\bar{z}$	*p*	1 45	1 00
$z\bar{x}$	*q*		
$x\bar{y}$	*r*		
x	*a*	1 00	0 69
y	*b*		
z	*c*		
yz	*l*	1 38	0 95
zx	*m*		
xy	*n*		

Object of Experiment —From a consideration of the planar and linear atomic densities, as outlined in Tables I and II, it appeared that the slip plane of antimony might be either the 111 plane or the planes of the $01\bar{1}$ type From previous work on other metals there seems to be little doubt that the tendency to slip is a function of the atomic density on the slip plane and of the linear density in the slip direction, moreover, some recent experiments* have indicated that the latter is perhaps the more important factor On these grounds, therefore, it might be anticipated that the lower atomic density on the 111 plane, as compared with the density on planes of the $01\bar{1}$ type, would be compensated by the higher linear density in the p, q, r directions contained by the O plane, as compared with the linear density in the l, m, n directions contained by the P, Q, R planes

It appeared, therefore, of primary importance to determine the slip plane and, if possible, the slip direction also

From the results of a preliminary experiment on a specimen of antimony consisting of several large crystals, it was concluded that, in antimony as in zinc, mechanical twins were produced by the action of alternating torsional stresses, and fairly definite evidence was obtained as to the type of the twinning plane A secondary object of the main experiment, therefore, was to check this conclusion both as regards the production of twins and as to the identity of the twinning planes

Choice of Specimen and Stressing System—For these very general objects of research no particular orientation of specimen was more desirable than any other, and in any case, at the time of the inception of this experiment, one single crystal bar only was at the authors' disposal

The choice of stressing system was at once more critical and more under the authors' control Practically any type of stressing should suffice to show the slip plane, though if more than one slip plane were found to exist, the stressing system should preferably be such as to cause slip on as many slip planes as possible

Direct evidence as to the direction of slip could only be obtained by tests in which marked change of shape occurred, but fairly definite evidence can usually be obtained from tests in which very little plastic deformation takes place by comparison of the distribution of slip with the distribution of shear stress resolved on the slip plane in the probable slip directions Observation of twins and determination of the twinning planes, however, are most easily made on specimens in which very little distortion has occurred

In view of all these circumstances, alternating torsional stresses appeared to be the system most generally satisfactory, and the choice was finally decided by the fact that specimens for this type of test are relatively easy to machine

Preparation of Specimens, etc—The single crystal (reference mark S I) used in the present experiment was prepared from the liquid—by the Bridgman method—and was ¾ inch diameter and 7 inches in length. Of this total length only 2½ inches was truly single crystal, the remaining portion being composed of several large crystals. Two specimens were machined from this bar, one from the single crystal portion (reference mark S IB) and the other from the remaining portion (reference mark S IA), both to a cylindrical form, 0.35 inch diameter and 0.7 inch in length with enlarged ends (joined by transition curves) of diameter 0.5 inch, the total length of each specimen being 2.9 inches. Reference marks on the enlarged ends were provided for the purpose of measurement of twist. Extreme care was found to be necessary in machining these specimens, as the material tended to chip, and even with the extremely fine cuts that were taken (0.001 inch maximum) the position of the 111 plane was, after machining, quite well defined by the holes left where the material at the edge of this plane had been chipped away; this remark applies especially to the single crystal specimen, but the effect was noticeable also in the case of the other specimen.

---

* Taylor and Elam, 'Roy Soc Proc,' A, vol. 112, p 337 (1926), Gough, 'Roy Soc Proc,' A, vol. 118, p 498 (1928)

After machining, the specimen S IB was etched and then X-rayed, but the X-ray photograph obtained showed that deeper etching was necessary to remove the layer distorted during the turning operations. The specimen was accordingly etched more deeply and then again X-rayed, but the result was still not entirely satisfactory and the specimen was subjected to a further light polish and etch. The X-ray photograph then obtained being deemed sufficiently good, the specimen was given a metallurgical polish prior to test. Even after this continued etching and polishing (by which the mean diameter was reduced to 0.34 inch), the chipping at the edges of the 111 plane was still very noticeable. In addition, the cross section at the centre of the test portion was reduced to a roughly elliptical section, the maximum and minimum diameters being about 0.347 inch and 0.327 inch respectively; the mean diameter being 0.338 inch. The surface of the specimen was thus something in the nature of a hyperboloid of one sheet.

Fig. 3 is a stereographic diagram showing the orientations of the principal crystallographic planes and directions relative to the specimen axis and to the reference mark on one of the enlarged ends of the specimen S IB; these orientations were determined by correction of values obtained by the final X-ray analysis, the corrections being made on the assumption that the lattice structure was of the form stated by Ogg and by James and Tunstall. The spherical co-ordinates of the principal planes and directions are tabulated in Table III.

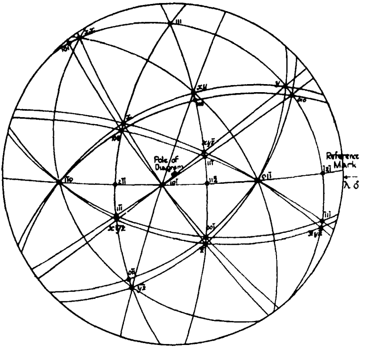

Fig 3 —Stereographic Diagram showing position of principal Planes

Preliminary Tests on S IA —The specimen S IA was used as a guide both as to the stresses the material was capable of supporting and as to the mode of deformation to be anticipated

The specimen was placed in the alternating torsion machine with the intention of subjecting it to a range of nominal shear stress of ± 0 5 ton per square inch, the specimen, however, fractured during the process of "loading-up" when this stress was little more than ± 0 4 ton per square inch The fracture was very complete, the main fractures being approximately parallel and perpendicular to the axis of torsion, there were some distinct cases of intercrystalline failure, but in the main the fractured surfaces appeared as cleavage planes, which were divided sharply into two types Actually the fracture was such that the whole parallel portion was disintegrated into three main portions and numerous splinters, although when first removed from the machine the pieces were more or less locked together in the manner of a jig-saw puzzle This complete disintegration, however, may have been due to the "hammering" action to which the specimen was subjected, while the machine was slowing down after the real fracture had occurred

Examples of the appearance of the two distinct types of cleavage planes are shown in figs 10 (Pl 7) and 12 (Pl 7) There can be no confusion as to which class any true cleavage belongs, for, even to the unaided eye, the two types of surface are easily distinguishable, the appearance of a surface such as is shown in fig 12 being very much brighter than such a surface as in fig 10

The straight bands apparent in fig 12 make with each other angles that are indistinguishable from 60°, moreover, these bands are clearly all of the same type Now the only plane of antimony having this trigonal symmetry is the plane O perpendicular to the trigonal axis, the cleavage plane shown in fig 12 and all other cleavage planes of this type must therefore be planes of the type 111, quite independently of the exact nature of the straight bands themselves

From the actual appearance of the straight bands it is reasonable to suppose that these bands represent the traces of twins on the O plane If this is so it should be possible by observation of the change of direction of one twin where it crosses another to deduce the identity of the twinning plane In fig 12 the traces of one twin within another are too short to permit of very accurate measurement, but it may be seen that approximately such traces divide the angle between the directions of the two twins concerned It may be shown that this indicates that the twinning planes are planes of the type 011

Assuming that the traces observed in fig 10 are the traces of the twinning and cleavage planes, it appears that the plane of fracture is such that the intersections on it of two of the twinning planes make equal and opposite angles with the intersection of the O plane It is easily shown that the necessary and sufficient condition that a plane should have this property is that the plane should contain one of the directions p, q, or r, and it appears further that on such planes the traces of the third twinning plane coincide with the traces of the O plane The absence in fig 10 of a fourth independent trace representing the third twinning plane was regarded as fairly definite evidence that the plane of fracture shown was of the above type, *i e*, of the type $\alpha 11$, $1\alpha 1$ or 11α, where α may have any value whatsoever

The principal planes of this type are the 111, 110, $11\bar{1}$ $11\bar{2}$ types of plane A comparison of figs 12 and 10 shows that the plane of fracture in fig 10 is not of the 111 type The angles between the intersections of the twinning planes and the intersection of the O plane on the remaining planes are as follows on the 110 plane ± 36 0°, on the $11\bar{1}$ plane ± 32 0°, and on the $11\bar{2}$ plane ± 33 5° The actual angles in fig 10 are almost exactly

± 36°, so that it appears that the second cleavage plane is actually the twinning plane

On the surface of this specimen after test very few markings were visible, and, since the orientations of the principal planes were not known, no deductions could be made as to the planes represented by the observed traces It is sufficient, therefore, to remark that the appearance of the few marks observed on the surface was very similar to the appearance of the marks subsequently observed on the surface of S IB after test

From this preliminary experiment it appeared probable that the cleavage plane (and hence, probably, also the slip plane) of antimony would prove to be the 111 plane and that twins would be formed on planes of the type 011, 101 and 110 It was also expected that the twinning planes would prove to be secondary cleavage planes

Stress Analysis of Antimony Single Crystal (S IB) *

Resolved Shear Stress—The equations to the shear stresses on the principal crystallographic planes resolved in the principal atomic directions contained by each plane were evaluated, using the co ordinates deduced from the corrected X-ray analysis The stress equation† is of the form $S_r/S = A \cos(\lambda - \alpha)$ where

S_r = value of resolved shear stress,

S = nominal maximum shear stress on the specimen

$\lambda = 2T/\pi r^3$ (T the applied torque and r the radius of the cross section of the specimen),

and where A and α are constants depending upon the orientations of the plane and direction considered

In Table III the values of A and α for the particular planes and directions considered are tabulated, and in fig 4 the values of S_r/S on some of these planes have been plotted against λ In fig 4, as elsewhere, the capital letter represents the plane and the small letter the direction of the resolved shear stress, this notation is in accordance with previous work

---

* The actual stresses upon the various crystallographic planes must have been to some extent modified by the actual shape of the test portion of the specimen, but it was not practicable to make any estimate of the nature or extent of this modification In any case it is not considered that this modification can have been serious, so that the ordinary stress analysis as for a circularly cylindrical specimen is used as a sufficiently good approximation.

† See 'J Inst Met,' vol. 36, pp 185–187 (1926)

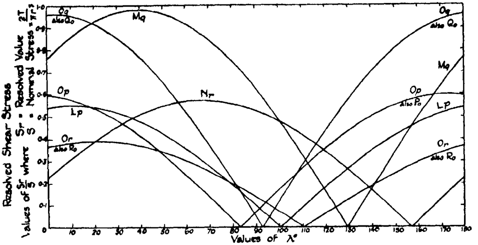

FIG 4 —Curves of Shear Stress, resolved on principal Crystallographic Planes, in the primitive Lattice Directions

Normal Stress —Using the equation* $N/S = \sin 2\theta_p \sin (\psi_p - \lambda)$ the values of the normal stresses N on the principal planes were evaluated and have been plotted in fig 5, the designating letters refer to the code shown in Table 1

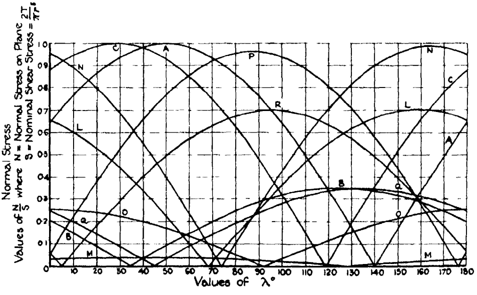

FIG 5 —Curves of Normal Stresses on Principal Planes

Traces of Planes —The slopes of the traces of the principal planes were calculated and are expressed graphically in fig 6

---

* *Loc cit*

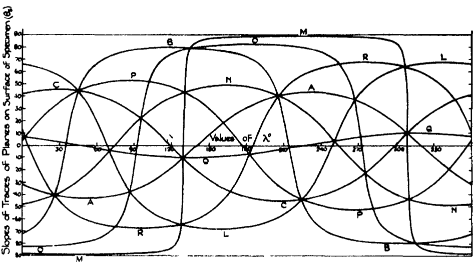

FIG 6 —Slopes of Traces of Principal Planes

Table III Spherical Co-ordinates and Stress Equation Constants

Plane					Constants in resolved shear stress equations			
Millerian indices	Relative density	Symbol	Spherical co ordinates		Symbol	Resolved direction	A	a°
			θ°	ψ°				
111	0 88	O	82 7	92 2	O*p*	$y\bar{z}$	0 601	172 2
					O*q*	$\bar{z}x$	0 961	3 2
					O*r*	$x\bar{y}$	0 389	20 4
$01\bar{1}$	1 00	P	52 6	356 8	P*l*	$\overline{yz}$	0 562	7 8
					P*a*	x	0 365	138 3
					P*o*	xyz	same as O*p*	
$10\bar{1}$		Q	10 1	225 3	Q*m*	zx	0 983	35 6
					Q*b*	y	0 934	128 8
					Q*o*	xyz	same as O*q*	
$1\bar{1}0$		R	67 7	185 1	R*n*	xy	0 548	63 7
					R*c*	$\bar{z}$	0 570	123 0
					R*o*	xyz	same as O*r*	
$0\bar{1}\bar{1}$	0 52$_5$	L	67 6	248 6	L*p*	$y\bar{z}$	0 368	10 5
					L*a*	x	0 594	133 5
101		M	88 8	129 4	M*q*	$\bar{z}x$	0 984	39 6
					M*b*	y	0 185	35 4
110		N	49 1	74 1	N*r*	$x\bar{y}$	0 571	66 8
					N*c*	$\bar{z}$	0 351	94 4

Record of Tests on the Specimen S IB (Single Crystal).—A record of all the tests made on the specimen S IB is given in Table IV below The twists recorded are reckoned positive when anti-clockwise and in every case denote the twists occurring in *each individual test*

Table IV —Record of Tests

Number of test	Range of nominal shear stress	Number of reversals	Permanent twist occurring during test	Treatment prior to next test
	ton per square inch		°	
1st	±0 1	51,000	0 7	None
2nd	±0 3	54,000	− 0 7	Repolished
3rd	±0 3	3 5 × 10^6	+3 1	Repolished
4th	±0 3	7 0 × 10^6	+0 5	None
5th	Fractured completely (while loading to ±0 6 ton per square inch) at about ±0 5 ton per square inch			

After each test the surface of the specimen was carefully examined in a metallurgical microscope, a survey made of all visible surface markings, and representative photo-micrographs were taken The apparatus used both for the visual examinations and for obtaining the photographic records has been described very fully in a previous paper (*loc cit*) As in previous reports, λ represents the angle subtended by the reference plane (containing the axis of the specimen and the reference mark on one of the enlarged ends) and the point on the surface to which reference is made Slopes of traces of planes, in the photo-micrographs as elsewhere, are reckoned positive and negative in the anti clockwise and clockwise senses respectively

Features exhibited by Microstructure of the Specimen S IB —After the first test (51,000 reversals of ± 0 1 ton per square inch) there were apparent on the surface of the specimen two main features firstly, a series of fine straight lines nearly parallel to the axis of the specimen , and secondly, two series of twin bands, the slopes of which varied between wide limits After the 2nd test (54,000 reversals of ± 0 3 ton per square inch) the same features were observed in greater profusion, together with indications of a third series of twin bands , in addition, several series of regular marks were observed within the twinned structures Prior to the third test (3 5 × 10^6 reversals at ± 0 3 ton per square inch) the specimen was repolished, and after this test the same features were again apparent on the surface All three sets of twin bands were easily measurable, and the two sets which appeared after the first test were now observed at nearly every value of λ. The fine straight lines were also apparent over the greater part of the surface and in one or two cases were readily identifiable as cracks In addition, within the two main sets of twin bands there were observed three main features that corresponded exactly with the three main features (i e, cracks, fine, straight lines and twin bands) apparent on the untwinned portions of the specimen Prior to the fourth test (7 0 × 10^6 reversals at ± 0 3 ton per square inch) the specimen was again repolished, but the most definite of the marks previously identified as cracks were not rendered entirely invisible by this treatment After test, these marks were very carefully examined for any sign of extension, but in this respect, as in all others, the appearance of the surface of the specimen was exactly the same as its appearance immediately before the test, no fresh marks of any kind being observed

It was intended, in the fifth test, to subject the specimen to a range of stress of ± 0 6 ton per square inch, but during the process of loading up the specimen fractured completely when the range of stress was still less than ± 0 5 ton per square inch Complete fracture parallel to one plane occurred in the test portion and another complete fracture parallel to two planes occurred across one of the enlarged ends within the collar holding this end in the chuck of the testing machine The appearance of the cleavage planes was similar to the appearance of the cleavage planes of the specimen S IA, the plane of fracture in the test length being of the type shown in fig 10 (Pl 7) and the planes of fracture in the enlarged end being one of the type shown in fig 10 and one of the type shown in fig 12 (Pl 7) The fracture in the test length was subsequently found to be parallel to the twinning plane L, and the two fractures in the enlarged end were found to be parallel to the planes O and N respectively

The surface of the specimen after fracture exhibited a few twin markings, mainly in the neighbourhood of the fracture Some of the cracks previously observed were again apparent and further photographs were taken to compare with those taken before test Photographs were also taken of the several cleavages (figs 11 and 13 (Pl 7)

Discussion of Features Exhibited by Microstructure—The slopes of the fine, straight lines on the untwinned portions of the specimen (and of the similar marks later recognisable as cracks) agreed closely with the calculated slope of the trace of the 111 plane (O) of the original structure The observed slopes of the primary twin bands agreed with the calculated slopes of the traces of the planes 110, 011 and 101 (N, L and M), the twins formed on the planes N and L being very much more numerous than those formed on the plane M The slopes of the fine straight lines (and of the subsequent cracks) within the twinned structures agreed closely with the calculated slopes of the traces of the 111 planes of the twinned structures The observed slopes of the secondary twin bands within the primary twins agreed with the calculated slopes of the traces of the planes of the type 011 of the particular twinned structure concerned

The distribution of the primary features after each test is shown in fig 7,

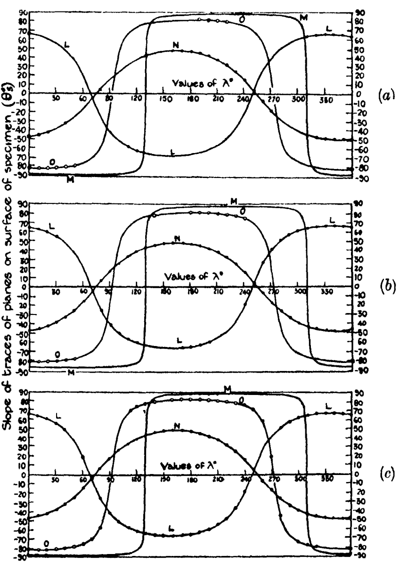

FIG 7 —Diagram showing recorded values of the slopes of twin bands and other surface markings observed within the primary structure of the crystal. Full circles refer to twin bands, open circles to fine lines or cracks.

(*a*) After first test, (*b*) after second test, (*c*) after third test in which the readings of the slopes of the fine lines and of the twin bands are recorded as open and closed dots respectively, upon curves representing the calculated traces of the planes O, L, M and N, the small experimental errors have been neglected in preparing these diagrams •

The distribution of the secondary features after the third test is shown in a similar manner in fig 9 This distribution was not sufficiently systematic to be of much theoretical interest, naturally it is largely dependent upon the distribution of the primary twin bands

Traces of the Plane O --The fine, straight lines observed in all the tests were identified beyond all doubt as traces of the 111 plane of the original structure Their distribution, particularly in the earlier tests (*cf* fig 7 (*a*)), was roughly in accordance with the expected distribution of slip bands deducible from the shear stress analysis (fig 4) Thus in fig 7 (*a*) which represents the marks observed after the first test, it will be seen that the fine lines were centred about $\lambda = 25°$ and $\lambda = 205°$, while from fig 4 it will be seen that the points of maximum resolved shear were at $\lambda = 3°$ and $\lambda = 183°$ The agreement is not sufficiently good to provide definite evidence as to the mode of formation of these fine lines, but by analogy with previous work it seems probable that they are formed as a result of the shear stresses resolved on the O plane in the p, q and r directions This hypothesis is supported by the results of all the tests in that, in each case, there are gaps centred about $\lambda = 93°$ and $\lambda = 273°$ corresponding to the minima of the resolved shear stress curves

The fine lines, however, had not the appearance of slip bands, rather, they appeared as very fine cracks without the continuity and regularity of spacing usually associated with true slip The characteristic appearance of the lines is illustrated by fig 15 (Pl 8) In the third test some of these lines developed into cracks that were easily recognisable as such, and it is not unreasonable to suggest that the lines observed in the earlier tests may also have been cracks, though they were not directly identifiable as such If this were the case, we have in antimony a material in which slip apparently does *not* occur, and the mode of failure under static stressing would seem to be of considerable interest

Twin Bands —The presence of twin bands in the surface of the specimen was made apparent by a difference in lustre (under normal lighting) and/or by the presence of regular marks within the twins Where the difference in lustre was slight and the marks within the twin faint, the twin bands were often difficult to see, but in these cases the twins could often be made more apparent by being thrown out of focus

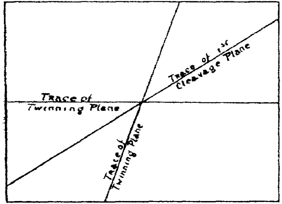

Fig 10 × 97

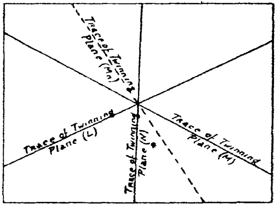
Trace of Twinning Plane (Mn)
Trace of Twinning Plane (L)
Trace of Twinning Plane (N)
Trace of Twinning Plane (M)

Fig 12 × 97

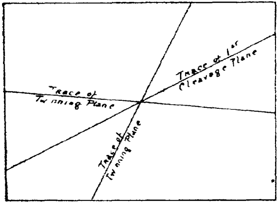

Fig 11 328

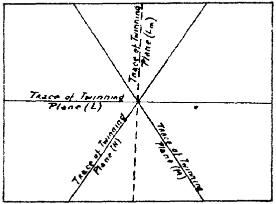
Trace of Twinning Plane (Lm)
Trace of Twinning Plane (L)
Trace of Twinning Plane (N)
Trace of Twinning Plane (M)

Fig 13 × 97

Figs 10 and 12 relate to specimen SIA Figs 11 and 13 relate to specimen SIB

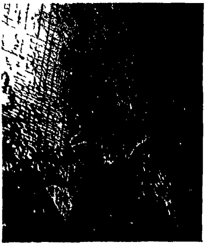

(*Facing p* 440)

Plate 8

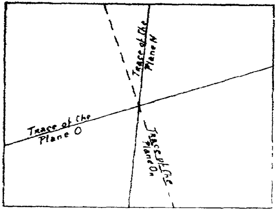

Fig 14 λ = 70° × 328

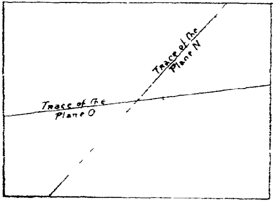

Fig 15 λ = 32 97

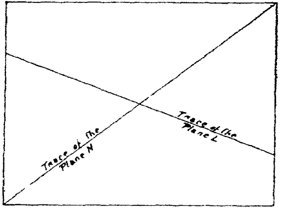

Fig 16 λ = 350° × 97

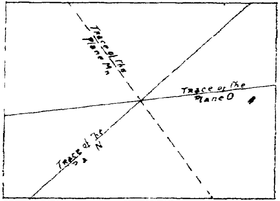

Fig 17 λ = 18° × 174

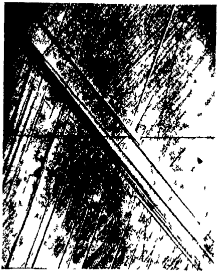

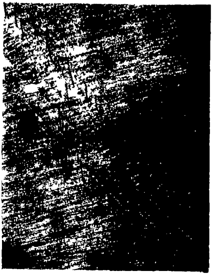

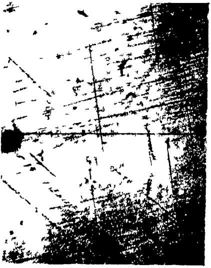

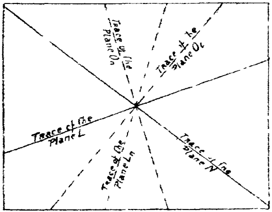

Fig 18 $\lambda = 164$ 179

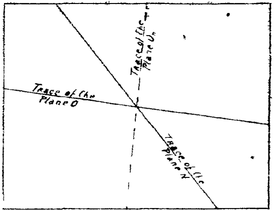

Fig 20 $\lambda = 215\frac{1}{2}°$ 328

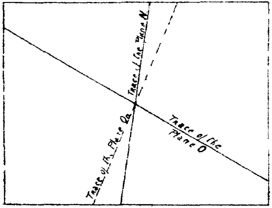

Fig 19 $\lambda = 260°$ 179

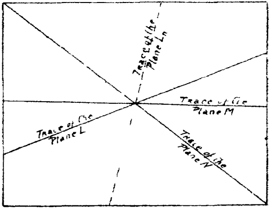

Fig 21 $\lambda = 173°$ 179

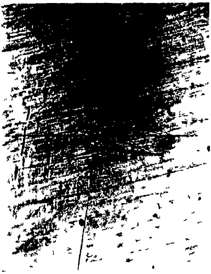

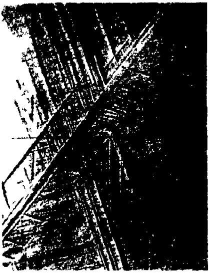

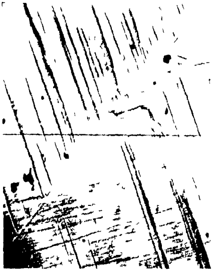

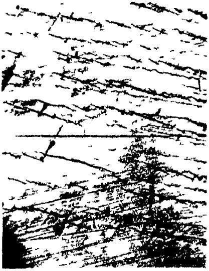

Plate 10

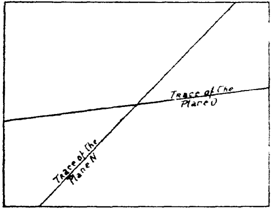

Fig 22 λ = 24½ 328

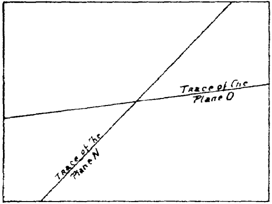

Fig 23 λ = 24½° 325

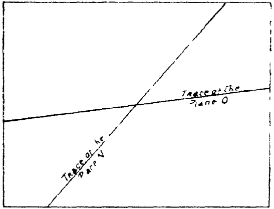

Fig 24 λ = 32° 97

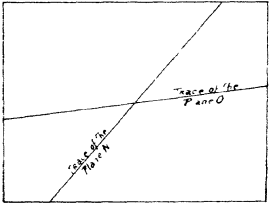

Fig 25 λ = 32° 97

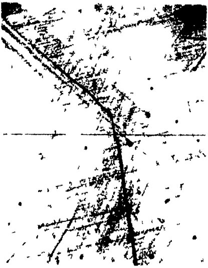

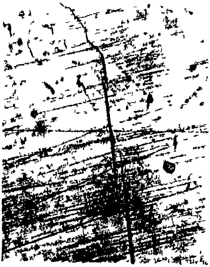

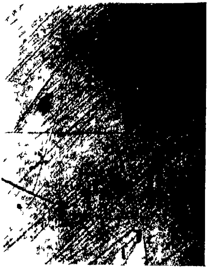

Plate 11

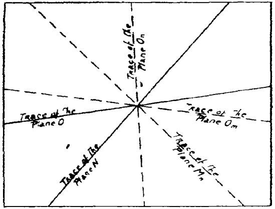

Fig 26 ι = 31° 179

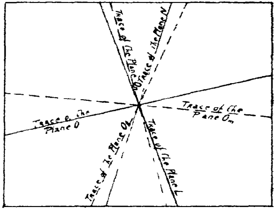

Fig 28 ι = 60° 179

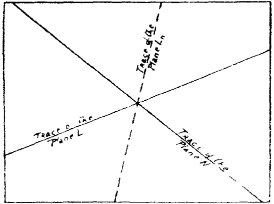

Fig27 ι = 18° 97

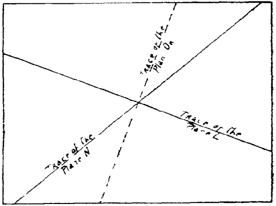

Fig 29 ι = 32° 97

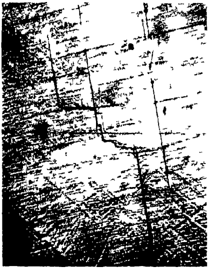

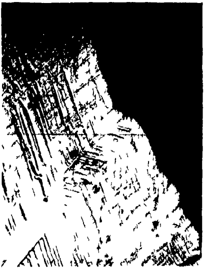

The twin bands observed were definitely identified as the traces of the N, L and M planes In the initial test, twins on the N and L planes only were observed, and in the final tests the twins on these planes were very much more numerous than the twins on the M plane thus from fig 7 (*c*) it will be seen that after the third test (3 5 × 10^6 reversals at ± 0 3 ton per sq inch) twins on the planes N and L were observed at practically every value of λ, whereas twins on the plane M were observed only in the ranges $\lambda = 0°$ to $40°$ and $\lambda = 180°$ to $210°$ Now, of the three possible twinning planes, the plane M alone contains the direction, which, according to shear stress considerations, should be the direction of deformation on the 111 plane

In a previous paper* on the deformation of a single crystal of zinc, the authors recorded the fact that of the six possible twinning planes (of zinc) the actual planes of formation of twins at any point never included the pair that contained the slip direction at that point, this fact has since been confirmed in the case of zinc by the results of further experiments

The predominance of N and L twins over M twins in the present experiment may be regarded as another example of the same phenomenon, although the evidence is not considered to be conclusive In view however, of the suggestion made in the previous paper† as to the possible effect of the normal stresses on the twinning planes, it should be noticed that the maximum normal stress on the plane M was very much lower than the maximum normal stress on either of the planes N or L, but it should also be remarked that, while at $\lambda = 72°$ (and $252°$) (*cf* fig 5) the normal stresses on all three twinning planes were practically equal, no traces of M twins were observed at either of these values of λ, though both N and L twins were recorded ‡

Of the N and L twins the former were slightly more numerous, and in the regions $\lambda = 50°$ to $90°$ and $\lambda = 230°$ to $270°$, twins on the plane L were very few indeed If, in accordance with the deductions drawn from the experiments on zinc, twinning is a direct result of deformation on the cleavage (or slip) plane, no twins would be expected to be formed in regions where deformation on the cleavage plane was not evidenced by the presence of the fine straight lines Thus, referring to the examination after the third test (fig 7 (*c*)) it seems that twins would not have been expected to appear in the neighbourhood of $\lambda = 90°$ and $\lambda = 270°$ (corresponding approximately also to the points of minimum resolved shear stress on the 111 plane) That twins do appear in these regions may be due to the "overrunning" effect proposed in the case of zinc,* and the predominance of N twins over L twins in these regions may be caused by some factor affecting the relative tendencies of each type of twin to overrun

---

* 'Roy Soc Proc,' A, vol 123, p 143 (1929)

† *Loc cit*

‡ At these values of λ the traces of the N and L planes have the same slope (fig 6) One type of twin could, however be distinguished from the other by the sense of the change of slope occurring in the field of the microscope

It is therefore suggested that the phenomena of mechanical production of twins, as observed in the present experiment, are in many ways analogous to similar phenomena observed in the case of zinc, and that the hypothesis proposed to account for one set of phenomena will, reasonably, account also for the other set

The present experiment definitely confirms the conclusions drawn from the results of the previous experiment (on the specimen S IA) as to the type of the twinning planes, and it is regarded as established that *the twinning planes of antimony are of the* 110 *type*

Structure within the Twin Perhaps the most interesting feature of the present experiment is the wealth of detail observable within the primary twin bands Not only fine lines and cracks (corresponding to the fine lines and cracks on the original structure), but secondary twin bands also, were observed within the primary twins, and the correlation of the directions of these secondary lines and bands with the theoretical directions of the cleavage and twinning planes within the twins yielded valuable corroborative evidence as to the types of the planes on which these deformations occur

Before entering upon the discussion of the marks observed within the twins it is necessary to extend the notation already described to include the crystallographic planes and directions belonging to the twinned structure

This is conveniently done by denoting each plane and direction of the twinned structure by the same letter as was used to denote the corresponding plane or direction of the original structure and adding as a suffix the letter denoting the primary twinning plane Thus O_l denotes the 111 plane of the structure twinned on the plane L, M_n the 101 plane of the structure twinned on the plane N, etc It should be noticed that by this convention each twinned structure is a mirror image of the original structure in the particular twinning plane concerned, and, as a result, the sense of the structure (or rather of the notation) is reversed

Fig 8 is a stereographic diagram of the structure of a single crystal of antimony (with the trigonal axis as pole) and of the three structures formed by twinning on the planes L, M, N of the original structure The conventions

---

* *Loc cit*

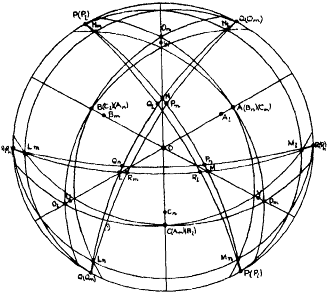

FIG 8 —Stereographic Diagram showing Positions of Twinned Planes (All twinned planes should be preceded by a negative sign)

and notation are as explained above The calculated slopes of the traces of the planes O, L, M and N for the three twinned structures are shown in fig 9

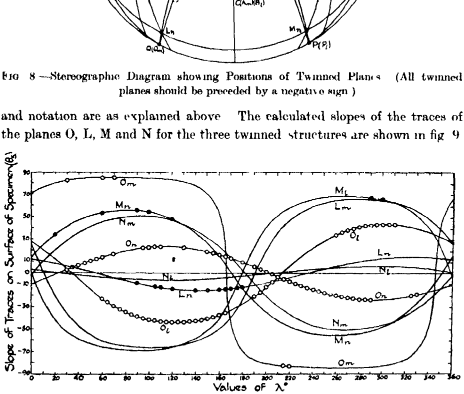

FIG 9 —Diagram showing recorded values of slopes of surface marks within the twinned structures ○ refers to fine lines or cracks, ● to secondary twin bands

After the first test (51,000 reversals of ± 0 1 ton per square inch) the twins observed on the surface of the specimen did not contain any internal marks

After the second test (54,000 reversals of ± 0 3 ton per square inch) the majority of the twins still lacked internal detail, but, at various points, there were observed within the twins fine lines very similar in appearance to the fine lines observed in the original structure, although shorter and less definite in direction The appearance of the twins in a typical region is shown in fig 14 (Pl 8), while fig 16 (Pl 8) shows their appearance where no internal marks were observed In fig 14 the twins shown are formed on the plane N and the agreement of their directions with the calculated slopes of the trace of this plane is evident but, in addition, it is clear that the fine lines within these twins agree in direction with the slopes of the trace of the 111 plane of the twinned structure It was concluded therefore, that these fine lines were exactly analogous to the fine lines observed in the original structure

After the third test (3 5 × 10^6 reversals of ± 0 3 ton per square inch) the above conclusion as to the nature of the fine lines within the twins was fully confirmed , figs 18, 19, 20, 26 and 28 (Plates 9, 11) afford ample proof of the identity of the fine lines and cracks within the twins with the traces of the O planes of the twinned structures In one or two cases, however, the lines " tended to follow the direction of the twins themselves (this effect is shown in figs 22 and 24 Pl 10) , but in these cases the lines were definitely recognisable as cracks

At this stage there were also observed within the primary twins, secondary twin bands that were found to agree in slope with the traces of the twinning planes of the twinned structure This agreement is illustrated in figs 17 (Pl 8), 18 and 21 (Pl 9) (Fig 21 also serves to illustrate a number of twins of the type M, which were observed only in this and in the complementary region)

In one or two photographs, particularly in fig 26 (Pl 11), small portions of the fine lines may be observed parallel to the trace of the O_m plane In the region of fig 26 ($\lambda = 31°$) M twins were actually recorded , but even where no M twins were observed there are very short traces parallel to the O_m plane These latter may have been due either to the presence of small M twins in the original structure, or more probably to the production of small twins on this plane by the stresses set up in the neighbourhood of the original fine lines

Cracks —In addition to the fine lines that were observed on the surface of the specimen after every test, there were apparent after the third test (3 5 × 10^6 reversals of ± 0 3 ton per square inch) a number of definite cracks following several fairly well-defined directions, being parallel either to the traces of the O plane or to the traces of the twinning planes either of the original or of one of the twinned structures In fig 28 (Pl 11) a crack is shown which follows the directions O of the original structure and the directions O_l, O_m and O_n of the structures twinned on the plane L, M and N respectively The strong resemblance in everything but in size between the main crack and the fine lines surrounding it tends to show that the fine lines are themselves small cracks

Two cracks are shown in figs 22 and 24 (Pl 10) where the main directions are parallel to the traces of the O and N planes Both photographs are particularly interesting in that the cracks shown were not obliterated by the repolishing of the specimen prior to the fourth test After this test ($7\ 0 \times 10^6$ reversals of ± 0 3 ton per square inch) these cracks were again photographed as nearly as possible in the same position These photographs are reproduced in figs 23 and 25 (Pl 10), and by comparison with figs 22 and 24 (Pl 10) it will be seen that the changes in appearance were negligible A comparison of fig 25 with fig 24 affords a decisive test of the similarity of the cracks before and after the fourth test In fig 24 the end of that portion of the crack which follows the direction of the N twin can be distinguished fairly clearly about 4 5 cms from the kink in the middle of the photograph, in fig 25 this same end can just be seen at the same distance from the kink These two photographs, therefore, provide definite evidence that the cracks formed during $3\ 5 \times 10^6$ reversals of a range of stress of ± 0 3 ton per square inch, did not extend during a further $7\ 0 \times 10^6$ reversals of the same range of stress, this is remarkable in view of the extreme "fine-ness ratio" of the crack and of the "brittle" nature of the material

After the fifth test in which complete fracture occurred these two cracks were again examined, and it was found that they had just joined Sufficient photographs were taken to make a panorama of the complete crack, this panorama served also to illustrate the main directions followed by all the cracks both in the original and in the twinned structures

Distribution of Cracks—The distribution of such recognisable cracks as were mainly parallel to the O plane was roughly in accordance with the distribution of resolved shear stress, thus the crack shown in figs 24 and 25 occurred at $\lambda = 32°$ On the other hand, the cracks which followed in the main the edges of the twins could not be expected to bear any relation to the resolved shear stresses and appeared to be independent of them It appears probable that the intensity of normal stress on the twinning planes would affect the propagation of cracks along the edges of the twins

Final Fracture—Final fracture in the test portion occurred completely across the specimen parallel to the L plane, a small portion at the vertex of the ellipse thus formed also broke away from the remainder of the specimen parallel to the N plane The surfaces of the fractures were not absolutely plane, but appeared to be "stepped" Figs 27 and 29 (Pl 11) show two views of the edge of the fracture in the test portion From these it can be seen that the fracture as a whole followed the L direction, but in crossing an N twin tended to follow either the L_n or the O_n direction At other points the edge of the fracture while still following the L (or N) direction was "splintered" parallel to the O plane and the edge of the fracture was thus rendered very irregular The apparent stepping of the plane of fracture appeared also to be due to "splintering" parallel to the O plane, and this "splintering" was in such a direction as to increase the inclination of the plane of fracture to the axis of the specimen

Cleavages — Photographs were also taken of the cleavage faces after fracture and two of these are reproduced in the present report, figs 11 and 13 (Pl 7) A comparison of these photographs with figs 10 and 12 (Pl 7) show that the deductions drawn from the results of the preliminary experiment on the specimen S 1A were fully justified

Summary of Results of Experiments

1 The specimen did not deform by "slip" and no slip bands were observed A number of "fine lines" or cracks were, however, observed which corresponded to the traces of planes perpendicular to the axis of trigonal symmetry, this plane, while not of the maximum atomic density, does contain the three principal lines of atoms, and hence might be expected to act as slip plane

2 The twinning planes of antimony have been identified as of the 011 type (making an angle of 52° 37′ with the axis of trigonal symmetry), twins were observed on all three planes (011, 101 and 110) of this type

3 The "mirror image" nature of the structure within the primary twin bands was established by observation of secondary twins and other markings within the bands

4 The cracks and fracture faces followed, in general, well-defined crystallographic planes The first cracks observed coincided with the traces of the 111 plane of the original structure or of the twinned structures, although some of the larger cracks tended to extend along the edges of the twins themselves Final fracture, however occurred by complete cleavage parallel to one of the twinning planes with a small secondary cleavage parallel to another twinning plane

5 Owing to the fact that no definite slip bands were observed, the nature of the dependence of slip on the maximum linear and planar atomic densities could not be investigated It is hoped, however, to repeat the experiment on a single crystal of bismuth, which is believed to be much more plastic

The experiment is an item of a general programme of research performed for the Engineering Research Board of the Department of Scientific and Industrial Research and the Aeronautical Research Committee the authors' thanks are due to these bodies for the research facilities afforded and for permission to publish the results

The crystal of antimony used in the present experiment was prepared by Mr V H Stott, M Sc, of the Metallurgy Department of the N P L, and was etched and polished in the same department under the direction of Mr J D Grogan, B A, the X-ray analyses were carried out in the Physics Department of the N P L by Mr I Backhurst, M Sc The present authors wish to express their indebtedness to Mr Stott, to Mr Grogan and to Mr Backhurst for their invaluable assistance in these directions

---

Further Experiments on the Behaviour of Single Crystals of Zinc subjected to Alternating Torsional Stresses

By H J Gough M B E D Sc, and H L Cox, B A

(Communicated by Sir Thomas Stanton, F R S Received January 15, 1930)

[Plates 12-15]

Object of Experiment From the results of a previous experiment* on a single crystal of zinc, it was concluded that the formation of twins in zinc occurred on planes of the $10\bar{1}2$ type and that the particular operative twinning plane (of the six available) was determined chiefly by the direction of slip on the original† basal plane and possibly, to some extent, by the relative magnitudes of the normal stresses on the possible twinning planes In this previous experiment the orientation of the crystal was such that slip on the original basal plane occurred in one direction only and one pair of complementary twins only was observed

From the results it was predicted that if a test were made on a crystal of suitable relative orientation of the crystallographic and straining axes such that *all three slip directions* became operative, then the *operative* twinning planes should change with the slip direction The present experiment was planned in order to test this prediction Again, in the previous experiment, of the two possible pairs of complementary twinning planes associated with any one slip direction, it appeared probable that the choice of the operative pair was influenced by considerations of normal stress on the twinning plane The present experiment would, it was hoped, throw further light on this aspect of twinning

---

* 'Roy Soc Proc,' A, vol 123, pp 143-167 (1929)

† Associated with the initial structure of the unstressed crystal

For the purpose of such a critical experiment the optimum orientation would have been that in which the basal plane was perpendicular to the axis of torsion , all three slip directions would then have been *equally* involved The zinc single crystal bars at our disposal were therefore subjected to preliminary X-ray analysis with the object of determining the bar, the orientation of which was nearest to the required orientation

One bar, reference mark Z5, was found in which the normal to the basal plane made an angle of about 15° with the axis of the bar Three specimens, reference marks Z5A, Z5B and Z5C, were therefore machined from this bar

Preparation of Specimens, etc – The single crystal bar used in this experiment was prepared from the liquid– by the Bridgman method and was ⅜ inch diameter and 10 inches in length The X-ray photograph taken at this stage revealed clearly-defined reflections free from "asterism" effects The first specimen, reference mark Z5A, machined from this bar was of a cylindrical form 0 35-inch diameter and 0 75 inch in length with enlarged ends (joined by transition curves) of diameter 0 5 inch, the total length being 2 9 inches , reference marks were carefully scribed on the enlarged ends for the purpose of measurement Extreme care had to be taken in machining specimens from this bar owing to the tendency of the crystal to cleave along the basal plane , and, as in the previous experiment, cuts of 0 001 inch were found to be the maximum permissible An X-ray photograph taken after machining revealed very little resolution from the concentric rings of a complete "powder pattern, showing, as was expected, that machining had produced severe surface distortion The specimen was then deeply etched , but the X-ray photograph then obtained was still not satisfactory After further etching the specimen was again X-rayed, and the resolution into spots being now considered sufficiently good the specimen was given a metallurgical polish prior to test The mean diameter of the polished surface before test was 0 340 inch

Subsequently two other specimens, Z5B and Z5C, were machined from the same bar to a cylindrical form 0 4 inch diameter and 0 6 inch in length with enlarged ends (joined by transition curves) of diameter 0 6 inch, the total length being 2 8 inches , as in the case of Z5A, reference marks were scribed on the enlarged ends The larger diameters and shorter lengths were adopted, in order to reduce both the amount of material to be removed by machining and the tendency of the specimens to fracture across the enlarged ends, as the specimen Z5A, which was tested before Z5B and Z5C were put in hand, had fractured in this way As a further means to avoid this type of failure special split collars for *each end of each specimen* were carefully machined to fit closely over the enlarged ends and to be a good sliding fit in the chucks of the machine in which the tests were made

Both the specimens, Z5B and Z5C, were then deeply etched and X ray photographs were taken , these photographs being satisfactory as regards definition of the spots, the specimens were given a metallurgical polish prior to test The mean diameters of the polished surfaces before test were 0 394 inch in the case of Z5B and 0 388 inch in the case of Z5C

The stereographic diagram of fig 1 shows the orientation, referred to the specimen axis and to the reference mark on the enlarged end of the specimen, of the principal crystallographic planes of the specimen Z5B, as determined

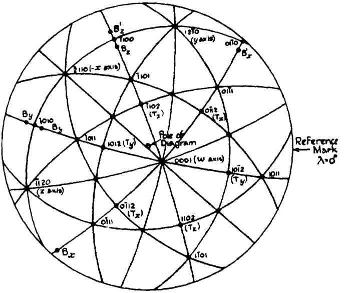

FIG 1 —Stereographic Projection showing Positions of Principal Planes and Twinned Positions of Basal Planes

from the corrected X-ray analysis The spherical co-ordinates of the principal planes of this specimen are listed in Table II

Record of Experiments - All the specimens were tested under alternating torsional couples Details of all the tests are given in Table I below The twists tabulated are the relative angular movements of the reference marks on the enlarged ends occurring during *each particular* test, the anti-clockwise sense is taken as positive

Table I

Specimen	Number of test	Range of nominal shear stress tons per square inch	Number of reversals	Permanent twist produced during individual test	History and treatment prior to next test
Z5A	1st	±0 5	25,000	None	Repolished
Z5A	2nd	±0 8	26 400	−1 3°	Repolished
Z5A	3rd	±0 8	0 10 10^6	+2 1°	Fractured across enlarged end Measurement of twist only approximate owing to the specimen being bent
Z5B	1st	±0 5	38,000	None	—
Z5B	2nd	±0 8	25 700	−0 8°	Repolished
Z5B	3rd	±0 8	6 02 × 10^6	+1 8°	Polished and etched for examination and finally repolished
Z5B	4th	failed during loading		—	Fractured in test length
Z5C	1st	±0 8	0 26 10^6		Fractured across enlarged end

After each test the surface of the specimen concerned was very carefully examined in a metallurgical microscope using a 4 mm Apochromat objective (Zeiss) The apparatus used for this purpose has been described very fully in a previous paper[*], as before, λ represents the angle subtended by the reference plane (containing the axis of the specimen and the reference mark on the enlarged end) and the point on the surface considered A number of representative photomicrographs were taken and some of these are reproduced in the present report In all the photographs of the surface of any specimen, the vertical black line is the line of zero slope used for measurement of the slope of the slip bands or twin markings, positive and negative angles are measured, respectively, anti-clockwise and clockwise from this datum line

Conventions and Symbols The conventions and symbols used in the previous experiment* have been adhered to throughout, save that, in Table II, and subsequently, the twinning planes p_x^2, p_x^{-2}, p_y^2, etc (which in the previous report were called T^3, T^4, T', etc), have been renamed T_x, T_x', T_y, etc , and in accordance with this alteration, B_x, B_x', B_y, etc , in the present report denote the basal planes belonging to the structures twinned on the planes T_x T_x' T_y, etc , respectively

---

[*] 'Roy Soc Proc,' A, vol 118, p 498 (1928)

Stress Analyses of Zinc Single Crystals Z5A, Z5B and Z5C

Resolved Shear Stress The equations to the shear stresses on the principal crystallographic planes resolved in the direction of the primitive lattice direction (*s*) contained by the planes were evaluated for each specimen The stress equation† is of the form

$$S_r/S = A \cos(\lambda - \alpha)$$

where S_r = value of resolved shear stress at surface of specimen

S = nominal maximum shear stress at surface of specimen

λ = angular distance of point considered from reference plane,

and where A and α are constants

Since the three specimens were cut all from the same bar, the θ co ordinates of corresponding planes were effectively the same in each specimen, the ψ co-ordinates differing by constant amounts For the same reason the constants ' A " (in the stress equations) did not differ appreciably for different specimens, while the constants " α " differed by the same constant difference as the ' ψ " co-ordinates For this reason, in Table II below, the spherical co-ordinates and the values of A and α for the principal crystallographic planes have been tabulated for the specimen Z5B only

In fig 2, the values of S_r/S have been plotted against λ for the following crystallographic planes of Z5B

Basal plane (B)

First order prismatic planes (P_x, P_y P_z)

Second order prismatic planes (P_{yz}, P_{zx}, P_{xy})

First order pyramidal (two) planes (p_x^2, p_x^{-2}, p_y^2, p_y^{-2}, p_z^2, p_z^{-2})

---

* ' Roy Soc Proc ,' A, vol 123, pp 143–167 (1929)

† See ' J Inst Met ,' vol 36, pp 185–187 (1926)

Table II —Spherical Co-ordinates and Stress Equation Constants for specimen Z5B

Plane				Spherical co-ordinates		Shear stress constants			
Millerian indices	Type	Relative density	Symbol	θ	ψ	Symbol	Resolved direction	A	a°
0001 (w axis)	Basal	1 00	B	15 7	315 5	Bx	$\bar{2}110$	0 852	49 5
						By	$\bar{1}2\bar{1}0$	0 931	165 9
						Bz	$\bar{1}\bar{1}20$	0 942	111 8
$01\bar{1}0$	First order prismatic	0 47	P_x	89 1	48 8	$P_x x$	$\bar{2}110$	0 273	143 8
						$P_x w$	0001	0 962	138 5
$\bar{1}010$			P_y	76 7	170 1	$P_y y$	$\bar{1}2\bar{1}0$	0 265	19 9
						$P_y w$	0001	0 885	82 3
$\bar{1}100$			P_z	75 8	100 0	$P_z z$	$\bar{1}\bar{1}20$	0 267	86 3
						$P_z w$	0001	0 874	16 0
$\bar{2}110$ (x axis)	Second order prismatic	0 54	P_y	74 2	139 2	$P_{yz} w$ (also Bx)	0001	0 852	49 5
$\bar{1}2\bar{1}0$ (y axis)			P_{zx}	81 5	78 0	$P_{zx} w$ (also By)	0001	0 931	165 9
$\bar{1}\bar{1}20$ (z axis)			P_{xy}	83 0	200 0	$P_{xy} w$ (also Bz)	0001	0 942	111 8
$01\bar{1}2$	First order pyramidal (two)	0 34	p_x^2 (T_x)	48 0	34 3	$p_x^2 x$	$\bar{2}110$	0 623	31 1
$0\bar{1}12$			p_x^{-2} (T_x)	50 0	243 0	$p_x^{-2} x$	$\bar{2}110$	0 604	68 7
$\bar{1}012$			p_y^2 (T_y)	34 6	181 0	$p_y^2 y$	$\bar{1}2\bar{1}0$	0 800	173 7
$10\bar{1}2$			p_y^{-2} (T_y)	60 5	343 0	$p_y^{-2} y$	$\bar{1}2\bar{1}0$	0 493	153 4
$1\bar{1}02$			p_z^2 (T_z)	61 3	293 7	$p_z^2 z$	$\bar{1}\bar{1}20$	0 481	123 3
$\bar{1}102$			p_z^{-2} (T_z)	33 5	99 1	$p_z^{-2} z$	$\bar{1}\bar{1}20$	0 818	105 5

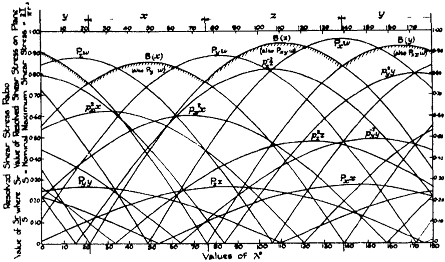

FIG 2 —Resolved Shear Stress Ratios on Principal Crystallographic Planes

The diagram shows that, from considerations of resolved shear stress, all three slip directions on the basal plane are involved, the ranges of λ over which each resolved shear stress is greater than either of the other two being approximately equal

Normal stress —Using the equation*

$$N/S = \sin 2\theta_p \sin(\psi_t - \lambda)$$

where N is the normal stress on the plane whose spherical co ordinates are $(\theta_p \psi_p)$ and where S and λ are as previously defined, the values of the ratio N/S were evaluated for the basal and first order pyramidal (two) planes of the specimen Z5B In fig 3 these values are shown plotted against λ

Traces of Planes -The slopes of the traces of the principal crystallographic planes of the specimen Z5B were calculated from the X-ray analysis and are expressed graphically in fig 4, the convention of sign of slope being as defined above

Diagrams for Z5A *and* Z5C —Figs 1, 2, 3 and 4 and all diagrams for Z5B, in which values of λ are used as abscissæ, apply equally to the specimens Z5A and Z5C, if, to the values of λ for Z5B, there is added 126 5° in the case of Z5A and 270° in the case of Z5C A similar alteration may be made to Table II, the values of ψ and α only being affected

---

* See ' J Inst Met ,' *loc cit*

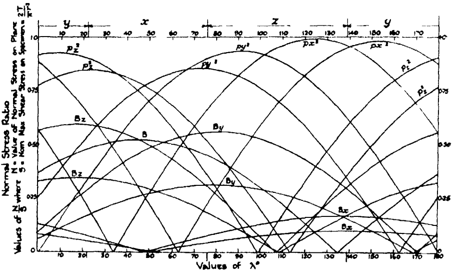

FIG 3 —Normal Stress Ratios on Principal Crystallographic Planes

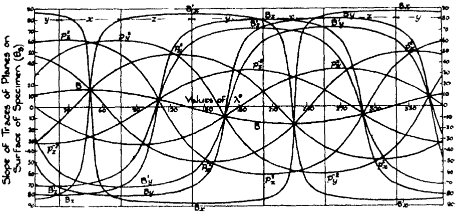

FIG 4 —Slopes of Traces of Principal Crystallographic Planes

(In figs 2–4, x, y, and z denote the operative slip direction over the area indicated)

Features Exhibited by Microstructure —The features exhibited by the microstructure of each specimen after test were always of two distinct types (1) a closely spaced system of slip bands nearly perpendicular to the axis of the specimen, (2) six distinct sets of twin bands agreeing very closely with the traces of the first order pyramidal (two) planes In the later stages of test on the specimen Z5B there appeared a third feature, a series of long, black lines nearly parallel to the axis of torsion and extending the whole length of the specimen It appears convenient to discuss briefly the appearance of each specimen after each test, and subsequently to review the results as a whole both in relation to the predictions made from the results of the previous experiment and with regard to any further conclusions that may be drawn

Specimen Z5A —The examination of the surface of Z5A before test revealed a few isolated marks having the general appearance of twin bands While these bands were too faint to be directly identifiable as twins, their direction in every case agreed well with the calculated slope of the trace of one of the six twinning planes It was therefore concluded that these marks were twins produced probably in the process of machining and not entirely removed by the subsequent etching and polishing processes The appearance of these twins before test is of some value in that it shows that the many more numerous twin bands recorded after test were indeed produced by the alternating torsional stresses, and were not present in the specimen before the tests were commenced

In figs 5 (*a*), (*b*) and (*c*) are plotted the calculated slopes of the traces of the slip and twinning planes of the specimen Z5A The vertical lines at $\lambda = 22°$, $86°$, $148°$ (and corresponding positions) divide these diagrams at the points where, according to shear stress considerations the slip direction on the basal plane should change from one primitive direction to another For all values of λ between any two such vertical lines one slip direction only should be concerned, each range is therefore marked with the particular slip direction involved Since the stresses applied to the specimen were alternating stresses, no distinction is made as to the sense of these directions

On fig 5 (*a*) are indicated the positions and slope of the slip and twin bands apparent on the surface of the specimen after the first test (25,000 reversals of $\pm 0\ 5$ ton per square inch), the readings being recorded by full black dots in the case of twin bands and by open dots in the case of slip bands The actual readings observed differed from the calculated values by small amounts not exceeding $\pm 2°$, these small differences have been neglected in preparing the diagram In the same way the slip and twin bands observed after the second test are shown in fig 5 (*b*) and after the third test (in which fracture occurred) in fig 5 (*c*) Details of these tests are given in Table I

Specimen Z5B —In figs 6 (*a*), 6 (*b*) and 6 (*c*) are plotted the calculated slopes of the traces of the slip and twinning planes of the specimen Z5B The vertical lines at $\lambda = 22°$, $76°$, $139°$, $202°$, $256°$ and $319°$ divide these diagrams into regions within each of which the slip direction is constant and each region is marked with the appropriate letter denoting the slip direction concerned

On fig 6 (*a*) are shown the slip and twin bands apparent on the surface of the specimen after the first test (38,000 reversals of $\pm 0\ 5$ ton per square

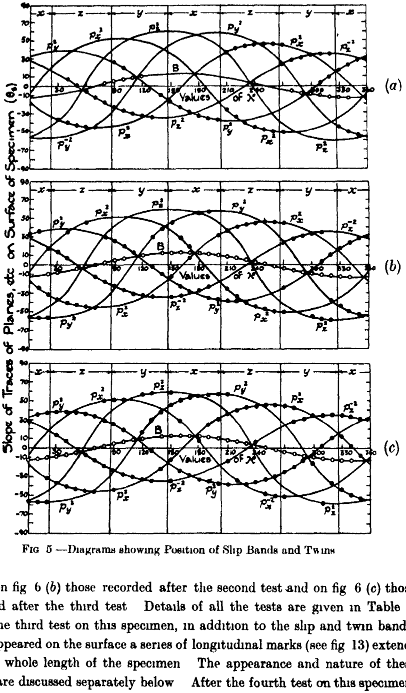

FIG 5 —Diagrams showing Position of Slip Bands and Twins

inch), on fig 6 (*b*) those recorded after the second test and on fig 6 (*c*) those recorded after the third test Details of all the tests are given in Table I After the third test on this specimen, in addition to the slip and twin bands, there appeared on the surface a series of longitudinal marks (see fig 13) extending the whole length of the specimen The appearance and nature of these marks are discussed separately below After the fourth test on this specimen, in which fracture occurred before the required stress range had been reached,

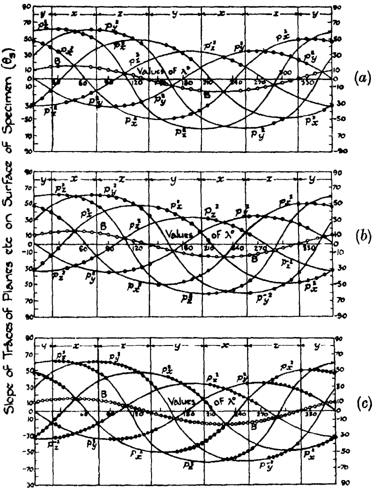

Fig 6 —Diagrams showing Positions of Slip Bands and Twins

the surface showed only a few isolated twins, which may have been formed during or after fracture, no record of these twins is therefore given The longitudinal marks observed after the third test were, however, again observed after the fourth test, and these, together with the appearance of the slip bands after fracture, are discussed later

Specimen Z5C —This specimen fractured across the enlarged end before the first test had been completed Fig 7 shows the calculated slopes of the traces of the slip and twinning planes of the specimen Z5C, the diagram being divided, as in the case of the other specimens, into regions of constant slip direction On this diagram are plotted the positions and slopes of the slip and twin bands observed after fracture (which occurred after 0·26 × 10^6 reversals at ± 0·8 ton per square inch)

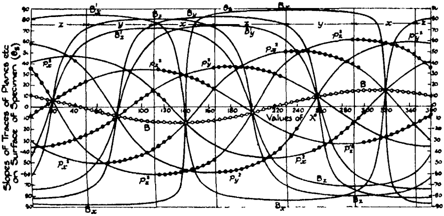

FIG 7 —Diagram showing Position of Slip Bands and Twins

Slip Bands —From the results of the previous experiment* on a single crystal of zinc it was shown conclusively that the slip plane operative under fatigue stresses was the basal plane, the position of maximum intensity of slip bands and its agreement with that of maximum resolved shear stress also completely identified the slip direction In the present experiments also, no slip, except that identified with basal plane slip, was observed Evidence of the actual slip directions is not so direct in the present experiments for reasons, however, which will be apparent In the later stages of each test (nominal shear stress ± 0·8 ton per square inch) a series of closely-pitched slip bands completely encircled the specimen Following the first stage (f_s ± 0·5 ton per square inch), faint slip bands were visible but were extremely difficult to detect at the points of calculated maximum resolved shear stress This, however, was undoubtedly due to the fact that at these maxima points the slip direction was tangential to the surface of the specimen, rendering visual observation extremely difficult (on a *perfect* surface *nothing* should be visible under a microscope) On the other hand, careful examination of the *intensity* of the slip bands in those regions where the slip direction would be expected to change showed that the frequency and intensity of the slip bands had minimum values at these change points There is also the evidence of the location of certain longitudinal marks and of the change points of the operative twinning planes (both of which are discussed later) These facts, together with all previous experience of zinc and other crystals, are sufficient to show that the law of deformation by slip obeyed in the present experiments was that of maximum resolved shear stress on the basal plane in the contained primitive directions

---

* 'Roy Soc Proc,' A, vol. 123, p 143 (1929)

With regard to the lowest stress value at which slip bands are produced, reference to figs 2, 5 (*a*) and 6 (*a*) shows that this value *must be less* than ± 0 38 ton per square inch When it is remembered that in the previous test (crystal Z3A) no slip bands were detected until the range of applied stress was nearly ± 1 0 ton per square inch, the effect of crystal orientation on the "visible slip limit" is apparent, this disparity is probably largely due to the restraining effect of the enlarged ends of the specimen, and perhaps to some extent is influenced by the relation of the slip direction to the surface of the specimen

The typical appearance of slip bands in the later stages of the tests is shown in fig 16 (Pl 13) (specimen Z5B after third test, taken at $\lambda = 90°$)

Twin Bands

(i) *Identification of Twinning Plane*—In the previous experiment the twinning planes of zinc were identified as first order pyramidal (two) planes of the general type $10\bar{1}2$ In the present experiments a profusion of twins were observed, the twinning plane in *every* case was of the $10\bar{1}2$ type, and twins on all the six possible $10\bar{1}2$ planes were observed

(ii) *Relation between the Twinning Plane and the Direction of Slip on the Basal Plane*—For reference purposes the developed half-surface of each specimen can be considered as divided (by lines parallel to the axis of torsion) into three regions denoted by x, z and y (in the order given) where these letters refer to the operative slip direction from maximum resolved shear stress considerations (see fig 2), as the three specimens considered were all cut from the same bar, and as the same nomenclature is employed throughout, these regions were in the same *sequence* in all three specimens and the actual differences of λ value may conveniently be disregarded

According to the prediction made from the results of the previous experiment, each such region should contain one or two complementary pairs of twins formed on particular $10\bar{1}2$ type planes, as indicated in Table III, the system being such that no operative twinning plane present in any region shall include the slip direction operative in that region

Table III

Area.	Twinning plane		
x	p_y^2, p_y^{-2}	and/or	p_z^2, p_z^{-2}
z	p_x^2, p_x^{-2}	and/or	p_y^2, p_y^{-2}
y	p_z^2, p_z^{-2}	and/or	p_x^2, p_x^{-2}

The actual distribution of twins that was observed on all three specimens was identical in general characteristics, being such that within any region of constant slip direction, twins were formed almost entirely on one pair of twinning planes The observed positions of the twins are indicated in figs 5 (*a*), (*b*) and (*c*) (specimen Z5A), figs 6 (*a*), (*b*) and (*c*) (specimen Z5B), and fig 7 (specimen Z5C) by the full circles It may be necessary to point out that this method of diagrammatic representation is somewhat misleading as no clear indication can be given of the relative occurrence and width of the twins recorded Quite a different impression of the appearance of the microstructure is often obtained from a searching visual examination For example, a system of twins may largely disappear at a certain value of λ, one or two small twins only extending beyond that point, and the occurrence of these exceptional twins must be, and has been, recorded The only satisfactory method of recording the appearance of the structure would be the reproduction of such a large number of photographs that is impracticable It must be sufficient to record that the visual examination of the structure showed that each region corresponding to any one slip direction was occupied by two sets of twins of major importance , when other twins were present, it was apparent that their presence was due to " over-running "* (as they obviously decreased in intensity and width) from a neighbouring region or were of an " occasional " nature The transition from one slip region to its neighbour was, in fact, marked by a change in the chief operative twinning planes The results of the observations are summarised as shown in Table IV

The outstanding features of these results can be summarised as follows --

In every specimen—

1 Twins formed on one *complementary* pair of $10\bar{1}2$ type planes were observed in each operative slip region

---

* *Note*.—The tendency of twin formation to " over run " or continue beyond the region in which the twin originated was noticed in the previous experiments, and it was shown that the mode of formation of mechanical twins would tend to extend the twins in the direction of the twinning planes concerned.

Table IV

Specimen	Region (operative slip direction)	Predicted twinning planes (from previous experiment)	Observed operative twinning planes
Z5A	x	p_y^2, p_y^{-2} and/or p_z^2, p_z^{-2}	p_y^2 and p_y^{-2}
Z5B			p_z^2 and p_z^{-2}
Z5C			p_z^2 and p_z^{-2}
Z5A	z	p_x^2, p_x^{-2} and/or p_y^2 p_y^{-2}	p_x^2 and p_x^{-2}
Z5B			p_y^2 and p_y^{-2}
Z5C			p_y^2 and p_y^{-2}
Z5A	y	p_z^2, p_z^{-2} and/or p_x^2, p_x^{-2}	p_z^2 and p_z^{-2}
Z5B			p_x^2 and p_x^{-2}
Z5C			p_x^2 and p_x^{-2}

2 The operative twinning planes changed with the change in operative slip direction (controlled by maximum resolved shear stress considerations)

3 Twins on all six possible twinning planes ($10\bar{1}2$ type) were observed on each specimen

4 In no case did the operative twinning plane in any region contain the operative slip direction in that region

The main prediction, based on the results of the previous experiment, regarding the dependence of the operative twinning plane on the slip direction has, therefore, been fulfilled in the present critical experiment The results must, however, be further examined, as the factors determining the choice of twinning plane are not obvious

(iii) *Choice of Twinning Planes*—According to the previous hypothesis, within any region of constant slip direction there are four possible planes on which twins might be formed, but figs 5, 6 and 7 and Table IV show conclusively that on only one of the two pairs of possible twinning planes are twins actually formed

In the previous experiment a similar result was obtained, and in that case it was suggested that, since the atomic movements by which twinning is effected are probably confined to a plane normal to the twinning plane, the relative values of the normal stresses on the twinning planes might determine on which of the possible twinning planes twins would actually be formed In the previous experiment the normal stress on both the actual twinning planes was very much greater than the normal stress on either of the other possible twinning planes, thus, consideration of the normal stress appeared to supply the criterion required in order to determine the actual twinning planes

By reference to fig 3, which shows the normal stresses on the twinning planes of the specimen Z5B, it will be seen that in the present experiments, normal stress considerations fail to explain the distribution of twins actually obtained Taking, on fig 3, the region $\lambda = 22°$ to $\lambda = 76°$, in which the slip direction is x, as an example it will be seen that from $\lambda = 22°$ to about $\lambda = 50°$ the normal stresses on p_z^2 and p_z^{-2} are greater than the stresses on p_y^2 and p_y^{-2}, but that from about $\lambda = 50°$ onwards the positions are reversed, the stresses on p_y^2 and p_y^{-2} being greater than those on p_z^2 and p_z^{-2} On the previous hypothesis it would be expected that from $\lambda = 22°$ to about $\lambda = 50°$ T_z and T_z' twins would predominate, and that from about $\lambda = 50°$ to $\lambda = 76°$, twins would be formed chiefly on T_y and T_y' Fig 6, however, shows that from $\lambda = 22°$ to $\lambda = 76°$ the twins observed on the surface were almost entirely on the T_z and T_z' planes *In a similar manner the normal stress fails in every other region of constant slip direction to provide an independent criterion between the two possible pairs of twinning planes This hypothesis must, therefore, be abandoned*

The shear stresses on the twinning planes, resolved in the direction of the primitive directions contained by the planes, *i e*, parallel to the basal plane, would not be expected to have any effect on twinning, the atomic movements by which such twinning is effected being presumably in a plane normal both to the twinning and to the basal planes In any case, a reference to fig 2, in which these shear stresses for the specimen Z5B are plotted, shows that consideration of these stresses would lead to similar conclusions as were drawn from the consideration of the normal stresses

The shear stresses on the twinning planes, resolved in the directions perpendicular to the primitive directions contained by the planes, might be expected to influence twinning, since, to a very limited extent, twinning is of the nature of shear in these directions These shear stresses have been calculated for the specimen Z5B and are plotted in fig 8 In this case also, again taking the region $\lambda = 22°$ to $\lambda = 76°$ as an example, the criterion would indicate a change from T_y and T_y' to T_z and T_z' approximately in the middle of the interval

It appears therefore that, in the present experiments, the choice of twinning plane can have been decided neither by the normal stresses nor by the shear stresses on the twinning planes, each considered independently, though the possibility remains that the true criterion may be some combination of these stresses

From the experimental results it appears conclusive that the conditions that cause twins to be formed on one twinning plane also cause twins to be formed on the complementary plane containing the same primitive direction, *e g*, if twins are formed on T_x they are formed on T_x' also This result was obtained

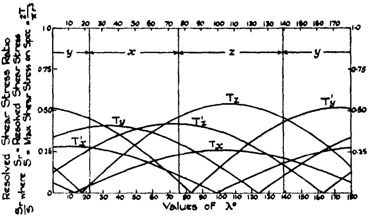

FIG 8 —Shear Stress on Twinning Planes resolved in a direction perpendicular to the primitive direction contained by the plane

also in the previous experiment, but since, in that case, the normal stress criterion appeared to account for all the facts, no particular importance was attached to it

The pair of twinning planes that contain the same primitive direction are to a large extent complementary also as regards the stresses on them The angle between them is 86°, *i e*, they are almost perpendicular to one another, so that the normal and shear stresses due to alternating torsional couples upon such a pair are very nearly identical, any *stress* condition, therefore, that would cause twins to be formed on one plane would tend also to produce twins on the other

Two such planes are complementary also in another sense directly concerned with twinning In the discussion of the results of the previous experiment it was shown that the mechanical process of twinning must result in what is, viewed macroscopically, a small shear along the twinning plane in the plane perpendicular to the primitive direction contained by the twinning plane Twinning on the complementary twinning plane results in a small shear in the opposite sense When a twin band is of a certain very small width (about 50 Å), or any multiple of this width, the actual movement of the atoms along the twinning plane at the farther edge of the twin is such as to move each atom into the position occupied by the next, thus the original structure can permit the formation of twin bands of this width (or any multiple of this width) without itself undergoing any deformation On the other hand, it is possible for the original structure at each side of a much broader twin to move " solid " with the edge of the twin and thus deform by the whole amount of the shear occurring within the twin

In any case, whether the original structure deforms by the whole amount of this shear or whether it remains more or less unchanged, during the process of formation of the twin, the shear must to a limited extent affect the original structure And, therefore, since the shears for a pair of complementary twinning planes are in opposite senses, it is possible that the production of both sets is due to the alternating nature of the applied stresses, and this appears to be the most plausible explanation of the experimental fact

An obvious method of testing whether the mutual occurrence of twins on complementary planes in the present and previous experiments is due to the alternating nature of the stress system employed, would be by carrying out careful experiments on zinc crystals employing static torsional loading, and it is proposed to make some experiments on these lines when opportunity permits Some information might also be obtained from static tensile tests

(iv) "*Sequence*" *Considerations* —Considerations of normal stress having failed completely to account for the selection of operative pairs of twinning planes, some interesting facts emerge from a consideration of the experimental results, *per se* The results show definitely —

(*a*) Twins on complementary twinning planes are always present in the same operative slip region, thus reducing the total of six possible twinning planes to three pairs

(*b*) Three slip directions are involved

(*c*) One pair of twinning planes only appear in each operative slip direction

(*d*) A change in slip direction is accompanied by a change in the pair of twinning planes operative

(*e*) In any operative slip region, the twinning planes containing that slip direction do not appear

Now the three crystals used in the present experiment were cut from the same bar and the same crystallographic nomenclature has been carefully adhered to throughout the present report Figs 5, 6 and 7 show, therefore, that, in order of increasing value of λ, the common sequence of operative slip regions is denoted by $x, z, y, x, z, y,$, etc Now, with this sequence, if conditions (*a*), (*b*), (*c*), (*d*) and (*e*) above are to be obeyed, only two possible sequences of operative twinning planes can exist , these sequences are shown in Table V

Table V

Direction		→ Increasing values of λ° →		
Sequence of operative slip regions		x	z	y
Corresponding sequence of operative twinning planes	Alternative A	$(p_y^2$ and $p_y^{-2})$	$(p_x^2$ and $p_x^{-2})$	$(p_z^2$ and $p_z^{-2})$
	Alternative B	$(p_z^2$ and $p_z^{-2})$	$(p_y^2$ and $p_y^{-2})$	$(p_x^2$ and $p_x^{-2})$

It is now apparent at once that alternatives A and B represent the *same* sequence of operative twinning planes, the difference between the two being merely one of *phase* *Reference to Table IV will reveal that alternative A represents the behaviour of specimen* Z5A, *while both the specimens* Z5B *and* Z5C *correspond to alternative B* Consider fig 7, for example, and the twinning plane p_x^{-2} at the point where the slip direction changes from z to y The simple conditions given above ((*a*), (*b*), (*c*) and (*d*)) can be fulfilled if twinning on p_x^{-2} spreads to the *left* of the dividing line and extends over the region denoted by z (in which case the twinning characteristics of specimen Z5A will be produced) or if twinning on p_x^{-2} spreads to the *right* of the dividing line and extends over the region denoted by y (in which case the twinning characteristics of specimens Z5B and Z5C will be produced) It will be seen from fig 7 that the dividing line coincides very nearly with the position at which the trace of the twinning plane has its maximum slope , these points also correspond to positions of maximum normal stress on the twinning plane under torsional straining It is obvious, therefore, that the direction (right or left) in which twinning proceeds cannot have been controlled by normal stress considerations

One is led to assume therefore that the sequence of twinning is dictated almost entirely by the sequence of slip direction and that the phase difference adopted by any particular specimen is influenced by secondary considerations Thus, specimen Z5A happened to adopt alternative A (of Table V), while specimens Z5B and Z5C conformed to alternative B The important point is that the behaviour of all three specimens is entirely consistent As to the unknown factor which serves to discriminate between alternatives A and B, the present experiments give no information

The outstanding conclusion is that the suggested process, which is simple and logical, makes consistent the apparently discordant characteristics exhibited by three specimens and renders unnecessary the formulation of any primary factor affecting the choice of twinning plane other than consideration of slip direction It is necessary, however, to point out that no *explanation* of the process has yet emerged

Slip Bands within the Twins —All the twin bands observed in the present experiments were small some of the broadest recorded being shown in fig 11 (Plate 12) For this reason, although slip within the twin bands was, in nearly every case, easily observable, the slope of the slip bands was not often accurately measurable The evidence as to the slip plane within the twins deduced from the large twins observed in the previous experiment is regarded as so very definite that no attempt has been made to confirm these previous results by purely independent measurements of the much smaller twins observed in the present experiment

In several cases, however, measurements were made on some of the broadest twins, and the slopes of the slip bands were found to be in good agreement with the slopes of the various twinned basal planes In figs 15 and 12 (Plates 13, 12) the difference of slope of the slip bands within two sets of complementary twins may clearly be seen

The process of twinning (as it occurred in the present experiments) produces twinned basal planes that are everywhere nearly parallel to the axis of the specimen and (at the points where slip bands are visible) are inclined at a large angle to the surface of the specimen The resolved shear stresses on the twinned basal planes are therefore everywhere very high, so that slip on the twinned basal planes would be expected wherever twins are formed An inspection of the photographs, which are representative of the general appearance of the surface of the specimens, shows that twins without internal slip were never observed

Fracture —All three specimens fractured completely under a range of nominal shear stress of ± 0 8 ton per square inch , specimens Z5A and Z5C fractured across the enlarged ends, the plane of fracture in each case being the basal plane (the cleavage plane) , specimen Z5B fractured approximately in the middle of the test length, the fracture being mainly parallel to the basal plane with a small irregular area of roughly prismatic form

From the appearance of the fracture of the specimen Z5B, it appears probable that cracks started on opposite sides of the specimen on two distinct basal planes, and that the roughly prismatic fracture occurred by tearing action after the specimen was almost completely severed, the fracture being thus completed

None of the fractures had the appearance of a fatigue failure, and from the nature of the failures, it appears that the initial cracks developed into complete fractures almost instantaneously It will be seen from the curves of shear stress (fig 2) that the shear stress on the basal plane did not vary greatly all round the specimen It is not unreasonable to suppose, therefore, that a crack once formed would be propagated round the specimen merely under the static effect of the maximum stress of the stress range On the other hand, with the particular orientation of the present crystals, the slightest bending stresses in a plane containing the axis of torsion is apt to reveal the inherent "brittleness" of the crystal and its marked tendency to cleave along the basal plane Although the very greatest precautions were taken to avoid bending stresses while placing the specimen in the testing machine grips the appearance of the fractures indicate that bending stresses were chiefly responsible for the actual final failure The value of the nominal shear stress being applied ± 0 8 ton per square inch, when fracture occurred has probably little relation to the fatigue range of the crystal The writers believe that no information regarding the actual value of the fatigue limit has been obtained in the present experiments

Prismatic Planes —In the present experiments, as in the previous experiment, no indication of deformation by slip on any of the prismatic planes (either first or second order) was observed After the third test (6 02 × 10^6) reversals of ± 0 8 ton per square inch) on the specimen Z5B, however, there were apparent on the surface six sets of long, black markings all nearly parallel to the axis of the specimen and the majority extending the whole length of the specimen

Sufficient photographs (magnification × 100) were taken to form continuous panoramas of the surface of the specimen, the first a circumferential development showing the appearance of the surface about midway between the enlarged ends from λ = 0 to λ = 180°, the second following the direction of the longitudinal lines and showing their appearance from end to end of the specimen at about λ = 115° The first of these panoramas is reproduced in diagrammatic form in fig 9 (*c*) to show the positions and approximate slopes of the longitudinal lines both in relation to the crystalline structure and to the applied stressing system , a diagram of the resolved shear stresses on the basal plane is appended (fig 9 (*b*))

It will be seen that the lines were grouped round the points of maximum resolved shear stress on the basal plane, *i e* , round λ = 49°, 107°, 170° (229°, 287° and 350°), that each group had a definite slope, and that these slopes were everywhere nearly perpendicular to the trace of the basal plane The slopes of any two of these lines separated by 180° λ were always equal and

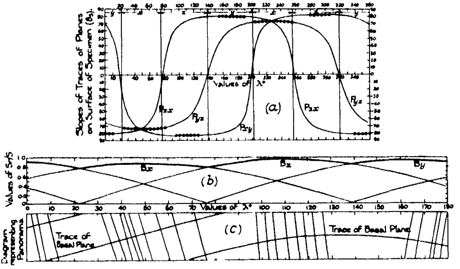

FIG 9 —Diagrams showing Positions of Longitudinal Markings

opposite, so that it was concluded that the lines represented the traces of crystallographic planes From the perpendicularity of these lines to the trace of the basal plane, it was evident that they could only represent the traces of planes of a prismatic form, and it was found that they agreed, within ± 2°, with the traces of the second order prismatic planes P_{yz}, P_{zx}, P_{xy} (of the $11\bar{2}0$ type) The particular plane concerned at any point was the plane perpendicular to the slip direction at that point, *e g*, P_{yz} in the x region In fig 9 (*a*) are plotted the calculated slopes of the traces of these three prismatic planes and the observed traces are recorded on this diagram as full black dots , as in the previous diagrams, the small differences between the calculated and the observed slopes have been neglected in preparing the diagram

It was thought at first that these longitudinal lines might be cracks or cleavages, although the general appearance and nature of the marks did not correspond with the usual type of fatigue crack or cleavage failure, and the almost simultaneous production of so many cracks seemed extremely unlikely However, in order to test this hypothesis, after the polished surface of the specimen had been fully examined and photographed, the specimen was lightly polished and etched and the surface was then re-examined and re-photographed The appearance of the marks after this treatment was not that of cracks One of the photographs taken is reproduced (fig 21, Plate 14), and by comparison with the photographs before polishing and etching it will be seen that the effect of the treatment has been to render the longitudinal lines less definite, a result that would not have been obtained had these marks been cracks

It was concluded, therefore, that these lines were more in the nature of ridges, an impression that had previously been conveyed directly after test by the appearance of the specimen to the unaided eye This conclusion was supported also by the slight differences of level existing in the neighbourhood of the longitudinal lines, these differences being evidenced by the slight adjustments necessary to bring each feature into focus in the microscope The difference of levels is shown also as a difference of focus in fig 17 (Plate 13)

In the vicinity of the longitudinal lines, it will be noticed that the basal slip lines, and, to a lesser degree, the twin bands also, are considerably distorted (figs 17 and 18) This distortion *may* be due entirely to the effect of the ridges, which, by causing the surface of the specimen to become inclined to the plane perpendicular to the axis of the microscope, alters the apparent slopes of the traces of the crystallographic planes The traces of planes which are perpendicular to the surface of the specimen would not be affected by this distortion of the surface, *e g*, at the points λ = 45 5° and λ = 225 5°, where the basal plane is normal to the surface, no bending of the slip lines would be expected An examination of fig 14 (λ = 48°) and fig 13 (λ = 40°) shows that experimental evidence on this point is indecisive In fig 14 the slip lines appear reasonably straight and continuous, but in fig 13 the lines, while straighter than elsewhere (*cf* fig 19, λ = 112°), are very far from continuous across the photograph

It is therefore suggested that, while the apparent *curvature* of the slip lines may be due to the optical effect of the corrugation of the surface of the specimen, the actual discontinuity of slope of these lines, as instanced in fig 13, is probably not due entirely to this cause It appears therefore that the experimental evidence, though very far from conclusive, does indicate that something in the nature of shear deformation in the direction of the longitudinal lines has taken place

It may be remarked here that, in the previous experiment on the specimen Z3A, one or two short dark lines were observed in the regions of maximum slip, corresponding in general appearance and orientation with respect to the crystallographic axes to the longitudinal lines observed in the present tests

At the time these short dark lines were regarded as being accidental, they were not sufficiently numerous to afford any indication of correlation with the crystallographic axes Now, however, it appears that these lines were the exact counterpart of the longitudinal lines observed in the present test and their occurrence in the regions of maximum slip confirms the deductions drawn as to the dependence of these lines on the process of slip

From the appearance, position and orientation of the longitudinal lines, it is natural to associate the *production* of the lines with the slip on the basal plane It was, at first, thought that the lines might represent the effect of non-uniformity of slip resulting in a "piling up" of material at the points where the actual amount of slip was changing most rapidly, but estimates of the variation of the actual amount of slip round the specimen seemed to indicate that this would lead to the production of longitudinal lines near the *change over points* rather than at the *crests* of the curves of resolved shear stress on the basal plane Moreover, on this hypothesis, the deformation of the slip lines by the longitudinal lines must be attributed entirely to the optical effect of the corrugation of the surface

In fig 10 are shown four diagrams intended to illustrate a tentative suggestion as to the manner in which these lines may be produced For convenience we consider a specimen in which the basal plane is perpendicular to the axis or torsion, the actual orientation of the specimens used in the present experiments was sufficiently close to this ideal orientation for the present purpose Fig 10 (*a*) shows a rectangle drawn on the surface of this ideal specimen (one pair of edges being parallel to the traces of the basal plane) in the vicinity of a point of maximum resolved shear stress Suppose, now, that the rectangle tends to slip into the form shown in fig 10 (*b*) In the neighbourhood of the change-over points, however, not only is the shear stress, and hence the tendency to slip less, but such slip as does occur is not entirely perpendicular to the radius vector and hence contributes in a lesser degree to the actual torsional movement This may have the effect of restricting the total torsional movement of the whole specimen to such an extent that the

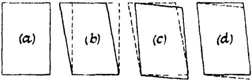

FIG 10

rectangle of fig 10 (*a*) can reach only the position shown in fig 10 (*d*) It is suggested that this final position may be reached from the position fig 10 (*b*) by a rotation into the position shown in fig 10 (*c*) and a shear deformation on the plane normal to the direction of slip on the basal plane, *i e* , on the prismatic plane It is not suggested that this shear deformation is effected by slip in the ordinary sense, but rather by mass movement mainly in the neighbourhood of the longitudinal lines

It is not desired to lay any emphasis on the explanation suggested above, since the experimental evidence is not regarded as sufficient to warrant anything more than a tentative hypothesis

After the specimen Z5B had been broken, the fractured surface was examined and photographed It was found that at six points practically equally spaced round the edge of the fracture and agreeing well with the positions of the longitudinal lines on the polished surface, the face of the fracture over a small area appeared corrugated, the degree of corrugation decreasing as the distance from the point of maximum stress increased Fig 23 shows the appearance of the fractured surface The shear stress values on the basal plane resolved along the primitive directions have been placed round the photograph in the form of a polar diagram Fig 22 (Plate 14) shows the corrugations (appearing as broad black bands) at about $\lambda = 110°$ photographed at a higher magnification The general directions of the corrugations on opposite sides of the specimen agreed well with each other and with the calculated trace of the particular second order prismatic plane concerned at each point It appears, therefore, conclusive that whatever deformation occurs to produce the longitudinal lines on the surface, the deformation is such that the second order prismatic planes normal to the direction of slip remain undisturbed

On the fractured surface of Z5B there was apparent a second set of marks, easily recognisable as twin bands and agreeing exactly with the traces of the twinning planes In fig 22 these twin bands may be seen crossing a corrugated area, the angle between the bands and the direction of the corrugations being almost exactly 30° (the theoretical angle)

The polished surface of Z5B after fracture showed no regular distribution of twins, a few isolated bands only being observed In the vicinity of the fracture, however, the longitudinal lines again appeared as fine lines, occupying exactly the same positions round the specimen as the broader marks observed after the third test

Summary of Results and Conclusions

1 *Slip Plane, Slip Directions and Twinning Planes*.—The slip plane of zinc is the basal plane (0001), the slip direction is the most highly stressed primitive direction, deformation by slip is controlled by the criterion of maximum resolved shear stress The twinning planes of zinc are the six planes of the general type $10\bar{1}2$

2 *Operative Twinning Planes*.—With the specimens employed in the present tests, due to the relative orientation of crystallographic and straining axes, and to the type of applied stressing, the circumference of the specimen can be considered as being divided into six consecutive portions (a sequence of three portions repeated twice), in each of which one slip direction is operative Thus three slip directions become operative in turn The results show definitely (*a*) One pair only of complementary twinning planes appear in the area associated with each operative slip direction, thus reducing the total of six possible twinning planes to three pairs, (*b*) a change in slip direction is accompanied by a change in the identity of the pair of operative twinning planes, (*c*) in any operative slip direction, the twinning planes containing that slip direction do not appear, (*d*) normal stress alone does not determine the choice of operative twinning plane If conditions (*a*), (*b*), (*c*) and (*d*) are fulfilled, only one sequence of operative twinning planes can result, offering two alternative phases of the sequence Both phases have been observed on different specimens

The important conclusion is thus reached that the occurrence of twins, as well as slip bands, is controlled by the simple criterion of maximum resolved shear stress on the slip plane

3 *New features observed in the Microstructure*.—Long widely-spaced black "marks" appeared on the surface of the specimen In every case their direction was parallel to the trace of the particular second order prismatic plane ($11\bar{2}0$ type) perpendicular to the slip direction operative at that portion of the specimen The exact meaning of these "marks" is not apparent, it is suggested that they may represent the effects of block shear movement on prismatic planes rendered necessary to preserve the continuity of the specimen and compensating for the fact that zinc has only one slip plane, with three slip directions

---

The experiment is an item of a general programme of research performed for the Engineering Research Board of the Department of Scientific and Industrial Research and the Aeronautical Research Committee, the authors' thanks are

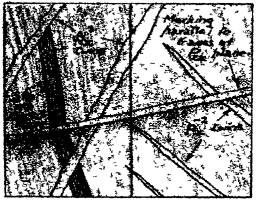

FIG 11 $\lambda = 2\frac{1}{2}$ 328

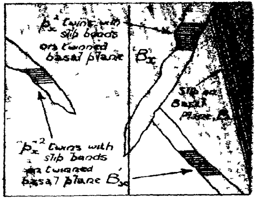
p_x^{2} twins with slip bands on twinned basal plane B_x
Slip on Basal Plane, B
p_x^{-2} twins with slip bands on twinned basal plane B_x

FIG 12 $\lambda =$ [illegible] 712

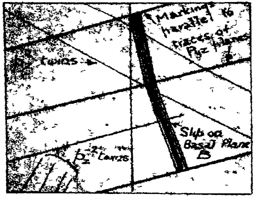

FIG 13 $\lambda = 40$ [illegible]

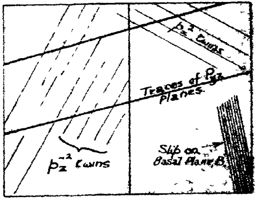

FIG 14 $\lambda = 48$ 97

Gough and Cox *Roy. Soc. Proc., A, vol. 127, Pl. 12*

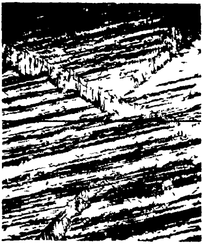

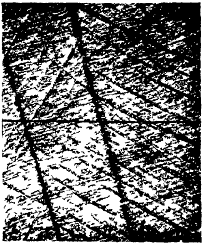

(*Facing p. 418.*)

Plate 13

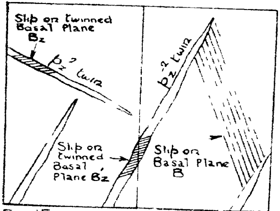
Slip on twinned Basal Plane Bz
p_z^2 twin
p_z^{-2} twin
Slip on twinned Basal Plane B_z'
Slip on Basal Plane B

Fig 15

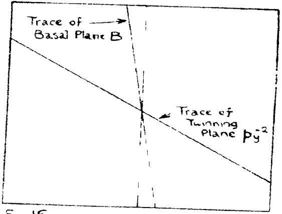

Fig 16

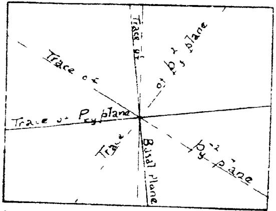

Fig 17

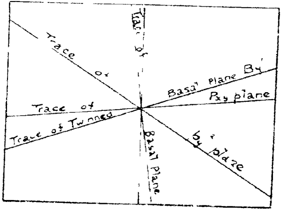

Fig 18

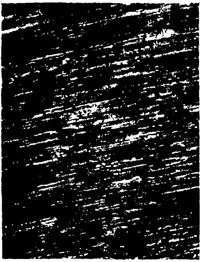

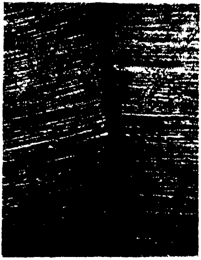

Plate 14

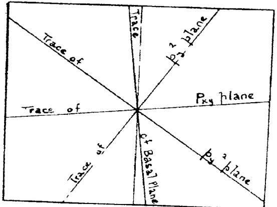

Fig 19

112 0°

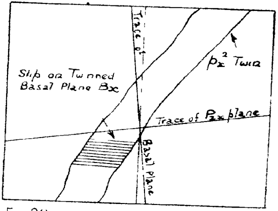

Fig 20

– 356° 712

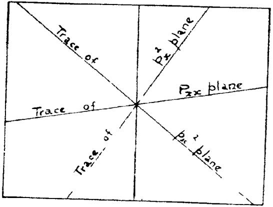

Fig 21

= 0° 0°

(Etched Surface)

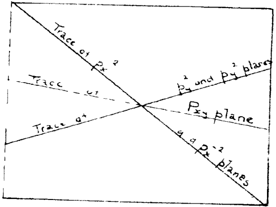

Fig 22

– 111 0°

(Cleavage on Cross Section)

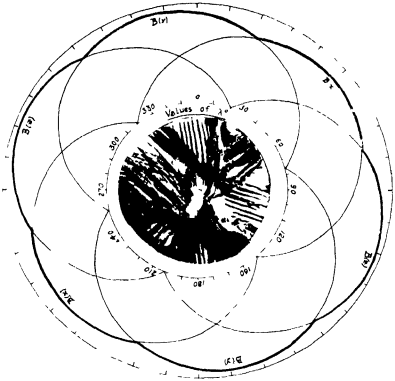
B(y)
B(x)
B(z)
Values of λ°
330
0
30
60
90
120
150
180
210
240
270
300

Fig 23

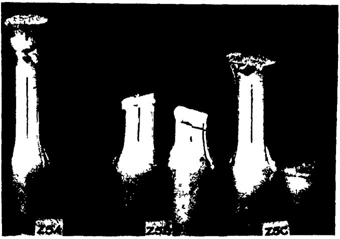
Z5A
Z5B
Z5C

Fig 24

due to these bodies for the research facilities afforded and for permission to publish the results.

The zinc crystal used was prepared by Mr V H Stott, M Sc, and the metallographic polishing was arranged by Mr J. D Grogan, B A, both of the N P L Metallurgical Department The X-ray analyses were carried out in the N P L Physics Department by Mr I Backhurst, M Sc

The authors take this opportunity of expressing their indebtedness to Messrs Stott, Grogan and Backhurst for their invaluable assistance in these directions

---

Structure in very Permeable Collodion Gel Films and its Significance in Filtration Problems

By WILLIAM JOSEPH ELFORD, National Institute for Medical Research

(Communicated by J E Barnard, F R S —Received January 31, 1930)

(Abstract)

1 Optical studies of permeable collodion films have revealed the existence of two very definite types of structure—(i) microgel structure of microscopic order, and (ii) ultragel structure of ultra-microscopic order The general nature of these structures has been established for several different nitro-cottons and the conditions determining them investigated

2 Gelation in this particular instance is a process of phase transition resulting from the coagulating influence of desolvation The precise nature and stability of the gel is a function of the specific characters of the nitro-cellulose and solvent, and the variation in free surface forces around the dispersed phase particles with differing degrees of molecular complexity of the system

3 The bearing of these observations upon ultra-filtration has been discussed A complete explanation of the general behaviour of ultra-filter membranes is afforded, and a sound basis established for the interpretation of filtration results

(*The full paper is published in Proceedings, B, vol* 106, *pp* 216–228)

Researches on the Chemistry of Coal Part VI —*Its Benzenoid Constitution as shown by its Oxidation with Alkaline Permanganate*

By William A Bone, D Sc, F R S, Laurence Horton, Ph D, and Stacey G Ward, M Sc

(Received March 13, 1930)

In Part IV of this series* a preliminary account was given of the discovery that the benzene pressure-extracted "residue" of a typical bituminous coal can readily be oxidised by means of an alkaline solution of potassium permanganate with formation of considerable quantities of benzenoid acids, among which benzene hexacarboxylic (mellitic) and 1 2 3 4 benzene tetracarboxylic acids had been isolated and identified, the total yield of such acids obtained amounting to between 25 and 40 per cent of the weight of the coal residue taken, according to the conditions under which the oxidation had been conducted Seeing that the benzene pressure-extracted 'residue" treated in the experiments was 88 6 per cent of the original coal substance, such results indicated that a considerable part of the original coal substance is of a benzenoid character, and the working out of the possibilities thereby opened up was reserved for further investigation because of its bearing upon the chemical constitution of coal

Since the publication of those results the subject has been under continuous investigation in the Fuel Research Laboratories of the Imperial College with the aid of grants from the Fuel Research Board of the Department of Scientific and Industrial Research, and the present paper gives an account of our further experiments

In drawing up the original programme of work the following points seemed to be of first importance, namely, (i) the optimum conditions for oxidising the coal substance so as to obtain a maximum yield of crystalline acids, (ii) the isolation and identification of the various acids produced, (iii) variations (if any) in the oxidation and its products according to the maturity of the coal substance, (iv) "stepwise" oxidation of the coal substance, with a view to discovering possible intermediate products, (v) the effects of progressive carbonisation of the coal substance upon the oxidation and the proportions of various products therefrom, and (vi) the oxidation of anthracites and various forms of charcoal and carbon

---

* 'Roy Soc Proc,' A, vol 110, p 537 (1926)

In this paper we propose dealing principally with the first five of these points in the light of our work up to date. It should be understood that, except when otherwise stated, the experiments recorded herein were carried out with the "residues" from the benzene-pressure-extraction of the coals in question, representing between 85 and 98.5 per cent of the original coal-substance in each case. It was deemed advisable to deal separately with these "residues" and the "corresponding extracts" although experiments have shown that such procedure is more a matter of convenience than of necessity. Indeed the original unextracted coal might have been employed in each case without materially affecting the results, but for our desire to investigate the oxidation of the "residue" and "extracts" separately.

Before proceeding, however, to detail the results of our further experiments, we will briefly indicate their character and what we consider to be their bearing upon the chemistry of coal.

We have examined in detail the permanganate oxidation of the "residues" from the benzene-pressure extraction of five typical coals of widely different geological ages and maturities, namely (i) Morwell brown coal from Victoria (Australia) of tertiary origin and in an incipient stage of maturity, (ii) a brown lignite from Estevan in the province of Saskatchewan (Canada), also of tertiary origin but considerably more matured, (iii) a well matured bituminous non-coking coal from South Africa (Witbank) of permocarboniferous origin, (iv) a fully matured hard coking bituminous coal from the "Busty" seam, N.W. Durham, and (v) a Canmore coal of semi-bituminous type from the Western Canadian Coalfield.

All these coal-residues have been oxidised giving much the same weight yields of crystalline organic acids chiefly consisting of benzene carboxylic acids, the proportions of which do not seem to vary materially from one coal to another, together with smaller amounts of oxalic and acetic acids. This would indicate that a considerable part of the organic debris originally deposited in the incipient coalfields either had or soon acquired a cyclic, and probably benzenoid, structure which has been preserved during the subsequent maturing process. Otherwise it would be difficult to account for the remarkable fact that we have found the permanganate oxidation of the Morwell brown coal to give much the same yields and types of benzenoid carboxylic acids as the highly matured "Busty" coking coal. Hence it would appear that, whatever its chemical nature may have been, the maturing process has not destroyed the essential chemical structure of the coal substance, however much it may have been modified in detail.

We have found that, under suitable conditions, the alkaline permanganate oxidation of 100 parts by weight of the original coal substance will yield something between 3 and 7 parts of acetic acid, from 15 to 35 (but usually about 20) parts of oxalic acid, and from 33 to 50 parts of chiefly benzene carboxylic acids of mean composition closely approximating to that of a benzene tricarboxylic acid From the last-named mixture of benzenoid acids we have isolated no less than 10 out of the 12 possible benzene carboxylic acids, including all three isomeric phthalic acids, all three benzene tricarboxylic acids, two out of the three possible benzene tetracarboxylic acids, and the pentacarboxylic and hexacarboxylic acids

Moreover, in the cases of two of the coals examined—namely the immature tertiary Morwell brown coal and the well-matured carboniferous Busty coking coal—complete "carbon balances" experimentally worked out for the oxidation under optimum conditions showed a very similar distribution of the original carbon in the coal substance among the various products, namely, approximately 42 per cent as carbonic anhydride, 2 per cent as acetic acid 7 per cent as oxalic acid, and 48 per cent as benzene carboxylic acids in each case In each case also about a third of the original carbon ultimately appeared as C_6-rings in the oxidation products

In carrying out "step-wise" alkaline permanganate oxidations of the coal substance, evidence was forthcoming that complex colloidal "humic acids" are formed intermediately, the crystalline benzenoid acids and probably also oxalic and acetic acids arising simultaneously from their further oxidation, this was confirmed by other experiments proving that on separate oxidation 100 parts by weight of such humic acids yield some 60 parts of a mixture of benzene carboxylic acids, 20 parts of oxalic acid, 3 parts of acetic acid and rather less than one part of succinic acid Moreover, certain observations lead us to suspect that the transition from "humic" to benzenoid acids may be through some crystalline acid of intermediate complexity, although we have not yet isolated it

From the fact that the "residues" resulting from the benzene-pressure-extraction of the coals under investigation constituted from 85 to 98 5 per cent of the original coal substance, and that nearly one-third of the carbon in such residues appeared as C_6-rings in the products of their alkaline permanganate oxidation, it may be inferred that a considerable part of the original coal substance has a "benzenoid" structure

This, however, is not all, for it has also been proved that (i) from 57 to 66 6 per cent of the benzene-pressure-extracts of the two immature brown coals examined were composed of phenols and phenolic esters, and (ii) at least two-thirds of the corresponding extract from the mature Busty coking coal, namely, the portion thereof (Fraction IV) which is mainly responsible for its coking propensities is also essentially " benzenoid " in character

Such results, revealing as they do that in great part the coal substance - no matter what its geological age or chemical maturity, or whether or not it is extractable by boiling benzene under pressure—has an essentially " benzenoid " structure, suggest the possibility of its having arisen through condensations of phenolic- and amino- with aldehydic-bodies, much as " bakelite " is synthesised nowadays from phenols and formaldehyde

This suggestion also accords well with the evidence contained in Part V hereof (*q v*) that the development during the maturity of the coal substance of the constituents mainly responsible for the coking propensities of bituminous coals is marked by the disappearance of the phenols and phenolic esters extractable from brown coals and brown lignities,* and it is reinforced by the proof now forthcoming that such " coking constituents " are largely benzenoid in structure

It should here be noted that various previous investigators have suggested a " benzenoid structure " for lignin,† and that on oxidising, in an alkaline medium with air at 55 atmospheres pressure, 1665 grams of the " Willstatter " lignin (obtained by treating wood with a large excess of strong hydrochloric acid), F Fischer and his collaborators obtained 138 grams of aliphatic (principally acetic) and 52 grams of benzene carboxylic acids ‡ Moreover, they obtained small amounts of benzene carboxylic acids by such pressure-oxidation of both brown and bituminous coals, which (they said) points to an essentially aromatic structure in them Apparently, however, the significance of such results in regard to the constitution of coals has been lost sight of, but in the light of ours can hardly now be doubted

It is not difficult to account for the production of benzene carboxylic acids by the alkaline permanganate oxidation of the coal substance (or the " humic acids " resulting therefrom) Thus 1 2 3 benzene tricarboxylic acid, for example, would result either from such fused rings as 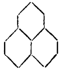 or from

* 'Roy Soc Proc,' A vol 120 p 523

† 'Abhand Kohle,' vol 5 pp 132–365 (1920), and vol 6, pp 1–26 (1921)

‡ 'Brennstoff Chemie,' vol. 2, p 216

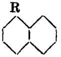
(where R = side chain), etc., while 1 3 4 benzene tricarboxylic acid might result from 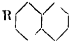 Indeed the production of any benzene carboxylic acid could be explained on similar lines. Also it would be equally possible for benzene carboxylic acids to arise by the oxidation of such structures as 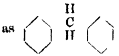

The production of oxalic acid might also arise simultaneously by the oxidation of "fused" benzene rings and/or alkyl side chains, while acetic acid obviously would arise by the oxidation of side chains.

It must also be borne in mind that (as already shown in previous papers) during the maturing process in all probability the organic matter of brown coals has also undergone "internal condensations" involving the elimination of both carbon dioxide and water; moreover under the influence of heat produced by igneous intrusion or exceptional earth pressures in certain cases, bituminous coals have lost their coking constituents and neutral oils, thereby being converted into "semi bituminous" types.

More experimental exploration of the subject will be needed to test it before such views can be advanced otherwise than tentatively for discussion and we are undertaking further work with that objective. Also, we propose extending the investigation so as to include comparative studies of the oxidation of celluloses, lignins, etc., as well as of the oxidation and carbonisation of "bakelite" and the like.

EXPERIMENTAL

A.—*The Coals Employed*

Although some details regarding the coals employed have already been given in previous papers of the series, the following may be repeated here as being essential to the proper understanding of this new work. It should be understood that, except when otherwise stated, the following analytical data refer to the dry-ashless coal substance or "residue" in each case.

(1) *Morwell Brown Coal*.—A tertiary earthy brown coal in a very early stage of development from the uppermost bed of the famous Morwell deposit

in Victoria (Australia) containing about 50 per cent of water and 4 per cent of ash in the raw state The dry-ashless coal-substance contained —

C = 66 4, H = 4 1, N and S = 1 0 and O = 28 5 per cent,

and at 900° C yielded 53 3 per cent of "volatiles" On being extracted with benzene at pressures between 40 and 48 atmospheres (corresponding with temperatures between 250° and 280° C) it yielded altogether 15 per cent of "extract," namely, 9 0 per cent of phenols (among which phenol, *p*-cresol and catechol were identified), 1 per cent of phenolic esters, 3 5 per cent of "neutral oils" and 1 5 per cent of amorphous solids insoluble in light petroleum

The dry-ashless "residue" as used in our present experiments contained -

C = 71 2, H = 3 75, N and S = 1 0 and O = 24 05 per cent

(2) *Estevan Brown Lignite* —A typical brown lignite, more matured than (1) from the top 7 foot seam of the Estevan Coal and Brick Company, S Saskatchewan The raw coal (as received in our laboratories) contained 37 8 per cent water and 7 65 per cent of ash The "dry ashless" coal substance contained

C = 67 75, H = 4 3, N = 0 95, S = 0 6, and O = 26 4 per cent,

and at 900° C yielded 44 9 per cent of "volatiles" On benzene-pressure-extraction, as aforesaid, it yielded altogether 4 5 per cent of crude extract comprising 2 25 of phenols (principally phenol, *p*-cresol and catechol) 0 3 of phenolic esters, 1 65 of "neutral oils" and 0 3 of solid amorphous bodies, there being a close similarity between the crude extract and its components and those obtained from the Morwell coal The dry-ashless "residue" used in the present experiment contained —

C = 71 5, H = 3 65, N and S = 1 6, O = 23 25 per cent

(3) *Busty Coking Coal* —A typical well-matured carboniferous hard-coking bituminous coal from the "Busty" seam in Langley Park Colliery, co Durham The dry coal contained 3 45 per cent of ash, and the "dry-ashless" coal substance contained —

C = 87 75, H = 5 0, N = 1 55, S = 0 75, and O = 4 95 per cent,

and at 900° C yielded 25 5 per cent of "volatiles" On benzene-pressure extraction, as aforesaid, it yielded altogether 15 6 per cent of crude extract which, in addition to neutral oils and small amounts of resinous bodies, was two-thirds composed of amorphous coking constituents (Fraction IV) the latter replacing the phenols and phenolic esters found in the corresponding extracts from the brown coals The dry-ashless "residue" used in our present experiments contained —

C = 85 65, H = 4 4, N and S = 2 35, and O = 7 6 per cent

(4) *Witbank Coal* —A non coking bituminous coal of permocarboniferous origin from the upper portion of the No 2 (or main working) seam of the Coronation Colliery, Witbank, E Transvaal, South Africa The dry coal contained 10 35 per cent ash, the "dry-ashless" coal substance contained —

C = 81 75, H = 4 5, N = 2 0, S = 0 55, and O = 11 2 per cent,

and at 900° C it yielded 27 6 per cent of 'volatiles' and an absolutely non-coherent powder On benzene-pressure extraction it yielded 7 5 per cent of crude extract, and the dry-ashless 'residue" contained —

C = 79 4, H = 3 6, N = 2 0, S = 0 6, and O = 14 4 per cent

(5) *Canmore Coal* from a seam in the lower cretaceous formation of the extreme western part of the W Canadian Coalfield Under the stress of mountain building subsequent to its formation, the coal had been converted into a non-coking "semi bituminous" type containing ("dry-ashless") —

C = 89 7, H = 4 0, N = 1 4, S = 1 0, and O = 3 9 per cent

and yielding at 900° C 14 1 per cent of "volatiles" On benzene pressure-extraction it yielded only 1 35 per cent of crude extract, the ultimate composition of the ashless "residue" being substantially that of the original "dry-ashless" coal

B —*Their Permanganate Oxidation*

Seeing that the benzene-pressure-extracts from all the foregoing coals had been fractionated and examined in detail, as already described in Part V hereof (*q v*),* it was decided to employ only the so-extracted "residues' in the main permanganate oxidation experiments, because these 'residues" comprised by far the greater part, *i e*, from 85 to 98 5 per cent of the coal substance And having regard to the purpose of our researches namely, the elucidation of the chemical constitution of the principal coal substance, it seemed advisable to oxidise these "residues" apart from the corresponding 'extracts," leaving the latter to be dealt with separately as a subsidiary part of the problem Accordingly it will be understood that in the experiments now to be described only the benzene-pressure-extracted residues of the coals in question were used

---

* *Loc. cit.*

Relative Proportions of $KMnO_4$/Coal Substance used.—When either a dry-coal or its "residue" after benzene-pressure-extraction is submitted to an alkaline permanganate oxidation according to our method, it is important first of all to determine the relative proportion of $KMnO_4$/coal substance to be used This will obviously depend partly upon the ultimate elementary composition of the material under investigation, and partly upon the extent of the desired oxidation

It may be recalled that in an alkaline permanganate oxidation two molecules of $KMnO_4$ yield three atoms of oxygen *plus* hydrated manganese dioxide, *e g*,

$$2KMnO_4 + 3H_2O = 2KOH + 2MnO(OH)_2 + 3O$$

In any particular case dependent upon the ultimate composition of the coal substance used, there would be a certain theoretical proportion of the potassium permanganate which would just suffice in an alkaline solution to oxidise the whole of the organic matter completely to carbon dioxide and water if such were possible This may be conveniently termed the ' theoretical proportion " and is denoted in the text by the expression $KMnO_4$ (theoretical) In point of fact, however, such a complete oxidation is never reached when the process is carried out according to our procedure (*q v*), there being always a definite " end point " corresponding with a $KMnO_4$-proportion which may be conveniently referred to as $KMnO_4$ *e p* proportion There is also in each particular case another $KMnO_4$-proportion which it is desirable to determine experimentally, namely the minimum actually needed to oxidise the whole of the coal substance to crystalline acid products without leaving any colloidal acidic bodies which will always be referred to as the $KMnO_4$ *c a* proportion in each case In our principal experiments we usually employed a proportion intermediate between the *e p* and the *c a* proportions For the original ' dry coals ' and their dry benzene-pressure extracted residues respectively, the foregoing $KMnO_4$/coal weight ratios would be as follows -

—	Theoretical calculated	*e p* found.	*c a* found	Actually used
Morwell residue	12 5	10 0	7 5	8 2
Estevan residue ..	12 9	11 7	8 4	9 75
Busty residue	16 9	13 7	8 5	12 8

We have found that, by employing a proportion of $KMnO_4$ intermediate between the *c a* and *e p* proportions, the whole of the coal substance in any case may be oxidised so that substantially the whole of its carbon is transformed into a mixture of carbonic, acetic, oxalic, succinic and benzene carboxylic acids, the first and last always being the main products

When, however, the proportion of $KMnO_4$ used in relation to the coal substance is progressively diminished below the *c a* limit, not only may complex colloidal acid products ("humic acids") be added to the other oxidation products, but also some of the coal substance may remain unoxidised

As already stated in our introduction, and will be proved later, the "humic acids" referred to in the preceding paragraph are intermediate oxidation products between the original coal substance and the benzene carboxylic acids, because we have found that these latter normally result from a properly regulated alkaline permanganate oxidation of the "humic acids" Also, we have some grounds for suspecting that the passage from the humic to the benzene carboxylic acids may not be direct, but possibly through some intermediate crystalline acids more complex than the latter which we have not yet been able to isolate This point, however, is reserved for future investigation

A Typical Oxidation Experiment —In our preliminary experiments described in Part IV hereof (*q v*)* the permanganate oxidation was carried out in a strongly alkaline medium in an autoclave Starting at 70° C the process always became so vigorous that the temperature of the system would rise automatically to anything between 140° and 175° C, corresponding with pressures in the latter case as high as 140 lbs per square inch

In later experiments, however, we have obtained better yields of crystalline organic acids by working at atmospheric pressure so that the temperature does not rise beyond the boiling point of the liquid medium thereat We will now describe, as a typical example, the procedure adopted in the case of the benzene pressure-extracted residue from Morwell Brown Coal

507 grams of the dried and finely pulverised coal "residue" (*i e*, equivalent to 478 grams of "ashless" residue) were suspended in open vessels containing 34 5 litres of water in which 345 grams of potassium hydroxide had been dissolved The temperature of the medium having been raised to between 60° and 70° C, 3896 grams in all of potassium permanganate were gradually added to it † The external heating was continued until the temperature of the medium had risen up to its boiling point, a condition usually attained after

---

* *Loc cit*

† Later on in the research it was found that an even smoother oxidation resulted on using an alkali/coal ratio of 1 6 and adding the said proportion of the permanganate quite slowly as a solution at the temperature stated

between one-quarter and one-third of the total permanganate had been added For some time thereafter the heat developed by the reaction sufficed to keep the liquid boiling at atmospheric pressure, but after about three-quarters of the whole permanganate had been added, it became necessary again to apply heat externally in order to maintain it so The whole operation of adding the permanganate usually extended over 2 to 3 hours

The heating was continued after the last addition of the permanganate until its colour had been discharged, whereupon the precipitated manganese hydroxide was removed from the hot medium by filtration, and the gelatinous mass of the hydroxide subsequently well pressed and thoroughly washed and extracted with boiling water

The resulting clear alkaline solution (*i e*, filtrate *plus* washings, etc) having been concentrated by evaporation to a convenient bulk, an amount of sulphuric acid (suitably diluted) theoretically required to convert all the potassium present into sulphate was gradually added, care being taken to prevent escape of any volatile organic acid (*e g*, acetic acid) during the operation, which was marked by a copious evolution of carbon dioxide The resulting acid liquid so produced was next steam distilled for removal of any volatile organic acids, and the latter then recovered from the distillate by suitable means, which need not be here described

The solution of non volatile acids was finally evaporated to dryness in a steam bath, and the hygroscopic residue of potassium sulphate *plus* organic acids was then ground to a suitable degree of fineness, dried at 80° C, and a pressure of *circa* one-fifth atmosphere and finally extracted with (*a*) ether and (*b*) acetone successively in a Soxhlet apparatus

The crude mixture of non volatile acids recovered in the usual way from the "dried ethereal or acetone solution formed a pale yellow to yellowish-brown crystalline mass which was afterwards subjected to prolonged investigation with the object of isolating and identifying its principal constituents This crude mixture of acids contained a small proportion of oxalic acid which, however, was subsequently estimated and removed by suitable means

The residual potassium sulphate after the foregoing extraction still contained the greater part of the oxalic acid produced by the oxidation, it was therefore dissolved in water and the oxalic acid recovered from the solution as calcium oxalate and finally converted into its methyl ester

Yields of Oxidation Products—The following figures will give an idea of the yields of the various acids already referred to obtained in typical oxidation experiments with the coal residues under investigation, they are given as parts by weight formed by 100 parts of the dry-ashless coal residue used in each case

Oxidation of residue from	Parts by weight per 100 of coal residue		
	Volatile acetic acid, etc	Oxalic acid	Crude benzenoid acids
Morwell brown coal	4.6	10.3	33.2
Estevan brown lignite	6.8	21.4	47.3
Busty coal	3.3	20.8	41.8
Witbank " coal	5.0	15.6	49.0
Canmore coal	3.2	35.35	43.2

It should be noted that (i) the term "acetic acid" in the foregoing possibly may have included small proportions of higher fatty acids, although none were ever actually found in the steam "volatile" monobasic acids (ii) that the "oxalic acid" was quite pure and anhydrous, and (iii) among the "crude benzenoid acids" in the third column, which consisted almost wholly of benzene carboxylic acids, might be included inconsiderable amounts of succinic acid in some cases Indeed no other acids than these were ever detected or isolated, for although we had rather expected to find some adipic acid among the oxidation products, we never actually did

The Mixture of Crude Benzenoid Acids

Ultimate analyses of the "crude benzenoid acids" (almost freed from oxalic acid in each case) obtained by the oxidation of the benzene extracted "residues" from Morwell Brown Coal and Busty Coal, respectively resulted as follows —

	"Morwell" acids	"Busty" acids	Mean
	Per cent	Per cent	Per cent
Carbon	50.9	49.6	50.25
Hydrogen	3.25	2.9	3.07
Oxygen (by difference)	45.85	47.5	46.68
Ratio C/H	15.7	17.1	16.4

The foregoing figures accorded well with the subsequent detailed examination of the crude acids, which resulted in the isolation of nothing but benzene carboxylic acids whose equivalents and ultimate compositions are shown in Table I The figures pertaining to our crude benzenoid acids— which it will

Table I – Showing Ultimate Compositions of Acids

Acid	Equivalent	Carbon	Hydrogen	Oxygen	Ratio C/H	Ratio O/H
		per cent	per cent	per cent		
Benzene dicarboxylic	83	57.82	3.64	38.54	16	10.7
Benzene tricarboxylic	70	51.41	2.85	45.74	18	16
Benzene tetracarboxylic	63.5	47.25	2.36	50.39	20	21.3
Benzene pentacarboxylic	59.6	44.30	2.01	53.60	22	26.7
Benzene hexacarboxylic	57	42.10	1.75	56.15	24	32
Oxalic	45	26.65	2.22	71.13	12	32
Succinic	59	40.67	5.08	33.25	8	10.3
Glutaric	66	45.45	6.05	48.50	7.5	8
Adipic	73	49.30	6.35	44.35	7.2	6.4
Azelaic	80	52.50	7.50	40.00	7.0	5.3
Suberic	87	55.20	8.05	36.75	6.85	4.6
$CH_2\ COOH$ $CH\ COOH$ $CH\ COOH$	58.7	40.90	4.54	54.51	9	12
$CH_2\ COOH$ $(CH\ COOH)$ $CH_2\ COOH$	58.5	41.03	4.27	54.70	9.6	13
$CH\ COOH$ $(CH\ COOH)_3$ $CH_2\ COOH$	58.4	41.10	4.11	54.79	10	13.3
$CH_2\ COOH$ $(CH\ COOH)_4$ $CH_2\ COOH$	58.3	41.14	4.00	54.86	10.3	13.5
$CH_2\ COOH$ $(CH\ COOH)_5$ $CH_2\ COOH$	58.3	41.18	3.92	54.90	10.5	14.0
$CH_2\ COOH$ $(CH\ COOH)_6$ $CH_2\ COOH$	58.2	41.20	3.86	54.94	10.7	14.2

be seen were very near to those for benzene tricarboxylic acid—should also be compared with those for the di- and tri-basic saturated open chain acids included in the table, when it will be seen also that the C/H ratios found for the crude acids were far higher than would be required for any mixture of the foregoing open-chain acids

The "equivalents" of the 'crude benzenoid acids' obtained from the 'Morwell" and Busty coals were found to be 77 5 and 76 7 respectively, or rather higher than the 70 theoretically required for a benzene tricarboxylic acid, to which the mean ultimate composition of the crude acids closely approximated This led us to suspect the presence among the crude acids of a small proportion of some crystalline acid more complex than any benzene carboxylic acid, i.e., of some crystalline acid coal oxidation product intermediate between the colloidal humic acids" and the crystalline benzene carboxylic acids This suspicion was confirmed when it was subsequently found that on submitting the crude benzenoid acid mixture to the action of warm alkaline permanganate some slight oxidation occurred, and on the crystalline acid being recovered almost quantitatively its equivalent" was found to have fallen to 71, or almost to that required for benzene tricarboxylic acid

In this connection it should perhaps be mentioned that trial experiments had shown that, when pure, neither oxalic acid nor any of the benzene carboxylic acids underwent appreciable oxidation on being boiled with alkaline permanganate solution of the strength employed during this research

Therefore, from the analytical results obtained with the crude benzenoid acids we think there can be little doubt but that—apart from their possibly containing some trace of oxalic acid, up to 1 per cent of succinic acid, and probably also small amounts of some much more complex crystalline acid of benzenoid type intermediate between them and colloidal "humic acids"—they were almost wholly composed of benzene carboxylic acids of mean composition closely approximating to that of a benzene tricarboxylic acid

Carbon Balance of the Oxidation —Besides determining the weight yields of the principal organic acids produced during the oxidation, we carried out special experiments each with 10-gram portions of dry "residues" from the benzene-pressure-extraction of the "Morwell" and "Busty" coals with the object of determining the distribution of their carbon contents among the various oxidation products Care was taken not only to use a high KOH/Coal ratio (1 6), but also to add the permanganate very slowly and as a solution to the alkaline medium in which the coal substance was suspended, such being the conditions most conducive to smooth working. We were thus enabled to account for practically the whole of the original carbon in each case, as the following figures indicate:—

Original carbon of the coal substance appearing as—	Morwell	Busty
	Per cent	Per cent
Carbonic anhydride	41.3	42.4
Acetic acid	2.5	1.7
Oxalic acid	7.7	6.5
Succinic acid	0.8	Nil
Benzenoid acids	47.4	48.8
Total accounted for	99.7	99.4

That two coals so different in geological age, geographical occurrence and chemical maturity as these are—the one an immature tertiary brown coal from Australia and the other a well matured Durham bituminous coal of carboniferous origin—is indeed very remarkable, showing as it does the essential constancy of the chemical structure of the main "coal substance" notwithstanding differences in geological age and maturity.

Also, seeing that in each case the ultimate composition of the mixture of crude benzenoid acids closely approximated to that of benzene tricarboxylic acid, two-thirds of whose carbon atoms form the benzene ring, it may be concluded that in each case nearly one third of the carbon originally present in the coal substance appeared as C_6-rings in the oxidation products.

Detailed Investigation of the Organic Acids produced by the Oxidation

The detailed investigation of the complex mixture of acids produced by the oxidation was a long, difficult and laborious matter, but eventually it was completed in the case of three of the coals investigated; in the other two cases it was taken sufficiently far to show that, had it been completed, the results would not have differed materially from those in the other three cases.

The procedure adopted varied somewhat in different cases, and to describe it all in detail would serve no useful purpose. We will, therefore, take the case of the Morwell coal oxidation acids as typical, and outline the procedure adopted in examining them; it may be assumed that in principle similar procedures were adopted in other cases.

Oxidation Products from Morwell Coal —The general procedure is shown diagrammatically as follows

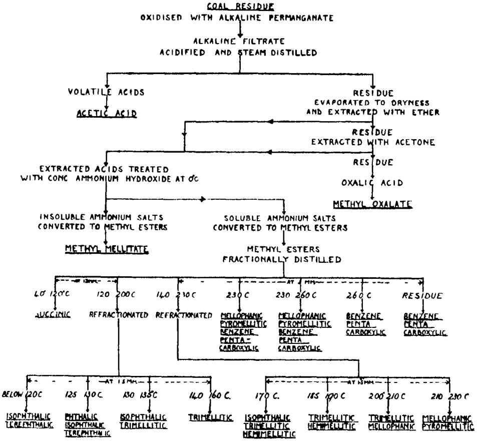

EXAMINATION OF OXIDATION PRODUCTS FROM MORWELL BROWN COAL RESIDUE

First of all, any "volatile" acids present (practically all acetic acid) were removed by steam distillation as already described The distillate was then neutralised with sodium hydroxide, and the solution of sodium salts obtained evaporated to dryness The dry salts were then treated in suspension in ether with phosphorus pentachloride, and the resulting acid-chloride solution was treated with an ethereal solution of *p*-toluidine The *p*-toluidides so formed were subsequently fractionally crystallised from a suitable solvent As only acet-*p*-toluidide (found *m p* 147 5° C, C = 72 88, H = 7 7 per cent required for $C_9H_{11}ON$, *m p* 147 5° C, C = 72 47, H = 7 38 per cent) could be isolated, it was concluded that the "volatile acids" were almost entirely composed of acetic acid The same applied to the oxidation products of all the other coals examined, the yields of acetic acid varying between 2 and 7 per cent of the weight of coal substance originally taken

The aqueous solution of the " non-volatile " acids *plus* potassium sulphate having been evaporated, and the residue dried under reduced pressure, it was powdered and then thoroughly extracted with (*a*) ether and (*b*) acetone successively In drying the residue care was taken to ensure the elimination as far as possible of water of crystallisation from any oxalic acid present, because of $C_2H_2O_4$ $2H_2O$ being much more soluble in ether than the anhydrous acid Provided such precautions were taken, most of the oxalic acid was left unextracted, though a little passed into solution The unextracted oxalic acid was subsequently separated out as calcium salt $CaC_2O_4 + H_2O$ which, after re-precipitation from acetic acid solution was finally converted into the methyl ester, and the last-named identified by its melting point and a mixed melting point with an authentic specimen of methyl oxalate The calcium salt was also analysed (Ca = 27 25, as compared with the theoretical 27 43 per cent)

The mixture of ether and acetone extracted non-volatile acids was cooled to 0° C and dissolved in a similarly cooled concentrated solution of ammonium hydroxide (0 880), the operation being carried out in well-cooled vessels at a low temperature In this way ammonium mellitate together with (may be) a little ammonium oxalate (both of which are sparingly soluble in strong ammonium hydroxide at 0° C) separated out from the other much more soluble ammonium salts This procedure was found to be an excellent way of freeing the ether soluble acids from any oxalic acid which they might contain, the amount so present depending on the extent to which the oxalic acid had been dehydrated before the ether extraction Indeed we found that either nearly all, or only part, or even none of the oxalic acid may appear in the ether soluble acids according to the thoroughness of the previous drying operation

In cases where the previous drying had been completed, the insoluble ammonium salts were found to consist mainly, if not wholly, of ammonium mellitate (benzene hexacarboxylate), albeit in cases where ammonia gas had been passed into the cold liquid to replace that lost by evaporation during the operation described in the previous paragraph, some ammonium benzene pentacarboxylate might also have been present It was found inadvisable to allow the insoluble ammonium salts to become too dry for fear of some imide formation

The solution of soluble ammonium salts was first boiled until free from excess of ammonia, and then cooled and exactly neutralised with ammonia During the boiling not only was all the *free* ammonia expelled, but also some more was eliminated owing to partial dissociation of ammonium salts, hence the need of subsequent exact neutralisation of the cold solution To the cold neutral solution of ammonium salts was added slight excess of a solution of silver nitrate, whereby insoluble silver salts were precipitated These were separated by filtration, washed with water and then dried The dried mixture of silver salts was subsequently converted into methyl esters by refluxing them with excess of methyl iodide in dry ethereal solution

The filtrates and washings from the so precipitated insoluble silver salts were found to contain in solution small amounts of silver salts which, however, on subsequent examination were found to be the same as the precipitated silver salts, and merely representing the small unprecipitated part thereof, the silver salts as a whole being very "sparingly soluble," but not absolutely insoluble, in water

The mixture of methyl esters obtained from the precipitated silver *salts* consisted of both neutral and acid esters; these were separated by the usual method, any acid ester subsequently converted as far as possible into neutral esters, *via* silver salts + methyl iodide Finally, having got them for the most part as neutral esters, the latter were fractionally distilled *under as low a pressure as possible* (starting at 13 and finishing up at 1 mm) some of the fractions being subsequently refractionated The "fractionation scheme" is detailed on p 494 and need not be further described It will be noticed that the successive fractions distilled over a temperature range commencing at 40° C ($p = 12$ to 13 mm) and extended up to 260° C ($p - 3$ mm), the distillation being stopped at that temperature for fear of decomposition setting in, leaving a residue, usually amounting to about one-fifth of the whole, which had not distilled over

The various successive ester fractions, as well as the residue so obtained, were all submitted separately to close investigation In some cases, methyl esters crystallised out and could be isolated, purified, analysed and separately hydrolysed to the corresponding acids Otherwise the ester fractions and/or uncrystallised parts thereof were separately hydrolysed to the corresponding acids which were then recrystallised from suitable solvents (usually mixtures of acetone and chloroform, but occasionally either dry ether or other media) and afterwards identified by (*a*) melting points, ultimate analyses and determinations of "equivalents," (*b*) direct comparisons with authentic specimens, including "mixed melting points" wherever possible, (*c*) conversions into crystalline methyl esters, and subsequent analyses and comparison thereof with authentic specimens

It should be stated that the silver iodide precipitated during the esterification of the mixed insoluble silver salts by means of methyl iodide was always boiled with hydrochloric acid solution with a view to hydrolysing and removing any esters adsorbed therein Any acids so obtained were subsequently reconverted into their neutral methyl esters which were added to, and fractionated with, the main bulk of the methyl esters

The foregoing procedure, together with the isolation, purification and identification of the various acids resulting therefrom, necessarily occupied several months in each case , but eventually, in the case of three of the coal-residues under investigation, it was successfully carried to completion, every part of the acid oxidation product being thoroughly examined It may be that, notwithstanding the searching character of the investigation and all care bestowed upon the various operations involved, some constituents of the acid products were overlooked , but we think that at any rate all the more important and conspicuous acids present in the crude oxidation products were identified as far as was possible in the circumstances

Acids isolated from the Oxidation Products of Morwell, Estevan and Busty Coal Residues

The list of acids actually isolated, purified and identified in the three cases where the investigation and refinement of the crude oxidation products were completed was as follows* - -

---

* For readers unfamiliar with the nomenclature of organic acids it may be explained that —

$$\left.\begin{array}{l}\text{Phthalic}\\ \text{Isophthalic}\\ \text{Terephthalic}\end{array}\right\}\text{acids}=\left\{\begin{array}{l}\text{ortho}\\ \text{meta}\\ \text{para}\end{array}\right\}\text{benzene dicarboxylic acids, respectively}$$

$$\left.\begin{array}{ll}\text{Hemimellitic acid} & = 1\ 2\ 3\\ \text{Trimellitic acid} & = 1\ 2\ 4\\ \text{Trimesic acid} & = 1\ 3\ 5\end{array}\right\}\text{benzene tricarboxylic acids.}$$

$$\left.\begin{array}{ll}\text{Pyromellitic acid} & = 1\ 2\ 4\ 5\\ \text{Mellophanic acid} & = 1\ 2\ 3\ 5\end{array}\right\}\text{benzene tetracarboxylic acids.}$$

Mellitic acid = benzene hexacarboxylic acid.

Oxidation of residue from—		
Morwell brown coal	Estevan brown lignite	Busty coking coal
Carbonic anhydride	Carbonic anhydride	Carbonic anhydride
Acetic	Acetic	Acetic
Oxalic	Oxalic	Oxalic
Succinic	Succinic	—
Phthalic	Phthalic	Phthalic
Isophthalic	Isophthalic	Isophthalic
Terephthalic	Terephthalic	Terephthalic
Hemimellitic	Hemimellitic	—
Trimellitic	Trimellitic	Trimellitic
—	Trimesic	—
Mellophanic	Mellophanic	Mellophanic
Pyromellitic	Pyromellitic	Pyromellitic
Benzene-penta-carboxylic	Benzene-penta-carboxylic	Benzene-penta-carboxylic
Mellitic	Mellitic	Mellitic

The accompanying Table II summarises how each acid was identified

It was thus proved that on oxidation all these coal residues had yielded carbonic anhydride, acetic, oxalic, the three phthalic, trimellitic, pyromellitic, mellophanic, benzene pentacarboxylic, and mellitic acids, that two others had also yielded both succinic and hemimellitic acids, while the Estevan coal residue had yielded trimesic acid in addition to all the others Indeed from one or other of the three coal residues there had been obtained every possible benzene carboxylic acid except benzoic and the 1 2 3 4 tetra-carboxylic acid, while the Estevan residue had yielded every one of the ten benzene carboxylic acids actually obtained And, with regard to the yields, it may be said that some 1 7 to 3 8 per cent of the carbon in the original coal residues appeared as acetic acid and some 6 to 8 per cent as oxalic acid, that the proportion appearing as succinic was undoubtedly small, so far as could be judged not more than 0 8 per cent of the whole, and that something between 45 and 50 per cent appeared as benzenoid acids, although it is difficult to say which of them predominated

As already stated, it is impossible for us to say whether any other acids present in the oxidation products had escaped detection and isolation during

Table II.—Acids obtained by the Alkaline Permanganate Oxidation of Morwell, Estevan, and Busty Coal Residues

Acid identified.	Substance obtained pure	Recorded melting point	Theoretical composition	Theoretical equivalent	Obtained from coal residue	Melting point found	Composition found.	Equivalent found.
Acetic acid	Acet *p*-toluidide	147.5° C	per cent C = 72.47 H = 7.38	—	Morwell Estevan Busty	147.5° C 147.5° C 147.5° C	per cent C = 72.88 H = 7.7	—
Oxalic acid	*Methyl ester	54° C	C = 40.66 H = 5.12	—	Morwell Estevan Busty	54° C 54° C 54° C	—	—
	$CaC_2O_4 \cdot H_2O$	—	Ca = 27.43	—	Estevan Busty	—	Ca = 27.25 Ca = 27.16	—
Succinic acid	Succinic acid	182.5° C	C = 40.67 H = 5.08	59.0	Morwell Estevan	182.5° C 181.5°–182° C	C = 40.21 H = 5.11	58.8 58.6
	p-bromphenacyl succinate	212° C –212.5° C	C = 46.88 H = 3.15	—	Morwell Estevan	212°–213° C 212°–212.5° C	—	—
Phthalic acid	Phthalic acid	191° C (dec.) (slow) 213° C (dec.) (rapid)	C = 57.82 H = 3.64	83.0	Morwell Estevan Busty	193° C (dec.) 192° C (dec.) 192° C (dec.)	—	82.9
	p-bromphenacyl phthalate	151.5° C –152.5° C	C = 51.43 H = 2.88	—	Estevan Busty	151.5°–152.5° C 151.5°–152.5° C	—	—
Isophthalic acid	Isophthalic acid	Above 300° C sublimes	C = 57.82 H = 3.64	83.0	Morwell Estevan Busty	>300° C subl. >300° C subl. >300° C subl.	—	82.9
	Methyl ester	67.5° C –68° C	C = 61.86 H = 5.15	—	Morwell Estevan Busty	67°–68° C 67.5°–68° C 67.5°–68° C	C = 61.65 H = 5.32	—

* The methyl esters referred to in this table are the neutral methyl esters.

Table II—(continued)

Acid identified	Substance obtained pure	Recorded melting point	Theoretical composition	Theoretical equivalent	Obtained from coal residue	Melting point found	Composition found	Equivalent found
Terephthalic acid	**Terephthalic acid**	Sublimes without melting	C = 57.82 H = 3.64	83.0	Morwell Estevan Busty	Sublime Sublime Sublime	per cent —	—
	Methyl ester	140° C	C = 61.86 H = 5.15	—	Morwell Estevan Busty	140° C 140° C 140° C	C = 61.65 H = 5.66	—
Hemimellitic acid	**Hemimellitic acid**	190° C (dec.)	C = 51.41 H = 2.85	70.0	Morwell Estevan	190°–193° C (dec.) 191.5°–192.5° C (dec.)	—	69.9
	Methyl ester	100° C	C = 42.86 H = 4.78	—	Morwell Estevan	99.5°–100° C 100° C	—	—
Trimesic acid	**Trimesic acid**	380° C sublimes	C = 51.41 H = 2.85	70.0	Estevan	Sublimed about 200° C	—	70.2
Trimellitic acid	**Trimellitic acid**	225° C (dec.)	C = 51.41 H = 2.85	70.0	Morwell Estevan Busty	225° C (dec.) 225° C (dec.) 225° C (dec.)	C = 51.32 H = 3.12	70.2 70.3
	Anhydride	158° C	C = 56.25 H = 2.10	—	Morwell Estevan Busty	160° C 161° C 160° C	—	—
Mellophanic acid	**Methyl ester**	133°–135° C	C = 54.19 H = 4.52	—	Morwell Estevan Busty	129.5°–130° C 129.5°–130° C 129.5°–130° C	C = 53.99 H = 4.61 C = 54.04 H = 4.67	—
	Mellophanic acid	238° C (dec.)	C = 47.25 H = 2.36	63.5	Morwell Estevan	Sintered 225° C 256°–264° C (dec.) Sintered 223° C 258°–264° C (dec.) sealed tube	C = 47.26 H = 2.60	63.15 63.0

Pyromellitic acid	**Methyl ester**	141 5° C	C = 54 19 H = 4 52	—	Morwell Estevan Busty	142 5 C 141 5°-142 5 C 141 5 -142 5 C	C = 53 93 H = 4 64 C = 53 96 H = 4 77	—
	Pyromellitic acid	$-2H_2O$ 242 5° C (dec) 273°–275° C (dec)	C = 47 25 H = 2 36	$+2H_2O=$ 72 5 63 5	Morwell Estevan	241 -242 C (dec) 275°-277 C (dec) 235 -237 C (dec) 274 -277 5° C (dec)	C = 47 07 H = 2 90	$+2H_2O$ 72 0 64 0
Benzene pentacarboxylic acid	**Methyl ester**	148° C	C = 52 18 H = 4 38	—	Morwell Estevan Busty	148 C 148 C 148 C	C = 52 00 H = 4 78 C = 51 84 H = 4 63	—
	Benzene pentacarboxylic acid	Melts with decomposition	C = 44 30 H = 2 01	59 6	Morwell Estevan	Sintered 225 C 242°–252° C (dec) Sintered 227 C 241°–243 C (dec) sealed tube	C = 44 06 H = 2 53	60 4
Mellitic acid	Methyl ester	187° C	C = 50 71 H = 4 23	—	Morwell Estevan Busty	187 C 187 C 187 C	C = 50 38 H = 4 35 C = 50 44 H = 4 58	—

the long and tedious series of operations involved in our examination, but even if some did we feel sure that the quantities would be quite small And we think it significant that, with the exception of a small proportion of succinic in two cases, nothing but benzene carboxylic acids were isolated from the oxalic-free mixture of the ether and acetone-soluble non-volatile acids, the mean ultimate composition of which (*q v*) approximated to that of benzene tricarboxylic acid Moreover, it should be noted that no acid containing more than one C_6-ring was ever isolated

We therefore feel justified in concluding that by far the most part of the oxalic-free, ether and acetone-soluble non-volatile acids were benzenoid acids, and seeing that these represented some 45 to 50 per cent of the carbon originally contained in the coal residue treated (which "residue" = from 85 to 98 per cent of the whole coal substance), the significance of this fact in regard to the chemical constitution of coal scarcely needs emphasising

Examination of the Crude Acids obtained by the Oxidation of the Witbank and Canmore Coal Residues

The permanganate oxidation of the benzene-pressure extraction residues from Witbank and Canmore coals was carried out in much the same way, and with much the same results, as in the three previous cases

It was not considered necessary, however, to examine exhaustively the crude acids obtained, but only so far as was needed to establish their essential similarity to those obtained from the three coal residues previously investigated

Following much the same procedure as that already outlined, from the crude oxidation products of the Witbank coal residue acetic, oxalic, phthalic, mellophanic, pyromellitic, benzene pentacarboxylic and mellitic acids were isolated and identified, while the crude oxidation products from the Canmore residue were found to contain (*inter alia*) acetic, oxalic, phthalic, terephthalic, mellophanic, benzene pentacarboxylic and mellitic acids There can be little doubt of the practical identity of the oxidation products from these two coal residues with those previously derived from the Morwell, Estevan, and Busty residues

Step-wise Oxidation of the Main Coal Substance

Having thus determined the nature of the complex acid products derived from the alkaline permanganate oxidation of typical coal residues, when the $KMnO_4$/Coal weight ratio was somewhere between *c a* and *e p* (*vide* p 487) it now seemed of interest to explore what would happen if and when the $KMnO_4$/Coal weight ratio were progressively reduced downwards starting from a point just below the *c a* ratio and continuing until it had reached unity

With such object in view a series of experiments was made with the "residues" from Estevan and Busty coals, respectively The general method employed was to oxidise a given weight (10 grams) of the pulverised coal-residue, suspended in an alkaline (KOH) solution of proper strength, by means of a variable weight ratio of the potassium permanganate, the operation being started at about 70° C but chiefly conducted at the boiling point of the medium at atmospheric pressure The acid oxidation products were subsequently recovered and separated into steam-volatile (acetic) acid, oxalic acid and ether- and acetone-soluble acids, much as in previous cases , but beyond satisfying ourselves that the ether- and acetone-soluble acids were essentially benzenoid in character, they were not further investigated The weight yields of each category of acids were, however, always determined

It was found possible in each case to find a "critical" $KMnO_4$/Coal ratio (somewhere above 8) at which all (or nearly so) of the coal substance could be oxidised to carbonic anhydride and crystalline organic acids only, without the formation of any colloidal humic acids, but so that on diminution of the $KMnO_4$/Coal ratio the last named appeared in the products

In carrying out our experiments with the said "critical" $KMnO_4$/Coal ratio, the latter was progressively diminished in successive experiments until it fell to unity And in each case, the proportions of the resulting (i) unoxidised coal residue (ii) humic acids, (iii) acetic, (iv) oxalic, and (v) ether- and acetone-soluble ("benzenoid") acids were determined

Without going into unnecessary details, the following are the tabulated summarised results of these experiments —

(*a*) With Estevan Coal residue

$KMnO_4$/Coal ratio	Weight yields per 100 of coal substance taken				
	Unchanged coal substance	Humic acids	Benzenoid acids	Oxalic acid	Acetic acid
8 25	Nil	1 45	50 2	21 4	5 6
7 0	3 9	4 0	54 9	19 2	4 8
5 0	5 6	37 0	33 6	12 4	3 8
3 0	20 9	45 3	24 6	5 5	3 1
1 0	52 2	27 9	18 2	1 2	3 4
Nil*	92 7	10 4	3 4	Nil	1 5

* This blank experiment was made to ascertain the effects of suspending the coal substance in a boiling alkali-solution of the same strength as that used in the experiments.

(*b*) With Busty Coal residue

KMnO$_4$/Coal ratio	Weight yields per 100 of coal residue taken				
	Unchanged coal substance	Humic acids	Benzenoid acids	Oxalic acid	Acetic acid
8 1	4 4	Nil	46 8	17 0	2 6
7 0	10 85	19 1	51 0	20 0	2 1
5 0	32 4	24 4	35 1	13 2	2 4
3 0	56 1	27 8	23 0	8 0	1 9
1 0	81 9	10 9	6 0	1 95	0 9
Nil	100 0	Nil	Nil	Nil	Nil

It is thus seen that not only are colloidal "humic acids" intermediately produced during the permanganate oxidation of the coal substance, but in the case of an immature brown coal some may be present originally

In order better to view the foregoing results in the proper perspective, however, it is advisable to disregard the "unchanged coal substance" remaining after each experiment and to express them in terms of the "coal substance" actually changed in each case, and this is shown in the following tables —

(*c*) With Estevan Coal residue

KMnO$_4$/Coal ratio	Weight yields per 100 of coal substance oxidised			
	Humic acids	Benzenoid acids	Oxalic acid	Acetic acid
8 25	1 45	50 2	21 4	5 6
7 0	4 15	57 15	20 0	5 0
5 0	39 2	35 55	13 1	4 0
3 0	57 2	30 9	6 8	3 9
1 0	58 4	38 1	2 5	7 1

(*d*) With Busty Coal residue

KMnO$_4$/Coal ratio	Weight yields per 100 of coal substance oxidised			
	Humic acids	Benzenoid acids	Oxalic acid	Acetic acid
8 1	Nil	48 9	17 8	2 72
7 0	21 4	57 1	22 4	2 35
5 0	36 1	52 1	19 5	3 6
3 0	63 3	52 3	18 2	4 33
1 0	60 2	33 2	10 7	4 95

Taken as a whole these results showed that most probably the colloidal "humic acids" are the initial oxidation products, the simpler crystalline benzenoid and oxalic acids subsequently arising from their further oxidation.

Oxidation of the Intermediate Humic Acids

The foregoing conclusion was confirmed by the results of a later series of experiments in which the "humic acids" in question were isolated free from the other oxidation products and then further oxidised by suitable proportions of alkaline permanganate, acetic, oxalic, succinic and various benzene carboxylic acids were thus obtained.

The "humic acids" were first of all obtained by the partial oxidation of "Estevan" coal residue by means of a suitable proportion of alkaline permanganate solution at its boiling point ($KMnO_4$/Coal residue = 3 : 1). The precipitated hydrated manganese oxides having been removed by filtration, the colloidal humic acids were precipitated from the clear alkaline solution of potassium salts on acidification by means of dilute sulphuric acid, they were then thoroughly washed and redissolved in a slight excess of potassium hydroxide solution, from which they were re-precipitated by means of dilute sulphuric acid, and afterwards thoroughly washed with hot distilled water until practically free from adsorbed salts.

The acids were next dried, first of all in an oven at 80° and then *in vacuo* at room temperature over sulphuric acid, the ultimate composition of the dried acids was

$C = 56.7$, $H = 3.35$, $N = 1.2$, $S = 0.6$, and $O = 38.15$ per cent.

About 60 grams of the so dried humic acids were oxidised by means of a suitable proportion of boiling alkaline permanganate ($KMnO_4$/Humic acid = 5 : 1) in our usual manner, and the resulting acid oxidation products subsequently separated and estimated as already described. These consisted of acetic, oxalic, succinic and benzenoid acids in the following proportions per 100 by weight of the original humic acids —

Acid	Weight yield per 100 of "humic acid"
Acetic	2.9
Oxalic	17.7
Succinic	1.0
Benzenoid acids	62.0

From the crude benzenoid acids were isolated terephthalic, mellophanic, pyromellitic, benzene pentacarboxylic and mellitic acids.

Weight Ratios of Acid Oxidation Products

The striking fact that two such different coals as the Morwell brown coal and the strongly coking Busty bituminous coal when similarly oxidised yielded nearly the same proportion of acetic, oxalic, and benzenoid acids, respectively, has already been commented upon , but there remains the further question as to whether these products arise simultaneously or independently during the oxidation

This point may be considered by reference to the benzenoid/oxalic and benzenoid/acetic acid ratios formed in the products at the different degrees of oxidation attained in our "step-wise" experiments (p 502) Commencing with the least and passing onwards to the greatest degree of oxidation attained in each case, these were as follows —

	Weight ratios				
Estevan coal residue—					
Benzenoid/oxalic	15 2	4 55	2 71	2 85	2 35
Benzenoid/acetic	5 35	7 92	8 87	11 43	8 96
Busty coal residue					
Benzenoid/oxalic	3 1	2 87	2 67	2 55	2 75
Benzenoid/acetic	6 85	12 1	14 5	24 3	17 98

Although the significance of these ratios, subject as they undoubtedly are to a fair margin of experimental error, ought not to be unduly stressed, it may be noted that, except during the initial stages of the oxidation of the Estevan residue, there was a marked tendency for the benzenoid/oxalic ratios to be fairly constant (*e g* , between 2 35 and 3 1) throughout, as though the benzenoid and oxalic acids were arising simultaneously from a common source The constancy of the ratio throughout the "Busty" experiments is remarkable and could scarcely have been a mere coincidence , in the case of the "Estevan" experiments, it seems likely that the higher ratio during the earlier oxidation phases may be due to the original coal substance already containing (as the "blank" experiments showed) some 3 4 per cent of benzenoid acids

In this connection it should be noted that the benzenoid/oxalic acid ratio observed in the case of the further oxidation of the humic acid prepared from the Estevan coal residue was 3 5, while the corresponding benzenoid/acetic acid ratio was 21 4

The absence of any constancy in the benzenoid/acetic acid ratios in the foregoing cases makes it difficult to say whether or not *all* the acetic acid arose simultaneously with the benzenoid acids, but that some of it does is proved by the experiments upon the oxidation of the humic acids intermediately found for the Estevan residue

Therefore on the evidence so far available, and pending further exploration of the subject, we are inclined to view the oxidation of the original coal residue as proceeding in accordance with the following provisional scheme

$$\text{Coal substance} \longrightarrow \text{Humic acids} \longrightarrow \left\{\begin{array}{l}\text{Possibly}\\ \text{Intermediate}\\ \text{Crystalline}\\ \text{Acids}\end{array}\right\} \begin{array}{l}\nearrow \text{Benzenoid acids}\\ \longrightarrow \text{Oxalic acid}\\ \searrow \text{Acetic acid}\end{array}$$

Further experimental work will, however, be required before any final conclusion would be justified, and as we have the matter now well in hand, we will reserve further discussion of it for a future communication

Oxidation of the Benzene Pressure-Extracts

Having dealt with the permanganate oxidation of the " residues " from the benzene-pressure-extraction of the various coals under investigation—and which constituted from 85 to 98 5 per cent of their whole " coal substance "—a short statement may now be added as to what we have already established regarding the constitution of our various fractions of the benzene-pressure-extracts

Reference to Part V hereof will show that the benzene-pressure-extracts from Morwell brown coal and the Estevan brown lignite, though differing in amounts (namely, 15 0 and 4 5 per cent respectively), were practically alike in their chemical character, in that each could be fractionated into similar proportions of (i) neutral oils soluble in light petroleum, (ii) neutral amorphous powder insoluble in light petroleum, (iii) phenolic esters, and (iv) phenols In the case of the Morwell coal two-thirds, and in the case of the Estevan coal 57 per cent, of the crude extract was composed of phenols and phenolic esters, and was therefore benzenoid in structure

In the case of the well-matured Busty bituminous coking-coal, the crude extract, which amounted to 15 6 per cent of the dry-ashless coal-substance, contained neither phenols nor phenolic esters, these being replaced by a large fraction (IV) of a nitrogenous amorphous solid of high softening point, which represented 9 6 per cent of the original coal substance and was responsible for the strong coking propensities of the coal The remainder of the crude extract was of chemically similar character to the "neutral oils" obtained from the two brown coals

It therefore seemed probable that the gradual development of "coking propensities" in coals has been due to "condensations" of phenolic with aldehydic and amino bodies in the coal substance during the long maturing process

This view of the matter has received further support from some recent experiments in our laboratories in which Fraction IV of the crude benzene-pressure extract from the Busty coking coal was oxidised by means of solutions of chromic acid and alkaline permanganate, successively applied yielding 2 4 parts of acetic, 24 parts of oxalic and 62 parts of benzenoid acids per 100 parts by weight of the original Fraction IV taken

It would therefore appear that the constituents which are mainly responsible for the "coking propensities" of bituminous coals, like the main coal-substance itself are also substantially benzenoid in character

The Oxidation of Carbonised Materials

During the later stages of our work, we have begun investigating the effects of a progressive carbonisation of our coal residues upon the relative yields of the various permanganate oxidation products, and although this part of the investigation is not yet completed it has advanced far enough to enable the following preliminary statement of results to be made

The experimental method has been (i) to carbonise the coal-residue out of contact with air to a steady state (such that no further volatile matter was expelled from it) at various selected temperatures up to about 1000°, and then (ii) to oxidise each so carbonised material with a suitable proportion of potassium permanganate in a boiling alkaline medium The oxidising procedure required longer time the more the material had been carbonised, also, as the carbonising temperature was progressively raised beyond a certain point the carbonised product became progressively less oxidisable, although evidence was obtained that it was only a question of time for all of it to become oxidised We found it advisable, however, in experimenting with highly carbonised materials, to suspend the oxidation before the whole of it had been completed, some of the original material being recovered at the end of the experiment

As typical examples of the results to date, we have selected the following obtained with the progressively carbonised Estevan and Busty coal residues, respectively, which are tabulated below —

(*a*) With Estevan Coal-residue

Carbonisation temperature	Weight yields per 100 of the dry ashless carbonised residues taken			
	Unchanged material	Benzenoid acids	Oxalic acid	Acetic acid
C° Original residue uncarbonised	Nil	47 3	23 5	6 8*
370	Nil	55 7	17 5	3 5
510	Nil	62 1	17 5	1 0
670	16 3	61 5	10 2	0 2
830	21 2	37 8	4 5	0 1
1000	50 1	22 0	1 3	Nil
or in terms of 100 parts of the material actually oxidised in each case —				
670	—	73 5	12 1	0 2
830	—	48 0	5 7	0 1
1000	–	44 0	2 6	Nil

* These results are included merely as a basis of comparison with those obtained with the various carbonised residues

(*b*) With Busty Coal residue

Carbonisation temperature	Weight yields per 100 of the dry ashless carbonised residue taken			
	Unchanged material	Benzenoid acids	Oxalic acid	Acetic acid
C° Original residue uncarbonised	Nil	41 7	20 8	3 3*
370	3 4	86 0	11 3	2 6
510	46 6	61 6	7 8	0 5
635	56 7	39 5	4 2	0 1
850	52 4	30 2	1 4	Trace
995	74 7	17 0	1 25	Nil
or, in terms of 100 parts of the material actually oxidised —				
510	—	115 7	14 4	0 9
635	–	91 2	9 7	0 2
850	—	63 5	3 0	Trace
995	—	67 3	4 9	Nil

* See footnote to Table (*a*)

It will be observed that in each case, as might be expected, the yields of "benzenoid acids" increased with the carbonisation temperature up to a certain point, probably between 500 and 600° C, where they were a maximum, and afterwards progressively diminished, but even with material which had been fully carbonised at 1000° C, considerable yields of benzenoid acids resulted, pointing to part of the resulting coke having retained its C_6-ring structure And it is conceivable that what is sometimes termed the "reactivity" of such a coke may depend on the proportion of C_6-rings comprising its structure

With Wood Charcoal—We have also made an experiment with a sample of wood charcoal, whose ultimate "dry-ashless" composition was —

$C = 82\ 3$, $H = 3\ 5$, $N = 0\ 45$, $S = 0\ 35$, and $O = 13\ 4$ per cent

This material was quite easily oxidised by the boiling alkaline permanganate medium, going wholly into solution, and ultimately yielding 59 parts of benzenoid acids (from which, *inter alia*, phthalic, benzene penta- and hexa-carboxylic acids have been isolated and identified), 4 2 parts of oxalic and 2 1 parts of acetic acid per 100 parts of the dry-ashless material taken

Carbons—We are also experimenting with various forms of "carbon," including graphite and the flocculent carbon deposited by the catalytic decomposition of carbonic oxide $2CO \rightleftharpoons C + CO_2$ at 450° C in contact with oxides of iron, but the results are not yet far advanced enough for publication, and therefore must be reserved for a future communication

The experimental exploration of the many questions opened up by the foregoing results is being continued in our laboratories with a view to elucidating further the chemical constitution of coal

In conclusion we desire to thank Dr C D Lawrence, and Mr J Taylor, M Sc, for valuable assistance in some of the experiments, as also the Fuel Research Board of the Department of Scientific and Industrial Research for generous annual grants out of which the principal expenses of the work, including personal grants to two of us and Dr Lawrence, have been defrayed

The Interaction of Oxygen with Nitrogen after Collision with Electrons

By O H Wansbrough-Jones, Ramsay Memorial Research Fellow

(Communicated by T M Lowry, F R S —Received November 28, 1929)

In previous communications* from this laboratory a method of examining the rates of reaction of gases after collision with electrons has been described, and in particular the use of a triode of special construction and dimensions for determining the critical potentials at which the reaction takes place has been noted This method has now been applied to the combustion of nitrogen, which has been shown to depend upon ionisation of the nitrogen, activation or ionisation of oxygen apparently playing no part This conclusion is supported by the measurements of critical potentials, by the chemical examination of the reaction products in the experiments to be described, and to some extent by measurements of the efficiency of the process

Previous Work

The synthesis of nitric oxide in the arc has been studied by many workers,† and it has long been recognised that the yields of oxides of nitrogen so obtained were too large to be given by a purely thermal formation in the arc The necessity for an electrical process is further shown by the possibility of synthesis by purely electrical means, such as the silent electric discharge,‡ the corona discharge,§ the spark discharge|| or a cold discharge from a heated oxide cathode ¶ This work was undertaken in the hope of defining this electrical process more completely It has been suggested that the reaction is one between the atoms** or that ionisation and dissociation of the reacting gases

---

* Cafess and Rideal, 'Roy Soc Proc,' A, vol 115, p 685 (1927), and vol 120, p 370 (1928)

† *Cf* Knox, "Fixation of Atmospheric Nitrogen," 2nd edition (Gurney and Jackson, 1921), Allmond and Ellingham, "Applied Electrochemistry" (Arnold, 1924)

‡ Warburg and Leithauser, 'Ann Phys,' vol 20, p 743 (1906), and vol 23, p 209 (1907), Berthelot, 'C R,' vol. 142, p 1367 (1905), and 'Ann Chim Phys,' vol 8, p 145 (1906)

§ Strong, 'Amer Chem J,' vol. 54, p 204 (1913)

|| Briner, 'J Chim Phys,' vol 13, p 18 (1915)

¶ Schwab and Loeb, 'Z Phys Chem.,' vol 114, p 23 (1924)

** Briner and Naville, 'J Chim Phys,' vol 17, p 329 (1919) plays an important part,* while Schwab and Loeb (*loc cit*) have proved that activation of the nitrogen was necessary Nitric oxide has never been made from its elements by a process in which a high degree of excitation was not attainable, but no attempts have hitherto been made to determine the degree necessary

When, as in these experiments, nitrogen and oxygen are allowed to react in a triode, the gas mixture is exposed either to an oxide-coated platinum wire or to a bare platinum wire at a temperature which may be as high as 1800° K — a condition in which the thermal formation of nitric oxide has been shown to take place † A preliminary investigation was necessary in order to discover whether oxidation at the surface of the hot filament could be detected at pressures low enough for the electronic oxidation of nitrogen to be studied

Experimental

1 Surface oxidation The apparatus used and the precautions taken were the same as described in a previous paper ‡ Purified oxygen and nitrogen were admitted to a reaction bulb cooled in liquid air, connected through a liquid air trap to a McLeod gauge, and pressure readings were taken as the filament was heated After running, the apparatus was roughly evacuated and an extra pressure on removing the liquid air, due to the evaporation of the oxides of nitrogen, was looked for In 16 runs lasting for some hours, at temperatures up to 1900° K, at pressures ranging from 40 to 300 bars, and at concentrations of nitrogen ranging from 10 per cent to 90 per cent, no nitrogen peroxide was detected with either platinum or oxide-coated platinum filaments Certainly at the higher pressure any nitric oxide that had been formed would have been oxidised to nitrogen peroxide The rate at which the oxygen was removed by reaction with the platinum filament was affected but slightly until the partial pressure of oxygen was reduced to 10 or 20 bars

A new series of experiments was then made, using a flow method Air was admitted through a fine capillary, passed through two liquid air traps to remove water vapour and carbon dioxide, and over a platinum filament wound in the form of a rectangular grid on a light silica frame held obliquely by stouter platinum leads across the axis of a tube 2 5 cm diameter After combustion the gases were passed through a 500-c c flask cooled in ice to allow time for the slow termolecular reaction

---

* *Cf* Karrer, 'Trans Am. Electrochem Soc,' vol 48, p 25 (1925)

† Clements, 'Ann Phys,' vol 14, p 334 (1904), Rossi, 'Gaz Chim Ital,' vol. 35, p 1 (1905), Fischer and Braumer, 'Ber D Chem Ges,' vol 39, p 940 (1906), Briner, Boner and Rothen, 'Helv Chim. Acta,' vol 9, p 634 (1926)

‡ Rideal and Wansbrough Jones, 'Roy Soc Proc,' A, vol 123, p 202 (1929)

$$2NO + O_2 \rightarrow 2NO_2$$

to take place, and the nitrogen peroxide was then condensed by liquid air By varying the speeds of pumping and the length of the capillary, the pressure was varied between 24 to 80 bars while the speed of flow reached 500 c c per hour

The platinum filament was heated to about 1800° K and air streamed over for from 3 to 6 hours The taps were then closed, and after pumping out the air, the liquid air was removed from the final trap and the nitrogen peroxide contained expanded into a known volume in connection with a McLeod gauge The flow speed was found by measuring the rate of leaking Careful blank runs were made with the conditions the same but for the temperature of the heating element, which was reduced to 1000° K Then no condensable gas was found in the last trap Chemical tests were made to detect and identify the nitrogen peroxide, a mixture of α-naphthylamine and sulphanilic acid giving a red colour Both bare platinum wires and oxide coated wires were used, and the relative difference is shown in Table I

Table I

Run	Pressure (bars)	Flow speed (c c /hour)	Time (hours)	Length of filament (cm)	Amount of NO_2 (c c) per hour per cm of filament × 10^4
Bare wire—					
1	24	161	3	24 0	9 7
2	47	220	4	24 0	12 5
3	49	270	5	17 3	12 0
4	60	401	5	17 3	12 7
5	80	500	5	29 0	13 8
Oxide coated—					
6	47	100	5	16 1	26 5
7	47	260	6	22 0	25 8
8	70	403	5	28 0	27 2

All measurements were made at a temperature of 1800° K The heated area of the platinum wire cannot be estimated with any accuracy, nor can the increase in area on coating it with oxide be determined The uncertainty of the areas is a factor which must be taken into account before these results can be said to confirm the observation that the efficiency of a catalyst is related closely to its thermionic work function * It is noticeable that the effect of pressure is far greater than the speed of flow, but the yields were small, and an investigation of the kinetics of the reaction was not practicable

From these experiments it is clear that the purely thermal synthesis of oxides of nitrogen in the triode would be too slow to affect the results

Oxidation after Electron Collision —A platinum filament 2 cm long, 0 15 mm diameter, was mounted axially inside a helical platinum wire grid having 10 turns, the mean distance being about 2 mm from the filament Outside was a platinum anode 2 5 cm diameter, and 3 cm long Connections were at first made by a nickel-iron alloy which could be sealed into glass, but these were afterwards replaced by nickel wires coated with platinum to which the thinner platinum wires were welded The three electrodes were at first held in a ground joint fitting into the reaction vessel, but in later experiments with oxygen alone small errors were found due to oxidation of the tap grease or wax at the ground joint which was then removed, and the wires were sealed through the glass The filament was coated with a mixture of barium and strontium carbonates for which thanks are due to the General Electric Company, Wembley

The reaction vessel A (see fig 1), cooled in liquid air, was connected through a liquid air trap B, to the McLeod gauge M, and thence through the tap T_1, to the pump line, the pure gas lines, or a known reaction mixture stored in C, a

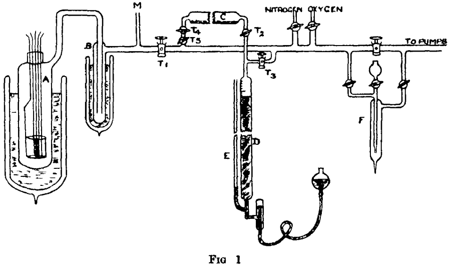

FIG 1

---

* Briner, 'Helv Chim Acta,' vol. 9, p. 634 (1926), *cf* Rideal and Wansbrough-Jones, 'Ann. Rep Chem. Soc,' vol. 25, p 345 (1928)

tube dusted with phosphoric anhydride, small amounts of gas mixture being admitted by the sampling taps T_4, T_5. The tube C could be filled with any mixture of oxygen and nitrogen by means of the burette D and the levelling tube E, the procedure being evident from the diagram. The reaction products could be pumped off through the trap F, which was cooled in liquid air, and identified. A vacuum of 10^{-5} mm was obtained by a double stage mercury diffusion pump backed by a "Hyvac," and the connecting tubing was heated with the flame of a Bunsen burner at this pressure before use, the pressure inside the apparatus being kept at 10^{-5} mm. Oxygen was prepared from manganese dioxide, hydrogen peroxide, and sulphuric acid in a small Kipp's apparatus and stored over potash and phosphorus pentoxide before use, and the nitrogen was taken from a cylinder, purified by passage over heated copper and copper oxide, and thence over potash and phosphorus pentoxide. In later experiments when experiments on pure oxygen were being conducted and oxidation of tap grease was found to occur, the tap T_1 was replaced by a mercury cut-off, and a second liquid air trap was inserted between the pump and this cut off. To obtain reproducible results it was essential to bake out the reaction vessel to 400° C between each run, and until no more gas was evolved, the glass connections being frequently heated.

Measurements

The applied potentials and the electron currents were measured in the same way as by Caress and Rideal, and the rate of reaction was determined by the rate of fall in the pressure. This rate of reaction is generally constant over a range of pressure from 180-130 bars for a particular voltage, when comparable results are obtainable, but below this range the effect of the fewer collisions between the ions, electrons or molecules becomes apparent. In comparable conditions the reaction rate at the same potential is found to be very nearly proportional to the number of electrons accelerated, and hence the number of electrons necessary for one molecule of nitrogen peroxide to be formed could be found. In order to identify the products of reaction, the total decrease in pressure was observed, when the reaction was apparently completed. With excess of nitrogen this value was readily determined, but a slow pressure decrease always took place when oxygen was in excess, the completion of the main reaction being shown by an alteration in the rate of decrease of pressure, generally sharply defined. The effect of oxygen in reducing greatly the emission of electrons, particularly from an oxide emitter, is, of course, well known,* and throughout the work was a source of trouble, though ultimately it was found possible to make a tenacious coating of oxide which would adhere long enough at the high temperature necessary to give an adequate emission , this effect was particularly noticeable in mixtures rich in nitrogen, the disappearance of the last trace of oxygen being accompanied by a marked change in the colour of the arc, from bluish-purple to reddish-purple, and a sudden increase in the electron emission amounting at times to a hundredfold , a very well-defined end-point for the reaction Further readings of the pressure were made after removing the liquid air and evaporating the nitrogen oxides The difficulty of correcting accurately for the difference in temperature due to the hot filament, and the slightly varying levels in the liquid air vessels might cause an error of not more than 5 per cent in these values, but in suitable conditions the measurements of the rate of reaction were more accurate

The reproducibility of the rate of reaction is a matter of great importance This rate is governed by a number of factors, the age of the filament, the thickness of the oxide coating, the form of the arc, the adequacy of the baking-out and the pre-treatment of the electrodes, some of which are not controllable Care was exercised on this account to make all runs comparable, and between every two or three runs, one at 26 volts was made Failure to return to the standard rate was generally cured by recoating the filament and baking-out for 8 to 12 hours , but some runs were found to give anomalous results and had to be rejected

The Rate of the Reaction

Fig 2 shows a number of runs plotted for various voltages and various gas mixtures It will be noticed that the composition of the gas mixture has little effect except for low nitrogen concentration In fig 3 the mean rates of reaction (excluding such mixtures) are plotted against the applied electron voltages , the units being the rate of decrease of pressure per milliampere, it having been first ascertained that these ratios were constant for a given voltage (see fig 5)

The features which may be observed on fig 3 are —

1 No reaction occurs unless the electron has an energy greater than 17 volts The very slight fall in pressure observed below this voltage was due to the oxygen alone

---

* Koller, ' Phys Rev ,' vol 25, p 671 (1925)

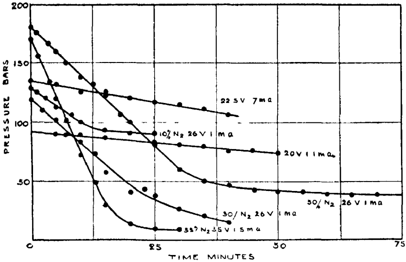

Fig 2

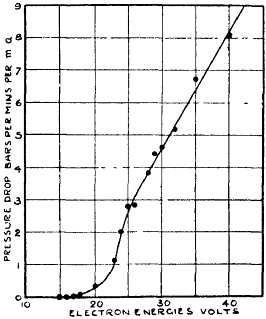

Fig 3

2 There exist two well-defined breaks, the one at 17 volts and the other at about 23 volts

3 There is a rapid and apparently regular rise above 30 volts, but with no breaks

4 The absence of any breaks attributable to oxygen, at any of the reported critical potentials, i e resonance at 8 9 volts[*], ionisation to O_2^+ at 12 5[§], 13 0,[†] 15 5,[‡] or at the O^+ potentials of 20,[†] 19 5[||] or 23 0,[‡]

1 The absence of a purely thermal reaction below the first arcing potential, even with emissions as large as 2 milliamperes, is in agreement with the previous runs I made with a closed system Many attempts, all unsuccessful, were made to find a reaction starting at the critical potentials of oxygen below 17 volts

2 At 17 volts the main reaction starts and at 23 volts it becomes much more rapid The absolute measurement of these voltages and their identification is important By the arrangement of the electrical circuit the potential is applied to the middle of the filament, but some correction due to the drop in voltage along the filament must be made and all voltages shown are corrected To make this correction the breaks in the current voltage curves in pure oxygen and nitrogen were identified with the known critical potentials and later a calibration was made with pure helium which gave identical results The correction was less than 1 volt

It is generally believed that the first ionising potential of nitrogen is 16 9 volts[¶] though Turner and Samson[**] have recently found 15 8 volts as its value The rate of reaction at this voltage is too small to discriminate between these values, but it is clear that the interaction is here initiated by the formation of positive molecular ions of nitrogen

The second ionising potential of nitrogen was believed to be 24 1 volts,[††] but this was based on the assumption that 16 9 volts is the first ionising potential Turner and Samson consider that 23 volts is the real value of the second ionising potential, the process being the formation of an excited positive ion which, on collision, dissociates into atoms and atomic ions The production of this excited molecular ion, therefore, greatly increases the rate of reaction

[*] Compton and Mohler, "Critical Potentials," 'Bull Nat Res Council,' vol 9, part I (1924)

[†] Hogness and Lunn, 'Phys Rev,' vol. 27, p 732 (1926)

[‡] Smyth, 'Roy Soc Proc,' vol 105, p 116 (1924)

[§] Mackay, 'Phil Mag,' vol 46, p 828 (1923)

[||] Lockrow, 'Astrophys J,' vol 63, p 205 (1926)

[¶] Compton and Mohler, *loc cit*

[**] Turner and Samson, 'Phys Rev,' vol 34, p 743 (1929)

[††] Hogness and Lunn, 'Phys Rev,' vol. 26, p 786 (1926), Smyth, 'Roy Soc Proc,' A, vol 105, p 116 (1924)

The rate of reaction between nitrogen and hydrogen is greatly increased at the same voltage *

3 The rapid increase in the rate of oxidation of nitrogen when the electrons are accelerated by more than 26 volts is shown below to agree well with the increase in the efficiency of ionisation

4 It has frequently been stated that activation of the nitrogen in the arc process is the most important process (*cf* Escales, Koenig and Lowry)† but it was suggested that parallel activation of oxygen was necessary Fischer and Hene‡ believed that only oxygen was activated in the arc, while Schwab and Loeb considered that nitrogen became reactive after a collision with excited oxygen It is clear that in these experiments no such activation of the oxygen was necessary

The simplest and most probable mechanism for the reactions are therefore

(1) At 17 volts $N_2^+ + O_2 \rightarrow 2NO$

and

(2) At 23 volts $N^+ + O_2 \rightarrow NO_2$ or $N_2^{+\prime} + O_2 \rightarrow NO_2 + N$

with other less important reaction possible

The vapour pressure of nitric oxide is not low enough for it to be frozen out by liquid air, and there would therefore be no change in pressure as it was formed, but its reaction with oxygen or nitrogen peroxide would give a condensible product, and it would also be strongly adsorbed on the walls of the glass vessel, which, after repeated baking at a high temperature under a vacuum, has a highly adsorptive surface

The End Point of the Reaction

1 Many runs were made on gas mixtures containing oxygen and nitrogen in widely varying proportions, the runs being continued to the end of the main reaction Some of these runs are shown plotted in fig 4 and are tabulated below The figures show the slow absorption of oxygen referred to above, when all the nitrogen had been used up

---

* Storch and Olson, 'J Am Chem Soc ' vol 45, p 1605 (1923), Caress and Rideal *loc cit*

† Escales, 'Z Elektrochem,' vol 12, p 539 (1906) Koenig, 'Ber D Chem Ges,' vol 46, p 132 (1913), Lowry 'J Chem Soc,' vol 101 p 1152 (1912), and 'Trans Faraday Soc,' vol 9, p 189 (1913)

‡ 'Ber D Chem Ges,' vol 45, p 3562 (1912), and vol 46, p 603 (1913)

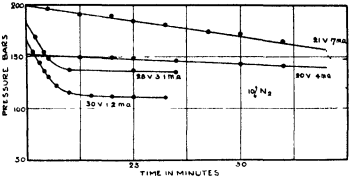

FIG 4

Table II 10 per cent N_2

1 Run	2 Voltage (volts)	3 Current (ma)	4 Initial pressure (bar)	5 Pressure fall (bar)	6 Fall calculated as NO_2 (bar)	7 Fall calculated as NO (bar)
F 1	30	0 61	180	59	54	36
F 2	30	1 2	165	54	49 5	33
F 5	21	0 7	200	52	60	40
E 6	20	0 4	151	33	45 3	30 2
E 7	28	3 1	193	58	57 9	38 6

Column 4 shows the total pressure of gas mixture originally present, and column 5 the total fall in pressure when the reaction is complete Column 6 gives the pressure decrease calculated from the initial amount of nitrogen on the assumption that it is all oxidised to nitrogen peroxide, and column 7 the decrease on the assumption that nitric oxide is the only product These pressures were measured with the filament cold, and liquid air round the traps and reaction vessel It will be noted that for the higher voltages even a slightly greater fall in pressure than that given in column 6 is found, and for the lower this value is not reached, but one corresponding to a mixture of nitric oxide and nitrogen peroxide There is always a slow electrical or electrochemical absorption of gas proceeding* which will account for small discrepancies (and the greater decreases than theory demands for the higher voltages) It is clear that mechanism (1) and the possible secondary reactions are operating to a greater extent at the lower voltages

---

* Research Staff, G E C, Wembley, 'Phil Mag,' vol 48, p 553 (1924), Dushman, "High Vacuum," p 165 (Schenectady, 1922)

2 Runs with nitrogen in excess allowed more accuracy, the end of the reaction being determinable with greater ease Measurements of the residual pressure of nitrogen oxides on re-evaporation were also made

Table III —10 per cent O_2

1 Run	2 Voltage (volts)	3 Current (ma)	4 Initial pressure (bars)	5 Pressure drop (bars)	6 Fall calculated as NO_2 (bars)	7 Calculated drop as NO (bars)	8 Pressure found on re evaporation (bars)	9 Pressure calculated as NO_2 (bars)	10 Pressure calculated as NO (bars)
C 3	30	1 6	180	28 2	27	36 0	19 3	18	36 0
C 4	30	1 6	171	25 4	25 6	34 2	15 9	17 1	34 2
C 5	19	0 4	210	37 0	31 5	42 0	33 6	21 0	42 0
C 7	20	0 9	222	29 2	33 3	44 4	34 0	22 2	44 4
D 2	30	4 1	141	20 9	21 1	28 2	15 5	14 1	28 2
D 6	26	2 6	172	27 0	25 8	34 4	20 1	17 2	34 4
D 7	21	1 1	190	33 2	28 5	38 0	28 3	19 0	38 0
D 8	22	0 4	201	37 1	30 1	40 2	35 1	20 1	40 2
D 14	21 5	1 1	180	31 4	27 0	36 0	27 8	18 0	36 0
D 15	21 5	1 0	160	30 1	24 0	32 0	27 1	16 0	32 0
D 16	21 5	0 6	160	28 7	24 0	32 0	26 2	16 0	32 0

Columns 4, 5, 6 and 7 are obtained in the same way as those in Table II Column 8 is the total pressure of nitrogen oxides found on removing the liquid air, column 9 gives the pressure calculated by assuming that all the oxygen has been used to give nitrogen peroxide, and column 10 the pressure of nitric oxide calculated by the same assumption , the same deductions can be made from this table as the previous one The striking difference between the two series of experiments is that in the first the fall in pressure found is larger, and in the second smaller than that given in column 6, in both cases as the mechanism demands Further, the runs at the higher voltages where the concentration of N^+ ions is greater show a much closer agreement with the simple formation of nitrogen peroxide The primary formation of nitric oxide could not give this result, since at these total pressures the number of termolecular collisions $2NO + O_2$ occurring before the nitric oxide ' struck," either adsorbed, or dissolved in the nitrogen peroxide on the walls, would be very few The experiments at lower voltages show nitrogen peroxide and lower oxides present in varying proportions , but an examination of the amounts of each is unprofitable

3 Experiments made with other proportions of oxygen gave results similar to those detailed above, and are not tabulated, since the extreme mixtures

show the point more clearly Frequently a mixture containing 33 per cent of nitrogen would react under 30-volt electrons until only 2 per cent of the total original pressure remained

Some of the discrepancies between the observed and calculated values for the total fall in pressure are too large to be accounted for by errors in reading The slow removal of oxygen as ozone is shown in a later paper to be negligible, while direct oxidation of the filament would also be very slow at a maximum temperature of 1600° K In the earlier runs, the presence of small traces of organic vapours would account for an apparent loss of oxygen, but the differences persisted when, as in the later experiments, this source of error was removed The admitted presence of oxygen ions and atoms suggests that reaction such as $N_2^+ + O \rightarrow N_2O$, will occur to some small extent, and these small errors must be ascribed to the sum of these causes, together with the well-known "clean-up" or absorption of gas in any type of discharge tube

The Examination of the Products

1 Three experiments were made, with an accelerating potential of 21 5 volts, in which the products of the reaction were mixed with excess oxygen A decrease in pressure would show that nitric oxide was reacting with oxygen

Table IV

1 Run	2 Pressure of oxides (bars)	3 Pressure of oxygen (bars)	4 Total (bars)	5 Found (bars)
D 14	27 8	40	67 8	60 1
D 15	27 1	13	40 1	32 1
D 16	27 2	20	46 2	34 1

Column 4 gives the sum of the pressures of oxygen and oxides of nitrogen, and column 5 the pressure half-an-hour after mixing

2 The products of the reaction were pumped off through the trap F, cooled in liquid air This trap was then isolated by the taps and reagent added through the top An alcoholic solution of α-naphthylamine and sulphanilic acid was the most convenient test and always gave a deep red colour, while brucine and sulphuric acid turned orange red Colorimetric estimations were made of the products from certain runs after addition of excess oxygen, by condensing them in small bulbs which were then sealed off at a constriction

and estimating the nitrogen peroxide by the colour tests described above Comparison tests made by heating a small quantity of pure lead nitrate greatly diluted with glass powder and condensing the products in the same way showed that the method was of sufficient accuracy

Table V

1 Run	2 Voltage (volts)	3 Residual pressure found (bars)	4 Calculated as NO_2 (bars)	5 Weight calculated for (3) $\times 10^5$ gm	6 Weight calculated for (4) $\times 10^5$ gm	7 Weight found by estimation $\times 10^5$ gm	8 Remarks
B 2	30	77	81	12 8	13 5	11 0	50 per cent N_2.
B 3	26	80	75	13 3	12 5	13 0	
B 4	20	120	128	20 0	21 3	19	33 per cent N_2
B 5	21	121	103	20 2	17 2	19	
B 6	26	124	121	20 7	20 2	20	
D 6	26	20 1	17 2	3 4	2 9	3 5	90 per cent N_2
D 7	21	28 3	19 0	4 7	3 2	4 6	
D 8	22	35 1	20 1	5 9	3 3	5 7	

Column 3 gives the actual amount of gas found on re-evaporating the nitrogen oxides, and column 4 the amount calculated from the initial total pressures assuming all the nitrogen had been oxidised directly to nitrogen peroxide Columns 5 and 6 respectively show the same amounts expressed as weight of nitrogen peroxide, while column 7 gives the actual weight found by the estimation

In the first five experiments the weight of nitrogen peroxide found by estimation is very nearly the same as the weight given in column 5, that is to say, the products of the reaction are almost entirely nitrogen peroxide Runs D4 and 5 show the largest errors, these runs being made with smaller applied potentials, and it was therefore to be expected that the products would contain more nitric oxide Runs D7 and D8 at 21 and 22 volts show clearly an initial oxidation to nitric oxide must have taken place, since considerably more nitrogen peroxide is found by the colorimetric estimation than the initial amount of oxygen would give The oxidation was therefore completed on adding more oxygen The small quantities of gas available reduces the accuracy of these estimations

The Electron Efficiencies

No method is available for use with this type of apparatus whereby the actual number of ions produced and reacting can be found directly

Instead, the number of molecules reacting for each electron emitted and accelerated can be found Fig 5 shows the plot of the rates of reaction against the current in milliamperes for the reaction at 26 volts Fig 6 shows the electron energies plotted against the electron efficiencies, i e, the number of electrons required to give one molecule of nitrogen peroxide, points being taken from experiments made in three different forms of the apparatus two with a ground joint, and one with no ground joint The currents were measured by a galvanometer with a calibrated shunt and the volumes of the three systems were respectively 790 c c, 823 c c and 630 c c

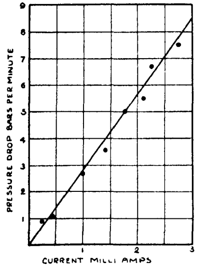

FIG 5

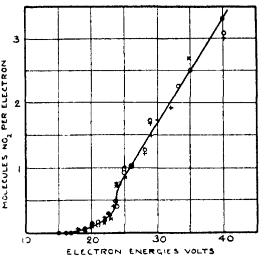

FIG 6

For convenience the mean number of electrons producing one molecule of nitrogen peroxide are shown below, for mixtures with more than 30 per cent nitrogen

It is necessary to estimate first how many electrons actually acquire their full energy, how many then escape collection by the grid and are available to make ions, and how many actually do so At a mean pressure of 150 bars the mean free path of the electron as given by the kinetic theory, $4\sqrt{2}$ the mean free path of the gas molecules, is 3 8 mm in nitrogen and 4 2 mm in oxygen at 25° C The temperature of the space between the filament and grid

Table VI

Voltage	No of electrons	Voltage	No of electrons
17	>3000	25	11
18	500	30	6
20	120	40	3

which we are considering is considerably higher than this, and an estimate made from the increase in pressure on heating up the filament puts it at about 500° C Assuming the validity of the Sutherland viscosity formula* and its applicability to this problem† the considerably longer free path of some 1 3 mm in either gas, or in this case, their mixtures is obtained Taking 2 mm as the mean distance between the filament and the grid—an upper limit—the free path of the electron is some 6 5 times the distance it must travel in order to reach its full velocity some 87 per cent will do this ‡

Experiments have shown, however, that this theory does not give the actual mean free path of an electron in a gas, both the Ramsauer and Lenard methods§ giving rather smaller values Thus Bruche gives as the total absorbing area for electrons of 1 c c oxygen at 1 mm pressure, 37 sq cm at 10 volts and 32 sq cm at 50 volts Assuming at 26 volts an absorbing area of 35 sq cm, the mean free path at 1 mm pressure is 0 29 mm, at 150 bars about 75 per cent of the electron would be fully accelerated before a collision with a gas molecule occurred The indirect method of Townsend and Bailey‖ gives figures leading to the result that about 80 per cent of the electrons reach their full velocity For mixtures of oxygen and nitrogen, whose absorbing areas differ by little, no anomalous results are to be expected

These results are obtained on the assumption that the equipotential surface containing the grid is a cylinder, whereas this is not strictly the case Attempts to correct for this by altering the number of turns per unit length in the grid indicated that the correction was both small and uncertain The number of electrons passing the grid is given by the difference between the total current from the filament, and that between the filament and anode It was found that about 85 per cent of the electrons actually passed into the space between the grid and anode

---

* Sutherland, ' Phil Mag ' vol 36, p 507 (1893)

† Sutherland ' Phil Mag ,' vol 18, p 341 (1909), *cf* also Erikson, ' Phys Rev ,' vol 6, p 345 (1915), and Compton, ' Phys Rev ' vol 21, p 717 (1923)

‡ Loeb, ' Kinetic Theory of Gases," p 41 (McGraw Hill Book Company, 1927)

§ Bruche, ' Ann Physik,' vol 83 p 1065 (1927), vol 81 p 537 (1926), Robinson, *ibid* , vol 31, p 805 (1910), Lenard, *ibid* , vol 12 pp 449 and 714 (1903), Mayer, *ibid* , vol 64, p 451 (1921), Ramsauer, *ibid* vol 64, p 513 (1921), Brode, ' Phys Rev ,' vol 25, p 636 (1925), Åkesson, Lunds, ' Univ Arsskr ,' vol 12 p 11 (1916)

‖ Townsend and Bailey, ' Phil Mag ,' vol 42, p 871 (1921), Townsend, ' J Franklin Inst ,' vol 200, p 563 (1925)

There will also be a few slow secondary electrons from the grid[*] but the spacing of the grid is comparatively wide and at potentials below 50 volts it is very improbable that these exceed 2 or 3 per cent of the whole Therefore some 70 per cent will be the fraction of the number of electrons emitted which can be taken as having their full energy in the grid anode space where reaction occurs For voltages greater than 25 volts the full energy is not required to ionise the gas, and hence more than this number are available, which should be taken as a lower limit

The best values for the number of ionising collisions made by an electron are obtained from the corrected curves of Compton and Van Voorhis[†] which give the number of ionising collisions per centimetre length of path at a pressure of 0 01 mm The distance between the grid and the anode was about 1 cm and assuming the temperature in this space was about 0° C , and the average pressure about 150 bars, the mean number of ionising collisions made by one electron in pure nitrogen ranged then from 0 21 at 25 volts to 0 84 at 50 volts From the value of the efficiency of ionisation appropriate to each voltage, it is now possible to find the number of electrons which must be emitted from the filament to give one ion , and hence to estimate the number of ions required to give one molecule of nitrogen peroxide

Table VII

1 Voltage	2 Total number of electrons required to give one molecule NO_2 by experiment	3 Number of electrons required to give 1 ion Estimated as above	4 Number of ions per molecule NO_2 obtained
18	500	50	10
20	120	17	7
25	11	6 7	1 6
30	6	4 2	1 4
40	3	2 2	1 3

---

[*] *Cf* Lehmann and Osgood, ' Proc Cam Phil Soc ,' vol 22, p 731 (1925)

[†] ' Phys Rev ,' vol 27, p 724 (1926)

In this table, column 3 gives the approximate number of electrons required to form one ion at this voltage assuming the mixture behaves as if it was all nitrogen There are no figures available giving the efficiencies in oxygen, though Penning reasons from its lower ionisation potential that these efficiencies should be higher than in nitrogen *

It will be noticed that the number of ions formed by each electron varies greatly with the voltage, but column 4 shows that this alteration is not sufficient to account for the changes in gradient in the curves showing the rate of reaction plotted against the applied voltage Since below 24 volts one ion really forms two molecules of NO_2, it will be seen that the change in rate above 24 volts is still greater It is interesting that above the second ionisation potential of nitrogen, although the electron efficiency is increasing, the number of ions per molecule is only changing slightly

Discussion

A lower limit of about 1 5 ions has been obtained as the number required to give one molecule of nitrogen peroxide This is the total number of ions, but if only nitrogen ions can react, their number will be proportionately less than this as the proportion of nitrogen in the mixture is decreased It seems then that with percentages of oxygen above 50 per cent , the M/N ratio becomes less than unity The possibility of one ion giving more than one molecule, by forming a " cluster " which then reacts as a whole, seems rather remote, and it is more likely that an error lies in the estimate of the number of ions The mean temperature of the space between the anode and grid may well be less than 0° C , since the valve is surrounded by liquid air, thus allowing more collisions between electron and molecules than has been assumed

More electrons are required to produce a molecule of nitrogen peroxide when the mixture is weak in either component This increase, noticeable in mixtures containing less than 33 per cent of nitrogen, is accounted for if only ions of this gas can react, while in mixtures rich in oxygen some of the nitrogen ions must escape collision with oxygen molecules

Schwab and Loeb (*loc cit*) found that 120 ions were required to give one molecule of nitrogen peroxide Their method of using a diode at a pressure of 6 mm of gas is not suited to give accurate values of this ratio, which is probably widely in error The work described above entirely supports their suggestion that activation of the nitrogen is the main factor, but does not support the possibility of activation of the nitrogen by collision with activated oxygen

---

* Penning, ' Physica,' vol 6, p 290 (1926)

Firstly, the only physical significance which can be attached to this process would be the formation of a molecular ion of nitrogen by collision with an oxygen molecule excited by a 19.5-volt electron, which is believed to suffer almost immediate ionisation and dissociation. The pressure is too low for more than a very few collisions between a nitrogen molecule and an excited oxygen molecule to occur before dissociation has taken place. Secondly, there is no increase in reaction rate at the critical potentials of oxygen. Thirdly, the efficiency of the process is reconcilable with the view that the nitrogen alone is activated.

Busse and Daniels,* synthesised oxides of nitrogen by passing high-speed electrons from a Coolidge tube through a metal window into a tube containing air. There is great uncertainty in finding the number of ions formed per electron, and probably it is most accurate to accept Lehmann's value of 43 volts per ion for 2000-volt electrons, giving an M/N ratio of about 0.5 in air, from their values for the total energy supplied by the electrons to the air in the reaction vessel.

Lind and Bardwell† from their work with α particles found the ratio $\frac{\text{molecules acid}}{\text{total ions}}$ to be unity. Among the products are NO_2, NO, O_3 and traces of N_2O, complicating the reaction. At the pressures used in the experiments described above no ozone is formed, and the N_2O, if present, is not noticeable.‡ It is not considered that these values are contradictory when consideration is taken of the different experimental methods. They are summarised in Table VIII.

Table VIII

Method	M/N	Observer
α particles	1	Lind and Bardwell
High velocity electrons	0.5	Busse and Daniels
Low voltage arc	120	Schwab and Loeb
Low voltage arc	1.5	Wansbrough-Jones

---

* 'J. Am. Chem. Soc.,' vol. 51, p. 3271 (1928).

† Lind, "The Chemical Effects of α particles and Electrons," Chemical Catalog Co., N.Y.' p. 101 (1928).

‡ *Note added in proof*.—Since this paper was communicated Brewer and Westhaver ('J. Phys. Chem.,' vol. 34, p. 554 (1930)) have examined this reaction in the glow discharge, obtaining substantially similar results. They attribute reaction to the N_2^+ ion, and conclude, by varying the proportions of the gases, that nitrogen alone is activated. An approximate maximum value of two molecules of nitrogen peroxide from one N_2^+ ion was obtained.

It may be mentioned that the yield of oxides of nitrogen in this apparatus is equivalent to about 20 gm of nitric acid per kilowatt hour, whereas an average commercial arc process has an efficiency of about 60 gm of nitric acid per kilowatt hour

Summary

(1) Oxides of nitrogen have been synthesised from their elements at pressures below 100 bars

(2) This reaction has been studied in these gases after excitation by electron collision, and is shown to depend on the ionisation of the nitrogen Excitation of the oxygen is unnecessary

(3) Evidence is brought forward that the two principal reactions are

$$N_2^+ + O_2 = 2NO$$

and

$$N^+ + O_2 = NO_2 \quad \text{or} \quad N_2^{+\prime} + O_2 \rightarrow NO_2 + N$$

and the independent production of either of these gases is established

(4) The efficiency of the process is discussed, and it is shown that at the higher voltages very nearly all the ions formed will react

Grateful acknowledgment is due to the Goldsmiths' Company and the Department of Scientific and Industrial Research for a grant, also to the Imperial Chemical Industries for assistance in purchasing some of the necessary apparatus My best thanks are due to Prof T M Lowry for his interest, and to Dr E K Rideal, for suggesting the problem for his constant advice, and for his sustaining encouragement

The Formation of Ozone from Oxygen after Collision with Electrons

By O H WANSBROUGH-JONES, Ramsay Memorial Research Fellow

(Communicated by T M Lowry, F R S —Received November 28, 1929)

Introduction

In a previous paper* the reactions between nitrogen and oxygen after collision with electrons have been described, and mention was made of some anomalies noticeable in the total absorption of gas It was natural to suppose that the formation of ozone played a part in these, and accordingly a more detailed study has been made of the behaviour of oxygen in the same apparatus

The results obtained agree best with a mechanism requiring neither atoms nor ions for the formation of ozone, but rather an excited ion of short life, a possibility which is not contradicted by previous experimental work

Experimental

In the previous paper it was noted that there was a slow removal of oxygen in the low-voltage arc The first experiments were made to find if this was connected with ozone formation

The first form of the apparatus was identical with that described in the previous paper After a most thorough evacuation, the apparatus was charged with oxygen to a pressure of about 200 bars, or in some experiments up to 1 mm The filament having been heated and the accelerating potential applied to the grid the rate of fall in pressure was examined No ozone was detected at any time, and the results of these experiments are summarised below

1 A very slow purely thermal reaction with the filament was found to depend on the temperature of the filament and the state of the coating of oxide, to be independent of the applied potential, and agreeing with earlier work† on the oxidation of platinum, normally to be negligible

2 When potentials slightly greater than the arcing potentials were applied the absorption of oxygen became more rapid, but was still very small indeed, so small that it is not possible to state that the absorption is then due to the

---

* *V supra*, p 511

† Rideal and Wansbrough Jones, 'Roy Soc Proc,' A, vol 123, p 202 (1929)

formation of ions Some evidence was, in fact, obtained suggesting that there was an " electrical " reaction below 12 volts additional to the thermal reaction mentioned above, but generally at 20 volts more ions were formed and an increased rate was noticeable

3 During the run liquid air surrounded the vessel At the end of each experiment it was removed and search made for any increase in the pressure of oxygen additional to that due to expansion Oxygen atoms stuck to the walls or ozone would both form oxygen molecules on striking the platinum anode, but no increase in pressure attributable to either of these two causes was ever found In a few runs an increase in pressure on removing the liquid air was found, but always it was due to imperfect baking having left some carbon or hydrogen

4 Applied potentials between 30 and 60 volts gave a higher rate of absorption, but even in 3 or 4 hours and with currents up to 4 ma the reduction of pressure would rarely exceed 30 bars Measurements of the electron efficiencies were unreproducible, ranging from about 100 to 5000 electrons per molecule removed a very different order from that found in mixtures of nitrogen and oxygen

5 The rate of absorption became slower after a series of runs between which air had not been admitted to the valve

6 In some runs the absorption stopped completely after a time, always those at a relatively low temperature where the thermal reaction with the hot filament was negligible

The tacit assumption that if ozone was produced it would be removed must not be allowed to pass without question The vapour pressure of ozone at —190° C is about 0 035 mm * so that in small concentrations it would not be frozen out, but it would be absorbed on the glass walls of the tube Attempts to increase the absorption by introducing small quantities of silica gel gave no alteration in the results If a very small concentration of ozone had been present in the gas, signs of ' tailing " on the mercury in the McLeod gauge might have been seen, but these were never observed Probably, however, such tailings would only be produced if a little water vapour was present The detection of ozone in these experiments then really tests on the power of the glass to absorb small quantities of it at low pressures and to give it up again when warmed

Ozone if formed might decompose on the platinum anode Removing this

---

* Spangenberg, 'Z Phys Chem,' vol 118, p 419 (1926), Schwab, 'Z Phys Chem ' vol 110, p 599 (1924)

altogether was not practicable, but it was replaced by an open platinum wire helix of the same diameter The arc could then be brought in apparent contact with the glass walls, and if ozone molecules had been present and the pressure low enough they would have been able to diffuse on to the cold surface At higher pressures the green glow of the arc closely surrounded the filament, and ozone might have been formed and decomposed without being detected, as seems likely from subsequent experiments

The removal of oxygen in these experiments depends primarily on the state of the glass walls, and is not due to the formation of ozone Taylor* has shown that oxygen, excited by an electrodeless discharge can react with hydrogen in the glass, while Dalton† has shown that oxygen, activated by impact with electrons having energies of over 8 volts, will react with solid carbon It is evident that oxygen so activated "combines" with the glass walls, and that ions need not be formed before this reaction can take place ‡

The absence of ozone in these experiments suggested that possibly a second gas was needed to carry away the surplus energy after a collision Warburg and Rump§ obtained a greater yield of ozone on ozonising air than the partial pressure of the oxygen warranted, and Juilard‖ showed that the addition of 40 per cent nitrogen more than doubled the yield of ozone Helium was therefore added to the oxygen up to a total pressure of 1 mm in some experiments, the percentage of helium being from 30 to 90 per cent The arc was obviously a mixture of both oxygen and helium, and this gas also increased the total ionisation current ¶ No traces of ozone were detectable, however, and helium serves merely as a diluent, modifying the rate of clean-up but slightly, and the character of it not at all

Experiment with a Flow Method

It was clearly desirable to find some more convincing proof of the absence of very small amounts of ozone, as, for example, by accumulating a quantity of the supposed ozone oxygen mixture The conditions in which it was desired to conduct the experiment rendered this a difficult matter, as low pressures of oxygen were essential, and it was important that water vapour should be rigorously excluded. An optical method is not suitable since dry ozone is very unstable, and after trials with such substances as solid potassium iodide, starch-iodide paper, or silica gel, or attempts to find mercury "tailings," or an oxide film on silver (all of which failed owing to the dryness of the system), concentrated sulphuric acid was used as an absorbent.*

---

* 'Roy Soc Proc,' A, vol 123, p 252 (1929)

† 'J Am Chem Soc,' vol 51, p 2366 (1929)

‡ *Cf* also Meirdal, 'Am Phys,' vol 85, p 612 (1928), G E C, Wembley, 'Phil Mag,' vol 8, p 553 (1924), etc

§ 'Z Phys,' vol. 32, p 245 (1925)

‖ 'Bull Sci Acad Roy Belg,' vol 12, p 914 (1926), Pinkus and Juilard, *ibid*, vol 24, p 379 (1927)

¶ *Cf* Duffendack and Smith, 'Phys Proc,' vol. 34, p 71 (1929)

The apparatus used is shown in fig. 1. Oxygen, at atmospheric pressure, prepared by the electrolysis of baryta solution, passes into the tube A and leaks through the pipeclay stem in A into the vacuum side of the apparatus. Raising or lowering the mercury reservoir B covers part of the stem and so controls the rate at which the oxygen flows through; the pressure can be varied easily

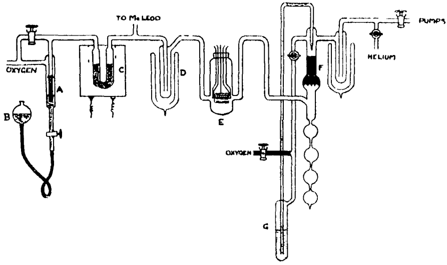

FIG. 1

from 0.1 mm. to 4 mm. and other ranges can be used. Traces of vapour from the wax cementing the pipe stem to the glass, or other impurities, are removed by passing the gas over copper oxide heated to 400° C. in the furnace C, from which the oxygen goes through a liquid air trap D to the valve E. The triode here is built up entirely of platinum, the filament about 1 cm. long being coated with barium and calcium oxides, and the middle of it, from which nearly all the electrons are emitted, is about 1 mm. from the grid. Thence the gas passes through the absorption apparatus F to the vacuum line. The tube F contains a column of glass beads supported on a glass spiral held in a wide part of the tube Pure sulphuric acid is forced up slowly from the reservoir G and drops on to the beads and keeping them moistened is collected in the series of bulbs, which are then sealed off one by one with the sulphuric acid containing the ozone found in one run Thus several consecutive runs could be made without allowing air to enter, or removing the liquid air traps, making them much more reproducible The column of beads had to allow free passage for the oxygen and in fact the pressure on the valve side of the column could be easily kept down to 0 05 mm At the end of a run the current was switched off and the oxygen allowed to flow through for half an-hour The beads were then washed with several small charges of sulphuric acid, allowed to drain for an hour, and the bulb removed About 10 c c of acid were generally removed in each bulb The electrical connections have been described previously

---

* Grafenburg, 'Z. Anorg. Chem.,' vol. 36, p. 350 (1903); Brand, 'Ann. Phys.,' vol. 9, p. 468 (1920).

It was soon found that with pressures above 1 mm traces of ozone were obtained in the sulphuric acid The method of procedure was thus to clean and bake out the apparatus completely and adjust the rate of flow and the pressure The furnace C was heated up, and after gas had been flowing for a time the heating current for the filament and the accelerating voltage were switched on, and the oxygen run through for 6 to 10 hours, so long a time being necessary for enough ozone to accumulate

On completing the run the sulphuric acid was neutralised, potassium iodide added, and the titration made with approximately N/1000 sodium thiosulphate Blank runs made by flowing oxygen through in precisely the same condition but with no applied potential never gave a trace of blue colour when starch and potassium iodide were added The valve was kept cooled in ice, pressure readings were taken periodically but varied very slightly indeed, and the rate of flow of the oxygen was found from the amount of oxygen which had been taken from the aspirator in which it was stored

No accurate information was obtainable as to the efficiency of the absorption apparatus and the total quantities of ozone found have little meaning, but that the relative concentrations in different runs were comparable was shown by the reproducibility of the results

Three variables can control the amount of ozone found, the rate of flow, the pressure, and the applied potential

1 The rate of flow varied from 500 to 100 c c of oxygen at atmospheric pressure per hour There was a slight increase of about 20 per cent in the ozone found when the flow speed was increased five times This is good evidence that there is little decomposition of ozone after formation, and that therefore the yields found are directly proportional to the amount of ozone

actually formed In the subsequent discussion values for yields at rates of flow above 300 c c per hour are used, beyond which rate alteration had no effect

2 No ozone was ever detected unless at least 25 volts were applied Increasing the voltage increased the yield slowly and regularly, and there are no definite voltages where any marked changes occur Relatively high pressures are used, and the actual meaning of this voltage requires more discussion Calibration of the apparatus was, as usual, made by determining the ionisation potential of helium

3 The pressure has the greatest effect on the yield as will be seen in fig 2 The number of molecules of ozone produced per hour at 30 volts are plotted against the pressure It is noticeable that the amount of ozone decreases with diminishing pressure, none being found below 0 8 mm The rate of increase decreases as the pressure increases

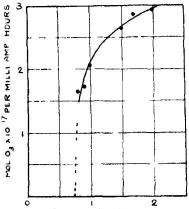

FIG 2

Discussion

Excitation of the oxygen is clearly necessary and the failure to obtain ozone at low pressures can only mean that a species of short life is being produced which, at the lower pressures, reverts to a state ineffective in making ozone before making a successful collision

The critical energy to which the electron must be accelerated was found in this apparatus to be about 25 volts, which is considerably above the ionisation and dissociation potential of oxygen of 20 volts The distance between grid and filament was about 1 5 mm and the pressure 1 mm The mean free path of the electron in oxygen at an assumed temperature of 500° C is 1 3 mm from the kinetic theory or about 1 mm from direct measurements at this pressure The mean free path of the electron is then distinctly shorter than the distance it must travel without loss of energy in order to acquire its full velocity, and only some 20 per cent will have the full velocity It was noticeable in these high pressure experiments that the low voltage arc was very near to the filament and did not extend to the grid

There must, therefore, be some uncertainty as to the true energy required for the formation of ozone, and the results from the efficiency of the process cannot dispel them 25 volts is undoubtedly a maximum, but the true minimum cannot be found with certainty except by greatly reducing the space between the grid and filament which is not practicable with a valve of this type, *i e*, where a hot wire is used as a source of electrons None the less the yields are undoubtedly low and in no way comparable to the number of ions produced, and hence it seems likely that further excitation of ion or atom is necessary The most probable interpretation is that atomic or molecular ions, or atoms which have a long life, are not able to form ozone, but that an ion must be in an excited state before it can form ozone The high energy required strongly suggests an excited ion rather than an excited atom or molecule

The yield increases slowly above 2 mm at which pressure the apparatus could not be conveniently used on account of the short mean free path of the electron and the likelihood of considerable decomposition From 0 8 mm to 1 8 mm there was a continuous increase in the yield, while below 0 8 mm no ozone was ever detected Turner* has calculated the average life of an excited mercury atom when dissociating hydrogen, a calculation based on the variation of yield with pressure, and a similar one has been made of the life of the oxygen active ion Turner shows that the probability that an ion will collide when excited is given by $P = \tau/(T + \tau)$ where τ is the mean life of the excited ion and T the mean time between collisions The uniformity of yield with flow speed shows that no back decomposition has taken place, and hence that the equilibrium concentration of ozone has not been reached The amount of oxone formed per unit current will then be proportional to this probability factor

Since T is given by $pT = 1/\sigma^2 A$, where σ is the mean distance between the centre of two colliding particles and q the quantity of ozone obtained by $q = C\,\tau/(T + \tau)$ thus

$$\frac{1}{q} = \frac{1}{CA\sigma^2\tau}\,\frac{1}{p} + \frac{1}{C},$$

and accordingly a straight line should be obtained on plotting $1/p$ against $1/q$, for which, moreover, the intercept divided by the gradient will give $A\sigma^2\tau$

These quantities are plotted in fig 3 and it will be seen that the points lie on a straight line for the middle values, from which values, therefore, an estimate of the mean life is obtained At the higher pressures, *i e*, above 1 5 mm, the yields do not increase as much as theory demands, but here some decomposition is undoubtedly taking place, and this easily accounts for the discrepancy It is more difficult to account for the absence of ozone below 0 8 mm According to Turner's equation at 0 5 mm an amount of ozone equivalent to 1 c c of thiosulphate solution should have been obtained, an amount detectable with certainty, whereas none was found It is possible that the absorbing apparatus was not efficient enough to trap such small quantities, and the yields might have been further reduced by the greater number of electrons escaping collision at lower pressures

---

* 'Phys. Rev,' vol 23, p 464 (1924)

In the middle of the range the agreement is fairly satisfactory, since such factors as variation in the form of the arc, the temperature of the gas and the alteration with pressure of the efficiency of ionisation and activation are not taken into consideration At first sight it might appear that the last effect would be large, but the pressure is so high in all these experiments that few electrons escape effective collision To allow for this effect is impossible since no knowledge is available as to the efficiency of the activation process The rough linearity of these points is therefore to be used not so much as proof of the existence of active species but more for the most satisfactory method of estimating their life

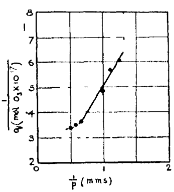

FIG 3

From fig 3 $1/C = 0\ 095$, and $1/A\sigma^2\tau C = 0\ 419$ and therefore $A\sigma^2\tau = 0\ 226$

A is equal to

$$2666\ 6 \times \sqrt{\frac{2\pi N}{K\theta}\ \frac{m + m_1}{mm_1}}\ *$$

where $N = 6\ 06 \times 10^{23}$, $k = 1\ 371 \times 10^{-16}$, 0 = absolute temperature, estimated at 773° A and m and m_1 are the molecular weights of the colliding molecules, p having been expressed in millimetres of mercury Assuming for the moment that this collision formula is applicable to ions, and that they are atomic ions, $m = 32$ and $m_1 = 16$, whence $A = 4\ 9 \times 10^{21}$ and hence $\sigma^2\tau = 4\ 6 \times 10^{-23}$

From the observed energy of excitation it seems most probable that an atomic ion is the active species, though Stueckleberg† gives some evidence for an excited oxygen molecular ion at 20 3 volts which quickly dissociates to an atom and atomic ion It should be noted that for a molecular ion, A is $4\ 0 \times 10^{21}$ and $\sigma^2\tau$ is then $5\ 65 \times 10^{-23}$ cm² sec

---

* Cario, 'Z Physik,' vol. 10, p 185 (1922)

† 'Phys Rev,' vol. 34, p 65 (1929)

Treating the two possibilities separately, for the molecular ion σ is at least $2\ 9 \times 10^{-8}$, the diameter of the oxygen molecule, and almost certainly more than this since all the available evidence shows that on excitation an ion has a larger size Moreover the collision formula used applies properly to uncharged particles, whereas charged particles would collide more frequently giving an apparent larger molecular diameter As a lower limit $\sigma^2 = 8\ 4 \times 10^{-16}$ giving an upper limit for τ of $6\ 7 \times 10^{-8}$ secs This is a rather short life for an excited state and is in agreement with Stueckleberg's suggestion that dissociation takes place very easily to atomic ions or atoms

For atomic ions direct, if contradictory, values have been found for the size of the ion,* the most probable diameter being between that of an oxygen atom and of an oxygen molecule The diameter of the atom is about $1\ 0 \times 10^{-8}$ cm and that of the ion is taken as $1\ 6 \times 10^{-8}$ cm and therefore $\sigma = 2\ 25 \times 10^{-8}$ cm if the atomic ion collides with an oxygen molecule and τ is about 10^{-7} secs a not unreasonable value Wien has shown that the life of one species of excited oxygen ion is about 2×10^{-7} secs No explanation other than the necessity for excited ion of short life as an intermediate product gives such a satisfactory explanation of the diminution in yield with pressure

The formation of ozone from oxygen at pressures between 3 mm and 0 1 mm in a direct discharge between metal electrodes has been examined by Hunt† who also reports a diminution in yield as the pressure decreases The yields are equilibrium yields which are not amenable to the same treatment, but as would be expected equilibrium was reached more slowly at the lower pressures

In no other experiments has the pressure been reduced sufficiently for this diminution in yield to be apparent

The suggestion that a highly energised ion is an active intermediary in chemical reaction in discharge tubes in general has been put forward by Elliott, Joshi and Hunt,‡ whose view was that before such a reaction could take place, ions having energy in excess of a critical value must have been formed Rusk§ suggested that the combination of hydrogen and oxygen in a low voltage arc was due to excitation of atoms or molecules, secondary to ionisation

---

* Ruttenhauer, 'Z Physik,' vol 4, p 267 (1921), Ruchardt, 'Ann Physik,' vol 71 p 377 (1923), Koenigsberger, 'Z Physik,' vol 43, p 883 (1927)

† 'J Am Chem Soc,' vol 51, p 30 (1929)

‡ 'Trans Faraday Soc,' vol 23, p 57 (1927)

§ 'Phys Rev,' vol 29 p 907 (1927)

It seems probable that the photochemical production of ozone is due to the presence of O_4 molecules in oxygen, but there could only be very few of these in the neighbourhood of the hot filament, and though Dopel* has found evidence for the existence of O_4 in the dark space of a discharge tube, it does not seem possible to correlate it with the formation of ozone in these experiments

The evidence from these experiments is therefore that, for dry ozone, the process of ozone formation is collision between an active ion and a neutral molecule Collision between ion and atom or generally between two active species would be rare and while showing efficiencies of the same order as in these experiments, they would not show the same dependence on the pressure

Summary

1 It is confirmed that the electrochemical absorption of oxygen is a chemical process with the glass walls, not necessarily connected with ions

2 Ozone is not formed by direct collision between normal ions and molecules or atoms and molecules when the gas is dry and at a low pressure

3 Ozone is formed by collisions between excited ions of life of the order of 10^{-7} secs and oxygen molecules

---

* Ann Physik,' vol 26, p 1 (1928)

On the Coefficient of Heat Transfer from the Internal Surface of Tube Walls

By ALBERT EAGLE, B Sc, and R M FERGUSON, M Sc, Manchester University

(Communicated by G G Stoney, F R S —Received September 9, 1929 —Revised January 21, 1930)

1 *Introductory*

The present work on the transfer of heat from a heated brass tube to water flowing through it was undertaken for the British Electrical and Allied Industries Research Association though the experimental methods pursued were left to the discretion of the experimenters Two important innovations compared with the methods of previous experimenters were First, the direct heating of the tube by a low tension alternating current, and secondly, the discarding of the use of thermocouples to obtain the temperature of the water, this being calculated for any cross section from the amount of heat put into the water up to that cross-section The temperature so calculated is what an engineer always understands as the temperature of the water The only other way of getting a definite water temperature is to take the temperature at points in the axis—a quite unimportant temperature in practice Naturally the value that is obtained for the coefficient of heat transfer depends considerably on what is taken as the water temperature

2 *Historical*

Many experiments on the transfer of heat across condenser tubes have been made with the outside of the tube steam heated, the amount of heat transfer being obtained from the rise of temperature of the water flowing through the tube None of this work has any scientific value, however, except in the few cases where the actual temperature of the tube was directly obtained by means of thermocouples Here are included the experiments of Webster,* Clement and Garland† and McAdams and Frost ‡ Also worthy of mention are some early experiments by Stanton* in which the temperature of the tube was obtained from its increase in length

---

* " Some experiments in the Condensation of Steam," ' Inst Engineers and Shipbuilders in Scotland,' vol 57 (1913)

† " A Study in Heat Transmission," ' Bulletin No 40 University of Illinois ' (1909)

‡ ' J Ind Eng Chem ,' vol 5, pp 13 18 and 1101 1105 (1922)

Webster's experiments suffer from the disadvantage, among other things, that the difference of temperature between the tube and the water was so great (the steam outside the tube being above atmospheric pressure and therefore above 100° C) that in view of the greatly varying properties of water over the range from 20° C to 100° C, his results have comparatively little application to the problems of modern condensers Clement and Garland's experiments suffer from the fact that they used an iron tube of about one-eighth of an inch (3 mm) thick Thermocouples gave the temperature of the outside of the tube whereas it was the temperature of the inside surface which was required , and it has been pointed out by McAdams and Frost that the uncertainty of the thermal conductivity of the iron render Clement and Garland s results uncertain by about 50 per cent Moreover the increasing film of iron oxide which must develop with use must make reliance on their results difficult

Probably the most accurate experiments published when the present work began were those of McAdams and Frost , but they had only obtained the coefficient of heat transfer for comparatively isolated cases, whereas, owing to its great variation, a systematic examination was required covering a wide range of water velocities, water temperatures, tube diameters and heat flow rates Only when this has been done can any useful theoretical deductions be made from the experimental results The experiments of Stanton also covered too limited a range , moreover Stanton's tubes were too short to give accurate coefficients of heat transfer since it is not till the water has traversed a sufficient length of the heated portion of the tube, to establish the limiting distribution of temperature over the cross section, that a definite coefficient can be obtained The present experimental values refer entirely to these limiting coefficients

3 *Range of Conditions covered by the present Experiments*

The present experiments on commercial brass tubes covered the desired wide range of conditions The water temperature was varied from about 40° F (5° C) to over 140° F (60° C) , the water velocity from 1 ft per second (30 cm per second) to 11 ft per second (330 cm per second) , the outside tube diameters from $\frac{1}{2}$ inch to $1\frac{1}{2}$ inches (inside diameters from 1 02 cm to 3 56 cm) , while the heat flow rates varied from 4000 British thermal units per square foot per hour to 20,000 British thermal units per square foot per hour (0 30 to 1 50 calories per square centimetre per second)

---

* 'Phil Trans.,' vol. 190, pp 67-88 (1897).

For each tube the water velocity was adjusted as nearly as possible to the desired round figure of so many feet per second, and tests were taken at various inlet water temperatures and rates of heat flow at this velocity

In the present experiments the experimental tube was cleaned at the commencement of every morning's or afternoon's experiments, by drawing a wash-leather plug through it Other experimenters do not seem to have sufficiently realised the necessity of this if accurate coefficients are to be obtained The dirt removed was chiefly hydrated oxide of iron from the connecting pipes and was especially pronounced at the higher water temperatures

4 *Symbols*

The following symbols are used, all the quantities being in C G S units —

$d = 2a$ = diameter of tube ,

θ = temperature of fluid (° C) ,

$\Delta\theta$ = the temperature difference between the inside tube surface and the calculated mean temperature of the fluid at that cross section ,

H = heat flow in calories per square centimetre per second of internal tube surface ,

k or $k_H \equiv H/\Delta\theta$ = coefficient of heat transfer

k_0 = value of k when $H = 0$,

ρ = density of fluid ,

s = specific heat of fluid (at constant pressure in the case of a gas) ,

c = thermal conductivity of fluid ,

μ = viscosity of fluid ,

v = mean velocity of flow ,

$v_m \equiv \rho v$ = " mass velocity " ,

f = " theoretical " thickness of viscous flow film at tube wall ,

ϕf = actual thickness of above film ,

$\sigma \equiv \mu s/c$ This measures the departure from the ideal gaseous state for thermal conductivity, and might appropriately be called the " coefficient of liquidity " ,

$\tau \equiv \rho v d/\mu$ This is known as Reynolds' number, and may appropriately be called the " coefficient of turbulence " ,

R = wall friction (in dynes per square centimetre) at tube surface causing the loss of hydrostatic head

$Z \equiv R/\rho v^2$ is a function of τ only which has been experimentally determined by Stanton and Pannell[*] Z is sometimes known as "Lees' function," he having given an empirical formula for it

5 *Dimensional Equations*

The consideration of the dimensions of the quantities involved, shows that if Q is the amount of heat gained or lost in unit time by a surface of any fixed shape, and of linear dimensions proportional to l, when a fluid of density ρ, specific heat s, viscosity μ, and thermal conductivity c, flows past it with a velocity v, and if the difference in temperature between the surface and any point in the fluid (in any given direction and at a distance proportional to l) is θ, then Q is given by

$$Q = \rho l^2 v^3 \quad F\{s\theta/v^2, \quad \mu s/c, \quad \rho v l/\mu\}, \tag{1}$$

where F is any function of its three arguments[†]

If we assume that the temperature difference, θ, is infinitesimal it is obvious that Q will be infinitesimal and that Q/θ will, in the limit, be independent of θ In this case Q can only involve θ through $s\theta/v^2$ as a factor Hence we have

$$\text{limit } Q/\theta l^2 = \rho v s \quad F\{\mu s/c, \quad \rho v l/\mu\} \tag{2}$$

As the left-hand side is proportional to the heat transfer coefficient, k_0, while, for a pipe of diameter d at points too far, both from the entrance and the point at which the heating begins to be affected by the initial irregularities due to these causes, no linear dimension is concerned save d, we get, on replacing l by d in (2) and inverting the formula for convenience,

$$\rho v s/k_0 \equiv v_m s/k_0 = F(\sigma, \tau), \tag{3}$$

where $\sigma = \mu s/c$, $\tau = \rho v d/\mu$ and $v_m = \rho v$ is the mass flow Experimentally, ρv is the quantity W/At, where W is the weight flowing past a cross section of area A in the time t For water, we have termed v_m the "nominal velocity"

Equation (3) does not accurately hold for finite rates of heat flow because some or all of the quantities μ, s, c and ρ change with the temperature, and hence to get k then by (3) would necessitate substituting the values of μ, s, c and ρ for some unknown temperature intermediate between that of the tube and the liquid

---

[*] 'Phil. Trans.,' A, vol. 214, p 199 (1914)

[†] See *e g* A H Gibson, "The Mechanical Properties of Fluids," p 180 This formula, of course, entirely neglects any transfer of heat through the fluid by direct radiation, and so is not applicable to most gases where this may be a considerable fraction of the whole transfer The external pressure to which the fluid is subjected is also assumed by this formula to have no effect on k This must practically be so for both gases and ordinary liquids, but need not be so for liquids and vapours near their critical point where the molecular complexity changes greatly with a change of pressure

By the principle of small variations and the theory of dimensions we get k_H, the coefficient for a small but not infinitesimal, rate of heat flow, H, given by

$$k_H - k_0 = \left\{\frac{\lambda_1}{\mu}\frac{d\mu}{d\theta} + \frac{\lambda_2}{s}\frac{ds}{d\theta} + \frac{\lambda_3}{c}\frac{dc}{d\theta} + \frac{\lambda_4}{\rho}\frac{d\rho}{d\theta}\right\} \mathrm{H}, \tag{4}$$

where the λ s are mere numerical constants or functions of the dimensionless quantities σ and τ In the case of many liquids $ds/d\theta$ and $d\rho/d\theta$ are negligible

6 *Osborne Reynolds' Theory of Heat Transfer and its Modifications*

Osborne Reynolds' well-known theory of heat transfer, founded on the similarity of the manner in which turbulent fluids convey both heat and momentum, gives, if we ignore the presence of a viscous flow film over the surface,

$$v_m s/k_0 = Z^{-1} \tag{5}$$

If a viscous film of small thickness is supposed to cover the tube wall and the whole of the turbulent core is supposed to have the velocity v and no thermal resistance, it is easily found, by calculating the thickness of the film from the viscosity, wall friction and transverse velocity gradient, that

$$v_m s/k_0 = \sigma Z^{-1} \tag{5A}$$

G I Taylor* allowed for the experimentally demonstrated fact that the velocity at the film boundary is only a fraction, say ϕ, of v, so that the film thickness is only ϕ of the above amount, in this case it can be shown that

$$v_m s/k_0 = (1 - \phi + \sigma\phi) Z^{-1} = \{1 + (\sigma - 1)\phi\} Z^{-1}, \tag{6}$$

an equation first explicitly given by Sir T E Stanton† though he derived it from, and it is implied in, Taylor's paper just cited which was originally published prior to Stanton's paper Equation (6) may conveniently be called the Taylor formula though neither Stanton nor Taylor specified that the heat flow rate was to be infinitesimal

It is to be noted that when $\sigma = 1$ -and it is not greatly different from unity for most gases and vapours—the presence or the viscous flow film is without effect on the thermal resistance as (6) then reduces to (5) But equation (6) is in strong contradiction to what the present results give when extrapolated to $\sigma = 1$ For $\sigma = 1$ it will be seen that the results in Table I (p 556) give

---

* 'Technical Report of Advisory Committee for Aeronautics,' vol 9, p 423 (1917)

† 'Technical Report of Advisory Committee for Aeronautics,' vol 8, p 16 (1916)

$$v_m s/k_0 = 1\ 48\ Z^{-1} \text{ when } \log \tau = 3\ 7$$

falling to

$$v_m s/k_0 = 1\ 04\ Z^{-1} \text{ when } \log \tau = \infty,$$

showing a very large discrepancy at low values of τ which indicates that when the turbulence is feeble the thermal resistance of the fluid is much larger than is given by Reynolds theory

Now Stanton and Pannell's results on the loss of hydrostatic head show that if the loss of head for turbulent flow is extrapolated past the unstable and discontinuous region, it will become identical with the loss of head for viscous flow when $\log \tau \simeq 3\ 07$, *i e*, say when $\tau \simeq 1175$ Since Z^{-1} is the main variable factor in (6) in the expression for $v_m s/k_0$ it may be expected with some reason that the k_0 s when extrapolated, first to $\sigma = 1$ and then to low values of τ, should agree with the calculable results for pure viscous flow at about $\log \tau = 3\ 07$ Also k_0 for viscous flow is calculated in Appendix A, as

$$v_m s/k_0 = 11\sigma/6Z \tag{7}$$

At $\sigma = 1$ this is $v_m s/k_0 = 1\ 833\ Z^{-1}$ The present results indicate a very satisfactory tending to this value at about $\log \tau = 3\ 07$

It is noteworthy that though the present results differ so markedly at low turbulence from the Taylor equation (6) they closely agree with a *general* linear formula in σ, say,

$$v_m s/k_0 = \{\alpha + \beta(\sigma - 1)\} Z^{-1}, \tag{8}$$

where α and β are functions of τ only In fact this equation could be made to represent the *whole* of the present results covering from $\sigma = 3\ 0$ to $\sigma = 10\ 6$ and all values of τ to within $1\frac{1}{2}$ per cent Nevertheless the deviation of the results from (8) was perfectly regular and systematic and in the manner which theory indicated was to be expected Taking (8) to represent the results with sufficient accuracy, (7) shows that both α and β must become $11/6$ for viscous flow

It is, of course, possible to calculate ϕ in (6) so as to make k_0 agree with any experimental k_0, but the ϕ's so calculated are not constants but vary with both σ and τ Now if ϕ has the physical meaning attributed to it, it is absurd to suppose it varies with σ since it obviously has nothing to do with the thermal conductivity which is involved in σ, nor can the heat flow upset the value of ϕ for we are only dealing with *infinitesimal* rates of heat flow

Since the thermal resistance of the viscous flow film cannot, apparently, be very different from ϕ times the value in (5A),* it appears that the expression in (5) cannot be considered as valid for the core but only as the value to which its thermal resistance would tend for very high rates of turbulence Comparing equations (6) and (8) for both the film and the core we see that $\beta = \phi$, and that the thermal resistance of the core is $(\alpha - \beta)/(1 - \phi)$ times its value given by Reynolds' theory At $\tau = 5000$ (i e, $\log \tau = 3\ 7$) this ratio is (see Table I below) $(1\ 483 - 0\ 480) \div (1 - 0\ 480) = 1\ 93$, at $\tau = 1{,}000{,}000$ this ratio has fallen to 1 055, and it is shown in § 14 that there is evidence that it is below this, and presumably, exactly unity

It is easy to see on theoretical grounds that the thermal resistance of the turbulent core must be considerably more than its value given by Reynolds' theory when the turbulence is feeble and sluggish It can also be seen that in this case the thermal resistance must depend appreciably upon the thermal conductivity for complete temperature equalisation, that is the thermal resistance of the core itself must vary (at least when τ is small) with σ It follows from this that it is impossible to apportion the thermal resistances of the core and film Since the resistance of the core will increase with $1/c$ it must increase with σ Hence the $\beta\sigma$ term in (8) will represent part of the thermal resistance of the core as well as the resistance of the film Consequently ϕ, the fractional thickness of the film, is less than β

7 *The Formula Adopted*

As there must be, between the film and the core a region whose mean behaviour is intermediate between the behaviour of these, theory indicates that $v_m s/k_0$ instead of being a linear function of σ should be a continually increasing function of it with a gradient continuously decreasing to some asymptotic value, which asymptotic value would give the value of ϕ for the viscous film This variation with σ is exactly what the present results indicate, except that in the variation with σ (for a constant τ) the curvature of the curves is so small for the range of σ covered (3 0 to 10 6) that no *rate of change* in the rate of change of slope could be detected

It follows that the present experiments can be exactly represented by

$$v_m s/k_0 = A' + B'\sigma - C\sigma^2,$$

or, as we prefer to write it, by

$$v_m s/k_0 = A + B(\sigma - 1) - C(\sigma - 1)^2, \tag{9}$$

---

* The effect of the curvature of the tube wall is easily calculated (since $f/d = 1/2\tau$) and will be found to be quite small

where A, B and C are positive functions of τ only Inserting Z^{-1} as a factor in the right-hand side, we may write

$$v_m s/k_0 = \{\alpha + \beta(\sigma - 1) - \gamma(\sigma - 1)^2\} Z^{-1} \qquad (10)$$

The experimental results gave ample justification for inserting Z^{-1} as a factor, in that α, β and γ were all found to be continuously decreasing functions of τ apparently tending asymptotically to definite limiting values

Tables of A, B, C, α, β, γ and Z^{-1}—the latter from Stanton and Pannell—are given below (p 556) It may be noted that Z^{-1} is, as is easily proved, equal to 8N, where N is the number of diameters of length in which the loss of hydrostatic head is equal to the velocity head It should also be noted that formula (10) has only been arrived at for the range $3\ 0 < \sigma < 10\ 6$, and it should not be used when σ is, say, > 15 The quantity $v_m s/k_0$ is *necessarily* always an increasing function of σ whereas (10) gives a maximum value when $\sigma - 1 = \beta/2\gamma$—a value in the neighbourhood of 40 to 50

As pointed out above, the resistance of both the core and the intermediate layer must increase with σ, so the resistance of the film is less than the $\beta\sigma$ term in (10), in fact, the β appertaining to the film resistance proper should be less than the *minimum slope* given by $\alpha + \beta(\sigma - 1) - \gamma(\sigma - 1)^2$ over the experimental range This slope is $\beta - 20\gamma$ when $\sigma - 1 = 10$, which is roughly equal to 0 25

From the present experiments none of the quantities A, B, C or α, β, γ appear to be simple analytic functions of τ so that no attempt is here made to find formulæ for them A set of large scale graphs which can easily be constructed from the tabulated values given below is far preferable to complicated empirical formulæ

Although the present experiments have been exclusively confined to water, it will be seen from the above analysis that the functions A, B, C and α, β, γ must be the same for all fluids, liquid and gaseous, just as Z is the same for all fluids The limitations on these results, viz, that they only apply to an infinitesimal rate of heat flow and after the initial irregularity has died down, must not be overlooked Also, in the case of gases, it must be remembered that the transfer of heat by direct radiation may be an appreciable fraction of the total amount

8 *Description of Apparatus*

A diagram of the experimental tube with its salient fittings is shown in fig 1 The dimensions there given apply to the ¾ inch tube, though tubes of nominal outside diameters of ½ inch, ¾ inch, 1 inch and 1½ inches and of mean internal

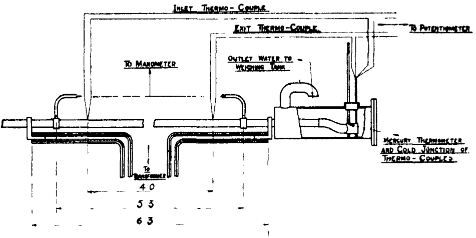

FIG 1 —Diagram of Apparatus

diameters of about 1 025 cm , 1 659 cm , 2 29 cm , and 3 56 cm , respectively, were all employed

A length of 6 feet 3 inches of a ¾-inch tube, which was 15 feet in total length, was heated electrically by a low tension alternating current, fed into it by six copper straps of section 1½ inches × ⅛ inch in parallel* at the heavy brass lugs shown, which were soldered on to the tube Two copper-constantan thermocouples were soldered on to the tube at 13½ inches respectively from the ends of the electrically heated portion, care being taken that the two wires emerge separately, but near together, from a small blob of solder To prevent any cooling of the thermo-junction the two wires were laid down close to the tube for about an inch and insulated from it by a thin flake of mica, and the wires and the tube at this place were then wrapped round with asbestos rope Two grooved rings were also soldered to the tube at two points 5 feet 3 inches apart where four small holes had been drilled through the tube wall These served to determine the loss of hydrostatic head over the included portion of the tube Immediately beyond the heated portion the tube projected into a water box, also shown A brass end piece shaped somewhat like a tobacco pipe fitted into the end of the ¾-inch tube and the "bowl" served to contain the bulb of a mercury thermometer, which was used to obtain the temperature of the outlet water, together with the "cold junctions," immersed in oil in thin glass tubes, of the two thermocouples mentioned above A third thermocouple with its hot junction in this bowl was used to obtain the temperature rise of the water and so to check the electrical heat supplied With the 1-inch and the 1⅛-inch tubes this " tobacco pipe " was not necessary, nor was it necessary with the ¾-inch tube at the higher velocities, while it was required in all cases for the ½-inch tube

---

* Twelve straps in parallel were used for the 1½ inch tube

The water supply came from a tank (not shown) 18 feet above the experimental tube The water in this tank could be heated by direct steam heating—the steam issuing from nozzles and mixing with the water A motor driven stirrer was also provided

The value of the electric current was given by a bus bar transformer and an ammeter which were calibrated together against a Kelvin current balance in the Electrical Standards Department of the Manchester College of Technology The electrical resistance of the heated portion was obtained by previously comparing on the potentiometer the drop of potential across the brass lugs with that across a standard low resistance of about 0 002 ohm in series with it when a direct current passed through both This was done with water at different temperatures flowing down the tube The electrical input was taken as given by C^2R, the error due to the unequal distribution of current over the cross section being utterly negligible The extreme currents employed varied from 520 to 2750 amperes for the different tubes

The third thermocouple mentioned above had its cold junction immersed in oil in a thin glass tube, inserted into the condenser tube about 2 feet before the commencement of the heated portion It served to check the electrical heat supplied , and the two heats were found to be in quite satisfactory agreement being often within 1 per cent and nearly always within 2 per cent The heat supplied could be determined with much greater *consistent* accuracy electrically than by this thermocouple, as the arrangement at the inlet water junction was not so satisfactory for getting the temperature of the water as that at the outlet end, and the diameter of the tube being too small to permit the temperature being taken up accurately by the thermojunction, so that it was the C^2R determination of heat which was always used in reducing the results The check served, however, to show that there was no reason for doubting the accuracy of the electrical heat to more than 1 per cent

The two thermocouples soldered on the tube were calibrated *in situ* by running water at various temperatures and a fairly high velocity through the tube and placing the " cold-junctions " either in ice or in a thermos flask which contained oil or water heated to any desired temperature up to about 230° F From these results a graph was constructed showing the ' thermoelectric power " plotted against the mean temperature of the junctions over a range from about

40° F to 190° F The E M F of the thermocopules was obtained on a potentiometer in the usual way with a Weston normal cell employed to ensure a constant potential gradient down the potentiometer The sensitivity was about 10 cm of wire to 1° F

The mean internal diameters of the tubes were determined by weighing them empty and full of water This readily gave the weight of water per second corresponding to a (nominal) velocity of 1 foot per second

The mean water temperatures at the positions of the thermocouples were calculated from the heat put into the water up to those positions , that is, it was taken to rise linearly along the tube The temperature drop across the tube wall was allowed for, but since the heat was generated throughout the bulk of the material this drop was only half what it would have been had the heat been supplied from outside the tube The loss of heat from the external surface of the tube was determined and allowed for, though it was nearly negligible

Three heat flow rates of approximately 4000, 12,000 and 20,000 B Th U per square foot per hour were adopted as the most convenient (save in the case of the 1½ inch tube where the rates had to be reduced to 4000, 8000 and 12,000 on account of the large currents required) As the bus-bar transformer had two windings which could be connected either in series or parallel, heat flows in the ratio 1 3 5 gave very comparable ammeter readings in the ratio 2 $\sqrt{3}$ $\sqrt{5}$ In the case of the ½-inch tube the current was so small that it was led twice through the bus-bar transformer

The alternating supply was from a separate turbo generator and the heating current was kept constant by continuous hand regulation of a liquid rheostat in the primary circuit of the transformer by an observer watching the bus bar ammeter

Nominal or " mass flow " water velocities of 2, 3, 5, 8 and sometimes 1 and 11 feet per second were mostly employed, and were set as near as possible beforehand till the right weight-flow in 5 minutes was obtained Correction to these exact velocities was made taking k to vary as $v^{0\,8}$ Inlet water temperatures in steps of about 20° F (or less) from 40–50° F to about 140–150° F were taken, this temperature, and the water velocity, being kept constant while the tests at the three heat flow rates were made

To obtain greater accuracy in the k's the three values of $\Delta\theta$ (the net temperature difference between the tube and the water) were plotted against the rate of heat flow and a smooth curve—a slightly curved parabola—was drawn through the origin among these three points The $\Delta\theta$'s used in calculating the *k*'s were those taken from this curve This method was especially valuable at the higher temperatures where it was difficult to get temperature differences correct to the desired 0 02 to 0 05° F , since it was difficult to keep the temperature of the inlet water constant to anything like this when it was being preheated by 50–100° F

It is perhaps worth while placing on record here the fact that the potentiometer used with the thermocouples was a Callendar and Griffiths bridge with the connections transposed for potentiometer use This had the effect of doubling the value of the coils in terms of a centimetre of wire and necessitated the electrical determination of the " end correction " of the wire With the ordinary student's metre-wire potentiometer first employed very considerable difficulty was experienced owing to the large kicks which the galvanometer gave on making and breaking its circuit owing to the alternating current flowing through the tube to which the thermocouples were soldered With this excellent instrument these difficulties, which threatened to make the use of an electrically heated tube impossible, disappeared

9 *A Sample Experiment*

In order to allow a critical estimate of the accuracy which the experimental method pursued is capable of, we subjoin here particulars of a sample experiment with one of the ¾-inch tubes The experiment selected was with a water velocity of 5 feet per second and an inlet water temperature of about 87° F , and was selected because, corresponding to fairly mean conditions, it gives a better idea of the magnitude of the temperature rises usually obtained than extreme cases

Sample Experimental Test with a ¾ inch Tube —A length of 178 80 inches held a weight of 2 1475 lbs of water at 61° F giving a mean internal diameter of 0 6513 inch (1 654 cm), an internal heated area of 1 0656 sq ft , and a flow of 216 4 lbs in 5 minutes for a ' nominal velocity " of 5 feet per second

	Heat flow	First	Second	Third
1	Heating current in amperes	840	1458	1876
2	Weight of water in 5 minutes (lbs)	218	218	216 5
3	Temperature of outlet water (°F)	88 9	92 6	96 3
4	Temperature rise on inlet (or first) thermocouple	1 87	5 50	8 90
5	Temperature rise on outlet (or second) thermocouple	2 91	8 89	14 37
6	Temperature of outside of tube at inlet t c	90 77	98 10	105 20
7	Temperature of outside of tube at outlet t c	91 81	101 49	110 67
8	Allowed drop through tube wall	0 12	0 36	0 60
9	Temperature of inside tube surface at outlet t c	91 69	101 13	110 07
10	Resistance of heated portion of tube in milli ohms	1 913	1 924	1 934

	Heat flow	First	Second	Third
11	C^2R heat in B Th U per foot per hour (1 watt = 3 412 B Th U per hour)	4320	13,110	21,800
12	Extra external heat loss due to rise in tube temperature with electric heat	10	40	60
13	Net heat flow rate H	4310	13,070	21 740
14	Calculated water temperature rise from electric heat and water weight	1 75	5 33	8 91
15	Water temperature at outlet t c below exit water (= 0 18 of above)	0 33	0 96	1 60
16	Water temperature at outlet t c [= (3) − (15)]	88 57	91 64	94 70
17	Temperature difference between tube and water at outlet t c [= (9) − (16)]	3 12	9 49	15 37
18	Above temperature difference corrected to exact water velocity	3 14	9 55	15 37
19	The same smoothed graphically against H to vanish with it [= $\Delta\theta$]	3 19	9 47	15 40
20	$K = H + \Delta\theta$	1352	1380	1410
21	K corrected for conicality of tube by adding 0 83 per cent (see below)	1363	1391	1421
22	Water temperature for above [= (16) repeated]	88 6	91 6	94 7

K extrapolated to zero rate of heat flow gives $K_0 = 1348$ at 87 0° F That is $k_0 =$ 0 1825 calories per square centimetre per second per °C at a water temperature of 30 5° C Now σ for water at 30 5° C is 5 25 (see Table II, below, p 559) while $\tau = v_m d/\mu = 152\ 4 \times 1\ 654 + 0\ 00792 = 31{,}830 = \log^{-1} 4\ 503$ Now Table I, below (p 556) using the values of A, B and C at $\log \tau = 4\ 50$, gives $v_m s/k_0 = 152\ 4/k_0 = 840$ or $k_0 = 0\ 1815$, while at $\log \tau = 4\ 503$ Table I gives $k_0 = 0\ 1818$ in very satisfactory agreement with the above value especially as the table was constructed long before the above tube was bought, and it was bought from a different maker to see, among other things whether the same value of k could be obtained from different makers' tubes

A source of error discovered rather late in the work was the conicality of the internal bore of the tubes mentioned in item (21) The outside diameters were remarkably constant and the same was therefore assumed of the internal bore However, testing the uniformity of potential drops over a measured length showed a variation of resistance per unit length of from 2½ to 13 per cent for the different tubes As this resistance varies inversely as the area of the metallic cross section it was possible to find the actual internal diameter at any point from its mean value This necessitated three corrections to the coefficients, k, (i) a correction to the heat supplied per unit length, (ii) a correction to the area of the internal surface of the tube, and (iii) a correction to the water velocity *

---

* There are certain other small errors which must be considered (1) The water will not rise at a uniform rate along the tube since its electrical resistance is not constant, the outlet end being warmer than the inlet end This was considered and the effect found to be negligible, (2) owing to the heat flow along the tube in the opposite direction to the water velocity some of the heat will enter the water before the point at which it was generated. If l is the heated length, S the area of metallic cross section, c_b the thermal conductivity of brass and θ_l the difference of temperature along the tube, the longitudinal heat flow

10 *Method of Reducing the Experimental Results*

The values of k recorded in this paper depend entirely upon the temperatures given by the thermocouple near the outlet end of the tube, the other one was chiefly used to obtain the mean temperature of the tube upon which its resistance depended The values of k, obtained in sets of three as described, were plotted against the water temperature at the position of the outlet-end thermocouple and were then interpolated and extrapolated to give k for the three exact heat flow rates of zero, 10,000 and 20,000 B Th U per square foot per

is $c_b S\theta_d/l$ so that the heat flowing into the water between the outlet end thermocouple and the end of the heated portion is not $2\pi a \times 0\ 18l \times \mathrm{H}$ ($0\ 18l$ is the distance of the thermocouple from the end) but is less than this by $c_b S\theta_d/l$ The ratio of these quantities is $c_b S\theta_d/0\ 36\pi a l^2\mathrm{H}$ In C G S units this becomes $\theta_d/180\ 000\mathrm{H}$ As θ_d is rarely over 10° C at the highest heat flow rate when $\mathrm{H} = 1\ 5$ calories per square centimetre per second this effect is completely negligible (3) The *differential* longitudinal heat flow, $c_b S \dfrac{d^2\theta}{dx^2}$ per unit length, becomes transverse heat flow into the water Assuming a parabolic distribution of temperature along the tube given by $\theta = 4\theta_m x(l - x)/l^2$, superposed on a uniform temperature gradient (this gives a mid point temperature in excess of the arithmetical mean of the end temperatures by θ_m) we see that this differential flow is $8c_b S\theta_m/l^2$ per unit length This bears a ratio of $4c_b S\theta_m/\pi a l^2\mathrm{H}$ to the heat flow into the water per unit length Numerically this ratio is $\theta_m/130\ 000\mathrm{H}$ and so is utterly negligible (4) The sudden drop of tube temperature which would occur at the point where the heating ceases if there were no longitudinal conduction of heat is smoothed off by such conduction and the effect of this will extend for some length along the tube Calculation shows that for a thin walled tube of thickness t the reduction of the tube temperature at a distance x before the end of the heated portion is approximately $\frac{1}{2}\Delta\theta\ e^{-nx}$ where $n^2 = k/tc_b$ Taking $c_b = 0\ 26$, $t = 0\ 125$ and a very low value of k of $0\ 050$—its value for water at 5° C and 2 feet per second—$n = 1\ 24$ So that at the position of the outlet thermocouple, $x = 34$ cm this effect is infinitesimal (5) Another error is due to the heat flow into or from the copper straps via the lugs Neglecting the $\mathrm{C}^2\mathrm{R}$ heat generation in the copper straps this error was compensated for by taking the thermocouple readings on the potentiometer when the heating current was zero and using these readings as a "false zero" This method is almost inevitable when it is required to determine small temperature differences accurately at temperatures considerably above room temperature by means of thermocouples Owing also to this method of working, the external heat loss to be allowed for in item (12), above, is not the whole heat lost by the outside of the tube but only the extra heat lost by the rise in temperature of the tube during heat flow (6) The remaining error, the flow into the tube of the $\mathrm{C}^2\mathrm{R}$ heat generated in the copper straps, could readily be detected with the largest of the three currents, by a noticeable creep in the thermocouple readings in those experiments, where, owing to the conditions not being sufficiently steady, delay was experienced in getting the readings Such experiments were repeated another time We do not think that an error of more than one or two parts in a thousand could have arisen in the majority of experiments from this cause hour calculated on the area of the internal surface of the tube The sets of points for these exact heat flow rates at different water temperatures, but the same velocity, were then connected by smooth curves From these curves values of k at definite temperatures were selected at the different velocities and log k was plotted against log v_m These curves were only slightly curved lines of a slope approximately 0 77 to 0 81 and enabled the k's for the intermediate velocities (which were generally 4, 6, 7, 9 and 10 feet per second) to be obtained

Having done this work for the four diameters of tubes, the velocities divided by the k_0's at 40° F (which gives $v_m s/k_0$ since $s = 1$ sensibly) were plotted on a single diagram against $v_m d$ for all the different velocities and tube diameters Similar diagrams were drawn for each of the temperatures 60°, 80°, 100°, 120° and 140° F By theory all the points on each of these diagrams should lie on a single curve This was found to be so to within $1\frac{1}{2}$ per cent , some tubes giving points consistently high and some consistently low *

The six mean curves on these six sheets were next replotted on a single large sheet with their abscissæ divided by the viscosity of water for the temperature in question The abscissa were then the τ's The quantity $\sigma = \mu s/c$ was next determined for these six temperatures using Kaye and Higgins' recent

---

* Some of this systematic deviation between one tube and another seems from later tests to be due to the conicality of the tube the three known effects of conicality were allowed for as above , but in a check test in which the same tube was reversed in direction, values of k differing by 2 to 3 per cent were obtained , the difference apparently being due to nothing save the reversal The values of k were greater for a converging than a diverging tube It is difficult to explain this We can only suggest that vortices of a certain diameter are formed in the tube, and when moving along a converging tube tend to cut away the viscous film more than they would in a parallel tube and thus decrease the thermal resistance But even this suggestion seems fantastic considering that the semi-angle of the conical surface was only about 1/40,000 of a radian Possibly the slight irregularities on the surface were such that they offered less resistance to water flowing towards the larger end than towards the smaller end , this would make the viscous film thicker in the former case , and this direction is, of course, the direction in which the man dril was withdrawn from the tube after manufacture , it was to facilitate this withdrawal that the tubes were made conical The k's for the $1\frac{1}{4}$ inch tube were among the high ones, but this was thought to be natural as with this tube it was impossible to take the tests as many diameters away from the initial disturbances as with the other tubes

Some tubes from another manufacturer were obtained and tested after the table of results in Table I below was constructed These tubes were found to have considerably less conicality than the previous ones, and the values of the heat transfer coefficient obtained from them were in very satisfactory accord with the table, as is seen by the sample experiment given above which was from one of these later tubes values for the conductivity of water,[*] in the absence of which the thermal conductivity of water could not be considered to be known well enough to make the present analysis reliable Ordinates were next drawn for selected values of τ and the values of $v_m s/k_0$ were replotted as functions of σ for these values of τ These curves, as previously stated, were found to be slightly curved parabolas for which the constants in the equation

$$v_m s/k_0 = \mathrm{A} + \mathrm{B}\,(\sigma - 1) - \mathrm{C}\,(\sigma - 1)^2 \tag{11}$$

were very easily found These constants were then plotted against the corresponding value of τ when very satisfactory smooth curves were obtained In fact the values of k_0 obtained from formula (11) by using the smoothed curves for A, B and C agreed with the values of the two large sheets to within one-third of 1 per cent practically everywhere

11 *Table of Results*

Table I, below, gives the values as above determined for A, B and C together with the values of Z^{-1} from Stanton and Pannell, and the values of α, β and γ defined by $\alpha = \mathrm{AZ}$, $\beta = \mathrm{BZ}$ and $\gamma = \mathrm{CZ}$

To get regular smoothed values of Z for this analysis the ordinates midway between the two limiting curves marked N P L on Stanton and Pannell's well-known diagram (fig 5 of their paper) were taken as giving Z A formula to represent these ordinates has been previously published by one of the present writers[†]

The above seven functions are given for regular intervals of log τ that being the most convenient variable to plot them against The next most convenient variable is $\tau^{-\frac{1}{2}}$ the values of which are also given Z when plotted against $\tau^{-\frac{1}{2}}$ is practically a straight line In the letter to 'Nature' above referred to, reason is given for thinking that any correct expression for Z should be intelligible, when τ is negative, which it is when Z is expressed in rational terms of $\tau^{-\frac{1}{2}}$ This follows since there should be no sudden discontinuity in Z when the curvature of the tube wall—which is $2/d$—passes through zero, *i e*, when $\tau^{-\frac{1}{2}}$ passed through zero For negative values of τ, $\rho v^2\mathrm{Z}$ represents the surface friction when a very long cylinder of diameter d is dragged axially through water with a velocity v, which is thus a matter of considerable theoretical interest

---

[*] 'Roy Soc Proc,' A, vol 117, p 459 (1928) The values of σ taken for the six temperatures were 10 60, 7 60, 5 73, 4 49, 3 62 and 2 99 respectively, the last figure being for 140° F

[†] 'Nature,' vol. 123, p 14 (1928)

Table I

$\log \tau$	$\tau^{-\frac{1}{2}}$	A	B	100 C	Z^{-1}	α	β	100γ
3 6	0 0631				195	(1 55)	(0 53)	(0 63)
3 7	0 0584	307	99_5	123	207	1 483	0 480	$0\ 59_5$
3 8	0 0541	311	97	124_5	220	1 414	0 439	$0\ 56_5$
3 9	0 0501	315	96	126	234	1 343	0 411	$0\ 53_5$
4 0	0 0464	321	97_5	127_5	250	1 284	0 390	0 51
4 1	0 0430	329	99	129	266	1 237	0 372	$0\ 48_5$
4 2	0 0398	341	101_5	130_5	284	1 202	0 358	0 46
4 3	0 0369	356	104_5	132	303	1 175	0 345	$0\ 43_5$
4 4	0 0341	372	108	133	323	1 152	0 333	0 41
4 5	0 0316	390	111_5	134	344	1 133	0 324	0 39
4 6	0 0293	409	116	135_5	366	1 118	0 316	0 37
4 7	0 0271	429_5	120_5	137_5	388	1 105	0 311	$0\ 35_5$
4 8	0 0251	450	126	140	411	1 094	0 307	0 34
4 9	0 0233	470_5	132	143	434	1 084	0 305	0 33
5 0	0 0215	491_5	138_5	146_5	457	1 075	0 303	0 32
5 1	0 0199	512_5	145	150	480	1 069	0 302	$0\ 31_5$
5 2	0 0185	535	151_5	155_5	503	1 064	0 302	0 31
5 3	0 0171	555	158_5	160_5	524	1 060	0 301	$0\ 30_5$
5 5	0 0147				565	(1 053)	(0 301)	(0 30)
6 0	0 0100				650	(1 045)	(0 300)	$(0\ 29_5)$
∞	0				860 ?	(1 040)	(0 300)	(0 29)

Numbers in brackets are extrapolated

The coefficients k_0 are given from the above table by the formulæ

$$\begin{aligned} \rho v s/k_0 &= \mathrm{A} + \mathrm{B}\,(\sigma - 1) - \mathrm{C}\,(\sigma - 1)^2 \\ &= \{\alpha + \beta\,(\sigma - 1) - \gamma\,(\sigma - 1)^2\}\ \mathrm{Z}^{-1} \end{aligned}$$

Values of σ for water are given in Table II, below, while a curve of $\log 1/\mu$ or $\mu^{\frac{1}{2}}$ for water (or other fluid) is very convenient for evaluating $\log v_m d/\mu$ or $\{\mu/v_m d\}^{\frac{1}{2}}$, i e, $\tau^{-\frac{1}{2}}$

12 *Coefficient of Heat Transfer at Infinite Velocity*

As pointed out, the equation (6) requires that $v_m s/k_0 = \mathrm{Z}^{-1}$ when $\sigma = 1$ for all values of τ That is, it requires that α in Table I should be unity throughout It is quite possible, and even likely, that this may be so when $\tau = \infty$, for then, and only then, are the conditions necessary to make Reynolds' theory exactly true completely satisfied Experimentally no values of σ less than 3 0 were employed so that the values for $\sigma = 1$ are a pure extrapolation But it was shown in § 7 that the rate of *decrease* of $v_m s/k_0$ must increase with increasing rapidity as σ decreases Thus it is quite likely that some extra term of this behaviour should be added to (10) giving, say, something like

$$v_m s/k_0 = \{\alpha + \beta(\sigma - 1) - \gamma(\sigma - 1)^2 - 0\ 04\sigma^{-2}\} Z^{-1} \qquad (12)$$

This expression would then satisfy Reynolds' theory at $\tau = \infty$ and over the range of the experiments would introduce a deviation of less than 0 3 per cent, which is well within the experimental errors No physical objection can be raised against the σ^{-2} term for giving an infinite value when $\sigma = 0$ since σ cannot be much below unity for any substance We mention this point chiefly for those who may desire to extrapolate our results below $\sigma = 3\ 0$

13 *Loss of Hydrostatic Head during Heat Transfer*

It was one of the original objects of this research to determine the loss of hydrostatic head at the same time as heat transfer was taking place For this purpose the loss of head over a length of about five sixths of the electrically heated portion of the tube was measured on a water manometer during each heat-flow test These determinations gave the extremely simple result, in nearly all cases, that the loss of head during heat transfer was the same as if the water had been at the *tube* temperature and no heat transfer was taking place When inlet water down to about 40° F could be obtained it was found that the law was slightly different from this, the loss of head then being the same as if there was no heat flow and the water was at its own temperature plus about 90 per cent of the difference of temperature between tube and water, but with rising temperature this fraction soon became sensibly 100 per cent It is shown in Appendix B that for purely viscous flow this fraction is theoretically $6/11 \simeq 54\ 5$ per cent

14 *Coefficients at Finite Rates of Heat Flow*

We have already given, in § 5 above, the theoretical form of the expression for the difference between k_H and k_0 at a heat flow rate H A concrete approximate expression may be obtained theoretically when τ is large In this case α and β are sensibly constants, that is, they will not vary with the temperature, which they do generally since τ varies with the temperature through μ Neglecting the γ term in (10) as being small compared with the other two, we have

$$v_m s/k_0 = (\alpha - \beta + \beta\sigma) Z^{-1},$$

where the $\alpha - \beta$ term and the $\beta\sigma$ term represent the resistance of the core and the film respectively Now we have just stated that Z is practically unaltered by heat flow at the same *tube* temperature Hence for a finite rate of heat flow with a given tube temperature we have merely to change $\beta\sigma$ into $\beta\bar{\sigma}$ where $\bar{\sigma}$ represents the mean value of σ through the film But

$$\bar{\sigma} = \sigma - \tfrac{1}{2}\frac{d\sigma}{d\theta}\,d\theta,$$

where $d\theta$ is the difference of temperature across the film, and the σ is the value of σ at the tube well temperature Now the difference of temperature from tube to water is $\mathrm{H}/k_{\mathrm{H}} \approx \mathrm{H}/k_0$, and the temperature difference across the film is clearly the fraction $\beta\sigma/(\alpha - \beta + \beta\sigma)$ of this amount Hence we have

$$v_m s/k_{\mathrm{H}} = \left\{\alpha - \beta + \beta\left(\sigma - \frac{\beta\sigma}{2\,(\alpha - \beta + \beta\sigma)}\,\frac{\mathrm{H}}{k_0}\,\frac{d\sigma}{d\theta}\right)\right\}\mathrm{Z}^{-1},$$

whence

$$\frac{k_{\mathrm{H}}^{-1} - k_0^{-1}}{k_0^{-1}} \approx \frac{k_0 - k_{\mathrm{H}}}{k_0} = -\left(\frac{\beta\sigma}{\alpha - \beta + \beta\sigma}\right)^2 \left(\frac{1}{2\sigma}\frac{d\sigma}{d\theta}\right)\frac{\mathrm{H}}{k_0} \tag{13}$$

Now $(k_0 - k_{\mathrm{H}})/k_0$ is small for ordinary rates of heat flow in practice, so that an approximate evaluation of (13) will suffice It is seen from fig 2 that

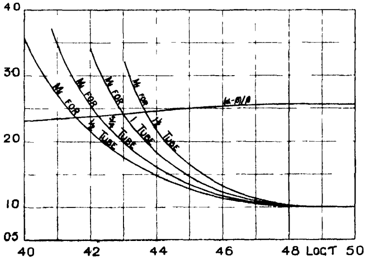

Fig 2 —Multiplying Factors and $(\alpha - \beta)/\beta$

$(\alpha - \beta)/\beta$ is remarkably constant over a wide range, from $\tau = 13{,}000$ to $\tau = \infty$ it only differs from 2 45 by less than 4 per cent Hence we have, approximately, for large values of τ,

$$k_{\mathrm{H}} - k_0 = -\left(\frac{\sigma}{2\ 45 + \sigma}\right)^2 \left(\frac{-1}{2\sigma}\frac{d\sigma}{d\theta}\right)\mathrm{H} \tag{14}$$

Table II, below, shows the value of σ and $\frac{-1}{2\sigma}\frac{d\sigma}{d\theta}$ for water in Centigrade units. The values of σ are required for use in conjunction with Table I, they involve a considerable extrapolation of Kaye and Higgins' linear values of c, but they have been given to 160° C because values of σ for such temperatures are required for modern feed-water heaters, for which purpose these values of σ are amply accurate enough, as when $\sigma = 1$ the percentage change in k_0 for a 1 per cent change in σ is only about one-third of what it is for cold water, moreover, k_0 being so much greater for hot water, the temperature differences causing the heat flow are so much less that the same accuracy in k_0 is not needed. The values of $\frac{-1}{2\sigma}\frac{d\sigma}{d\theta}$ were deduced from the values of σ by the finite difference formula

$$D = \Delta - \tfrac{1}{2}\Delta^2 + \tfrac{1}{3}\Delta^3 -$$

Table II

° C	σ	$q = \frac{-1000}{2\sigma}\frac{d\sigma}{d\theta}$	$\left(\frac{\sigma}{2.45+\sigma}\right)^2 q$
0	12.45	18.0	12.6
5	10.46	16.5	11.0
10	8.93	15.1_5	9.5
15	7.73	13.9_5	8.0
20	6.75	13.0	7.0
25	5.96	12.0_5	6.0
30	5.30	11.2_5	5.3
40	4.29	9.9	4.0
50	3.55	8.8_5	3.1
60	2.99	8.0	2.4
70	2.56	7.3_5	1.9
80	2.22	6.7_5	1.5
90	1.95	6.2	1.2
100	1.74	5.7	1.0
110	1.56	5.2	0.8
120	1.40	4.8	0.6
130	1.27	4.3	0.5
140	1.17	3.9	0.4
150	1.09	3.4_5	0.3
160	1.02	3.0_5	0.2

It must be remembered that k_H and the corresponding k_0 are at the same *tube* temperature and that therefore k_H is at a *water* temperature of H/k_H below the water temperature of the corresponding k_0.

At the higher velocities or higher water temperatures the above calculated differences between k_H and k_0 agreed excellently with the experimental results but deviated markedly at the lower temperatures and velocities.

However, on comparing the actual $(k_H - k_0)$'s with the values calculated for them by (14), it was found that the ratios between them (for various water temperatures and velocities) when plotted against τ all lay on the same curve for results on the same tube. This ratio was taken as an empirical multiplying factor. Denoting it by M_t, (14) may be written in the revised form,

$$\frac{k_H - k_0}{H} = -\left(\frac{\sigma}{2 \cdot 45 + \sigma}\right)^2 \left(\frac{-1}{2\sigma}\frac{d\sigma}{d\theta}\right) M_t \tag{15}$$

Table 11, above, in addition to giving values of $\frac{-1}{2\sigma}\frac{d\sigma}{d\theta}$ for water also gives the same quantity multiplied by $\left(\frac{\sigma}{2 \cdot 45 + \sigma}\right)^2$, while fig. 2 shows the multiplying factors arrived at for the four tubes of nominal outside diameters of ½ inch, ¾ inch, 1 inch and 1½ inches respectively. In all cases the multiplying factors decrease to their theoretical value for unity for values of τ above 60 to 70 thousand.

For cold water at low velocities $k_0 - k_H$ becomes relatively large, but if k_H is compared with k_0 for the *same water temperature* (k_0' say) the difference $k_H - k_0'$ (which is then positive) remains of nearly the same magnitude.

The above theory of the difference between the k_H's and the k_0's should be applicable to all fluids when once the function $\frac{1}{2\sigma}\frac{d\sigma}{d\theta}$ has been determined for that fluid. An exception must be made in the case of gases where the change of density consequent upon a change of temperature is so great that entirely fresh convection currents may be set up by this cause alone. This means that the above theory fails because it does not take into consideration the $\frac{\lambda_4}{\rho}\frac{d\rho}{d\theta}$ term in (4).

15. *The variation of k at the commencement of heating*

A crude investigation, perhaps better than nothing, may be made as follows into this difficult problem. Treating γ and f/d as negligible, and identifying β and ϕ, as an approximation, we will represent the temperature, θ, at a distance r from the axis by

$$\theta = \frac{\alpha - \beta}{\alpha - \beta + \beta\sigma}\{1 - \sqrt{(1 - r^2/a^2)}\}\,\theta_w, \tag{16}$$

where θ_w is the temperature of the tube wall, and the temperature at the axis has been taken as zero. This intentionally makes the temperature gradient infinite at the wall to agree with the gradient through the film, which must be infinite if its thickness is negligible It also makes the temperature drop across the film and core in the correct ratio $\beta\sigma \quad (\alpha - \beta)$ Now it is easily found that the above temperature distribution necessitates an amount of heat of at least equal to

$$\frac{\pi}{3} a^2 \rho s \left(\frac{\alpha - \beta}{\alpha - \beta + \beta\sigma}\right) \theta_w$$

per unit length being put into the water before such distribution is possible But the heat put in per unit length per unit time is $2\pi a H$ which is approximately $2\pi a k_0 \theta_w$ Substituting $\rho c s Z(\alpha \quad \beta + \beta\sigma)$ for k_0 we get $a(\alpha - \beta)/6Zv$ as the *time* required to impart this heat But in this time the liquid flows a distance of $(\alpha - \beta)/12Z$ diameters down the tube As $Z^{-1} = 8N$ where N is the number of diameters in which the loss of head is equal to the velocity head, this is $\frac{2}{3}(\alpha - \beta)N$, or, roughly, since $(\alpha - \beta)$ is of the order of 0 7 to 0 9, say, $\frac{1}{2}N$ diameters It is fairly evident that the value of k_0 will reach its limiting value, roughly, exponentially, and that in two or three times this distance the initial effect will have become insensible

As, for ordinary velocities, N varies between about 25 50 this calculation is in no way inconsistent with the experiment which gave values of k at the first thermocouple of anything up to about 5 per cent greater (when compared for the same water temperature) than those given by the second couple, while one test made with the first thermocouple only 3 inches from the commencement of heating gave values of k about 50 per cent greater

If, instead of generating heat at a constant rate along the tube, the tube had been maintained (by a variable heat flow) at a *constant temperature* above the water, which is more the condition in a steam condenser, the effect of this ' entrance effect ' will be to cause an *extra* heat flow into the water of the amount required to produce the equilibrium distribution of temperature over the cross section Thus we see that the tube will behave as if its length were somewhere about $\frac{2}{3}(\alpha - \beta)N$ or $\frac{1}{2}N$ diameters longer than it actually is

The above investigation may be extended to determine roughly the difference in the value of k obtained by taking the water temperature as its axial value and the temperature given by allowing the water at any section to flow into a vessel and to become thoroughly mixed

We will take the velocity u at a distance r from the axis to be given by

$$u = u_0\{\beta + (1 - \beta)\sqrt{(1 - r^2/a^2)}\}, \tag{17}$$

where u_0 is the axial velocity This makes the velocity at the boundary with the film a fraction β of the axial velocity, and agrees approximately with

Stanton and Pannell's determination of the velocity distribution From (16) and (17) we easily find the " mixing temperature " over the cross section to be

$$\frac{1+\beta}{4+2\beta}\ \frac{\alpha-\beta}{\alpha-\beta+\beta\sigma}\ \theta_w ,$$

so that the temperature difference between tube and water, instead of being θ_w, is less by the above amount Hence taking the water at its axial temperature would give smaller k's in the ratio

$$\left\{1-\frac{1+\beta}{4+2\beta}\ \frac{\alpha-\beta}{\alpha-\beta+\beta\sigma}\right\} \quad 1$$

If, say, roughly, $\alpha = 1\ 3$ and $\beta = 0\ 4$ this gives a ratio of $5 + 3\sigma \quad 7 + 3\sigma$ (approximately) making a difference of about 10 per cent with water at 80° F It must not be assumed that with cold water when σ is large this ratio is nearly unity for the thickness of the viscous flow film has been assumed negligible, and that it is only so at high velocities with cold water It is shown in Appendix A that for purely viscous flow the ratio of the k's given by these two ways of taking the water temperature is 11 18

The authors desire to thank the authorities of the Manchester College of Technology, in the Engineering Department of which this research was carried out , they also owe a debt of gratitude to Dr G Stoney under whose kindly help and supervision the work was commenced

Summary

The present paper records the determination of the coefficient of heat transfer, k, from brass tubes to water flowing through them, the tubes being directly heated by large alternating currents No definite coefficient of heat transfer is obtainable till the temperature distribution over the cross section has attained its limiting form The coefficient of course varies with what the water temperature at any cross section is considered to be In these experiments this temperature is taken as the mixing temperature of the water flowing past the section

It is shown that the limiting coefficient is, apart from a simple factor, a function of Reynolds' number $\tau \equiv \rho v d/\mu$ and $\sigma \equiv \mu s/c$ (*i e*, viscosity × specific heat — thermal conductivity) only The results for very small rates of heat flow can be expressed in the form

$$\rho v s/k_0 = A + B(\sigma - 1) - C(\sigma - 1)^2,$$

where A, B and C are functions of τ only given in Table I on p 556 This holds for all values of σ up to about 15, and for values of τ from about 5000—which is only $2\frac{1}{2}$ times the lower critical velocity and is the lowest at which the flow is stable enough to obtain readings - to infinity

A theory, agreeing with experiments, is given showing the difference between k_0 and k_H, the coefficient at a heat flow rate H, when τ is large and also a simple empirical rule for the difference when τ is not so large

An approximate estimate of the distance before k settles down to its limiting value is also given which is not inconsistent with the experiments

APPENDIX A

Calculation of k_0 for Viscous Flow

This problem, though it has been solved before,* contains points to which we wish to draw attention

When the temperature distribution over the cross section has reached its limiting form we must have

$$\theta = gx + f(r)$$

where g is the gradient along the direction of x, the axis of the tube The velocity u at any point is known to be given by

$$u = 2v\,(1 - r^2/a^2)$$

where v is the mean velocity

The excess of heat flowing radially into a thin cylinder of unit length and of radii r and $r + dr$ per unit time over that flowing out is clearly

$$\frac{\partial}{\partial r}\left\{c2\pi r\,\frac{\partial \theta}{\partial r}\right\} dr$$

As the temperature remains steady this is equal to the heat removed by the flow which is

$$(2\pi r\,dr)\,\rho s u\,\frac{\partial \theta}{\partial x}$$

per unit time

Writing g for $\dfrac{\partial \theta}{\partial x}$ and substituting for u, we get on equating

$$\frac{\partial}{\partial r}\left(r\,\frac{\partial \theta}{\partial r}\right) = \frac{2\rho v s g}{c}\,(r - r^3/a^2)$$

The solution of this, calling the axial temperature zero is

$$\theta = \frac{2\rho v s g}{c}\left(\frac{r^2}{4} - \frac{r^4}{16a^2}\right)$$

---

* See, *e g*, Nusselt's paper cited below

This gives $3\rho vsga^2/8c$ as the temperature at the tube wall and $\rho vsga/2c$ as the temperature gradient at the tube wall As the heat flow per unit area is c times the latter quantity we get

$$k_0 = 4c/3a$$

on taking the axial temperature of zero as the water temperature

Had we taken the static mean temperature over the cross section viz,

$$\frac{1}{\pi a^2}\int_0^a 2\pi\theta r\, dr = \frac{5}{24}\frac{\rho vsga^2}{c}$$

as the temperature of the water we should have obtained

$$k_0 = 3c/a$$

while if we take the kinematic mean or "mixing temperature" given by

$$\frac{1}{\pi a^2 v}\int_0^a 2\pi u\theta r\, dr = \frac{7}{48}\frac{\rho vsga^2}{c}$$

we get

$$k_0 = 24c/11a = 2\ 182c/a\,*$$

It is interesting to express this last result in the form $\rho vs/k_0$ equal to something with Z^{-1} as a factor We have

$$\rho v^2 Z = R = \mu\left(\frac{\partial u}{\partial r}\right)_{r=a},$$

giving $Z = 4\mu/\rho va$ But we have found

$$\rho vs/k_0 = 11a\rho vs/24c$$

whence, eliminating a we get

$$c_m s/k_0 = 11\sigma/6Z,$$

so that (10) will hold in this case also if we take $\gamma = 0$ and $\alpha = \beta = 11/6$ This known value of α and β for viscous flow was a useful guide in drawing their graphs

APPENDIX B

Calculation of $(k_H - k_0)$ *for Viscous Flow*

This calculation, though quite elementary, is long and tedious so that only the step by step results are given here We will assume that $d\rho/d\theta$ and $ds/d\theta$

---

* It should be stated that this result does not agree with the value given by Nusselt in 'Z Ver Deut Ing,' vol 54, p 1156 (1910), where as the result of a more elaborate analysis, during which he also obtains the initial increase in k_0 before it settles down to its limiting value he gives $k = 2\ 576c/a$ (probably meant for $18c/7a$) There seems, however, no doubt about the correctness of the present result

are negligible and will denote $d\mu/d\theta$ and $dc/d\theta$ by μ' and c'. We will suppose that the temperature at the axis is taken as zero and that μ and c refer to this temperature. We will further suppose that the velocity is adjusted so that the wall friction is *exactly* the same as when μ and c are constant, and that θ is the wall temperature in this *latter* case.

With μ and c variable we find that the wall temperature becomes

$$\theta' = \theta\left\{1 + \left(\frac{29}{324}\frac{\mu'}{\mu} - \frac{1}{2}\frac{c'}{c}\right)\theta\right\}$$

while the temperature gradient at the tube wall and the heat flow per unit area are

$$1 + \left(\frac{7}{18}\frac{\mu'}{\mu} - \frac{c'}{c}\right)\theta \qquad \text{and} \qquad 1 + \frac{7}{18}\frac{\mu'}{\mu}\theta$$

times their previous values respectively. We also find the total flow of liquid through the tube is

$$1 - \frac{13}{18}\frac{\mu'\theta}{\mu}$$

times its previous value; the total heat carried away by the liquid is

$$1 - \left(\frac{97}{126}\frac{\mu'}{\mu} + \frac{29}{105}\frac{c'}{c}\right)\theta$$

times its former value; and the kinematic or "mixing" temperature of the liquid is

$$1 - \left(\frac{1}{21}\frac{\mu'}{\mu} + \frac{29}{105}\frac{c'}{c}\right)\theta$$

times its former value; thus making the difference of temperature between tube and water

$$1 + \left(\frac{35}{198}\frac{\mu'}{\mu} - \frac{106}{165}\frac{c'}{c}\right)\theta$$

times its former value. Dividing the ratio in which the heat flow has been increased by this, we see that

$$k_H/k_0 = 1 + \left(\frac{7}{33}\frac{\mu'}{\mu} + \frac{106}{165}\frac{c'}{c}\right)\theta$$

But this is comparing the new k_H with k_0 for the same *axial* water temperature; if it is compared with k_0 for the same tube temperature (which is greater in the ratio $(c + c'\theta) : c$) we get

$$k_H/k_0 = 1 + \left(\frac{7}{33}\frac{\mu'}{\mu} - \frac{59}{165}\frac{c'}{c}\right)\theta$$

Remembering that by Appendix A, $k_0 = H \div 11\theta/18$ we get

$$k^{H} - k_0 = \left(\frac{42}{121}\frac{\mu'}{\mu} - \frac{354}{605}\frac{c'}{c}\right) H ,$$

that is

$$k_{H} - k_0 = (0\ 347\ \mu'/\mu - 0\ 585\, c'/c)\ H$$

If k_H be compared with k_0 at the same kinematic water temperature it will be found that

$$k_{H} - k_0 = \left(\frac{210}{605}\frac{\mu'}{\mu} - \frac{31c'}{605c}\right) H = \left(0\ 347\frac{\mu'}{\mu} - 0\ 051\frac{c'}{c}\right) H$$

Since we have assumed such a mean velocity that the wall friction, and therefore the loss of head is the same as before , and for viscous flow the loss of head is proportional to the velocity, and as we have seen the total flow is increased in the ratio

$$\left(1 - \frac{13}{18}\frac{\mu'}{\mu}\theta\right)\ 1,$$

it follows that for the *same* total flow the loss of head would be increased in the ratio

$$\left(1 + \frac{13}{18}\frac{\mu'}{\mu}\theta\right)\ 1$$

But, as the loss of head is proportional to the viscosity, this is the same as if there were no heat flow (so that the temperature was constant throughout) and the temperature of the liquid was $13\theta/18$ As $7\theta/18$ is the kinematic temperature of the liquid, and $11\theta/18$ is the difference between this and the tube wall temperature, $= \Delta\theta$, say, it follows that the loss of head is the same as if there was no heat flow and the temperature of the liquid was $6\Delta\theta \div 11$, that is, as if the actual kinematic water temperature was increased by 6/11 of the difference between this temperature and the tube temperature and no heat transfer was taking place

Vertical Electric Currents below Thunderstorms and Showers.

By T. W. Wormell, Ph.D., the Solar Physics Observatory, Cambridge.

(Communicated by C. T. R. Wilson, F.R.S.—Received February 3, 1930.)

[Plates 16, 17.]

1. *Introduction.*

In a previous paper* an account has been given of apparatus which was found to be suitable for studying the discharge of electricity from a raised metal point in the strong electric fields which occur at the surface of the ground during thunderstorms and showers. The two methods of observation which were employed consisted, first, in measuring the quantity of electricity of each sign which was discharged from the point in a definite period of time, usually the duration of a storm; and secondly, in obtaining a continuous record of the current from the point throughout a storm. Observations on a number of thunderstorms and showers over a period of several months, by the first method, showed that there was a considerable preponderance of upward discharges of positive electricity, indicating that negative gradients of potential predominated at the surface of the ground in such disturbed weather conditions. Some examples of records obtained by the second method were also given.

In the present paper, results obtained by the first method over a period of two years are discussed, the observations including all occasions, during that time, on which intense electric fields existed at the observing station for a sufficiently long time to cause a measurable quantity of electricity to be discharged from the point. (The smallest quantity which would be detected by the integrating device is about 0·1 milli-coulomb.) The preponderance of negative potential gradients during periods of intense electric field has been confirmed over the longer period of time. Records obtained by the second method are also described, and their bearing on the question of the polarity of the clouds is discussed. For this purpose, the method of observation is simply a convenient way of obtaining an unambiguous continuous record of the sign of the potential gradient, and a rough estimate of its magnitude throughout periods of heavy rain. Finally, the problem of the total interchange of electricity between the earth and the atmosphere from known causes is re discussed, utilising the results already given

---

* 'Roy. Soc. Proc.,' A, vol. 115, p. 443 (1927).

Throughout this paper the usual convention is adopted of describing the vertical potential gradient at the surface of the ground as positive, when the electric field is directed downwards, and the charge on the ground in the immediate vicinity is negative A bipolar cloud is said to be of positive polarity if the mean height of the positive charge exceeds the mean height of the negative charge

2 *Apparatus*

A full description of the apparatus which was employed in these observations was given in the paper to which reference has already been made It will suffice, here, to say that the integration of the current was performed by a specially designed gas microvoltameter, which gave the quantities of electricity which had passed through the instrument in each direction with an accuracy of about ± 0 5 milli-coulomb The current itself could also be observed by allowing it to charge up a condenser until the potential difference was sufficient to cause a spark to pass across a small gap, the process of the charging and sudden discharge of the condenser being recorded photographically by means of the movement of the meniscus of a special type of capillary electrometer Thus each vertical step on the records of Plate 16 indicates a discharge of the condenser, and the passage to earth of 8 5 micro-coulombs of electric charge The records of the current from the discharging point were supplemented when possible by observations of the electric field The methods used for this purpose were those developed by Prof C T R Wilson* for measuring the electric fields at the surface of the ground due to thunderclouds, and consisted in measuring, by means of the same electrometer as was used for the observations of current, the charge on a raised metal sphere, or other conductor, which was maintained at zero potential Thus, when the field was not large enough to cause an appreciable discharge current, and when no rain was falling, a record of the field itself could be obtained on the plate

3 *The Magnitude of the Currents from the Discharging Point*

(*a*) *Results of Observations with the integrating Apparatus* —It will be convenient to discuss first the results obtained with the discharging point and voltameter This instrument is examined daily, and usually in fine weather no gas collects In showery or thundery weather, the volume of gas produced at each electrode† is measured after each shower or storm whenever the other observations in hand permit, but if the showers are at short intervals, it is often impossible to read the instrument until the other observations are completed for the day. On a few occasions, owing to absence from Cambridge, the reading includes effects produced on several days. On such occasions the values deduced are only approximate, owing to the slow solution of the gas.

---

* 'Roy Soc Proc,' A, vol 92, p 555 (1916), 'Phil. Trans,' A vol 221, p 74 (1920)

In 1926 the voltameter was attached to the discharging point only when no other observations were being made, and the table of results previously published (*loc. cit.*) is therefore somewhat incomplete. At the beginning of 1927 a new discharging pole was erected at a considerable distance from the hut. The discharging point is similar to the old one but the new pole is taller, being 12·3 metres high. The exposure, however, is not so good as at the hut, the new pole being in the centre of a field fringed by fairly high trees. (The nearest tree is about 70 metres from the pole.) The voltameter is permanently connected between this discharging system and earth in order to obtain a complete record of the quantities of electricity discharged from the pole in periods of intense electric fields. The results obtained are not strictly comparable with the results previously published owing to the different dimensions of the new pole. The results of observations with this apparatus from January, 1927, to December 31, 1928, are tabulated below. All the quantities are in *milli-coulombs*. The column headed q_1 gives the quantity of positive electricity discharged from the point, q_2 is the quantity of negative electricity discharged, and the next column gives the net upward discharge from the point. Notes concerning the weather conditions are frequently given. The accuracy of each individual entry is about ± 0·5 milli-coulomb.

Table I

Date		Milli coulombs			
		q_1	q_2	$q_1 - q_2$	
1927					
January	26	0	0·7	− 0·7	Fine weather *
	27	0	0·1	− 0·1	Slight showers
	28	18·0	2·5	+15·5	Hours of heavy rain with gale
	30	0·7	0·7	0	Slight rain

* *See* para. 3, p. 574.

† From the separate measurements of the volume of gas liberated from each electrode it is possible to deduce the quantity of electricity of each sign which has been discharged from the point.

Table I -(continued)

Date		Milli coulombs			
		q_1	q_2	$q_1 - q_2$	
1927					
February	2	1 1	0	+ 1 1	
	5	0 1	0 1	0	
	8	1 1	0	+ 1 1	
	14	0	1 0	− 1 0	Three days of dense fog *
	16	0	0 2	0 2	Fog *
	21	6 0	0 5	+ 5 5	Several hours of rain
	22	0 1	0	0 1	Slight rain
	24	28 5	3 3	25 2	Heavy shower followed by hours of steady rain
	26	1 5	0 5	1 0	
	28	9 1	0	9 1	Several hours of heavy rain
		1 2	0	1 2	Brief shower
March	1	2 7	0 3	2 4	Shower
	3	0 1	0	0 1	
	5	2 2	1 3	0 9	Very heavy shower
	8	8 1	2 6	5 5	Brief but heavy showers
	14	2 1	4 5	2 4	
	18	0	0 6	− 0 6	Several days of fine weather *
	22	0 1	0 1	0	
	23	0 8	0	+ 0 8	Brief shower
	24	0 6	0	0 6	Shower
	25	9 1	1 5	7 6	Heavy showers
		5 5	5 5	0	Heavy showers with hail
	26	1 1	0	1 1	Shower
		4 3	2 3	2 0	Heavy showers
	27	18 6	2 6	16 0	Heavy showers A few lightning discharges took place, the nearest ones being approximately 5 kms from the observatory
	30	0 7	2 5	− 1 8	Several showers of which only the extreme edges passed overhead
		0 4	1 0	− 0 6	Further showers
April	1	5 0	0	+ 5 0	
	2	0 6	5 3	− 4 7	Showers
	4	2 5	0	+ 2 5	
	6	0 4	0	0 4	Slight shower
	8	1 5	0 4	1 1	Shower cloud developing not quite overhead
	9	1 1	0 1	1 0	Shower
		4 5	2 0	2 5	Showers
	24	1 9	0 4	1 5	
	25	1 1	1 1	0	
	26	1 1	0	+ 1 1	Showers and prolonged heavy rainfall
		0	2 3	− 2 3	Shower with sleet
May	16	0 3	0	+ 0 3	Slight showers
		1 8	0 5	1 3	Heavy shower
	21	0 4	0	0 4	Slight shower
		4 6	3 0	1 6	Showers
	23	2 5	4 5	− 2 0	Showers These did appear to pass overhead
	31	0 8	1 2	0 4	Rain.
June	8	2 5	3 9	− 1 4	Showers during the night
		1 8	1 8	0	Steady rain for an hour
	19	7 9	2 4	+ 5 5	Heavy showers
	21	0 3	0	0 3	

Table I (continued)

Date		Milli coulombs			
		q_1	q_2	$q_1 - q_2$	
1927					
June	23	3·3	2·7	0·6	Heavy shower
		1·2	0·5	0·7	
	24	13·2	4·6	8·6	Heavy thunder shower passed overhead
	26	0·5	0·7	0·2	Showers
	27	9·5	1·5	+8·0	Showers
		0·2	0	0·2	
	28	4·6	1·3	3·3	Showers and distant thunderstorms
July	6	4·0	4·0	0	
	7	15·3	11·5	+3·8	Heavy rain for most of the night
		1·2	0·6	0·6	
		4·7	2·4	2·3	Moderate thunderstorm passed overhead
	9	3·2	0	3·2	Rain
	27	0·8	0	0·8	Showers
		3·1	3·1	0	Thunderstorm
August	22	7·2	2·8	+4·4	Result of absence for 3 weeks
		0·1	0·3	−0·2	
	24	0·2	0·9	−0·7	
	25	0·4	0	+0·4	
		0·3	0·1	0·2	
September	10	1·8	2·3	−0·5	Thunderstorm nearest flashes about 6 kms away
	15	0·3	0	+0·3	
	24	5·0	0	5·0	Heavy rain and strong wind
	24	0·3	1·3	−1·0	
	26	1·7	0·5	+1·2	
	30	0·6	0	0·6	
October	8	0	0·5	−0·5	Fog *
	15	0·2	0·2	0	
	24	3·7	0·5	+3·2	Prolonged rainfall
	28	0	0·2	−0·2	Rainfall for 24 hours
	31	0·6	0	+0·6	Heavy rain
November	7	1·4	0·1	1·3	
	8	2·1	0·9	1·2	A shower
	12	3·0	4·0	−1·0	Showers
	28	2·0	1·5	+0·5	Drizzle and rain
	29	13·0	0	13·0	Heavy rain for several hours
December	12	0	0·7	−0·7	Overcast sky little rain
	16	0	0·2	−0·2	Slight fall of snow
	19	0	3·0	−3·0	Slight fall of snow
	26	8·8	25·8	−17·0	Heavy drifting snow which lay till January 1 The voltameter was read on January 3 after a day of rain
1928					
January	6	2·8	0·8	+2·0	Showers
	13	0	1·4	−1·4	Rain.
	19	0·4	0·8	−0·4	Prolonged rain
	21	0·8	0·5	+0·3	Fog followed by drizzle
	24	1·0	1·0	0	
	31	0·6	1·3	−0·7	Rain and sleet

Table I—(continued)

Date		Milli coulombs q_1	Milli coulombs q_2	Milli coulombs $q_1 - q_2$	
1928					
February	2	9·3	0·7	+ 8·6	Very heavy shower.
	4	0	1·5	− 1·5	Rain and drizzle.
	5	2·0	0	+ 2·0	Showers with hail.
	10	7·5	0·8	6·7	Very heavy hail showers. A few lightning discharges occurred.
	16	1·2	0·3	0·9	
March	8	0	1·6	− 1·6	
	9	2·0	1·4	+ 0·6	Shower.
	23	0·4	0·3	0·1	
		0·7	0·4	0·3	
		3·0	2·7	0·3	
	30	1·6	0·8	0·8	
	31	1·0	0·7	0·3	
		15·2	10·3	4·9	Several hours of heavy rain during the night.
April	4	2·0	1·0	1·0	Showers.
	5	10·7	0·2	10·5	Shower-cloud passing and developing. Fringe of cloud overhead. One peal of audible thunder.
	8–17	0·8	0·6	0·2	Several showers.
	18	0	3·7	− 3·7	Heavy shower.
		0·1	0·5	− 0·4	Slight showers.
	20	1·3	0·2	+ 1·1	Heavy shower with sleet followed by several hours of rain.
	22	2·6	0	2·6	Overcast with occasional slight rain.
May	3	6·3	5·4	0·9	A sharp thunderstorm about 3.0 a.m. Flashes were occurring at about 4 per minute and many were striking the ground. A tree was struck 150 metres from the discharging pole. Rainfall extremely heavy.
	16	17·3	16·1	1·2	Several hours of heavy rain followed by showers.
		0·7	0	0·7	Slight rain.
	17	8·0	1·1	6·9	Several showers. One peal of thunder audible.
	18	3·1	0·8	2·3	Several showers.
	20	24·8	13·1	11·7	Thunderstorm of moderate intensity passed slowly right overhead. Several flashes were within 1 km.
		4·9	0	4·9	
June	5	0·5	0·3	0·2	Heavy rain.
	6	3·6	1·2	2·4	Moderate thunderstorm passed rapidly overhead.
	13	3·3	1·8	1·5	Very heavy showers.
	16	1·2	2·3	− 1·1	Showers. One lightning discharge about 10 kms. away.
	19	0·7	0·3	+ 0·4	Slight showers.
	26	1·5	1·2	0·3	Heavy shower which developed into a thunderstorm after passing over.
	30	0·7	1·3	− 0·6	Moderate showers.
July	3	0·5	0	+ 0·5	Hours of steady rain.
	27	2·9	4·6	− 1·7	

Table I—(continued)

Date		Milli-coulombs			
		q_1	q_2	$q_1 - q_2$	
1928					
July	27	3·2	1·2	+ 2·0	Showers of thundery type Distant thunder
	30	0·7	0·1	0·6	Heavy rain
August		25·2	16·1	9·1	
September	18	3·0	1·0	2·0	
	25	3·7	0	3·7	
	28	0·8	0	0·8	Short shower
October	8	1·4	2·9	− 1·5	Showers of moderate intensity
	9	5·5	3·6	+ 1·9	Showers
	19	3·9	0	3·9	Showers and continuous rain
	23	7·2	1·2	6·0	Heavy rain
	24	0·7	0	0·7	Heavy shower
	26	0·5	0·7	− 0·2	Showers
November	12	0	1·3	− 1·3	Continuous rain for several hours
	24	1·3	0	+ 1·3	Heavy rain and showers
	26	4·6	2·1	2·5	Heavy showers and squalls
December	19	2·6	2·2	0·4	
	21	2·9	0	2·9	Moderate rainfall
	31	22·5	0·5	22·0	Much heavy rain and some snow
		0	0·3	− 0·3	Showers

Over the whole period there is a definite excess of upward discharges of positive electricity from the point, the total expressed in *coulombs* being as follows* —

	1927	1928	Total
Positive or upward discharges	$0·28_4$	$0·23_7$	$0·52_1$
Negative discharges	$0·14_2$	$0·11_6$	$0·25_8$
Net upward transfer of electricity from the single point	$0·14_2$	$0·12_1$	$0·26_3$

In order to demonstrate the consistency with which this excess of upward discharges occurs, the totals for periods of three months have been drawn up in the table below, the quantities here being expressed in *milli-coulombs*

---

* In 1929, the results were again of about the same magnitude, the net discharge of positive electricity being 0·11 coulomb

——	q_1	q_2	$(q_1 - q_2)$
1927			
1st quarter	123	34	89
2nd ,,	75	40	35
3rd ,,	50	30	20
4th ,,	35	38	−3
1928			
1st quarter	49	27	22
2nd ,,	94	51	43
3rd ,,	40	23	17
4th ,,	53	15	38

The one exception to the uniform positive sign of the quantities in the last column is due mainly to the large excess of downward current (indicating a predominance of positive potential gradients) which accompanied the exceptionally heavy snowstorm of December 25 26, 1927, when heavy snow drifts formed near the discharging pole †

A few of the entries in Table I call for special mention There is normally no detectable discharge current from the point in fine weather, but on a few occasions near the maximum in the annual variation of the fine weather electric field a small downward discharge current could be detected, of the order of 10^{-8} ampere, when the sky was free from cloud It would appear that occasionally this current may become big enough to give bubbles in the voltameter which are sufficiently large to be measured Thus the entries of January 26 and March 18, 1927, were apparently due to fine-weather current Again, during fogs, appreciable downward currents were sometimes recorded, *e g*, February 14 and 16, 1927 The occurrence of fairly large positive gradients of potential in fogs is a well-established phenomenon

If we exclude the few cases which come under these two heads, marked with an asterisk in Table I, all the remaining entries are effects of the potential gradients associated with precipitation Of the 147 entries in the table when the effects were associated with precipitation, 103 show an excess of upward current, 34 an excess of downward current, and in 10 the net discharge was zero

If we now classify these readings according to the magnitude of the quantity discharged up or down, whichever happened to be greater, we obtain the

---

† Previous observers have remarked on the association of high positive gradients of potential with the occurrence of drifting snow See, for example, Simpson, "British Antarctic Expedition, 1910–13," 'Meteorology,' vol 1, p 309

A

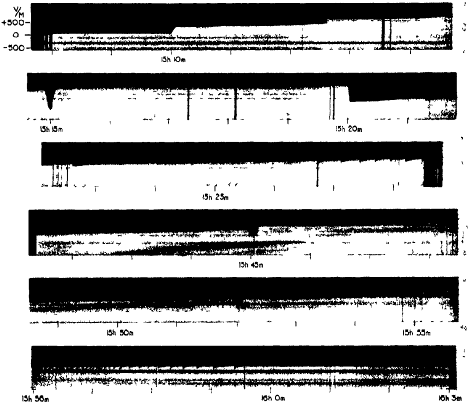
V/M
+500
0
-500
15h 10m
15h 15m
15h 20m
15h 25m
15h 45m
15h 50m
15h 55m
15h 56m
16h 0m
16h 5m

B

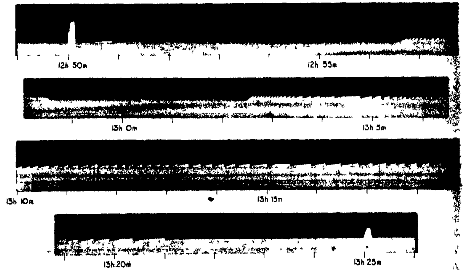
12h 50m
12h 55m
13h 0m
13h 5m
13h 10m
13h 15m
13h 20m
13h 25m

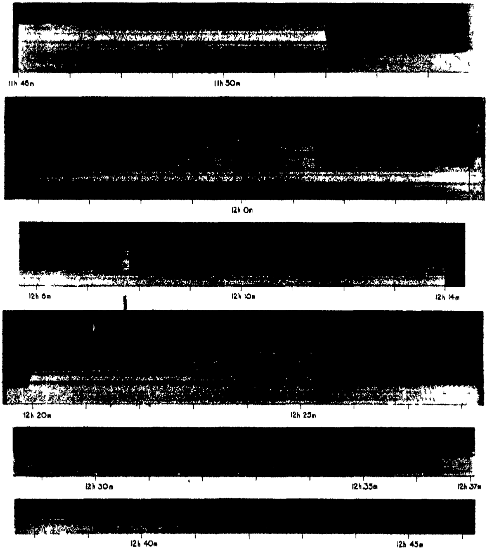
11h 46m
11h 50m
12h 0m
12h 6m
12h 10m
12h 14m
12h 20m
12h 25m
12h 30m
12h 35m
12h 37m
12h 40m
12h 45m

following table showing the number of occasions on which the net effect was an upward or downward discharge current.

Greatest quantity discharged in one direction, in *milli coulombs*	Number of occasions of		
	Excess of upward current	Excess of downward current	Net effect zero
> 20	4	1	0
10–20	8	0	0
5–10	15	1	1
3–5	18	7	2
1–3	32	14	3
< 1	26	11	4

This table may be summed up in the statement that, when the quantity discharged in either direction was greater than 5 milli-coulombs, there were 27 occasions of a net upward discharge and only 2 of a net downward discharge (one of these being in exceptional weather conditions), when the discharge in each direction was less than 5 milli-coulombs there were 76 occasions of a net upward discharge and 32 with a net downward discharge.

It must be borne in mind that the duration of the electric fields, which caused the discharge of these various quantities from the point was very different on different occasions. The results indicate, however, that the predominance of upward currents and of negative gradients of potential is much more marked when fields are very intense (frequently of the order of 10,000 volts per metre), than during rainfall in which the maximum fields are only of moderate intensity (of the order, perhaps, of 1000 volts per metre). In cases of the latter type, although occasions of preponderating positive potential gradients are relatively more frequent than in the cases where very intense fields occur, yet, even in such cases they are less frequent than occasions of preponderating negative potential gradients.

This generalisation would appear to be true both of isolated shower clouds, and of occasions of persistent rainfall.

(*b*) *The Variation of the Current and Electric Field as a Single Shower passes overhead.*—In Plate 16, A, and fig. 1 are reproduced a series of enlargements from the original records, and a curve deduced from them, showing the variations in current and field obtained during a very heavy shower on March 27, 1927. The cloud was a typical cumulo-nimbus cloud with "anvil" top. On this occasion there were no other clouds in the vicinity throughout the period of the observations There were, however, some distant shower-clouds in some of which lightning discharges were occurring The record shows the variation

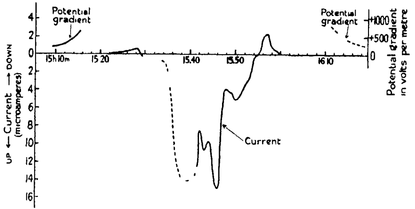

Fig 1 —March 27, 1927

In all the figures the curve is drawn as a continuous line where it is deduced from a photographic record, and as a broken line where it is plotted from visual observations

of current and field as the cloud travelled overhead The first portion of the record is of the potential gradient, while the cloud was approaching from a distance The sphere* was raised at 15 h 10 m , the potential gradient was then positive and had a value of about + 200 volts per metre The value of the positive potential gradient soon began to increase steadily as the cloud drew nearer, if the effects of some distant lightning discharges are neglected, and at 15 h 15 m , when the sphere was lowered for a few seconds, had reached a value of + 600 volts per metre At 15 h 20 m , when the sphere was lowered and shielded, a downward discharge current had commenced and it gradually increased in magnitude until 15 h 28 m , indicating that the positive potential gradient was still increasing Visual observations showed that the potential gradient remained positive until about 15 h 33 m , when it reversed in sign, and very soon there was a large upward discharge current Heavy rain began to fall at the observing station at about the same time that the reversal of the field occurred The record shows that this upward current, and consequently a negative potential gradient, persisted until 15 h. 55 m , heavy rain falling throughout this period The centre of the shower was overhead at about 15 h 45 m From 15 h 55 m onwards a slowly decreasing downward discharge current, indicating a positive potential gradient, was observed After the end of the photographic record, visual observations showed that as the cloud receded into the distance the positive potential gradient gradually decreased

* C T R Wilson, *loc cit*

until it approached the fine weather value Values of + 600, + 400 and + 200 volts per metre were observed at 16 h 13 m, 16 h 15 m, and 16 h 24 m, respectively By this time the cloud had receded to some considerable distance, and overhead the sky was quite free from cloud

During the period of heavy rainfall the test plate was exposed for a few seconds at 15 h 45 m, 15 h 48 m, and 15 h 52 m It must be pointed out, however, that the test plate* is quite close to the discharging pole —(4 metres from the base of the pole)—and that consequently the field measured at the test plate may be diminished by the space charge discharged from the point, and also that the charge on the rain may be affected by falling through part of this space charge Thus, neither the observed value of the field, nor the observed sign of the charge on the rain, can be taken as fair samples of the effects which would be observed over open ground Definite evidence has since been obtained that the discharging point does exercise an appreciable shielding effect on the test plate in intense fields The record shows, however, that, on this occasion, the electric field at the surface of the test plate was about 8000 volts per metre at 15 h 45 m and about — 4000 volts per metre at 15 h 48 m and 15 h 52 m The charge on the rain when it reached the test plate was positive at 15 h 45 m, negative at 15 h 52 m, and could not be detected by this rough observation at 15 h 48 m

Plate 16, B, and fig 2 show the variations in discharge current and electric field as a shower cloud passed overhead on March 26, 1927 Before the shower-cloud approached, the sky was clear overhead and there were no other clouds in the neighbourhood The first observation, as the cloud was approaching, showed at 12 h 50 m when the sphere was raised for a few seconds, a positive

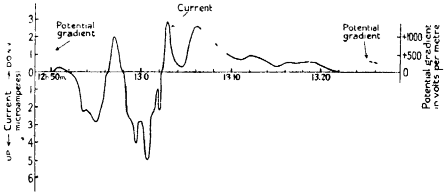

FIG 2 —March 26, 1927

---

* C T R Wilson *loc cit*

potential gradient of 550 volts per metre, which was increasing A minute later, the downward discharge current had become appreciable and just one spark passed The front edge of the cloud was now just about overhead and slight rain was beginning to fall The positive potential gradient now decreased again, and reversed, and just before 12 h 53 m sparks began to pass, due to an upward discharge current Just as this upward current started the rain became very heavy and some hail fell The upward current reached a maximum value of 2 8 microamperes and just after 12 h 56 m its sign reversed again, remaining downwards for about 2 minutes The current then became upwards again, this reversal again being associated with an increase in the intensity of rainfall after a temporary lull In this period the upward current reached a maximum value of 5 0 microamperes At 13 h 2 5 m the current became downward and remained so until it gradually became inappreciable at about 13 h 22 m The rear edge of the shower was overhead at about 13 h 10 m and another shower-cloud was now passing fairly near, but to one side of the observing station This second cloud was never sufficiently close to cause rain at the discharging pole The long persistent downward current and positive gradient of potential at the end of this record are almost certainly due, partly to the effect of this second cloud passing on one side, and partly to the receding shower which has passed over At 13 h 25 m the potential gradient had diminished to + 260 volts per metre, measured with the sphere , this is still somewhat greater than the fine weather field The sky overhead was now free from cloud

Plate 17 and fig 3 represent the results of records obtained on March 30, 1927 On this occasion several shower-clouds passed near the apparatus but in no case did the centre of the cloud pass overhead As the first cloud was approaching, the potential gradient was observed to increase from + 50 volts per metre to about + 100 volts per metre The photographic record then

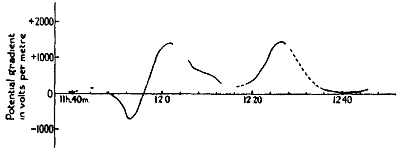

Fig 3 —March 30, 1927

commences At 11 h 46 5 m the potential gradient had decreased to + 37 volts per metre, the sphere being raised for a few seconds It was then raining slightly The rainfall increased and became heavy for a few seconds but there was no appreciable discharge current At 11 h 50 m the sphere was raised again for a few seconds, the potential gradient being — 130 volts per metre The rain now stopped and at 11 h 52 m the sphere was raised and left in position The potential gradient was now — 600 volts per metre and soon after this there was a small upward discharge current The subsequent variations in the field are shown in the curve of fig 3 The active portion of the cloud was never very near and, as the positive potential gradient decreases from 12 h 5 m onwards, the cloud was definitely receding Later, the positive gradient of potential increased again as the fringe of another shower-cloud passed overhead

Fig 4 represents the variations in discharge current and electric field as a shower passed over on March 26, 1927 The cloud covered a fairly wide area

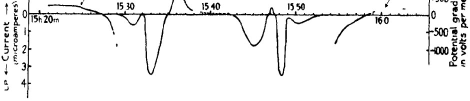

FIG 4 —March 26, 1927

and passed overhead, but the rainfall at the observing station was never very heavy Regions of heavier rainfall appeared to pass on both sides and this rather suggests that these may have been two regions of electrical activity A positive gradient of potential was observed at the beginning and end although the field scarcely exceeded the fine-weather value in either case The positive potential gradient near the centre, at 15 h 36 m coincided with a temporary cessation of rainfall at the observing station In the most intense fields, which occurred when the rainfall was heaviest, the potential gradient was negative Fig 5 shows a record with a distribution of field of an unusual type As the shower-cloud approached, it had the appearance of a grey sheet of stratiform cloud and was therefore probably of rather small vertical thickness The electric field had been very small for some time and the approaching cloud did not produce any appreciable effect until the front edge of the cloud was almost overhead, when the potential gradient became negative and increased rapidly The subsequent variations in field are shown by the curve The heaviest

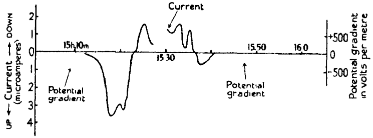

FIG 5 —May 21, 1927

rainfall occurred during the period of negative potential gradient near the beginning The rain was slight during the period of positive potential gradient in the middle of the record and ceased altogether about 15 h 37 m As the cloud receded, a slowly decreasing negative potential gradient was observed

4 *Interpretation of the Records*

In endeavouring to interpret these results it must be noted that the intense electric fields which have been studied have been almost invariably associated with precipitation or with clouds of cumulus type, and consequently with vertical air convection currents Thus, whatever the mechanism of the production of the electrical charges in such cases, the primary effect will consist in the vertical separation of equal and opposite charges The various processes of dissipation of the charges will be very different for the upper and lower charges, and consequently the two charges in the cloud may become very unequal, but a vertically bipolar cloud will tend to be produced One would expect that a shower-cloud or a thunder-cloud in which the lightning discharges were infrequent, would after a time reach an approximately steady condition such that the rate of dissipation of each charge was equal to the rate of separation of charges in the cloud This suggestion derives considerable support from the form of the "recovery-curves" of the electric field after a lightning-discharge, which are such a remarkable feature of the records of the electric fields of thunderstorms obtained by Wilson (*loc cit*) If one examines the record of the field due to a fairly distant and approximately stationary thunder-cloud in which the discharges are not very frequent, it will be observed that immediately after a discharge, the field varies rapidly, the magnitude of the rate of variation per second being frequently about one-seventh of the sudden change in field produced by the discharge The rate of variation of the field soon decreases, however, and the field frequently reaches a steady value which may remain constant for several minutes until another discharge occurs There is thus some justification for hoping that one may in some cases observe, as a shower cloud passes overhead, variations in field due mainly to the motion of the cloud as a whole, in an approximately steady condition, over the observing station There will in all cases be some uncertainty in deciding what part of the variation in the field at a given point with time, can be ascribed to a motion of the cloud as a whole, and what part is due to variations of the electrical charges in the cloud It seems worth while, however, to compare the observations of the mode of variation with time of the electric field at a single point on the ground, with the effects which would be produced if a cloud with constant electrical charges passed overhead

The observed preponderance of negative gradients of potential would seem to indicate at once, that, in the majority of clouds, either the negative charge is below the positive charge, or that the negative charge is much greater than the positive charge In order to decide between the two possible interpretations, it is necessary to consider the actual distribution of fields which has been found to occur beneath shower-clouds The distribution of electric field at the ground, produced by a vertical bipolar cloud of the type considered, depends very greatly on the way in which the charges are distributed through the volume of the cloud The case in which the two charges are so distributed that they can be treated as if each was concentrated at a point was first discussed by Wilson (*loc cit*) It is possible however, to obtain some information from observations of the field without making any assumptions as to the actual distribution of the charges

The field due to a cloud at a distance, L, large compared with the dimensions of the cloud is given by the equation

$$F = 2\{Q_1h_1 - Q_2h_2\}/L^3,$$

where Q_1 and Q_2 are the magnitudes of the total positive and negative charges respectively in the cloud, and h_1 and h_2 are the mean heights of these two charges Thus the sign of the potential gradient due to a distant cloud is the sign of the quantity $2(Q_1h_1 - Q_2h_2)$, which may be called the electric moment of the cloud

In practice a difficulty may arise in that, at very great distances from the shower-cloud, the vertical field which it produces will be so small that it cannot be disentangled either from the normal positive potential gradient, which occurs in the absence of clouds, or from the effects of other clouds , on the other hand, it is necessary to make the observations at a considerable distance from the shower-cloud in order to obtain definite evidence of the sign of the moment of the cloud In a number of cases, however, the effects of isolated shower-clouds can be traced to distances exceeding 10 kilometres When, in such cases, the potential gradient due to the distant cloud has the same sign, both when the cloud is approaching and when the cloud is receding after passing over, and in each case diminishes in intensity with increasing distance, then one may deduce fairly definitely the sign of the total electric moment of the cloud If moreover the predominating sign of the intense potential gradient when the cloud is overhead, is the reverse of the smaller gradients observed while the cloud is distant both when approaching and when receding, the evidence becomes still more conclusive, and strongly suggests that the sign, both of the electric moment of the cloud, and of its polarity, is the same as the sign of the potential gradient due to the cloud when at a considerable distance from the observing station These points can best be elucidated further during a study of individual records from the point of view of this paragraph

The shower recorded in fig 1 gave a positive potential gradient as it was approaching and again as it was receding This shower was, moreover, observed until its distance was estimated to be at least 15 kilometres There were throughout the record no other clouds sufficiently close to cause any ambiguity in the sign of the field due to the cloud which was being studied One can thus say definitely that this cloud had a positive electric moment while it was approaching and also while it was receding Thus in the notation previously employed, $Q_1h_1 > Q_2h_2$ Again, while the cloud was overhead, and throughout the period of heavy rainfall, the potential gradient was uniformly negative and was much greater than any positive gradients of potential which occurred during this record The conclusion would seem to be that this was a cloud of positive polarity, the negative charge being, on the whole, below the positive In the notation employed above, $h_1 > h_2$

The only possible way of escaping from this conclusion would be to postulate a very rapid change in the charges in the cloud just as the front edge was passing over the observing station, and, again, an opposite series of changes, equally rapid, just as the rear edge was passing over the station Even if it is possible for such changes to occur with sufficient rapidity, it would be a remarkable coincidence that this double series of changes had occurred just at the correct instants to cause the whole record to simulate so closely the effects which would be produced if a cloud of positive polarity, with approximately constant charges, had passed overhead It is much more probable that we were indeed actually observing the effects of a cloud of positive polarity Moreover, there is no escape from the conclusion that the moment of the cloud was positive while the cloud was approaching, and while it was receding

Unfortunately, the records obtained are rarely so simple as in the case just discussed In the record of fig 2, for example, a positive potential gradient was again observed as the cloud was approaching When the cloud had passed over, the observations were complicated by the proximity of a second cloud, the two clouds together producing a positive gradient when in the distance A great preponderance of negative gradients of potential was observed beneath the central portion of the cloud, and the gradient was always negative in regions of heavy rainfall Again it would seem that we are dealing with clouds of positive polarity

Fig 3, again, was a record obtained while two clouds passed successively somewhat to one side of the observing station, the fields never becoming very intense

The edge of the first cloud passed overhead and some rain fell, just at this time the potential gradient was negative The second cloud also passed definitely to one side, very little rain falling from it at the place of observation The second cloud was nearest to the observing station at about 12 h 30 m The record suggests that the electric moment of both clouds was positive, *i e*, $Q_1h_1 > Q_2h_2$ The small region of negative potential gradient just as the centre of the first cloud was nearest to the observing station suggests that this cloud, at least, was also of positive polarity The persistence of the positive potential gradients was, however, unusual The whole record is in accordance with the view that two clouds of positive polarity were being observed, and that in each case the upper positive charge was greater than the lower charge It was noted at the time that the vertical thickness of these clouds appeared to be rather small The rate of dissipation of the upper charge might consequently have been less than usual

Fig 4 was inserted as an example of the complicated records which are sometimes obtained, and from which it is scarcely possible to draw any definite conclusions with regard to the polarity of the cloud concerned

The record of fig 5 is an example which definitely suggests a cloud of negative polarity, in that the main phenomena observed were two regions of negative potential gradient with a region of positive potential gradient between them In this case, however, the most intense fields and the heaviest rainfall occurred in the region of negative potential gradient at the beginning of the shower

The few records which have been discussed in detail have been selected more or less at random, or on account of the suitability of the plates for reproduction and of the occurrence of fairly definite and unambiguous meteorological conditions , they are quite typical of the type of record which has frequently been obtained The records considered were interpreted tentatively as follows The first two, represented in figs 1 and 2, were interpreted as indicating the presence of clouds of positive polarity Fig 3 did not give very definite evidence but suggested a cloud of positive polarity rather than the reverse Fig 4 could yield no definite conclusion as to polarity Finally fig 5 was interpreted as due to a cloud of negative polarity Similar records were obtained when the conditions were fairly definite and the effects could be ascribed apparently to single shower-clouds on 22 occasions during 1927 An attempt has been made to interpret all these records on similar lines The results were as follows —

Definite indication of a cloud of positive polarity	6	occasions
Definite indication of a cloud of negative polarity	2	,,
Interpretation doubtful but positive polarity suggested .	4	,,
Interpretation doubtful but negative polarity suggested	2	,,
No definite evidence of polarity of either sign	8	,,

In the majority of records included under the last head, the changes of sign of the current and electric field were very complicated, and frequently the sign of the field when the cloud was approaching was the reverse of that observed when the cloud was receding

Of these 22 records, in 14 cases the maximum upward current was greater than the maximum downward current, in 7 cases the reverse was true, in 1 case the maximum current in the two directions was equal Again, if we select the occasions when the electric fields were very intense by considering only these records in which the current in one direction or the other exceeded 5 microamperes at some time during the shower, we are left with only 6 records Of these 4 were interpreted as being definitely due to a cloud of positive polarity, 1 as being probably due to a cloud of positive polarity, and 1 yielded no definite indications of polarity

To sum up, the observations have definitely shown that shower-clouds have, frequently, positive electric moments Indeed, in the majority of cases where definite observations could be made, the moment of the cloud was found to be positive This result and the previously established result of the great preponderance of negative fields below the clouds, which has been shown to be true both generally by observations with the voltameter, and also, in detail, for the particular clouds now being considered, have been interpreted as indicating that many of the clouds were of positive polarity This result is in agreement with the interpretation which Appleton,* Watson-Watt and Herd, and Schonland† have placed upon the observations by Wilson and by themselves, of the changes of electric field produced by lightning discharges The result, on the other hand, is not considered to be in agreement with the very definite distribution of electric charges in a typical cumulo-nimbus cloud, which Simpson‡ has suggested, to account for the observations on lightning discharges

5 *The Total Exchange of Electricity between the Earth and the Atmosphere*

It seems desirable to attempt a rediscussion of the problem of the interchange of electricity by known processes between the ground and the atmosphere, using the results of the observations which have been tabulated in this paper An endeavour will be made to estimate as accurately as possible the sign and magnitude of the total effect, in the course of a year, of the main processes which are known to transfer electrical charges from the atmosphere to the earth or in the reverse direction The four main processes which will be considered are, first, the ionisation current of fine weather, secondly, the convection of electrical charges by precipitation, thirdly, the charges transferred by lightning discharges, and, fourthly, the currents carried by point-discharges in periods of disturbed weather conditions For definiteness, a circular area of 1 square kilometre, surrounding the observatory where the observations on point discharges were made, will be considered For the mean value of the fine-weather current, a downward current of 2×10^{-6} amperes per square kilometre will be assumed If the duration of disturbed weather conditions is neglected, the total effect in the course of a year would be about 60 coulombs per square kilometre

No systematic series of observations of the charge caused by rain has been made in Cambridge, but an estimate of the order of magnitude of the effect may be made from the results of numerous observers elsewhere The values of the mean charge per cubic centimetre of precipitation, found by various observers vary from + 0 176 e s u according to Simpson at Simla,§ to + 0 029 e s u according to Schindelhauer at Potsdam * Assuming an annual rainfall of 60 cm , Simpson's value would indicate the convection of + 34 9 coulombs per square kilometre to the ground per year, that of Schindelhauer + 5 7 coulomb per square kilometre per year Simpson's value is almost certainly too high for conditions in this country, the great majority of his observations being made on thunderstorm rains We shall assume a value of + 20 coulombs per square kilometre per year It would thus appear probable that the two processes considered, transfer a positive charge of the order of 80 coulombs per square kilometre per annum to the ground

---

* 'Roy Soc Proc,' A, vol 111, p 654 (1926)

† 'Roy Soc Proc,' A, vol. 114, p 229 (1927), and vol 118, p 233 (1928)

‡ 'Roy Soc Proc,' A, vol 114, p 376 (1927)

§ 'Phil Trans,' A, vol 209, p 379 (1909)

The transfer of electricity between the atmosphere and the ground by the mechanism of lightning discharges must next be considered It is necessary to obtain an estimate of the mean number of lightning discharges which actually reach the ground within the given area per annum Discharges which do not reach the ground may cause a transfer of electricity to the ground, but the chief mechanism will be that of the point-discharge currents in the intense electric field existing near the ground immediately after the discharge The electrical charges which reach the ground in this way will be included in the estimate of the total discharge current based on the quantities discharged from the artificial point and registered by the voltameter The records of the changes of electric field accompanying lightning discharges, which have been obtained by Wilson and others, make it possible to estimate what fraction of the total number of lightning discharges occurring over the area, reach the ground, and also the relative numbers of these discharges carrying positive and negative charges to the ground respectively Wigand† has discussed this problem but his method of treatment of the available data is unsatisfactory and it seems desirable to discuss the matter in some detail

In discussing the effect of lightning discharges on the electric field, a sudden increase of a positive potential gradient or a decrease or a reversal of a negative potential gradient will be described as a positive field-change Wilson (*loc cit*) records that at Cambridge for discharges within 5 km of the observing station, the numbers of positive and negative field-changes were in the ratio 4 6 1 On the other hand, Appleton, Watson-Watt, and Herd (*loc cit*) observed at Cambridge for discharges at a considerable distance, a ratio of the numbers of positive and negative field changes of 1 1 5_3 Let us suppose that out of every 100 lightning discharges occurring at Cambridge, N_1 bring a negative charge to the ground, N_2 a positive charge to the ground , the N_1

---

* 'Abh K Preuss Met Inst ,' No 263 (1913)

† 'Phys Z ,' vol 28, p 2 (1927)

discharges will cause positive field-changes, and the N_2, negative field-changes, at all distances It is probable that the only other common type of discharge is a flash which does not reach the ground but which effectively lowers the height of a positive charge in the atmosphere The effect of such a discharge on the field reverses beyond a certain distance Let N_3 be the number of discharges which cause a positive field change when near the observing station, a negative field change when distant

If we neglect other types of discharge we have at once

$$N_1 + N_2 + N_3 = 100$$
$$N_1 + N_3 = 4\ 6\ N_2$$
$$N_2 + N_3 = 1\ 5\ N_1,$$

whence $N_1 = 40$ per cent , $N_2 = 18$ per cent , $N_3 = 42$ per cent

If we suppose there are also N_4 discharges causing negative field changes among the near discharges, but positive changes among the distant ones, then —

$$N_1 + N_2 + N_3 + N_4 = 100$$
$$N_1 + N_3 = 4\ 6\ (N_2 + N_4)$$
$$N_2 + N_3 = 1\ 5\ (N_1 + N_4)$$

We deduce at once

$$N_2 + N_4 = 18 \text{ per cent}, \quad N_1 + N_4 = 40 \text{ per cent},$$

and again

$$N_1 - N_2 = 22 \text{ per cent}$$

It remains to consider the possibility that a lightning discharge may completely discharge a cloud to the earth, the effect being recorded as a single net field change If the two charges in the cloud were very unequal, the effect would be the same as if a single charge, of the sign of the greater charge in the cloud, had been transferred to the earth, and discharges of this category will have been automatically included in the correct class, N_1 or N_2 according to the sign of the predominating charge If, however, the two charges in the cloud are not very different in magnitude a discharge of this type will produce an effect on the field, which reverses beyond a certain distance, and it becomes possible that some of the N_3 (or N_4) discharges were of this type, and therefore transferred a charge to the ground The data do not suffice to determine the proportion of discharges of this type Multiple changes of field are, however, observed so frequently in the records that one may expect that a discharge of this type would be usually separated into different steps, each stage being assigned to its correct category Moreover, the effect of the discharge is to transfer to the ground a charge equal to the difference between the magnitudes of the two charges in the cloud This difference may be small and of either sign The effect of such discharge will therefore be neglected, and it will be assumed that, approximately, the total net effect of the lightning flashes is that one-fifth of the total number bring down a negative charge to the ground The main source of uncertainty in the estimate is probably that the number of close discharges which have been recorded, is rather small for it to be regarded as a reliable sample of the average thunderstorm The electric charge carried by an average lightning flash is known quite reliably to be of the order of 20 coulombs The average number of days on which thunder is reported at Cambridge per annum is 12 Brooks* has estimated roughly that thunder is audible from all storms in an area of 200 square miles and that an average storm lasts 1 hour and produces 200 flashes If the same estimate be adopted here, the average annual number of lightning flashes over 1 square kilometre would appear to be about five Thus the annual effect of lightning discharges on the square kilometre under consideration is to transfer to it a negative charge of the order of 20 coulombs

It remains to consider the effect of the currents caused by point discharges from trees and vegetation in general The single artificial point, from which the current has been studied, discharges in the course of a year about 0 13 coulomb of positive charge from the earth to the atmosphere Data as to the comparative efficiency of the artificial point and natural dischargers, such as the various types of trees, are lacking It has been found, however, that when placed in an intense artificial electric field between two plates, a metal point similar to the point on the pole gives currents of the same order of magnitude as those discharged from various types of twigs and leaves at about the same height One is perhaps justified in saying that the artificial pole might be expected to give a current of the same order of magnitude as that from a tree of the same height In order, therefore, to obtain a rough estimate of the total magnitude of the effect of the point-discharge currents over a given area, the trees surrounding the pole have been counted It is probable that the magnitude of the current from a single source of discharge depends on the number of other discharges in the immediate neighbourhood, the field near the ground automatically reaching such a value that the vertical current per unit area is equal approximately to the charge per unit area generated per second by the cloud above It was decided, arbitrarily, to count the trees in a circular area of 0 25 sq km surrounding the pole, omitting all trees whose height did not exceed that of the artificial discharging point It was found that there were in this area, rather more than 200 fairly well-exposed trees all exceeding appreciably the height of the artificial point Some of these were much larger than the pole This number neglects entirely the large number of smaller trees and other types of vegetation which must presumably carry some current when the exposure to the electric field is good It also omits entirely two small plantations containing several hundred closely placed trees, many of them taller than the artificial pole It seemed, however, quite impossible, at present, to make any estimate of the contribution of these, to the total current It does not seem unreasonable therefore to estimate roughly that this area of 0 25 sq km provides 200 dischargers equivalent to the artificial one which has been studied The area would then gain in one year about 26 coulombs of negative charge, or 104 coulombs per square kilometre The estimate of the annual charge per square kilometre brought to the ground by the four processes considered is thus as follows –

---

* 'Geophysical Memoirs,' No 24 (vol 3, No 4), 1925.

Fine weather current	+ 60	coulombs
Precipitation	+ 20	,,
Lightning discharges	20	,,
Currents carried by point discharges	−100	,,

The estimates are admittedly very rough ones , it would appear, however, to be quite possible that the four processes balance one another approximately, or even that in this locality the earth on the whole gains a negative charge It appears very probable that the current carried by lightning and the point discharges together exceeds considerably the current carried down by rain, which is in the opposite direction, and therefore that there is effectively a vertical upward current through a cumulo-nimbus cloud from the earth to the upper atmosphere This conclusion is in accord with previous results based on evidence of a different type that shower clouds were predominantly of positive polarity Schonland* in South Africa has reached a similar conclusion with regard to the total current through a cumulo nimbus cloud The results of all the observations which have been discussed are thus in entire agreement with Wilson's theory that the fine-weather current into the ground over the whole earth is balanced by the currents maintained between the earth and the upper atmosphere by shower-clouds

---

* 'Roy Soc Proc ,' A, vol. 118, p 252 (1928)

In conclusion it is a pleasure to express my gratitude to Prof C T R Wilson for his continued interest and advice during the course of these observations My thanks are also due to Prof H F Newall, lately Director of the Solar Physics Observatory, for his interest in the work Further, I wish to thank Messrs L J Stanley and W H Manning of the Observatory for their assistance in the setting up of some of the apparatus

---

The Spread of Vorticity in the Wake behind a Cylinder

L Rosenhead, Ph D, St John's College, Cambridge

(Communicated by H Jeffreys F R S —Received February 3, 1930—Revised April 7, 1930)

1 *Introduction*

This paper is an attempt to investigate the effect on the configuration of vortices in the wake behind a cylinder of an allowance for the thickness of the vortices The vortices themselves are assumed to be initially rectilinear and of equal circular section, and we assume also that they arrange themselves in an " unsymmetrical double row " We therefore find a relationship between the " stability ratio " of the double row—that is, the ratio of the distance between the rows to the distance between consecutive vortices on the same row, in the stable configuration— and the diameters of the vortices The problem in its initial stages can no longer be treated as one in two dimensions, for the " self induction " of a vortex only enters when we deal with a three-dimensional disturbance, and it is the self-induction that produces the difference between this and the original treatment of the subject By the " self-induction " of a vortex we mean the effect of the vortex on itself The isolated rectilinear vortex is treated separately and the results obtained from it are extended to meet the case of the double row of rectilinear vortices The three-dimensional stability of the Bénard-Karman street has already been discussed,* but the present treatment introduces various simplifications which, while not altering the general nature of the problem, make the expressions more amenable to treatment and yield results that appear to have been masked by the complexities of the algebra in the previous investigation

---

* Karl Schlayer, ' Z Angew Math ,' vol. 8, p 352 (1928)

I would like to express my thanks to Dr H Jeffreys for many helpful criticisms which have had the effect of altering entirely certain sections of this paper

2 *Summary*

The stability of a rectilinear vortex of circular section for three dimensional disturbances is discussed and the vortex is found to be stable for a most general displacement This verifies a result obtained in another fashion by Levy and Forsdyke The work is extended to meet the case of the double row of vortices set up in the wake behind a cylinder moving in an infinite sea of liquid

In a two dimensional disturbance the Benard-Karman street is stable for the stability ratio 0 281 for all values of the thickness of the vortices In a three-dimensional disturbance, if the wave length of the disturbance along the axis of the street is large, then the system is stable for all values of the thickness of the vortices In a general disturbance however, in which there occur components whose wave-lengths are small, these components give instability, and they tend to break up the configuration The vortices will become increasingly distorted and the distance between the rows will either decrease or increase In the first of these cases the system will always be unstable and the double row will disappear In the second case a position of transitional stability will ultimately be reached and the distance between the rows will no longer tend to increase nor will the vortices become more distorted The increase in the thickness of the vortices will now become the dominating factor, and with the spread of vorticity the system, though always stable, will tend to close up its ranks and to disappear In a general three dimensional disturbance, therefore, the pattern is always completely destroyed and it is only a matter of time before this occurs

Hence in the trail behind a cylinder we should expect that the first few vortices in the steady part of the wake are given by a stability ratio of about 0 281 and that the ones further away become increasingly distorted and either come together and lose their identity, or at first show a tendency to increase the distance between the rows and then ultimately to come together as the vorticity diffuses

3 *The Isolated Rectilinear Vortex*

In a recent paper by Prof H Levy and A G Forsdyke,* the stability of a rectilinear vortex of circular section was discussed as a particular case of a more general problem, the straight vortex being taken as the limiting form of a helical vortex when the pitch tends to infinity The investigations showed that the vortex was stable to a wave like disturbance along its length, but the equations from which stability was inferred involved complicated infinite integrals the convergence of which was not examined Stability can be inferred, however, by direct reference to some remarks made by Lord Kelvin in his discussion on the vibrations of a columnar vortex *

---

* 'Roy Soc Proc,' A, vol 120, p 670 (1928)

In Lord Kelvin's work the vortex was considered to consist of a core of radius ε in which, in the undisturbed state, the liquid was rotating with an angular velocity ω Outside the core the motion was in circles round the vortex with velocity $\omega\varepsilon^2/r$, r being the distance from the axis of the vortex The most general disturbance was then discussed and the components of velocity were found to be —

When $r < \varepsilon$,

$$r = \rho \cos lz \sin(\lambda t - n\theta),$$

$$r\theta = \omega r + \tau \cos lz \cos(\lambda t - n\theta),$$

$$z = \phi \sin lz \sin(\lambda t - n\theta),$$

where

$$\rho = (\lambda - n\omega)\left\{(\lambda - n\omega)\frac{d\phi}{dr} - \frac{2n\omega}{r}\phi\right\}\Big/ l\,[4\omega^2 - (\lambda - n\omega)]^2,$$

$$\tau = (\lambda - n\omega)\left\{2\omega\frac{d\phi}{dr} - \frac{n(\lambda - n\omega)}{r}\phi\right\}\Big/ l\,[4\omega^2 - (\lambda - n\omega)^2],$$

and where ϕ satisfies the equation

$$\frac{d^2\phi}{dr^2} + \frac{1}{r}\frac{d\phi}{dr} + \left(\nu^2 - \frac{n^2}{r^2}\right)\phi = 0,$$

ν being given by the equation

$$\nu^2 = l^2\,[4\omega^2 - (\lambda - n\omega)^2]/(\lambda - n\omega)^2$$

ϕ was taken to be $CJ_n(\nu r)$, where C is some constant

When $r > \varepsilon$, r, $r\theta$ and z are given by expressions similar to those above, but in the expression for $r\theta$ we have $\omega\varepsilon^2/r$ instead of ωr This makes

$$\rho = -\frac{1}{l}\frac{d\phi}{dr}, \quad \tau = \frac{n\phi}{lr},$$

---

* Thomson, 'Phil. Mag,' vol 10, p 155 (1880), Kelvin, "Collected Papers," vol. 4, p 152

and ϕ satisfies the equation

$$\frac{d^2\phi}{dr^2} + \frac{1}{r}\frac{d\phi}{dr} - \left(l^2 + \frac{n^2}{r^2}\right)\phi = 0$$

ϕ was taken to be $\mathrm{DK}_n(lr)$, where D is some constant

The condition of no slip at the boundary of the vortex becomes

$$\frac{\mathrm{J}'_n(q)}{\mathrm{J}_n(q)} + \frac{n}{q^2\mathrm{X}} = \frac{-\mathrm{K}'_n(l\varepsilon)}{l\varepsilon\mathrm{K}_n(l\varepsilon)},$$

where

$$q^2 = l^2\varepsilon^2(1 - \mathrm{X}^2)/\mathrm{X}^2,$$

and

$$\mathrm{X} = (n\omega - \lambda)/2\omega$$

Lord Kelvin remarked that if this equation is treated as a transcendental equation in X, then this equation has an infinite number of roots between -1 and 0, and a similar number between 0 and $+1$ Further it was remarked that this equation has no roots other than those between -1 and $+1$ Hence X, and therefore λ, must always be real This is just the condition that the system is stable, for if λ were complex, the disturbances would involve exponentials that would increase with the time Hence the rectilinear vortex of circular section is stable for the most general disturbance

Let us now discuss the various modes of vibration The case $n = 0$ is just a swelling or contraction of the filament without displacing the centre, for we see that r at the surface of the vortex is independent of θ The amount of swelling or contraction varies, of course, with z The case $n = 1$ represents a displacement of the centre of the vortex for it is easily seen that if we compare the radial velocities at the points θ and $\theta + \pi$ we get $(\dot{r})_\theta = -(\dot{r})_{\theta+\pi}$ Kelvin showed that, in the case $n = 1$, the wave of deformation on the surface of the vortex rotates with angular velocity λ where*

$$\lambda = -\tfrac{1}{2}\omega l^2\varepsilon^2 \log(1/l\varepsilon) = -\frac{\kappa}{4\pi} l^2 \log(1/l\varepsilon)$$

The equations of motion of the centre of the vortex would then be

$$\left.\begin{aligned} \frac{4\pi}{\kappa}\dot{x} &= l^2 \log(1/l\varepsilon)\, y, \\ \frac{4\pi}{\kappa}\dot{y} &= -l^2 \log(1/l\varepsilon)\, x \end{aligned}\right\} \quad (1)$$

Lord Kelvin also showed that for $n > 1$, the motion was also a rotation, but in this case the angular velocity was $(n-1)\,\omega = \frac{\kappa}{2\pi\varepsilon^2}(n-1)$ The equations of motion would now be

---

* Kelvin, *loc cit*, equation (61)

$$\left.\begin{aligned}\frac{4\pi}{\kappa}\,x &= \frac{-2(n-1)}{\varepsilon^2}\,y \\ &= C_n\,\frac{4\pi}{\kappa}\left(\frac{3}{4}\right)^{n/2}\frac{1}{(n-1)\,!}\,(lr)^{n-1}\cos lz \sin (n-1)\,[\omega t-\theta] \\ \frac{4\pi}{\kappa}\,y &= \frac{2\,(n-1)}{\varepsilon^2}\,x \\ &= -\,C_n\,\frac{4\pi}{\kappa}\left(\frac{3}{4}\right)^{n/2}\frac{1}{(n-1)\,!}\,(lr)^{n-1}\cos lz \cos (n-1)\,[\omega t-\theta]\end{aligned}\right\}\qquad(2)$$

The centre of the vortex therefore is at rest The cases $n > 1$ represent wave motions over the surface of the vortex without displacing the centre of the vortex

The equations obtained above are so simple that it was thought interesting to obtain a verification from another point of view The case $n = 1$ was taken as one that would show least complication, but in spite of this, the discussion involves quite a deal of algebra but finally reduces to the form obtained from Lord Kelvin's elegant treatment

Briefly our method is as follows We assume that in the undisturbed state the vortex is parallel to the axis of z The vortex is now disturbed and assumes a wave-like form The three components of velocity at a point on the surface of the vortex are obtained by integration and the equations of motion are thus determined These give the normal modes of vibration for that particular form of disturbance It will be seen that the equation in λ derived from the x and y components of velocity will not involve z, for the factor e^{ilz} will cancel throughout, and the equation in λ derived from the z component of velocity will only introduce the value $\lambda = 0$ (see equation 3 9) which can be neglected

We may notice here that the small disturbances in velocity are not of the same order of magnitude The alteration in r and $r\theta$ is of the order ε^{n-1}, where that in z is of the order ε^{n} Hence a good approximation will be obtained if we neglect entirely the z component of velocity This will be verified incidentally in the case of $n = 1$, but it is equally true in any other case If we adopt this simplification the general displacement can be treated in the same way as we treat the two-dimensional problem, the only difference being that we must introduce the x and y components of velocity due to the vortex tself These are the self-induction effects

We must now investigate the wave-like form assumed by the centre-line of the vortex corresponding to $n = 1$. By letting $r \to 0$ in the expressions for the velocities in the core of the vortex we get

$$(r)_0 = -p\cos lz \sin(\lambda t - \theta), \quad (r\theta)_0 = p\cos lz \cos(\lambda t - \theta),$$

where

$$p = \mathrm{C}\nu(\lambda - \omega)/2l(\lambda + \omega)$$

This means

$$(x)_0 = -p\cos lz \sin \lambda t, \quad (y)_0 = p\cos lz \cos \lambda t$$

Hence the general displacements of the centre-line must be of the form $\alpha e^{\lambda t + ilz}$, $\beta e^{\lambda t + ilz}$, where α and β are constants and where λ is not the same as that in the expressions for $(x)_0$ and $(y)_0$.

If κ be the strength of a vortex, supposed uniform along its length, then the component velocities u, v, w at a point (x, y, z) are given by the line integrals

$$\left.\begin{aligned} \frac{4\pi}{\kappa}u &= \int\{(z - z')\,dy' - (y - y')\,dz'\}/\mathrm{R}^3 \\ \frac{4\pi}{\kappa}v &= \int\{(x - x')\,dz' - (z - z')\,dx'\}/\mathrm{R}^3 \\ \frac{4\pi}{\kappa}w &= \int\{(y - y')\,dx' - (x - x')\,dy'\}/\mathrm{R}^3 \end{aligned}\right\} \qquad (3)$$

where (x', y', z') are the current co-ordinates, and

$$\mathrm{R}^2 = (x - x')^2 + (y - y')^2 + (z - z')^2$$

If we have a single line vortex at (x_1, y_1) parallel to the axis of z, we get the usual results that the vortex itself is at rest and that the velocity at points off the axis is

$$-\kappa(y - y_1)/2\pi r^2, \quad \kappa(x - x_1)/2\pi r^2, \quad 0,$$

where

$$r^2 = (x - x_1)^2 + (y - y_1)^2$$

If now the axis is slightly displaced owing to a disturbance along its length of wave-length $2\pi/l$, the position of an element originally at (x_1, y_1, z_1) is now at (x', y', z') where

$$x' = x_1 + \alpha e^{\lambda t + ilz_1}, \quad y' = y_1 + \beta e^{\lambda t + ilz_1}, \quad z' = z_1 + \gamma e^{\lambda t + ilz'},$$

where α, β and γ are some constants and λ is to be determined. For stability the real part of λ must be either negative or zero.

In the above line integrals we now put

$$dx' = il\alpha e^{\lambda t + ilz'}\,dz', \quad dy' = il\beta e^{\lambda t + ilz'}\,dz',$$

and for points at an appreciable distance off the axis we put

$$1/\mathrm{R}^3 = \left[1 + 3\,\frac{x - x_1}{\mathrm{R}_0^2}\,\delta x_1 + 3\,\frac{y - y_1}{\mathrm{R}_0^2}\,\delta y_1\right]\Big/\mathrm{R}_0^3,$$

where

$$\mathrm{R}_0^2 = (x - x_1)^2 + (y - y_1)^2 + (z - z_1)^2, \quad \delta x_1 = \alpha e^{\lambda t + \iota l z'}, \quad \delta y_1 = \beta e^{\lambda t + \iota l z'}$$

We get

$$\left.\begin{aligned} \frac{4\pi}{\kappa}u &= -(y - y_1)\int_{-\infty}^{\infty}\frac{dz'}{\mathrm{R}^3} + \iota l\beta e^{\lambda t}\int_{-\infty}^{\infty} e^{\iota l z}\,\frac{z - z'}{\mathrm{R}^3}\,dz', \\ \frac{4\pi}{\kappa}v &= (x - x_1)\int_{-\infty}^{\infty}\frac{dz'}{\mathrm{R}^3} - \iota l\alpha e^{\lambda t}\int_{-\infty}^{\infty} e^{\iota l z'}\,\frac{z - z'}{\mathrm{R}^3}\,dz', \\ \frac{4\pi}{\kappa}w &= \iota l\,\{\alpha(y - y_1) - \beta(x - x_1)\}\,e^{\lambda t}\int_{-\infty}^{\infty} e^{\iota l z'}\,\frac{dz'}{\mathrm{R}^3} \end{aligned}\right\} \qquad (4)$$

These integrals split up into several integrals of the form $\int_0^\infty \frac{\cos s\eta}{(1 + \eta^2)^{p+\frac{1}{2}}}\,d\eta$, which are, of course, only special cases of Bessel functions of imaginary argument, and in Watson's* notation we have

$$\int_0^\infty \frac{\cos s\eta}{(1 + \eta^2)^{p+\frac{1}{2}}}\,d\eta = \left(\frac{s}{2}\right)^p \frac{\Gamma\left(\frac{1}{2}\right)}{\Gamma\left(p + \frac{1}{2}\right)}\,\mathrm{K}_p(s)$$

This gives

$$\left.\begin{aligned} u &= -\frac{\kappa(y - y_1)}{2\pi r^2} + \frac{\kappa}{2\pi}\,l^2 e^{\lambda t + \iota l z}\Big[\beta\mathrm{K}_0(lr) \\ &\qquad\qquad - \left\{\frac{(x - x_1)(y - y_1)}{r^2}\,\alpha + \frac{(y - y_1)^2}{r^2}\,\beta\right\}\mathrm{K}_2(lr)\Big], \\ v &= \frac{\kappa(x - x_1)}{2\pi r^2} - \frac{\kappa}{2\pi}\,l^2 e^{\lambda t + \iota l z}\Big[\alpha\mathrm{K}_0(lr) \\ &\qquad\qquad - \left\{\frac{(x - x_1)^2}{r^2}\,\alpha + \frac{(x - x_1)(y - y_1)}{r^2}\,\beta\right\}\mathrm{K}_2(lr)\Big], \\ w &= \frac{\iota\kappa}{\pi}\,l^2 e^{\lambda t + \iota l z}\left\{\frac{(y - y_1)}{r}\,\alpha - \frac{(x - x)_1}{r}\,\beta\right\}\mathrm{K}_1(lr) \end{aligned}\right\} \qquad (5)$$

When s is large the following asymptotic expansion is permissible

$$\int_0^\infty \frac{\cos s\eta}{(1 + \eta^2)^{p+\frac{1}{2}}}\,d\eta$$

$$= 2\sqrt{2}\,\pi\,\frac{s^{p+\frac{1}{2}}e^{-s}}{1\ 3\ 5\ \ (2p+1)}\left|\,1 + \frac{\left(p^2 - \frac{1}{2^2}\right)}{(2s)} + \frac{\left(p^2 - \frac{1}{2^2}\right)\left(p^2 - \frac{3^2}{2^2}\right)}{(2s)^2}\qquad\right],$$

so that as $s \to \infty$

$$\mathrm{K}_p(s) \to 0$$

---

* "Bessel Functions" (1922), p 185

This indicates that the disturbance becomes zero at large distances from the axis We cannot use the expressions for (u, v, w) to give the values of the velocity components on the vortex itself even if we insert those expansions for $\int_0^\infty \frac{\cos s\eta}{(1+\eta^2)^{p+\frac{1}{2}}}\,d\eta$ which are valid for small r This is so because the expressions for (u, v, w) were obtained on the assumption that $(\delta x_1/R_0)^2$ and $(\delta y_1/R_0)^2$ were negligibly small for all values of x and y This is no longer true if (x, y) lies on the vortex itself Further, if we consider the velocity at a point on the axis of the vortex the integrals involved in have an infinity at $R = 0$ and are divergent, thus making (u, v, w) indeterminate The fact is that the expressions (u, v, w) are not true for points on the axis Singularities of a similar kind occur in the theories of attractions * This difficulty is avoided if we discuss the motion of a point on the surface of the vortex Let ε be the radial distance of this point (x, y, z) from the point (x', y', z'), (x', y') being, of course, the point in which the axis of the vortex cuts the z plane Let ν be the angle made by this radius vector and the axis of x Then

$$x = x_1 + \alpha e^{\lambda t + ilz} + \varepsilon\cos\nu, \qquad y = y_1 + \beta e^{\lambda t + ilz} + \varepsilon\sin\nu,$$
$$x' = x_1 + \alpha e^{\lambda t + ilz}, \qquad y' = y_1 + \beta e^{\lambda t + ilz}$$

We now have

$$R^2 = (z - z')^2 + \phi^2,$$

where ϕ^2 is of the second order in α and β, and we see that

$$\phi^2 = \varepsilon^2 + 2\varepsilon e^{\lambda t}[\alpha\cos\nu + \beta\sin\nu][e^{ilz} - e^{ilz'}] + e^{2\lambda t}[\alpha^2 + \beta^2][e^{ilz} - e^{lz'}]^2 \quad (6)$$

If the system is in absolute equilibrium, that is, if the real part of λ is negative, then ϕ^2 approaches ε^2 as t increases If the system is in neutral equilibrium, that is, if the real part of λ is zero, then

$$\varepsilon^2 \leqslant |\phi^2| \leqslant (\varepsilon + 2\sqrt{\alpha^2 + \beta^2})^2$$

This fixes limits $\phi_1 = \varepsilon$ and $\phi_2 = \varepsilon + 2\sqrt{\alpha^2 + \beta^2}$, and gives an indication of the accuracy of the approximation Further, if ε is large compared with the displacement of the centre line, and if the section of the vortex is circular, we may put $\phi = \varepsilon$ The substitution of ε for ϕ in R^3 over the whole range of

---

* *Cf* Leathem, "Cambridge Tracts," No 1

integration will be immaterial If the system is unstable, the above approximation will lead to an inconsistency We now get

$$\left.\begin{aligned}
\frac{4\pi}{\kappa}u &= \int_{-\infty}^{\infty} il\beta e^{\lambda t+ilz}\,\frac{(z-z')\,e^{il(z'-z)}}{[(z-z')^2+\varepsilon^2]^{3/2}}\,dz' \\
&\qquad -\beta e^{\lambda t+ilz}\,\frac{(1-e^{il(z'-z)})}{[(z-z')^2+\varepsilon^2]^{3/2}}\,dz' - \frac{\varepsilon\sin\nu}{[(z-z')^2+\varepsilon^2]^{3/2}}\,dz', \\
\frac{4\pi}{\kappa}v &= \int_{-\infty}^{\infty} il\alpha e^{\lambda t+ilz}\,\frac{(z-z')\,e^{il(z'-z)}}{[(z-z')^2+\varepsilon^2]^{3/2}}\,dz' \\
&\qquad +\alpha e^{\lambda t+ilz}\,\frac{(1-e^{il(z'-z)})}{[(z-z')^2+\varepsilon^2]^{3/2}}\,dz' + \frac{\varepsilon\cos\nu}{[(z-z')^2+\varepsilon^2]^{3/2}}\,dz', \\
\frac{4\pi}{\kappa}w &= \text{order }(\alpha^2) = 0
\end{aligned}\right\} \tag{7}$$

The integrals

$$\int \frac{\varepsilon\sin\nu}{[(z-z')^2+\varepsilon^2]^{3/2}}\,dz' \quad\text{and}\quad \int \frac{\varepsilon\cos\nu}{[(z-z')^2+\varepsilon^2]^{3/2}}\,dz',$$

which are equal to $\frac{2\sin\nu}{\varepsilon^2}$ and $\frac{2\cos\nu}{\varepsilon^2}$ are the components of velocity in the undisturbed state of a point on the surface of the vortex, and therefore cancel with corresponding terms in the values of u and v Hence

$$\begin{aligned}
\frac{4\pi}{\kappa}\lambda\alpha &= \beta\left\{-\frac{2}{\varepsilon^2}+2l^2\mathrm{K}_0(l\varepsilon)+\frac{2l}{\varepsilon}\mathrm{K}_1(l\varepsilon)\right\} \\
&= \beta\left\{-\frac{2}{\varepsilon^2}+2l^2\log(1/l\varepsilon)+\frac{2l}{\varepsilon}\left[\frac{1}{l\varepsilon}-\frac{l\varepsilon}{2}\log(1/l\varepsilon)\right]\right\} \\
&= \beta\{l^2\log(1/l\varepsilon)\}
\end{aligned} \tag{8}$$

Similarly

$$\left.\begin{aligned}
\frac{4\pi}{\kappa}\lambda\beta &= -\alpha\{l^2\log(1/l\varepsilon)\}, \\
\frac{4\pi}{\kappa}\lambda\gamma &= 0
\end{aligned}\right\} \tag{9}$$

Hence

$$\left(\frac{4\pi}{\kappa}\right)^2\lambda^2 = -[l^2\log(1/l\varepsilon)^2]^2, \quad\text{or}\quad \lambda = 0, \tag{10}$$

and the system is in neutral stability $\lambda = 0$ is just a general displacement of the vortex These equations are true for any point on the surface of the vortex and as the diameter of the vortex remains constant the equations are also true for the centre of the vortex. This verifies the results that were obtained before, for the equations of motion are seen to be

$$\frac{4\pi}{\kappa}\,x = l^2 \log(1/l\varepsilon)\,y, \quad \frac{4\pi}{\kappa}\,y = -\,l^2 \log(1/l\varepsilon)\,x, \quad \frac{4\pi}{\kappa}\,z = 0 \tag{11}$$

The above approximations were made on the understanding that $(l\varepsilon)$ is small. This makes the expression $l^2 \log(1/l\varepsilon)$ positive. We now define the symbol $\eta = 2b^2l^2 \log(1/l\varepsilon)$ where b is a constant at present undefined. η is a measure of the self-induction of a vortex, for we see that if u and v are the components of velocity of a point on the surface of the vortex, then we see at once that the thinner the vortex the more stable it is. Also, if ε is fixed, and l becomes very small, $\eta \to 0$. This means that as the wave-length of the disturbance becomes infinite, the effect of self-induction becomes zero. This is true for all ε. For pure translation of rectilinear vortices $\eta = 0$ for all ε, and the investigations of the stability of a double row of vortices, each of radius ε, reduce to the investigations of von Karman. Hence the Karman street in which the stability ratio is 0.281 is stable for a disturbance of purely translatory type, and for a disturbance of large wave-length, for all values of the thickness of the vortex. This was noted by Schlayer (*loc. cit.*)

4. *The Double Row of Vortices*

In actual experiment the vortices are not of infinite length, but we imagine the vortices to be continued indefinitely on both sides of a surface of discontinuity, such as the bounding wall of the vessel, or the free surface (which is considered as a slightly deformable boundary), so as to satisfy the condition that there shall be no flow through the bounding surface.

In the undisturbed position the Karman street of vortices in an infinite sea of liquid consists of cylindrical vortices of radius ε whose axes are at right angles to the z plane and cut it as follows :—

Vortices of strength $+\,\kappa$ at the points $(2mb,\, a)$,
Vortices of strength $-\,\kappa$ at the points $(\,(2n+1)\,b,\, -\,a)$,

where m and n assume all integral values from $-\,\infty$ to $+\,\infty$. We intend to discuss the vortex $m = 0$. We now assume that all the vortices are slightly displaced and that a representative vortex on the upper row takes the shape

$$x' = 2mb + \alpha e^{\lambda t + \iota l z + \iota 2m\phi}, \qquad y' = -\,a + \beta e^{\lambda t + \iota l z + \iota 2m\phi}, \tag{1}$$

and that a representative vortex on the lower row takes the shape

$$x' = (2n+1)\,b + \alpha' e^{\lambda t + \iota l z + \iota (2n+1)\phi}, \quad y' = -\,a + \beta' e^{\lambda t + \iota l z + \iota (2n+1)\phi}, \tag{2}$$

where α, β, α', β' are constants and ϕ is a constant such that $\pi \geqslant \phi \geqslant 0$ The factor e^{ilz} introduces a periodicity into the disturbance along the axes of the individual vortices and the term $e^{i2m\phi}$ introduces a periodicity along the axis of the wake We investigate the x and y velocities of the points of section of the axes of the vortices with an arbitrary z plane In this plane we put

$$\left.\begin{aligned} x_m &= \alpha e^{\lambda t + ilz + i2m\phi}, & y_m &= \beta e^{\lambda t + ilz + i2m\phi}, \\ x'_n &= \alpha' e^{\lambda t + ilz + i(2n+1)\phi}, & y'_n &= \beta' e^{\lambda t + ilz + i(2n+1)\phi} \end{aligned}\right\} \tag{3}$$

The factor exp (ilz) can very well be absorbed into the constants α, β, α', β' in this plane For stability we must have that the real part of λ is either zero or negative In the two-dimensional treatment of this problem the equations of motion are

$$\left.\begin{aligned} \rho x_0 &= - A\beta - B\alpha' - C\beta', \\ \rho y_0 &= - A\alpha - C\alpha' + B\beta', \\ \rho x_0' &= - B\alpha + C\beta + A\beta' \\ \rho y_0' &= C\alpha + B\beta + A\alpha', \end{aligned}\right\} \tag{4}$$

where

$$\rho = 8\pi b^2/\kappa, \qquad k = a/b, \tag{5}$$

and where

$$\left.\begin{aligned} A &= -\sum_n \frac{(n+\frac{1}{2})^2 - k^2}{(n+\frac{1}{2})^2 + k^2} + \sum_m{}' \frac{1 - e^{i2m\phi}}{m^2} = -\pi^2 \operatorname{sech}^2 k\pi + 2\phi(\pi - \phi), \\ B &= \sum_n \frac{(2n+1) k e^{i(2n+1)\phi}}{\{(n+\frac{1}{2})^2 + k^2\}^2} = i \left\{\frac{2\pi\phi \sinh k(\pi - 2\phi)}{\cosh k\pi} + \frac{\pi^2 \sinh 2k\phi}{\cosh^2 k\pi}\right\}, \\ C &= \sum_n \frac{\{(n+\frac{1}{2})^2\}}{\{(n+\frac{1}{2})^2\}^2} e^{i(2n+1)\phi} = \frac{\pi^2 \cosh 2k\phi}{\cosh^2 k\pi} - \frac{2\pi\phi \cosh k(\pi - 2\phi)}{\cosh k\pi} \end{aligned}\right\} \tag{6}$$

These equations of motion are the same as those given by Lamb* but a few alterations in notation have been made If now we take account of the alteration in velocities due to the distortion of the individual vortices we get that the equations of motion are

$$\left.\begin{aligned} \rho x_0 &= (\eta - A)\beta - B\alpha' - C\beta', \\ \rho y_0 &= -(\eta + A)\alpha - C\alpha' + B\beta', \\ \rho x_0' &= - B\alpha + C\beta - (\eta - A)\beta', \\ \rho y_0' &= C\alpha + B\beta + (\eta + A)\alpha' \end{aligned}\right\} \tag{7}$$

---

* "Hydrodynamics," p 211 (1924)

If now we put $x_0 = \lambda\alpha$, $y_0 = \lambda\beta$, $x_0' = \lambda\alpha'$, $y_0 = \lambda\beta'$, we can get the quartic for λ in the usual way, but the displacement resolves itself into two types In the first type we have $\alpha = \alpha'$, $\beta = -\beta'$, giving equations

$$\left.\begin{aligned} \rho x_0 &= \qquad\qquad -B\alpha \quad + (\eta - A + C)\,\beta, \\ \rho y_0 &= -(\eta + A + C)\alpha \qquad\qquad -B\beta \end{aligned}\right\} \tag{8}$$

This gives rise to exponentials $e^{\lambda t}$ where

$$\rho\lambda = -B \pm \sqrt{A^2 - (C + \eta)^2} \tag{9}$$

In the second type we have $\alpha = -\alpha'$, $\beta = \beta'$, giving

$$\left.\begin{aligned} \rho x_0 &= B\alpha + (\eta - A - C)\,\beta, \\ \rho y_0 &= -(\eta + A - C)\,\alpha + B\beta \end{aligned}\right\} \tag{10}$$

The solution of these equations involves exponentials $e^{\lambda t}$ where

$$\rho\lambda = B \pm \sqrt{A^2 - (C - \eta)^2} \tag{11}$$

For stability we must have that $A^2 < (C + \eta)^2$ and $A^2 < (C - \eta)^2$ for all values of ϕ We see at once that if the vortex is sufficiently thin for fixed values of κ and l, that is, if η is large enough to swamp the values of A and C, then the system will be stable for all values of a/b We have

$$A = 2\phi\,(\pi - \phi) - \pi^2 \operatorname{sech}^2 k\pi,$$

$$C = \pi^2 \operatorname{sech}^2 k\pi \cosh 2k\phi - 2\pi\phi \operatorname{sech} k\pi \cosh k\,(\pi - 2\phi),$$

where $0 \leqslant \phi \leqslant \pi$ Let us now put $k\pi = \mu$, $2k\,(\phi - \tfrac{1}{2}\pi) = \theta$ From this point, the symbol θ will be used consistently with this interpretation, and it should not be confused with the polar co-ordinate θ used previously We get

$$k^2A = \tfrac{1}{2}\mu^2\,(1 - 2\operatorname{sech}^2\mu) - \tfrac{1}{2}\theta^2,$$

$$k^2C = \mu \operatorname{sech}\mu\,[\mu \tanh\mu \sinh\theta - \theta\cosh\theta],$$

where $-\mu \leqslant \theta \leqslant \mu$ The stability conditions now become

$$(A + C - \eta)\,(A - C + \eta) < 0 \quad \text{for all } \theta \text{ in the range } -\mu \leqslant \theta \leqslant \mu,$$

$$(A + C + \eta)\,(A - C - \eta) < 0 \quad \text{for all } \theta \text{ in the range } -\mu \leqslant \theta \leqslant \mu$$

If in the first of these conditions we put $\theta_1 = -\theta$, A remains unaltered but C changes sign, and the first condition is transformed into the second The two stability conditions are therefore identical We will deal with the first of them

On account of the symmetry of the expressions we will first discuss the forms of the curves $(A + C)$ and $(A - C)$ Even this is not necessary, for if we plot the curve $(A + C)$ with abscissa θ and ordinate y, then the curve $(A - C)$ is the image of $(A + C)$ with respect to the y axis Hence we need only discuss the shape of $(A + C)$ For this purpose the following table is useful

Table I

θ	$-\mu$	0	μ
$k^2(A+C)$	0	$\frac{1}{2}\mu^2(1 - 2\operatorname{sech}^2\mu)$	$-2\mu^2\operatorname{sech}^2\mu$
$k^2\frac{d}{d\theta}(A+C)$	0	$\mu\operatorname{sech}\mu(\mu\tanh\mu - 1)$	-2μ
$k^2\frac{d^2}{d\theta^2}(A+C)$	$(\mu^2\operatorname{sech}^2\mu + 2\mu\tanh\mu - 1)$	-1	$-(\mu^2\operatorname{sech}^2\mu + 2\mu\tanh\mu + 1)$

We note that

$$k^2\frac{d}{d\theta}(A + C) = -\theta + \mu\operatorname{sech}\mu\,[(\mu\tanh\mu - 1)\cosh\theta - \theta\sinh\theta]$$

$$= -\theta + k^2\frac{dC}{d\theta},$$

$$k^2\frac{d^2}{d\theta^2}(A + C) = -1 + \mu\operatorname{sech}\mu\,[(\mu\tanh\mu - 2)\sinh\theta - \theta\cosh\theta]$$

$$= -1 + k^2\frac{dC}{d\theta},$$

$$k^2\frac{d^3}{d\theta^3}(A + C) = \mu\operatorname{sech}\mu\,[(\mu\tanh\mu - 3)\cosh\theta - \theta\sinh\theta] = k^2\frac{dC}{d\theta}$$

The above details and the following considerations enable us to draw the curves $k^2(A + C)$

A knowledge of the positions of the maxima and minima (if any) of $k^2(A + C)$ is of great help and these will now be investigated The solutions of

$$k^2\frac{d}{d\theta}(A + C) = 0$$

are obtained from the equation

$$k^2\frac{d}{d\theta}(A + C) = -\theta + \mu\operatorname{sech}\mu\,[(\mu\tanh\mu - 1)\cosh\theta - \theta\sinh\theta] = 0$$

This can be put into the form

$$(\sinh\theta + \cosh\mu/\mu)\left\{\frac{(\mu\tanh\mu - 1)\cosh\theta}{\sinh\theta + \cosh\mu/\mu} - \theta\right\} = 0$$

The factor $(\sinh\theta + \cosh\mu/\mu)$ has at most one zero in the range $-\mu \leqslant \theta \leqslant \mu$, and at this zero we have

$$k^2 \frac{d}{d\theta}(\mathrm{A} + \mathrm{C}) = (\mu\tanh\mu - 1)\cosh\theta,$$

which does not vanish unless $\mu\tanh\mu - 1 = 0$. But if $\mu\tanh\mu - 1 = 0$ then the zero of $(\sinh\theta + \cosh\mu/\mu)$ occurs at the point $\theta = -\mu$. But there is a zero at $\theta = -\mu$ for all values of μ. Hence the factor $(\sinh\theta + \cosh\mu/\mu)$ contributes nothing to the zeros of $k^2 d(\mathrm{A} + \mathrm{C})/d\theta$, and we need only discuss the curve

$$\xi = \frac{a\cosh\theta}{\sinh\theta + b} - \theta,$$

where $a = (\mu\tanh\mu - 1)$ and $b = \cosh\mu/\mu$. The zeros of ξ and $k^2 d(\mathrm{A} + \mathrm{C})/d\theta$ are identical. We have

$$\frac{d\xi}{d\theta} = \frac{a(b\sinh\theta - 1)}{(\sinh\theta + b)^2} - 1 = -\frac{\sinh^2\theta - b(a-2)\sinh\theta + a + b^2}{(\sinh\theta + b)^2},$$

$$\frac{d^2\xi}{d\theta^2} = \frac{a\cosh\theta}{(\sinh\theta + b)^3}\left[(2 + b^2) - b\sinh\theta\right]$$

When a is negative then the minimum value of $(\sinh\theta + b)$ in $-\mu \leqslant \theta \leqslant \mu$ is

$$-\sinh\mu + b = \cosh\mu\,(1 - \mu\tanh\mu)/\mu = -ab = \text{positive}$$

Hence $(\sinh\theta + b)$ is always positive in the range $-\mu \leqslant \theta \leqslant \mu$. Hence ξ can have no zero for a positive θ. Also $d^2\xi/d\theta^2$ is always negative for negative θ and hence a straight line can cut ξ in at most two points in the negative range. Hence the curve $\xi = 0$ has at most two zeros in the negative range, and one of these is always $\theta = -\mu$. We see at once that ξ has no zeros other than that at $\theta = -\mu$ if $(d\xi/d\theta)_{\theta=-\mu}$ is negative, that is if

$$\sinh^2\mu + b(a-2)\sinh\mu + a + b^2 \geqslant 0,$$

which reduces to the condition

$$(2\mu - 1) \leqslant e^{-\mu} \quad \text{or} \quad \mu \leqslant 0{\cdot}639$$

Hence when $\mu \leqslant 0{\cdot}639$ the curve $k^2(\mathrm{A} + \mathrm{C})$ is of the form (1) in fig 2. When $a = 0$, $\mu = 1{\cdot}200$ and so in the range $0{\cdot}639 < \mu < 1{\cdot}200$, $d\xi/d\theta$ is positive at $\theta = -\mu$. But $(\xi)_{\theta=-\mu} = 0$ and $(\xi)_{\theta=0} = a/b =$ negative, and so there is one zero for ξ in the range $-\mu < \theta \leqslant 0$ when a is negative. This zero and the one at $\theta = -\mu$ are the only ones that ξ possesses. When $a = 0$

$$k^2 \frac{d}{d\theta}(\mathrm{A} + \mathrm{C}) = -\theta(1 + \mu\,\mathrm{sech}\,\mu\sinh\theta) = -\theta\left(1 + \frac{\sinh\theta}{\sinh\mu}\right)$$

and the only zeros for ξ are those at $\theta = 0$ and $\theta = -\mu$ Hence when a is negative typical members of $k^2(A + C)$ are given by the curves (1), (2), (3), (4), (5) of fig 2 Curve (3) corresponds to the case $\cosh^2 \mu = 2$ and cuts the abscissa at the origin This curve will be referred to later The curve (5) corresponds to $a = 0$ and has its maximum on the ordinate axis We have now to investigate the state of affairs when a is positive

We see at once that $(\sinh \theta + b)$ will be zero for some negative value of θ This will correspond to an asymptote to the curve ξ parallel to the ordinate axis Let θ_1 be that value of θ that makes $(\sinh \theta + b) = 0$ Then in the range $-\mu < \theta < \theta_1$, $d^2\xi/d\theta^2$ is negative and ξ has no zero In the range $\theta_1 < \theta \leqslant 0$, $d\xi/d\theta$ is always negative and $(\xi)_{\theta=0}$ is a/b which is positive Hence ξ has no zero in the range $-\mu < \theta \leqslant 0$ When a is positive the only possible zeros for ξ occur in the positive range of θ $(\xi)_{\theta=0}$ is positive and $(\xi)_{\theta=\mu} = -2\mu/(1 + \mu \tanh \mu) =$ negative Hence there are an odd number of roots between $\theta = 0$ and $\theta = \mu$ Also $d\xi/d\theta$ is zero for two values of θ, and hence ξ has one or three roots in the range $0 \leqslant \theta \leqslant \mu$ $d\xi/d\theta$ is zero when

$$2 \sinh \theta = b(a-2) \pm \sqrt{b^2(a-2)^2 - 4(b^2 + a)}$$

The expression within the square root sign can be put into the form

$$a(a-4)\left(b^2 - \frac{4}{a-4}\right),$$

and we see that this is negative when $a < 4$ If $a > 4$ the critical case is given by the solution of the equation $b^2 = 4/(a-4)$ which is $\mu = 5\ 018$ Hence when $1\ 200 < \mu < 5\ 018$, $d\xi/d\theta$ has no zero and the equation $\xi = 0$ has only one solution in the range $0 \leqslant \theta \leqslant \mu$ When $\mu = 5\ 018$, $d\xi/d\theta$ is zero for $\theta = 3\ 415$, and, as might be expected, $d^2\xi/d\theta^2$ is zero here since $b^2 = 4/(a-4)$ When $\theta = 3\ 415$, $\xi = -1\ 394$ Hence ξ only has one zero and that occurs at a value of θ less than 3 415 It occurs in fact somewhere near 0 27

When $\mu > 5\ 018$, $d\xi/d\theta$ has two real zeros The values of θ for which this occurs lie within the range $0 < \theta < \mu$ That this is so can be shown as follows Let θ' be the larger of the two values of θ corresponding to the roots of $d\xi/d\theta = 0$ If this lies outside the range $0 \leqslant \theta \leqslant \mu$ then $\sinh \theta' > \sinh \mu$, that is

$$2 \sinh \mu < [b(a-2) + \sqrt{b^2(a-2)^2 - 4(b^2 + a)}$$

or

$$2 \sinh \mu < \sinh \mu - \frac{3 \cosh \mu}{\mu} + \sqrt{\left(\sinh \mu - \frac{3 \cosh \mu}{\mu}\right)^2 - 4(b^2 + a)},$$

which becomes

$$12 \sinh \mu \cosh \mu/\mu < -4\,(b^2 + a),$$

which is obviously impossible. Hence the larger value of θ, and the smaller one, lie within the required range. The smaller value of θ will correspond to a minimum of ξ and the larger one will correspond to a maximum of ξ. If we can prove that the value of ξ at this maximum is negative, then it is obvious that ξ has only one zero within the range. This is the case and the following investigation proves it. When μ is large, greater than 5, say, we pay put $\tanh \mu = 1$ with an accuracy of 1 in 10^4, and the equation giving the roots of $d\xi/d\theta = 0$ is

$$\sinh \theta = \tfrac{1}{2}\left[b\,(a-2) \pm \sqrt{b^2\,(a-2)^2 - 4\,(b^2 + a)}\right]$$
$$= \tfrac{1}{2}\left[\cosh \mu\left(1 - \frac{3}{\mu}\right) \pm \sqrt{\frac{(\mu-1)(\mu-5)}{\mu^2}\left(\cosh^2 \mu - \frac{4\mu^2}{\mu-5}\right)}\right]$$

For large values of μ, $4\mu^2/(\mu-5)$ can be neglected in comparison with $\cosh^2 \mu$, *e.g.*, when μ is 6, $4\mu^2/(\mu-5) = 144$ and $\cosh^2 \mu = 40{,}689 \cdot 1833$. The ratio of disparity increases with μ. Hence we have

$$\sinh \theta = \tfrac{1}{2} \cosh \mu \left[1 - \frac{3}{\mu} \pm \left(1 - \frac{6}{\mu} + \frac{5}{\mu^2}\right)^{\frac{1}{2}}\right]$$
$$= \tfrac{1}{2} \cosh \mu \left[1 - \frac{3}{\mu} \pm \left(1 - \frac{3}{\mu} - \frac{2}{\mu^2}\right)\right]$$

neglecting terms of smaller order than $1/\mu^2$. Hence the smaller value of θ is given by

$$\sinh \theta = \cosh \mu/\mu^2$$

and the larger value by

$$\sinh \theta = \cosh \mu \left[1 - \frac{3}{\mu} - \frac{1}{\mu^2}\right]$$

We see that θ in both cases becomes large with μ, and putting $\sinh \theta = \frac{1}{2} e^{\theta}$ we get that

$$\theta_{\max} = \mu - \frac{3}{\mu} - \frac{11}{2\mu^2}$$

The value of ξ for this value of θ is easily found to be

$$-2 + \frac{2}{\mu} + \frac{5}{2\mu^2}$$

correct to $(1/\mu^2)$ and we can see that this is negative even for moderately large values of μ. Hence ξ has at most one zero in the range. We note also that $(\xi)_{\theta=0} = a/b = \mu\,(\mu \tanh \mu - 1)/\cosh \mu$. This tends to zero as μ increases and hence the zero of ξ tends towards $\theta = 0$ as μ becomes large Hence the curve (α) of fig 1 represents a typical ξ curve in the range $1\,200 < \mu < 5\,018$, and the curve (β) represents a typical curve when $\mu > 5\,018$

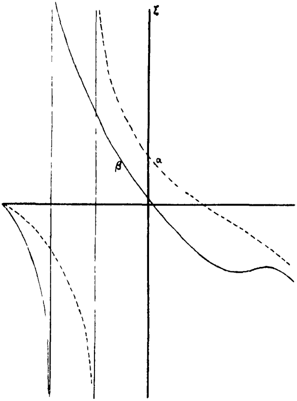

FIG 1 —The ordinate in this figure is $\xi = \dfrac{a\cosh\theta}{\sinh\theta + b} - \theta$ where $a = \mu\tanh\mu - 1$ and $b = \cosh\mu/\mu$ θ varies from $-\mu$ to μ, and so ξ has been plotted against the abscissa θ/μ Curve α represents a typical ξ curve in the range $1\,200 < \mu < 5\,018$, and the curve β represents a typical curve in the range $\mu > 5\,018$

The corresponding changes in the form of the curve $k^2(A + C)$ is given by the following fig 2

We are now in a position to determine those values of η that make $(A+C+\eta)(A - C - \eta) < 0$ for all θ in the range $-\mu \leqslant \theta \leqslant \mu$ There are three possible ways in which this can occur —

(1) $(A + C + \eta)$ always positive, and $(A - C - \eta)$ always negative ,

(2) $(A + C + \eta)$ always negative, and $(A - C - \eta)$ always positive ,

(3) $(A + C + \eta)$ and $(A - C - \eta)$ being of opposite sign for a particular value of θ, but intersecting on the θ axis in one or more points

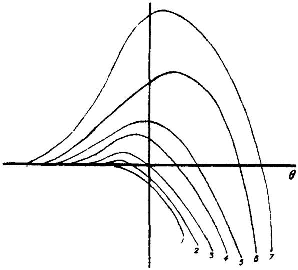

FIG 2 —The ordinate in this figure is $k^2(A + C)$ and the abscissa θ The figure shows the change in form of $k^2(A + C)$ with increasing μ

The state (2) is impossible, for if it were possible, then

$$(A + C + \eta) - (A - C - \eta) = 2(\eta + C)$$

would have to be negative for all θ, and for $\theta = 0$ in particular, that is η would have to be negative, which is impossible The state (3) is also impossible, for suppose it were possible that $(A + C + \eta)$ and $(A - C - \eta)$ should cut the axis of θ at the same point, then both $(A + C + \eta)$ and $(A - C - \eta)$ must have both positive and negative values in the range $-\mu \leqslant \theta \leqslant \mu$ Now the stability condition at the point $\theta = \mu$ is

$$(-2\mu^2 \operatorname{sech}^2 \mu + k^2\eta)(-k^2\eta) < 0,$$

that is,

$$k^2\eta > 2\mu^2 \operatorname{sech}^2 \mu$$

But if $k^2\eta > 2\mu^2 \operatorname{sech}^2 \mu$, then from the form of the curve $(A + C)$ we see that $k^2(A + C + \eta)$ is always positive, for the maximum modulus of the negative ordinate is $2\mu^2 \operatorname{sech}^2 \mu$ Hence state (3) cannot exist There is, however, the singular and isolated case in which state (3) can exist This corresponds to curve (3) of fig 1 Hence $\eta = 0$ and $\mu = 0\ 881$ This particular case corresponds to the case investigated by von Karman and its relevance will be discussed later We must, therefore, return to the first of the three alternatives given above

We have seen already that if $(A + C + \eta)$ is to be positive always, then

$k^2\eta > 2\mu^2 \operatorname{sech}^2 \mu$ The sole remaining question is whether this value of η makes $k^2(\mathrm{A} - \mathrm{C} - \eta)$ negative for all values of θ This is obviously so if the maximum positive ordinate is less than $2\mu^2 \operatorname{sech}^2 \mu$ A consideration of the curves shows us therefore that the minimum value of $k^2\eta$ for stability is the greater of $2\mu^2 \operatorname{sech}^2 \mu$ and the maximum positive ordinate of $k^2(\mathrm{A} + \mathrm{C})$ We find that when $\mu \leqslant 1\ 531$, then $k^2(\mathrm{A} + \mathrm{C})_{\max} \leqslant 2\mu^2 \operatorname{sech}^2 \mu$ Hence when $\mu \leqslant 1\ 531$, then $k^2\eta = 2\mu^2 \operatorname{sech}^2 \mu$ When $\mu \geqslant 1\ 531$, $k^2\eta = k^2(\mathrm{A} + \mathrm{C})_{\max}$ We note that as μ increases the position of the maximum tends towards $\theta = 0$ and that the value of the maximum tends towards $\frac{1}{2}\mu^2$, as can be seen from the formula for $k^2(\mathrm{A} + \mathrm{C})$ This and other points can be verified from the following table

Table II

μ	$\theta_{\max}$	$k^2(\mathrm{A} + \mathrm{C})_{\max}$	$2\mu^2 \operatorname{sech}^2 \mu$
1 200	0 0000	0 2809	0 8781
1 500	0 2027	0 7430	0 8131
1 530	0 2231	0 7985	0 8013
1 531	0 2237	0 8009	0 8009
1 600	0 2618	0 9348	0 7708
1 800	0 3584	1 3602	0 6710
2 000	0 4360	1 8295	0 5652
2 500	0 5595	3 1299	0 3323
3 500	0 5410	6 2217	0 0892
5 000	0 2746	12 5323	0 0091

We note that $k^2\eta = 2a^2l^2 \log(1/l\epsilon)$, and that if ϵ is some definite quantity, as it is in actual experiment, then $k^2\eta \to 0$ in two ways The first is when $l \to 0$, and the second when $a \to 0$ The limiting processes must therefore be applied with some care We may summarise the results of the stability considerations as follows As long as the disturbances of the vortices are purely translations then the Karman street given by $k = 0\ 281$ is stable no matter what the thickness of the vortices But as soon as the wave-length of the disturbance along the vortex becomes sensible there is, from a consideration of fig 2, a distinct domain of instability in the neighbourhood of $\phi = \frac{1}{2}\pi$ This, however, is of no importance if ϕ for the actual disturbance is small, in which case the system is stable If there are any components of the general disturbance in the neighbourhood of $\phi = \frac{1}{2}\pi$ they will give instability and break up the configuration We must now make an assumption of a physical nature if we are to explain the subsequent motion The assumption is that the vortices tend to spread as much as possible owing to viscosity Owing to instability the individual vortices will twist about and give an irregular three-dimensional motion, and also the distance between the rows will either tend to increase or to decrease If the tendency is to decrease the distance between the rows, then the system will always be unstable and the double row will close up its ranks and will disappear If there is a tendency to increase the distance between the rows then, assuming that ϵ does not alter appreciably, a state will ultimately be reached where the parameters of the system are such that they correspond to a point on the stability curve By "stability curve" we mean the curve showing the relation between the minimum value of η that will ensure stability for a given value of a/b—as is shown in fig 3 In a position of stability there will be no tendency for a to increase, nor for the vortices to increase their distortion The change in ϵ is now the dominating factor Therefore for a given value of l, η increases till it cuts the curve obtained from Table II Since there is a tendency for ϵ to increase, the parameters of the system will now be given by this curve ϵ increases slowly and η diminishes Hence a now tends towards zero (The small bump in the curve $k^2\eta$ which may give rise to complications, such as a gradual increase in ϵ and then a decrease, may be ignored The bump is merely due to the mathematical peculiarities of the curves—and since we are only dealing with the problem very approximately we cannot pay too much attention to it The general tendency is, however, as given) This is true for all ϵ Generally we may say that for disturbances of large wave length along the axes of the street and vortices the Karman street is stable whatever the thickness of the vortex For smaller wave lengths there is instability and the vortices become increasingly contorted The double row may meanwhile tend to close up its ranks and disappear, or to increase the distance between the rows In the latter case a position of stability is reached - but this is merely transitional, for the increase in the diameter of the vortices becomes the dominating factor and the vortices twist up till they are no longer recognisable The following fig 3 demonstrates what happens The broken line is the curve $k^2\eta$, and the unbroken lines show the increase in η for various values of l, resulting from the increase of a and ϵ The curve giving the relationship between η and μ is therefore as follows —

Schlayer* eliminated ϵ from the equations in a manner which is open to criticism. The work done by the body (put equal to [Karman's expression for the resistance] × [velocity of the body]) per unit time, was equated to an expression involving the energy associated with the vortices. The energy associated with the vortices was taken from an expression given by Lamb, namely, $E = \frac{1}{2}\rho\Sigma\kappa\psi$, where the appropriate signs for κ are taken, and ψ is the value of the stream function at the different vortices It was remarked

---

* Schlayer, *loc. cit*, pp 361-2

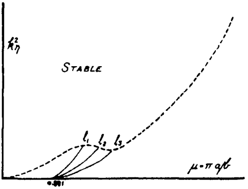

FIG 3 —The ordinate is $k^2\eta = 2a^2l^2 \log(1/l\epsilon)$ and gives a measure of the self induction effect of the vortices Systems represented by points on and above the broken line are stable for all components of the motion All systems represented by points below the line (except the isolated case corresponding to the two dimensional disturbance of the Karman street) have certain components which are unstable The unbroken lines represent changes in the value of $k^2\eta$ produced by changes in a (the distance between the rows) and ϵ (the radius of the vortices), l being kept unchanged along each unbroken line

correctly that ψ at each vortex was infinite, and therefore the author took a small domain of radius ϵ round each vortex, found the energy, and so introduced ϵ into the equations But the expression $E = \frac{1}{2}\rho\Sigma\kappa\psi$, used by the author, is only valid if $\Sigma\kappa$ is zero Apart from the difficulties involved in the assumption that we may consider the Karman street as a system in which $\Sigma\kappa$ is zero, there is also the fact that the energy does not depend on ϵ and can easily be evaluated If we consider an individual vortex, say at $z = \alpha$, we have that ψ in the neighbourhood of this vortex is given by

$$\psi = \frac{\kappa}{2\pi} \log r + \text{regular function},$$

where r is the distance from the point α. The infinity at a vortex is due to the term $\log r$ But if $\Sigma\kappa$ is zero, then all these infinities cancel and the total energy is $\frac{1}{2}\rho\Sigma\kappa\psi$ where ψ is the value of the stream function at a vortex due to all the other vortices, and is no longer infinite The energy can thus be evaluated without introducing the thickness of the vortex The relation obtained by Schlayer therefore cannot be accepted.

[*Note added March* 20, 1930 —It has been suggested that some definite numerical case of unstable motion be given—and the following may be regarded as a typical example. Let us assume that the undisturbed double row is the Karman street—that is, $a/b = 0{\cdot}281$. For the remaining figures we shall take values derived from certain experimental data which, it is hoped, will be published shortly. The depth of the water tank used was 13 cm. and if we assume that the free surface of the water is a slightly deformable bounding wall, then the distance between the two boundaries is some integral multiple of half the wave length of the disturbance along the axis of a vortex of the street, for at the bounding wall the velocity of the fluid must be entirely along the wall. That is

$$13 = n\,(\pi/l), \tag{1}$$

where n is an integer, and $(2\pi/l)$ is the wave length along the axis of the vortex tube. Let us investigate the case $n = 10$. This makes $l = 0{\cdot}4138$. The radius of the vortices is approximately 0·16 cm. Approximately also $a = 5\epsilon = 0{\cdot}80$ cm. These figures make $\lambda^2\eta = 0{\cdot}60$. A brief investigation shows that $(\mathrm{A} + \mathrm{C} + \eta)$ is negative in the range $0{\cdot}775 < \theta \leqslant 0{\cdot}881$, and positive in the range $-0{\cdot}881 \leqslant \theta < 0{\cdot}775$. $(\mathrm{A} - \mathrm{C} - \eta)$ is found to be negative in the whole of the range $-0{\cdot}881 \leqslant \theta \leqslant 0{\cdot}881$. Hence the components in the range $0{\cdot}775 < \theta \leqslant 0{\cdot}881$ are unstable. This refers to the disturbance which, in the theoretical investigation, was given by (4·9). That of (4·11) will be unstable in the range $-0{\cdot}881 \leqslant \theta < 0{\cdot}775$. The component that will increase most rapidly with time is the one that has the largest value of $\sqrt{\mathrm{A}^2 - (\mathrm{C} + \eta)^2}$. In the case we are discussing, this is given by $\theta = 0{\cdot}881$, which gives

$$\lambda = \frac{\kappa}{8\pi b^2}\frac{1}{\lambda^4}(0{\cdot}3224) = 0{\cdot}0408\omega,$$

where ω is the angular rotation of the vortex. ω itself cannot be measured, but it is obviously very large. If we give it only a moderate value, say $\omega = 10$, we get that the component of the initial disturbance corresponding to $l = 0{\cdot}4138$, $\phi = 0$ (*i.e.*, $\theta = 0{\cdot}881$) is doubled in 1·7 seconds and trebled in 2·8 seconds. If we adopt different values for n we get correspondingly different ranges of instability, and different amounts of instability—but the general phenomenon is the same.

Since the communication of this paper the results of an interesting investigation have been published by Levy and Hooker* and the results indicate that there is another factor that makes for instability in the Karman street, and this is the velocity distribution in the fluid upon which the vortex system is superposed The discussion in the present paper deals with three-dimensional disturbances of the vortices in an infinite sea of liquid, in which, of course, the basic velocity is assumed to be constant The paper of Levy and Hooker investigates two-dimensional disturbances of the vortex system in a channel of finite breadth, in which the distribution of the basic velocity is such that it has a maximum at the centre-line of the channel and decreases smoothly to the barriers Any such distribution makes for instability The disturbing effect depends upon the rate of change of the velocity between the axis and the walls of the channel with respect to the distance from the axis It was remarked correctly that, in general, when the channel is wide, the basic velocity in the middle of the channel is approximately constant The result of this will be to diminish the disturbing effect if the distance between the rows is small compared to the distance between the channel walls There will however, be the self-induction effect of the vortices which will tend to destroy the pattern In general we may say then that both factors are operative The effect of three-dimensional disturbances is always present and the effect of the distribution of the basic velocity is operative with varying degrees of importance, thus, if the object is wide compared with the channel, the distribution of velocity is the all-important factor, but if the object is of small diameter, the effect is negligible It should be noted, however, that the analysis of Levy and Hooker is only valid when the channel is wide in comparison with the obstacle]

---

* 'Phil. Mag.,' vol. 9, p. 489 (1930).

Photo-conductance Phenomena in the Silver Halides, and the Latent Photographic Image.—Introduction and Part I

By F. C. Toy, D.Sc., and G. B. Harrison, B.Sc., British Photographic Research Association Laboratories

(Communicated by T. Slater Price, F.R.S.—Received February 8, 1930—Revised March 22, 1930.)

[Plate 18.]

Introduction

In studying the mechanism of the photographic process the question naturally arises as to the part played by the silver halides, which form the basis of practically all photographic emulsions. It becomes important to determine whether, or not, the photographic mechanism can be linked up with one or more particular characteristics of these silver salts. Especially is this so in view of the fact that some investigators have developed theories* in which the silver halides play no direct part in the photo reaction taking place on exposure. They have assumed that the absorption of the active light and the resulting process occurs in other light sensitive substances associated with the silver halides in the emulsions, and that the function of the silver halide is merely to act as a source from which metallic silver is produced by the process of development. Weigert especially supports this idea at the present time.

It seems to us, however, that the evidence which now exists is not only strongly against this view, but is in favour of the idea that the primary photographic process is intimately concerned with the absorption of light by the silver halides themselves, and may indeed be identified with certain of their characteristic properties.

We may take silver bromide as typical of the silver halides, and as the one most commonly used in photography. There are three well-known effects of the action of light upon crystals of this salt :—

(1) The splitting up of the silver bromide by light into free bromine and metallic silver, which under ordinary conditions can be observed by the detection of free bromine in the medium surrounding the crystal and by the residue of metallic silver. This is what is known as "photochemical decomposition" ; the process by which it takes place will be discussed later.

---

* Schanz, 'Phot. Korr.,' vol. 58, p. 8 (1921) ; Weigert, 'Proc. VII Int. Congress of Photography,' London, p. 87 (1928).

(2) The external photo-electric effect when the light is of suitable frequency.*

(3) The internal photo-electric effect, or photo-conductivity effect, by which is meant the change in the electrical conductance of the crystal which takes place on illumination †

It has now been shown beyond any reasonable doubt that (2) can only be indirectly connected with the photographic process ‡ This conclusion has been drawn because experiments have shown that the critical wave-length for the external photo-electric emission from silver bromide is in the region of λ 3000, whereas a silver bromide emulsion is photographically sensitive to wave-lengths longer than λ 5000

On the other hand, when we consider the two other characteristic properties (1) and (3), the evidence strongly points to the photo-chemical decomposition and the change of electrical conductance on illumination being intimately connected and governed by the same mechanism as the photographic process This suggestion will be developed in what follows

There is now a large measure of general agreement that the process of latent image formation by light may be considered theoretically as divisible into two stages --

(1) The formation of free bromine and metallic silver as the immediate result of the light absorption by the silver bromide This is known as the *primary process*

(2) Complicated chemical reactions between the bromine and other substances, such as gelatin, present in the emulsion and surrounding the grains of silver bromide, the distribution of the liberated silver possibly being influenced in some way in order that nuclei of a certain minimum size, capable of initiating the development process, may be built up These reactions whereby the bromine is to some extent prevented from recombining with the silver make up what is known as the *secondary process*

The Primary Process

We shall be concerned here with the primary process only Although the conception of it given above agrees better with observed facts than any other idea, yet actual photo-chemical decomposition of silver bromide into its elements has not definitely been proved to take place in exposures of the order of those used in photography In the latter case proof of decomposition is at present beyond the accuracy of available analytical technique It will now be shown how a study of the photo conductance effect will furnish a method by which the primary process can be observed under conditions of time and intensity comparable with those used in photography

---

* W Wilson, 'Ann Physik,' vol. 23, p 107 (1907)

† Wilson, *loc cit* , Scholl, 'Ann Physik,' vol 16, pp 193, 417 (1905), and Arrhenius, 'Eder's Jahrb ,' p 201 (1895)

‡ Toy, Vick and Edgerton, 'Phil Mag ,' vol 3, p 482 (1927), Butler, 'Proc Iowa Acad ,' vol 34, p 277 (1927)

In the silver bromide lattice, the single valency electron in the outer shell of each silver atom may be regarded as associated with bromine rather than with silver, giving silver and bromide ions The action of the light in splitting up the crystal into free bromine and metallic silver may be regarded as the release of valency electrons from the bromide ions Thus during illumination there are a certain number of free electrons present in the crystal, which were not free in the dark The presence, on illumination, of a sufficient number of these additional free electrons should be detectable as a change in the electrical conductance of the crystal At this stage we do not, of course, exclude the possibility of the photo-current being partly ionic

The idea here suggested is that the electron shift necessary for the photo-chemical decomposition is the same as that which produces the change in conductance, or in other words, the *photo current observed by applying a potential difference to the silver halide is due to the same mechanism as that which brings about decomposition*

If this be true, then it should be a general fact that compounds which can be decomposed by light will show the photo-conductance effect over the same spectral region as is effective in causing decomposition This point has been emphasised by Toy,* and only a brief reference need be given here It is certainly true for the silver halides , Fajans has shown† that if pure silver bromide, free from gelatin, be prepared in such a way that its surface is not contaminated by certain adsorbed ions, such as silver or hydroxide ions, the longest wave-lengths which are effective in causing appreciable visible decomposition in a reasonable time are in the blue green region of the spectrum, the sensitivity increasing rapidly towards the ultra-violet This is also true for the direct decomposition (called the " print out " effect) of a pure bromide photographic emulsion, and the spectral range over which this decomposition is observed is precisely the same as that over which silver bromide exhibits the photo-conductance phenomenon For both silver bromide and silver chloride it may be noted that this region is, in fact, the long wave-length edge of the absorption bands of these salts

---

* 'Proc VII Int Congress of Photography,' London, p 23 (1928)

† 'Z Elektrochem ,' vol 28, p 499 (1922)

In addition to these special cases where the spectral sensitivity data are known, it seems to be a general fact that all compounds which can be split up into their elements by light show the photo-conductance effect, while most of those which are very stable to light, such as many fluorides, nitrates and sulphates, do not show any photo-conductance whatever These facts are well brought out in a paper by Gudden and Pohl *

There seems, therefore, to be little doubt that in studying the photo-current in silver bromide we are dealing fundamentally with the same mechanism as that which brings about photo decomposition A *permanent* chemical change can only occur if some secondary process is allowed to prevent the liberated bromine from recombining with the silver The secondary process can to some extent be controlled For instance, it will be given every chance to occur if the silver bromide is surrounded by a medium with which free bromine reacts very readily, while it will be prevented entirely if the surrounding medium is an impervious substance which does not react with bromine, such as glass or quartz In this latter case no permanent change in the silver salt can take place no matter how long the exposure to light may be, and it will be in precisely the same state after exposure as it was before But the point to emphasise here is that even if there is no permanent decomposition the process of liberation of the valency electrons still takes place when the silver bromide is illuminated, only in this case there is an equilibrium existing between the rate of their liberation from the bromide ions and the rate at which they go back again The photo-conductance effect should therefore be observed whether decomposition takes place or not In the former case, it will, however, be complicated by the changing nature of the system, whilst in the latter it can be observed as a completely reversible process In the experiments to be described later, the conditions were always chosen so that the secondary reactions were prevented

Now if in the *photographic plate* the light action is the same as that taking place both in photo-conductance and in photo-chemical decomposition then the spectral sensitivity range common to these two latter processes for a given halide should be the same as that of the latent photographic image (made visible by the process of development) in an emulsion made with the same halide This also has been shown to be true (Toy, *loc cit*) Both in emulsions made with silver bromide and silver chloride the spectral regions active

---

* 'Z Physik,' vol 16, p 42 (1923)

photographically correspond closely with the light absorption curves of the pure halides. Another striking example of the similarity between the photo-conductance and photographic effects is given by mercuric iodide, which Lüppo-Cramer* showed in 1903 could be used with gelatin to make a photographic emulsion. He stated that such an emulsion had a maximum sensitivity at about λ 5600 when exposed to the spectrum of the sun. Later and more accurate experiments by G. Athanasiu† showed that for an equal energy spectrum this maximum sensitivity is at λ 5100, a value which agrees closely with that found by Volmer‡ for the position of maximum photo conductance effect in pure mercuric iodide.

From the standpoint of the mechanism of the formation of the latent image in silver halide emulsions the investigation of the photo conductance phenomenon in the silver halides themselves thus appears to be of great importance. It furnishes a means of studying the mechanism of the primary photo-chemical process during the actual light exposure. Also it is capable of detecting extremely small light effects, the limiting accuracy depending only on the sensitivity of the electrical apparatus used for the observations. It therefore brings within the range of attack latent image problems for the solution of which the available methods of chemical analysis are quite inapplicable.

Gudden and Pohl have published many very important papers on the photo-conductance effect in crystals. Little reference is made to their work here, largely because in the different types of crystal (diamond, zinc sulphide, selenium) mainly studied by them, the photo-currents seem to be of a less simple nature than those we have observed in silver bromide.

The precise meaning of "photo-conductance" throughout this paper is as follows: if σ and R be the conductance and resistance in the dark, and σ' and R′ the corresponding values in the light, then photo-conductance equals $\sigma' - \sigma = 1/R' - 1/R$.

The first part of the paper describes the experiments which have been undertaken in connection with the study of this photo-conductance effect in silver bromide. The experiments have been devised with the main object of elucidating the following problems:—

(1) The relation between the effect and the time of exposure.

(2) The relation between the effect and the light intensity.

(3) The nature of the carriers of the photo-currents.

---

* 'Eder's Jahrb.,' p. 34 (1903).

† 'C. R.,' vol. 176, p. 1389 (1923).

‡ 'Z. Wiss. Phot.,' vol. 16, p. 152 (1916).

The last problem involves a study of both the dark and the photo-conductance effect over a large temperature range, and the influence on the temperature effect of annealing the silver bromide

The second part of the paper deals with the interpretation of the experimental results and their significance from the standpoint of photographic theory

PART I *

The first essential in carrying out the work outlined in the introduction is to find a method of mounting the silver halide in a satisfactory and convenient form The main conditions to be fulfilled are the following good contact between the salt and electrodes, a uniform electric field between the electrodes, layer of salt of uniform and controllable thickness, area illuminated made as large as possible and the resistance between the electrodes kept low

It would, of course, be desirable to use single crystals, such as are found in photographic emulsions, for these experiments, but owing to the difficulty of handling such small objects it was thought advisable to work first with the salt in a more convenient form It was therefore decided to used fused silver bromide, which Wilsey† has shown to have the same crystal structure as the grains in a photographic plate However, the technique of working with small crystals is being developed and it is hoped that as soon as possible they will be tested in the same way as the fused salt

The silver bromide was prepared as follows 30 gms triple re-crystallised silver nitrate were dissolved in about 700 c c of distilled water, and 20 gm of ammonium bromide, re-crystallised once from water, were dissolved in 200 c c distilled water The silver nitrate solution was slowly added to the ammonium bromide solution in red light with violent shaking and agitation When all had been added the precipitate was allowed to settle, and the whole allowed to stand overnight The supernatant liquid was decanted off and the precipitate, after washing by decantation six times, was collected on a hardened filter paper (so as to minimise contamination by organic matter) on a Büchner funnel and further washed 12 times with distilled water It was then transferred to a watch glass and dried for 5 hours at 130° C, and further for 14 hours at 180° C

Fig 1 shows a transverse section of the type of specimen first used (type G) The silver bromide was fused on to a circular quartz plate A, 25 mm in diameter,

---

* By G B HARRISON

† 'Phil Mag,' vol 42, p 262 (1921)

with optically worked surface, and spread by a quartz rod into a long strip along a diameter While still hot the optically worked edge of another quartz

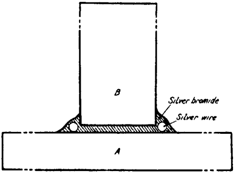

Fig 1

plate B was pressed down on the strip, being kept at a given distance from the base plate by means of two small pieces of microscope cover slip The dimensions of the edge of this upper plate were 25 × 1 5 mm Sufficient silver bromide was used to fill the gap between the two plates and leave enough on both sides of the upper plate for making contact with the electrodes The electrodes were of fine silver wire 0 2 mm in diameter and were carefully cleaned by immersion in dilute nitric acid until the surface just started to etch, followed by washing in distilled water This etched surface seemed to produce better contact than if the wire were mechanically cleaned so as to leave a fairly smooth surface The wire was then embedded in the molten salt on each side of the upper plate and the whole allowed to cool When its temperature had fallen to about 100° C the surface of the bromide was painted with paraffin wax to exclude moisture The use of silver for the electrodes has the advantage that with the silver bromide it forms a reversible system, a point which will be referred to later In all the experiments silver electrodes are used unless stated otherwise

It will be seen from fig 1 that there is a uniform layer of salt between the plates, and since practically the whole of the resistance is due to this part of the salt the field will be uniform whatever the position of the wires in the outer salt The thickness of the layers may be measured by means of an accurate screw gauge, a zero being taken with the two plates pressed in close contact. In this way a thickness down to 2 or 3 μ can be estimated with sufficient accuracy Qualitatively the results given in the paper are not affected by variation in thickness from 1 μ to 200 μ, which are the limits used throughout the work

These preparations were found to be very satisfactory, the electrode contact was good and they could easily be repeated Their dark resistances at ordinary temperatures were of the order of 10^{-8} ohms

Electrical Circuit

The potential gradients used across the silver bromide throughout this work did not exceed 4 volts per millimetre at ordinary temperatures, giving a current of the order of 10^{-8} amps. The magnitude of the additional current on illuminating the silver bromide varied enormously with the conditions, but in some cases it was at least 100 times smaller than the " dark " current It was therefore necessary to find a suitable method of measuring a small fraction of a small current

The specimen of silver bromide (S, in fig 2) was set up in series with a constant

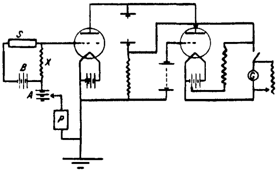

FIG 2

50-megohm resistance (X) and a 6-volt dry battery (B) One end of the 50-megohm resistance was connected to the grid of the first valve, and the other end through an adjustable dry battery A, and a Cambridge potentiometer P, to the filament of the first valve Two stages of amplification using resistance coupled D E.5*b* valves were found suitable, the anode current of the second valve being passed through the galvanometer (G) together with a " compensating " current adjusted to the same value, and fed from part of the battery supplying the second valve filament Precautions had to be taken to ensure that the first valve acted as a voltmeter of infinite resistance

Two kinds of galvanometer were used—for ordinary work a comparatively insensitive Gambrell instrument was found to be satisfactory, its period being about 2 seconds For investigating the time of reaction, etc, an Einthoven string galvanometer* with synchronous timing and photographic recording gear was used The quickest period of this instrument in the circuit described is about 1/200th second

To measure the photo-currents, the adjustable potentials A and P (fig 2) in the grid circuit of the first valve were arranged so that there was no deflection of the galvanometer The silver bromide was illuminated and in consequence its resistance changed, producing a redistribution of potential around the circuit SXB The change of potential across the fixed resistance X was then compensated by altering the potentiometer to bring the galvanometer back to zero The battery B was then disconnected and the potentiometer reading required to bring the galvanometer to zero again taken These three readings gave the potential difference between the ends of the fixed resistance both in the dark and light Dividing these values by the magnitude of the resistance X gave the total " dark " and the total ' light " currents The photo-current was the difference between the two

The great disadvantage of this circuit is that every change of resistance of the silver bromide is accompanied by a change of potential across it, and it was necessary in order to obtain comparable results to reduce all readings to some standard potential This could, of course, only be done if the current-potential curve in silver bromide follows some known law, for instance, Ohm's law This point was tested, using silver electrodes for both the light and dark currents at various temperatures from −180° C to + 60° C, and the law was found to hold rigidly in every case But it was found that if platinum electrodes are substituted for the silver ones, a potential of about 1 volt has to be applied before any current flows, due to a polarisation e m f which builds up quite slowly This appears in the light as well as in the dark, as would be expected These results showed that provided silver electrodes were used the circuit described above could be employed, and the observed current always reduced to the value corresponding with a fixed potential by the application of Ohm's law The reduced values were strictly proportional to the conductances

If a freshly prepared melt of silver bromide be exposed to light, complicated effects which will be referred to later are at first noticed It is sufficient for the moment to say that the effect expected (a quick increase in conductance on illumination, called the ' positive effect " and resulting in the photo-current) could be observed under suitable conditions, and isolated from all complicating factors. It was therefore possible to investigate the time of appearance of the photo-current after the silver bromide was illuminated

---

* Kindly loaned by the Director of the Science Museum

Experiments were first made using one valve amplification combined with the Einthoven string galvanometer, but recently increased sensitivity (to be dealt with later) has made it possible to use a simple circuit consisting of battery, Einthoven galvanometer, and specimen, thus doing away with any lag introduced by the amplifier The period of the instrument under these conditions was about 0 005 second For the actual experiment it was necessary to record on the film the trace of the galvanometer string, the timing marks, and some record of the time when illumination of the bromide was commenced and finished In order to do this the apparatus was arranged as shown in fig 3

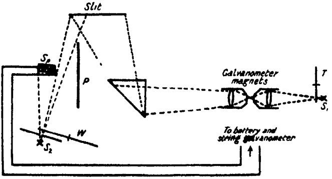

FIG 3

The cinematograph film may be taken as equal in width to the length of slit shown in fig 3, and moving in a direction perpendicular to the plane of the paper The two sources of light, S_1 and S_2, illuminate the film in the manner shown in the figure, the partition P being placed so that S_2 can only illuminate part of the slit and S_1 practically the whole of it The specimen of silver bromide S_p is mounted in the beam from S_2 so that part of the beam illuminates the specimen and the other part the slit The specimen is connected to a battery and the string galvanometer The source S_1 is focussed on the string and a lens forms an image of the latter on the film A synchronised toothed wheel T interrupts the beam from S_1 at intervals of 0 01 second and thus produces lines across the film corresponding to this interval With this arrangement the moment of illumination of the crystal S_p is registered by the darkening on the film due to the direct light from S_2, while the moment at which the photo-current starts to flow in S_p is registered by the movement of the image of the galvanometer string on the other part of the film Any "lag"

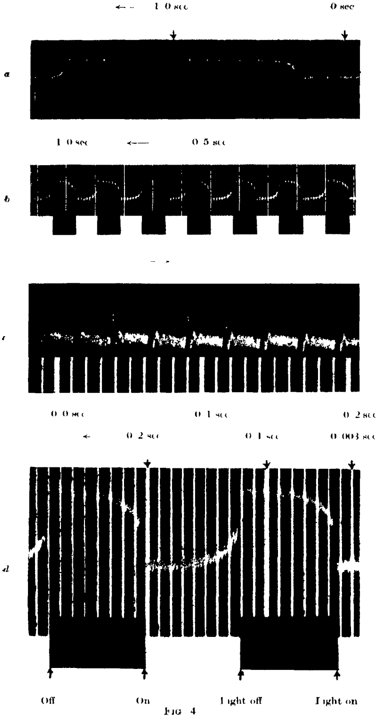

Fig 4

(Facing p 623)

between the time of illumination and the initiation of the photo-current could thus be detected

The photographs in fig 4 (Plate 18) show some of the results thus obtained (*a*) shows a comparatively long exposure of about 1·36 seconds, it will be seen that equilibrium is established after about 0·1 second However long the exposure lasts after this there is no change, and on cutting off the light the specimen returns to its original state (*b*) was obtained by means of a motor-driven disc W (fig 3) cut so that the specimen was illuminated during half a revolution and was in the dark during the other half The "shutter" gave exposures of 0·08 second, taking 0·004 second to open and the same time to close (*d*) is an enlargement of part of (*b*) showing clearly the exact agreement between the edges of the black portions, representing the moments of exposure and cut off, and the beginning and end of the string movements due to photo-currents (*c*) shows exposures of 0·0005 second made about every 0·02 second by a revolving wheel, it can clearly be seen that even at this short exposure some considerable effect occurs

It is interesting to note in passing that this arrangement is an illustration of the idea of the primary and secondary photographic processes discussed in the introduction The single beam of light from S_2 may be regarded as producing only the primary part of the photographic process in one layer of silver bromide (S_0) and the *whole* photographic process (primary + secondary, giving latent image) in another layer, *i e*, the emulsion on the film

The complication referred to earlier as occurring with a freshly prepared specimen is a slow *decrease* of conductance with time (negative effect), due to a gradual alteration in the crystalline state, until equilibrium is established after 5 or 6 days As will be seen later the establishment of equilibrium can be hastened by annealing This decrease is accelerated by light, so that on first illumination a freshly prepared specimen may show an increase, or a decrease, or very little change in its conductance, depending on its crystalline state at the moment of test Moreover, the observed result will vary with time In the recent work of Kirillow* on these effects it appears that he has not recognised that the negative effect is merely a subsidiary property of an agglomeration of silver bromide crystals, and is not a fundamental characteristic of silver bromide itself

---

* 'Z Wiss Phot,' vol 26, p 235 (1929)

Relation between Intensity of Illumination and Photo-conductance Effect

From a theoretical standpoint it might be expected that the effect would be proportional to the incident light intensity, as in the photo-electric case The experiment to test this was carried out by mounting one of the usual type of specimens behind the slit of the spectroscope, and placing in front of the slit a movable Ilford neutral optical wedge The blue line λ 4358 from the mercury arc was then adjusted to pass through the slit and readings of the photo-current taken by the usual valve amplifier method for various positions of increasing density of the wedge until the effect became too small to be measured The density of the wedge was then gradually decreased and readings taken in the reverse direction The mean of these two sets was taken so as to eliminate any possible errors due to small changes of sensitivity of the specimen during the experiment The Ilford wedge was calibrated accurately for the particular light used

The light intensity was varied in the ratio of 100 to 1 approximately, and many curves were obtained on different specimens, all of which gave a straight line relation between photo-current and intensity within the limits of experimental error The greatest intensity of the light employed was 50×10^{-6} cals per square centimetre per second

So as to prove beyond all doubt that the photo-currents were actually observable with light intensities within the normal photographic range (*i e*, those which require ordinary exposures) an intensity of ultra-violet light was adjusted so that it only just produced a developable effect on a plate of H and D speed 550 in an exposure of 1/25th second The photo-current which this intensity produced in silver bromide was easily observable on the galvanometer

Investigation of the Effect of Temperature on the Dark Conductance and on the Photo conductance

The dark conductance was found to vary very rapidly with temperature, being practically exponential in form as shown in fig 5 (1) The relation found can be represented by the following formula,

$$\log \sigma = A - B/T,$$

when σ is the conductance, T the absolute temperature and A and B are constants As can be seen from curve 2 (fig 5) the results fit this formula extremely well, and it has been shown to hold over the range from 20° C to −150° C[*] (Since the specific conductance could not be obtained owing to uncertainty as to the dimensions of the specimen, the current at constant voltage has been plotted against 1/T) Every specimen tested whether annealed or not, gave the same relation, the slope of the curves agreeing within experimental error The effect of annealing was, however, to decrease the dark conductance enormously in all cases

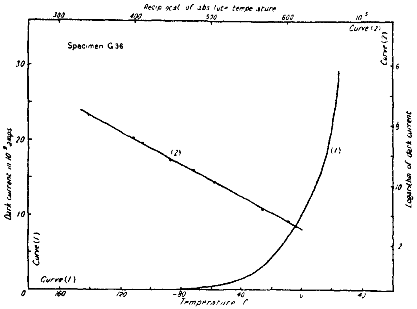

FIG 5

The experimental results obtained from the investigation of the effect of temperature on the photo conductance are very complicated The various curves obtained are shown in fig 6 The first experiments yielded curve A which will be seen to have a sharp maximum at about – 5° C This was repeated for four specimens of the standard (G) type Then for no apparent reason types (B) and (C) appeared which have a maximum at – 90° C Sometimes this maximum was very pronounced (B) and sometimes almost negligible (C) This occurred in more than 12 consecutive specimens of the standard type, and no change in the mode of preparation could produce curve A again

Many explanations of the peculiar shaped curves were considered but they all failed when put to experimental test One, however, led to an interesting piece of work of which the results only will be given for lack of space It was suggested that the effect might be due to a variation of absorption of silver bromide with temperature, direct observation having already made it

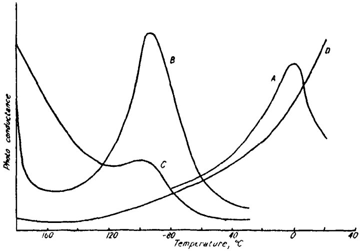

Fig 6

clear that the salt was more transparent to blue light at low temperatures The experimental results are given in fig 7 , relative values only were obtained,

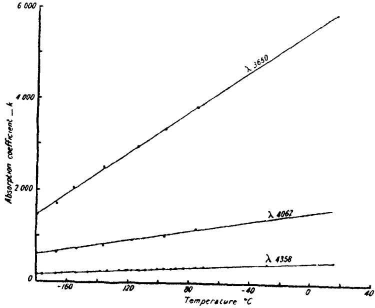

Fig 7.

and the values obtained by Slade and Toy* at room temperature were used for standardisation The values of the absorption coefficient k are plotted against temperature for the wave-lengths λ 4358, λ 4062 and λ 3650 It will be seen that the variation is very considerable, but the results cannot explain the maximum in the photo-conductance curves at — 90° C

---

* 'Roy Soc Proc ,' A, vol 97, p 91 (1920)

At this point further tests were made on a specimen which had been made four months previously A comparatively large quantity of silver bromide had been fused on to a glass plate and in it had been placed a grid of 10 platinum wires, 0 07 mm diameter—the bromide spreading over all the wires The whole had been allowed to cool in the absence of any cover plate The specimen had been given a test for sensitivity at room temperatures, and had then been put away and left for four months before being tested at various temperatures The result of this test is shown in fig 6 (D) This curve is seen to be different from all those previously obtained, and it was thought that the reason for this change might throw some light on the peculiarities already encountered Other specimens made up exactly as the one just described and tested immediately, gave temperature curves of the type B and C, so that the form of the curve appeared to be connected with the time the specimen is kept before testing

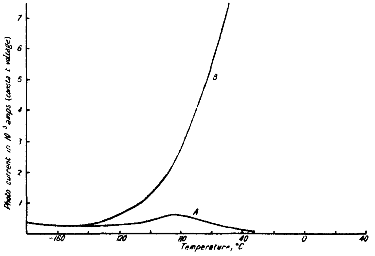

Fig 8

This suggested that the shape of the curve would depend on the extent to which the silver bromide had been "annealed," and that if a specimen were kept at a temperature just below its melting point for a day or two and then allowed to cool slowly, it might produce the same effect as keeping it for several months at room temperatures This was found to be the case, for on annealing a specimen similar to the one described above, which for convenience we will call the Z type, for 2 days, curve D was obtained The curves drawn in the figure are not all on the same ordinate scale Various degrees of annealing produce different shaped curves—some having maxima at various temperatures above – 90° C Fig 8 shows the results of annealing one particular specimen—curve A was taken immediately after preparation when the specimen (Z type) has been cooled very rapidly It was then annealed for 48 hours at about 20° C below its melting point—it then gave curve B It may be stated here that although it has never been possible to extend a curve of type D (fig 6) or B (fig 8) to a sufficiently high temperature owing to the breaking down of the specimen, it is practically certain that the curve will reach a maximum, since all measurements done at high temperatures above 30° C show a very rapid falling off of photo-conductance

From the above experimental data the following fact is explained In the standard type of specimen, when the bromide is enclosed between two plates, it would be expected that annealing would be more difficult than in the open "Z" type, consequently curves of type D (fig 6) have never been observed on the standard specimens however long they have been kept or to whatever extent they have been annealed However, the few that gave curve A (fig 6) were evidently annealed to a greater degree than the usual ones

This evidence definitely seems to prove that the shape of the photo-conductance, temperature curve is largely controlled by the crystalline state of the silver bromide

It may be noted here that the increased sensitivity at room temperatures due to annealing, and the fact that the "Z" type is naturally more sensitive than the standard G type, has made it possible to use a simple circuit containing only the specimen, battery, and Einthoven galvanometer, the dark current being compensated by means of a potentiometer At room temperatures the increase of conductance on illumination of carefully annealed specimens can easily be made as much as 30-fold whereas unannealed specimens of the same type exposed to the same illumination would only show increases of a few per cent, or less.

Photo-conductance Phenomena in the Silver Halides and the Latent Photographic Image.—Part II.

By F. C. Toy and G. B. Harrison.

(Communicated by T. Slater Price, F.R.S.—Received February 8, 1930.)

The Nature of the Photo current.

Although the experiments which have been described do not permit definite conclusions to be drawn regarding the nature of the photo current, it is very probable that it is to a large extent, if not entirely, electronic, as predicted in a preliminary note to 'Nature' (May 4, 1929). As, however, the method of attacking the problem has been by a comparison with the dark current, the mechanism of which is known from the work of previous investigators it is advisable first to refer briefly to the question of electrical conduction through unilluminated fused salts.

The work of many previous investigators has definitely shown that in the dark at room temperature the conduction process is purely electrolytic, there being no evidence of any electronic current in salts of the silver chloride-silver bromide type. Tubandt and his co-workers* have shown that in silver bromide all the dark current is carried by the silver ion only. The experiments of Phipps, Lansing and Cooke,† of Phipps and Leslie ‡ and of Phipps and Partridge,§ show that the transport of electricity by means of the kation only is a common characteristic of many solid salts. These authors found that from room temperatures up to the melting points the kation is the only carrier of electricity in the case of the chlorides and bromides of silver, lead and thallium, but that in the case of sodium and potassium chlorides, the anion also conducts at the higher temperatures. In all these cases the relation between the conductance (σ) and the absolute temperature (T) was found to be

$$\log \sigma = A - B/T,$$

where A and B are constants, which is the same equation as we have found to hold in our experiments over the entirely different range, from room temperatures to −180° C.

---

* Tubandt and Lorenz, 'Z. Phys. Chem.,' vol. 87, p. 573 (1914); Tubandt and Eggert, 'Z. Anorg. Chem.,' vol. 110, p. 196 (1920); Tubandt, 'Z. Elektrochem.,' vol. 26, p. 358 (1920); Tubandt, 'Z. Anorg. Chem.,' vol. 115, p. 105 (1921).

† 'J. Amer. Chem. Soc.,' vol. 48, p. 112 (1926).

‡ 'J. Amer. Chem. Soc.,' vol. 50, p. 2412 (1928).

§ 'J. Amer. Chem. Soc.,' vol. 51, p. 1331 (1929).

The process of electrical conduction in single crystals and crystal aggregates has also been the subject of many other papers, notably by A Smekal * A brief reference to his work must be made here, since it may be of considerable importance from the point of view of photographic theory According to Smekal, crystal properties may be considered as divisible into two classes according to whether alteration of crystal structure leaves the property unchanged or not The former he calls "structure insensitive" properties and the latter, to which electrical conduction belongs, properties which are "structure sensitive" The latter are greatly influenced by the conditions of crystallisation, whereas the former are not Smekal distinguishes two types of conducting ion One of them (the 'pore" ion) is the ion which is on an internal or external "surface" of the crystal In the case of an aggregate mass of salt these "surfaces" or edges of discontinuity in crystal structure, may be largely internal, due to imperfect crystallisation This type of ion Smekal supposes to be more loosely held and much freer to move in the crystal than the second or 'lattice ion type, by which he means an ion in a part of the crystal where it is surrounded by a perfect lattice The more mobile "pore" ions are identified with the edge' ions suggested by Blüh and Jost † On this idea the dark conductance is due to the pore ions and depends on the extent to which these are present, their number being least in the most perfect crystal and becoming greater as the state of crystallisation becomes less and less perfect Smekal quotes in support of this idea the fact that the imperfect crystalline aggregates formed by the solidification of molten salts at a high temperature have an electrical conductance enormously greater (in one case it was found to be nearly one thousand times greater) than for crystals of the same material deposited from solution The experiments of Joffe and Zechowitzer,‡ which show that the electrical conductivity of a single crystal of rock salt heated between 500° C and 600° C and subjected to increasing strain remains unchanged as long as no new "surface" or 'cracks' are formed in it, are also quoted by Smekal as supporting his "surface" theory of electrolytic conduction

Our own experiments on the dark conductance are in complete agreement with these ideas Fig 5 shows that the same relation holds between the dark

---

* 'Z Physik' vol 36, p 288 (1926), 'Phys Z,' vol 27, p 837 (1926), 'Z Elektrochem,' vol. 34 p 472 (1928), 'Z Phys Chem,' vol 5, p 60 (1929), 'Z Physik,' vol. 55, p 289 (1929), 'Z Elektrochem,' vol 35 p 567 (1929)

† 'Z Phys Chem,' vol 1, p 270 (1928)

‡ 'Z Physik,' vol 35, p 446 (1926)

conductance and temperature as previous workers found This relation holds whether the silver bromide is annealed, or not, though the magnitude of the dark conductance depends enormously on the state of crystallisation and varies with it in the way demanded by Smekal's theory This is shown by our experimental observation that the dark conductance of a silver bromide melt which had been prepared by very sudden cooling was decreased some thirty times by subsequent slow annealing

It seems, therefore, that the dark conduction of silver bromide may be attributed very largely, if not entirely, to silver ions which are situated at such places as "surfaces" and interfaces between elementary crystals, and that, apart from its true surface conduction, a single perfect crystal of silver bromide would be practically an insulator This conclusion seems a natural one, since it is difficult to imagine how conduction can occur in such a crystal, made up of highly electropositive and highly electronegative atoms the latter having a strong affinity for the excess or valency electron of the former

The problem whether the photo current is carried by electrons or by ions could be directly solved if it were possible to test Faraday's Second Law for the photo-current as Tubandt did for the dark current But unfortunately the currents through silver bromide layers of dimensions suitable for giving a photo-current comparable with the dark current are so small that a measurable quantity of silver cannot be deposited on an electrode within a reasonable time Nevertheless, the facts just quoted in regard to the dark conduction are of considerable value in arriving at a conclusion as to the probable nature of the carriers of the photo-current For if we compare the results obtained in our experiments on the photo-conductance with those for the dark conductance, to which reference has just been made, striking differences are at once noticed Firstly, the variation of photo conductance with temperature (figs 6 and 8) is in sharp contrast to that of the dark conductance with temperature, the shape of the former depending enormously on the conditions of crystallisation and in all cases being different from the form of the relation between the dark conductance and temperature Further, while at room temperatures the effect of annealing the silver bromide is to decrease the dark conductance (some thirty times in the case already quoted) it increases the photo-conductance enormously Thus in fig 8 even at − 50° C the photo conductance after annealing is some forty times greater than the value at the same temperature before annealing

These facts strongly suggest that the photo current is largely, if not entirely, electronic If it were ionic, it could only be due to the silver ions, just as is the dark current, for if the action of light is to change certain of the bromide ions into neutral bromine atoms, there seems no reason why the bromide ions should carry the current in the light if they do not do so in the dark But the idea of an ionic photo-current not only leads to the suggestion that it must be carried by silver ions but also that these ions must be "surface" ions like those carrying the dark current, for we rule out the possibility of ions in a perfect lattice having any appreciable mobility If this were the case then it might be expected that the photo-conductance would decrease with an increase in the annealing just as the dark conductance does, and for the same reason The fact that the photo-conductance changes on annealing in just the opposite way to the dark conductance therefore makes it difficult to suppose that the photo-current is ionic, but has a simple explanation if it is carried by electrons For, since free electrons can move easily through a metal, there seems no reason why they should not do so even in the perfect silver bromide lattice, assuming, of course, that during the light action some electrons which previously were bound to the bromine atoms may then be regarded as ' free ' Also, the continuity of the crystal structure might favour their easy flow and hence increase the conductance instead of decreasing it as in the case where it is due to the "surface" silver ions

In connection with this question of the nature of the photo-current, there is one more point which must be mentioned Referring again to figs 6 and 8 it will be noticed that for every silver bromide specimen, whatever its state of crystallisation, the photo-conductance tends to increase with decreasing temperature below about − 150° C This is again in disagreement with the facts for the dark current, which decreases continuously from the melting point down to −180° C While we cannot yet explain why the general shape of the photo-conductance, temperature curve depends to such an extent on the annealing, it is possible that at the lower temperatures the photo conductance, being electronic, increases with decreasing temperature for the same reason (whatever that may be) that it does so in a metal At temperatures above −150° C it may be that this simple metallic conduction (which is approximately inversely proportional to the absolute temperature) is becoming more and more masked by some other, and at present unknown factor Of course it may be dangerous to push this analogy to the case of a metal too far, since in silver bromide the "free" electrons are generated artificially by light, and in metals they are present naturally as a characteristic property

The Relation of the Photo-conductance to the Light Intensity

It has already been stated in Part I that the photo-conductance is directly proportional to the intensity of the light, a result which can very probably have only one interpretation For, since the mobility of the electrons is almost certainly independent of the light intensity for large variations of the latter, the change in photo-conductance with intensity can only be ascribed to a change in the number of additional free electrons present on illumination Thus we conclude that the number of electrons free at any moment during illumination and taking part in the conduction process is proportional to the light intensity If for every free electron there exists a neutral bromine atom, then the number of such atoms is also proportional to the intensity of the light

The Relation of the Photo conductance to the time of Exposure

Our experiments (fig 4) can be explained by supposing that the rate of production of free electrons is proportional at each instant to the incident light intensity This uniform growth of free electrons will be checked, however, by recombination with discharged atoms As a result of this an appreciable time must elapse before equilibrium conditions are established Fig 4 shows that this period is of the order of 0 07 second

In connection with this question of the time of appearance of the photo-currents, some recent important experiments by Vanselow and Sheppard* must be quoted, for although they do not deal directly with changes of current, the experimental observations certainly fit in with the assumption of an almost instantaneous liberation of electrons from the silver halides on illumination Vanselow and Sheppard have been investigating electrode potentials in photo-voltaic cells, a problem which has been the subject of much previous work, though not from the special view-point of photographic theory The phenomenon studied was originally discovered by Becquerel† who found that if two similar electrodes consisting of a layer of silver iodide on metallic silver be immersed in a solution containing iodide ions, a difference of potential is established between the two electrodes when one of them is illuminated. Using silver electrodes coated with silver bromide and a solution containing bromide ions Vanselow and Sheppard have shown that although the effects which occur on illumination are rather complicated, in general the illuminated electrode becomes negative relatively to the other when the light is first turned on, and then gradually assumes a positive potential as the illumination is continued In a further communication Sheppard* describes later experiments which show that the rise of negative potential begins within 1/600th second and attains a maximum within 1/65th to 1/20th second, although on turning off the light the positive potential only falls off very slowly, taking several seconds to drop in value by 10 per cent Vanselow and Sheppard suggest that the effects observed are due to the liberation of electrons from the silver bromide by the action of light and to accompanying liberation of bromine The almost instantaneous initial negative potential is supposed to be due to the fact that "the electrons penetrating into the silver electrode increase the electron pressure and thereby produce the initial negative surge," while the positive potential is explained as being due to the action of the slower moving bromine atoms on the inner silver part of the electrode when they reach it They test this assumption as to the positive effect in two ways Firstly, they argue that if it is due to the action of bromine on the silver electrode, then the presence in the solution of a "bromine acceptor," *i e*, a substance which will react with bromine and thus prevent it attacking the silver, should decrease or eliminate the positive potential They find this to be true Secondly, they say that if both electrodes are kept in the dark and one only is surrounded by a solution containing bromine which should diffuse through the silver bromide layer on to the silver, then this electrode should become positive relative to the other and there should be no negative effect at all This again is what is observed experimentally, the value of the positive potential varying with the concentration of the bromine in solution

---

* 'J Phys Chem,' vol 33, p 331 (1929), 'Nature,' vol 123, p 979 (1929)

† 'La Lumière,' p 121 (1868)

Owing to the known complicated nature of the electrode potentials in such cells as Sheppard and Vanselow have used, it is not easy to see to what extent their results and ours are in agreement But if their explanation of the effects they observed be correct, then both their experiments and ours confirm the fact that the primary light action is to remove an electron from the bromide ions, leaving neutral atomic bromine In their experiments this bromine diffuses towards the metal silver electrodes, in ours it is entirely prevented from moving

Sheppard has suggested† that the investigation of the photo-conductance phenomenon has not proved that the electrons involved are the valency electrons of the bromine atoms as is believed to be the case in the direct decomposition effect and also in the latent image formation But the whole of the spectral sensitivity data previously referred to in the introduction to this paper shows definitely that it is due to the removal of this valency electron that the photo-currents are produced Whether this is the electron involved in Vanselow and Sheppard's experiments will be more apparent when they have published further data on the spectral sensitivity of the effect they have observed The data already published on this point by them* shows no sensitivity at wave-lengths beyond about λ 3650, which is nearly 1500 A U less than the range active photographically and over which we have observed photo-conductance On the other hand, their experiments clearly suggest that bromine is liberated, a fact which, if true, necessarily involves the removal of the valency electron, which in the lattice is associated with the bromine giving the bromide ion Probably further experiments by Sheppard and Vanselow will clear up this uncertainty

---

* 'Nature,' vol 123, p 979 (1929)

† 'Nature' (*loc cit*)

Application to Photographic Theory

The conclusions which have been reached above may have a very important bearing on the theory of the formation of the latent photographic image, and in connection with this we will consider certain conclusions which our experiments indicate -

(1) The dark conductance of silver bromide is ionic, is carried by certain silver ions, and decreases to about one hundred thousandth part of its value at room temperatures at the temperature of liquid air This decrease may be due to a change in the number of silver ions free, or to a change of mobility, or both

(2) The photo-conductance is probably largely, if not entirely, electronic If any part of it is ionic, that part is presumably carried by the same kind of silver ion as that which carries the dark current , also, if the rapid falling off in ionic dark conductance is largely due to changing mobility, then the *ionic part* (if any) of the photo-conductance will also decrease rapidly with temperature

These facts bear directly on any theory of latent image formation which depends on the production of elementary electric currents in the silver bromide crystal. Such a theory has been proposed by A P H Trivelli† of the Kodak Research Laboratories It is probable that the silver bromide grains of certain photographic emulsions contain traces of silver and silver sulphide Trivelli supposes that these substances form the electrodes of an elementary voltaic cell of the type Ag | AgBr | Ag_2S having silver bromide as the electrolyte, the external circuit being completed by contact between the silver and silver sulphide The developability of the grain is assumed to depend on the existence of a "speck" of metallic silver large enough to act as a reduction centre for development Such a centre is supposed to be formed by growth of the original small silver particle (which acts as one of the electrodes) due to the deposition of more silver from the electrolyte, the silver sulphide electrode or anode thus losing silver to the profit of the silver electrode or kathode

---

* 'Phot J ,' vol 68, p 407 (1928)

† J Franklin Inst ,' vol 204, p 649 (1927)

The light action is supposed to facilitate the accumulation of additional silver on the silver speck in two ways, firstly by increasing the conduction of the silver bromide electrolyte and also by increasing the potential of the cell, so that the silver electrode speck grows more rapidly in the light than in the dark

Such a theory is very difficult to accept in the light of our experimental results, for the reasons which we now give

A fraction of a second is a normal light exposure in order to make developable a photographic emulsion which, in the dark, will probably remain without a developable image for several years On Trivelli's theory this would imply that the rate of growth in size of the silver speck, or the magnitude of the electrolytic current to which the growth is due, must be hundreds of millions of times greater in the light than in the dark This increase on illumination in the rate of transport of silver ions would, on Trivelli's theory, have to be accounted for either by an enormous increase in the voltage of the cell or by a corresponding increase in the *electrolytic* conduction of the electrolyte, *i e*, the silver bromide The former alternative is almost inconceivable and the latter appears very improbable in the light of our experiments, since it is doubtful whether the ionic conduction is increased *at all* by the light

There is also the effect of varying temperature to be considered It has already been shown that *if* any part of the photo current were ionic, it would probably decrease rapidly with decrease of temperature (on the assumption that an appreciable part of the hundred-thousand-fold decrease of dark conductance is due to changing mobility) to a value at −180° C, which was only a small fraction of its value at room temperatures Quite apart from any decrease in the efficiency of the secondary chemical processes at low temperature and considering only the primary process, we should therefore expect, on the idea of an ionic part of the photo-conductance being responsible for latent image formation, that the sensitivity of a photographic emulsion would be very much less at −180° C than at ordinary temperature This is contrary to the facts, for at the temperature of boiling liquid oxygen the sensitivity of a photographic plate is still some considerable fraction of its sensitivity at room temperature

We are thus led to the conclusion that the formation of the latent photographic image probably does not depend on the transport of silver by elementary electrolytic currents Rather does it appear to us that in the primary photographic process we are concerned with stationary silver and bromide ions, and that in the light some of the bromide ions momentarily become free atomic bromine and as such can readily react with other atoms, or molecules, such as those in the surrounding gelatin, thus producing a permanent change with metallic silver as one of the resulting products

In conclusion, we wish to express our thanks to Dr T Slater Price, F R S , Director of The British Photographic Research Association, for his interest and advice throughout this research and to Prof A W Porter, F R S , for many helpful suggestions at all stages of the work We are also indebted to our colleague, Dr S O Rawling, for much useful criticism

Summary

Existing experimental evidence indicates that in the formation of the latent photographic image, and in the photo conductance phenomena in the silver halides, and in the direct decomposition of the silver halides by light, the primary light action is the release of valency electrons from the bromide ions For a complete understanding of the process of formation of the latent image a study of the photo conductance phenomena is therefore of importance Experiments are described in which these phenomena have been investigated in silver bromide, under different conditions of crystallisation and over a temperature range from room temperatures to -180° C

It is shown that provided the silver bromide is exposed in such a way that no permanent decomposition can take place, the photo-current very probably commences to flow at the instant of illumination, and within about 0 07 second rises to a constant final value which is strictly proportional to the light intensity

The results of varying the conditions of crystallisation and the temperature indicate that in all probability the photo current is electronic This suggests that latent image formation is not due primarily to elementary electrolytic photo-currents in the silver bromide crystals Rather does it seem that in the light some of the bromide ions are momentarily changed into free bromine atoms, which are not present in the dark and which react with other atoms or molecules, such as those in the surrounding gelatin A permanent change thus takes place, metallic silver being one of the resulting products

The Absorption Band Spectrum of Chlorine— II

By A Elliott, B Sc , Fellow of the Rockefeller Foundation, Physical Institute of the University of Utrecht

(Communicated by O W Richardson, F R S —Received February 28, 1930)

Introduction

As the results of measurements and analysis of the absorption bands of chlorine, communicated in a previous paper,* seemed to justify further work on the same problem, particularly with regard to intensity measurements, these bands have been further investigated and the results form the subject of this paper

In the publication referred to, the analysis of three bands due to $Cl_{35}Cl_{35}$ was described, and the discovery of the corresponding isotope band $Cl_{35}Cl_{37}$ in the case of one of them enabled the absolute numbering for the vibrational quantum number in the upper electronic level to be determined, if one assumed that the vibrational quantum numbers for the lower level were known

Throughout, we shall use the notation given by Birge,† in which the vibration quantum number, which is integral, is denoted by v, with $v = 0$ for the lowest existing state Since in formulæ for the vibrational isotope effect it is always the parameter $v + \frac{1}{2}$ which appears, the symbol n is used in place of $v + \frac{1}{2}$ in these formulæ For zero vibration, therefore, $n = 0$, and for the lowest existing state $n = \frac{1}{2}$ As in the older notation, the molecular constants for the lowest existing state are denoted by the subscript 0, *e g* , ω_0, B_0, etc The constants in the case of zero vibration are denoted by the subscript e

The three bands referred to above were designated the 2 → 17, 2 → 18 and 2 → 19 bands, but as Birge (*loc cit*) has shown from the writer's new data, this is certainly wrong, and the correct v'' v' numbering is 1 → 11, 1 → 12, and 1 → 13, This will be dealt with later in the section on the isotope effect, but is introduced now in order that the corrected numbering may be employed throughout

---

* 'Roy Soc Proc ,' A, vol 123, p. 629 (1929)

† I am informed by Prof Birge that his paper on the isotope effect will not be published for some time, and he has asked me to state that, as there are objections to the use of n, it is proposed to employ u in place of it I am greatly obliged to him for placing the results of his calculations at my disposal, and take this opportunity of expressing my thanks for his kindness

The new bands measured belong to the third progression, and are due to the transitions (corrected numbering) 2 → 6, 2 → 7, 2 → 8, and 2 → 12 These bands are to be attributed to the molecule $Cl_{35}Cl_{35}$ In the case of the 2 → 6 and 2 → 12 bands, the weaker bands due to $Cl_{35}Cl_{37}$ have been found and measured In no case has it been possible to identify the very weak bands which may be expected from the molecule $Cl_{37}Cl_{37}$

Experimental

Since the new bands belong to a higher progression (higher v'') than the ones first described, they are considerably weaker (at least at room temperature, which has been employed in these experiments), and it has been found necessary to use longer tubes of chlorine in order to get a satisfactory absorption Two tubes each of 150 cm length and 5 cm diameter were filled with chlorine at a pressure of ½ atmosphere Light from a carbon arc was made to pass three times through each tube by an arrangement of plane and concave mirrors The glass surface of a plane mirror was cemented to one end of each tube and an aperture 12 mm × 3 mm was scraped from the silvering of each mirror Plate glass was cemented to the other ends of the tubes, "picien" being employed for this purpose Since the ends were ground only a very small surface of "picien" was exposed to the chlorine, and the danger of contamination from this source was very small

The light from the arc was focussed first on the aperture of the mirror of the first tube, after traversing the latter, it was reflected by a concave mirror back through the tube, to be reflected again by the plane mirror and brought to a focus immediately in front of the concave mirror, having then traversed the tube three times Small plane mirrors served to direct the light on to the aperture in the mirror of the second tube, through which it passed in similar fashion and was finally focussed on the spectrograph slit by a lens The total length of the light path in the chlorine was 9 metres

The chlorine was procured from a cylinder washed and dried in the same way as in the first experiments

The 6-metre grating of the Utrecht Institute was employed, and the new bands were observed in the first order, with a dispersion of 2 5 Å U per millimetre, with which the exposure times were about 2½ hours In order to take exposures in the second order, very much longer exposures would have been necessary, and comparison with the second order plates taken in the first investigation, using a grating of nearly the same dispersion, showed that little resolution was lost by using the first order

The measurements of frequencies were made from iron arc standards in the same way as in the first experiments, and the same measuring micrometer was employed On account of the smaller dispersion, the errors of measurement are greater in the present measurements, but are probably not greater than 0 07 cm $^{-1}$ In addition to the error of measurement, however, the position of a line may be in error on account of its being overlaid by neighbouring lines The frequencies and intensities of the band lines are given in Table I, in which integral values for j are used, since the form $E = Bj(j+1)$ is used for the rotation term in the present work

Table I —Frequencies and Intensities in Chlorine Band Lines

Band 2 → 6

$Cl_{35}Cl_{35}$

j_P	j_R	ν vac (cm $^{-1}$)	Int
7	10	17833 42	0 0030
8	11	81 63	85
9	12	79 53	76
10	13	77 37	80
11	14	74 93	83
12	15	72 46	64
13	16	69 68	85
14	17	66 65	85
15	18	63 55	67
16	19	60 26	65
17	20	56 69	65
18	21	53 03	83
19	22	48 97	64
20	23	44 90	63
21	24	40 58	87
22	25	36 13	88
23	26	31 39	65
24	27	26 51	90
25	28	21 46	83
26	29	16 14	77
27	30	10 67	68
28	31	04 96	72
29	32	17799 17	63
30	33	93 14	51
31	34	86 88	46
32	35	80 39	72
33	36	73 83	60
34	37	66 98	59
35	38	59 95	Too weak for measurement
36	39	52 70	
37	40	45 48	
38	41	37 73	
39	42	30 01	

$Cl_{35}Cl_{37}$

j_P	j_R	ν vac (cm $^{-1}$)	Int
15	18	17866 07	0 0034
16	19	62 68	70
17	20	59 28	55
18	21	55 69	69
19	22	51 75	51
20	23	47 97	55
21	24	43 83	71
22	25	39 34	69
23	26	34 69	77
24	27	30 08	62
25	28	25 29	49
26	29	20 02	59
27	30	14 79	63
28	31	09 19	74
29	32	Overlaid by Fe	32
30	33	17797 61	41
31	34	91 42	29
32	35	85 42	33
33	36	78 96	47
34	37	72 19	49
35	38	65 42	60
36	39	58 50	

Table I—(continued)

Band $(2 \rightarrow 7)_{35-35}$

J	P branch		R branch	
	ν vac (cm $^{-1}$)	Int	ν vac (cm $^{-1}$)	Int
17	18041 11	0 0050		
18	37 18	0 0044		
19	33 27	0 0056		
20	28 95	0 0023	18040 65	0 0037
21	24 64	0 0062	36 73	0 0058
22	20 00	0 0047	32 73	0 0035
23	15 14	0 0046	28 37	0 0046
24	10 14	0 0019	23 92	0 0054
25	04 00	0 0040	19 27	0 0054
26	17999 43	0 0037	14 40	0 0058
27			09 28	0 0047
28			04 06	0 0028
29			17998 51	0 0051

Band $(2 \rightarrow 8)_{37-35}$

J	P branch		R branch	
	ν vac (cm $^{-1}$)	Int	ν vac (cm $^{-1}$)	Int
14	18225 36	0 0105		
15	22 01	0 0131		
16	18 51	0 0098		
17	14 79	0 0183	18224 29	0 0140
18	10 85	0 0113	20 92	0 0108
19	06 66	0 0149	17 37	0 0160
20	02 10	0 0124	13 55	0 0160
21	18197 63	0 0108	09 60	0 0146
22	92 82	0 0064	05 37	0 0108
23	87 82	0 0205	00 74	0 0119
24	82 71	0 0060	18196 12	0 0100
25	77 19	0 0097	91 11	0 0097
26	71 16	0 0054	86 17	0 0051
27	65 53	0 0125	80 86	0 0095
28	59 68	0 0087	75 42	0 0091
29			69 76	0 0087
30			63 78	0 0077
31			57 65	0 0100

Table I—(continued)

Band 2 → 12

$Cl_{35}Cl_{35}$

J_P	J_R	ν vac (cm $^{-1}$).	Int
4	6	18836 97	Too confused for measurement
5	7	35 54	
6	8	33 77	
7	9	31 97	
8	10	29 84	
9	11	27 40	0 0269
10	12	24 89	0 0253
11	13	22 03	0 0295
12	14	18 93	0 0152
13	15	15 51	0 0246
14	16	12 04	0 0170
15	17	08 18	0 0215
16	18	04 18	0 0209
17	19	18799 91	0 0241
18	20	95 31	0 0254
19	21	90 57	0 0240
20	22	85 54	0 0200
21	23	80 29	0 0314
22	24	74 89	0 0164
23	25	69 19	0 0308
24	26	63 16	0 0346
25	27	56 89	0 0337
26	28	50 51	0 0338
27	29	43 88	0 0395
28	30	37 06	0 0231
29	31	29 78	0 0237
30	32	22 41	0 0205

$Cl_{35}Cl_{37}$

J_P	J_R	ν vac (cm $^{-1}$)	Int
7	9	18829 33	Too confused for measurement
8	10	27 31	
9	11	24 82	
10	12	22 46	
11	13	19 61	0 0236
12	14	16 55	0 0162
13	15	13 31	0 0259
14	16	09 95	0 0148
15	17	06 28	0 0095
16	18	02 43	0 0101
17	19	18798 27	0 0186
18	20	93 66	0 0178
19	21	89 18	0 0285
20	22	84 46	0 0146
21	23	79 11	0 0172
22	24	74 01	0 0218
23	25	68 39	0 0258
24	26	63 12	Overlaid by lines of $Cl_{35}Cl_{35}$,
25	27	56 87	
26	28	50 53	
27	29	43 89	
28	30	37 44	
29	31	30 62	0 0165
30	32	23 15	0 0126

Analysis

As before, only P and R branches are found, and from these, term differences for the upper and lower states ($\Delta F'$ and $\Delta F''$, respectively) are found, and are given in Tables II and III for the $Cl_{35}Cl_{35}$ molecules, and in Table IV for $Cl_{35}Cl_{37}$ In the case of $Cl_{35}Cl_{35}$ the term differences for the upper state agree for the bands 1 → 12 and 2 → 12, and for the lower state agreement is found for the bands 2 → 6, 2 → 7, 2 → 8 and 2 → 12 This confirms simultaneously Kuhn's and Nakamura's* vibrational analysis, and the present rotational analysis

---

* Kuhn, 'Z Physik,' vol 39, p. 77 (1926), Nakamura, 'Mem Coll. Sci. Imp Univ Kyoto,' A, vol 9, p 315 (1926)

Table II — Combination Differences for the Normal State ($Cl_{35}Cl_{35}$)

$$R(j-1) - P(j+1) = 2\Delta F''(j)$$

j	2 → 6	2 → 7	2 → 8	2 → 12	Average	$\Delta F''(j)/j+\frac{1}{2}$
7				7 13		
8				8 14		
9				8 88		
10				9 94		
11	10 96			10 91		
12	11 95			11 89		
13	12 88			12 85		
14	13 82			13 85		
15	14 67			14 75		
16	15 77			15 60		
17	16 65			16 73		
18	17 68		17 63	17 61	17 64	0 4757
19	18 65		18 73	18 64	18 67	0 4787
20	19 68		19 72	19 62	19 67	0 4798
21	20 56	20 65	20 73	20 42	20 57	0 4784
22	21 64	21 59	21 78	21 38	21 60	0 4800
23	22 44	22 59	22 66	22 38	22 49	0 4785
24	23 44	23 47	23 55	23 40	23 46	0 4788
25	24 44	24 49	24 96	24 38	24 59	0 4822
26	25 46		25 58	25 31	25 45	0 4802
27	26 43		26 49	26 10	26 34	0 4789
28	27 36			27 11		
29	28 32			28 10		
30	29 26					
31	30 23					
32	31 13					
33	32 19					
34	33 19					
35	34 18					
36	34 91					
37	36 10					
38	36 97					
					*Average	0 4790

* From strong lines

Table III — Combination Differences for the Excited State ($Cl_{35}Cl_{35}$)

$$R(j) - P(j) = 2\Delta F'(j)$$

j	$2 \rightarrow 6$		$2 \rightarrow 7$		$2 \rightarrow 8$		$2 \rightarrow 12$	
	$2\Delta F'(j)$	$\Delta F'(j)/j+\frac{1}{2}$	$2\Delta F'(j)$	$\Delta F'(j)/j+\frac{1}{2}$	$2\Delta F'(j)$	$\Delta F'(j)/j+\frac{1}{2}$	$2\Delta F'(j)$	$\Delta F'(j)/j+\frac{1}{2}$
6							3 20	0 2462
7							3 57	0 2380
8							3 93	0 2312
9							4 57	0 2405
10	6 05	0 2881					4 95	0 2357
11	6 70	0 2913					5 37	0 2335
12	7 07	0 2828					5 96	0 2384
13	7 69	0 2848					6 52	0 2415
14	8 28	0 2855					6 89	0 2376
15	8 91	0 2874					7 33	0 2365
16	9 42	0 2855					7 86	0 2382
17	9 96	0 2846			9 50	0 2714	8 27	0 2363
18	10 52	0 2843			10 07	0 2722	8 87	0 2397
19	11 29	0 2895			10 71	0 2746	9 34	0 2395
20	11 79	0 2876	11 70	0 2854	11 36	0 2771	9 77	0 2383
21	12 45	0 2895	12 09	0 2812	11 95	0 2779	10 28	0 2391
22	12 84	0 2853	12 73	0 2829	12 55	0 2789	10 65	0 2367
23	13 51	0 2874	13 23	0 2815	12 92	0 2749	11 10	0 2362
24	14 05	0 2867	13 78	0 2812	13 41	0 2737	11 73	0 2394
25	14 67	0 2876	14 37	0 2818	13 92	0 2729	12 30	0 2412
26	15 25	0 2877	14 97	0 2825	15 01	0 2732	12 65	0 2387
27	15 86	0 2884			15 33	0 2787	13 01	0 2365
28	16 50	0 2895			15 74	0 2761	13 45	0 2360
29	16 97	0 2876					14 10	0 2390
30	17 53	0 2874					14 65	0 2402
31	18 08	0 2870						
32	18 78	0 2889						
33	19 31	0 2882						
34	19 90	0 2884						
35	20 44	0 2879						
36	21 13	0 2895						
37	21 50	0 2867						
38	22 22	0 2886						
39	22 69	0 2872						
*Average		0 2874		0 2815		0 2750		0 2382

* From strong lines

The isotopic bands 2 → 6 and 2 → 12 also show agreement in the term differences for the lower state, and comparison with the previous communication (Elliott, *loc cit*) shows that the term differences for the upper state for 1 → 12 and 2 → 12 agree Ample confirmation of the correctness of the assignments of these new weaker bands to the isotopes is thus provided The rotation constants may be found in Table IX at the end of this paper They have been calculated in the same way as previously, and again terms in $(j)^4$ are found to

Table IV—Combination Differences for the Normal and Excited States ($Cl_{35}Cl_{37}$)

	Normal state				Excited state			
j	2 → 6		2 → 12		2 → 6		2 → 12	
	$2\Delta F'(j)$	$\Delta F''(j)/j+\frac{1}{2}$	$2\Delta F'(j)$	$\Delta F''(j)/j+\frac{1}{2}$	$2\Delta F'(j)$	$\Delta F'(j)/j+\frac{1}{2}$	$2\Delta F'(j)$	$\Delta F(j)/j+\frac{1}{2}$.
9							4 51	0 2374
10			9 72	0 4629			4 85	0 2312
11			10 76	0 4678			5 21	0 2265
12			11 51	0 4604			5 91	0 2364
13			12 51	0 4633			6 30	0 2333
14			13 33	0 4597			6 60	0 2276
15			14 12	0 4555			7 03	0 2268
16			15 04	0 4558			7 52	0 2279
17			16 29	0 4654			8 01	0 2289
18			17 10	0 4622	10 38	0 2805	8 77	0 2370
19	18 10	0 4641	17 97	0 4608	10 93	0 2803	9 09	0 2331
20	18 85	0 4598	19 16	0 4673	11 31	0 2759	9 20	0 2244
21	19 94	0 4637	19 65	0 4570	11 86	0 2758	10 07	0 2342
22	21 00	0 4667	20 79	0 4620	12 41	0 2758	10 45	0 2322
23	21 67	0 4611	21 34	0 4540	13 28	0 2826	10 72	0 2281
24	22 68	0 4629	22 24	0 4539	13 75	0 2806	10 89	0 2222
25	23 81	0 4660	23 48	0 4604	14 05	0 2755	11 52	0 2259
26	24 55	0 4632	24 50	0 4623	14 67	0 2768	12 59	0 2375
27	25 50	0 4636	25 68	0 4669	15 29	0 2780	12 98	0 2360
28			26 25	0 4605	16 10	0 2825	13 09	0 2296
29	27 68	0 4692	27 38	0 4641			13 27	0 2249
30	28 60	0 4689			17 18	0 2816	14 29	0 2343
31	29 37	0 4662			17 77	0 2821		
32	30 23	0 4651						
33					18 65	0 2784		
34	32 19	0 4665			19 23	0 2787		
35	32 86	0 4628			20 00	0 2817		
36					20 40	0 2795		
Average		0 4647		0 4611		0 2792		0 2307

be too small to detect * The bands 2 → 6 and 2 → 12 have the same peculiarity of structure as was observed in the 1 → 12 band, namely, superposed P and R branches, and this, of course, applies to the main band and to the isotope It results in a great simplification of structure as well as an increase in intensity, and it is doubtless for this reason that the isotopic bands have here been detected In the case of bands in which the two branches are separated, the complexity is so great that the isotopic bands cannot be identified

* The differences in B for the strong and weak lines previously reported has not been confirmed in the present work Only small, non systematic differences are found; presumably the fact that slightly larger B values were found for the 1 → 11, 1 12 and 1 → 13 bands from the strong lines was accidental

The Vibrational Isotope Effect

A knowledge of the rotation constants of a band enables the frequency of the origin to be calculated from the frequencies of the band lines with considerable precision, and this has been done for all the chlorine bands which have been analysed; the origin frequencies are given in Table VI, along with the vibrational isotopic separations which are given directly by the differences in origin frequencies of the isotopic and main bands. In accordance with the usual practice, the separation or shift is given as $\nu^i - \nu$, where the superscript i denotes the less abundant molecule, in this case $Cl_{35}Cl_{37}$.

Since isotope shifts for different values of both v' and v'' are known, it is possible to find the correct numbering for both levels from the observed shifts. This has been done by Birge (*loc cit*), using a method which has been given by Gibson,* and there can be no doubt that Kuhn's conclusion (Kuhn, *loc cit*) that the progression in which $v'' = 0$ does not occur but is replaced by continuous absorption, is wrong.† The calculated isotopic shifts for the new numbering are given in Table V.

Consequent upon the change in the v'' v' numbering, a revision of the vibration constants for the lowest state becomes necessary, and this will be dealt with later. A further consequence is that the value for the heat of dissociation of the normal chlorine molecule given by Kuhn (*loc cit*) must be reduced by one quantum of vibration. The heat of dissociation is then given simply by

$$D = \nu_c - (2^2P_2 - 2^2P_1)$$

where ν_c is the frequency of the convergence point.

Taking Kuhn's figures for the quantities on the right-hand side of this equation, D becomes 56 9 C. This value agrees better with the chemically determined value 57 00 C than did Kuhn's original result (58 5 C).

Molecular Constants of $Cl_{35}Cl_{35}$

(*a*) *Rotation Constants.* The rotation constants of $Cl_{35}Cl_{35}$ are now known for two vibration states ($v'' = 1$ and 2) for the normal electronic level, and for six states ($v' = 6$, 7, 8, 11, 12 and 13) in the case of the excited level (Table IX). If we assume a linear relation between B_v'' and v'' for the normal level, a simple extrapolation through 1 unit of v'' leads to the value of B_v'' for the lowest possible state (B_0'') and since the extrapolation is through such a short distance, the values so obtained must be fairly reliable

---

* 'Z Physik,' vol 50, p 692 (1928).

† *Note added in proof*.—Dr Kuhn has informed me that, after hearing about the new results on isotopes in Cl_2, he has repeated his temperature experiment. The new experiment indicates that the observed absorption series converging to a limit, arises from the lowest level $V'' = 0$. The earlier result $V'' = 1$ was due to an error.

For the excited state the B_v' values have been plotted against v' in fig 1, and a marked divergence from linearity is to be observed The values for $v' = 11$, 12 and 13 are fairly linear, as are those for $v' = 6$ 7 and 8 but the two linear portions have quite different slopes It would perhaps be possible to draw a smooth curve through all the points, but it would show a very quick change of slope and the impression is very strong that we have here to deal with two more or less linear curves, with something very like a discontinuity at the point $v' = 8\frac{1}{2}$ It is to be regretted that more points on the curve are not available, especially in the direction of decreasing v', but the bands in which v' is lower than 6 are exceedingly weak and their analysis has hitherto proved impossible Assuming that a linear extrapolation holds the value of B_0' is given in Table IX but this must be taken as the upper limit to this quantity

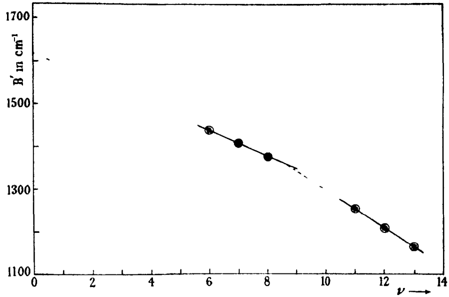

Fig 1 —Rotation Constants B′ for Excited State

The fact that an abrupt change of slope, or discontinuity, occurs in the $B' - v'$ curve is very striking, and suggests at once that here we may have a connection with the point of discontinuity in $\omega_e' - v'$ curves which Birge* has found in certain molecules, including the halogens This will be discussed in the section on vibration constants which follows

---

* 'Trans Faraday Soc,' vol 25, p 707 (1929)

For the molecule $Cl_{35}Cl_{37}$ the rotation constants are now determined for $v'' = 1$ and 2 for the normal state, and for $v' = 6$ and 12 for the excited state These, along with the observed and calculated ratios B_{35-35}/B_{35-37} are also given in Table IX The calculated value of this ratio is obtained as follows —

For the main molecule we have

$$B_v = B_0 - \alpha v$$

For the isotope, the appropriate factor is ρ^2 for B_0 and ρ^3 for α

Hence

$$B'_v = \rho^2 (B_v + \alpha v (1 - \rho)$$

and

$$B_v/B_v' = B_v/(B_v + \alpha v (1 - \rho))$$

It may be seen from the calculated values of this ratio that the influence of the term $\alpha v (1 - \rho)$ is negligible for values of v lower than 6 Except in the result for $v' = 12$, the observed and calculated values are in very good agreement, and in that case the difference is 1 7 per cent

(*b*) *Vibration Constants* —The measurements of band heads and the analyses carried out by Kuhn and by Nakamura (*loc cit*) permit the calculation of the frequencies of vibration of the nuclei (ω_v), and Kuhn gives a list of these frequencies from his own data Hitherto, however, the correct vibrational numbering has been uncertain, and the determination of the fundamental frequencies ω_0' and ω_0'' (that is, the nuclear vibration frequencies in the lowest existing states) has in consequence also been in doubt Since reliable determinations of the absolute values of v' and v'' have now been made, and since also more accurate data for some of the band origins is available, a discussion of the vibrational constants seems to be useful at this stage

The measurements of Nakamura were made with an instrument of higher dispersion than were those of Kuhn, but are not necessarily more accurate on this account, since high dispersion makes it difficult to observe the heads In fact, the figures of Nakamura do not give such a consistent $\omega_v'' - v''$ curve as those of Kuhn, though the $\omega_v' - v'$ curves of both agree fairly well Nakamura's measurements are, however, more extensive and include values for the heads of bands which were not observed by the latter, due no doubt to the long absorption tubes used by the former The frequencies of the band heads are arranged in a vibrational scheme in Table V The analysis of the rotation structure has enabled the origins of seven bands to be calculated

(Table VI), and from these, four reliable values for ω_v' and one for ω_v'' are obtained , these are given in Table VIII, and are probably accurate to $\pm$ 0 2 cm^{-1} Kuhn's and Nakamura's measurements are of the frequencies of the R-heads, and the writer's measurements are of the band origins, but the difference on this account is small A simple calculation, using the known rotation constants, shows that the heads of the 2 → 6 and 2 → 7 bands, for example, are situated at 0 36 and 0 34 cm^{-1} from the origin The error in ω_v if one uses measurements of heads instead of origins is therefore 0 02 cm^{-1} and is quite negligible

Table V -Band Heads

Frequencies from Nakamura's measurements (*loc cit*), with vibrational assignments as in this paper

v' \ v''	0	1	2	3
4			17495 4	
5			17701 9	
6			17893 9	17352 1
7			18088 8	17536 5
8		18809 0	18261 8	17707 0
9		18969 9	18417 9	17866 7
10	19673 4	19120 5	18578 7	18024 5
11	19808 7	19259 7	18710 1	18167 0
12	19948 1	19388 9	18844 1	18295 9
13	20070 7	19506 9	18966 7	18414 5
14	20177 6	19617 5	19073 4	18523 0
15	20277 8	19714 5	19171 8	18627 2
16	20364 1	19808 7	19262 5	18714 7
17	20444 1	19891 4	19340 1	18798 8
18	20519 6	19961 6	19421 3	18874 7
19	20581 6	20025 6	19481 4	18936 5
20	20633 5	20082 7	19536 0	18993 7
21	20682 1	20133 7		
22	20727 5	20178 0		
23	20757 7	20210 2		
24	20793 0	20240 5		
25	20808 2			
26	20827 7			
27	20836 4			

Table VI —Origin Frequencies and Isotope Separations

Band	Origin frequency		Isotope separation		Observed-calculated
	$Cl_{35}Cl_{35}$	$Cl_{35}Cl_{37}$	Observed	Calculated	
	cm $^{-1}$	cm $^{-1}$	cm $^{-1}$	cm $^{-1}$	cm $^{-1}$
1 → 11	19258 0				
1 → 12	19389 0	19379 4	−9 6	−9 98	−0 38
1 → 13	19509 2				
2 → 6	17890 9	17892 5	−1 6	−1 74	−0 14
2 → 7	18076 1				
2 → 8	18250 4				
2 → 12	18840 2	18837 6	−2 6	−2 68	−0 08

The available data from all three sources has been combined, the greatest weight being given to the measurements of origin frequencies The ω_v values for the excited state are plotted against v' in fig 2 The points of this curve show a very large spreading, though this is not so great in the case of Kuhn's results for high values of v'

The determination of the exact form of the $\omega_v - v'$ curve is very uncertain in view of the spreading of the points, but it is evidently of the non-linear type, and seems to be of the form which Birge (*loc cit*) has found to be general for non-linear types Over the portion for which determinations of ω_v from band origins are available, the curve is linear to a high degree

It has been examined by plotting ΔE_ω ($= \delta E_v/\delta\omega_v$) against ω_v, and this curve, which is reproduced in fig 2, gives fairly clear evidence of the break which Birge (*loc cit*) has found in such curves for the excited state of molecules such as O_2 and the halogens In Cl_2 the break occurs at a point where ω_v has the value 135 cm $^{-1}$, corresponding to $v' = 11$ Unfortunately, the values of ω_v do not permit of the determination of this position within less than about ± 2 units of v'

The discontinuity or at least abrupt change of slope in the $B_v' - v'$ curve occurs at $v' = 8\frac{1}{2}$, or perhaps 9 In view of the uncertainty of the position of the break in the $\Delta E_\omega - \omega_v$ curve, it appears quite possible that the point of discontinuity occurs at the same value of v' in the two cases, and that they are both evidences of the same change in structure of the molecule The point $v' = 9$ corresponds to (very approximately) 59 per cent dissociation

Since the $\omega_v - v'$ curve is linear over the range for which the origin frequencies have been determined, these latter can be fitted to a Kratzer formula

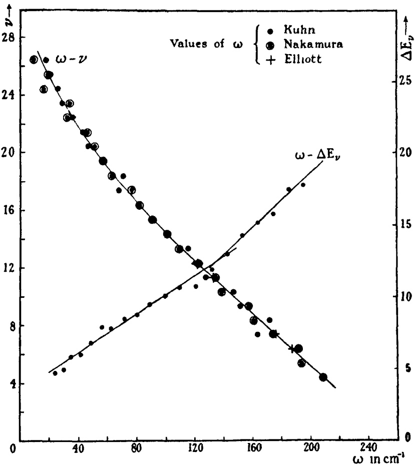

FIG 2

quite accurately, using the vibration constants in Table VIII The following formula fits the data satisfactorily

$$\nu = 17657\ 7 - (255\ 7v' - 5\ 42v'^2) - (560\ 9v'' - 4\ 0v''^2)$$

The first term in the expression for the origin frequency is, of course, the frequency of the 0 — 0 band, assuming that a linear extrapolation to $v' = 0$ is permissible The mean value of the ' observed-calculated " values for the seven bands measured is 0 25 cm $^{-1}$

Intensity Measurements

Since the $Cl_{35}Cl_{35}$ bands show alternating intensities, the determination of the ratio of strong to weak lines in this spectrum is a matter of considerable interest, as it leads to the evaluation of the nuclear spin A tentative value of this ratio has already been given* but it was highly desirable to obtain more measurements, and intensity measurements have been carried with this point in view

The relative abundance of the isotopes can, in some cases at least, be determined from band spectrum intensities, but in the present case it is subject to considerable uncertainty As has been pointed out by Giauque and Johnston,† it is possible that the absorption coefficient of a non-symmetrical molecule may be greater than that of a symmetrical molecule, which is similar in other respects, in considering the abundance of $Cl_{35}Cl_{35}$ relative to that of $Cl_{37}Cl_{37}$ from intensity measurements, we must keep this possibility in mind The present results, when compared with Aston's figure for the relative abundance of Cl_{35} and Cl_{37}, show that such an effect may be present here, though the accuracy of measurement does not admit of certainty on this point

With regard to the question of the absence of alternating intensities in the non-symmetrical molecule $Cl_{35}Cl_{37}$, not much new evidence is provided, since the intensities in one of the isotope bands (2 → 12) are very much disturbed by overlying lines, and in the other (2 → 6) the strong lines (odd j numbering) of one branch are superposed on the weak lines (even j numbering) of the other for both main and isotope bands, and no alternation of intensity results The results of the first communication were fairly conclusive on this point, however, and the effect has also been found in the band spectrum of oxygen ‡

The intensity of an absorption line is measured by the value of $\int_{-\infty}^{+\infty}\alpha_\nu d\nu$ where α_ν is the absorption coefficient for the frequency ν in the usual absorption formula $I = I_0e^{-\alpha\rho c}$, and the determination of the absolute intensities would involve the integration of α_ν over the whole breadth of the line, for every line Since the determination of the absolute intensities was not the chief object of this work, the integration has not been carried out for these lines, and only the maximum value of α_ν, *i e*, the coefficient of absorption for the centre of the line, has been determined

If all the lines measured were of the same shape, then it is clear that the ratio of intensities of two lines 1 and 2 would be given equally well by the ratio $\int_{-\infty}^{+\infty}\alpha_{\nu_1} d\nu \Big/ \int_{-\infty}^{+\infty}\alpha_{\nu_2} d\nu$ or by $\alpha^{(\max)1}/\alpha^{(\max)2}$, and no error could be introduced by employing the latter There is no reason for thinking that the shape of single band lines will alter, at least within one band, and the different shapes of the lines which appear on the photometer curves must be chiefly due to blending with other lines Now the integrated absorption coefficient would be at least as much in error as the central absorption coefficients on this account, and might conceivably be even more disturbed than the latter, which has consequently been employed as a measure of the intensity

---

* Elliott, *loc cit*

† 'Nature,' vol. 123, p 831 (1929)

‡ Giauque and Johnston, 'J Amer Chem Soc,' vol 51, p 1436 (1929), also Babcock, 'Proc Nat. Acad Sci,' vol 15, p 471 (1929)

In all the intensity measurements, the usual method employed at Utrecht* has been employed, and from the photographic densities (measured from the microphotometer record) the corresponding intensities were found from a calibration curve The latter was obtained from a plate developed simultaneously with the chlorine plate, on which spectra of a tungsten lamp were photographed , the intensity of these spectra was varied in a known manner by means of " step reducers,' and the densities corresponding to these intensities (at the required wave length) were measured From these, a density-intensity curve was drawn, one for each band This was desirable since the form of the calibration curve alters somewhat with wave length, though within one band it was sufficiently constant The absorption coefficients α for the centres of the lines were calculated as in the former work, and are given under the heading " Int " in Table I

In all absorption measurements, the finite resolution of the spectrograph and the width of the slit cause the absorption lines to appear less deep than they are in reality So far as relative measurements are concerned, this would not matter if all the lines were of the same shape, but the lines as actually observed differ somewhat in this respect

To determine the correction for each line would have necessitated very great labour, but the influence on the intensity relations could be investigated as follows The band 1 → 12 (which on account of its strength could be observed with a single tube and consequently did not require very long exposures) was photographed in the first order with the slit width employed throughout this work (namely 0 02 mm) and also with a slit width 0 04 mm , and in the second order with slits of 0 03 and 0 04 mm The intensities of seven of the narrowest lines were then measured from these four plates Although the absolute intensities varied considerably, the values of the intensity ratio for strong and weak lines only differed from the mean by — 4 5 per cent , 0 per cent , — 2 per cent , and 1 per cent for the slit widths

---

* Ornstein, 'Proc Phys Soc ,' vol 37, p 334 (1925), also Baly, "Spectroscopy," vol. 3, p 156

0 04 mm (first order), 0 02 mm (second order), 0 04 mm (second order), and 0 03 mm (second order) These results indicate that the true ratio may perhaps be somewhat larger than the measured one, but it is also possible that the differences are accidental Since the lines on which these test measurements were made are narrower than most of the lines whose intensities have been measured, the effect (if real) will in general be smaller than that above and has been neglected in the final result for the intensity ratio

The differences in the absolute absorption coefficients are irregular and much greater, being even as large as 100 per cent This is not in the direction which would be expected if it were due to the finite resolution of the spectroscope and is probably due to developer effects, which are known to occur when there is a steep density gradient on a photographic plate, as in narrow absorption lines The figures under the column ' Int " in Table I therefore only give a rough estimate of the absolute value of the central absorption coefficient

Alternating Intensity Ratio

The average value of the intensity of the lines in one branch having odd *j* values (*i e*, the strong lines) has been compared with that of the even *j* lines in the same branch, for the bands 1 → 11, 1 → 12, 1 → 13, 2 → 7, 2 → 8, and 2 → 12 This is equivalent to finding the ratio of intensity of a strong line to that of the mean of the two adjacent weak lines, since the intensity of the chlorine band lines does not vary very rapidly with *j*, this procedure does not introduce any appreciable error The results are given in Table VII The mean of the ratio for the P and R branches for each band is fairly consistent A weighted mean value for all the bands has been taken, in which the value for each band has been weighted according to its closeness to the arithmetic mean This final value for the ratio of the alternating intensities (1 36 1), has been

Table VII —Intensity Ratios

(*a*) Alternating intensities (ratio of intensity of strong to weak lines in $Cl_{35}Cl_{35}$).

Band	P branch	R branch	Mean
1→ 11	1 28	1 22	1 25
1→ 12	1 40 (superposed P and R)		1 40
1→ 13	1 43	1 34	1 38
2→ 7	1 49	1 21	1 35
2→ 8	1 62	1 18	1 40
2→ 12	1 34 (superposed P and R)		1 34
		Weighted mean	1 36

Table VII—(continued)

(*b*) Isotopes (ratio of intensity of $Cl_{35}Cl_{35}$ to $Cl_{35}Cl_{37}$)

Band	Ratio
1 → 12 1 → 6 2 → 12	1.35 1.28 1.42
Mean	1.35

derived from more than 170 lines, and may therefore be considered fairly reliable, the mean error calculated from the divergence of the individual values for each band from the mean is 0.057.

By taking an average over a very large number of lines in this way, one can to a considerable extent get rid of the errors due to blending, *i.e.*, to the fact that a number of lines are overlaid by other lines. But even if a sufficient number of lines has been taken to ensure that, on the average, the same intensity of overlying lines has been added to both strong and weak lines, the measured ratio of these latter will still be in error, and will be smaller than the true ratio by an unknown amount. Consequently the figure 1.36 must be regarded as a lower limit. It appears probable that the true ratio is not greatly in excess of this, since even if the average intensity of the overlying lines amounted to 20 per cent. of the intensity of the weaker lines, the ratio would then only be raised to 1.45, and this estimate of the intensity of the overlying lines is probably too high. In view of these considerations, it is probable that the true ratio is very close to 1.4 : 1, which is the theoretical one corresponding to a nuclear spin of 5/2, and the latter is therefore taken as the most probable value for this quantity. The fact that an odd number of units of spin is found is in agreement with the fact that $Cl_{35}Cl_{35}$ has an odd number of nuclear particles (18 + 35).

Relative Abundance of Isotopes

In the first results published on Cl_2, an estimate of the relative abundance of the molecules $Cl_{35}Cl_{35}$ and $Cl_{35}Cl_{37}$ was made from three lines in the 1 → 12 band, and a ratio 1.75 : 1 was found. It has seemed better in the present work to compare as many lines as possible, and the intensities of $Cl_{35}Cl_{35}$ and $Cl_{35}Cl_{37}$ have been compared by taking the average (over lines having the same *j* values) for the bands 1 → 12, 2 → 6, and 2 → 12 (see Table VII). The mean value for the ratio (from 50 lines) is 1 45 1, but this is again a lower limit The same assumption as to the intensity of the overlying lines would raise the figure to 1 45 1, and this is still considerably below the value 1 67 calculated from Aston's value for the isotope ratio On account of the much smaller number of lines from which the ratio has been derived, it is more open to doubt than the alternating intensity ratio, especially as in many cases the isotope lines were imperfectly separated from other lines It is, however, possible that here we have evidence of a greater absorption coefficient for the non-symmetrical molecule $Cl_{35}Cl_{37}$, but it is not conclusive

Table VIII —Vibration Constants for $Cl_{35}Cl_{35}$

	v	ω_v (cm $^{-1}$)	b	Data employed
Normal level	0	560 9		Extrapolated from results of Kuhn, Nakamura, and this paper
	1½	548 9	4 0	ω from origins of bands calculated from rotational analysis, b from curve using above data
Excited level	0	255 7	5 42	From origins of bands (this paper)
	6½	185 2		
	7½	174 3		
	11½	131 0		
	12½	120 2		

Table IX —Rotation Constants

	v	$Cl_{35}Cl_{35}$			$Cl_{35}Cl_{37}$			B_{35-35}/B_{35-37}	
		B.	I	r	B	I	r	Calculated.	Observed
		cm $^{-1}$	gm cm ^{2} $\times 10^{-40}$	cm $\times 10^{-8}$	cm $^{-1}$	gm cm ^{2} $\times 10^{-40}$	cm $\times 10^{-8}$		
Normal state	1	0 2412	114	0 992	0 2347	118	0 994	1 028	1 032
	2	0 2395	115 3	0 996	0 2324	118 8	0 997	1 028	1 030
Excited state	6	0 1437	192 2	1 286	0 1396	197 7	1 286	1 026	1 029
	7	0 1408	196 1	1 301					
	8	0 1375	200 7	1 317					
	11	0 1254	220 2	1 376					
	12	0 1209	228 3	1 401	0 1164	237 1	1 409	1 022	1 039
	13	0 1166	236 8	1 429					
Extrapolated values— Normal	0	0 2429	113 7	0 988	0 2350	117 4	0 991		
Excited	0	0 162	170	1 21					

Summary

(*a*) The rotation structure of four bands assigned to $Cl_{35}Cl_{35}$ and of two assigned to $Cl_{35}Cl_{37}$ has been analysed, and only P and R branches are found.

(*b*) The vibrational isotope shifts observed demand a revision of the vibrational quantum numbers for both the normal and excited states. The former is decreased by 1, and the latter by 6, as compared with the results of a previous communication.

(*c*) A peculiarity in the $B_v - v$ curve for the excited state, amounting probably to a discontinuity, is observed; it is suggested that this is connected with a discontinuity observed by Birge in curves for the vibrational constants of certain types of molecules.

(*d*) Tables of vibrational and rotational constants are given, and probable extrapolations for these constants are made for the lowest vibrational state, in both electronic levels.

(*e*) Intensity measurements have been carried out on a large number of lines, and a lower limit for the alternating intensity ratio 1·36 : 1 found. From a consideration of the sources of error, it is shown that the ratio is probably not higher than 1·45 : 1. The only theoretically possible nuclear spin which gives a ratio between these limits is 5/2, which is consequently taken as the nuclear spin of Cl_{35}.

(*f*) The abundance of $Cl_{35}Cl_{35}$ relative to $Cl_{35}Cl_{37}$ is estimated from intensity measurements, and a lower value is found than would be expected from Aston's ratio of isotopes. This may be due to inaccuracies of measurement, but may also be caused by a greater absorption (per molecule) for $Cl_{35}Cl_{37}$ than for $Cl_{35}Cl_{35}$.

Finally, the author wishes to express his thanks to Prof. L. S. Ornstein for the facilities and assistance afforded him at Utrecht, to Prof. W. E. Curtis for the use of a measuring micrometer and calculating machine when he was in England, and to the Fellowship Committee of Armstrong College for a grant during the first part of his stay in Utrecht.

The Scattering of Electrons by Atoms.

By N F Mott, Lecturer in Theoretical Physics, The University, Manchester

(Communicated by W L Bragg, F R S —Received March 8, 1930)

The scattering of a stream of charged particles by a spherically symmetrical electrostatic field was first investigated, from the point of view of the wave mechanics, by Born [*] Various authors have developed his ideas and have applied them to the scattering of electrons by atoms, which for the purpose have been treated simply as fields of force The purpose of the present note is to obtain formulæ for the scattered intensity by methods similar to those used in calculating the scattering of X-rays by an atom The formulæ obtained have all been published elsewhere, either by the present author, or by others , it has, however, appeared worth while to publish the present method of obtaining them, partly because the analysis is particularly simple, secondly because the results are expressed in a form easy to compare with those for X-rays, and thirdly because the method makes it clear under what conditions the approximations used will lead to a sufficiently accurate result

Experiments on the scattering of streams of charged particles measure the "scattered intensity", we shall first define just what we mean by this Suppose we have a beam of particles of such intensity that one particle crosses unit area in unit time Suppose that the beam fall on one scattering centre—that is to say, on one atom, at a point O Suppose that a disc, of area $R^2\,d\omega$, be placed at a point P, distant R from O, and such that OP makes an angle θ with the original direction of motion of the particles The disc is to be normal to OP, so that it subtends a solid angle $d\omega$ at O Then if $I_\theta\,d\omega$ be the number of particles striking the disc per unit time, I_θ is what we call the scattered intensity

The fundamental assumptions that we make in dealing with the scattering are as follows A beam of particles, all with the same energy, behaves like a beam of waves The rate of flow of particles is proportional to the square of the amplitude of the waves If the waves fall on a small region of space, in which there is an electrostatic field of force, they are scattered From the amplitude of the scattered wave we deduce the number of electrons scattered in any direction Thus, if when a wave of unit amplitude falls on the centre of force, the wave scattered has amplitude $R^{-1}f(\theta)$ at distance R from the centre and in a direction making an angle θ with that of the incident beam, then

---

[*] Born, 'Z Physik,' vol. 38, p 803 (1926)

$$I_\theta = |f(\theta)|^2$$

The law that determines how these waves are scattered can be deduced from the wave equation We shall state it first and then prove it Each element of volume $dxdydz$ in which there is any field scatters a spherical wavelet If $V(xyz)$ be the potential energy that one of the *particles* would have in that element of volume, then the amplitude of the scattered wavelet at distance R from (xyz) is

$$\frac{1}{R}\,\frac{2\pi m}{h^2}\,V(xyz)\,dx\,dy\,dz,$$

times the amplitude of the wave at the point (xyz) If V is greater than zero, then the wavelet starts with the same phase as that of the whole wave at (xyz), if V is less than zero it starts with opposite phase This law is exact The amplitude of the resultant wave scattered by the whole region in which there is any field is obtained by considering the interference of all these wavelets

It will now be shown that this law is derivable from, and indeed equivalent to, the wave equation of Schrodinger Let ψ be the wave function, a complex function, giving the amplitude and the phase of the wave at any point The wave equation is

$$\nabla^2\psi + \frac{8\pi^2 m}{h^2}(E - V)\,\psi = 0 \tag{1}$$

E is the energy of each particle in the stream that the wave is to describe m is the mass of each particle Let us write $8\pi^2 m\,E/h^2 = k^2$, so that $2\pi/k$ is the wave-length of the waves Then (1) may be written

$$(\nabla^2 + k^2)\,\psi = 8\pi^2 m V\psi/h^2$$

Now it is a well-known result that if $f(xyz)$ be a known function, then the most general solution of

$$(\nabla^2 + k^2)\,\psi = f(xyz)$$

is

$$\psi(xyz) = G(xyz) + \frac{1}{4\pi}\iiint \frac{e^{ik|\mathbf{r}-\mathbf{r}'|}}{|\mathbf{r}-\mathbf{r}'|}\,f(x'\,y'\,z')\,dx'\,dy'\,dz'$$

where $G(xyz)$ is the *general* solution of

$$(\nabla^2 + k^2)\,G = 0$$

Therefore, if ψ is any solution of (1), then ψ must satisfy the "integral equation,"

$$\psi(xyz) = G(xyz) + \frac{1}{4\pi}\iiint \frac{e^{ik|\mathbf{r}-\mathbf{r}'|}}{|\mathbf{r}-\mathbf{r}'|}\,\frac{8\pi^2 m}{h^2}\,V(x'\,y'\,z')\,\psi(x'\,y'\,z')\,dx'\,dy'\,dz' \tag{2}$$

Now, let ψ be that solution of (1) which describes the scattering, namely, that solution which consists of an incident wave and a scattered wave.

For large r, the integral on the right tends to

$$Ar^{-1}e^{ikr},$$

where A depends on $\mathbf{r}/|\mathbf{r}|$ only. The integral therefore represents the scattered wave. G must be chosen to represent an incident wave; that is to say

$$G = e^{ikz}.$$

The form of the integral in (2) shows that the scattered wave is made up as we have stated, by the interference of wavelets scattered by each element of volume, each with amplitude and phase given by

$$(2\pi m/h^2)\,V(xyz)\,\psi(xyz)\,dx\,dy\,dz/R.$$

To calculate the scattered intensity then, we must consider the interference of the wavelets. This will be particularly easy if the amplitude and phase of the waves inside the region in which there is any field are not very different from what they would be if the field were not there. In other words, if the scattered wave, inside the atom, is negligible compared to the incident wave. The amplitude and phase of each scattered wavelet is thus known. Born's method of obtaining approximate formulæ for the scattering is equivalent to this assumption; he sets

$$\psi = e^{ikz}$$

in the integral in (2), and evaluates it for large r. However, we can obtain his results by a simpler method.

We use a formula that is familiar in X-ray analysis. Suppose that a wave of wave length λ falls on a spherically symmetrical distribution of scattering medium. Suppose that an element of volume $dx\,dy\,dz$ at distance r from the centre scatters a wavelet of amplitude $R^{-1}\,P(r)\,dx\,dy\,dz$. Then, so long as the amplitude and phase of the incident wave inside the medium are not very much disturbed, the amplitude of the resultant scattered wave at a great distance R, and in a direction making an angle θ with the direction of the incident wave is

$$R^{-1}\,4\pi\int_0^\infty \frac{\sin\mu r}{\mu r}\,P(r)\,r^2\,dr, \tag{3}$$

where

$$\mu = 4\pi\sin\tfrac{1}{2}\theta/\lambda.$$

The formula is applied to the scattering of X-rays by an atom in the following way. The atom is treated as though it were a spherically symmetrical distribution of electric *charge* The charge density at distance r from the nucleus of the atom we denote by $\varepsilon|\psi(r)|^2$ This density may be calculated by the methods of Thomas and of Hartree Now, according to a theory due to J J Thomson, an element of charge $d\rho$ should scatter a spherical wavelet of amplitude $\mathrm{R}^{-1}\,\varepsilon d\rho/mc^2$ times the amplitude of the wave at that point If therefore a wave train of X-rays of unit amplitude fall on an atom, and if the amplitude and phase of the waves are not very much altered inside the atom* then the amplitude of the total scattered wave is

$$\frac{1}{\mathrm{R}}\frac{\varepsilon^2}{mc^2}\,\mathrm{F}(\theta),$$

where

$$\mathrm{F}(\theta) = 4\pi\int_0^\infty \frac{\sin \mu r}{\mu r}\,|\psi(r)|^2\,r^2\,dr \tag{4}$$

The curves F have been calculated for a great many atoms It is noteworthy that F is a function of $\sin\frac{1}{2}\theta/\lambda$ only

The same formula can be used to calculate the scattering of particles by a field of force Suppose a wave of unit amplitude fall on the scattering centre In this case every volume element of space in which there is any *field* scatters a wavelet of amplitude

$$\frac{1}{\mathrm{R}}\frac{2\pi m}{h^2}\,\mathrm{V}(r)\,dx\,dy\,dz$$

The amplitude of the resultant scattered wave will then be

$$f(\theta)/\mathrm{R},$$

where

$$f(\theta) = \frac{8\pi^2 m}{h^2}\int_0^\infty \frac{\sin \mu r}{\mu r}\,\mathrm{V}(r)\,r^2\,dr \tag{5}$$

Note that $\mathrm{V}(r)$ is the potential energy of any one of the particles at distance r from the centre of the force μ, as before, denotes $4\pi\sin\frac{1}{2}\theta/\lambda$ which in this case is equal to

$$4\pi mv/h \;\sin\tfrac{1}{2}\theta$$

§ 2 Scattering of a beam of charged particles by an inverse square law centre of force

The wave equation can be solved exactly,† so that the amplitude and phase of the scattered wave are known If a stream of particles, of mass m and charge ε, fall on a point charge, of charge Q and infinite mass, then the amplitude of the scattered wave at unit distance is given by

---

* The assumption is valid, for the scattered wave has amplitude of the order of magnitude $\mathrm{R}^{-1}\,\varepsilon^2/mc^2$ times that of the incident wave ε^2/mc^2 is the "radius of the electron," so inside the atom the amplitude of scattered wave is much smaller than that of the incident waves

† Gordon 'Z Physik,' vol. 48, p 180 (1928)

$$f(\theta) = \varepsilon Q/2mv^2 \quad \operatorname{cosec}^2 \tfrac{1}{2}\theta \tag{6}$$

The scattered intensity is therefore

$$I_\theta = (\varepsilon Q/2mv^2)^4 \operatorname{cosec}^4 \tfrac{1}{2}\theta,$$

which is Rutherford's formula for the scattering of a stream of α particles by a heavy nucleus

The formula (6) can also be obtained from equation (5) of the last section with $V(r)$ equal to $\varepsilon Q/r$ However, it is seen at once that the integral in (5) does not converge, an expression of the form

$$\int_0^\infty \sin \mu r \quad dr$$

being obtained This is because the assumption that (5) involves, that the amplitude and phase of the wave in the field is the same as it would be in the absence of the field, is not strictly true , if the change in amplitude were taken into account, the integral would be found to converge

In order to make the integral converge, we suppose that

$$V(r) = \varepsilon Q\, r^{-1} e^{-\kappa r}$$

and put κ equal to zero in the final result This can hardly be regarded as more than an artifice which gives the right answer We obtain for $f(\theta)$

$$f(\theta) = \frac{8\pi^2 m}{h^2} \int_0^\infty \frac{\sin \mu r}{\mu r} \varepsilon Q\, e^{-\kappa r}\, dr = \frac{8\pi^2 m\varepsilon Q}{h^2} \frac{1}{\mu^2 + \kappa^2}$$

Putting $\kappa = 0$ this reduces to the same result as (6) The Rutherford scattering formula was first obtained by this method by Wentzel *

§ 3 *Scattering of Electrons by Atoms*—The problem is very similar to that of the scattering of X-rays by an atom The atom is, as before, treated as a static distribution of electric charge, of density $\varepsilon|\psi(r)|^2$ at distance r from the nucleus It is now the electrostatic potential at any point that determines the amplitude of the wavelet scattered by an element of volume The electric intensity $\kappa(r)$ at any point, due to the charge, and to the nucleus, is

$$\kappa(r) = \frac{\varepsilon}{r^2}\left[\int_0^r |\psi(r)|^2 4\pi r^2 dr - N\right]$$

Therefore, the potential energy of an electron at distance r from the nucleus is given by

$$V(r) = -\varepsilon \int_\infty^r \kappa(r)\, dr$$

---

* 'Z Physik,' vol. 40, p 590 (1926)

Subject, therefore, to the approximation that the wave is not much deformed inside the atom, the amplitude $f(\theta)$ of the scattered wave is given by (5), with this value of $V(r)$.

It is useful to express $f(\theta)$ in terms of the functions $F(\theta)$, defined by (4), since these have been worked out for a great many atoms. We can transform the integral (5) by partial integration; we obtain

$$\left.\begin{aligned} f(\theta) &= \frac{8\pi^2 m\varepsilon^2}{h^2}\,E(\theta) \\ \text{where}\qquad E(\theta) &= \frac{N-F}{\mu^2} \end{aligned}\right\} \tag{7}$$

This formula is equivalent to

$$f(\theta) = \frac{\varepsilon^2}{2mv^2}[N - F(\theta)] \operatorname{cosec}^2 \tfrac{1}{2}\theta \tag{8}$$

The formula (8) has a striking similarity to the formula (4), which gives the amplitude of the X-ray wave scattered in any direction. The significance of this becomes apparent if we obtain the formula (8) by a slightly different method. In deducing the formula (8) we considered that each element of volume scattered a wavelet of amplitude proportional to the *potential* of the field at that point. But we can obtain the same formula by supposing that each element of volume scatters a wavelet proportional to the amount of charge $d\rho$ that it contains. Now we know from §2 the amplitude of this wavelet; it is not the same in all directions, but is equal to

$$R^{-1}\,\varepsilon d\rho/2mv^2 \quad \operatorname{cosec}^2 \tfrac{1}{2}\theta$$

in the direction θ. The nucleus also scatters a wave of amplitude

$$N\varepsilon^2/2mv^2 \quad \operatorname{cosec}^2 \tfrac{1}{2}\theta$$

The phase of this wave will be opposite to that of the waves scattered by the surrounding charge, because the charge on the nucleus has opposite sign. If we consider the interference of all these waves, we see that the amplitude of the resultant scattered wave is just (8).

The formula (8) is, as we have stated, only approximate; it assumes that the amplitude and phase of the wave inside the atom are not very much disturbed. We can easily see under what conditions this assumption is true. Let us consider any single electron of the atom; it will scatter a wave of order of magnitude $\epsilon^2/mv^2\ R^{-1}$ If there are N electrons, and R_a be the radius of the atom, then the order of magnitude of the scattered wave, inside the atom, cannot be greater than

$$\frac{N\epsilon^2}{mv^2}\Big/R_a \qquad (9)$$

times the amplitude of the incident wave If the constant (9) is very much less than unity, then the scattering should be given by our formula

The formula (8) neglects, also, the effect of the polarisation of the atom by the incident electron The exact effect of this polarisation is not at present known, it seems probable, however, that if the velocity of the colliding electron is much greater than that of the electrons in the atom, then the electron will get past without having time to polarise the atom much

We conclude then that our formulæ are only valid for electrons of greater energy than that of a K electron in the atom

The author has compared the formula (8) with experimental data from two sources, the scattering of a beam of 210 volt electrons by helium gas, carried out by Dymond and Watson,* and the experiments on the diffraction of 20,000 volt cathode rays by a gold foil, carried out by G P Thomson † In both cases the agreement between theory and experiment was within the limits of experimental error, although in the latter case the energy of the electrons is less than that of the K ring In neither case has a comparison been made for more than one value of the velocity of the electrons, so it is not known if the scattering really is a function of $v \sin \frac{1}{2}\theta$ Further, in neither case do the experiments give a measure of the absolute scattered intensity, it has only been possible to compare the scattering at various angles

It is, however, extremely probable that the formula (8) does give the correct absolute magnitude of the scattering For fast electrons and large angles it reduces to the Rutherford formula for the scattering of particles by a nucleus which is known to be correct Therefore the formula is at any rate correct for the limiting case of large μ

In conclusion, we give a graph of F and E for oxygen F is a pure number, E has the dimensions of an area, and is plotted in arbitrary units It will be seen that F falls away more sharply than E F has been worked out by

---

* 'Roy Soc Proc,' A, vol 122, p 571 (1928) For comparison with theory see Mott, 'Proc Camb Phil. Soc,' vol. 25, p 304 (1929)

† 'Roy Soc Proc,' A, vol. 125, p 352 (1929) For theory see 'Nature,' vol. 129, p 986 (1929)

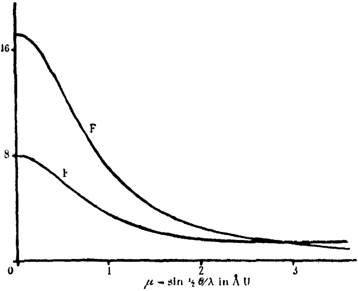

Fig 1

James,* using Hartree's field E is calculated from the formula (7) The scattered intensity is, of course, proportional to E^2, per unit solid angle

* I am much indebted to Mr James for providing me with these data

Scattering of Fast Electrons and Nuclear Magnetic Moments

By H S W MASSEY, B A , M Sc , Trinity College, Cambridge , Aitchison
Scholar, University of Melbourne

(Communicated by R H Fowler, F R S —Received March 12, 1930)

Scattering of Fast Electrons and Nuclear Magnetic Moments

Summary —The problem of the nuclear scattering of fast electrons has been considered by Mott * His method consists in using the wave equation of Dirac† and applying the usual theory of collisions thereto The result obtained is not in good agreement with experiment and it is thus of interest to consider the possibilities of other effects In this note the effect of a nuclear magnetic moment is considered and shown to be negligible Thus the only explanation of the disagreement between theory and experiment seems to be the effect of radiation as suggested by Mott *

It is convenient to consider the second order form of Dirac's equations

$$\nabla^2\psi + \frac{4\pi^2}{h^2}\left[\frac{E^2}{c^2} - m^2c^2 + \frac{ieh}{2\pi c}\,A\ \ \text{grad} - \frac{e^2A^2}{c^2} - \frac{eh}{2\pi c}\,\boldsymbol{\sigma}\ \ \text{curl}\ A - \frac{2eVE}{c^2} + \frac{e^2V^2}{c^2}\right]\psi = 0$$

Here E is the energy of the electron, V, A‡ the scalar and vector potentials respectively of the field of force in which the electron moves, ρ_1, the four rowed matrix

$$\begin{pmatrix} 0 & 0 & 1 & 0 \\ 0 & 0 & 0 & 1 \\ 1 & 0 & 0 & 0 \\ 0 & 1 & 0 & 0 \end{pmatrix},$$

and $\boldsymbol{\sigma}$ a vector matrix whose components σ_x, σ_y, σ_z are given by

$$\sigma_x = \begin{pmatrix} 0 & 1 & 0 & 0 \\ 1 & 0 & 0 & 0 \\ 0 & 0 & 0 & 1 \\ 0 & 0 & 0 & 0 \end{pmatrix}, \quad \sigma_y = \begin{pmatrix} 0 & -i & 0 & 0 \\ i & 0 & 0 & 0 \\ 0 & 0 & 0 & -i \\ 0 & 0 & -i & 0 \end{pmatrix}, \quad \sigma_z = \begin{pmatrix} 1 & 0 & 0 & 0 \\ 0 & -1 & 0 & 0 \\ 0 & 0 & 1 & 0 \\ 0 & 0 & 0 & -1 \end{pmatrix}$$

---

* 'Roy Soc Proc ,' A, vol 124, p 425 (1929)

† P A M Dirac, 'Roy Soc Proc ,' A, vol 117, p 610 (1928)

‡ V, A are assumed to be independent of time

e, h, c, m have their usual significance. As Born's method of approximation* gives good results for the case considered by Mott (*loc. cit.*), it will be used here as it is very convenient.

Write the equation (1) in the form

$$\nabla^2 \psi + (k^2 - S)\,\psi = 0, \tag{1}$$

where

$$k^2 = \frac{4\pi^2}{h^2}\left(\frac{E^2}{c^2} - m^2c^2\right), \tag{2}$$

and S denotes the remaining terms. Then the form of solution required is taken as $\psi_1 + \psi_2$ where

$$\nabla^2 \psi_1 + k^2\psi_1 = 0, \tag{3}$$

ψ_1 thus representing the incident plane wave. ψ_2 is given to a first approximation by

$$\nabla^2 \psi_2 + k^2\psi_2 = S\psi_1, \tag{4}$$

so that

$$\psi_2 = \frac{e^{ikr}}{r}\int_{-\infty}^{\infty} S e^{ik(\mathbf{n}-\mathbf{n}_0)\cdot\mathbf{r}}\,dv, \tag{5}$$

where $e^{ik\mathbf{n}_0\cdot\mathbf{r}}$ represents the incident wave in direction $\mathbf{n}_0$, and $\mathbf{n}$ is a unit vector in the direction of observation.

The terms in S involving scalar potentials have been evaluated by Mott (*loc. cit.*) so we are concerned only with the vector potentials. The portion of ψ_2 due to these is given by

$$\psi_2' = \frac{e^{-ikr}}{r}\int_{-\infty}^{\infty}\frac{4\pi^2}{h^2}\left[\mathbf{A}\cdot\text{grad} - \frac{e^2A^2}{c^2} - \frac{eh}{2\pi c}\,\boldsymbol{\sigma}\cdot\text{curl}\,\mathbf{A}\right]e^{ik(\mathbf{n}-\mathbf{n}_0)\cdot\mathbf{r}}\,dv \tag{6}$$

We take $\mathbf{A} = \boldsymbol{\nabla}\left(\frac{1}{r}\right) \times \mathbf{M}$,† where $\mathbf{M}$ is the vector magnetic moment of the scattering centre, $= \alpha i + \beta j + \gamma k$, say, i, j, k being unit vectors along the co-ordinate axes. Then

$$\int_{-\infty}^{\infty}\mathbf{A}\cdot\text{grad}\,e^{ik(\mathbf{n}-\mathbf{n}_0)\cdot\mathbf{r}}\,dv = \int_{-\infty}^{\infty}\boldsymbol{\nabla}\left(\frac{1}{r}\right)\times\mathbf{M}\cdot\text{grad}\,e^{ik(\mathbf{n}-\mathbf{n}_0)\cdot\mathbf{r}}\,dv \tag{7}$$

---

* 'Z. Physik,' vol. 39, p. 803 (1926).

† Here × is used to denote a vector product.

Now

$$\nabla\left(\frac{1}{r}\right)\times \mathbf{M}\,.\,\mathrm{grad}=\left[\gamma\frac{\partial}{\partial y}\left(\frac{1}{r}\right)-\beta\frac{\partial}{\partial z}\left(\frac{1}{r}\right)\right]\frac{\partial}{\partial x}$$
$$+\left[\alpha\frac{\partial}{\partial z}\left(\frac{1}{r}\right)-\gamma\frac{\partial}{\partial x}\left(\frac{1}{r}\right)\right]\frac{\partial}{\partial y}$$
$$+\left[\beta\frac{\partial}{\partial x}\left(\frac{1}{r}\right)-\alpha\frac{\partial}{\partial y}\left(\frac{1}{r}\right)\right]\frac{\partial}{\partial z} \qquad (8)$$

Taking the polar axis along the direction of the vector $\mathbf{n}-\mathbf{n}_0$ we have only the last term in (8) to consider. But it is obvious that it will contribute nothing to the integral as it contains trigonometric functions of first degree in the azimuthal angle ϕ, i.e.,

$$\frac{\partial}{\partial x}\left(\frac{1}{r}\right)=\frac{\sin\theta\sin\phi}{r^2} \qquad (9)$$

These vanish when integrating for ϕ. Hence the term $\mathbf{A}$. grad, contributes nothing to the first approximation. Consider now

$$\int \boldsymbol{\sigma}\,.\,\mathrm{curl}\,\mathbf{A}\,e^{ik(\mathbf{n}-\mathbf{n}_0).\mathbf{r}}\,dv \qquad (10)$$

We have

$$\mathrm{curl}\,\mathbf{A}=\nabla\times\nabla\left(\frac{1}{r}\right)\times\mathbf{M},$$
$$=\nabla\left(\nabla\left(\frac{1}{r}\right).\mathbf{M}\right)-\nabla^2\left(\frac{1}{r}\right)\mathbf{M},$$
$$=\nabla\left(\nabla\left(\frac{1}{r}\right).\mathbf{M}\right), \qquad (11)$$

so

$$\boldsymbol{\sigma}\,.\,\mathrm{curl}\,\mathbf{A}=\left\{\alpha\frac{\partial^2}{\partial x^2}\left(\frac{1}{r}\right)+3\beta\frac{xy}{r^5}+3\gamma\frac{xz}{r^5}\right\}\sigma_x+,\text{ etc} \qquad (12)$$

The terms in $\frac{xy}{r^5}$, $\frac{xz}{r^5}$, vanish on integration as they include $\cos\phi$, $\sin\phi$ respectively. Consider then

$$\int_{-\infty}^{\infty}\frac{\partial^2}{\partial z^2}\left(\frac{1}{r}\right)e^{ik(\mathbf{n}-\mathbf{n}_0).\mathbf{r}}\,dv \qquad (13)$$

Change to cylindrical co-ordinates ρ, z, ϕ with z axis along $\mathbf{n}-\mathbf{n}_0$ so the integral becomes

$$\int_0^{\infty}\int_{-\infty}^{\infty}\int_0^{2\pi}\frac{\partial^2}{\partial z^2}(z^2+\rho^2)^{-\frac{1}{2}}\exp\{-ik[(1-\cos\delta)z-\rho\sin\delta\cos\phi]\}\,\rho\,dz\,d\rho\,d\phi, \qquad (14)$$

where δ, the angle between $\mathbf{n}$, $\mathbf{n}_0$ is the angle of scattering.

Now

$$\int_{-\infty}^{\infty} \frac{\partial^2}{\partial z^2}(z^2+\rho^2)^{-\frac{1}{2}}\exp\{-ik(1-\cos\delta)z\}\,dz$$

$$= \left[\frac{\partial}{\partial z}(z^2+\rho^2)^{-\frac{1}{2}}\,e^{-ik(1-\cos\delta)z}\right]_{-\infty}^{\infty}$$

$$+\,ik(1-\cos\delta)\int_{-\infty}^{\infty}\frac{\partial}{\partial z}(z^2+\rho^2)^{-\frac{1}{2}}\,e^{-ik(1-\cos\delta)z}\,dz,$$

$$= k^2(1-\cos\delta)^2\int_{-\infty}^{\infty}(z^2+\rho^2)^{-\frac{1}{2}}\,e^{-ik(1-\cos\delta)z}\,dz \tag{15}$$

Hence the integral (13) is

$$k^2(1-\cos\delta)^2\iiint(z^2+\rho^2)^{-\frac{1}{2}}\exp\{-ik[(1-\cos\delta)z-\rho\sin\delta\cos\phi]\}\,\rho\,dz\,d\rho\,d\phi$$

This integral has been evaluated by Oppenheimer,* who gives

$$-1/k^2\sin^2\tfrac{1}{2}\delta, \tag{16}$$

so the integral (13) is simply $-4\sin^2\frac{1}{2}\delta$ and the contribution to ψ_2 is

$$-\frac{e^{-ikr}}{r}\,\frac{8\pi e\gamma}{ch}\,\sigma_z\sin^2\tfrac{1}{2}\delta \tag{17}$$

Now

$$\frac{\partial^2}{\partial x^2}\left(\frac{1}{r}\right)+\frac{\partial^2}{\partial y^2}\left(\frac{1}{r}\right) = -\frac{\partial^2}{\partial z^2}\left(\frac{1}{r}\right)$$

and x and y being arbitrary when the z axis is chosen, so that

$$\int_{-\infty}^{\infty}\frac{\partial^2}{\partial x^2}\left(\frac{1}{r}\right)e^{ik(\mathbf{n}-\mathbf{n}_0)\cdot\mathbf{r}}\,dv = -\tfrac{1}{2}\int_{-\infty}^{\infty}\frac{\partial^2}{\partial z^2}\left(\frac{1}{r}\right)e^{ik(\mathbf{n}-\mathbf{n}_0)\cdot\mathbf{r}}\,dv,$$

$$= 2\sin^2\tfrac{1}{2}\delta \tag{18}$$

Thus the total contribution of these terms is

$$-\frac{e^{-ikr}}{r}\,\frac{4\pi e}{ch}\,(\alpha\sigma_x+\beta\sigma_y-2\gamma\sigma_z)\sin^2\tfrac{1}{2}\delta \tag{19}$$

The remaining terms in $\psi_2{}^r$ due to A^2 will be negligible as they are only a correction to the effect of terms of first order in A. Hence

$$\psi_2{}^r = \frac{e^{-ikr}}{r}\,\frac{4\pi e}{ch}\,(\alpha\sigma_x+\beta\sigma_y-2\gamma\sigma_z)\sin^2\tfrac{1}{2}\delta \tag{20}$$

---

* 'Z. Physik,' vol. 43, p. 413 (1927).

The contribution to the scattering will then be of the order $|\psi_2'|^2$, i e, of order $\frac{\pi^2e^2}{c^2h^2}$ × square of magnetic moment of scattering centre

Now the scattering due to a Coulomb centre of force has been shown* to be given by

$$\frac{Z^2e^4}{4m^2v^4}\left(1-\frac{v^2}{c^2}\right)\left[\operatorname{cosec}^4\tfrac{1}{2}\delta-\frac{v^2}{c^2}\operatorname{cosec}^2\tfrac{1}{2}\delta+\frac{2\pi^2Ze^2v}{hc^2}\,\frac{\cos^2\frac{1}{2}\delta}{\sin^3\frac{1}{2}\delta}\right] \tag{21}$$

Hence if the magnetic effect is to be of the same order

$$\frac{16\pi^2e^2}{c^2h^2}\,\mathrm{M}^2\simeq\frac{Z^2e^4}{4m^2v^4},$$

where M is the scalar magnetic moment of the scattering centre This means

$$\begin{aligned}\mathrm{M}^2&\simeq\frac{Z^2e^2c^2h^2}{64m^2v^4},\\&\simeq\left(\frac{eh}{mc}\right)^2\frac{Z^2c^4}{64v^4},\end{aligned} \tag{22}$$

i e, M of the order of a Bohr magneton This is an impossibly high value for the magnetic moment of a nucleus so it can be concluded that the nuclear magnetic forces have a negligible effect on the scattering of electrons However, this does not apply to scattering due to electrons themselves, for in such case the moment is of the order of a Bohr magneton This effect may be of importance in the scattering of fast β-particles by matter To calculate it correctly requires the use of Dirac's relativistic equations for a two electron problem in some such form as used by Gaunt† in calculation on the helium spectrum

---

* Mott, *loc cit*

† 'Roy Soc Proc,' A, vol 122, p 513 (1929), and 'Phil Trans,' A, vol 228, p 151 (1929)

Remarks on the Anomalous Scattering of α-Particles from the Quantum Mechanical Point of View

By H S W Massey, B A, M Sc, Trinity College, Cambridge, Aitchison Scholar, University of Melbourne

(Communicated by R H Fowler, F R S —Received March 20, 1930)

§ 1 It has been established experimentally by Bieler and Rutherford and Chadwick* that α-particle scattering by light nuclei does not obey the Rutherford formula† if the velocity of the incident particles be sufficiently large (of the order 2×10^9 cm per second) Bieler showed that the scattering becomes less than the classical value for moderate angles (up to 70° scattering angle), while Rutherford and Chadwick found that it increases again for 135° scattering angle It is at once obvious that these results indicate a departure from the Coulomb law of force, and various laws have been invoked to explain the deviations Thus Bieler‡ showed how the inverse fourth power law was capable of explaining his results, and he found the radius of the neutral surface of the nucleus to be $3{\cdot}44 \times 10^{-13}$ cm Hardmeier|| used an inverse fifth power polarisation law and was able to explain the increase again at high velocities However it is desirable to consider the validity of these calculations from the standpoint of the new mechanics

§ 2 *Dimensional Considerations* —Consider scattering by a centre of force exerting a potential $\mathrm{F}r^{-n}$ This scattering will depend not only on the mass m, and velocity v of the incident particles, and on F, but also on Planck's constant h The possible dependence on h is not taken into account in any of the above attempts to explain anomalous scattering Put the scattering cross section proportional to $h^s v^t m^u \mathrm{F}^w$ Then we must have the dimensional equation

$$[h]^s\,[v]^t\,[m]^u\,[\mathrm{F}]^w = [\mathrm{L}]^2, \tag{1}$$

and also

$$[\mathrm{F}]\,[\mathrm{L}]^n = [\text{energy}] \tag{2}$$

---

[*] Bieler, 'Roy Soc Proc,' A, vol. 105 p 434 (1924), Rutherford and Chadwick, 'Phil Mag,' vol 50, p 889 (1925)

[†] Rutherford, 'Phil Mag' vol 21, p 669 (1911)

[‡] 'Proc Camb Phil Soc,' vol 28, p 181 (1925)

[||] 'Phys Z' vol 27 p 574 (1926)

Therefore from (1)

$$\left.\begin{aligned} s + u + w &= 0 \\ 2s + t + 2v + nw &= 2 \\ -s - t - 2w &= 0 \end{aligned}\right\}, \tag{3}$$

giving

$$s = 2 - nw, \quad t = (n-2)w - 2 \quad u = (n-1)w - 2 \tag{4}$$

If the scattering is independent of h

$$2 - nw = 0$$

or

$$w = 2/n \tag{5}$$

Therefore the scattering formula includes h for $n > 2$ unless we may expect dependence on proper fractional powers of F which is extremely improbable. All methods of treatment consist in expansion in powers of F which is in general very small, in which case we must have $w \geqslant 1$. Hence it is almost certain that h appears in formulæ representing scattering by higher power laws. Even in the case of $n = 2$, w would have to be unity, and in all wave mechanical treatments F appears in no lower power than the second, so in this case also h appears.

Now it is a general rule that when h appears explicitly in a formula there is little possibility of classical calculations giving the correct result, but when h does not so appear we expect classical formulæ to hold. This is clearly illustrated in the scattering by a Coulomb law of force. Here $n = 1$ and h does not occur so we have the classical Rutherford formula agreeing with that obtained wave mechanically. However, when relativity mechanics is introduced, which is equivalent to including an inverse cube law of force, h appears and Darwin's classical formula* for this case is in no way similar to Mott's† wave mechanical formula. We must then expect that Bieler and Hardmeier and Debye's theories (*loc. cit.*) have little significance, the classical formulæ breaking down entirely in the case of higher power laws.

§ 3. *Scattering by Higher Power Laws and Wave Mechanics.* We now proceed to consider in more detail the effects of higher power laws from the point of view of wave mechanics. Unfortunately it is not possible to carry out investigations in this field with any rigour at present, and what follows can only be taken as a probable suggestion.

The most convenient formula to use when scattering by unusual potentials is considered is that given by Born* which is a method of successive approximations. To the first approximation the fraction of particles scattered in a direction making an angle δ with the direction of incidence by a potential V, is given by

---

* 'Phil. Mag.,' vol. 25, p. 201 (1913).

† 'Roy. Soc. Proc.' A, vol. 124, p. 25 (1929).

$$\frac{4\pi^2m^2}{h^4}\left|\int_0^\infty\int_0^\pi\int_0^{2\pi} V \exp\left(\frac{4\pi i m v}{h} r \sin\tfrac{1}{2}\delta\cos\theta\right) r^2 \sin\theta \, dr \, d\theta \, d\phi\right|^2 \tag{6}$$

If V is a function of r only this reduces to

$$\frac{4\pi^2m^2}{h^4}\left|\frac{2\pi h}{2\pi m v \sin\frac{1}{2}\delta}\int_0^\infty V r \sin\left(\frac{4\pi m v r}{h}\sin\tfrac{1}{2}\delta\right) dr\right|^2$$

$$= \frac{4\pi^2}{v^2h^2\sin^2\frac{1}{2}\delta}\left|\int_0^\infty V r \sin\left(\frac{4\pi m v r}{h}\sin\tfrac{1}{2}\delta\right) dr\right|^2 \tag{7}$$

In general this integral diverges but by making suitable modifications in V it may be made to converge. This may seem high handed but it is a common feature of quantum theory that such must often be done. It consists formally in introducing a parameter ε in V so as to modify the potential only slightly but such that

$$\operatorname*{Lt}_{\varepsilon\to 0}\int_0^\infty V(\varepsilon, r)\, r \sin\left(\frac{4\pi m v r}{h}\sin\tfrac{1}{2}\delta\right) dr \tag{8}$$

is finite. We shall assume that appropriate ε's may be obtained to make the above formula yield "physical" values for the scattering. This, of course, is a very doubtful step and cannot be justified mathematically but must be done to proceed.

The scattering in the above case will be proportional to F^2. Hence we have from (4)

$$s = 2 - 2n, \quad t = 2n - 6, \quad u = 2n - 4 \tag{9}$$

Hence the formula for the scattered wave amplitude, which is given by

$$r^2|\text{Amplitude}|^2 = \text{scattering cross-section},$$

must be of the form

$$C' h^{1-n} v^{n-3} m^{n-2}$$

Now, since v and $\sin\frac{1}{2}\delta$ always occur together as a simple product in expression (7) we must have a scattered wave amplitude of the form

$$C' h^{1-n} (v \sin\tfrac{1}{2}\delta)^{n-3} m^{n-2} \tag{10}$$

---

* 'Z Physik,' vol. 39, p 803 (1926)

Hence if we have the potential V expanded in the series

$$e^2 \Sigma_1 \frac{a_s}{r^s}, \qquad (a_s, \text{ constants}) \tag{11}$$

the scattered wave amplitude will be of the form

$$\Sigma_1 a_s' (v \sin \tfrac{1}{2}\delta)^{s-3}, \tag{12}$$

where the a_s' are new constants If the leading term is that for $s = 1$, which we take as giving the classical formula, the observed scattering by such a potential as (11) will be given by

$$a_1'^2 \left|\left(1 - \sum_{s=2} a_s'' v^{s-1} \sin^{s-1} \tfrac{1}{2}\delta\right)\right|^2 \tag{13}$$

where

$$a_s'' = a_s'/a_1' = a_s' (e^4/4m^2v^4 \sin^4 \tfrac{1}{2}\delta)^{-\frac{1}{2}} \tag{14}$$

for $a_1'^2$ just gives the classical Rutherford formula If this theory is valid then, if the scattering is due to a spherically symmetrical field of force, it should be a function of $v \sin \frac{1}{2}\delta$ It is easy to test this for any experimental values and if it is found to be the case, the powers of the additional potentials can be determined Since the deviation from the classical formula becomes greater the greater v and $\sin \frac{1}{2}\delta$, it is obvious from (13) that the only spherically symmetrical potential function capable of giving the results is one either expansible in powers of $1/r$, or in a series whose leading terms are in powers of $1/r$ Thus a pure exponential form of potential is of no value

§ 4 *Application to Experimental Values* —In figs 1 and 2 the ratio of observed to classical scattering is plotted as a function of $v \sin \frac{1}{2}\delta$ for magnesium and aluminium using all the points obtained by Bieler and by Rutherford and Chadwick For magnesium it is apparent that the ratio is of the form

$$C f (v \sin \tfrac{1}{2}\delta),$$

where C is independent of v and δ No such simplicity appears to characterise the aluminium results Whether this is due to failure of the theory, the law of force being not spherically symmetrical, or to experimental error in the determinations must remain an open question for the moment However as magnesium does seem to satisfy the required conditions we may proceed to find the law of force We have from (13)

$$R = \frac{\text{Observed}}{\text{Classical}} = \left|1 - \sum_{s=2} a_s'' v^{s-1} \sin^{s-1} \tfrac{1}{2}\delta\right|^2 \tag{15}$$

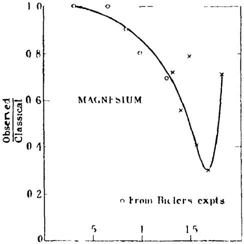

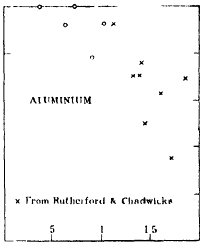

FIG 1 Scattering Ratio for Magnesium FIG 2—Scattering Ratio for Aluminium

Abscissa represent $v \sin \frac{1}{2}\delta \times 10^{-9}$ cm per second

Hence

$$R^{\frac{1}{2}} = 1 - \sum_{s} a_s'' v^{s-1} \sin^{s-1} \tfrac{1}{2}\delta \qquad (16)$$

If the predominating term in the expansion is for $s = n$ then if we plot $R^{\frac{1}{2}}$ as a function of $v^{n-1} \sin^{n-1} \frac{1}{2}\delta$ we should obtain an approximate straight line In fig 3 this has been done for $n = 3$, 4 and 5, and it is at once obvious that the

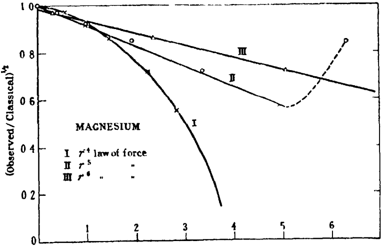

FIG 3—Illustrating relative probability of different laws of force causing anomalous scattering in magnesium

Scale—For curve I $(v \sin \frac{1}{2}\delta)^2 \times 10^{-18}$ (cm per sec)^2
For curve II $(v \sin \frac{1}{2}\delta)^3 \times 10^{-27}$ (cm per sec)^3
For curve III $(v \sin \frac{1}{2}\delta)^4 \times 10^{-36}$ (cm per sec)^4

last two give the best straight line We are thus led to consider the possibilities of the inverse fifth power law of force It is also clear from fig 3 that if we are to place reliance on the remaining experimental point we must introduce a further higher power repulsive law of force, but it is hardly allowable to draw such conclusions from a single point

§ 5 *Determination of Force Constant* a_4 —Let us introduce a potential

$$\frac{a_4 e^2}{r^2(r^2-l^2)} \tag{17}$$

We have then to evaluate

$$a_4 e^2 \int_0^{\infty} \frac{\sin\left(\frac{4\pi\, mvr}{h}\sin\frac{1}{2}\delta\right)dr}{r(r^2-l^2)} \tag{18}$$

Consider the Cauchy principal value of

$$\int \frac{\exp\left(\frac{4\pi i\, mvz}{h}\sin\frac{1}{2}\delta\right)dz}{z(z^2-l^2)} \tag{19}$$

taken over the usual semicircular contour indented at $z=0,\ \pm l$ This is equal to πi times the sum of the residues at the poles $0,\ \pm l$, of the integrand These residues are

$$-1/l^2, \quad e^{4\pi i\, mvl \sin\frac{1}{2}\delta/h}/2l^2, \quad e^{-4\pi i\, mvl \sin\frac{1}{2}\delta/h}/2l^2,$$

respectively, giving for the integral (19) the value

$$2\pi^2 \sin^2(2\pi\, mvl \sin\tfrac{1}{2}\delta/h)/l^2$$

But (19) is simply

$$2\int_0^{\infty} \frac{\sin\left(\frac{4\pi\, mvr}{h}\sin\frac{1}{2}\delta\right)dr}{r(r^2-l^2)}$$

Therefore the required principal value of (18) is

$$\frac{a_4 e^2\pi}{l^2}\sin^2\left(\frac{2\pi\, mvl}{h}\sin\tfrac{1}{2}\delta\right)$$

Making $l \to 0$ gives $a_4 e^2\, 4\pi^2 m^2 v^2 h^{-2} \sin^2\frac{1}{2}\delta$ for the 'physical" value of the integral in (7), for a law of force

$$4a_4 e^2 r^{-5}$$

Hence a_4' is

$$\frac{8\pi^4 a_4 v \sin\frac{1}{2}\delta\, m^2 e^2}{h^3} \tag{20}$$

using (7) Therefore from (14)

$$a_4'' = \frac{16\pi^4 m^3 a_4 v^3}{h^3 Z}\sin^3\tfrac{1}{2}\delta$$

If r_0 is the radius of the neutral surface in the nucleus

$$4a_4/r_0^5 = Z/r_0^2 \qquad (21)$$

so that

$$r_0 = \left(\frac{4a_4}{Z}\right)^{1/3} = \frac{h}{m}\left(\frac{a_4''}{4\pi^4}\right)^{1/3} \qquad (22)$$

Now from fig 3 we find $a_4'' = 0 \cdot 1/1 \cdot 5 \times 10^{27}$ so that

$$r_0 = 0 \cdot 6 \times 10^{-13}\ \text{cm} \qquad (23)$$

This is one sixth of the value deduced by Bieler with inverse fourth power law of force and classical mechanics Also

$$a_4 = 1 \cdot 1 \times 10^{-39}\ \text{cm}^3 \qquad (24)$$

which is very much less than Hardmeier's value (*loc cit*) of the "polarisability,"

$$0 \cdot 1 \times 10^{-36}\ \text{cm}^3$$

§ 6 *Conclusion* – It thus appears that if Born's theory of collisions can be approximately applied to scattering by higher power laws of force, the anomalous scattering results obtained with magnesium are due to a spherically symmetrical field of force which is at first that of an inverse fifth or sixth power attractive force In view of the sudden rise of scattering obtained at a certain point it appears that a higher power repulsive force may be coming into play This is of interest in view of the general explanation offered by Rutherford and Chadwick of their results as due to successive shells in the scattering nucleus the first attracting the α particle, the second repelling it. The radius of the neutral surface in the magnesium nucleus taking the fifth power law works out at $0 \cdot 6 \times 10^{-13}$ cm considerably smaller than the classical value of $3 \cdot 41 \times 10^{-13}$ cm Aluminium appears to show no irregularities of the same type as magnesium but until further experimental data is obtained the reason for this is not clear Despite the good results obtained from magnesium it is impossible to be certain of the validity of the above conclusions until very many more experimental observations have been made on various elements using angular ranges much smaller than those previously used

In conclusion, the author wishes to thank Sir Ernest Rutherford, Dr Chadwick and Mr R H Fowler for much discussion and the interest they have taken in this work

An Application of the Stern-Gerlach Experiment to the Study of Active Nitrogen

By L. C. Jackson, M.Sc., Ph.D., and L. F. Broadway, B.Sc., The University, Bristol

(Communicated by A. P. Chattock, F.R.S.—Received March 14, 1930.)

Introduction

Many theories have been put forward at one time or another to explain the chemical activity of active nitrogen and the mechanism of the production of the yellow "after glow." Reunion of nitrogen atoms to form molecules, metastable molecules and interactions between atoms and molecules have all been drawn upon to explain the after glow.*

At the time the work described in the present paper was commenced the theory holding the field was that of Sponer.† According to this theory two normal nitrogen atoms collide in a triple collision with a normal nitrogen molecule with the resultant formation of one normal nitrogen molecule and one excited molecule. Since the carrier of the after glow is known to be an excited nitrogen molecule with about 11·5 volts energy, and since the dissociation energy was then believed to be 11·5 volts, the theory seemed to explain the energy relations of active nitrogen satisfactorily. The comparative rareness of such a triple collision was in agreement with the long life of the after-glow. On this theory the chemical activity would be attributed to the nitrogen atoms (in their ground state). A support for this theory would have been obtained if it could have been shown that nitrogen atoms in their ground state, which is known to be a ^4S state, are present in active nitrogen. Later work has, however, shown that the dissociation energy of the nitrogen molecule is about 9·1 volts and not 11·5 volts as supposed by Sponer, and hence the theory cannot be valid.

What now appears to be a correct explanation of all the facts has been given by Cario and Kaplan.‡ They suppose that the production of the 11·5-volt excited molecules of the after-glow is due to an interaction between a metastable molecule in the $^3\Sigma$ state (8 volts) and a metastable nitrogen atom in the ^2P

---

* For a recent summary of the active nitrogen problem, see Kneser 'Ergebnisse der Exakten Naturwissenschaften,' vol. 8, p. 229.

† 'Z. Physik,' vol. 34, p. 622 (1924).

‡ 'Z. Physik,' vol. 58, p. 769 (1929); 'Nature,' vol. 121, p. 906 (1928).

state (3 5 volts) Interactions between metastable molecules in the $^3\Sigma$ state and metastable atoms in the ^2D state (2 4 volts) also give excited molecules required to explain the intensity distribution in the spectrum of the after-glow This spectrum is merely that of the first positive bond group of nitrogen but with a distribution of intensity different from that obtained in ordinary nitrogen The existence of these ^2P and ^2D metastable states of the nitrogen atom is predicted by Hund's theory* and they have been found spectroscopically by Compton and Boyce † who have verified that their energies are as required in the above theory The chemical activity of active nitrogen will on this view be due to the metastable atoms This theory would, therefore, receive confirmation if it could be shown that these metastable nitrogen atoms are present in active nitrogen and that they are chemically active

The work described in the present paper was undertaken with the hope of furnishing definite evidence as to the nature of the chemically active constituent or constituents of active nitrogen A stream of active nitrogen was submitted to investigation by means of the Stern Gerlach method using a chemical method for the detection of the stream From the traces produced evidence was obtained of the presence of metastable atoms of nitrogen in the $^2P_{\frac{1}{2}}$ state No other chemically active entities were recorded

Description of Apparatus

Several different experimental arrangements and methods of excitation were tried before any success was obtained These unsuccessful attempts will not be described but only the apparatus which was finally found to function satisfactorily

The main part of the apparatus is shown in the figure With the exception of the electrodes and the screen carrier, the whole was constructed of pyrex glass, so as to avoid any contact between the beam of active nitrogen and metal The nitrogen was purified by passing it from the cylinder in which it was contained through an alkaline solution of sodium hydrosulphite and a solution of potassium hydroxide A reservoir of about 1 5 litres capacity was filled with the gas to a pressure of about 6 cm The nitrogen passed from this reservoir through a spiral of fine capillary tubing (to give a considerable pumping resistance) into the discharge tube at A The greater part of the gas which enters the discharge tube leaves it again at B, it having been found that a

---

* " Linienspektren und Periodisches System der Elemente "

† ' Phys Rev ,' vol 33, p 145 (1929) See also Ingram, ' Phys Rev ,' vol 34, p 421 (1929)

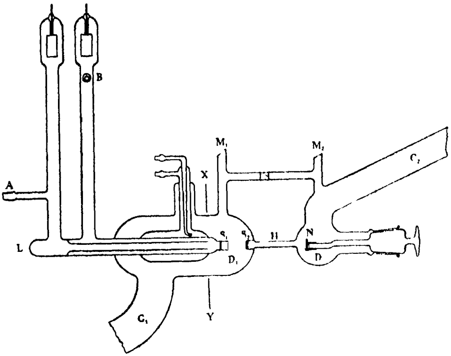

better after-glow could be obtained with a stream of gas larger than could be made to pass through the exit slit

The discharge tube is of the type described by Johnson* in his work on the reflection of hydrogen atoms from rock salt crystals Its construction will be obvious from the diagram The inner part of the discharge tube is water-cooled as shown to prevent these parts from becoming too hot The outer vertical tubes were kept cool by a current of air from an electric fan This type of discharge tube ensures that the activated gas is always present immediately behind the first slit and that it has not a long path to travel before reaching the latter as in the apparatus used by Wrede† for the determination of the magnetic moment of the hydrogen atom

A smaller part of the nitrogen passes through the fine slit S_1 This was made by sealing a piece of platinum foil of the required width and thickness into the end of a piece of pyrex tubing, sealing on a second piece of tubing to the first and blowing out flat the partition of glass so produced The platinum was then dissolved out with aqua regia Platinum was used as it gives the cleanest slits, quite free from bubbles or oxide By this means slits of any required length and width can readily be produced and the required pumping resistance can be obtained by suitably choosing the thickness of wall of the partition The slit S_1, actually used had a length of 1 5–2 mm , a width of about 0 05 mm , and a wall thickness or length of the canal of about 1 5 mm

---

* J Franklin Inst ,' vol. 206, p 301 (1928)

† Z Physik,' vol. 41, p 569 (1927)

The nitrogen then traversed the evacuated space, D_1, and passed through the second slit, S_2, so producing a fine beam of atoms (or molecules) along the narrow tube, H This second slit was made by sealing glass jaws, on which a bevelled edge had been ground, on to the flat, partially closed end of a glass tube The sealing was done with the aid of a miniature oxygen coal gas blowpipe The length of the slit is defined by the diameter of the hole left in the partially closed end of the tube, the required width being obtained by placing a piece of platinum foil of the required thickness between the jaws during the sealing on process The tube having been cut off short was sealed into the apparatus as shown The dimensions of this slit in the apparatus as first used were length 2 mm , width 0 05 mm The part D_1 of the apparatus was evacuated by a fast diffusion pump through a short length of 4 cm tubing shown at G_1

The narrow tube H was situated between the poles of a Weiss electromagnet, having the usual wedge-and-slot shape of the Stern Gerlach arrangement This tube bedded up against a brass block fitted into the slotted pole-piece in such a way that the vertical diameter of the tube lay nearly in the plane of the pole face *

After passing through the non homogeneous magnetic field, the beam was received on a screen N, coated with a suitable chemical indicator This screen was placed in a holder attached eccentrically to a ground-joint as shown, so that, as in Wrede's apparatus for the investigation of atomic hydrogen, the screen could be rotated, if desired, after an exposure with the magnetic field on, and a second with the field off, obtained on the same screen under the same conditions The tube H and the space D_2 were evacuated through the tube G_2 Side tubes at M_1 and M_2 served to measure the pressure in D_1 and D_2 respectively with a MacLeod gauge

The left half of the apparatus up to and including the narrow tube H was first constructed, the end L of the discharge tube being left open The whole was made up with the two slits as nearly in alignment as could be judged by eye They were then finally aligned as follows The apparatus was cut along

---

* For a diagram of and reasons for this arrangement, see Leu 'Z Physik,' vol. 41, p 551 (1927), and Wrede, 'Z Physik,' vol 41, p 569 (1927)

the line XY and the two halves supported in retort stands A brilliant line source of light was then focussed on the inside of the slit S_1 through the discharge tube at L Then by adjusting the position of the second half of the apparatus which carries the knife-edge slit S_2, it was possible to arrange that the light from the slit S_1 brilliantly illuminated the slit S_2 and that the beam of light also passed accurately along the axis of the tube H The adjustment was found to be very critical so that the alignment could be carried out with considerable accuracy and with relative ease The stands were then clamped in position and the apparatus again joined along XY, continual observation along the tube H ensuring that the slits were still in alignment when the joint was finished

The space D_1 in the apparatus first employed was evacuated by means of a Gaede steel three-stage diffusion pump backed by a Megavac rotary oil pump which also served to pump out the nitrogen at B A large liquid air trap of low resistance and of a design similar to that described by Johnson* was attached immediately to the ground-joint of the Gaede pump The space D_2 was evacuated through a similar trap by a pair of large single-stage glass diffusion pumps in parallel, backed by a third two-stage diffusion pump and a Hyvac rotary oil pump With this pumping system and with a pressure of about 1/10 mm in the discharge tube, the pressures in D_1 and D_2 were $2 - 3 \times 10^{-4}$ mm and less than 10^{-5} mm respectively

The indicator used in the present experiments was silver nitrate Preliminary trials in a separate apparatus had shown that this substance possesses advantages both as regards contrast and speed over the other substances which undergo a colour change through the action of active nitrogen † Silver nitrate possesses the disadvantages of being definitely crystalline and of darkening slowly under the action of light Neither of these is, however, fatal as the surface obtained when the salt is ground as finely as possible shows up the details of the trace quite adequately, and as the traces were measured and photographed soon after a run the eventual blackening of the whole screen was immaterial

The following dimensions of the apparatus may now be recorded discharge tube slit, 2 mm long, 0 045 mm wide, second slit, 2 mm long, 0 05 mm wide, distance between slits 3 cm, distance from second slit to screen 7 5 cm length of path in the magnetic field 4 cm

---

* 'J Franklin Inst,' vol 205, p 99 (1928)

† Several such substances are mentioned by Wrede, though in his experiments the substances were really acted upon by atomic nitrogen Our own observations afforded a general confirmation of his statements See 'Z Physik,' vol 54, p 53 (1929)

The apparatus was first calibrated by passing hydrogen through the discharge tube and so obtaining a trace for atomic hydrogen The theoretically expected splitting of the trace corresponds in this case to $mg = \pm 1$ and this has been confirmed experimentally by Wrede* and by Phipps and Taylor † The trace with the magnetic field on was first visible in about 20 minutes, and a completely exposed trace was obtained in 1½ hours The trace so obtained consisted of two clearly separated parallel lines each rather wider than the trace without the field on, exactly as in the photograph reproduced by Wrede Measurements of this trace, width of line without field width over outside edges of lines with field, width of gap between inside edges gave the necessary information for evaluating any other trace obtained with the same current through the magnet and for the same position of the screen ‡

Nitrogen was then run through the discharge tube and an attempt made to obtain a trace with it It was to be expected that the length of exposure would be much greater than with atomic hydrogen both because active nitrogen is not so reactive towards silver nitrate as atomic hydrogen and because the percentage of activated gas (about 2 per cent with the usual methods of activation) is very much less than in the case of hydrogen It was soon found that the exposures required with nitrogen were very long Again, there was no consistency in the results of the various runs, sometimes a run would result in a trace being obtained and sometimes not Though runs were made up to 36 hours' continuous exposure, the results obtained were quite unsatisfactory Thus it was necessary to decrease the length of exposure required by some means It was, therefore, reluctantly decided to increase somewhat the width of the second slit 0 05 mm was already as wide as could be allowed when it was desired to obtain clear resolutions of the split trace Widening the slit, therefore, meant sacrificing the resolution somewhat to speed of recording It would, however, result in determining *definitely* whether a molecular beam of active nitrogen can be satisfactorily recorded under the conditions demanded by the experiment, and, if so, whether the entity which is thus recorded possesses a magnetic moment or not It *might* also be possible to interpret the trace so obtained if it happened to correspond to certain particularly simple cases If a trace was obtained and could not be immediately interpreted, it was our intention to return to a narrower slit and to find some other means of evading or successfully obtaining the long exposures required in the light of the experience gained This latter step was not, however, found necessary as it was found that the trace finally obtained could be interpreted definitely though the lines were not actually resolved when developed to their full width.

---

* 'Z Physik,' vol 41, p 569 (1927)

† 'Phys Rev ' vol 29, p 309 (1927)

‡ Kurt and Phipps ('Phys Rev ' vol 34 p 1357 (1929)) in their recent work on the "Magnetic Moment of the Oxygen Atom " have also used atomic hydrogen to calibrate the apparatus

The second slit was, therefore, now given a width of rather more than 0 06 mm , the other dimensions of the apparatus remaining exactly as before The arrangement was again calibrated with atomic hydrogen, given purposely only a short exposure (a visible trace could now be obtained with atomic hydrogen with the magnetic field on in 2 minutes) to ensure that the trace was resolved The previous calibration was satisfactorily confirmed Runs were then made with nitrogen and though the results were now more satisfactory, it was found that exposures of more than one day's run would have to be given to obtain a completely developed trace To do this it was desirable to be able to shut down the apparatus over night and run again the next day This was quite possible as far as repeating the conditions as to the pressure in the discharge tube, the vacuum in the rest of the apparatus and the current in the electromagnet, but the special low resistance mercury vapour traps did not permit of liquid air being maintained in them after the pumps had been shut off Since it was quite necessary to prevent mercury vapour from reaching the silver nitrate screen (which is rapidly blackened thereby), it was necessary to re-design the pumping system The following arrangement was, therefore, adopted The two parts D_1 and D_2 of the apparatus were each evacuated by means of a large single-stage umbrella pattern diffusion pump using oil* as the working substance backed by a two-stage mercury diffusion pump with a mercury vapour trap of the usual pattern between them Liquid air could be kept on this trap indefinitely and the mercury vapour prevented from reaching the silver nitrate when the apparatus was shut down over night The oil diffusion pumps possess the advantage of requiring no trap so that they can be connected directly to the apparatus through a short length of tubing, so improving the pumping speed

This pumping system proved quite satisfactory and the apparatus immediately worked consistently with nitrogen and the time of exposure was reduced somewhat further This change in the behaviour of the apparatus was to be attributed to the elimination of a small trace of mercury vapour which passed the low resistance traps and partially deactivated the beam of active nitrogen That a very small amount of mercury vapour did get past was shown by the fact that with the earlier form of the apparatus the trace obtained with nitrogen was black, due to a developing action of the mercury and with the new pumping system was brown

---

* This oil was supplied by Mr Burch of the Metropolitan Vickers Co , Manchester, and has a vapour pressure of 10^{-7} mm at room temperature

Exposures were now made with the magnetic field on, and with it off The current through the electromagnet was always 9 amps A clearly visible, well-developed trace was obtained with the magnetic field off in 2–5 hours Exposures made with the field on, resulted in traces which were broadened compared with those obtained in the absence of the field, but broadened to an extent which corresponded to a splitting of the beam much smaller than that of atomic hydrogen Longer runs were, therefore, made to determine whether the full width of the trace had been reached or whether with a longer run the trace would broaden further, indicating the presence of other more deviated components With this object exposures were made up to as long as 40 hours, but no appreciable broadening of the trace was produced It was not found feasible to give much longer exposures, say longer than 50 hours, as the "background" due to general scattering then became undesirably noticeable Since it was intended to investigate active nitrogen in its ordinary state in which it gives the well-known yellow after glow, it was desirable to run the discharge tube under such conditions that an after-glow was always present The after-glow is relatively weak at the pressures at which it was found necessary to run the discharge tube 1/10–1/5 mm, and it was found that the after-glow disappeared after the tube had been running for more than, say, 2 hours This observation is in agreement with the known fact that no after-glow is produced in glass apparatus which has been thoroughly baked out, the walls becoming very catalytically active and destroying one of the components required to produce the after glow Herzberg* has shown that if a trace of hydrogen is introduced the after glow returns to its full intensity in such baked-out apparatus A trace of hydrogen, insufficient to give any record on the silver nitrate screen, was, therefore, added to the nitrogen during some of the runs The yellow after glow then persisted in parts of the discharge tube throughout the whole exposure No difference in the trace was, however, observed when the discharge tube was run under these conditions and when it was run with the after-glow absent This shows that the chemical activity of active nitrogen may persist in the non-glowing state as observed by several other workers * In view of this hydrogen was not added to the nitrogen in later exposures

---

* 'Z Physik,' vol 46, p 878 (1928)

Experimental Results and Discussion

It was found that moderately long exposures, 12–24 hours, produced traces with the magnetic field on which were not resolved into two components, and which had widths about 60 per cent greater than the line obtained in the absence of the field It was thus immediately seen that the splitting, to which these unresolved traces corresponded, was much smaller than that of atomic hydrogen, *i e*, mg was less than 1 As mentioned above longer exposures were then given, up to 40 hours, to determine whether the width of the trace obtained with, say, 24 hours' exposure, really represented the whole trace or whether components of larger mg value, which on account of the spreading due to the Maxwellian distribution of velocities would require a longer exposure to make them visible, would be recorded The width of the trace remained sensibly the same for increases of exposure beyond a definite minimum

It, therefore, seemed that the whole trace was to be accounted for by a single pair of components corresponding to an mg value of less than 1 On this assumption the breadth of the unresolved trace to be expected was calculated for the possible cases satisfying these conditions The calculation was made with the aid of the formula given by Stern,† using the data of the atomic hydrogen calibration It was then found that the width of the trace, whether it was as small as possible (lowest pressure in the discharge tube) or whether it was broadened somewhat by collisions (higher pressure), could be explained by a value of the magnetic splitting equal to $mg = \pm 1/3$ To give the numerical results, the width of the line in the absence of the field was in one instance, 0 33 mm , and with the field on, was 0 57 mm , with a probable error of about 5 per cent The calculated value of the width of the trace in the magnetic field, assuming 0 33 for the width without field, was 0 57 mm

Although each trace was photographed it was decided not to publish these photographs because, on the increased scale required for reproduction, the grain of the silver nitrate is shown so clearly that it confuses the details of the actual traces Furthermore, since the traces were brown, the photographic contrast always came out less than the visual contrast, and as this would be emphasised in the reproductions, the figures would give a very poor idea of the appearance of the original traces

---

* See Willey, J Chem Soc,' p 2831 (1927), Kneser, *loc cit*, pp 236, 251

† 'Z Physik,' vol 41, p 563 (1927)

A curious development phenomenon was observed with the traces obtained on silver nitrate with active nitrogen, in that they "developed" in the air in the dark for several days after removal from the apparatus. In fact unless an exposure of over 12 hours had been given (with the field on) no trace was visible on removing the screen from the apparatus. It soon, however, began to appear and continued to darken gradually for at least 3 days. This phenomenon permitted a satisfactory confirmation of the splitting $\pm 1/3$ to be obtained. A short exposure of about $1\frac{1}{2}$ hours was given with the field on. No trace was visible on removing the screen from the apparatus but, on watching the screen, a trace was seen to appear gradually. Because of this phenomenon it was possible to see the trace before the components had reached their full width and intensity. They were then seen as two very fine, clearly resolved lines, which as time went on became darker and broader and finally overlapped. It was found possible to obtain a measurement not of the actual separation, but of the total width across the outer edges of the lines. Now the calibration with hydrogen had shown that if the splitting with nitrogen corresponded to $mg = \pm 1/3$, the centres of the lines should be 0·13 mm apart. If now the lines were just visibly resolved the width of each component could not have been more than, say, 0·12 mm in this case. The width across the whole trace would thus be 0·25 mm or rather less. The mean of a series of measurements on traces, when just resolved, gave a width of 0·24 mm in excellent agreement with the above value. Many attempts were made to obtain photographs of the trace in the resolved condition. Although photographs were obtained, it was not found possible to obtain one which would reproduce satisfactorily on account of the faintness of these traces.

The whole of the evidence obtained pointed to the fact that the entity which produced the trace on the silver nitrate screen had a magnetic moment such that the splitting was $\pm 1/3$ and no evidence was obtained of the presence of atoms or molecules in other states. This fortunately means that the trace, in spite of the components not being resolved when they had reached their full width, was definitely interpretable.

In discussing the meaning of this result, we may first consider what states (atomic or molecular) might have been expected to have been present in the beam passing through the magnetic field. If Sponer's theory had been correct, one would have expected to obtain a trace corresponding to the nitrogen atom in its ground state. Since this is a ^4S state, the trace would have corresponded to ± 3, ± 1. Sponer's theory is, however, undoubtedly incorrect, so that one would not actually expect to observe this splitting. The theory of Cario and Kaplan, which requires the presence of metastable molecules in the $^3\Sigma$ state and metastable atoms in the ^2P and ^2D states, gives a larger number of possibilities The $^3\Sigma$ molecules (since a Σ diatomic molecule behaves in a magnetic field like an S atom) would lead to a trace $\pm 2, 0$ It is however, probable from available evidence that these metastable molecules are not chemically active, at any rate, to the extent of blackening silver nitrate The likelihood of the trace corresponding to $\pm 2, 0$ is, therefore small The two types of metastable atoms might each give rise to two traces, thus ± 2, $\pm 2/3$ for $^2P_{3/2}$, $\pm 1/3$ for $^2P_{1/2}$, ± 3, $\pm 9/5$, $\pm 3/5$ for $^2D_{5/2}$, $\pm 6/5$ $\pm 2/5$ for $^2D_{3/2}$ The ^2P state is the more important for Cario and Kaplan's theory and should be present to a greater extent than ^2D The finding of a splitting $\pm 1/3$ indicates that what registered its presence on the screen was the nitrogen atom in the metastable $^2P_{1/2}$ state This thus furnishes a confirmation of Cario and Kaplan s theory in so far as it proves the existence of atoms in the metastable ^2P state and that these atoms are chemically active

Since there seems to be no theoretical reason why if $^2P_{1/2}$ is present $^2P_{3/2}$ should not also be present, the failure to obtain evidence of the presence of the latter state must presumably be attributed to the exposure being insufficient to record it It was calculated, however, that if the two ^2P states were present to equal extents, and no other state which could produce a record on the silver nitrate screen, the longest exposures should have been adequate to show up the presence of the $\pm 2/3$ components at least and probably also the ± 2 components If, however, the ^2D state were also present to an extent less than the ^2P state, the exposures given might just fail to record anything but the $^2P_{1/2}$ state Longer exposures could not, however, be given as then the whole screen would have been unpleasantly darkened by general scattering and any fainter extensions of the trace would probably have been missed

The fact that the ^2P metastable state was recorded whether the discharge-tube was run under conditions which gave the after-glow or in the glowless state when the walls were catalytically active, indicates the correctness of the suggestion of Cario and Kaplan that the absence of the after-glow is due to the deactivation of the metastable $^3\Sigma$ molecules by the walls of the discharge-tube

Summary

The Stern-Gerlach experiment has been applied to study the nature of a beam of active nitrogen The nitrogen was activated by means of a condensed electrical discharge and the presence of the beam was recorded by means of a

chemical indicator, silver nitrate The results obtained indicated that the traces produced on the silver nitrate screen were due to nitrogen atoms in the metastable $^2P_{\frac{3}{2}}$ state This observation provides a confirmation of the theory of Cario and Kaplan as to the nature of active nitrogen and the mechanism of the production of the after-glow

---

The Energy of Crystal Lattices

By H Jones, Trinity College, Cambridge

(Communicated by R H Fowler, F R S —Received March 20, 1930)

Introduction

In order to calculate the potential energy of a collection of a large number of atoms it is necessary to use the quantum mechanical perturbation theory The choice of the initial wave functions with which the perturbation calculation is to be carried out, is equivalent to deciding what model of the system shall be taken as the starting point * In the case of crystals the model which involves the simplest assumptions is that in which the crystal is regarded initially as a large number of atoms in their lowest energy state, arranged in a lattice , the lattice constant being great The perturbation theory is then applied to find how the energy of the system changes as the atoms are brought slowly together , the lattice retaining its original form It is not necessarily true, however, that when the separation has been reduced to that actually occurring in a given crystal that the system of normal atoms, adiabatically brought together, will be identical with the crystal itself Thus, for example, Hertzberg has shown that the deepest state of N_2^+ does not arise from the adiabatic approach of a normal N atom, and a normal N^+ ion

When the atoms of the lattice are still well separated it is possible to calculate the mean first order energy using a method given by Heitler † The determinant of the secular equation can be reduced, as Wigner has shown, to a number of irreducible sub determinants to each of which corresponds a particular term system, and of these, those which satisfy the exclusion principle determine a given total spin moment The sum of all the energies belonging to one-term system is then given by summing along the diagonal of the corresponding sub determinant This procedure, however, assumes that the initial wave functions form an orthogonal set In the case of a crystal the initial wave functions are to be taken as the product of the wave functions of the separate atoms, and these will only be even approximately orthogonal when the distance between nearest atoms is great

---

* In a paper by J C Slater, in course of publication, dealing with the cohesive forces in metals, the problem of finding suitable initial wave functions is considered in detail. I have to thank the author and Dr J H Bartlett for kindly allowing me to see the manuscript

† 'Z Physik,' vol 46, p 47 (1928)

Such calculations, then, give but little indication of what the potential energy of a crystal will really be For example, one would find that a cubic lattice of hydrogen atoms with no resultant spin moment would always have a very much lower mean energy than the same number of atoms formed in pairs, the distance between the two atoms of a pair being the same as that between two nearest neighbours of the lattice The fact that hydrogen forms a diatomic gas shows that this is actually not the case, and indicates that the calculation of the energy has been too rough It is to be remembered that liquid and solid hydrogen are still essentially molecular, as appears from the density The binding forces here arise from the van der Waal's attractive forces between the molecules, which in turn probably come from polarisation effects They certainly do not appear from the first order perturbation interchange terms

As a closer approximation to the actual case the perturbation calculation has here been carried out without assuming that the initial functions are orthogonal Of course, if the equation for the first order perturbation energy were actually solved, and the zero order functions formed, which are just linear combinations of the initial product functions, these would then form an orthogonal set The immediate result of retaining the factor which expresses the non-orthogonality of the initial functions (the S of Heitler and London's paper) is that in the determinant of the secular equation the energy, for which the equation is to be solved, will appear in other elements than just the diagonal ones, and the summation along the diagonal will no longer give the sum of the roots

Unlike Heitler's method the method adopted here does not depend upon using the representation of the symmetric permutation group as a group of linear substitutions It is found sufficient to use an expression first given by Frobenius* for the irreducible factor of degree f of the group determinant In this expression the coefficients of the variables of the group matrix are just functions of the characteristics Applied to the case of a crystal, taking into account only those integrals which involve interchanges between nearest neighbours, the result emerges that the coefficient of the interchange term in the expression for the mean energy decreases as the points of the lattice come closer together. Thus the mean energy of the crystal depends to a much greater extent on the simple electrostatic potential energy given by the inter-lapping of the Schrodinger space charge, and to a much less extent on the interchange integral than does the binding energy in a diatomic molecule.

---

* A general account of Frobenius' work is given by Dickson in the 'Ann. Math.,' vol 34 (1901–1903)

For the case in which hydrogen atoms are regarded as placed in a simple cubic lattice, it is shown that the mean energy of the crystal is of the same order of magnitude as the energy of the same number of atoms forming a diatomic gas, instead of being much less as the simple calculation assuming orthogonal functions would suggest. One could not expect to get much more definite results so long as the interchanges between three and more nearest neighbours are neglected. This is particularly the case with hydrogen atoms, since here, as there is no repulsive core, the minimum of the energy curve occurs for small separations of the atoms, where the approximation of considering only nearest neighbours begins to fail badly. It is also shown that when the atoms do possess a closed shell lying behind the single valency electron, the potential energy of the crystal form always lies lower than the energy of the same number of atoms arranged as a diatomic gas. Moreover one sees also that in this case the closest distance of approach of the atoms will be greater, and the approximation of considering only nearest neighbours not so serious.

§ 1. There are $2n!$ different solutions to the wave equation for a system comprised of $2n$ widely separated hydrogen like atoms. Each function is a product of $2n$ functions $\psi\binom{k}{l}$ of the individual atoms where the upper number refers to the nucleus k, and the lower to the electron l. The different solutions arise by operating on the lower numbers of $\Psi_L = \prod_k^{2n} \psi\binom{k}{k}$ separately by the $2n!$ permutations which can be made on $2n$ symbols. The functions of zero order are linear combinations of these initial functions Ψ_E, Ψ_P, etc.,

$$u_k = \sum_P a_k{}^P \Psi_P,$$

the summation being taken over all the permutations. If H be the Hamiltonian operator, the perturbation calculation as carried out by Heitler and London consists in making $(H - E)\,\Psi_Q$ orthogonal to each of the $2n!$ functions u_k. E is the total energy of the system.

$$\sum_P a_k{}^P \int \Psi_P\,(H - E)\,\Psi_Q\,d\tau = 0$$

As H is symmetrical in all the electrons, the integrals involved become

$$x_{Q^{-1}P} = \int \Psi_{Q^{-1}1} (H - E) \Psi_F \, d\tau$$

and the secular equation for the first order perturbation energies is

$$|x_{Q^{-1}P}| = 0 \tag{1}$$

The left-hand side of this equation is just the group determinant in the variables x_R of the symmetric group of degree $2n$

If each of the z nearest neighbours to the nucleus k be denoted by some number j_k which can take z values for a given k, and $r_{j_k}^{k}$ is written for the distance between the nucleus k and the electron j_k, $r_{k\,j_k}$ for the distance between the electrons k and j_k, and $r^{k\,j_k}$ for the distance between the nuclei k and j_k, then putting

$$v(k, j_k) = \left(\frac{2}{r_{j_k}^{k}} - \frac{1}{r_{k\,j_k}} - \frac{1}{r^{k\,j_k}}\right)$$

one finds that the terms of $(H - E)\Psi_E$ which do not vanish identically can be written

$$\{\tfrac{1}{2}\sum_{k\;j_k} v(k, j_k) - \varepsilon\}\Psi_E,$$

where k goes over the numbers $2n$, and j_k takes z values for each k of course, $k \neq j_k$ ε is the perturbation energy Lengths are measured in units of a_H the radius of the first hydrogen orbit, and ε in units of the energy corresponding to this orbit

The wave functions $\psi\binom{k}{k}$ for the separate atoms are taken to be normalised but not orthogonal, when k and l are nearest neighbours,

$$\left\{\begin{aligned} 1 &= \int \psi^2\binom{k}{k} d\tau_k, \\ \xi &= \int \psi\binom{k}{k}\psi\binom{k}{l}\psi\binom{l}{l}\psi\binom{l}{k} d\tau_k \, d\tau_l \end{aligned}\right. \tag{2}$$

The variables of the group determinant are

$$\left\{\begin{aligned} x_E &= \int \{\tfrac{1}{2}\sum_{k\;j_k} v(k, j_k) - \varepsilon\} \Psi_F^2 \, d\tau_1 \quad d\tau_{2n}, \\ x_P &= \int \{\tfrac{1}{2}\sum_{k\;j_k} v(k, j_k) - \varepsilon\} \Psi_E \Psi_P \, d\tau_1 \quad d\tau_{2n}, \end{aligned}\right. \tag{3}$$

Defining

$$\left\{\begin{aligned} J_F &= \int v(k, j_k)\, \psi^2\binom{k}{k} \psi^2\binom{j_k}{j_k} d\tau_k \, d\tau_{j_k}, \\ J_0 &= \int v(k, j_k)\, \psi\binom{k}{k} \psi\binom{k}{j_k} \psi\binom{j_k}{j_k} \psi\binom{j_k}{k} d\tau_k \, d\tau_{j_k} \end{aligned}\right. \tag{4}$$

one sees that J_E can be regarded as the potential energy of two spherical charge distributions about two positive nuclei which are nearest neighbours, J_0 as the potential energy of two ellipsoidal charge distributions occupying the same space, and interacting, of course, with the nuclei as well as between themselves. Now if P be a permutation of order greater than 2, say 3, each term of x_P will involve integrals which can be regarded as the potential energy of two ellipsoidal charge distributions about two different pairs of nuclei, but with one nucleus common to both pairs. Integrals of this type will always be much smaller than ξ, J_E or J_0 except when the nuclei are very close together. The approximation is made here of neglecting all integrals except the three just mentioned. Thus, all x_P are taken to be zero when P is of order greater than 2. All the variables x_P for which P is of order 2 must be considered, i.e. P may contain many cycles of order 2 so long as no symbol occurs twice. Let such a permutation with α cycles be written P_α, e.g. $P_2 = (ab)(cd)$.

Hence from equations (2), (3), (4) one finds at once

$$(5) \qquad \begin{cases} x_E = znJ_E - \varepsilon, \\ x_{P_\alpha} = \alpha J_0 \xi^{\alpha-1} + (n-\alpha)\, zJ_1\, \xi^\alpha - \varepsilon\xi^\alpha \end{cases}$$

It is to be noticed that in each case except x_E there are $\alpha(z-1)$ terms which have been omitted as they are integrals of the form

$$J_1 = \int v(k, m)\, \psi\binom{k}{k}\, \psi\binom{j_k}{k}\, \psi^2\binom{m}{m}\, d\tau_k d\tau_m,$$

m being one of the $(z-1)$ nearest neighbours to k other than j_k. This integral is of the same order of smallness as those arising from permutations of order 3, and is therefore to be neglected in our approximation. Actually there would be no difficulty in retaining these terms if it were worth while to do so.

The highest value which α can take is n, so that the irreducible factor of degree f of the group determinant will be a homogeneous function in the $(n+1)$ variables $x_E, x_{P_1}, \dots x_{P_n}$. It may therefore be written

$$\prod_{\kappa=1}^{f} (x_E + \beta_1^\kappa x_{P_1} + \beta_2^\kappa x_{P_2} + \dots + \beta_n^\kappa x_{P_n})$$

The numbers $\beta_1^\kappa \dots \beta_n^\kappa$ will, of course, in general be different for each factor, to each of which there will correspond one value of the perturbation energy. If one writes

$$(6) \qquad w_\kappa = 1 + \beta_1^\kappa \xi + \beta_2^\kappa \xi^2 + \dots + \beta_n^\kappa \xi^n,$$

there follows at once by (5)

$$\varepsilon_\kappa w_\kappa = z\mathrm{J}_\mathrm{E}\{nw_\kappa - (\beta_1{}^\kappa\xi + 2\beta_2{}^\kappa\xi^2 + \quad + n\beta_\kappa{}^\kappa\xi^n)\} \\ + \mathrm{J}_0(\beta_{1\kappa} + 2\beta_2{}^\kappa\xi + \quad + n\beta_\kappa{}^\kappa\xi^{n-1})$$

or

$$\varepsilon_\kappa = zn\mathrm{J}_\mathrm{E} + \frac{1}{w_\kappa}\frac{du_\kappa}{d\xi}(\mathrm{J}_0 - z\mathrm{J}_\mathrm{E}\xi)$$

Forming now the mean energy for the whole term system, and writing

$$\Phi = \prod_{\kappa=1}^{f} u_\kappa$$

one has

$$\bar{\varepsilon} = zn\mathrm{J}_1 + \frac{1}{f}\;\frac{1}{\Phi}\frac{d\Phi}{d\xi}\;(\mathrm{J}_0 - z\mathrm{J}_\mathrm{E}\xi) \tag{7}$$

As can be seen from its definition Φ is just the irreducible factor of the group determinant which is being considered, but now the variables are $\xi_{\mathrm{P}_a} \equiv \xi^a$ instead of the x_{P_a} It remains therefore to determine $\frac{1}{\Phi}\frac{d\Phi}{d\xi}$ as a function of ξ It may be mentioned that if the integrals J_1 had been retained a term approximately $(z-1)\,\mathrm{J}_1\xi^4$ would appear in the factor $(\mathrm{J}_0 - z\mathrm{J}_\mathrm{E}\xi)$ The effect of this would be to keep the interchange term finite as the nuclei approached infinitely closely together , for ordinary values of the separation it is unimportant

§ 2 An expression for the irreducible factor of degree f is as follows —

$$\Phi = \Sigma\,\frac{(-1)^{\lambda_1+\lambda_2+\quad+\lambda_f}}{\lambda_1!\,\lambda_2!\quad\lambda_f!}\left(\frac{\mathrm{S}_1}{1}\right)^{\lambda_1}\left(\frac{\mathrm{S}_2}{2}\right)^{\lambda_2}\quad\left(\frac{\mathrm{S}_f}{f}\right)^{\lambda_f} \tag{8}$$

The summation is over all λ for which

$$\lambda_1 + 2\lambda_2 + \quad + k\lambda_k + \quad f\lambda_f = f$$

The numbers λ_k are either 0 or positive integers, and

$$\mathrm{S}_k = \sum_{\mathrm{R}_1\quad\mathrm{R}_k}\chi(\mathrm{R}_1\mathrm{R}_2\quad\mathrm{R}_k)\,\xi_{\mathrm{R}_1}\,\xi_{\mathrm{R}_2}\quad\xi_{\mathrm{R}_k} \tag{9}$$

Here the summation is taken over all R_k as each goes separately through every permutation of the group $\chi(\mathrm{P})$ is the characteristic belonging to the irreducible factor of degree f and the class of which P is a member We define a function ϕ_j by the equation

$$\phi_j = \Sigma\,\frac{(-1)^{\lambda_1+\lambda_2+\quad\lambda_j}}{\lambda_1!\,\lambda_2!\quad\lambda_j!}\left(\frac{\mathrm{S}_1}{1}\right)^{\lambda_1}\quad\left(\frac{\mathrm{S}_j}{j}\right)^{\lambda_j}$$

where

$$\lambda_1 + 2\lambda_2 + \quad + j\lambda_j = j \tag{10}$$

and the S's are still given by (9), *i.e.*, they belong to the factor Φ Differentiating ϕ_j partially with respect to S_k

$$\frac{\partial\phi_j}{\partial S_k} = -\frac{1}{k}\Sigma\frac{(-1)^{\lambda_1+\cdots+\lambda_j-1}}{\lambda_1!\cdots(\lambda_k-1)!\cdots\lambda_j!}\left(\frac{S_1}{1}\right)^{\lambda_1}\cdots\left(\frac{S_k}{k}\right)^{\lambda_k-1}\cdots\left(\frac{S_j}{j}\right)^{\lambda_j},$$

and condition (10) may be written

$$\lambda_1 + 2\lambda_2 + \cdots + k(\lambda_k - 1) + \cdots + j\lambda_j = j - k \tag{11}$$

If $\lambda_k > 0$ then all $\lambda_{j-k+m} = 0$ for $m = 1, 2, \ldots k$, so that (11) becomes

$$\lambda_1 + 2\lambda_2 + \cdots + k\lambda'_k + \cdots + (j-k)\lambda_{j-k} = j - k,$$

where all λ's including λ'_k are 0 or positive integers Thus

$$\frac{\partial\phi_j}{\partial S_k} = -\frac{\phi_{j-k}}{k} \tag{12}$$

when $\lambda_k > 0$ As $\Phi = \phi_f$ it follows that

$$\frac{d\Phi}{d\xi} = -\sum_{k=1}^{f}\phi_{f-k}\frac{1}{k}\frac{dS_k}{d\xi},$$

because when $\lambda_k = 0$ $\frac{dS_k}{d\xi} = 0$ The required function may therefore be written

$$\frac{1}{\Phi}\frac{d\Phi}{d\xi} = -\sum_{k=1}^{f}\frac{\phi_{f-k}}{\phi_f}\frac{1}{k}\frac{dS_k}{d\xi} \tag{13}$$

When $\xi = 0$, $S_k = f(E) = f$ and if one puts $(\phi_j)_{\xi=0} = p_j$ one sees that these are the coefficients in the equation

$$x^f + p_1x^{f-1} + p_2x^{f-2} + \cdots + p_f = 0$$

when this has f roots equal to unity, *i.e.* the p_j are just the binomial coefficients $(-1)^j\binom{f}{j}$ Forming now the expression

$$F(\xi) = -\sum_{k=1}^{f}\left\{\frac{\phi_{f-k}}{\phi_f} - \frac{p_{f-k}}{p_f}\right\}\frac{1}{k}\frac{dS_k}{d\xi} \tag{14}$$

one shows that $F(\xi) \equiv 0$ for all ξ, *i.e.*

$$F(0), \left(\frac{dF}{d\xi}\right)_{\xi=0}, \left(\frac{d^2F}{d\xi^2}\right)_{\xi=0}, \ldots$$

are all zero Of course, both $\frac{\phi_{f-k}}{\phi_f}$ and $\frac{dS_k}{d\xi}$ are functions of ξ and the vanishing of F (ξ) identically does not imply that the summand vanishes for each value of k One obtains in this way the simple formula for the required function

$$\frac{1}{\Phi}\frac{d\Phi}{d\xi} = -\sum_{k=1}^{f}\frac{p_{f-k}}{p_f}\frac{1}{k}\frac{dS_k}{d\xi} \tag{15}$$

From the expression giving S_k one sees that (15) can readily be obtained in ascending powers of ξ, the coefficients being functions of the characteristics which are easily calculable

The derivatives of F at $\xi = 0$ can be shown to vanish by employing equation (12) to carry out the differentiation , and then as when $\xi = 0$ ϕ_k becomes just the binomial coefficient p_k each $F^{(n)}(0)$ can be obtained It is convenient first to consider the following expression in which $g(k)$ is a function of the number k, not of ξ

$$\sum_{k=1}^{f} g(k)\frac{d}{d\xi}\left(\frac{\phi_{f-k}}{\phi_f}\right) = -\sum_{k=1}^{f-1}\sum_{l=1}^{f-k}\frac{\phi_{f-k-l}}{\phi_f}g(k)\frac{1}{l}\frac{dS_l}{d\xi}$$
$$+\sum_{k=1}^{f}\frac{\phi_{f-k}}{\phi_f}g(k)\sum_{l=1}^{f}\frac{\phi_{f-l}}{\phi_f}\quad\frac{1}{l}\frac{dS_l}{d\xi}$$

Also $\left(\frac{dS_l}{d\xi}\right)_{\xi=0} = lh_1\chi(\mathrm{P})$, h_P being the number of considered permutations of class P Using the properties of the binomial coefficients it follows at once that

$$\frac{-p_f}{h_\mathrm{P}\chi(\mathrm{P})}\left\{\sum_{k=1}^{f} g(k)\frac{d}{d\xi}\left(\frac{\phi_{f-k}}{\phi_f}\right)\right\}_{\xi=0} = \sum_{\mu=0}^{f-1} p_\mu\sum_{k=1}^{f-\mu-1} g(k) + \sum_{\mu=0}^{f-1} p_\mu g(f-\mu) \tag{16}$$

Taking special values of $g(k)$ one has the following results

$$\left\{\sum_{k=1}^{f}\frac{d}{d\xi}\left(\frac{\phi_{f-k}}{\phi_f}\right)\right\}_{\xi=0} = 0, \tag{17}$$

$$\left\{\sum_{k=1}^{f}(k-1)\frac{d}{d\xi}\left(\frac{\phi_{f-k}}{\phi_f}\right)\right\}_{\xi=0} = 0 \tag{18}$$

$$\left\{\sum_{k=1}^{f}(k-1)(k-2)\frac{d}{d\xi}\left(\frac{\phi_{f-k}}{\phi_f}\right)\right\}_{\xi=0} = 0 \tag{19}$$

It is easy to see that this type of relation is general and will hold for any number of factors $(k-1)(k-2)(k-3)$ less than f

For the first derivative of F one has

$$\frac{dF}{d\xi} = -\sum_{k=1}^{f}\frac{d}{d\xi}\left(\frac{\phi_{f-k}}{\phi_f}\right)\frac{1}{k}\frac{dS_k}{d\xi} - \sum_{k=1}^{f}\left\{\frac{\phi_{f-k}}{\phi_f} - \frac{p_{f-k}}{p_f}\right\}\frac{1}{k}\frac{d^2S_k}{d\xi^2}$$

Since $\left(\frac{1}{k}\frac{dS_k}{d\xi}\right)_{\xi=0}$ is independent of k the first term for $\xi = 0$ vanishes by (17) and clearly the second term also is zero when $\xi = 0$ Therefore $\left(\frac{dF}{d\xi}\right)_{\xi=0} = 0$

For the second derivative one has

$$-F''(\xi) = \sum_{k=1}^{f} \frac{d^2}{d\xi^2}\left(\frac{\phi_{f-k}}{\phi_f}\right)\frac{1}{k}\frac{dS_k}{d\xi} + 2\sum_{k=1}^{f}\frac{d}{d\xi}\left(\frac{\phi_{f-k}}{\phi_f}\right)\frac{1}{k}\frac{d^2S_k}{d\xi^2}$$
$$+\sum_{k=1}^{f}\left\{\frac{\phi_{f-k}}{\phi_f} - \frac{p_{f-k}}{p_f}\right\}\frac{1}{k}\frac{d^3S_k}{d\xi^3}$$

When $\xi = 0$ the last term vanishes Also as

$$(20) \qquad \left(\frac{d^2S_k}{d\xi^2}\right)_{\xi=0} = 2k\,h_{P_2 f}(P_2) + k(k-1)\sum_{P_1P_1'} f(P_1P_1')$$

the first term of the second member vanishes by (17), and the second term by (18) The first term is

$$\sum_{k=1}^{f}\frac{d^2}{d\xi^2}\left(\frac{\phi_{f-k}}{\phi_f}\right)\frac{1}{k}\frac{dS_k}{d\xi}$$
$$= \sum_{k=1}^{f-1}\sum_{l=1}^{f-k}\frac{d}{d\xi}\left(\frac{\phi_{f-k-l}}{\phi_f}\right)\frac{1}{k\ \ l}\frac{dS_k}{d\xi}\frac{dS_l}{d\xi} + \sum_{k=1}^{f}\sum_{l=1}^{f-k}\frac{\phi_{f-k-l}}{\phi_f}\frac{1}{k\ \ l}\frac{d^2S_l}{d\xi^2}\frac{dS_k}{d\xi}$$
$$-\sum_{k=1}^{f}\sum_{l=1}^{f}\frac{d}{d\xi}\left(\frac{\phi_{f-k}}{\phi_f}\ \ \frac{\phi_{f-l}}{\phi_f}\right)\frac{1}{k\ \ l}\frac{dS_k}{d\xi}\frac{dS_l}{d\xi}$$
$$-\sum_{k=1}^{f}\sum_{l=1}^{f}\frac{\phi_{f-k}}{\phi_f}\ \ \frac{\phi_{f-l}}{\phi_f}\frac{1}{k\ \ l}\frac{d^2S_l}{d\xi^2}\frac{dS_k}{d\xi}$$

When $\xi = 0$ the third term of this expression vanishes by (17) whilst the first term is apart from a constant factor

$$\sum_{k=1}^{f-1}\sum_{l=1}^{f-k}\frac{d}{d\xi}\left(\frac{\phi_{f-k-l}}{\phi_f}\right) = \sum_{k=1}^{f}(k-1)\frac{d}{d\xi}\left(\frac{\phi_{f-k}}{\phi_f}\right)$$

which vanishes when $\xi = 0$ by (18) The second and fourth terms do not vanish individually, but reduce to the same value and cancel each other Noticing that

$$(21) \qquad \sum_{k=1}^{f}\frac{p_{f-k}}{p_f}(k-1)(k-2) \qquad (k-r) = (-1)^{r+1}r!$$

for $r < f$, and using (20) it is easy to reduce both to

$$2h_{P_2 f}(P_2)\,h_{P_1\chi}(P_1) - h_{P_1\chi}(P_1)\,\Sigma\chi(P_1P'_1)$$

Thus one shows that $F''(0) = 0$, and as can easily be seen the same process may be applied to other derivatives, when it will be found that the third and higher ones also vanish As it is in any case only possible to obtain the first few powers of ξ in $\frac{1}{\Phi}\frac{d\Phi}{d\xi}$ it would be no essential advantage to prove rigorously that every derivative of $F(\xi)$ vanishes at $\xi = 0$

§ 3 To find the coefficients of the powers of ξ in $\frac{1}{\Phi}\frac{d\Phi}{d\xi}$ according to equation (15) one has first to express $dS_k/d\xi$ in ascending powers of ξ S_k is given in equation (9) and remembering that $\xi_{R_\mu} = \xi^{\alpha_\mu}$ where α_μ is the number of cycles of order 2, no symbol in the whole permutation being repeated

$$\text{(22)} \qquad \frac{d}{d\xi}(\xi_{R_1}\xi_{R_2} \quad \xi_{R_k}) = (\alpha_1 + \alpha_2 + \quad + \alpha_k)\,\xi^{\alpha_1+\alpha_2+ \quad \alpha_k - 1}$$

The r^{th} power of ξ in S_k is the one for which

$$\alpha_1 + \alpha_2 + \quad + \alpha_k = r + 1,$$

and the coefficient of ξ^r will be obtained by considering the ways in which this can be satisfied To obtain the coefficient of ξ^2 will be a sufficient illustration

$$\alpha_1 + \alpha_2 + \quad + \alpha_k = 3$$

This may be satisfied in k ways in which one $\alpha = 3$ in $\frac{k(k-1)}{2!}$ ways in which $\alpha_k = 2$, $\alpha_l = 1$ so that $\alpha_k > \alpha_l$ when $k < l$ and again in $\frac{k(k-1)}{2!}$ ways so that $\alpha_k < \alpha_l$ when $k < l$, and finally in $\frac{k(k-1)(k-2)}{3!}$ ways in which $\alpha_k = \alpha_l = \alpha_m = 1$ the rest being zero The coefficient of ξ^2 in $dS_k/d\xi$ is therefore

$$\text{(23)} \quad 3k\Sigma\chi(P_3) + \tfrac{3}{2}k(k-1)\Sigma\chi(P_2P_1) + \tfrac{1}{2}k(k-1)\Sigma\chi(P_1P_2) + \frac{3k(k-1)(k-2)}{3!}\Sigma\chi(P_1P_1'P_1'')$$

the summations being over all permissible values of each permutation indicated The prime is used to distinguish different permutations of the same class The permutations arising from the products P_1P_2 may be of three different classes, viz , $(ab)(cd)(ef)$, $(abc)(de)$, $(abcd)$ There will, however, be the same number of each class given by P_1P_2 as by P_2P_1, so that although frequently $P_1P_2 \neq P_2P_1$ the second and third terms of (23) are equal

Multiplying (23) by $\frac{1}{k}\ \frac{p_{f-k}}{p_f}$ the summation over all k is carried out at once by (21) and one has finally (the other coefficients being obtained in a similar manner)

$$\frac{1}{\Phi}\frac{d\Phi}{d\xi} = a_0 + a_1\xi + a_2\xi^2 + a_3\xi^3 +$$

where

$$a_0 = \Sigma\chi(\mathrm{P}_1)$$
$$a_1 = 2\Sigma\chi(\mathrm{P}_2) - \Sigma\chi(\mathrm{P}_1\mathrm{P}_1')$$
$$a_2 = 3\Sigma\chi(\mathrm{P}_3) - 3\Sigma\chi(\mathrm{P}_1\mathrm{P}_2) + \Sigma\chi(\mathrm{P}_1\mathrm{P}_1'\mathrm{P}_1'')$$
$$a_3 = 4\Sigma\chi(\mathrm{P}_4) - 4\Sigma\chi(\mathrm{P}_1\mathrm{P}_3) - 2\Sigma\chi(\mathrm{P}_2\mathrm{P}_2') + 4\Sigma\chi(\mathrm{P}_2\mathrm{P}_1\mathrm{P}_1') - \Sigma\chi(\mathrm{P}_1\mathrm{P}_1'\mathrm{P}_1''\mathrm{P}_1''')$$

As a special case one may put $\xi = 0$ when

$$\bar{\varepsilon} = zn\,\mathrm{J}_{\mathrm{F}} + \frac{zn}{f}\chi(\mathrm{P}_1)\,\mathrm{J}_0$$

which is just Heitler's result applied to a crystal lattice there being just zn values of P_1

One has now to consider the values of these coefficients when the $2n$ atoms form a special type of lattice The only case considered is that of a simple cubic lattice for which $z = 6$ Although one still writes z for clarity it is to be remembered that the following expressions are obtained just for this value of z The number of permutations of a given class R is written h_{R}, so that

$$a_0 = h_{\mathrm{P}_1}\chi(\mathrm{P}_1) \tag{25}$$

It is convenient to have different letters for the different classes of permutations consisting of a single cycle Thus one may put

$$\mathrm{Q} = (abc), \quad \mathrm{R} = (abcd), \quad \mathrm{S} = (abcde),$$

then one can write

$$\sum_{\mathrm{P}_1\mathrm{P}_1}\chi(\mathrm{P}_1\mathrm{P}_1') = h_{\mathrm{P}_1}\chi(\mathrm{E}) + h_{\mathrm{Q}}\chi(\mathrm{Q}) + 2h_{\mathrm{P}_2}\chi(\mathrm{P}_2)$$

The 2 occurs in the last term because each P_2 arises twice from the products $\mathrm{P}_1\mathrm{P}_1'$ There follows also an equation between the h's

$$h_{\mathrm{P}_1}{}^2 = 2h_{\mathrm{P}_2} + h_{\mathrm{Q}} + h_{\mathrm{P}_1} \tag{26}$$

Thus

$$a_1 = -\{h_{\mathrm{P}_1}\chi(\mathrm{E}) + h_{\mathrm{Q}}\chi(\mathrm{Q})\} \tag{27}$$

The determination of the other coefficients is a little more difficult First

$$\sum_{\mathrm{P}_1\mathrm{P}_1\mathrm{P}_1'}\chi(\mathrm{P}_1\mathrm{P}_1'\mathrm{P}_1'') = 2\sum_{\mathrm{P}_2\mathrm{P}_1}\chi(\mathrm{P}_2\mathrm{P}_1) + \sum_{\mathrm{QP}_1}\chi(\mathrm{QP}_1) + h_{\mathrm{P}_1}{}^2\chi(\mathrm{P}_1)$$

Therefore

$$a_2 = 3\Sigma\chi(\mathrm{P}_3) - \Sigma\chi(\mathrm{P}_2\mathrm{P}_1) + \Sigma\chi(\mathrm{QP}_1) + h_{\mathrm{P}_1}{}^2\chi(\mathrm{P}_1) \tag{28}$$

For each value of P_2 there are two P_1 such that $\mathrm{P}_2\mathrm{P}_1 = \mathrm{P}_1'$ Thus $\Sigma\chi(\mathrm{P}_2\mathrm{P}_1)$ gives $2h_{\mathrm{P}_2}$ values of $\chi(\mathrm{P}_1)$ For each possible Q there are two P_1 so that $\mathrm{QP}_1 = \mathrm{P}_1'$ Hence $\Sigma\chi(\mathrm{QP}_1)$ gives $2h_{\mathrm{Q}}$ values of $\chi(\mathrm{P}_1)$ Altogether, therefore, a_2 contains $(-2h_{\mathrm{P}_2} + 2h_{\mathrm{Q}} + h_{\mathrm{P}_1}{}^2)$ values of $\chi(\mathrm{P}_1)$ Now the permutations P_2 fall into three different types which must be treated separately They are written T_1, T_2, T_3, and are defined by $\mathrm{T}_1 = (ab)(cd)$ where a and c, b and d are nearest neighbours $\mathrm{T}_2 = (ab)(cd)$ where only a and c are nearest neighbours, and for T_3 neither a and c nor b and d are nearest neighbours It is then easy to see that $\Sigma\chi(\mathrm{P}_2\mathrm{P}_1)$ contains $(2h_{\mathrm{T}_1} + h_{\mathrm{T}_2})$ values of $\chi(\mathrm{R})$ Also one finds that there are $(3z - 4)$ values of P_1 which make $\mathrm{QP}_1 = \mathrm{R}$ so that $\Sigma\chi(\mathrm{QP}_1)$ contains just $(3z - 4)\,h_{\mathrm{Q}}$ of $\chi(\mathrm{R})$ All terms involving h_{T_2}, h_{P_2}, etc, so that higher powers of n than the first occur cancel each other This is readily verified in the coefficients up to a_3 which are given here, and clearly must always be the case, otherwise $\dfrac{1}{\Phi}\dfrac{d\Phi}{d\xi}$ would depend on a higher power of n than the first which physically is absurd Using the expressions given and equation (28)

$$a_2 = (3h_{\mathrm{Q}} + h_{\mathrm{P}_1})\,\chi(\mathrm{P}_1) + \{(3z - 4)\,h_{\mathrm{Q}} - (2h_{\mathrm{T}_1} + h_{\mathrm{T}_2})\}\,\chi(\mathrm{R}) \tag{29}$$

In the same way one can show that

$$\begin{aligned} a_3 = &- \{2h_{\mathrm{Q}} + h_{\mathrm{P}_1}\}\,\chi(\mathrm{E}) - \{(4z - 1)\,h_{\mathrm{Q}} + 8h_{\mathrm{T}_1} + 4h_{\mathrm{T}_2}\}\,\chi(\mathrm{Q}) \\ &- \{(3z - 1)(z - 2)\,h_{\mathrm{Q}} - 8(z - 2)\,h_{\mathrm{T}_1} - 2(2z - 3)\,h_{\mathrm{T}_2}\}\,\chi(\mathrm{S}) \end{aligned} \tag{30}$$

and

$$\left\{\begin{aligned} h_{\mathrm{P}_1} &= nz, \\ h_{\mathrm{Q}} &= 2(z - 1)\,nz, \\ h_{\mathrm{T}_1} &= \tfrac{1}{2}(z - 2)\,nz, \\ h_{\mathrm{T}_2} &= (z^2 - 3z + 3)\,nz \end{aligned}\right. \tag{31}$$

The characteristics are readily calculated by Schur's method described by Heitler, and one finds that for the term system corresponding to no total resultant spin moment, and for large values of n so that only the highest powers need be considered

$$\chi(\mathrm{E}) = f, \quad \chi(\mathrm{P}_1) = \tfrac{1}{2}\,f, \quad \chi(\mathrm{Q}) = \tfrac{1}{4}\,f, \quad \chi(\mathrm{R}) = \tfrac{1}{8}\,f, \quad \chi(\mathrm{S}) = \tfrac{1}{16}\,f$$

Hence

$$\begin{cases} a_0 = \frac{1}{2} nzf, \\ a_1 = -\frac{1}{2}(z+1)\, nzf \\ a_2 = \frac{1}{8}(5z^2 + 12z - 13)\, nzf, \\ a_3 = -\frac{1}{8}(z^3 + 22z^2 - 7z - 8)\, nzf \end{cases}$$

These values, as has already been said, will only be actually true for a simple cubic lattice In this case the coefficient of the interchange integral in the expression for the mean energy of the crystal is shown as a function of ξ in fig 1 The dotted line is merely a possible extrapolation

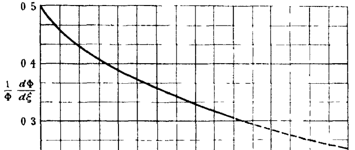

FIG 1 —Curve showing $\frac{1}{\Phi}\frac{d\Phi}{d\xi}$ as a function of ξ

As a special case which provides a check on the calculations the case of a system of $2n$ hydrogen atoms taken in pairs may be considered From Heitler and London's calculation the mean energy over the f states must be of the form

$$\bar{\varepsilon} = (n - m)\frac{J_E + J_0}{1 + \xi} + m\,\frac{J_F - J_0}{1 - \xi},$$

m being some integer less than n When the mean energy is put in the form of equation (7) one finds that the coefficient of $(J_0 - J_E\xi)$ is

$$\frac{n - m}{1 + \xi} - \frac{m}{1 - \xi} = (n - 2m) - n\xi + (n - 2m)\,\xi^2 - n\xi^3 +$$

The values of the coefficients a_0, a_1, etc , are easily calculated when each atom has only one nearest neighbour One finds

$$\frac{1}{f}\frac{1}{\Phi}\frac{d\Phi}{d\xi} = \tfrac{1}{2}n - n\xi + \tfrac{1}{2}n\xi^2 - n\xi^3 +$$

When $m = n/4$ the two expressions become identical One could not say *a priori* what value m should have The mean it is to be noticed is taken over $f = 2n!/n!(n+1)!$ states of the system

The application to a system of hydrogen atoms placed at the points of a simple cubic lattice is shown in fig 2 Curve (1) gives the electrostatic potential energy of the interlapping space changes, (2) is the interchange term assuming orthogonal initial functions, (3) the interchange term taking ξ into account

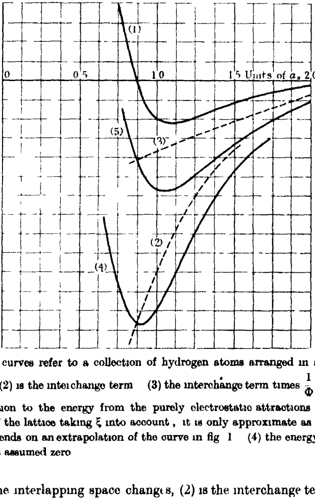

FIG 2—The curves refer to a collection of hydrogen atoms arranged in a simple cubic lattice (2) is the interchange term (3) the interchange term times $\frac{1}{\Phi}\frac{d\Phi}{d\xi}$ (1) is the contribution to the energy from the purely electrostatic attractions (5) gives the energy of the lattice taking ξ into account, it is only approximate as the lower part of (3) depends on an extrapolation of the curve in fig 1 (4) the energy of the lattice when ξ is assumed zero

The lowest energy state of the same number of atoms as a diatomic gas will be approximately one-third of the value of the minimum of curve (4) The energy of the crystal form is given by (5) and one sees that the minimum of this is still lower than that of the lowest gaseous state, though not nearly so deep as when the non-orthogonality of the initial wave functions is entirely neglected To get a closer approximation one would have to consider other interchange integrals than just those arising between pairs of nearest neighbours

If there exists a closed shell behind the single valency electron, it does not reduce the value of J_E, but very greatly reduces the value of the interchange integral The curves (2) and (3) would therefore have smaller gradients, and the ratio of the minimum of (4) to that of (5) would be less on account of the J_E curve remaining the same As the energy of the gaseous, *i e*, the diatomic, state is determined by (4), being very nearly one third of this it is seen that the presence of an inert gas-like shell, by reducing the importance of the interchange integral, results in giving the crystal configuration a deeper energy minimum relative to that of the molecular state than is the case for hydrogen atoms

I wish to express my thanks to Mr R H Fowler for his valuable suggestions, and stimulating encouragement during the course of this work

The Geographical Representation of the Mountains of Tibet

By Colonel Sir Sidney Burrard, K C S I , F R S

(Received March 18, 1930)

Tibet is the great protuberance of the Earth's surface, and many branches of science rely upon geographers for the accurate representation of its features The most definite features of mountain masses are the high peaks, and the determination of their positions is the first geographical step As the area of Tibet exceeds a million square miles, it has been necessary to classify its myriads of peaks, and the method of classification adopted has been to group the peaks according to the mountain ranges upon which they stand Geographers have utilised the ranges as their basis of classification, and geologists have relied upon the curvatures of the ranges in their consideration of the pressures which have caused the uplift of the continent of Asia By " ranges " we mean features of original structure, a line of mountains that has been carved by rivers out of an older mass we call a ' ridge "

The southern wall of Tibet is the range of the Himalaya which separates it from India The northern wall is the Kuen-Lun range which separates it from Turkestan Between these two border ranges the Karakoram forms the central backbone which is the second highest range of mountains upon the earth The width of each of these ranges is of the order of 100 miles In this paper I am considering the form and the alignment of the Karakoram range, and I will divide this consideration into three sections (1) The alignment, (2) the northern slopes, (3) the southern slopes

(*a*) *The Karakoram Alignment across Western Tibet* (1865)

(See Map I)

The alignment of this range has proved more difficult than that of the Himalaya The latter rise out of the low lying plains of India and are so conspicuous that all other features are dwarfed But the Karakoram rise from a plateau, where the ground-level is 16,000 feet high, and only the highest features emerge above the surface of the table-land In tracing the course of such a range we have to rely upon three classes of observation (i) altitude, (ii) the lines of drainage, (iii) the continuity of the curvilinear alignment

The main features of the Karakoram were determined in 1855–1865 by Colonel Montgomerie's surveys, and are shown here in map I The crest-line of high peaks extends from A on the map to E, a length of 170 miles The peaks are named as follows —

A—group of 4 Hunza-Kunji peaks, 3 of which exceed 25,000 feet

B—group of 3 Kunjut peaks, one of which exceeds 25 000 feet

C—the peak of K2, the second highest point on the globe, height 28,250 feet

D—Teram Kangri peak, height 24,430 feet (discovered 1909)

E—peak near the Rimo glacier, 23,320 feet (discovered 1914)

From F to G, a length of 110 miles there is another line of peaks somewhat lower, and 20 miles distant from the higher crest-line The probable explanation of this parallel line is that the original summit was a wide flat topped zone A difference noticeable between the Himalayan and Karakoram maps is that the glaciers of the former tend to flow in directions transverse to the range, whilst those of the latter have formed longitudinal beds This difference is probably due to the original formations of the summits

The watershed between the drainage basins of the Indus and Yarkand rivers is shown on map I by a dotted line This is the Central Asian divide , for a length of 140 miles it coincides with the Karakoram crest but on the west and on the east, in Hunza and Depsang the feeders of the Indus have cut back and have caused the watershed to recede behind the crest to a distance of 40 miles on the west, and of 20 miles on the east in Depsang

From A to E the crest line is so lofty that from longitude 74° to 77° the alignment is not open to doubt, but east of the Rimo peak at E the following changes in the topography occur together

(1) The crest-line decreases in height, and peaks of 23,000 feet are no longer seen

(2) Owing to the rainfall on the southern slopes being heavier than on the northern, the Upper Shyok river has been able to cut back through the range and to capture a small drainage area, Depsang, from the Yarkand river

(3) East of the Shyok river the rainfall almost ceases, and the river is replaced by inland lakes The Central Asian divide gives place here to the inland basin of Tibet The erosion by glaciers and rivers which has given to the Karakoram range its sharp and rugged character also ceases, and in the dry climate of Tibet the decomposition of rock fills the hollows with sand and gives to the mountains a rounded appearance

(*b*) *The Prolongation of the Alignment into Central Tibet* (1874 *to* 1909)

In 1870 the opinion held by Colonel Montgomerie was that from longitude 74° to 77° the range was aligned as shown in map I, and that near longitude 78° the range was cut across by the gorge of the Shyok river, and that its easterly prolongation was not known. In 1874 the survey sent the pundit Nain Singh to explore Central Tibet, but his explorations were begun south east of Montgomerie's surveys, and no connection was established between the two. Nain Singh's route lay to the east of map I, in latitude 32°, he was impressed by the high snowy range he saw to his south. This range was 120 miles north of a range known as "the Kailas," which had been fixed by earlier explorers, 1846–1850. (Many years later, 1904–5, Ryder and Wood made a survey of the Tsangpo river in southern Tibet and observed peaks on the Kailas range between latitude 29° and 30°.) The view adopted by the Survey, 1878 to 1880, was that Nain Singh's range was probably the easterly continuation of the Karakoram. The possibility of such a continuation was faintly indicated in the map of the Mountains of India, prepared

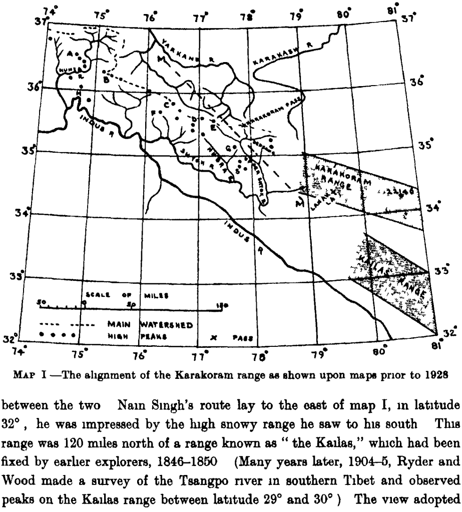

Map I —The alignment of the Karakoram range as shown upon maps prior to 1928 for the House of Commons, 1880 Up to 1908, however, the range lines were broken on charts to show that their continuity was hypothetical

In 1909 Sven Hedin published the results of his explorations in Tibet, 1906 to 1908 He had explored the whole country between Nain Singh's range and

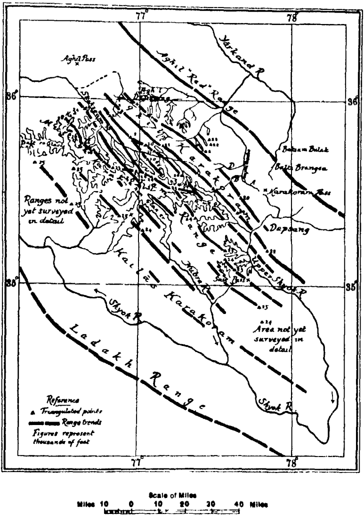

MAP II —The alignment of the Karakoram range as shown in 1928

the Kailas range, and he had discovered that these two apparent ranges were the north and south borders of one great range, over 100 miles wide This immense range was called by Sven Hedin the Trans Himalaya He showed that the Trans-Himalaya embraced the range, known to the Survey as the

"Kailas" In his book published in 1909 Sven Hedin also showed that the prolongation of the Karakoram range through Central Tibet was 2° further north than had been thought On the north his explorations fitted in with those of Deasy and Rawling The straightening of the eastern prolongation of the Karakoram range by Sven Hedin enables us with confidence now to continue the alignment of this range to the eastern limit of map I

(c) *Recent Confirmations of Montgomerie's Alignment* (1908 *to* 1922)

In 1909 Dr Longstaff explored the Karakoram crest, near the point D on map I he found that a bay in the watershed, 30 miles across, had arisen from an error in the original survey of the Siachen glacier By this discovery Longstaff straightened out the watershed, and showed that it conformed to the crest line Also by his further discovery of the peak of Teram Kangri he proved that the high crest-line was continuing on the same alignment, as it had followed from Hunza to Gasherbrum

Since 1914 the surveys of de Filippi and Wood* have given additional confirmation to the correctness of the accepted alignment Their maps of the Karakoram watershed (well known in geography from the Karakoram pass that crosses it) shows that this watershed is a "ridge" carved out of the northern slopes of the Karakoram range

(d) *The New Alignment advocated in* 1928

In 1928 a Report on the "Exploration of the Shaksgam Valley" by Major Mason was published by the Geodetic Branch Office of the Survey of India In this report the alignment of the Karakoram range, as described in this paper and as illustrated in map I, has been altered Map II of this paper is a copy of the map given in the report to illustrate the new alignment The two maps can be compared, as the high crest-line on map I can also be seen on map II running from the point marked K2(28) to the Rimo glacier (across three of the new alignments), the Karakoram pass is also shown on both maps I had to draw map I on a smaller scale than map II, because it was necessary to embrace a larger area in order to test the results of the new changes Major Mason has complicated map II by introducing many ranges, where his predecessors had shown only one The high crest-line in map I trends from W N W to E S E, the range-lines of map II trend from N W to S E The change in direction amounts to 20°, and in order to illustrate its effects I have drawn on map I one of Mason's new lines and marked it M–M This line on map I enables the proposed change in the Karakoram alignment to be appreciated Major Mason's several range lines are more or less parallel, and the range which I have copied from map II into map I is that which runs from Aghil Depsang to Depsang Major Mason, referring to the old alignment which had been adopted by his predecessors in consultations with geologists, writes as follows "The Karakoram range has been allowed to cut across the mountains that I have shown asbelonging to the Aghil chain" And he goes on to say that his "conception of the Aghil chain must necessarily change all this"

---

* Colonel Wood worked with the de Filippi expedition, 1913–14

The Surveyor-General (Brigadier E A Tandy) expressed his approval of map II in the preface which he contributed to the report He drew attention to the special interest attaching to "the great divide between the drainage of Central Asia and the Indian Ocean," and he added that "the interesting character of the drainage can best be studied" from map II A study of map II shows that five of the new ranges have been made to intersect the "great divide," as if drainage was independent of altitude On map II the Karakoram pass, which is on the great divide, seems to be standing on nothing

My objections to Major Mason's alignments may be summarised as follows -

(1) His mountain ranges have no relation to the drainage

(2) His ranges are shown cutting across the high Karakoram crest line which is the dominant feature of the region

(3) His alignments if prolonged beyond the western and eastern borders of his map II become further and further removed from the real Karakoram range

The map showing Mason's new alignments has been given wide publicity I take this opportunity of advising geologists and meteorologists and all who are interested in small-scale maps to consider the questions at issue before they accept the new geographical representations

(e) *The Northern Slopes of the Karakoram*

Between 1890 and 1900 the idea came to be held that a separate range, the Aghil range, was standing north of the Karakoram, between the latter and the Kuen-Lun There were grounds for believing that high mountains were standing there The possibility of an Aghil range was occasionally indicated on maps, but without further surveys it was known to be hypothetical In 1914 Colonel Wood made a survey of the Central Asian divide and of a considerable area beyond His map showed that there was no Aghil range The ground level is high and rugged, but not more so than is to be expected, when we consider that it is the flank of the second highest mountain chain in the world The general slope of the ground is downwards from the Karakoram crest to the Yarkand river, and this is an indication that the whole area was involved in the crustal fold which raised the Karakoram Not only does the ground slope gradually downwards, but its highest points, a few of 22,000 feet and one of 23,000, occur immediately opposite that section of the Karakoram crest in which the greatest altitudes have been observed The ranges of Tibet are the governing lines of the plateau, and it appears from Wood's and Mason's surveys that there is no such governing line in the Aghil area The evidence furnished by the drainage leads to the same conclusion, for the feeders of the Yarkand and Karakash rivers flow straight away from the main divide without encountering any serious obstacle

The interesting problem of the Aghil area is the deep trough of the Shaksgam river, it was discovered by Sir Francis Younghusband in 1887 That this trough owes its origin to the glaciers of the Karakoram seems beyond doubt, for it only exists, as a trough, below that section of the range (from C to D on map I) where the altitude of the range is greatest The drop from the crest to the trough is abnormally steep, but it cannot be said to be unique, there is an equally steep drop behind the Himalayan peak of Dhaulagiri, and there may be other similar instances

The "Karakoram pass" has had an important place in geography It is the only feature of the country that has been well known for centuries to the travelling population of Ladak and Turkestan, and it has been a landmark in modern geography From 1865 to 1880 the opinion held by the Survey of India was that the Karakoram pass was situated north of the mountain crest upon a minor ridge, to which the Shyok river had been able to cut its way from the south From 1890 to 1900, when the existence of an Aghil range in rear of the Karakoram was considered probable, an idea grew up that the Shyok river might have cut back into the trough between the two ranges This idea was conjectural and had been borrowed from the Himalayan analogy, a trough exists behind Mount Everest and Dhaulagiri, into which the rivers draining the front Himalayan slopes have been able to cut back The publication of de Filippi's and Wood's surveys has taught us that no trough exists behind the Karakoram Their maps showed that the Karakoram pass is situated on a ridge in rear of the crest-line, and that this ridge has probably been carved by the Shyok tributaries out of the massive flank of the range

An interesting confirmation of this view is to be obtained also from de Filippi's map[*], he shows that the Rimo glacier is situated upon the great divide, so that on one side it is feeding the Yarkand river and on the other it is feeding the Indus The idea is thereby suggested that the watershed is receding northwards, and that in its recession it has robbed the Yarkand river of a part of the Rimo glacier, and that it will in time rob it of all

(*f*) *The Southern Slopes of the Karakoram*

The southern slopes present more difficult problems than the northern Not only does the great range of southern Tibet come into contact with the Karakoram range, but there are two isolated masses surmounted with high peaks, marked upon map I as S and H, which cannot be allotted with certainty to either of the two ranges The Kailas range is the prominent feature of Southern Tibet from east to west, its position is shown on map I near the south-east corner Sven Hedin describes this range as it traverses Central Tibet as follows "It is 1400 miles long, in breadth it is inferior to the Himalaya, and its peaks are lower, but the height of its passes are greater than those of the Himalaya On the north and south its boundaries are sharply defined" Nain Singh observed its northern boundary, Ryder and Wood surveyed its southern flank from the Tsangpo

On map I the Karakoram and Kailas ranges are seen to be converging towards one another, as they trend westwards As far as we can judge from surface observations, these two ranges must be in actual contact when they reach the Upper Shyok river (longitude 78°) What happens to them when they meet cannot be discovered without geological investigations Along the line of their contact we see the two high isolated ridges, the Sasir and the Haramush, marked S and H, such isolated masses, 25,000 feet high, are abnormal in that they do not occur in the Himalaya so far from the crest-line There are reasons for thinking that there is an interrelation between the two ranges and the two isolated masses, the Sasir mass, S, rises out of the flank of the Karakoram range where the latter comes into contact with the Kailas, so long as the two ranges remain in actual contact, the Karakoram attains an altitude considerably higher than anywhere else Finally when the two ranges again separate, as they appear to do in Hunza (longitude 75°) the Karakoram declines in altitude whilst the second isolated mass, known as Haramush ridge, H, rises like the Sasir mass out of the flank of the range

---

[*] 'Spedizione Italiana de Filippi,' ser 2, vol IV, pl XI

Geographical surveyors have to draw their conclusions from observations of the Earth's surface The valuable testimony of the rocks out of which the mountains have been built is not available But the geological results of the de Filippi expedition will shortly be published The requirements of nomenclature occasionally lead geographers into the regions of hypothesis, in the course of the long Karakoram investigation the hypothesis was at one time adopted that Nain Singh's range was the easterly prolongation of the Karakoram, but this was afterwards shown to be wrong Such an hypothesis serves, however, a temporary purpose, in that it shows the way for future research

When two great earth-folds like the Karakoram and Kailas come into contact and become temporarily merged, it is not possible from surface observations to discover exactly what has happened But the necessities of classification and of nomenclature have been pressing the Survey to include the two isolated mountain masses, Sasir and Haramush, in their system of ranges, and to allot them either to the Karakoram as spurs, or to the Kailas as high points of its crest-line But any such steps, though in some ways helpful and suggestive to future surveyors, are merely hypotheses Our inability to understand the complexities of the orography should not, however, lead us to minimise the great amount of geographical knowledge that has been built up during the last 100 years, or to forget the debts that we shall always owe to the self-sacrifice of the geographical explorers

OBITUARY NOTICES.

CONTENTS

PAGE

HENRY JOHN HORSTMAN FENTON i

SIR HENRY BRADWARDINE JACKSON (with portrait) vi

PERCY ALEXANDER MACMAHON (with portrait) x

SEBASTIAN ZIANI DE FERRANTI (with portrait) xix

HENRY JOHN HORSTMAN FENTON—1854-1929

HENRY JOHN HORSTMAN FENTON was born at Ealing in 1854 He received his earlier education at Magdalen College School, Oxford, and afterwards went to King's College, London, where he studied chemistry under Bloxam During the time that Fenton was at King's College the Clothworkers' Company instituted an exhibition in physical science tenable for three years by a non-collegiate student at Cambridge Fenton applied successfully for this exhibition and, in accordance with its conditions, entered the University of Cambridge in the Lent Term, 1875 In his first year at Cambridge he gained an entrance scholarship at Christ's College, where he was admitted in May, 1876 He was then 22 and thus older than the majority of undergraduates His chemical knowledge and experience were also greatly in advance of those of men of the same university standing, and while still an undergraduate he was made an assistant demonstrator by Prof Liveing He had a very independent spirit, and it was therefore perhaps not unnatural that he chafed at the discipline then imposed on members of the University *in statu pupillari* and not infrequently came into conflict with University and College authorities In fact, to the end he cherished a certain antagonistic attitude towards university authority He took the Natural Sciences Tripos in 1877—it was at that time not divided into two parts—and was placed in the First Class along with, amongst others, Adam Sedgwick, the zoologist, F O Bowen, afterwards Professor of Botany at Glasgow, and Alex Hill sometime Master of Downing

On the resignation of the then University Demonstrator of Chemistry, John Wale Hicks, of Sidney Sussex, afterwards Bishop of Bloemfontein, W J Sell was appointed to succeed him, and an Additional Demonstratorship of Chemistry " was instituted by the University and the post was assigned to Fenton

The University Department of Chemistry was then accommodated in a building, since removed, which stood on the southern part of the east side of the Old Botanic Garden site and afterwards served as part of the Pathological Laboratory

Several of the colleges had their own chemical laboratories and these were run in competition with the University laboratory This competition continued for many years after the erection in 1887 of the new University Chemical Laboratory facing Pembroke Street, though in an ever-lessening degree as the college laboratories one by one were given up The greater part of the teaching in the University Laboratory was carried on by Sell and Fenton, and in spite of their different temperaments the two men worked together in harmony until their association was terminated by the death of Sell in 1915

Fenton's lectures were for many years an outstanding feature in the instruction given in the University Laboratory He took immense pains in their preparation and although in lecturing he affected an air of indifference and a somewhat indolent manner, actually he delivered them with very great care, and he was extraordinarily successful in stimulating the interest of the abler men He scrupulously avoided dogmatism He endeavoured, so far as possible, to present each subject as a debatable question on which there were diverse views to be discussed, to balance the evidence for and against every inference and to induce his hearers to use their own judgment and draw their own conclusions The value of his lectures was greatly enhanced by the informal discussions which he encouraged , at the close of every lecture a number of eager young men would come down to the lecture table and engage with him in a discussion, often prolonged, of the subjects in which he had aroused their interest Those who brought their difficulties to him found him unexpectedly sympathetic, and he would deal exceedingly gently with one who asked a thoughtless or an ill-considered question

The course of experimental work in general and physical chemistry which he devised to illustrate his lectures was very carefully thought out, and during the eighties, and even later, the type of laboratory work being done by his class was probably unique Although his chief interest always seemed to lie in general and physical chemistry, the greater part of his original work was carried out in organic chemistry His earlier work consisted of a series of investigations on the action of hypochlorites on urea and related compounds A pupil of his (Mr Street), wishing to estimate urea, happened to use, instead of sodium hypobromite, a strongly alkaline solution of sodium hypochlorite and found that only half the expected quantity of nitrogen was evolved Fenton followed up this observation and discovered that the missing half of the nitrogen was present in the solution as sodium cyanate He gave an explanation of the phenomenon a few years later At the same meeting of the Chemical Society (June 20, 1895) at which Walker and Hambly communicated their well-known experiments on the transformation of ammonium cyanate into urea Fenton read a paper giving an account of experiments he had been making on the same subject, using the action of sodium hypobromite to measure the rate of change Finding that the transformation of the ammonium cyanate was never complete, he inferred that ammonium cyanate and urea were in tautomeric equilibrium and concluded that, whilst the more reactive hypobromite attacked both the urea and the ammonium cyanate (liberating all the nitrogen from the former and that present as ammonium from the latter), the hypochlorite attacked the ammonium cyanate only and thereby disturbed the equilibrium of the system so that the whole of the urea was finally converted into nitrogen and sodium cyanate In other papers he showed that hypochlorites and hypobromites liberated different amounts of nitrogen from several nitrogenous compounds and in this manner he proved that ammonium carbonate in presence of water was in equilibrium with a small proportion of ammonium carbonate

$$NH_4' + CO_3'' \rightleftharpoons NH_2\,CO_2' + H_2O$$

What is probably to be regarded as his most important work is that connected with the discovery and investigation of dihydroxymaleic acid It extended over many years, for the initial observation from which it grew was made during his first year as an undergraduate at Cambridge The story current in the laboratory in later years was that a fellow student, amusing himself by mixing reagents at random, chanced to obtain a violet coloration which he showed to Fenton Fenton was keenly interested in the observation, and he found out the essential reagents which were concerned in the production of the colour, namely, tartaric acid, a ferrous salt, hydrogen peroxide and excess of caustic alkali He reported the discovery in a letter to the 'Chemical News,' entitled "On a New Reaction of Tartaric Acid,' and dated Christ's College, Cambridge, April 25, 1876 He was at first disposed to regard the colour as being due to the production of a ferrate, but in a few years later (in 1881) he published a second letter in the 'Chemical News' in which he showed that the colour arose from an iron derivative of an oxidation product of tartaric acid since the colourless solution obtained after removal of the iron gave the colour again on the addition of a ferrous or ferric salt

After several years he took up the problem again, and in 1894 he discovered how the new oxidation product could be isolated—it could be salted out from the reaction mixture by the addition of fuming sulphuric acid – and in a series of papers extending over the years 1894 to 1902 he described its reactions and relationships It had the formula $C_4H_4O_6$ its formation from tartaric acid thus involved only the loss of two atomic proportions of hydrogen It was a dibasic dihydroxy-acid , it showed no ketonic reactions, it could be reduced to racemic acid and oxidised to dihydroxytartaric acid It was therefore either dihydroxyfumaric acid or dihydroxymaleic acid It readily gave a diacetyl cyclic anhydride with acetyl chloride and was transformed into an isomeric acid by hydrobromic acid Fenton therefore regarded it as dihydroxymaleic acid —

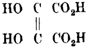

$$\begin{array}{c}HO\ \ C\ \ CO_2H\\ \|\\ HO\ \ C\ \ CO_2H\end{array}$$

Its production from *d*-tartaric acid thus involves the *trans* elimination of the two hydrogen atoms lost, and its reduction to racemic acid the *trans*-addition of hydrogen

The most interesting reaction of the new acid was perhaps that brought about by heating with water. Two molecules of carbon dioxide were eliminated and glycollic aldehyde was formed:—

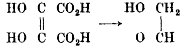

$$\begin{array}{l} HO\,C\,CO_2H \\ \quad\;\;\| \\ HO\,C\,CO_2H \end{array} \longrightarrow \begin{array}{l} HO\,CH_2 \\ \quad\;\;| \\ O\,CH \end{array}$$

On re-examining this reaction with H. Jackson the resulting glycollic aldehyde was obtained in a bimolecular crystalline form. It had a sweet taste (it could be regarded as the simplest sugar) and Fenton showed subsequently that it could be degraded by Wohl's method to formaldehyde. With Ryffel he showed that dihydroxymaleic acid could be oxidised to mesoxalic semialdehyde, a compound of considerable interest on account of its close relationship to the hypothetical trihydroxyacrylic acid of which uric acid is the diureide.

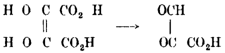

$$\begin{array}{l} H\,O\,C\,CO_2\,H \\ \qquad\;\| \\ H\,O\,C\,CO_2H \end{array} \longrightarrow \begin{array}{l} OCH \\ \;\;| \\ OC\,CO_2H \end{array}$$

Nevertheless attempts to synthesise uric acid by condensing this compound with urea yielded only glycouril and carbon dioxide.

Further investigations showed that the new reagent—hydrogen peroxide in conjunction with ferrous salts—which acted on tartaric acid in so characteristic a manner, constituted a specific and valuable oxidant for certain classes of compounds. With H. Jackson, Fenton showed that di- or polyhydroxy-alcohols with vicinal hydroxy groups were smoothly and rapidly oxidised to hydroxy aldehydes, thus, glycol gave glycollic aldehyde, glycerol glyceric aldehyde, erythritol erythrose and mannitol mannose. Monohydric alcohols, however, were not attacked. With H. O. Jones he examined the effect on the new reagent on acids: α-hydroxy-acids were oxidised rapidly and with evident heat-evolution to the corresponding keto-acids, acids of other classes were unaffected. Thus glycollic acid was shown to be oxidised to glyoxylic acid, lactic acid to pyruvic acid, tartronic acid to mesoxalic acid and glyceric acid to hydroxypyruvic acid, whilst from malic acid there was formed the previously unknown free oxalacetic acid. Fenton and Jones examined the reactions of this acid in some detail and among other observations found that its phenylhydrazone heated with water decomposed in two ways, either losing carbon dioxide to give pyruvic acid phenylhydrazone, or undergoing dehydration to a pyrazolone derivative. The relative proportion of these products depended on the hydrogen ion concentration of the solution, and on this fact an approximate method of comparing the strengths of acids could be based.

The observation that dihydroxymaleic acid was converted with its diethyl ester by the action of an ethereal solution of hydrogen bromide led him to examine the action of this mixture on compounds of other classes. With

Miss M M Gostling he found that various carbohydrates, in particular fructose, gave a purple colour when dissolved in ether and treated with hydrogen bromide, and this proved to be due to an oxonium salt of a yellow crystalline compound which could be thus obtained in considerable quantity and was shown to be ω-bromomethylfurfuraldehyde

Among other observations of interest which he made may be mentioned the reduction of carbonic acid by magnesium to formaldehyde and the formation of a crystalline explosive compound of formaldehyde and hydrogen peroxide of the composition $C_2H_6O_4$ and the probable constitution $HO\ CH_2\ O\ O\ CH_2\ OH$

His papers are characterised by the conciseness with which they were written and by their lucidity, as well as by their scientific restraint and freedom from speculation He was gifted with keen powers of observation and acuteness of interpretation and the whole of his experimental work is marked by its elegance

Of his books, those best known are his " Notes on Qualitative Analysis," which was based originally on a small book published by Liveing, but was greatly expanded in successive editions, and his " Outlines of Chemistry " He was elected into the Royal Society in 1899, and served on the Council from 1913 until 1916 He was made an honorary fellow of his College in 1911

He was naturally a shy man and was exceedingly sensitive to chaff or criticism , he endeavoured to conceal his shyness by assuming a certain *hauteur* which tended to repel some of those who would have sought his friendship He had a very strong sense of fairness, but his pertinacity in defending views in which he was in a minority of one sometimes made him a difficult member of University bodies He married in 1892, Edith, daughter of George Ferguson, of Richmond He left no children He gave up his lectureship in 1924 and went to live at Hove, but the last years of his life were greatly clouded by illness He died in a nursing home in London on January 13, 1929, at the age of seventy-four

W H M

SIR HENRY BRADWARDINE JACKSON—1855-1929

Henry Bradwardine Jackson was born at Barnsley in 1855 and when 11 years of age he entered the Navy He served on the African station during 1878 and 1879 and took part in the Zulu War On returning to England he was appointed to the " Vernon," where he qualified as a torpedo lieutenant , subsequently he studied torpedo design and construction at the Whitehead establishment at Fiume

In 1891 the idea first came to Jackson of employing Hertzian waves as a means of communication between a torpedo boat and a friendly ship He was at this time serving at sea and it was not possible to put his ideas into a practical form until four years later In 1895, while commanding the " Defiance," he became aware of the experimental work of Dr (now Sir Jagadis) Bose on coherers From the end of 1895 until July, 1896, he carried out a careful series of experiments in the " Defiance " with the object of obtaining a reliable coherer The form finally adopted consisted of a tube of metal filings between two metal plugs He carried out further experiments with various substances during the next 12 months This early coherer was tapped by hand For observing the radiations, a receiving circuit in the form of a circle of wire was employed for a considerable time In August, 1896, an electric bell of high resistance inserted in the circuit was successfully rung from a distance Naturally the idea of tapping the coherer by the bell was the next development, and before the end of the month Morse signals on the electric bell were received across the after-cabin of the ship The ship's induction coil which, under favourable circumstances would occasionally give a spark of 2 inches, was used as the transmitter He continued these experiments with increasing success and managed by the end of the year to effect communication by electromagnetic radiation over distances of several hundreds of yards In 1896 he met Marconi at a conference at the War Office The two pioneers of radio telegraphy exchanged information regarding their apparatus and found that they had been experimenting on practically the same lines and had apparently obtained the same results The next year they kept in close touch and gave each other much useful assistance In 1897 Jackson was appointed Naval Attaché in Paris

In 1899 he was appointed to command the " Vulcan " and in 1900 wireless telegraphy apparatus was installed in a number of His Majesty's ships, a contract being placed with the Marconi Company for the supply of installations The new means of communication proved to be successful From this time to his promotion to flag rank in 1908, Sir Henry Jackson played the foremost part in the development of radio telegraphy in the Navy Both he and

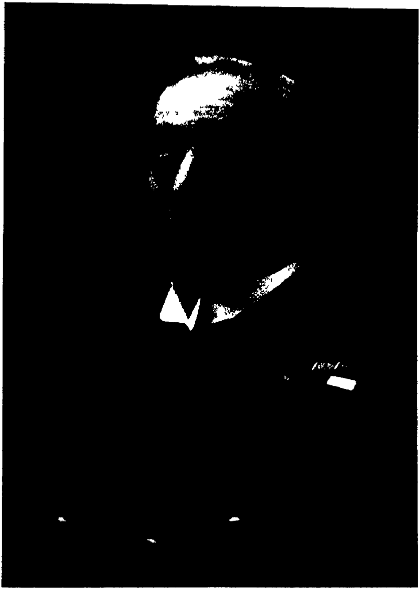

H. B. Jackson

Marconi found that increased ranges were possible by earthing one end of the oscillator and attaching to the other an elevated aerial wire Apparatus of this simple character, however, gave considerable trouble at sea owing to the fact that it was necessary to use an aerial which was highly insulated

Jackson was elected a Fellow of the Royal Society in 1901, and the next year communicated a paper entitled 'On some Phenomena affecting the Transmission of Electric Waves over the Surface of Sea and Earth' The subjects dealt with in it include a study of the effect of intervening land in reducing the practical signalling distance between two ships, observations on the effect of the height, thickness, contour and nature of the land being recorded as well as interesting observations on the effects of atmospherics The paper is a good illustration of the careful and methodical manner in which Sir Henry Jackson always made and recorded his observations In modern radio research in particular in wave propagation, considerable attention is given to the results of mutual interference of several waves arriving at a point with various phase differences Observations of such interference effects were made by Jackson in 1900 'This phenomenon," he writes "manifests itself by the gradual weakening and occasionally by the total cessation of signals, as the distance of two ships increases, up to a certain point, and their reappearance as the distance is further increased" At that time he believed this effect was due to want of synchronism in the oscillatory discharge between the spark balls of his transmitter, so that there was a change in frequency between the successive discharges of the transmitter Such want of synchronism would produce successive oscillations out of phase with each other which would at one point annul each other, while at a further distance they would reinforce each other The cause, however, of the weakening of signals he put down not so much to the interference of oscillations arriving out of phase as to the fact that the coherer required the building-up effect produced by several successive oscillations arriving in phase in order to actuate it satisfactorily

To get over the difficulties introduced by this effect and the high aerial insulation required, Sir Henry Jackson then proceeded to experiment with improved methods of tuning the apparatus and with coupled circuits Independently of Marconi he produced about this time an installation in which energy was introduced into the aerial by electro-magnetic coupling through a transformer, the primary of which was attached to the spark balls of the induction coil and was tuned by means of a condenser His system differed from those employed by other workers in that, in addition to the electromagnetic coupling through the transformer, electrostatic coupling was also employed by adding an extra plate connected to the aerial and to the condenser in the oscillating circuit Tuned receivers were also developed In order to obtain accurate tuning, careful experiments were made of the capacity of the condensers and aerial and of the self-induction of the coils of the coupling transformer for various numbers of turns in the secondary It is interesting to note that the self-capacity of the coils of the transformer was taken into account and also the capacity of the leads connecting the condenser The effective range of ships fitted with this type of apparatus was found to be about 55 miles

Although the final adoption and development of wireless telegraphy in the Fleet took some years nevertheless it achieved full recognition more rapidly than many other inventions of similar importance The comparatively rapid adoption of the invention is a tribute to Sir Henry Jackson's enthusiasm and to the scientific character of his work Jackson used to say that all new inventions seemed to go through the same sort of stages in His Majesty s service Firstly, " the sceptical," in which people would have nothing to do with the new thing, secondly, the " nibbling "—that is, ' there seems to be something in it, let us try it " , thirdly, the preliminary, in which trials are made and strong recommendations for adoption are put forward by enthusiasts fourthly, the adoption, in which as many sets are obtained as possible, although there may be no one to work them , fifthly, the practical, in which the defects are discovered , sixthly, the " low-water stage," in which it is said that the invention can never be any good and committees begin to sit , seventhly, the perfect development when the defects are made good and its uses demonstrated

In 1905 Lord Fisher appointed him Third Sea Lord and Controller At that time the design and equipment of warships were undergoing rapid changes, and Jackson was specially qualified to take charge of the application of science to naval equipment He was appointed First Sea Lord on May 23 1915, after Lord Fisher left the Admiralty During his period of office—from May, 1915, until December, 1916—the foundations were laid for various schemes for fighting the submarine menace, including the raid on Zeebrugge The Battle of Jutland was fought while Jackson was First Sea Lord, and he has stated that the evidence which finally convinced him that the German High Sea Fleet was coming out for action was the result of observations made by a radio direction-finding station, a change of 5° being shown in the angular position of a German warship

Jackson was appointed Admiral of the Fleet in 1916, and from April, 1917 to July, 1918, he had the honour of serving as First and Principal Aide-de-camp to the King In July, 1924, he retired from the Navy

In 1920 the Lord President of the Council appointed him as the first Chairman of the Radio Research Board of the Department of Scientific and Industrial Research The task of taking up once more experimental work in radio telegraphy was most welcome to him Under his guidance more than 100 important papers were published under the auspices of the Board, the main subjects dealt with being the propagation of waves, the nature and origin of atmospherics, radio direction-finding and radio frequency measurements He gave his personal attention to the work described, spending much time in visits to the laboratories and discussing aspects of the work with the staff, yet he always disclaimed credit for any of the results obtained While supervising the work of the Radio Research Board, Sir Henry Jackson himself carried out much experimenting in his own house With apparatus of his own design and manufacture he carried out work of a pioneer character on the reception of short waves Some of the results obtained were referred to by him in a contribution to a discussion at the Royal Society on the electrical state of the upper atmosphere

In 1926 the Royal Society awarded him the Hughes medal in recognition of the high merit of his work This honour gave him great gratification

Jackson was Secretary and later Chairman of the British National Committee on Radio Telegraphy, formed in connection with the International Union for Scientific Radio Telegraphy and he regularly attended the meetings of the general assemblies of the Union It is no exaggeration to say that British prestige in the scientific aspects of radio telegraphy owes much to his guidance

In 1890 he married Alice, daughter of Mr S H Burbury, F R S Many early experiments were carried out by Jackson and the Burburys, the latter also being enthusiastic experimenters in radio telegraphy

Sir Henry Jackson was a Knight Commander of the Royal Victorian Order, a Knight Grand Cross of the Bath honorary D Sc of the Universities of Oxford and Leeds, honorary LL D of the University of Cambridge, and Vice-President of the Seamen's Hospital Society He was a member of the Institution of Electrical Engineers, and honorary Vice-President of the Institution of Naval Architects

F E S

PERCY ALEXANDER MACMAHON 1854–1929

PERCY ALEXANDER MACMAHON was born at Malta, September 26, 1854, the second son of Brigadier-General P W MacMahon In view of his speculations on space filling solids, it is, perhaps, worth recording that he remembered at the age of 70 his boyish observations of the manner in which the ordnance was piled After being at school at Cheltenham, he was entered as a gentleman cadet at Woolwich in February, 1871 He became lieutenant in 1872, Captain in 1881 and Major in 1889 After some five years' service in India and Malta, he became Instructor in Mathematics at the Royal Military Academy, in 1882, until 1888, and Assistant Inspector at the Arsenal until 1891 He was then Instructor and, later, Professor of Physics at the Artillery College, retiring with retired pay in 1898 From 1904, for 16 years, he was Deputy Warden of the Standards of the Board of Trade involving in due course membership of the *Conférence Générale* and the *Comite International des Poids et Mesures*, and from 1902, for 12 years, was one of the General Secretaries of the British Association, of which he became a Trustee in 1914 He had been made Fellow of the Royal Society in 1890, and served as President of the London Mathematical Society in 1894-96, becoming also, in 1917 President of the Royal Astronomical Society He was also a member of the Permanent Eclipse Committee, and of the Council of the Royal Society of Arts In 1901 he was President of the Section A at the meeting of the British Association in Glasgow He received many academic honours D Sc at Dublin in 1897, Sc D at Cambridge in 1904, LL D at Aberdeen and S Andrews in 1911, was an honorary member of the Royal Irish Academy and of the Cambridge Philosophical Society The Royal Society conferred on him a Royal Medal in 1900, and a Sylvester Medal in 1919, the London Mathematical Society awarded him the De Morgan Medal in 1923 He was also, by the nomination of the Royal Society, a Governor of Winchester College

In the late years of the last century he will be remembered by some for the promptitude and distinction with which he would make an *impromptu* communication at the meetings of the London Mathematical Society, when other sources failed, later, after his marriage, for his hospitality at his home in Westminster During his life in London he was also a distinguished billiard player at the Athenæum Club In 1922 he gave up the majority of his London associations, became a resident member of St John's College, Cambridge, and mixed very willingly in social gatherings, until ill-health compelled his retirement to Bognor, where he died on Christmas Day, 1929 He had been a member of St John's College from November, 1904 His absorption in the mathematical problems he was considering, which was noticeable in his

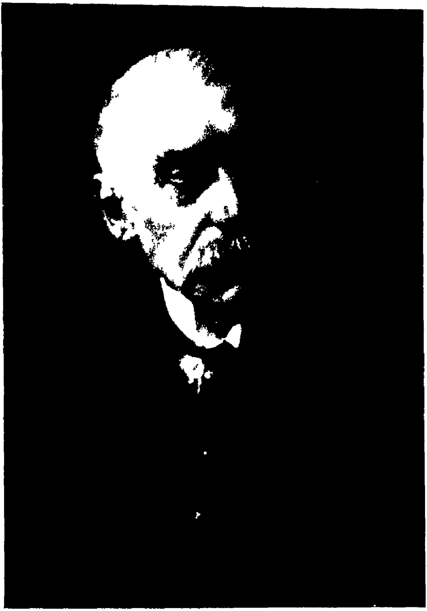

Percy A MacMahon

Woolwich days, became more pronounced in later life, but another trait, also noticed at Woolwich, was manifest to the end, namely, his formal kindly courtesy towards all with whom he had dealings, and he had always a desire to know the names of the more distinguished younger mathematicians, and to get some idea of the work they were doing Many of his friends will always remember his personal cordiality, in which he was so ably assisted by his wife

His mathematical achievements were in an abstract field, and it seems difficult to describe them in detail without being over-technical The plan followed here is to give an account of some of his more salient results, and otherwise to refer to the Bibliography appended Save for his first paper (in 1883), on what was then called the modern geometry of the triangle, his early work was inspired by the problems, connected with the Invariants of Algebraic Forms, with which Cayley and Salmon and Sylvester and Hammond were concerned He followed that by developments of the work of Sylvester and Cayley for the Theory of Partition of Numbers, with incidental reference to some problems of probability, and in the last years of his life his activity was largely taken up by consideration of repeating patterns, of which he constructed and coloured with his own hand, a vast number, together with proposals for generalising the theory of determinants Throughout he was, after Sylvester's pattern, always more anxious to invent than to know, and it seems right to avow that his knowledge of modern mathematics was not wide, especially of the modern logical theory of functions He stands indeed between that great efflorescence of the British realistic school of explicit algebraic form, associated with the names we have mentioned, and the more recent students of quantitative logic, or geometrical construction

It is easy to understand how Cayley, having seen the first explicit invariant forms, for instance, $a_0a_4 - 4a_1a_3 + 3a_2^2$, desired to see the actual expressions of other invariants, and how great this desire was with his successors is well shown by Salmon's reprint, extending to 13 pages, of the invariant of degree 15 of a binary sextic, which vanishes when the roots are in involution ("Higher Algebra," 1866) And it is easy to understand the fascination, when the number and length of known invariants began to make the concrete management difficult, of being able to specify the number of existing invariants of given character by means of the terms of an expansion in powers of a variable For the lower cases, too, such *generating functions* could be devised whose form indicated even the polynomial identities, or *syzygies*, connecting the invariants For the case of covariants it was found, originally through an early use by Sylvester of what Sophus Lie called an infinitesimal transformation, that if the coefficient of the highest power of the variable, x, in the covariant, were known, the other coefficients, functions of the coefficients in the fundamental algebraic form, could be calculated by use of a linear differential operator

Hence arose the importance of tabulating the possible forms of such highest covariant coefficients, or *seminvariants,* and of determining the syzygies connecting them And zest was added to the study by Cayley's frank discussion of his own results (' Amer Jour ,' vol 7, 1885) , while the kind of earnestness put into this enumerative work is well illustrated by Sylvester's papers of a few years previous (*e g* , "Coll Papers,' vol 3, p 283, 1879), Into the discussion of the problems thus arising MacMahon was encouraged to enter by two pieces of good fortune One of these was his remark of the identity of the linear partial differential equation of the first order, satisfied by seminvariants, with that satisfied by general symmetric functions (of a certain limited kind, known as *non unitary*), if only the form of the coefficients in the fundamental algebraic form be slightly modified The other was the publcation, by Hammond, of a symbolical calculus of differential operators acting upon symmetric functions, whereby a connection is made between the functions $\Sigma(\alpha^p\beta^q\gamma^r\quad)$, and $\Sigma(\alpha^q\beta^r\quad)$ The two things are intimately related The former, the relation of symmetric functions and seminvariants, was immediately acclaimed by Cayley , the latter was afterwards often used by MacMahon, as may be seen in his two volumes on Combinatory Analysis, where the Hammond operators are used in seven of the eleven sections of the book For his actual contributions to the generating functions of seminvariants, the later paper of 1895 (' Proc L M S ,' vol 26), and the paper in ' Trans C P S ,' vol 19 (1904) may be consulted

But some brief explanation in regard to the two initial steps of his career referred to, may perhaps be given For the fundamental form, written as $x^n + na_1x^{n-1} + \frac{1}{2}n(n-1)a_2x^{n-2} +$, with binomial coefficients, the differential operation for seminvariants, expressing, when the result is zero, that these are functions of the differences of the roots, is $\delta_1 + 2a_1\delta_2 + 3a_2\delta_3 +$, where δ_r means partial differentiation in regard to a_r On the other hand, for a form $x^n + p_1x^{n-1} + p_2x^{n-2} +$, the operation $\varpi_1 + p_1\varpi_2 + p_2\varpi_3 +$, where ϖ_r means partial differentiation in regard to p_r, is equivalent, when acting upon a function of $p_1, p_2,$, regarded as expresssed in terms of the sums of powers of the roots, to (the negative of) differentiation in regard to the sum, s_1, of the first powers A function whose expression in terms of these power sums, $s_1, s_2, s_3,$, does not contain s_1 is thus reduced to zero by this operator , such a symmetric function of the roots is that called non-unitary Now, if we put $p_r = a_r/(r\,!)$ we have $p_s\varpi_{s+1} = (s+1)\,a_s\,\delta_{s+1}$, and the latter operator becomes the former This is MacMahon's remark, which renders the tabulation of non-unitary symmetric functions the same problem as the tabulation of seminvariants

Hammond's operator, denoted by D_m, is obtained by m repetitions of the operator $\varpi_1 + p_1\varpi_2 + p_2\varpi_3 +$, spoken of above, where, however, this repetition is formal, the succeeding operations being upon the differential coefficients , for instance, two repetitions lead to $\varpi_1^2 + 2p_1\varpi_1\varpi_2 + p_2^2\varpi_3^2 + \quad$, every term involving two differentiations Precisely, if d_1 denote the negative of the first order operator, $D_m = (m!)^{-1}(d_1^m)$ A simpler definition, not so useful, however, for MacMahon s applications, is that, if the symmetric function which is to be the operand is expressed by the power sums of the roots, and σ_r denote partial differentiation in regard to s_r, then the series $1 + hD_1 + h^2D_2 + \quad$, with arbitrary h, is the same as the expansion of the exponential operator exp (Σ), where Σ denotes $h\sigma_1 + h^2\sigma_2 + \quad$ The use most often made of the operator depends upon two facts (i) that if $\alpha_1, \alpha_2, \quad$ denote the roots of the fundamental form, the symmetric function of which the single representative term is

$$(\alpha^p{}_1\alpha^p{}_2 \quad \alpha^p{}_l)(\alpha^q{}_{l+1}\alpha^q{}_{l+2} \quad \alpha^q{}_{l+m})(\alpha^r{}_{l+m+1} \quad \alpha^r{}_{l+m+n})$$

is reduced to zero by any operator D_m other than D_p, or D_q, or $D_r \quad$, while, denoting this symmetric function by $(p^lq^mr^n \quad)$, it is reduced by D_p to the function $(p^{l-1}q^mr^n \quad)$, by D_q it is reduced to $(p^lq^{m-1}r^n \quad)$, and so on In this statement the order of the fundamental form is supposed indefinitely great (that is, so high that the expression in terms of the coefficients of all the symmetric functions under consideration would be the same if the order of the form were greater) For a product of symmetric functions, say k functions $\phi_1, \phi_2, \quad \phi_k$, we have the second characteristic property of the operator D_m, namely (ii), the result of the operation $D_m(\phi_1\phi_2 \quad \phi_k)$ is obtained by expressing m as a sum of positive integers $m_1 + m_2 + \quad + m_r$, and then, if $\phi_{s_1}, \phi_{s_2}, \quad, \phi_{s_r}$ be any selection of r of the functions $\phi_1 \ \phi_2 \quad, \phi_k$, taking the term $(D_{m_1}\phi_{s_1})(D_{m_2}\phi_{s_2}) \quad (D_{m_r}\phi_{s_r})(\psi)$, where the brackets denote multiplications, and ψ is the product of the functions $\phi_1, \quad, \phi_k$ other than $\phi_{s_1}, \phi_{s_2}, \quad, \phi_{s_r}$ The sum of all possible terms so obtainable is to be taken , in many cases their number is not large because of the vanishing of one of the factors $D_{m_i}\phi_{s_i}$

These details will enable us to give an explanation of the nature of one method by which MacMahon proposed to compute the explicit form of all Latin squares of a specified number of rows A Latin square, of which the name is merely a survival of Euler's name for a more difficult square in which every element was characterised by two letters, one Latin and one Greek, may be explained as being a square arrangement, of say ν rows, in which ν letters are written down, ν times, in different rows, with such permutations that each letter occurs once not only in each row, but also once in each column Now consider a compound operator $D_{\mu_1}D_{\mu_2} \quad D_{\mu_k}$, acting upon a product of symmetric functions $\phi_1, \phi_2, \quad, \phi_s$ There will be several terms in the result Each such term is to be represented by a rectangular diagram of k rows and s columns In the first instance, let $\rho_1, \sigma_1, \quad, \tau_1$ be positive integers, s in number, some of which may be zero, whose sum is μ_1 Then one term of $D_{\mu_1}(\phi_1\phi_2, \quad \phi_s)$

is the product $(D_{\rho_1}\phi_1)\ (D_{\sigma_1}\phi_2)\quad (D_{\tau_1}\phi_s)$ Correspondingly we place in the first row of a rectangular scheme the numbers $\rho_1, \sigma_1, \quad, \tau_1$ Denoting now the factors $D_{\rho_1}\phi_1, D_{\sigma_1}\phi_2, \quad, D_{\tau_1}\phi_s$ by $\psi_1, \psi_2, \quad, \psi_s$, we may proceed to operate similarly with D_{μ_2} upon the product $\psi_1\psi_2 \quad \psi_s$, the s numbers, including zeros, which form the chosen partition of μ_2 being placed in order in the second row of the rectangular scheme , and so on till we find components for the k-th row which are a partition of μ_k Now, in particular, suppose $s = k$, and $\mu_1 = \mu_2 = \quad = \mu_k, = \mu$, say, while all of $\phi_1, \quad, \phi_s$ are the same, each being the symmetric function $\Sigma(\alpha_1{}^p\alpha_2{}^q \quad \alpha_s{}^r)$, say ϕ, where $p, q, \quad, r$ are different and $p + q + \quad + r = \mu$ Then, as ϕ is reduced to zero by any operator D_m other than D_p, or $D_q, \quad$ or D_r, or unity, the only possible partitions of μ_1, to fill the first row of a diagram, must consist of numbers chosen from $p, q, \quad, r$ and zero Suppose now that the only set of numbers, s in number, every one of which is one of $p, q, \quad, r$, or zero, whose sum is μ, consists of these numbers $p, q, \quad, r$, each occurring once , of this a numerical example is given immediately Then the first row of the diagram must consist of the number $p, q, \quad, r$ in some order The second row of the diagram, obtained by distributing the operator D_{μ_2}, must similarly consist of these same numbers $p, q, \quad, r$, but, as $D_p(\alpha_1{}^p\alpha_2{}^q \quad \alpha_s{}^r)$ is $\Sigma(\alpha_2{}^q \quad \alpha_s{}^r)$, in which the exponent p does not enter, it follows that, in the second row, the number p cannot occur in the same column as in the first row , and similarly with $q \quad r$ Thus, after operating with $D_\mu{}^s$, the diagram will consist of s rows and columns in which each row contains the numbers $p, q, \quad, r$, and each column likewise contains these numbers Such a diagram is a Latin square Further, the operation of $D_\mu{}^s$ upon $(\Sigma\alpha_1{}^p\alpha_2{}^q \quad \alpha_s{}^r)^s$ results in a number, the dimension of the operand being equal to the total order of the operator This number then gives the total number of Latin squares of s rows and columns This number is evidently independent of the choice of the numbers $p, q, \quad, r$, subject to the condition of the unique partition which has been explained To explain this condition we may take the particular case when μ is 30, and $p, q, \quad, r$ consist of the four numbers 19, 8, 2, 1 The only partition of 30 into a sum of four or fewer numbers chosen from these four, consists of these numbers each taken once , if, however, $p, q, \quad, r$ consist of 11, 8, 7, 4 we can express 30 not only as $11 + 8 + 7 + 4$, but also as $8 + 8 + 7 + 7$ or as $11 + 11 + 8$ In general, if $\mu = 2^s - 1$, we may always take $p, q, \quad, r$ to be the numbers $2^{s-1}, 2^{s-2}, \quad, 2, 1$ (This is, moreover, what MacMahon called a Perfect Partition of μ, every number less than μ being also uniquely expressible by a partition from these numbers)

A more technical application of Hammond's operator is to give a proof of a theorem of symmetry in tables of symmetric functions, which may be expressed by

$$D_{p_1}D_{p_2} \quad D_{p_t}k_{q_1}k_{q_2} \quad k_{q_t} = D_{q_1}D_{q_2} \ . \ D_{q_t}k_{p_1}k_{p_2} \quad k_{p_t},$$

wherein the sum of the positive integers $p_1, \ldots, p_s$ is equal to the sum of the positive integers $q_1, \ldots, q_t$, and k_r means the sum of the homogeneous products of dimension r of the roots of the fundamental algebraic form, mutilated, however, by the omission of every term which contains a power greater than k of any one root. The case $k = 1$ was well known, for this case the functions $k_1, k_2, \ldots$ are the coefficients, say $a_1, a_2, \ldots$, in the fundamental form, written as $x^n - a_1x^{n-1} + a_2x^{n-2} \ldots$. In the case in which there is no restriction of order ($k = \infty$), it is usual to use the notation h_r for the sum of the homogeneous products of r dimensions. If we then consider the form $x^n - h_1x^{n-1} + h_2x^{n-2} + \ldots$, it is noticeable that the power sums for the roots of the latter, s_r', are connected with those for the former by $s_r' = (-1)^{r-1}s_r$, and we recall that the operator D_m is expressible, with constant coefficients, by differentiations in regard to the power sums.

Another theorem of MacMahon's, which he called a Master Theorem, was designed to display the permutations of an aggregate of things, not all different, which should be subject to certain restrictions, in particular should exclude certain specified permutations. For instance, consider the familiar problem of the number of ways in which n written letters can be put into n addressed envelopes so that no letter is inserted in the envelope designed for it. The possible ways are evidently displayed by the various terms in $x_1x_2 \ldots x_n$ which occur in the developed product

$$(\quad + x_2 + x_3 + \ldots + x_n)(x_1 + \quad + x_3 + x_4 + \ldots + x_n) \ldots$$
$$(x_1 + x_2 + \ldots + x_{n-1} + \quad),$$

in which x_s does not occur in the sth factor. More generally we may seek a rule for computing the coefficient of $x_1^{p_1}x_2^{p_2} \ldots x_n^{p_n}$ in the development of the product $y_1^{p_1}y_2^{p_2} \ldots y_n^{p_n}$, where y_s is any general linear homogeneous function of $x_1, x_2, \ldots, x_n$, say $y_s = a_{s1}x_1 + \ldots + a_{sn}x_n$. The procedure suggested by MacMahon is equivalent to seeking, in the expansion in ascending powers of $t_1, t_2, \ldots, t_n$, of the inverse product

$$\left(1 - t_1\frac{y_1}{x_1}\right)^{-1}\left(1 - t_2\frac{y_2}{x_2}\right)^{-1} \ldots \left(1 - t_n\frac{y_n}{x_n}\right)^{-1},$$

the terms which are independent of $x_1, x_2, \ldots, x_n$, and then selecting from these terms the term in $t_1^{p_1}t_2^{p_2} \ldots t_n^{p_n}$. His theorem is that these terms, independent of $x_1, x_2, \ldots, x_n$, are obtainable by expanding, in ascending powers of $t_1, \ldots, t_n$, the inverse of the determinant

$$\begin{vmatrix} 1 - t_1a_{11}, & -t_1a_{12}, & \ldots, & -t_1a_{1n} \\ -t_2a_{21}, & 1 - t_2a_{22}, & \ldots, & -t_2a_{2n} \\ \cdot & \cdot & \cdot, & \cdot \\ -t_na_{n1}, & -t_na_{n2}, & \ldots, & 1 - t_na_{nn} \end{vmatrix}$$

This determinant, when developed before its inverse is expanded in powers of $t_1, \ldots, t_n$, consists of terms such as $(-1)^s t_1 t_2 \ldots t_s \Delta_s$, where Δ_s is a coaxial minor, of s rows and columns, from the determinant $|a_{rs}|$. MacMahon considered also the converse problem, of finding values for the elements a_{rs} such that the coaxial minors of the determinant $|a_{rs}|$ should have given values; he reached the conclusion that when n is even, the determinant can be expressed in two ways as a function of its coaxial minors (other than itself), a result in regard to which more detail seems desirable.

We may also refer to another curious theorem given by MacMahon which seems very illustrative of his work. Suppose that we have an aggregate $y_1^{p_1} y_2^{p_2} \ldots y_n^{p}$ of μ, that is $p_1 + p_2 + \ldots + p_n$, numbers, which for clearness of explanation we suppose to be positive and in ascending order of magnitude, so that $y_1 < y_2 < \ldots < y_n$. Take then, on squared paper, n horizontal rows of nodes and on these μ vertical columns of nodes for which the abscissa is respectively $x = 1$, $x = 2$, $\ldots$, $x = \mu$. We represent a permutation of the μ numbers by marking p_1 nodes upon the lowest row chosen anywhere in the μ nodes of this row; then marking p_2 nodes upon the second row of nodes $(y = y_2)$, also chosen anywhere but so that no one is upon the same ordinate as any of the marked nodes of the first row; then marking p_3 nodes in the third row $(y = y_3)$, but so as to avoid all the $p_1 + p_2$ ordinates already occupied in the first two rows; and so on. The permutation represented is then obtained by reading the μ columms in turn, with ascending abscissa, each containing one marked node and furnishing one letter, y_s, of the permutation, when the marked node in that column is in the s-th row from below. Taking now any such ordinate containing, say, y_s, consider the ordinates which have greater abscissæ. It may be that for each of these the marked nodes have the same ordinate y_s, or a greater one, containing nodes y_t for everyone of which $t \geqq s$. But it may be that among the ordinates of greater abscissa than y_s there are σ for which the marked nodes have less ordinate than y_s, these corresponding to σ elements y_t for which $t < s$. We then speak of these as furnishing σ *inversions* in the permutation. If now, for the particular permutation under consideration, the inversions be noted for every y_s, and all the numbers σ so found be added together, we may call the result the *inversion index* for this permutation. All this, in less graphical mode, is familiar. But we may, after MacMahon, obtain another index for the permutation, namely, proceeding as before from any ordinate, with marked node y_s, pass to the immediately following ordinate, and note whether the marked node in this ordinate has a less ordinate than y_s, namely, represents y_t with $t < s$. If so, we may say there is a *fall*. If then y_s is in the μ_s-th ordinate, counting from (and including) the ordinate of least abscissa (the first ordinate), we count the fall as having weight μ_s. Examine now all the first $\mu - 1$ ordinates (all except the last, that is), and take the sum of the weights of all the existing falls, and call this sum the *fall index* of the particular permutation. Then, if all the possible permutations be taken the set of inversion indices any one of which may occur with the same value in several of the permutations is the same save for order of occurrence, as the set of fall indices. And there is more than this. Let the product $(1-x)(1-x^2)\ldots(1-x^p)$ be denoted by (p), consider the expansion in ascending powers of x of the fraction

$$\frac{(p_1+p_2+\ldots+p_n)}{(p_1)(p_2)\ldots(p_n)}$$

which is in fact a polynomial of terms such as rx^{ρ}, where r is a positive integer. This term indicates that there are exactly r of the permutations for which the inversion index is ρ, as well as exactly r of the permutations for which the fall index is ρ. This seems a remarkable result, and it is evidently capable of treatment on the lines of Kronecker's characteristic. We may also consider instead of the falls, the *rises* in the ordinates similarly defined, and it is not difficult to see that if we reverse the order of the rows in the diagram, the falls change into rises, and the inversion indices severally change into complementary values. What we have called a fall, MacMahon calls a *major contact*.

Another part of MacMahon's work is that dealing with the treatment of partitions by the method of Diophantine inequalities. For this we must refer to the second volume of his book on Combinatory Analysis (Cambridge, 1916).

An activity of a different kind which occupied him for several of the later years of his life, the construction of repeating patterns to fill a plane, has already been spoken of. For this we can refer to his little volume, 'New Mathematical Pastimes' (Cambridge, 1921), which, however, gives a most inadequate idea of the vast enthusiasm and industry with which he pursued the matter. It must be added, however, that it seems curious that he did not in connection therewith, make himself acquainted with the theory of discontinuous groups represented in the plane of the complex variable, or with the mathematical theory of crystallography.

But to those who knew him and watched the constant keenness of his interest in what he was doing, and his never failing courtesy and frankness of demeanour the memory will remain of a personality striking and distinctive, whose loss is to be deplored.

BIBLIOGRAPHY

The following list, not complete as regards the smaller earlier papers, will enable the reader who wishes to follow out the development of the work* —

---

* 'Mess' = 'Messenger of Mathematics'. 'Q J' = 'Quarterly Journal of Mathematics', 'P L M S' = 'Proceedings of the London Mathematical Society'. 'Am J' = 'American Journal of Mathematics'. 'Phil Trans' = 'Philosophical Transactions of

the Royal Society (A), 'Trans C P S' = 'Transactions of the Cambridge Philosophical Society' The dates (of the volumes) are in some cases later than the actual dates of the papers

1883 "A generalisation of the nine point properties of a triangle," 'P L M S,' vol 14
1884 "On symmetric functions and certain inverse operators," 'P L M S' vol 15
1885 'The multiplication of symmetric functions," 'Mess,' vol 14
1886 "On perpetuant reciprocants," 'P L M S,' vol 17
1886 "Certain special partitions of numbers" 'Q J' vol 21
1884 "On the development of an algebraic function" 'Am J' vol 6
1884 'Seminvariants and symmetric functions" 'Am J' vol 6
1885 "On perpetuants," 'Am J' vol 7 pp 26, 259
1886 'Memoir on seminvariants," 'Am J' vol 8
1888 The expression of syzygies, etc," Am J,' vol 10
1887 "The law of symmetry in symmetric functions," 'Q J' vol 22
1887 "The theory of a multilinear operator," P L M S,' vol 18 (see also vol 19 1889 and 'Q J vol 24 (1890))
1887 "Symmetric functions and the theory of distributions" 'P L M S,' vol 19
1888–1890 "A new theory of symmetric functions,' Am J' vols 10 to 14
1889 "On play 'à outrance'" 'P L M S' vol 20
1890 'Symmetric functions of roots of systems'' 'Phil Trans' vol 181
1891 "The theory of perfect partitions" 'Mess' vol 20
1891 "Yoke chains and 'trees'," 'P L M S vol 22
1892 "Applications of a theory of permutations," 'P L M S' vol 23
1893 "A memoir on the compositions of numbers" 'Phil Trans' vol 184
1907 "A second memoir on the compositions of numbers," 'Phil Trans' vol 207
1893 "On the thirty cubes constructed with six coloured squares," 'P L M S, vol 24
1894 "A certain class of generating functions" 'Phil Trans,' vol 185
1895 "The perpetuant invariants of binary quantics,' P L M S' vol 26
1896 "Combinatory Analysis, A review (Presidential Address)," 'P L M S,' vol 28
1895 "Self conjugate permutations," 'Mess,' vol 24
1897–1912 "Six memoirs on the partitions of numbers," 'Phil Trans' vol 187 to 211
1898 "A new method in Combinatory Analysis Latin Squares," 'Trans C P S' vol 16
1899 'Partitions whose graphs possess symmetry," 'Trans C P S,' vol 17
1900 "Partition Analysis and any system of consecutive integers," 'Trans C P S' vol 18
1900 "Combinatorial Analysis The foundations of a new theory" 'Phil Trans' vol 194
1901 "Glasgow British Association Presidential Address'
1902 "The sums of the powers of binomial coefficients" 'Q J,' vol 33
1902 "Friday evening discourse on Magic Squares" 'Royal Inst,' vol 17 (Feb 1902) *See also* "Magic squares and problems on a chessboard" 'Nature,' vol 65
1904 "The Diophantine inequality $\lambda x > \mu y$," 'Trans C P S,' vol 19
1907 "Afternoon lectures on standards of weight and measure," 'Royal Instn, January 30 and February 7 1907

SEBASTIAN ZIANI DE FERRANTI

1912 ' The problem of derangement," 'Trans C P S ' vol 21
1913 " Permutations of any assemblage of objects Am J vol 35
1916 ' Two applications of general theorems ' P L M S ' vol 15 (Sec Series)
1915, 1916 " Combinatory Analysis Two Volumes (Cambridge Press)
1920 " An Introduction to Combinatory Analysis ' (' Cambridge Press)
1921 ' New mathematical pastimes ' (Cambridge Press)
1923 ' On compound denumeration ' Trans C P S ' vol 22
1930 Researches in the theory of determinants Trans C P S vol 23

H F B

SEBASTIAN ZIANI DE FERRANTI 1864 1930

SEBASTIAN ZIANI DE FERRANTI was born at Liverpool on April 9, 1864 of parentage comprising Italian and English elements He was educated at Hampstead School and at St Augustine's College Ramsgate, and attended University College London, for a brief period At about 17 years of age he entered the works of Siemens Bros at Woolwich, and there gained experience in miscellaneous electrical applications including the development of electric furnaces and the construction of submarine cables and electrical machines

In 1882 he filed his first patent which described a dynamo Many dynamos were being invented and built at this time but Ferranti's form gave a large output for its weight, partly because of the happy choice of proportions, partly because of the excellence of its mechanical design A 20 horse power alternator of this type was installed in 1882 for lighting Cannon Street railway station, and drew so much attention that in 1883, when the inventor was only 19 years of age, a company was formed to exploit this and other inventions now crowding his mind Among these early inventions was the mercury meter for measuring the current supplied by an electric supply company to its customers, a meter which depends on counting the revolutions produced in a pool of mercury through which the current flows radially within the influence of a vertical magnetic field This meter is still widely used

In 1885 Ferranti began to improve the construction and the modes of employing transformers in conjunction with his machines and in 1886 he became engineer to a company which had been promoted to erect generating plant under the Grosvenor Gallery in Bond Street for lighting the gallery and neighbouring buildings Here he installed two alternators of about a thousand horse power each and distributed current by overhead lines throughout a gradually extending area north of the Thames, which eventually reached from the City to Chelsea Now came the opportunity of employing his far-seeing constructive imagination he dreamt of supplying the whole of London with electricity from one giant generating station, distributing the current at 10,000 volts through underground cables But the scheme was throttled by the Electric Lighting Act of 1888, and, in effect, reduced to parochial dimensions Nevertheless, at Deptford, where sea borne coal and condensing water were available, a station of about 10,000 horse-power was erected and running by 1892 During the construction of this station and its distribution network innumerable problems concerning engines, air pumps, alternators, transformers, switchgear, measuring instruments and high voltage cables, were successfully solved It may be said that in this single job Ferranti worked out the main principles and methods which governed high voltage electrical engineering for several years in every country It is true that his slow speed engines and great flywheel alternators have now been superseded by the turbo-generator, but even in this supersession he himself added considerably by his work on the steam turbine, both mechanical and thermodynamical In steam turbine development he was largely responsible for the conception of expanding something less than the whole of the steam at each stage of expansion and using the rest for heating the boiler feed water instead of doing mechanical work, thereby increasing the overall efficiency In the gas turbine, moreover he was a daring pioneer and came nearer to success than perhaps any other worker In both forms of prime mover he demonstrated that because of inherent defects in actual engines it is advisable to make certain departures from the Carnot cycle, and besides he made many ingenious improvements in purely mechanical details

It will be appreciated from the preceding paragraphs that Ferranti's genius was principally exhibited in the solution of problems arising in the supply and utilisation of electricity on the large scale But his wonderful facility in the mechanical domain had many applications in other directions, for his patents deal with such miscellaneous matters as machines for the high speed winding of coils for radio apparatus, motor car wheels and tyres, carburetters, steam valves, bicycle parts, projectiles, furnaces and, not least, a long series of improvements in cotton-spinning machinery His name is therefore permanently attached to a great many appliances and improvements in engineering, and it is worth remarking as evidence of one of the outstanding qualities of his character that he allowed his name to be attached only to those inventions which were genuinely his own in conception and development

The mere catalogue of his 176 inventions indicates Ferranti's mastery of mechanical technique and materials but conveys no adequate idea of his influence in his epoch It is therefore necessary to put explicitly on record that in his own view his life's mission was to spread the gospel of the use of electricity for every possible purpose. He was the earliest and most convincing advocate in England of the advantages to the community of turning heat into electrical energy at central stations and distributing it to the consumer for driving machinery and for heating and lighting homes, thus preparing the way for recent advances towards the all-electric age. More than twenty years before the Electricity Act of 1926 removed the legislative obstacles, he preached the importance of generating electricity on the large scale at a few sites and of interlinking these throughout the country. Fortunately, in addition to foresight and vision he had an engaging personality which induced commercial leaders to believe in and support him, and thus he was able to expedite the realisation of some of his dreams. In these ways it is now clear he exerted great influence on contemporary thought in electrical engineering all over the world.

Ferranti was a member of the Institutions of Civil, Mechanical and Electrical Engineers and served as President of the last named in 1910 and 1911. He was given the honorary degree of D.Sc. by Manchester University in 1911, awarded the Faraday Medal in 1924, made honorary member of the Institution of Electrical Engineers in 1925, elected to the Royal Society in 1927 and was President of the Electrical Development Association in 1929. He died at Zurich on January 13, 1930.

W. H. E.

INDEX TO VOL CXXVII (A)

Absorbing power of materials, measurement (Davis and Evans) 89
Aerofoil, effect of rotation (Bickley), 186
Alpha particles, measurements on ranges (Harper and Salaman) 175
Alpha particles, scattering from quantum mechanical point of view (Massey), 671
Analysis by X ray spectroscopy (Eddy and Laby) 20
Antimony, single crystal under torsional stresses (Gough and Cox) 431
Armstrong (H. E.) The Origin and Nature of Coal and Chars 268

Bengough (G. D.), Stuart (J. M.) and Lee (A. R.) The Theory of Metallic Corrosion in the Light of Quantitative Measurements, III 42
Benzene, kinetics of oxidation (Fort and Hinshelwood) 218
Bhagavantam (S.) and Venkateswaran (S.) The Raman Spectra of some Organic Halogen Compounds, 360
Bickley (W. G.) The Effect of Rotation upon the Lift and Moment of a Joukowski Aerofoil, 186
Bone (W. A.), Horton (L.) and Ward (S. G.) Researches on the Chemistry of Coal, VI 480
Broadway (L. F.) See Jackson and Broadway
Bromine, ionised, spectrum (Chandra Deb) 197
Burrard (Sir Sidney) The Geographical Representation of the Mountains of Tibet, 704

Carbazole series, antimonial analogues (Davies and Morgan) 1
Catalytic reactions at high temperatures—discussion 240
Chandra Deb (S.) On the Spectrum of Bromine in Different Stages of Ionisation, 197
Chlorine, absorption band spectrum, III (Elliott), 638
Coal and chars, origin and nature (Armstrong) 268
Coal chemistry of, VI (Bone and others), 480
Conductivity of thiocyanates in alcohol (Unmack and others) 228
Corrosion, metallic, III (Bengough and others) 42
Cox (E. G.) and Shaw (W. F. B.) Corrective Factors in the Photographic Measurement of X Ray Intensities in Crystal Analysis, 71
Cox (H. L.) See Gough and Cox
Crystal lattices, energy (Jones), 689
Crystals of antimony and zinc under torsional stresses (Gough and Cox), 431, 453

Davies (G. R.) See Morgan and Davies
Davis (A. H.) and Evans (E. J.) Measurement of Absorbing Power of Materials by the Stationary Wave Method, 89
Dirac's operators, group properties (Temple), 339
Discussion on Catalytic reactions at high temperatures 240

Eagle (A.) and Ferguson (R. M.) On the Coefficient of Heat Transfer from the Internal Surface of Tube Walls, 540
Eddy (C. E.) and Laby (T. H.) Quantitative Analysis by X Ray Spectroscopy 20

Electrons, fast, scattering and nuclear magnetic moments (Massey), 666
Electrons from incandescent solids, energy losses (Rudberg), 111
Electrons, liberation from metal surfaces (Oliphant and Moon), 373, 388
Electrons, scattering by atoms (Mott), 658
Elford (W J) Permeable Collodion Gel Films and Filtration Problems, 479
Elliott (A) The Absorption Band Spectrum of Chlorine, II, 638
Evans (E J) See Davis and Evans

Fenton (H J H), obituary notice, i
Ferguson (R M) See Eagle and Ferguson
Ferranti (S Z de), obituary notice, xix
Freeman (L J) The Spectra of O IV and N IV, 330
Fort (R) and Hinshelwood (N) The Kinetics of the Oxidation of Gaseous Benzene 218

Gough (H J) and Cox (H L) The Behaviour of a Single Crystal of Antimony subjected to Alternating Torsional Stresses, 431 Further Experiments on the Behaviour of Single Crystals of Zinc subjected to Alternating Torsional Stresses, 453

Hamshere (J L) The Mobility of Ions in Air, 298
Hargreaves (J) The Effect of a Nuclear Spin on the Optical Spectra, II, 141 , III 407
Harper (G I) and Salaman (E) Measurements on the Ranges of α Particles, 175
Harrison (G B) See Toy and Harrison
Hartley (Sir Harold) See Unmack and others
Hill (A V) A Thermal Method of Measuring the Vapour Pressure of an Aqueous Solution 9
Hinshelwood (N) See Fort and Hinshelwood
Horton (L) See Bone and others
Hydrogen atom, operational wave equation (Temple), 349

Ions in air, effect of water vapour (Nolan and Nevin) 155
Ions in air, mobility (Hamshere), 298

Jackson (Sir Henry), obituary notice, vi
Jackson (L C) and Broadway (L F) An Application of the Stern Gerlach Experiment to the Study of Active Nitrogen, 678
Jones (H) The Energy of Crystal Lattices, 689

Laby (T H) See Eddy and Laby
Lee (A R) See Bengough and others
Lowry (T M) and Snow (C P) The Optical Rotatory Power of Quartz on either side of an Infra red Absorption Band, 271

MacMahon (P A), obituary notice, x
Massey (H S W) Scattering of Fast Electrons and Nuclear Magnetic Moments, 666 Remarks on the Anomalous Scattering of α Particles from the Quantum Mechanical Point of View, 671
Methyl formate, thermal decomposition (Steacie), 314
Mica, splitting strength (Obreimoff), 290
Moon (P B) See Oliphant and Moon
Morgan (G T) and Davies (G R) Antimonial Analogues of the Carbazole Series, 1
Morgan (G T) and others Discussion on Catalytic Reactions at High Temperatures, 240

Mott (N F) The Scattering of Electrons by Atoms, 658
Müller (A) The Crystal Structure of the Normal Paraffins, 417
Murray Rust (D M) See Unmack and others

Nevin (T E) See Nolan and Nevin
Nitrogen, active (Jackson and Broadway), 678
Nitrogen, trebly ionised spectrum (Freeman), 330
Nolan (J J) and Nevin (T E) The Effect of Water Vapour on Diffusion Coefficients and Mobilities of Ions in Air 155
Nuclear spin effect on optical spectra (Hargreaves) 141 407

Obituary Notices —
Fenton, H J H, i
Ferranti, S Z de, xix
Jackson Sir Henry vi
MacMahon P A x

Obreimoff (J W) The Splitting Strength of Mica 290
Oliphant (M L E) and Moon (P B) The Liberation of Electrons from Metal Surfaces by Positive Ions, 373, 388
Optical rotatory power of quartz (Lowry and Snow), 271
Oxygen, formation of ozone after collision with electrons (Wansbrough Jones), 530
Oxygen interaction with nitrogen after collision with electrons (Wansbrough Jones), 511
Oxygen, trebly ionised, spectrum (Freeman), 330

Paraffins crystal structure (Muller), 417
Photo conductance (Toy and Harrison), 613 629

Quartz optical rotatory power (Lowry and Snow), 271

Ramakrishna Rao (I) Study of Electrolytic Dissociation by the Raman effect, I, 279
Raman effect, electrolytic dissociation of nitric acid (Ramakrishna Rao), 279
Raman spectra of organic halogen compounds (Bhagavantam and Venkateswaran), 360
Rosenhead (L) The Spread of Vorticity in the Wake behind a Cylinder, 590
Rudberg (E) Characteristic Energy Losses of Electrons scattered from Incandescent Solids, 111

Salaman (E) See Harper and Salaman
Shaw (W F B) See Cox and Shaw
Snow (C P) See Lowry and Snow
Spectra See also Raman.
Spectra, optical, effect of nucleus spin (Hargreaves), 141, 407
Spectra, trebly ionised oxygen and nitrogen (Freeman) 330
Spectrum absorption band, of chlorine, III (Elliott), 638
Spectrum of ionised bromine (Chandra Deb) 197
Steacie (E W R) The Kinetics of the Heterogeneous Thermal Decomposition of Methyl Formate, 314
Stern Gerlach experiment and active nitrogen (Jackson and Broadway), 678
Stuart (J M) See Bengough and others

Temple (G) The Group Properties of Dirac's Operators 339 The Operational Wave Equation and the Energy Levels of the Hydrogen Atom, 349
Thunderstorms, vertical electric currents (Wormell), 567
Tibet, representation of mountains (Burrard), 704

Toy (F. C.) and Harrison (G. B.) Photo-conductance Phenomena in the Silver Halides and the Latent Photographic Image, 613, 629
Tube walls, coefficient of heat transfer (Eagle and Ferguson), 540

Unmack (A.), Murray Rust (D. M.) and Hartley (Sir Harold) The Conductivity of Thiocyanates in Methyl Alcohol, 228

Vapour pressure of aqueous solution (Hill), 9
Venkateswaran (S.) *See* Bhagavantam and Venkateswaran
Vorticity, spread behind a cylinder (Rosenhead), 590

Wansbrough Jones (O. H.) The Interaction of Oxygen with Nitrogen after Collision with Electrons, 511 The Formation of Ozone from Oxygen after Collision with Electrons, 530
Ward (S. G.) *See* Bone and others
Wormell (T. W.) Vertical Electric Currents below Thunderstorms and Showers, 567

X ray intensities, photographic measurement (Cox and Shaw), 71
X ray spectroscopy, quantitative analysis (Eddy and Laby), 20

Zinc, single crystals under torsional stresses (Gough and Cox), 453

END OF THE ONE HUNDRED AND TWENTY SEVENTH VOLUME (SERIES A)

I. A. R. I.

IMPERIAL AGRICULTURAL RESEARCH
INSTITUTE LIBRARY
NEW DELHI.

Date of issue.	Date of issue.	Date of issue.